‘Morphological and Process Dynamics of the Lower Mississippi River’

by Oliver P. Harmar, BSc

Thesis submitted to the University of Nottingham
for the degree of Doctor of Philosophy, May 2004

CONTENTS

CHAPTER 1. INTRODUCTION 1

1.1 Rationale and principal research questions 1
1.2 History of large-scale studies in geomorphology 3
1.3 The renewed significance of large-scale studies 4
1.4 Technological developments 5
1.5 The complexity of alluvial channel systems 6
1.6 Geomorphological approaches 9
1.7 Considering large-scale behaviour 11
1.8 Multiple scales of dynamics: The Lower Mississippi River 13
1.9 Research outline 15

CHAPTER 2. RESEARCH DESIGN, FIELD AREA, AND DATA SETS 17

2.1 Chapter synopsis 17
2.2 Research design 17
2.2 Geographic, physiographic and hydrological setting 21
2.2.1 The Mississippi drainage Basin 21
2.3.2 The Lower Mississippi River 22
2.4 Geomorphological complexity 26
2.5 Physical controlling variables 29
2.5.1 Geological influences 29
2.5.2 Neotectonic influences 30
2.5.3 Climatic influences 32
2.5.4 Sea level 32
2.5.5 Internal adjustments at timescales greater than 2000 years 33
2.6 Human-induced controls 35
2.6.1 Early modifications (pre-1927) 35
2.6.2 Sustained channel engineering (1927 to late 1960s) 38
2.6.3 Environmental approaches (late 1960s to present) 47
2.6.4 Geomorphological implications 50
2.7 Geomorphological understanding 50
2.7.1 Investigation of spatial and temporal variation in channel form 52
2.7.2 Investigation of spatial and temporal patterns of sediment transport 57
2.7.3 Investigation of the spatial and temporal variation of the efficiency of channel form (flow resistance) 58
2.7.4 Understanding of regional-scale geomorphological response to engineering intervention 59
2.8 Available data sets 60
2.8.1 Data set coverage and resolution 61
2.8.2 Reliability of data sets 63
2.8.3 Historic maps of river planform 63
2.8.4 Late Holocene maps of abandoned channels 66
2.8.5 Hydrographic survey data sets 68
2.8.6 Flow stage and discharge data sets 72
2.8.7 Sub-reach scale data sets 72

CHAPTER 3. METHODOLOGICAL FRAMEWORK AND ANALYTICAL TECHNIQUES 78

3.1 Methodological framework 78
3.2 Regional-scale and reach-scale methods and techniques 78
3.2.1 One-dimensional parameterisation 79
3.2.2 Serial analysis 87
3.2.3 Morphological feature extraction and analysis 98
3.3 Sub-reach scale methods and techniques 101
3.3.1 Initial data processing 101
3.3.2 Morphological analysis 103
3.3.3 Flow analysis 105

CHAPTER 4. PLANFORM DYNAMICS 107

4.1 Chapter synopsis 107
4.2 Quantifying planform variation 107
4.2.1 Scales of planform variation 107
4.2.2 Determination of a suitable sampling interval 108
4.3 Identification of planform reaches 113
4.3.1 Development of zonation methodology using the 1880 direction change series 113
4.3.2 Determining the most appropriate window size and number of boundaries 119
4.3.3 Planform reach dynamics 121
4.3.4 The statistical significance of identified boundaries 125
4.4 Variation of channel length 126
4.4.1 Method 126
4.4.2 Analysis of results 129
4.5 Variation of channel width 136
4.6 Variation of the process regime 137
4.7 Integrating morphological and process variation: unit stream power 140
4.8 Variation of radius of curvature 143
4.9 Variation of meander wavelength and amplitude 152
4.9.1 Autocorrelation and partial autocorrelation 152
4.9.2 Second-order autoregressive modelling 154
4.9.3 Spectral analysis 161
4.9.4 Meander bend statistics 167
4.9.5 Meander wavelength estimation: comparability between techniques 175
4.9.6 Empirical relations between meander wavelength, channel width and channel discharge 185
4.10 Reach History: The importance of longer-term controls 190
4.10.1 Magnitude and rates of planform changes during the Holocene period 190
4.10.2 Planform dynamics at the 2000 year timescale 194
4.10.3 Linking the 2 000 year and 165 year timescales 200
4.11 Discussion 204

CHAPTER 5. THE REGIONAL-SCALE LONG PROFILE 209

5.1 Chapter synopsis 209
5.2 Obtaining a consistent data series 209
5.3 Detecting variation in profile slope at the regional, reach, and sub-reach scales 215
5.4 Variation in profile slope at the regional-scale 216
5.5 Variation in profile slope at the reach-scale 222
5.5.1 Geological controls 223
5.5.2 Tributary controls 225
5.5.3 Neotectonic controls 225
5.5.4 Engineering controls 227
5.6 Variation in profile slope at the sub-reach scale 230
5.7 Variation in pool and crossing amplitude and wavelength 232
5.7.1 Downstream trend removal by regression 232
5.7.2 Second-order autoregressive modelling 234
5.7.3 Spectral analysis 234
5.7.4 Pool and crossing parameterisation by regression 239
5.7.5 Pool and crossing parameterisation by the cumulative elevation change technique 248
5.7.6 Pool and crossing classification: comparability of regression and the cumulative elevation change technique in relation to meander length spacing 257
5.9 Discussion 260
5.9.1 Explaining the concave long profile 260
5.9.2 Downstream trends in large-scale bedform resistance 263

CHAPTER 6. REACH-SCALE LONG PROFILE DYNAMICS 265

6.1 Chapter synopsis 265
6.2 Obtaining representative data series 265
6.3 Discharge variation in relation to the data collection 266
6.4 Referencing long profiles to a common channel distance 268
6.5 Temporal variation in long profile slope at the reach-scale 275
6.6 Temporal variation in the amplitude and wavelength of pools and crossings 281
6.6.1 Removal of regression trends 281
6.6.2 Serial analysis 281
6.6.3 Pool and crossing parameterisation by regression 282
6.6.4 Pool and crossing parameterisation by the cumulative elevation change technique 286
6.6.5 Relating changes in the pool-crossing configuration to changes in profile slope 289
6.7 Spatio-temporal variation in cross-section morphological and process parameters 292
6.7.1 Obtaining a water surface profile 292
6.7.2 Variation of the roughness coefficient (n) 298
6.7.3 Computation of morphological parameters 301
6.7.4 Comparability of computed bankfull width to measured bankfull width 305
6.7.5 Analysis of morphological and hydraulic relations in the 1949-89 time period 310
6.8 Discussion 320

CHAPTER 7. SUB-REACH SCALE DYNAMICS 324

7.1 Chapter synopsis 324
7.2 Pool-crossing dynamics at annual timescales 325
7.2.1 Method of standardising channel distance 325
7.2.2 Thalweg elevation changes between December 1991 and February 2001. 325
7.2.3 Thalweg elevation changes at 1-2 year intervals 326
7.2.3 Significance for longer-term and larger-scale dynamics 332
7.3 Bed material movement at sub-annual timescales 333
7.3.1 Studies of bed material movement on smaller-scale alluvial rivers 333
7.3.2 Method 335
7.3.3 Bed material movement: multiple scales of dynamics 336
7.3.4 Form resistance at the sub-reach scale 351
7.3.5 Estimating bed material movement at the sub-reach scale 352
7.3.6 A re-appraisal of bed material movement 356
7.4 Form-process interrelationships: velocity field dynamics 358
7.4.1 Method 358
7.4.2 Evaluation of existing theories of pool-crossing maintenance 358
7.4.3 Analysis of ADCP velocity data sets 361
7.5 Discussion 372
7.5.1 Multiple scales of morphological and process dynamics 372
7.5.2 Issues of representation 374

CHAPTER 8. CONCLUSION 376

8.1 Understanding of geomorphological response 376
8.2 Significance of geomorphological response 381
8.3 Representing dynamic geomorphological behaviour 382
8.4 Methodological approaches 386
8.5 Recommendations for further research 388
8.5.1 Further research based on existing data sets 388
8.5.2 Further research requiring new data sets 389

APPENDIX A 391

REFERENCES 392

LIST OF FIGURES

Chapter 1. Introduction

Figure 1.1 Interrelationships between channel form and process (Richards, 1982). 8

Figure 1.2 Time and space scales of morphological adjustment (after Knighton, 1998) 8

Chapter 2. Research design, field area and data sets

Figure 2.1 The relationship between measured parameters and alluvial river channel dynamics. 19

Figure 2.2 The scale continuum of morphological data sets available to the study. 20

Figure 2.3 The Lower Mississippi River within: a) its drainage basin and; b) its alluvial valley. 23

Figure 2.4 Flow duration curve for Vicksburg, 1938-2001 water years. 25

Figure 2.5 The discharge record at Vicksburg. Discharge has been computed daily from measured records at approximately fortnightly intervals. 25

Figure 2.6 The complexity of large alluvial rivers: physical and human induced controls and the role of geomorphology. 28

Figure 2.7 Neotectonic and geological controls in the Lower Mississippi alluvial valley (adapted from Autin *et al*., 1991). 31

Figure 2.8 A timeline of channel engineering on the Lower Mississippi River considered within the context of key advances in geomorphological understanding, socio-political influences and extreme events. 36

Figure 2.9 Cutoffs on the Lower Mississippi River between 1929 and 1942: a) adapted from Stanley Consultants (1990) and; b) adapted from Winkley (1977). 42

Figure 2.10 Increase in levee heights 1844-1978 (modified from Smith and Winkley, 1996). 44

Figure 2.11 a) Application of an articulated concrete mattress to aid bank stabilisation and b) a stone dike field (Biedenharn, 2000). 44

Figure 2.12 Bank revetment and dike field construction in the USACE Vicksburg District (confluence of Arkansas River to Old River distributary) in the period 1860-1980 (Winkley, 1977). 45

Figure 2.13 Number of crossings dredged in the USACE Vicksburg District (confluence of Arkansas River to Old River distributary) in the period 1896-1975 (Winkley, 1977). 45

Figure 2.14 The space-time domain of each controlling variable. 51

Figure 2.15 Regional-scale adjustments to the long profile in the period 1950-94, as proposed by Biedenharn and Watson (1997). 55

Figure 2.16 a) Aerial photograph mosaic of the 'Cat-Fish Point' bend sub-reach of the Lower Mississippi River, collected by the USACE Vicksburg District in 1999 at an original scale of 1:20 000. b) A team undertaking subsurface borings in the alluvial valley (Moore, 1972). 67

Figure 2.17 The relation between the original USACE decadal-interval hydrographic survey maps and the digitised data. 70

Figure 2.18 The location of the local-scale study reaches. 73

Figure 2.19 The density of observed velocities in each flow cross-section. 75

Figure 2.20 The morphology of the Red Eye crossing and Missouri bend sub-reach. 77

Chapter 3. Methodological framework and analytical techniques

Figure 3.1 Summary of initial processing to allow quantitative analysis of planform. 81

Figure 3.2 Digitising and initial data processing from historic planform maps. 82

Figure 3.3 Digitising and initial data processing from abandoned channel maps. 83

Figure 3.4 Hydrographic survey data sets following removal of 'problem' cross-sections. In a), 1962-64 survey overlays the 1948-51 survey and in b), the 1973-75 overlays the 1962-64 and 1948-51 surveys. 84

Figure 3.5 Summary of the automated data processing procedure developed to sort an unstructured table of *(x,y,z)* coordinates into delineated cross-sections. 86

Figure 3.6 Initial data processing performed on the hydrographic survey data sets. 88

Figure 3.7 The decomposition of a series into its constituent components (adapted from Richards, 1979). 90

Figure 3.8 Hypothetical boundaries identified using the global zonation method. 94

Figure 3.9 Identification of pool and riffle bedforms based on the bedform differencing technique (modified from Robinson, 2003). 102

Figure 3.10 Computation of the channel centreline using the flow cross-sections. 104

Chapter 4. Planform dynamics

Figure 4.1 a) The direction series for the 1880 planform of the Lower Mississippi River between Cairo and the Head of Passes, based on a sampling interval of 2 km. b) The corresponding planform with the five 'direction reaches' identified. 109

Figure 4.2 a) Direction and direction change series from Cairo to the Head of Passes for the 1880 planform series; b) the selected reach from 730-1200 km and; c) the selected series. 110

Figure 4.3 The direction and direction change series for reaches: a) in the vicinity of the Greenville bends and; b) immediately downstream from New Orleans. 111

Figure 4.4 Experimenting with sampling intervals in the range 0.5-4 km: a) direction change series for the reach 200-400 km downstream from Cairo and b) representation of planform for the selected reach 250-290 km downstream from Cairo. 114

Figure 4.5 Spectral density plots for the 1930 planform series at sampling intervals of a) 1 km and b) 2 km. 115

Figure 4.6 Direction change and moving standard deviation for the 1880 planform series. Moving standard deviation has been calculated using window sizes of 40 km, 80 km and 120 km. 116

Figure 4.7 Boundaries identified in the 1880 standard deviation series generated using a window size of 80 channel km. 118

Figure 4.8 a) A box plot illustrating the distribution of standard deviation within the six reaches (identified by five boundaries) and b) identified boundaries superimposed on the 1880 planform. 118

Figure 4.9 Percentage of total variation explained against number of zonation boundaries for the a) 1765 and b) 1930 planform series. 120

Figure 4.10 Boundaries identified in the 1930 standard deviation series for window sizes of 60 km, 80 km and 100 km. 122

Figure 4.11 Boundaries identified by applying the zonation procedure to the moving standard deviation of direction change series in the period 1765-1975. 124

Figure 4.12 Statistical significance of adding additional boundaries to the 80 km moving standard deviation of the 1930 direction change series. In a) the p-value is plotted on a linear y-axis and in b) a logarithmic y-axis is used. 127

Figure 4.13 Statistical significance of adding additional boundaries to the: a) 40 km and; b) 120 km moving standard deviation of the 1930 direction change series. Logarithmic y-axes are used. 127

Figure 4.14 Histograms of the distribution of reach length for: a) 20; b) 40; c) 60; d) 80; and; e) 100 boundaries. 128

Figure 4.15 A summary of the processing routine used to delineate sub-reaches based on equal valley distance. 130

Figure 4.16 Channel length changes between Cairo and Baton Rouge in the period 1765 1975: a) total length change; b) percentage mean annual rates of channel length change. 133

Figure 4.17 Channel length changes in the period 1765-1930 based on division of the valley axis into 200 sub-reaches of equal length. 134

Figure 4.18 Average percentage rates of length change per km for the pre-cutoff period 1765-1930. Rates in a) are presented as a modulus of gross length changes whereas rates in b) are presented as net changes over the period. 135

Figure 4.19 a) Mean top-bank channel width and b) standardised rates of top-bank channel width change in the period 1830-1975 (based on data collected by Winkley, 1977). 138

Figure 4.20 Trends in mean annual discharge at Vicksburg in the period 1817-1975 based on data from Winkley (1977). 138

Figure 4.21 The implications of channel length and width variability for unit stream power. 141

Figure 4.22 Plots of average length against width in the period 1830-1975 for: a) the Lower Mississippi River from Cairo to Old River and; b) the individual planform reaches identified in Figure 4.11. 141

Figure 4.23 Determination of radius of curvature at each sampling point. 145

Figure 4.24 Median radius of curvature in relation to survey reach and survey year. 145

Figure 4.25 Median radius of curvature against reach sinuosity for each reach and planform survey in the period 1765-1975. 146

Figure 4.26 The relationship between meander wavelength, meander amplitude and sinuosity. 148

Figure 4.27 Mean radius of curvature against the relative size of meander bends, measured by proportional increases in both wavelength *and* amplitude. 148

Figure 4.28 Spatial and temporal variability of the median radius of curvature/width (R_c/w) relationship. 151

Figure 4.29 The definition of meander amplitude and wavelength parameters according to Inglis (1947) and Leopold and Wolman (1960). 153

Figure 4.30 a) The ACF and b) the PACF for the Lower Mississippi River between Cairo and Baton Rouge in 1930. 155

Figure 4.31 PACFs of the 1930 direction change series for the reaches identified in Figure 4.11. 155

Figure 4.32 Modelled direction change in relation to observed direction change for the 1930 planform series. 157

Figure 4.33 Predicted direction change against observed direction change for the 1930 planform series. 157

Figure 4.34 a) Mean wavelength classified by both reach and survey year; b) mean wavelength for each survey year and; c) mean wavelength for each reach. 159

Figure 4.35 Variation explained (R^2) against: a) survey year and; b) reach. 160

Figure 4.36 Spectral density plots for the Lower Mississippi River between Cairo and Baton Rouge, in 1930 and 1975. 163

Figure 4.37 Spectral density plots for the six planform reaches of the Lower Mississippi River from Cairo to Baton Rouge (Figure 4.11) for the 1930 and 1975 planform series. 164

Figure 4.38 Plots of peak spectral density against wavelength for the six reaches identified in Figure 4.11. 165

Figure 4.39 a) Peak spectral density and b) peak wavelength for each survey year for the Lower Mississippi River between Cairo and Baton Rouge. 166

Figure 4.40 Number of identified inflexion points against original sampling interval for the 1930 planform survey. 169

Figure 4.41 Identification of inflexion points in the 1930 planform survey by applying a tolerance value specifying a minimum distance between inflexion points. 169

Figure 4.42 Identification of inflexion points in the 1930 planform survey by specifying an additional tolerance based on angle change. 170

Figure 4.43 The final set of identified inflexion generated by specifying a minimum distance tolerance of 1 km and an angle change tolerance value of 0.25 radians. 170

Figure 4.44	Identifying parameters from 'unpaired' meander bends (after Brice, 1983).	172
Figure 4.45	Plots of mean bend amplitude against mean bend wavelength for the six reaches identified in Figure 4.11.	173
Figure 4.46	a) Mean bend amplitude and b) mean bend wavelength for each survey year for the Lower Mississippi River between Cairo and Baton Rouge.	174
Figure 4.47	Comparison of meander wavelengths estimated by spectral, second-order autoregressive and inflexion point techniques.	176
Figure 4.48	Hypothetical spectra for direction change series.	178
Figure 4.49	The relationship between bend amplitude and bend wavelength for first order points of inflexion identified from the 1930 planform series.	178
Figure 4.50	Hypothetical superimposition of meander bends.	179
Figure 4.51	Generation of a hierarchy of meanders and higher order undulations in the 1930 planform series by the inverse renormalisation method.	181
Figure 4.52	The distribution of wavelengths computed between identified points of inflexion in the first and second order hierarchy for the 1930 planform series.	181
Figure 4.53	The distribution of wavelengths for bends with a sinuosity greater than 1.5 in comparison to all bends for the 1930 planform series.	184
Figure 4.54	Spatial and temporal variability of the channel wavelength/width (λ/w) relationship.	187
Figure 4.55	Wavelength-width ratios for each reach identified by spectral and inflexion point techniques plotted onto the regression relationship identified by Leopold and Wolman (1957).	188
Figure 4.56	The classification of channel pattern based on sediment load, total sinuosity and relative stability (modified from Schumm, 1985).	193
Figure 4.57	Abandoned channel data processing and analysis routine.	195
Figure 4.58	The distribution of abandoned channels in the alluvial valley in relation to: a) the broad distribution of Late Wisconsin valley train deposits; b) two areas of active neotectonic uplift and; c) tributary inputs and major settlements.	197
Figure 4.59	The range of channel length experienced in each of the 200 valley reaches in the pre-cutoff (1765-1930) period in relation to the distribution of Late Holocene abandoned channels.	202

Chapter 5. Regional-scale long profile

Figure 5.1	The variability of cross-sectional spacing in the 1974-75 hydrographic survey from Cairo to the Head of Passes.	211
Figure 5.2	Representation of the 1974-75 long profile using a variety of sampling intervals.	213
Figure 5.3	Spectral plots for the detrended long profile in reach 7 at sampling intervals of: a) 1.0 km; b) 0.5 km and; c) 0.25 km.	214
Figure 5.4	The fitting of a second order polynomial trend and linear trends to the 1974-5 long profile of the channel thalweg.	219
Figure 5.5	Daily discharge trends for seven gauging stations in the 1986 water year.	219
Figure 5.6	a) Composition of bed material in 1989 thalweg survey and b) comparison of median grain diameters for the 1989 and 1932 thalweg surveys (modified from Queen, 1994).	221
Figure 5.7	a) Smoothing the 1974-5 long profile using a 40 km moving average. b) An 80 km moving average applied to the long profile plotted alongside the coefficient obtained by applying equation 5.2 using a 160 km split windowing procedure.	224
Figure 5.8	The five Holocene delta complexes recognised in the most recent interpretation of delta chronology (modified from Frazier, 1967; in Saucier, 1994).	226
Figure 5.9	a) Reach sinuosity in relation to the 1974-75 long profile and; b) temporal trends in reach sinuosity in the period 1765-1975.	229
Figure 5.10	Moving standard deviation plotted alongside the coefficient obtained by applying equation 5.2 using a 160 km split windowing procedure.	231
Figure 5.11	Definition of pool and crossing amplitude, length and spacing (pool-to-pool wavelength) based on a regular sine wave.	233
Figure 5.12	Comparison of the ACFs and PACFs for: a) reach 4 and; b) reach 7.	235
Figure 5.13	Spectral plots of the detrended long profile in each of the eight reaches.	237
Figure 5.14	Variation in wavelength downstream estimated by second-order autoregressive and spectral techniques.	238
Figure 5.15	Downstream trends in reach-averaged pool-to-pool wavelength using the regression techniques at three sampling intervals: 0.25; 0.5 and; 1.0 km.	240
Figure 5.16	Downstream trends in reach-averaged: a) amplitude; b) length and; c) amplitude/length ratio; as identified by the regression technique.	242

Figure 5.17 Variation in bedform shape between the upstream (reaches 1-5) and downstream reaches (reaches 6-8) of the Lower Mississippi River in 1975. 246

Figure 5.18 Roughness due to triangular blocks on a plane bed (modified from Richards, 1982). 246

Figure 5.19 Contrasting bedform shapes and their implications for removal of regression trends (modified from Robinson, 2003). 247

Figure 5.20 Identification of both significant and insignificant bedforms in the reach 1260-1340 km downstream from Cairo (reach 7). 247

Figure 5.21 The identification of pools and crossings between 1220 and 1320 km downstream from Cairo (reach 7) using tolerance values of: a) 8 m; b) 6 m; c) 4 m and; d) 2 m. 251

Figure 5.22 The increase in mean pool-to-pool spacing as tolerance value is increased for each reach. 252

Figure 5.23 Comparison of wavelengths estimated from second-order autoregressive modelling with mean pool-to-pool spacing at tolerances of 4 m, 6 m and 8 m using the cumulative elevation change technique. 254

Figure 5.24 Defining the length of a pool and crossing using mid-point elevations. 255

Figure 5.25 Trends in pool and crossing: a) amplitude; b) length and; c) amplitude/length ratio for the eight reaches of the Lower Mississippi River. 256

Figure 5.26 The distribution of pool-to-pool wavelength obtained by: a) regression classification and; b) the cumulative elevation change technique in relation to the distribution of meander bend lengths defined by points of inflexion. 258

Figure 5.27 Mean crossing to crossing spacing against mean distance between identified points of inflexion for the eight reaches of the Lower Mississippi River. 261

Figure 5.28 Cross-correlation of detrended thalweg elevation with the modulus of direction change for: a) reach 4 and; b) reach 7. 261

Chapter 6. Reach-scale long profile dynamics

Figure 6.1 Discharge against percent of time exceeded at the Vicksburg gauge for two timescales: a) ten water years prior to each hydrographic survey and; b) two water years prior to each hydrographic survey. 269

Figure 6.2	Percent of time exceeding 17 000 m^3s^{-1} and 30 000 m^3s^{-1} in each water year during the 1940-2001 period.	270
Figure 6.3	Longitudinal thalweg profiles for the four hydrographic surveys in the 1949-89 period.	272
Figure 6.4	Deep pools at the apex of highly sinuous bends in the 1949-1989 period.	274
Figure 6.5	The development of pools in the 1949-89 period in the sub-reach labelled *c)* in Figure 6.3.	274
Figure 6.6	Linear regression of downstream elevation change in the period 1949 - 1989 within the reach 570 – 1020 km downstream from Cairo.	276
Figure 6.7	a) Cumulative elevation change from 570 km downstream from Cairo in the period 1949-1989; and b) cumulative elevation change within three sub-periods dictated by the dates of intermediate hydrographic surveys.	277
Figure 6.8	Comparing long profiles in the 1949-89 period that have been smoothed by applying an 80 km moving average.	279
Figure 6.9	Spectral plots in the period 1948-1988 for reaches 4 and 5.	284
Figure 6.10	Temporal trends in reach-averaged: a) amplitude; b) length and c) amplitude/length ratio as identified by regression for the four hydrographic surveys in the period 1949-1989.	287
Figure 6.11	The increase in average pool-to-pool spacing as tolerance value is increased for the four hydrographic surveys in the period 1949-1989.	288
Figure 6.12	Temporal trends in reach-averaged: a) length and; b) direction change as identified by the cumulative elevation change technique for the 1949-89 period.	290
Figure 6.13	Derivation of the equation for gradually varied flow (after Richards, 1982).	293
Figure 6.14	Stage against discharge relationships: a) Flow stage against computed daily discharge for the Vicksburg gauge in the period 1983 – 1993 and; b) flow stage against discharge measured intermittently in the period 1967-1998.	297
Figure 6.15	Longitudinal thalweg profile and computed water surface profile for a discharge of 10 000 m^3s^{-1}.	299
Figure 6.16	The roughness coefficient (*n*-value) entered into the 1-D step-backwater model in order to calibrate the computed water surface with average flow stages at each gauging station.	302
Figure 6.17	Determination of: a) channel width (*w*) and; b) the asymmetry ratio (*a*) parameters.	303

Figure 6.18 Determination of channel area based on verticals of equal channel width. 304

Figure 6.19 Obtaining a channel width series. In a) the top-banks are digitised from aerial photographs of the river in 1999 and in b) a centre-line is digitised based on these bank lines. 309

Figure 6.20 Variation in channel width with distance downstream. 311

Figure 6.21 Histogram of channel widths: i) measured from aerial photographs and; ii) computed using the 1-D step backwater model. 311

Figure 6.22 Average depth against width for pools and crossings in reach 4. 314

Figure 6.23 Average depth against width for pools and crossings in reach 5. 315

Figure 6.24 Average depth against asymmetry ratio for pools and crossings in reach 4. 318

Figure 6.25 Average depth against asymmetry ratio for pools and crossings in reach 5. 319

Chapter 7. Sub-reach scale dynamics

Figure 7.1 a) The location of the annual dynamics study reach of the Lower Mississippi River and b) thalweg elevation against distance downstream in December 1991 and February 2001. 327

Figure 7.2 Changes in thalweg elevation in relation to variation in discharge for seven sub-periods between December 1991 and February 2001. 328

Figure 7.3 Thalweg dynamics between December 1991 and November 1994. 330

Figure 7.4 Thalweg dynamics between November 1992 and November 1996. 331

Figure 7.5 Elevation change of the thalweg through Red Eye crossing. 338

Figure 7.6 Flow stage at Baton Rouge from October 1998 to April 2002. 339

Figure 7.7 Surfaces of difference for four time periods between the 12th January 1999 and 7th August 2001. 340

Figure 7.8 a) Dune height and length dynamics identified by the cumulative elevation change technique using a tolerance value of 0.1 m and b) crossing elevation against flow stage at Baton Rouge in the 2000 and 2001 water years. 343

Figure 7.9 Temporal variations in: a) dune length as a multiple of flow depth and; b) dune height as a percentage of flow depth. 343

Figure 7.10 Multi-beam sonar survey of Red Eye crossing and Missouri Bend on the 8th March 2001. 345

Figure 7.11 1-D profile of the channel thalweg showing the crossing and downstream pool. 346

Figure 7.12 a) Area *A* of Figure 7.11 enlarged to show mega-dunes within the crossing reach and; b) an enlarged area of a) showing the migration of smaller-scale dune bedforms over an eight hour period, superimposed upon the larger dune forms. 346

Figure 7.13 Area *B* of Figure 7.11 enlarged to show the movement of dunes over an eight hour period. 347

Figure 7.14 Area *C* of Figure 7.11 enlarged to show the variation in bedform superimposition within the pool. 347

Figure 7.15 The length of bedform undulations in the thalweg profile disaggregated at three scales using the cumulative elevation change technique. 349

Figure 7.16 Area *D* of Figure 7.11 enlarged to compare dune characteristics obtained from multi-beam sonar with dune characteristics obtained from single beam sonar. 354

Figure 7.17 Typical bend and crossing sections in a large alluvial river (modified form Lane and Borland, 1953). 360

Figure 7.18 Change in area of selected velocity sections through the pool-crossing sub-reach. 360

Figure 7.19 TIN surfaces of resolved downstream velocities (parallel to the channel centre-line) at each selected flow cross-section for low flow stage. 362

Figure 7.20 TIN surfaces of resolved downstream velocities (parallel to the channel centre-line) at each selected flow cross-section for high flow stage. 363

Figure 7.21 TIN surfaces of resolved cross-stream velocities (perpendicular to the channel centre-line) at each selected flow cross-section for low flow stage. 364

Figure 7.22 TIN surfaces of resolved cross-stream velocities (perpendicular to the channel centre-line) at each selected flow cross-section for high flow stage. 365

Figure 7.23 Comparison of asymmetry in the resolved downstream velocity distribution between channel locations within the sub-reach at low and high flow stage 366

Figure 7.24 Percentage area of cross-section less than a series of threshold velocities for four selected cross-sections at a low and high flow stage. 368

Figure 7.25 Change in mean bed velocity with flow stage, calculated as the average between 0.7 and 1.0 multiples of the depth. 368

Figure 7.26 The distribution of near-bed velocities over the wetted perimeter at a) low flow stage and b) high flow stage. 369

Figure 7.27 Comparison of the velocity distribution coefficient (α) of resolved downstream velocity between channel locations within the sub-reach, and at low and high flow stage. 371

Chapter 8. Conclusion

Figure 8.1 Representing spatially-distributed form-process feedback mechanisms in a scale-hierarchical framework 384

LIST OF TABLES

Chapter 1. Introduction

Table 1.1 Research approaches in geomorphology. 9

Table 1.2 The status of variables in the alluvial channel system at different time scales (after Schumm and Lichty, 1965). 14

Table 1.3 Scale and mode of geomorphological explanation (after Church, 1996). 14

Chapter 2. Field study and available data sets

Table 2.1 Hydrological characteristics of the major tributary basins of the Mississippi Basin. 24

Table 2.2 The variability of mean discharge on the Lower Mississippi River. 24

Table 2.3 A process-response model showing regional responses of the Lower Mississippi River to glacial/interglacial cycles (modified from Autin *et al*., 1991). 34

Table 2.4 Base data sets available to the study. 62

Table 2.5 Techniques used to measure depth on the Lower Mississippi River. 64

Table 2.6 Techniques to measure horizontal position on the Lower Mississippi River. 65

Table 2.7 Historic planform maps of the Lower Mississippi River, published in the period 1765-1932. 67

Table 2.8 The sub-reach scale morphological data sets in relation to data sets employed in other recent case-intensive investigations. 75

Chapter 4. Planform dynamics

Table 4.1 Autoregressive coefficients, R^2, and estimated mean wavelength based on fitting second order autoregressive models to direction change series with sampling intervals in the range 0.5-4.0 km. 115

Table 4.2 Detection of pseudo-periodicity and mean wavelength estimation using second-order autoregressive models for each survey year for the Lower Mississippi River between Cairo and Baton Rouge. 154

Table 4.3 Detection of pseudo-periodicity and mean wavelength estimation by fitting second order autoregressive models to each reach. 158

Table 4.4 Published meander wavelength-width relationships. 185

Table 4.5 Calculation of meander wavelength according to published meander wavelength-discharge relationships. 189

Chapter 5. Regional-scale long profile

Table 5.1 Differences in data collection between the three USACE Districts for the 1974-1975 hydrographic survey. 212

Table 5.2 Comparing the variation in sampling spacing between the three USACE Districts using ANOVA. 212

Table 5.3 Removing the trend from the longitudinal thalweg profile of each reach by linear and second order polynomial regression and detection of pseudo-periodicity by second order autoregressive modelling. 236

Chapter 6. Reach-scale long profile dynamics

Table 6.1 Differences in data collection between the 1949-51, 1962-64, 1975 and 1988-89 hydrographic surveys in the USACE Vicksburg District (reaches 4 and 5). 267

Table 6.2 The behaviour of selected pool/crossing reaches within the 1949-1989 period. 273

Table 6.3 Vertical trends in long profile gradient in the period 1949 – 1989. 277

Table 6.4 Removing the trend from the longitudinal thalweg profile in reaches 4 and 5 by linear and second order polynomial regression and detection of pseudo-periodicity by second order autoregressive modelling. 283

Table 6.5 Gauge locations, flow stage and values of Mannings roughness coefficient (n) used in the flow model computation. 300

Table 6.6 Standard morphological and process parameters. 302

Table 6.7 Percent of time exceeded, mean channel width, and number of cross-sections where the measured elevation extends beyond the computed left and right banks in the 1988-89 hydrographic survey. 307

Table 6.8 Comparison of morphological and hydraulic characteristics of pools and crossings in reaches 4 and 5 based on independent samples t-tests. 316

Chapter 7. Sub-reach scale dynamics

Table 7.1 Height, length, H/L ratio and k_{form} characteristics of dunes measured by the weekly-interval single beam sonar and the hourly-interval multi-beam sonar surveys of Red Eye crossing. 353

ACKNOWLEDGEMENTS

This research was undertaken whilst in receipt of a studentship from the University of Nottingham, and the thesis was written whilst employed as a postdoctoral researcher at the University of Nottingham.

The research would not have been possible without support from the U.S. Army Corps of Engineers. At the Engineering Research and Design Center in Vicksburg, Mississippi, David Biedenharn helped to develop initial ideas and provided a network of contacts with whom I could discuss the research. Lisa Hubbard provided great logistical support whilst based in Vicksburg. My thanks also go to Donald Williams and Terecia Price at the Mississippi Valley Division Offices, Glenda Hill and Jack Smith at the Vicksburg District Offices and Donald Rawson in the New Orleans District Office for providing access to a range of data sets used within the research.

At Nottingham, my thanks go to the many members of staff and postgraduate students in the School of Geography who provided help at various stages of the research. In particular, I would like to thank three people: Colin Thorne for creating the opportunity to embark on such an ambitious project and for providing continued support since initially arriving in Nottingham; Nick Clifford for providing countless suggestions, corrections, and stimulating discussions; and Gary Priestnall for providing support on early research visits to Vicksburg.

Most of all, I would like to thank my family and friends for the tremendous support they have given me, particularly in the final stages of writing the thesis.

ABSTRACT

This thesis uses data sets at a range of spatial and temporal scales to examine the geomorphological response of the Lower Mississippi River to engineering and management. During the twentieth century the geomorphology of the Lower Mississippi River has been transformed by a series of engineering modifications to improve flood control and aid navigation. These have included steepening of the longitudinal profile by removal of the most sinuous bends, fixing the river to a constant planform through extensive bank stabilisation, and regulating sediment movement through the channel system by dike field construction. Prior to these modifications, the Lower Mississippi River adjusted its planform morphology to satisfy large-scale flow resistance requirements. However, this mode of adjustment has been effectively removed and adjustments are now restricted to the long profile and cross-sectional form.

Morphological analysis reveals that the river has responded to engineering intervention at two principal scales: by vertical changes in the elevation of the channel bed at the reach-scale; and by increasing large-scale bedform resistance at the sub-reach scale through longitudinal and cross-sectional adjustments. These mutual changes are consistent with the changes in water surface elevation in the post-modification period noted by Biedenharn and Watson (1997). However, analysis of morphological and process dynamics at shorter timescales shows that geomorphological response remains difficult to explain. This is because geomorphological behaviour at any scale, and in any location within an alluvial channel, is a product of complex spatially-distributed feedbacks between operating processes and multiple scales of channel morphology. This has general significance in terms of research design because detecting the complexity at each scale of adjustment, and forming linkages between scales of adjustment, is dependent on taking into account all possible degrees of freedom, and applying a range of complementary analytical techniques.

KEYWORDS: geomorphological response; engineering intervention; large-scale behaviour; form-process feedback; multivariate dynamics.

CHAPTER 1. INTRODUCTION

1.1 Rationale and principal research questions

Large alluvial rivers are complex and highly dynamic geomorphological systems that have immense socio-economic and political significance. Yet, owing to large spatial and often long temporal scales of change, and the associated problems of reliable data collection, they have remained relatively understudied in the geomorphological community. Instead, geomorphological research since the mid-twentieth century has been dominated by studies at small spatio-temporal scales. From an applied perspective, this trend represents something of a paradox, because the sustainable use of water resources and flood control in large drainage basins have become priorities on the global political agenda during a period of rapid socio-economic change (Petts, 1995; Newson, 1995). Fortunately, marked technological developments in both data monitoring and computerised analytical procedures over the past decade provide the opportunity to re-address large-scale geomorphological behaviour with a range of more rigorous quantitative and visual techniques.

This thesis addresses the extent to which morphological and process data sets gathered at a range of spatial and temporal scales may be used to investigate process-response dynamics on the Lower Mississippi River. At each scale, Geographic Information System (GIS) software-based routines are used in conjunction with customised data processing algorithms to derive a series of indicative morphological and process indices. A series of both traditional and more novel analytical techniques are then used to characterise the spatial and temporal variation in these indices.

The Lower Mississippi River is one of the world's largest alluvial rivers, flowing southwards through the central USA for approximately 1550 km to the Gulf of Mexico. During the twentieth century, the actively meandering planform of the river has been stabilised through a suite of engineering interventions to provide flood control and navigation benefits to the Lower Mississippi Valley. At the large-scale, this has effectively confined any long-term morphological response to adjustments

within the vertical dimension and hence, attention must focus on adjustments to the long profile and cross-sectional form. Three specific research questions are posed regarding the nature of pre and post-modification geomorphological behaviour:

1. *In the pre-modification period, how did the Lower Mississippi River adjust its planform characteristics and to what extent did these vary both spatially and temporally according to variations in the process regime and other physical controls?*
2. *In the post-modification period, how has the Lower Mississippi River adjusted its geomorphology to accommodate a steeper long profile and a stable planform imposed by engineering interventions?*
3. *At the sub-reach scale, how does the channel morphology adjust at shorter timescales in response to variations in discharge and bed material supply, and how can these be used to inform larger-scale and longer-term behaviour?*

Three further research questions are addressed regarding the nature of geomorphological behaviour at each spatio-temporal scale and the value of adopting a multi-scaled research design:

4. *To what extent can the Lower Mississippi River be considered a dynamic-process response system with form-process feedback mechanisms operating at a variety of scales?*
5. *To what extent can the multi-variate and multi-scaled nature of alluvial channel dynamics be revealed by adopting a GIS-based methodology and by utilising a range of novel and more traditional analytical techniques?*
6. *To what extent can data sets collected primarily from routine data monitoring programmes be used to inform morphological and process dynamics?*

These questions lead onto a set of research objectives listed in section 2.7.4. It is hoped that this research will contribute significantly to understanding how the Lower Mississippi River has responded geomorphologically to imposed engineering intervention and illustrate the benefits of adopting a scale integrated approach in order to understand large-scale behaviour. The remainder of this chapter reviews the

history of large-scale studies in geomorphology and justifies the critical need to improve understanding at this scale. The problems associated with representing the complexity of the fluvial system are then discussed and the merits of adopting a multi-scaled approach are stated. Finally, an outline of the research is presented.

1.2 History of large-scale studies in geomorphology

Although large-scale studies in geomorphology since the mid-twentieth century have become relatively rare, geomorphological research from its early origins as a sub-discipline of geology was primarily interested in large-scale behaviour. In the early twentieth century, geomorphological thought was strongly influenced by ideas of large-scale landform evolution introduced by William Morris Davis. Davis's (1899) most famous paper, titled 'the geographical cycle,' was based on the concept of a sequence of landform changes evolving through time following uplift of the landsurface. This model may never have been accepted by the majority of geomorphologists (Summerfield, 1991). However, it led to the proposition of alternative models of landform evolution (Penck, 1924; King, 1950) and firmly established geomorphology as a discipline concerned with the description and classification of landscapes (Coates and Viteck, 1980).

From the mid-twentieth century onwards, many geomorphologists distanced themselves from such 'historical explanation' and became increasingly concerned with the quantitative analysis of landform morphology (e.g. Leopold and Maddock, 1953) and the field measurement of geomorphological processes. This followed publication of influential papers in hydrology (e.g. Horton, 1945) and civil engineering (e.g. Bagnold, 1941, 1960). This change of focus reflected increasing doubts that qualitative Davisian geomorphology could advance understanding as to the nature and rate of landscape change through time (Summerfield, 1991; Beckinsale and Chorley, 1991). Strahler (1950; 210) epitomised this thought:

'Geomorphology is not a simple, pleasant, nature-lovers hobby, but a geophysical science of almost terrifying complexity.'

Strahler (1952) perceived geomorphology as lagging behind developments in the core sciences of chemistry, physics and biology, and therefore recommended that geomorphologists turn to physical and engineering sciences to research into the fundamental principles and laws of earth science. Thus, increasing emphasis on quantification represented an attempt to align geomorphology more closely with scientific thought and method, and therefore be more persuasive to the scientific community at large. The changing focus of geomorphological research also represented an attempt to develop a more practical agenda for the discipline at a time of increasing recognition of the negative environmental impacts of large-scale engineering intervention in river systems, and the increasing requirement for sustainable water resources management (Worster, 1985; Reisner, 1986; Graf, 2001).

Emphasis on the quantification of form and process has inevitably led to a decline in the space and time-scales at which geomorphological research is conducted. Although this has greatly enhanced our knowledge of process-form relationships at small spatio-temporal scales, geomorphologists have increasingly questioned its relevance to improving understanding of larger-scale and longer-term geomorphological behaviour (Douglas, 1982; Gardner, 1983; Summerfield, 1991; Sugden *et al*., 1997; Lane and Richards, 1997). The small-scale bias in contemporary geomorphology is paradoxical because, as the following discussion demonstrates with specific reference to large alluvial rivers, the demand for large-scale geomorphological understanding is continually increasing (Goudie, 1990; Gregory, 2000).

1.3 The renewed significance of large-scale studies

There is a pressing need for better understanding of the geomorphological behaviour of large alluvial rivers for four principal reasons. First, climate change predictions suggest a likelihood of more dynamic river channels in this century (Newson, 1992; IPCC, 1996). Because large alluvial rivers drain large catchments that may cover several physiographic and climatic regions, it remains difficult to predict likely changes in geomorphological behaviour associated directly with climate change. However, since large alluvial rivers are of immense economic, political and social

importance (section 2.4) in addition to their environmental significance, the likely effect of climate change demands further research. Second, in the developing world, demographic explosions have led to dramatic increases in people living in areas of high flood risk. The floodplains of large alluvial rivers such as the Yangtze, the Ganges-Brahmaputra, and the Nile are already some of the most densely populated regions of the world. During the twentieth century, the flooding of large alluvial rivers has often had catastrophic consequences for human life and livelihoods (Jones, 1997). Thus, in the twenty first century, human populations in such areas are likely to become even more susceptible to extreme flood events linked to large-scale geomorphological changes. Third, but related to the second, although large alluvial rivers have played an important role in the history of humankind ever since early civilisations settled along the banks of the Nile, Indus, Yellow and Euphrates (Schumm and Winkley, 1994), it is probably only in the modern era that human impact has become sufficiently large to exert a significant interference with respect to large-scale geomorphological dynamics. For example, the effects of large-scale vegetation clearance, floodplain reclamation and siltation have been linked to the increased incidence of flooding in the Yangtze River Basin in China (Chen *et al*., 2001; Yin and Li, 2001). Increasing demand for water resources in some counties is being addressed through larger-scale and more innovative engineering designs. Hence, large-scale interference may well increase further during the twenty-first century. Fourth, in the developed world, a philosophy stressing the need to work with rather than against the natural dynamics of the environment has risen as a backlash to over two centuries of engineering regulation and control (Petts, 1995). Although the overwhelming policy driver remains flood control, water supply and navigational requirements, this more environmental philosophy demands an improved understanding of what constitutes natural geomorphological dynamics on large rivers, and related to this, how these have been modified through engineering intervention and management.

1.4 Technological developments

Almost all studies that have addressed the large-scale character of alluvial rivers have been either remained largely descriptive and qualitative (e.g. Schumm and

Galay, 1994), or if quantitative, generalising from the use of relatively sparse spatial and temporal data sets (e.g. Biedenharn *et al.*, 2000). However, technological developments over the past decade, in both data monitoring and computerised analytical procedures, provide the opportunity to readdress large-scale geomorphological behaviour with a range of more rigorous analytical techniques. In terms of data collection, advances in satellite remote sensing (Curran *et al.*, 1998), remote hydrographical techniques (Gilvear *et al.*, 1995; Dinehart; 2002) and photogrammetric techniques (Dixon *et al.*, 1998; Westaway *et al.*, 2000) now allow relatively rapid and fully three-dimensional representations of morphology. This is particularly the case for large rivers which, because of their physical scale, are more easily monitored from remote sources than by direct measurement in the field. Developments in monitoring technology have enabled research to take place at a spatial and temporal scale that could not have been envisaged several decades ago (Summerfield, 1991; Gregory, 2000). Analytical procedures have advanced through increases in computer processing power in parallel with the advent of more powerful GIS software. Such software has been widely used in fluvial geomorphology since the mid-1990s as a platform to handle a variety of different data types and aid parametisation of large data sets (Milne and Sear, 1997; Gurnell *et al.*, 1998; Walsh *et al.*, 1998; Sear and Milne, 2000; Downs and Priestnall, 1999).

1.5 The complexity of alluvial channel systems

To readdress large-scale geomorphological behaviour in alluvial channels, it is necessary to consider the complexity of the relationship between form and process and explore how geomorphologists have attempted to understand the dynamics of alluvial channel systems more generally.

The relationship between form and process in alluvial channels can be considered in terms of the balance between force and resistance. Alluvial channels are open physical systems in which the energy available to perform hydraulic and geomorphological work is balanced by the energy expended overcoming resistance to flow. The rate of potential energy expenditure per unit bed area is represented by the stream power per unit width:

$$\rho_w g Q s / w \qquad (1.1)$$

where:

Q = discharge

s = channel slope

w = width

g = acceleration due to gravity (constant)

ρ_w = bulk unit weight of water

Resistance to flow can be divided into three major sources: skin resistance, which is dependent on the size distribution of the sediments which form the channel boundary; form resistance, which arises from the shape of channel morphology in its three dimensions (longitudinal, cross-sectional and planimetric) and spill resistance, where local flow acceleration or deceleration is rapid (Leopold *et al.*, 1960). Morphological changes can occur through sediment transport, when excess energy is available to entrain material from the channel bed and erode material from the channel banks. However, channel morphology also determines friction losses and hence, controls total resistance to flow. Thus, channel morphology controls, and is controlled by, the prevailing process regime.

Characterising adjustments between form and process in alluvial channels requires a large number of variables whose interdependence is not always clear. This is illustrated by Richards's (1982) representation of the alluvial channel system (Figure 1.1). Because of the large number of interacting feedbacks between variables, the specific response of the system to a change in any single variable is very difficult to predict. As a result of this complexity, the behaviour of alluvial channels is essentially indeterminate over even very short time and space scales (Maddock, 1969). At larger time and space scales, characterising adjustment is further complicated by the multi-scaled nature of fluvial morphology (Figure 1.2). Measurable morphological variables adjust over a range of spatial and temporal scales to the instantaneous process regime. Hence, process-form relations are complicated by lags or hysterisis effects between changes in the process regime and changes in channel morphology. Adjustments in the alluvial channel system can therefore be considered the product of the relationship between the 'immanent' ahistorical process domain and historical 'configurational' properties of fluvial morphology (Simpson, 1963).

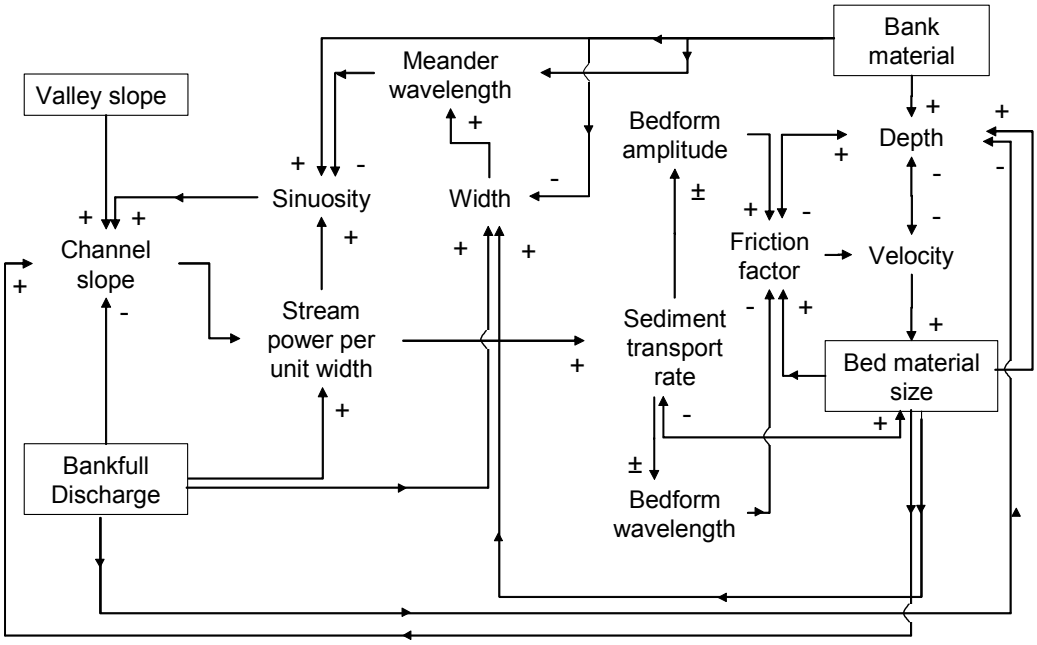

Figure 1.1 Interrelationships between channel form and process (Richards, 1982). Independent variables are contained within a box. Direct relationships are shown by +, inverse relationships are shown by –. Arrows shows the direction of influence; double headed arrows indicate reversible relationships.

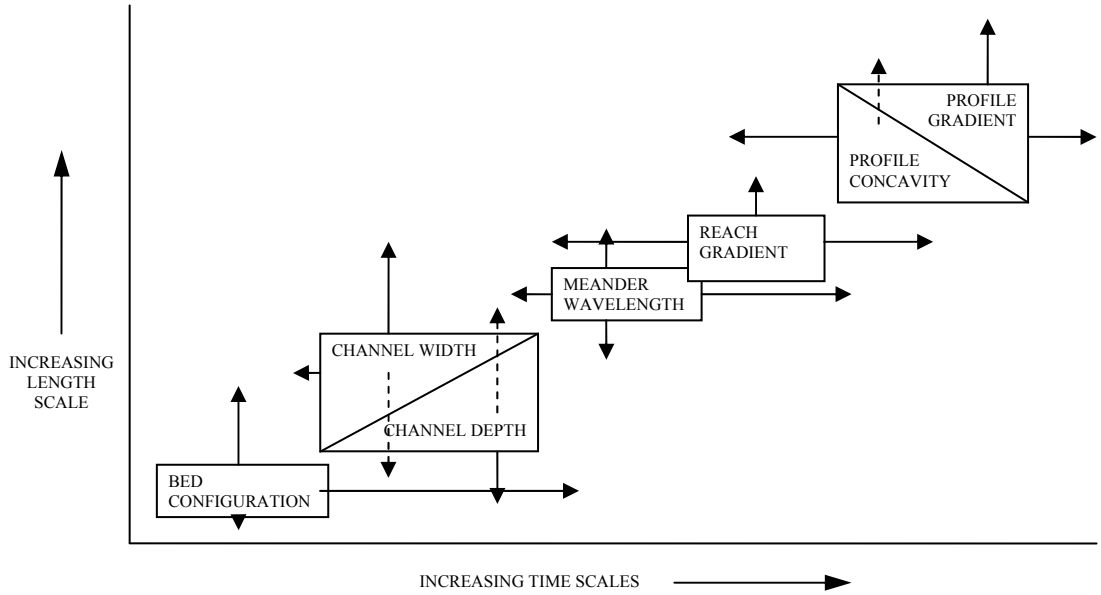

Figure 1.2 Time and space scales of morphological adjustment (after Knighton, 1998).

1.6 Geomorphological approaches

Faced with this complexity, researchers in fluvial geomorphology have taken to the challenge of developing the most rigorous explanations of river channel dynamics with the technology available to them. Over the last twenty years, the general approach has been cited as having undergone a transformation (Richards, 1990; Lane, 1995), moving from a classic 'black box' approach, where fluvial form was typically explained from operating processes by a series of unidirectional relationships, to a 'grey box' approach where the complex interrelations between process and form are identified. This represents a broader ontological shift from functionalism towards realism. The two approaches are summarised in Table 1.1.

Approach/Ontology	**Realist**	**Functionalist**
Research Design	Intensive	Extensive
Epistemology	Rational	Empirical
Explanation	Causal Explanation	Descriptive Generalisation
Typical Method	Small scale case study	Large-scale statistical analysis
Direction	Bottom-up	Top-down
Limitations	May not be representative or generalisable	Limited explanatory power

Table 1.1 Research approaches in geomorphology (modified from Sayer, 1992)

Embedded within the functionalist approach is general systems theory (Chorley, 1962) which encourages identification of all relevant variables in a defined system. All physical changes can be described by changes to the variables which describe the system and hence, a degree of explanatory closure is obtained. A qualitative example of this approach is provided by Schumm's (1969) qualitative relationships demonstrating how channel morphology adjusts to increases or decreases in discharge and bed material load, the dominant controls of channel form adjustment (Knighton, 1998).

$$Q^{+} = w^{+}, d^{+}, \lambda^{+}, s^{-} \quad (1.2)$$

$$Q^{-} = w^{-}, d^{-}, \lambda^{-}, s^{+} \quad (1.3)$$

$$L^{+} = w^{+}, d^{-}, \lambda^{+}, s^{+}, P^{-}, F^{+} \quad (1.4)$$

$$L^{-} = w^{-}, d^{+}, \lambda^{-}, s^{-}, P^{+}, F^{-} \quad (1.5)$$

where:

d = average channel depth

λ = meander wavelength

P = sinuosity

F = width-depth ratio

According to these relationships, an increase or decrease in discharge changes the dimensions of the channel and its gradient, but an increase or decrease in bed-material load at constant mean annual discharge changes not only channel dimensions, but also the shape of the channel (width-depth ratio) and its sinuosity. These relationships are admirable for their simplicity; however, changes in discharge and sediment load rarely occur alone. Where this is the case, it is often not clear in what manner morphological variables will change because complex variations in process can be accommodated by a series of mutual adjustments between different morphological variables. This is illustrated by considering a scenario where both discharge and bed material load increase:

$$Q^{+}, L^{+} = w^{+}, d^{\pm}, \lambda^{-}, s^{\pm}, P^{+}, F^{-} \qquad (1.6)$$

Channel depth and channel gradient should change in opposite directions, however, it is not clear whether gradient should steepen and depth decrease, or conversely, gradient flatten, and depth increase. For more complex scenarios, Schumm's qualitative relationships therefore demonstrate that cause and effect in the fluvial system are difficult to distinguish (Chorley *et al.*, 1984). Quantitative examples of classical functional relationships are provided by hydraulic geometry (Leopold and Maddock, 1953) and regime theory (Blench, 1969) which describe a stable channel morphological configuration as a function of the prevailing process regime.

The functional approach implicitly assumes that the causes of long-term and large-scale geomorphological behaviour may be discovered from repeated observations of events. However, this assumption has been criticised by more realist researchers who suggest that the link between empirical observations and the fundamental generating mechanisms is, at best, weak. Instead, realist theory recognises three levels of reality at which a phenomenon can be structured; the fundamental generating mechanism, the events that produced these mechanisms and the

experimental observations of these events (Sayer, 1992). These are termed the real, the actual and the empirical by Richards *et al*. (1996). Hence, realist theory advocates that in open physical systems, the action of a particular mechanism may not always produce the same event because it is dependent on the interaction with a wider set of mechanisms and on the particular contingent conditions. In practical terms, instead of viewing morphology as the outcome of process, realist approaches recognise their interdependence and interpret the interrelationships in terms of a series of spatially distributed feedbacks between process and form variables (e.g. Figure 1.1). This has been recognised by several researchers at small spatio-temporal scales (Ashworth and Ferguson, 1986; Clifford *et al*, 1993; Lane *et al.*, 1996) but has never been applied at larger scales of enquiry. This is partly because the realist approach is typified by intensive, case study research which is not often feasible to apply at larger scales of analysis.

1.7 Considering large-scale behaviour

Neither functionalist nor realist approaches are alone able to satisfactorily explain large-scale geomorphological behaviour. This is illustrated by considering conventional approaches to studying adjustments to the long profile of rivers. Most previous attempts have either modelled the shape of the geological profile using trend fitting procedures and compared the output to the classic concave equilibrium profile identified by (Hack, 1960); or, at much smaller spatio-temporal scales, examined the formation of the pool-riffle sequence and the associated mechanisms of adjustment (Clifford, 1993). However, few, if any, studies have attempted to link these two scales of analysis through an investigation of large-scale adjustments of the long profile at a timescale corresponding to the design life of the typical engineering project (Richards *et al*., 1987).

To improve understanding of large-scale geomorphological behaviour, it is necessary to consider how relationships between process and form change at different spatio-temporal scales. Schumm and Lichty (1965) state that the status of controlling variables, and the nature of their interrelationships, change with the time and space scale adopted (Table 1.2). Over geological timescales, Schumm and Lichty consider

channel morphological variables to be indeterminate in relation to instantaneous flow and sediment transport characteristics whereas at the shortest 'present' timescale they are considered independent. At an intermediate or 'graded' timescale however, at which steady state conditions persist, 'equilibrium channel forms' are considered to adjust to the prevailing process regime (Brunsden and Thornes, 1979). By recognising discrete spatio-temporal scales of behaviour, Schumm and Lichty therefore imply that an understanding of geomorphological behaviour at any one spatio-temporal scale can be gained by identifying the dependent and independent variables operating at that scale and considering their interaction. With regard to large-scale behaviour, this therefore suggests that understanding can be gained through repeated observations of large-scale dynamics.

More recent research differs from Schumm and Lichty by stressing the importance of reconciling linkages between scales in the understanding of large-scale behaviour. Lane *et al*., (1996) and Lane and Richards (1997) envisage morphological dynamics at a single scale as being conditioned by, and involved in, the conditioning of both larger and smaller spatio-temporal scales. Viewed in this context, adjustments to the channel systems may be categorised as either 'bottom-up' or 'top-down'. In the former, changes to the incoming discharge and sediment regime may result in changes to the operation of spatially distributed form-process feedback mechanisms at the local scale. Over a defined period of time, the cumulative action of these mechanisms may be sufficient to cause a larger-scale morphological change. For example, an increase in sediment load may initially lead to cross-sectional scale changes but through longer-term process-form interactions, may be sufficient to initiate regional planform and long profile changes. Such morphological adjustment higher up the hierarchy may then directly modify morphology at smaller spatio temporal scales in a top-down manner. For example, a meander cutoff will locally exert a change in long profile and channel cross-sections as well as locally changing the nature of spatially distributed form-process feedback mechanisms.

Despite the assumed importance of both 'bottom-up' and 'top-down' conditioning, neither a functionalist nor a realist research approach has been able to offer a rigorous insight into the nature of scale relations. Improving understanding of scale relations is considered by Petts (1995) to be one of the greatest challenges for studies

of river channel adjustment in the twenty-first century. In this thesis, the importance of scale linkages to developing understanding large-scale behaviour is examined by adopting a multi-layered approach and by utilisation of a range of analytical techniques at each spatial and temporal scale selected. The concept of reality being observed through 'multiple layers of explanation' has been discussed by Church (1996) with specific reference to the variation of velocity in rivers (Table 1.3) but it has never been examined by quantitative means. As the scale of enquiry is increased, Church envisages the level of contingency to increase and hence, empirical regularity to therefore decrease. However, at any scale of analysis, the importance of contingency may vary and hence, different reaches may exhibit different geomorphological behaviour. With this in mind, an initial question regarding the multi-layered approach is the extent to which dynamics at any single scale can be adequately identified and represented. Examination of the nature of variation at each scale may highlight both the relative importance of external and internal controls, and the strength and direction of scale-linkages within the system.

1.8 Multiple scales of dynamics: The Lower Mississippi River

The Lower Mississippi River provides an ideal field site to study large-scale geomorphological behaviour for two reasons. First, in the twentieth century, a suite of engineering interventions and other anthropogenic driven changes have transformed the geomorphology of the river. Interventions include steepening of the long profile by removal of the most sinuous bends, fixing the river to constant alignment through extensive bank stabilisation, and regulating sediment movement through the channel system by dike field construction (chapter 2). Second, the Lower Mississippi River has historically been one of the most intensely studied large alluvial rivers in the world. Consequently, a comprehensive record of geomorphological response to these changes is provided by a suite of observed data sets extending back to 1765, and reconstructed data sets covering the Late Holocene period.

River Variables	Geologic (10^3 + yrs.)	Modern (10^1 to 10^2 + yrs.)	Present (1 to 10 yrs.)
Geology	Independent	Irrelevant	Irrelevant
Climate	Independent	Independent	Independent
Vegetation	Dependent	Independent	Independent
Relief	Dependent	Independent	Independent
Palaeohydrology	Dependent	Independent	Independent
Valley Dimensions	Dependent	Independent	Independent
Mean discharge of water and sediment	Indeterminate	Independent	Independent
Channel morphology	Indeterminate	Dependent	Independent
Observed discharge of water and sediment	Indeterminate	Indeterminate	Dependent
Observed flow characteristics	Indeterminate	Indeterminate	Dependent

Table 1.2 The status of variables in the alluvial channel system at different time scales (after Schumm and Lichty, 1965).

Spatio-temporal scales	Mode of explanation
Very small	Stochastic
Small	Deterministic
Medium	Deterministic chaos
Large	Descriptive

↓ Increasing contingency

Table 1.3 Scale and mode of geomorphological explanation (after Church, 1996).

To investigate large-scale geomorphological behaviour, morphological and process data sets have been compiled from a range of U.S. Army Corps of Engineer (USACE) archival sources. The actual data sets together with all previous research into the long-term and large-scale geomorphological behaviour of the Lower Mississippi River are discussed in chapter 2. In general, previous researchers have been restricted to using process-based data sets at spatial and temporal resolutions which are too coarse to detect the full complexity of change (Grebau, *pers com*). This thesis advances previous research by taking advantage of technological developments in both data monitoring equipment and data processing operations which have transformed the way in which research can be conducted. Older data sources including historic maps of river planform and hydrographic surveys are re-examined using a plethora of new and often more consistent analytical techniques. In parallel with this, a variety of new high resolution morphological and process data sets, collected over the last decade, are analysed for shorter sub-reaches of the Lower Mississippi River.

1.9 Research outline

The principal aim of the thesis and the key research questions are explored in the following seven chapters. Chapter 2 introduces the formal research design, considers the Lower Mississippi River as a field site, and evaluates previous research into large-scale geomorphological response to engineering and management. This is followed by a description of the range of data sources available to the study. The methodological framework and range of analytical techniques are then presented in chapter 3.

The analytical results of the thesis are presented in four chapters. In chapter 4, a series of complementary analytical techniques are used to examine how the Lower Mississippi River adjusted its planform morphology in the pre-modification 1765-1930 time period. The spatial and temporal distribution of adjustments is considered against changes in the process-regime and other physical controls operating over much longer temporal intervals. Chapter 5 applies a similar analytical approach to the contemporary long profile. The profile is considered a morphological

configuration which can be disaggregated at three principal scales. At the regional-scale, an assessment is made of the extent to which downstream variations in the form of the long profile can be explained by the contemporary flow and sediment regime of the Lower Mississippi River, as imagined in Mackin's (1948) concept of a graded state. At the intermediate reach-scale, the importance of long-term geological, neotectonic and tributary controls in determining the reach-scale profile is established. Finally, at the sub-reach scale, downstream trends in the characteristics of pool-crossing formations in the long profile are assessed to see the extent to which they are adjusted to larger reach and regional-scale characteristics. Hence, in chapters, 4 and 5, analytical techniques are used to examine the extent to which a range of morphological properties associated with the contemporary planform and long profile are adjusted to the prevailing process regime, or reflect the operation of longer-term contingent controls.

Chapter 6 examines the nature of geomorphological response to engineering intervention. Because extensive bank stabilisation has effectively restricted response to the planform, attention is focused on the longitudinal and cross-sectional form. Fourteen artificial cutoffs constructed on the river between 1932 and 1942 steepened the long profile and removed the most sinuous bends (Winkley, 1977). These changes are consistent with an increase in stream power. Thus, it is hypothised that the river may have responded by increasing large-scale bedform resistance by increasing the amplitude and/or the frequency of pool-crossing undulations in the long profile. In chapter 7, a detailed study of a single sub-reach using relatively new high resolution data sets at sub-annual timescales, is coupled with annual-interval hydrographic surveys of a larger reach to explore the dynamics of pools and crossings at shorter timescales. This is undertaken to examine whether changes in morphological configuration can be identified at annual and sub-annual timescales that are consistent with the longer-term and larger-scale changes identified in chapter 6. The conclusions to the thesis are presented in chapter 8.

CHAPTER 2. RESEARCH DESIGN, FIELD AREA, AND DATA SETS

2.1 Chapter synopsis

This chapter introduces the formal research design, considers the Lower Mississippi River as a field site, and evaluates previous research into large-scale geomorphological response to engineering and management. This is followed by a description of the range of data sources available to the study. The Lower Mississippi River represents a challenging case study because it encompasses great physical and human-induced complexity at such a large scale. Although geomorphological behaviour has been widely studied, most previous research has relied upon the use of relatively sparse spatial and temporal data sets and hence, significant gaps in understanding remain. These gaps are addressed in this thesis by exploring geomorphological behaviour at a variety of spatio-temporal scales.

2.2 Research design

The research design couples analysis of selective morphological data with analysis of selective process data sets, in order to identify dynamic geomorphological behaviour. This behaviour is explained in terms of the relationship between energy availability and energy expenditure, as shown in Figure 2.1. Because alluvial river channels can adjust their morphologies through multiple degrees of freedom, a number of parallel investigations are undertaken into different components of adjustment. Each component is examined by computation of a series of appropriate parameters and then analysing their mutual adjustment in time and space.

The time and space scales selected for analysis are determined in part by the coverage and resolution of available morphological and process data sets. Figure 2.2 shows that in terms of total data set coverage, the available morphological data sets are clustered at two predominant scales. These clusters can be delineated most clearly at a spatial scale of approximately 10^4 m and each data set is therefore referred to as either regional-scale ($>10^4$ m) or local-scale ($<10^4$ m). However, the

regional-scale data sets are of an exceptional spatial and temporal resolution and hence, the data sets together allow an evaluation of the scale continuum presented in Figure 1.2. Planform dynamics are examined at a maximum 210 year timescale using historic planform maps and hydrographic surveys for the period 1765-1975; and at a longer (2000 year) timescale using reconstructed maps of abandoned channels. The regional-scale longitudinal profile is examined based upon the 1974-75 hydrographic survey from Cairo to the Gulf of Mexico. Approximately decadal-interval hydrographic surveys for the USACE Vicksburg District are used to study the reach-scale morphological changes in the post-cutoff channel from 1949 to 1989. Finally, shorter-term morphological dynamics are studied at the reach-scale using annual-interval hydrographic surveys, and at the smaller sub-reach scale using selected single-beam sonar and multi-beam sonar surveys of the channel. Analysis of process data sets includes long-term routine measurements of flow stage and discharge, and shorter-term acoustic doppler current profiler (ADCP) data sets, collected at both high and low flow stage.

The range of observed data sets include measurements collected as part of long-term routine monitoring programmes, undertaken primarily to meet statutory responsibilities, and localised data sets of specific reaches, collected as part of programmes commissioned by local USACE Districts. Thus, in addition to academic consideration, an important question in this thesis concerns the management value of observed data sets that have not been collected primarily to undertake regional-scale geomorphological research. From an applied perspective, this issue has wider applicability in geomorphology because the investigation of large-scale and long-term behaviour often requires the use of data sets which may have been collected for either a different primary purpose, or increasingly, a range of interdisciplinary purposes.

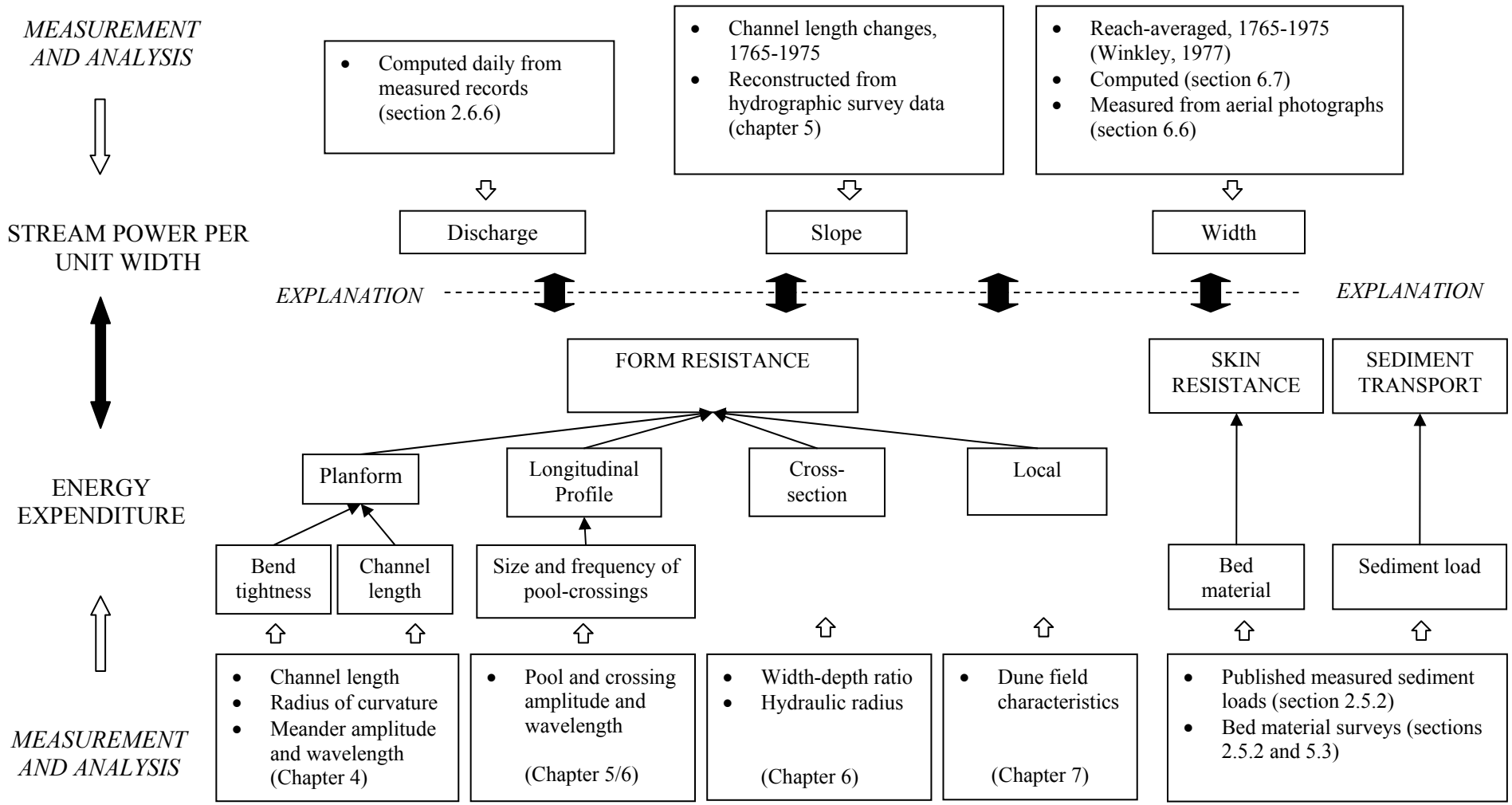

Figure 2.1 The relationship between measured parameters and properties of alluvial river channels.

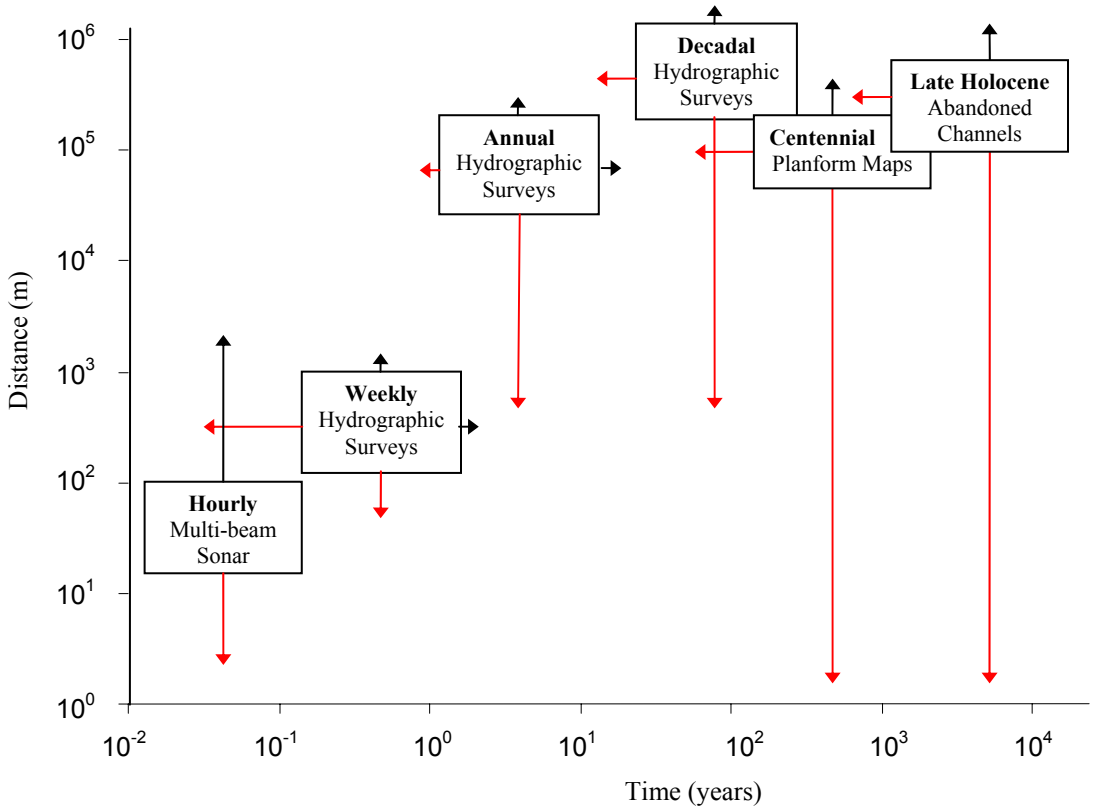

Figure 2.2 The scale continuum of morphological data sets available to the study. Red arrows indicate the minimum spatio-temporal longitudinal resolution of each data set and black arrows indicate the spatio-temporal coverage of each data set.

2.2 Geographic, physiographic and hydrological setting

2.2.1 The Mississippi Drainage Basin

The Mississippi River, together with the Missouri River, its longest tributary, flows for 6 260 kilometres through the central USA to the Gulf of Mexico (Figure 2.3a). The total drainage area of the Mississippi River and its tributaries is 3.2 million square kilometres which constitutes forty one per cent of the continental USA (Biedenharn *et al*., 2000). In comparison to other large rivers, the Mississippi River and its tributaries rank third in terms of channel length (from the outlet to the source of the longest tributary), fourth in terms of basin area, and eleventh in terms of mean annual discharge (Schumm and Winkley, 1994).

The Lower Mississippi River flows downstream from the confluence of the Ohio River at Cairo, Illinois, to the Gulf of Mexico. The input flow and sediment discharge to the Lower Mississippi River can be considered the product of three major tributary basins which together drain over 98 percent of the total basin area upstream from Cairo. The relative size and hydrological characteristics of these three basins, plus a major downstream sub-basin (the Arkansas Basin), is presented in Table 2.1. Each tributary basin has a unique physiography in terms of climate, geology and topography and consequently, a unique flow and sediment transport regime. The largest tributary basin, the Missouri Basin, drains into the Mississippi River near St. Louis, Missouri. The Missouri River drains the relatively dry inner plain states and the eastern side of the semi-arid and geologically active Rocky Mountain range, contributing an average of 44 percent of the discharge and 80 percent of the sediment regime to the Middle Mississippi River (Tuttle, 1998; Changnon, 1996). The remaining discharge and sediment load is supplied by the wetter, but geographically much smaller, Upper Mississippi Basin. The third large basin, the Ohio Basin, drains part of the more humid eastern United States and the western fringe of the geologically mature Appalachian mountain range. It is therefore characterised by a relatively high discharge and low sediment load (Tuttle, 1998). The Ohio Basin contributes an average of 54 percent of the discharge to the Lower Mississippi River. This is greater than the combined contribution of the

Upper Mississippi and Missouri Basins (which form the flow of the Middle Mississippi River) despite representing just 16 percent of the total drainage basin.

2.3.2 The Lower Mississippi River

The Lower Mississippi River flows through its alluvial valley and deltaic plain to the Gulf of Mexico, a channel distance of approximately 1 550 km (Figure 2.3b). The alluvial valley is bounded to the east by a distinctive bluff line separating the valley from the loess uplands of Tertiary age. To the west, the boundary is more difficult to define because of the merging of valleys of principal tributaries with the main Mississippi alluvial valley (Saucier, 1994). The present course of the Lower Mississippi River generally flows close to the eastern bluff line except between Memphis and Vicksburg where it flows across the central alluvial valley. Historically, the entire width of the alluvial valley, ranging from 48 kilometres to 200 kilometres, was inundated during periods of high flow. However, today it is protected by levees which confine the flood flows to a floodplain with an average width of only eight kilometres (Biedenharn and Thorne, 1994). The alluvial valley eventually merges with the deltaic plain where the deposition of sediment has historically been the most important process. Previous authors have consistently established the head of the most upstream distributary, the Atchafalaya River, as the boundary between the alluvial valley and deltaic plain (Hudson and Kesel, 2000).

The mean discharge characteristics of the Lower Mississippi River are presented in Table 2.2. The long-term (1938-2001) mean discharge at Vicksburg was 17 140 m^3s^{-1}. According to Figure 2.4, this is equalled or exceeded approximately 40 percent of the time. Over the same period, the mean annual maximum discharge was 43 500 m^3s^{-1} and the mean annual minimum discharge was 5 700 m^3s^{-1}. Over a shorter 15 year period (1983-97) the mean discharge was over 2 000 m^3s^{-1} greater than the long-term mean, suggesting that the record may display significant shorter-term variation (Winkley, 1977). The hydrograph is strongly seasonal with a peak discharge typically occurring in early Spring and a minima occurring in early Autumn. Figure 2.5 shows that the annual hydrograph was characterised by a relatively regular form throughout the 1990s with the exception of the 1992 and 1993

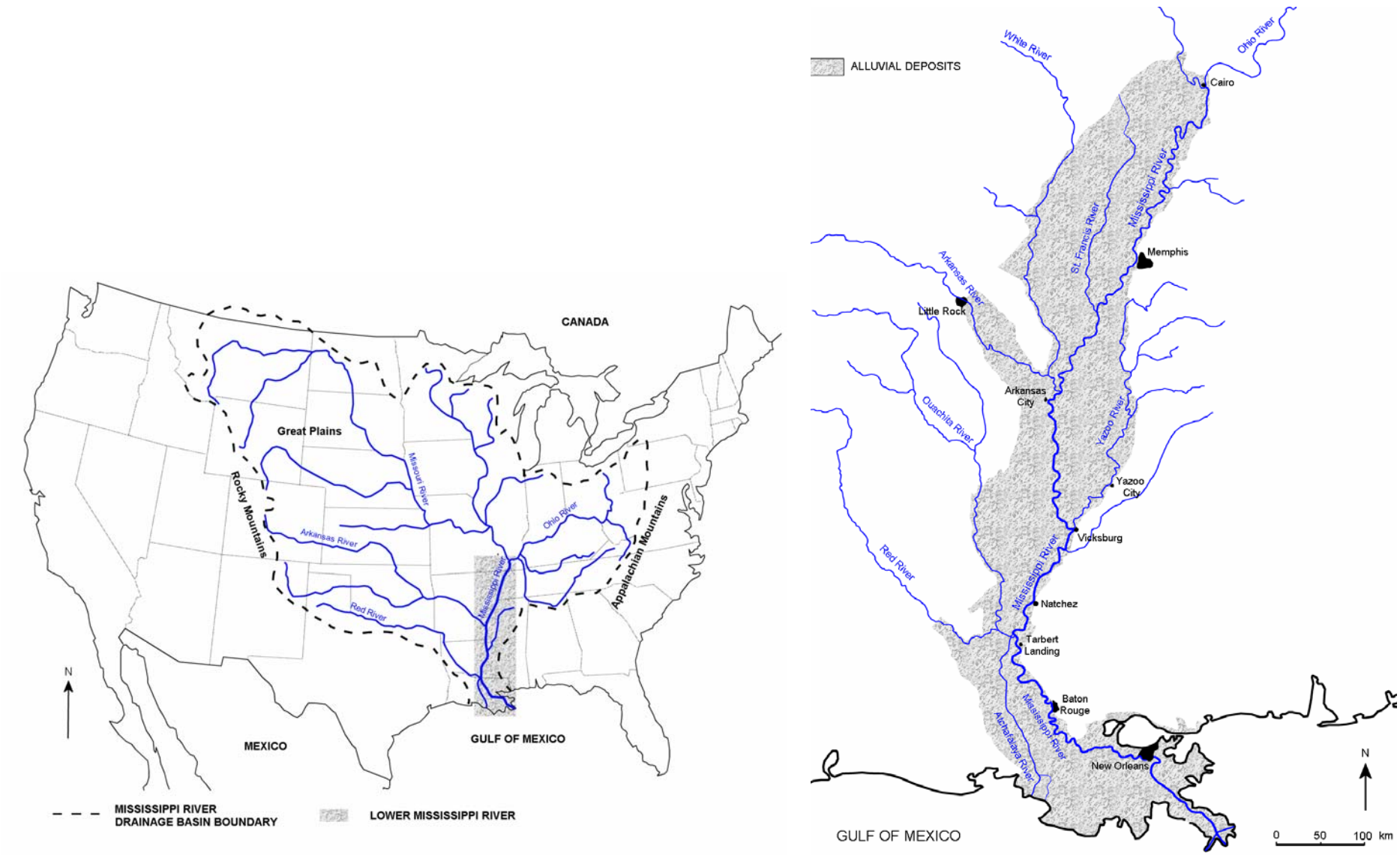

Figure 2.3 The Lower Mississippi River within: a) its drainage basin and; b) its alluvial valley.

Major Tributary Basins	Drainage area as a percent of total drainage area	Average contribution *	Minimum monthly contribution*	Maximum monthly contribution*
Upper Mississippi	13.8			
Missouri	42.4	44	35 (January)	52 (July)
Ohio	16.4	54	34 (July)	76 (January)
Arkansas/ White	14.6	14	11 (July/August)	17 (June/October)

*percent to existing flow at the tributary confluence

Table 2.1 Hydrological characteristics of the major tributary basins of the Mississippi Basin.

Gauging Station	Channel distance downstream from Cairo†	Mean Discharge (m^3s^{-1})	
		1938-2001*	1983-97*
Hickman	61		14 955
Memphis	351		16 135
Arkansas City	642	16 471	18 656
Vicksburg	827	17 140	19 272
Natchez	944	17 122	19 170
Tarbert Landing	1025		16 142

*water year

† based on 1975 distance

Table 2.2 The mean discharge of the Lower Mississippi River at gauging stations between Cairo and Head of Passes. Channel distance is the 1975 distance downstream from Cairo.

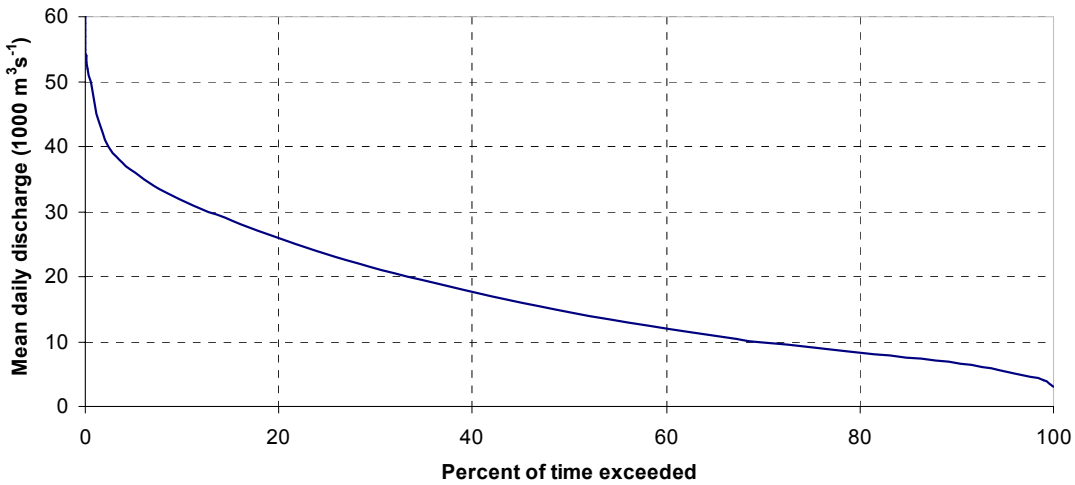

Figure 2.4 Flow duration curve for Vicksburg, 1938-2001 water years.

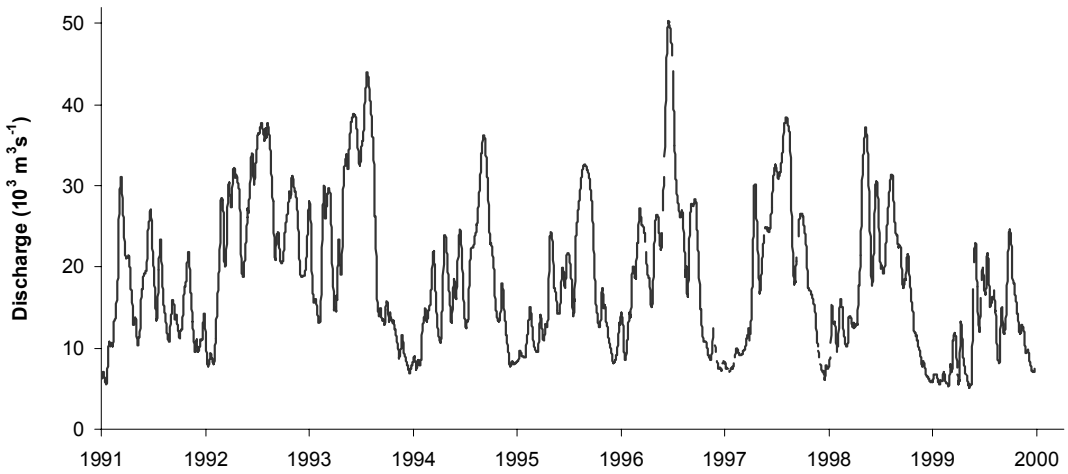

Figure 2.5 The discharge record at Vicksburg. Discharge has been computed daily from measured records at approximately fortnightly intervals.

water years when a sustained period of high flow was observed. In these two years, computed daily discharge exceeded 13 000 m^3s^{-1} for over 620 consecutive days. The geomorphological significance of annual and longer-term variation in discharge is investigated further in chapters four, six and seven.

The mean discharge is relatively stable downstream because there are no major discharge contributing tributaries downstream from Cairo. The largest tributaries of the Lower Mississippi River are the Arkansas and White Rivers which confluences just upstream from Arkansas City. Together, these tributaries contribute an average of approximately 2 350 m^3s^{-1}. This accounts for the majority of the difference in mean discharge between Helena and Arkansas City during the period 1983-97. The remaining increase is attributable to input from the St. Francis basin, a sub-basin of the alluvial valley. Similarly, the relatively small increase in mean discharge between Arkansas City and Vicksburg is caused by the flow input from the Yazoo tributary just upstream from the Vicksburg gauging station.

Further downstream, the decline in mean discharge by approximately 3 000 m^3s^{-1} between Natchez and Tarbert Landing is explained by the loss of flow to the Atchafalaya distributary. The flow in the Atchafalaya distributary is further supplemented by input discharge from the Red River, an historic tributary of the Lower Mississippi River. At high flows, the discharge of flow between the Lower Mississippi and Atchafalaya distributary systems is regulated by the Old River control structure so that a maximum of 33 percent of the flow at high discharges is diverted to the Atchafalaya distributary.

2.4 Geomorphological complexity

The Lower Mississippi River is one of the most challenging case studies for fluvial geomorphologists because it encompasses great physical and human-induced complexity at such a large-scale. This complexity is typical of large alluvial rivers which, owing to their physical scale and socio-economic and political significance, operate, and are managed, in unique ways.

A generalised geomorphological conceptualisation of the complexity of large alluvial rivers is provided in Figure 2.6. A range of physical and human controls together determine both, the short and long-term flow and sediment transport process characteristics, and the materials in which morphological adjustment can take place. The relative importance of each physical control varies between and within large drainage basins, along with the time and space domains within which the controls act. From a human-modification perspective, economic, political, social and environmental conditions together determine societal requirements, resulting in a range of different management approaches. Geomorphologists are tasked with the responsibility of observing, interpreting, and ultimately developing theories that explain the interactions between fluvial morphology (form) and operating processes. Within the conceptualisation, two types of feedback are evident. From a purely physical perspective, geomorphological response may be preserved as an 'inherited morphology' and thus, lead to a conditioning of future form-process interactions (Lane and Richards, 1997). Second, improved understanding of geomorphological form-process dynamics may influence future engineering policy and therefore, condition the operation of future human-induced controls. In practice, this second feedback is more of an ideal for geomorphologists than a reality because management is rarely undertaken solely on the basis of geomorphological principles, but usually in combination with economic, political and social factors which control the desire for flood control, water supply and navigational requirements.

The following discussion uses this model to highlight the true complexity of the Lower Mississippi River. A key focus of this thesis is to explore how a range of observed data sets can be better used to formulate geomorphological understanding that will feed into future management decisions on the river. This necessitates an appreciation of the range of physical and human-induced controlling variables, and the likely internal adjustments.

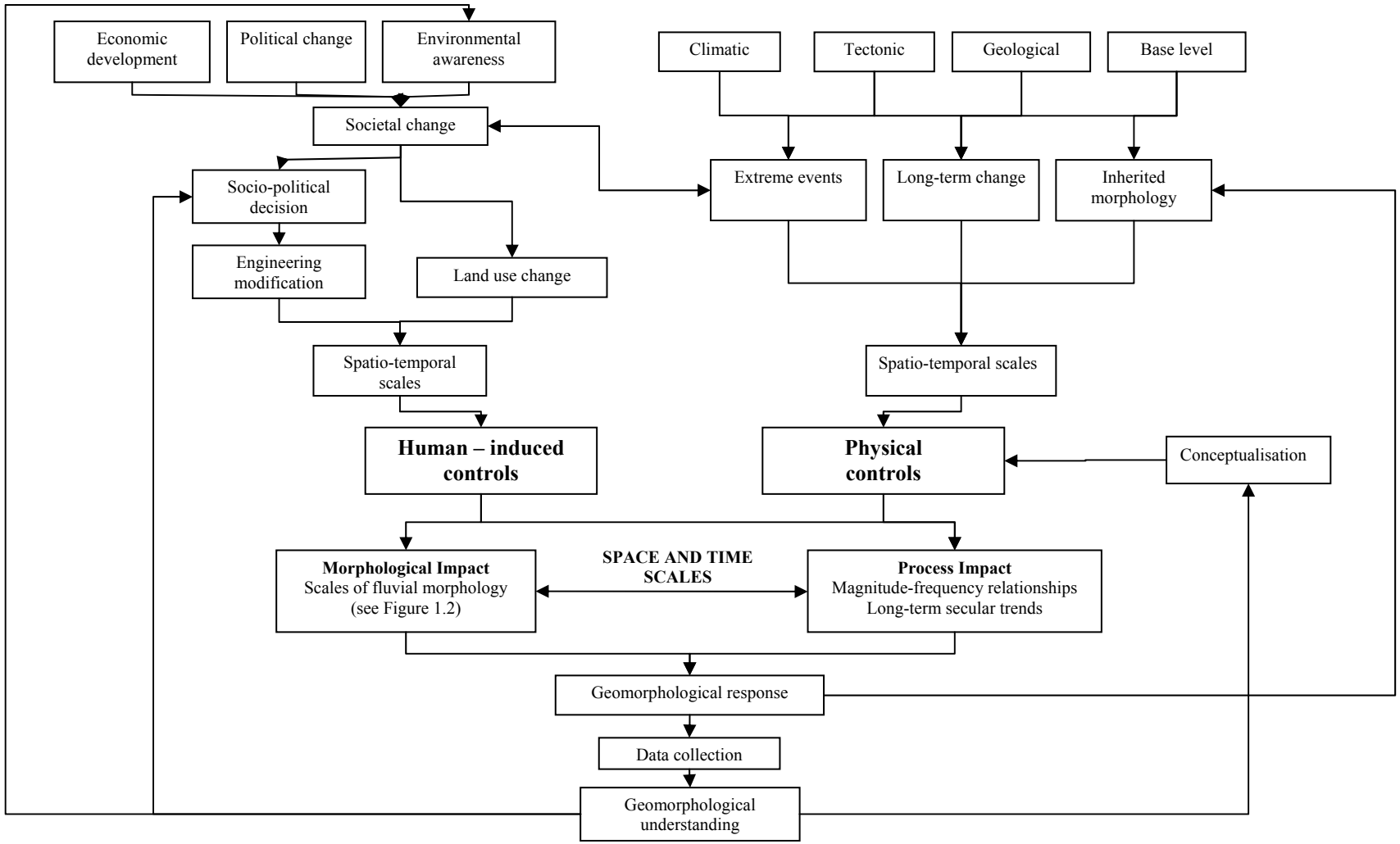

Figure 2.6 The complexity of large alluvial rivers: physical and human induced controls and the role of geomorphology.

2.5 Physical controlling variables

Physical controlling variables can be divided into those at the basin scale which affect the input discharge and sediment regime and those at smaller regional and local scales which affect the characteristics of morphological adjustment.

2.5.1 Geological influences

The geographic setting of the Lower Mississippi River is predominately determined by the regional geological framework. The course of the river follows a geologic syncline or physiographic 'trough' (Saucier, 1994) known as the Mississippi Embayment which formed through the gradual downwarping of Paleozoic rocks (Figure 2.7). Because of the influence of several secondary structural features, this north-south trending syncline follows a slightly sinuous route. The embayment widens noticeably in eastern Arkansas into the eastern portion of the larger Arkoma Basin. In western Mississippi, the embayment narrows and its axis is diverted to the southeast as a consequence of the Monroe Uplift to the west and the Jackson Dome to the east (Saucier, 1994).

Over shorter timescales, the complex surficial geology of the alluvial valley represents an important control on local channel geometry and the direction of planform adjustment (Fisk, 1951; Saucier, 1994). The vast majority of deposits date back only to the Wisconsin glaciation and the recent Holocene period (Fisk, 1951). At a regional-scale, the distribution of coarse sands and gravels, deposited during the Late Wisconsin period, represent relatively easily erodible materials where they outcrop within the channel banks (Saucier, 1994). These massive deposits are mainly confined to the northern third of the alluvial valley (Figure 2.7). At a much smaller scale, abandoned channel fill deposits known as clay plugs play a critical role in constraining rates of meander bend migration and hence, are a significant control in determining meander bend morphology (Hudson and Kesel, 2000).

2.5.2 Neotectonic influences

There are two currently active neotectonic processes within the Lower Mississippi alluvial valley which have geomorphic significance to fluvial processes on the Mississippi River. Firstly, two major geologic uplift features within the alluvial valley have been reported by Schumm and Watson (1982), Burnett and Schumm (1983), and Gregory and Schumm (1987): the Lake County Uplift in southeastern Missouri; and the larger Monroe Uplift feature in western central Mississippi, and southeastern Arkansas (Figure 2.7). Precise levelling surveys of these areas have reported movements of up to 4 mm yr^{-1}. The significance of this rate of movement over a timescale of fifty years is emphasised when it is compared to the gradient of the Lower Mississippi River which Schumm and Watson (1982) report to be approximately 55 mm km^{-1}. Because it is difficult to attribute geomorphological changes at the scale of the Lower Mississippi River directly to neotectonic uplift, no study has specifically addressed this. However, Burnett and Schumm (1983) found that smaller streams in southwest Mississippi and southern Louisiana do exhibit a spatial pattern of morphological response to a third uplift feature, the Wiggins anticline structure, which is located to the east of the river.

The second important neotectonic process is seismiscity. Seismic episodes represent pulsed disturbances (Brunsden and Thornes, 1979) which may be sufficient to trigger long-term changes in the system. No part of the Lower Mississippi Valley is completely aseismic but the area of active seismiscity is the New Madrid Seismic Zone located in the vicinity of the Lake County Uplift. Four of the largest earthquakes in historic times in eastern North America occurred in 1811 and 1812 (Saucier 1994). Narrative accounts and subsequent research by Jibson *et al*. (1988) suggest this series of earthquakes triggered widespread landslides and bank caving. This in turn surcharged local streams with an excess of sediment and debris, and in some cases caused a complete reversal of river flow (Saucier 1994). Hence, the contemporary river system may still be adjusting to this event.

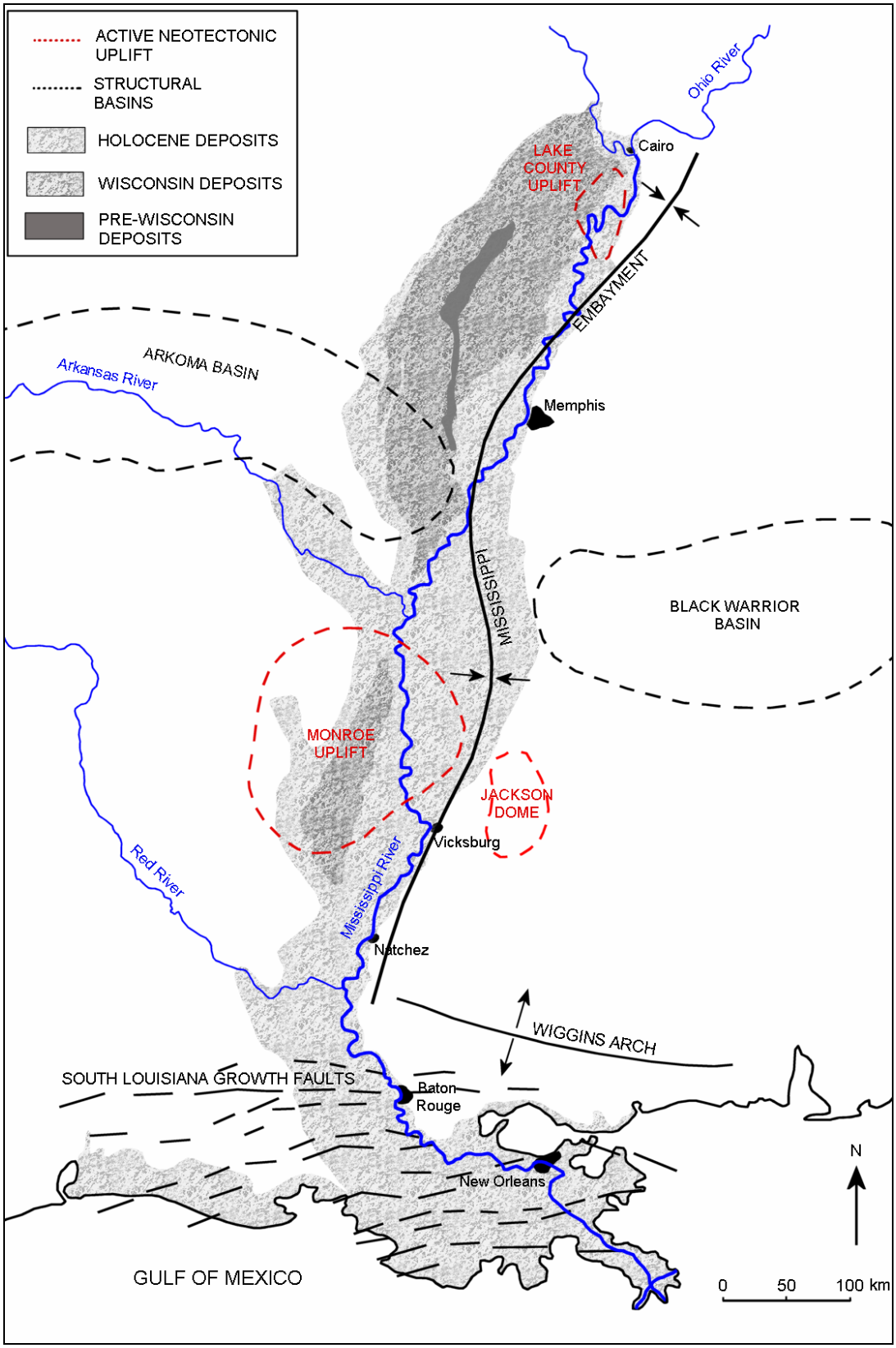

Figure 2.7 Neotectonic and geological controls in the Lower Mississippi alluvial valley (adapted from Autin *et al*., 1991).

2.5.3 Climatic influences

During the Quaternary period, the Lower Mississippi Valley has been directly influenced by at least 17 complete glacial-interglacial cycles, each persisting for an average of 100 kA (thousand years) to 150 kA (Morrison, 1991). The events of the most recent glacial period, the Wisconsin glaciation, are well recorded within the sediments of the alluvial valley. The cycle began around 120 kA BP (before present) but full glacial conditions were not reached until around 18 kA BP. Stratigraphic evidence suggests that the early and late Wisconsin periods can in fact by separated by an interstadial period in which temperatures and sea level rose, but not to interglacial levels (Saucier 1994). The Laurentide ice sheet, which covered much of the North American continent during the Wisconsin glaciation, decayed rapidly from approximately 12 kA BP following an amelioration of climate.

Winkley (1994) has proposed that morphological adjustment to the Wisconsin glacial period is likely to have only terminated approximately 500 years ago. Other researchers such as Biedenharn (*pers com.*) suggest the timescale of response is unknown and therefore, the system may still be adjusting. At the other end of the timescale spectrum, extreme hydrologic events such as the 1927 flood perform significant geomorphological work at the decadal timescale.

2.5.4 Sea level

The elevation of sea level, the ultimate base level determines the overall valley slope and therefore its variation is a significant control on fluvial processes. Fisk and McFarlan (1955) estimate that sea level at the last glacial maximum (18 kA. BP) was approximately 135 metres below present. Fisk (1944) initially suggested that the effect of glacial sea level lowering on the Lower Mississippi River was degradation and hence, entrenchment through the entire alluvial valley. However, more recently, Saucier (1994) has suggested that only the lower portion of the alluvial valley experienced valley degradation due to sea level change during the Quaternary.

2.5.5 Internal adjustments at timescales greater than 2000 years

Although this thesis is concerned with timescales extending up to only approximately 2000 years, observed geomorphological dynamics are nested within the context of those operating over much longer timescales. Over the Quaternary period, the nature of the relationship between the above external variables and channel changes on the Lower Mississippi River have been considered by several authors. Fisk (1944) first introduced the concept of a glacial response model by proposing that a falling sea level during glacial stages initiated extensive degradation throughout the alluvial valley, whereas a major rise in sea level during interglacial stages initiated valley aggradation and deltaic progradation. This relationship between sea level change and alluvial valley behavior has subsequently been criticised by Saucier (1994) who suggests that it does not account for the response times and relaxation times in the system. Autin *et al*. (1991) propose an improved conceptual model of process-response for a time-dimensionless glacial-interglacial cycle (Table 2.3). However, although this model accounts for a time lag in response between the deltaic plain and the alluvial valley, it still envisages geomorphological changes in the alluvial valley being ultimately driven by variations in sea-level at the Quaternary timescale. Yet, the geomorphology of the alluvial valley is more directly controlled by the discharge and the sediment regime of the Lower Mississippi River which is a product of continental scale glacio-climatic variability, not global glacio-eustatic variability.

Providing a more rigorous quantitative basis to the conceptual model has proved difficult because establishing regional-scale correlations between stratigraphic sedimentary sequences in the alluvial valley and deltaic plain is extremely difficult (Saucier, 1994). At shorter timescales, at least two distinct spatio-temporal scales of geomorphological dynamics can be recognised. First, at timescales in the order of magnitude 10^3 years, corresponding to the Holocene period, dynamics are characterised by abrupt shifts in channel course within the alluvial valley and the development of new meander belts. Since the adoption of a meandering planform at approximately 9.8 kA. BP (Guccione *et al.*, 1988), six meander belts have been recognised in the most recent interpretation of alluvial valley history (Autin *et al.*, 1991), each extending up to several hundred miles in length. Second, at 10^2 year timescales, dynamics are characterised by meander bend growth and eventual cutoff

Glacial Cycle		Sea Level Response	Coastal/Deltaic Response	Alluvial Valley Response
Interglacial		Highstand minor oscillations	Deltaic plains	Aggradation Meander belt formation
Glacial	**Waning glaciation**	Rising	Delta lobes on shelf Rapid shoreline transgression Trench filling	Minor degradation Valley train development Maximum aggradation
	Glacial maximum	Lowstand	Broad exposed shelf Shelf margin deltas	Outwash deposition and initial aggradation Degradation
	Waxing glaciation	Falling	Entrenchment Rapid shoreline regression	Planform change (meandering to braided)

Table 2.3 A process-response model showing regional responses of the Lower Mississippi River to glacial/interglacial cycles (modified from Autin *et al*., 1991).

cycles (Fisk, 1944; Autin *et al*., 1991), indicating that the river was highly active in its planform.

2.6 Human-induced controls

The following discussion analyses the history of human-induced modifications on the Lower Mississippi River. These modifications have been authorised by political decisions driven by a variety of factors including broad socio-economic changes, developments in scientific understanding and the occurrence of extreme flood events (Figure 2.8). The discussion is divided into three key periods which, although defined by key events in the history of Mississippi River management, are also somewhat arbitrary: early modifications (pre-1927); sustained channel engineering (1928 to late 1960s); and environmental approaches (late 1960s to the present).

2.6.1 Early modifications (pre-1927)

The earliest documented channel modification was the construction of a levee-based flood protection scheme between 1717 and 1726 at New Orleans. Subsequent levee constructions along the Lower Mississippi River during the eighteenth and early nineteenth centuries were the responsibility of riparian landowners. Hence, a levee system developed which was highly fragmented, built to a wide variety of design specifications, and was consequently frequently breached (Moore, 1972). This localised and non-coordinated approach was typical of widespread channel management in the United States following settlement throughout most of the nineteenth century (Brookes, 1988; Graf, 2001).

The creation of the Mississippi River Commission by an act of Congress in 1879 symbolised the beginning of a doctrine of comprehensive, integrated and unified river basin planning and development within the United States (Brookes, 1988). The Commission was established as a centralised organisation in response to demands for improved flood control, following the flood of 1874 which breached the levee system in several places, and to address methods to improve navigation as the river became recognised as a key trading route (Moore, 1972). The prioritisation of water

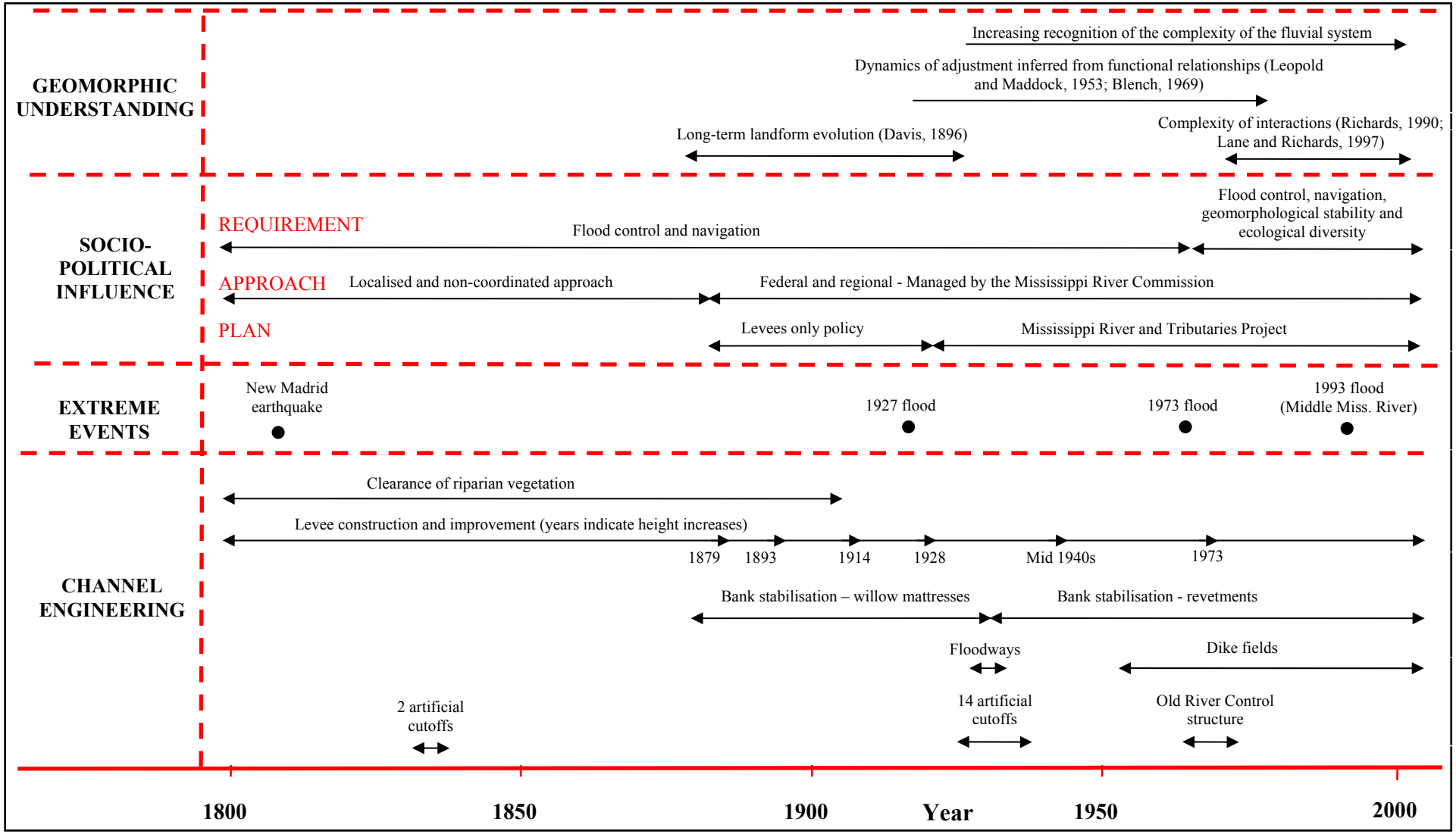

Figure 2.8 A timeline of channel engineering on the Lower Mississippi River considered within the context of key advances in geomorphological understanding, socio-political influences and extreme events.

resources development was later reflected on a national scale by the creation of the Bureau of Reclamation out of the 1902 Newlands Act. Alongside the U.S. Army Corps of Engineers, the agency was responsible for the planning and construction of large engineering projects to dam rivers and effectively control their courses. Engineering expertise developed rapidly, permitting the construction of increasingly sophisticated structures, but this was done largely without concern for geomorphological response.

Flood control policies initially adopted by the Mississippi River Commission generally followed the earlier publication of two influential reports by Ellet (1851) and Humphreys and Abbot (1861). Both reports supported the construction of levees as the primary policy for flood defence, albeit for different reasons. Humphreys and Abbott went as far as dismissing the construction of artificial cutoffs as a management strategy on the premise of being both too dangerous and too costly. Following these recommendations, the Commission based their flood control policy on a continuous levee system built to a standard design specification and extending from Cairo, Illinois to the Gulf of Mexico. Between 1882 and 1914 several legislatory acts were passed to increase the design height of the levees (Elliot, 1932) with the result that until 1927, no levee, built to the standards adopted by the Mississippi River Commission, had ever failed (Changnon, 1996).

From a geomorphological standpoint, the levee system effectively isolated the channel from its floodplain and therefore, restricted flow and sediment transport to within the confines of the channel. Following the River and Harbors Act of 1896, other engineering modifications undertaken included the first hydraulic dredging to maintain a channel at least 2.75 metre deep for navigational requirements, and localised bank protection aimed at reducing rates of bank erosion and consequently, maintaining a more stable alignment (Moore, 1972; Winkley, 1977). This latter modification was part of the 'no-cutoff' policy adopted by the Commission between 1884 and 1929. Geomorphologically therefore, both the planform alignment of the Lower Mississippi River, and the local cross-sectional morphology were significantly modified by human activities prior to 1928.

In addition to channel modifications associated with the Mississippi River Commission, riparian vegetation clearance and extensive land use change in parts of the Mississippi basin may have had a dramatic influence on the hydrology and geomorphology of the Lower Mississippi River before 1927. According to Winkley (1977), clearance of riparian vegetation together with land clearance along the natural levees for the purposes of agricultural development was commonplace throughout the nineteenth century. This may have increased river bank instability and consequently sediment input, in turn creating a more dynamic channel system. Prince (1997) provides an intricate account of artificial drainage practices for agricultural purposes following settlement of the wet prairies in the Upper Mississippi basin. In the states of Ohio, Indiana, Illinois, Iowa and southwest Minnesota, tile drainage and ditching were most active between 1870 and 1920. Gleick (1993) suggests that in the nation as a whole, nearly half of the wetland areas have been drained for agricultural development since 1780.

2.6.2 Sustained channel engineering (1927 to late 1960s)

i) The 1927 flood event

The catastrophic flooding of the Lower Mississippi Alluvial Valley in 1927 led to dramatic shift in flood control policy in the post-flood era. Close to one million people, in a nation of 120 million, were made homeless as the levee system was breached (Barry, 1997). Adjacent to Vicksburg, Mississippi, an area up to 80 miles (128 km) in width was flooded in the event which changed America (Barry, 1997). The flooding led to an almost immediate reappraisal of the *'levees-only'* policy and subsequently the adoption of the *Jadwin Plan* in legislation passed in 1928 (Elliot, 1932). This plan, later becoming known as the *Mississippi River and Tributaries (MR & T) Project*, marked the beginning one of the most intense and sustained programme of engineering on any large alluvial river in the world.

ii) Changes in river engineering policy

Although the 1927 flood triggered the dramatic policy shift, the decision to proceed with the Jadwin Plan cannot be divorced from the socio-economic and political conditions in the United States in the late 1920s and early 1930s. In the period of the

Great Depression, the government's priority to develop and improve water resources stemmed from not only a desire to expand public agencies and consequently employment opportunities, but also a political mission to publicly demonstrate the high standard of engineering capability and associated technological progress in society at large (Reisner, 1986). This was achieved through a proliferation of large-scale engineering projects, typified by dam building and widespread channelisation, combined with institutional changes which led to a more integrated and basin wide approach to river channel engineering. During the period from 1935 to about 1970, dams dramatically changed the hydrology of the Mississippi basin. Dam building reached its peak only in the 1960s when a quarter of the 80 000 existing dams in the USA were constructed (Graf, 2001). With specific reference to dam building, Reisner (1986; 154) suggests how:

> *'The Great Depression and the Roosevelt administration, together with the pyramid scheme economics of the river-basin accounts, were more than enough to launch the federal dam building program on a forty year binge.'*

The creation of powerful, regionalised basin institution is typified by the Tennessee Valley Authority (TVA). Charged with both land development and water management and following vast sums of public funding, the TVA constructed nine dams on the Tennessee River, itself a tributary of the Ohio, and forty two on major tributaries of the Tennessee River. The hydrological impact was the creation of a total lake shoreline longer than on the Great Lakes (Newson, 1992). The approach nurtured a widespread public belief that large-scale planned engineering projects would trigger economic growth and consequently poverty alleviation. At this time, hydrology and geomorphology were still relatively undeveloped and:

> *'Science emerged as the handmaiden of public policy with the aim of controlling rivers at a variety of scales for the economic and social benefit of the nation' (Graf, 1992, 9).*

iii) Protection from the maximum possible flood

The Jadwin Plan on the Lower Mississippi River was not based on a desire to control flooding up to a flow event of a pre-defined return interval but rather symbolised the then prevailing *'man against nature'* philosophy by being designed to protect against

the *maximum possible* flood event. Based on investigations by both the Mississippi River Commission and the National Weather Bureau, design calculations used the maximum possible Ohio River flood, combining with the maximum possible flood from the Middle Mississippi River to enter the Lower Mississippi River at Cairo (Moore, 1972). Not only did this require the extreme flood events to occur simultaneously in each basin, but each calculation was in turn based on the probability that extreme flood events would occur simultaneously in each of the major sub-tributary basins such as the Upper Mississippi and Missouri basins. Thus, the project is designed to alleviate the maximum flood event which is deemed climatically possible. The original project flood from 1928 was subsequently recalculated in 1941 and 1956 to take account of reservoirs on the tributary basins (Moore, 1972).

Engineering interventions incorporated in the original plan included the construction of three emergency floodways outlets, the strengthening of the levee system, the revetment of migrating banklines and continued dredging where it was deemed necessary. Although these interventions all have geomorphological implications, an intervention incorporated only within later plans has commanded greatest attention regarding regional-scale geomorphological response: the artificial cutoff program.

iv) The artificial cutoff programme

Between 1932 and 1942, fourteen artificial cutoffs were made along an 805 kilometre reach of the Lower Mississippi River from Memphis to Old River. The location of each cutoff is illustrated in Figure 2.9a. The cutoff programme was undertaken: firstly, as a method of flood control, to reduce flood stages by increasing slope and consequently velocity; and secondly, for navigational purposes by shortening its length (Winkley, 1977). In total, including two natural cutoffs occurring between 1929 and 1932, the river was shortened by 243 kilometres. This distance was later increased by a further 88 kilometres between 1935 and 1955 when 380 million cubic metres of material was dredged to facilitate the development of chute cutoffs (Moore, 1972). Figure 2.9b shows the Greenville Bends, the most sinuous reach of the Lower Mississippi River prior to the artificial cutoff programme. The construction of three cutoffs in this reach led to over an 80 percent reduction in

channel length. At the time, the cutoff programme represented a considerable engineering feat. According to Winkley (1977; 13):

> *'The laws of physics as pertain to rivers and sediment movement are not well defined today, and in 1932, the knowledge was certainly even more incomplete.'*

Indeed, General Ferguson, who approved the cutoff programme immediately after becoming president of the Mississippi River Commission in 1932 (Winkley, 1977), viewed the project as a short-term *'technical fix'* without consideration of longer term implications. According to Winkley (1977; 17), Stewart (1945) stated:

> *'Ferguson fixed the river, transforming it into a quite different stream, in the face of longstanding precedent and vigorous opposition.'*

This resonates once again with the prevailing technological philosophy within the river engineering community during this period, a philosophy of being able to control nature without exacting any negative responses.

The predicted immediate reduction of flow stage for any defined discharge has since been confirmed by examination of the change in relationship between stage and discharge in the post-cutoff period (Biedenharn and Watson, 1997). However, although a regional-scale geomorphological response has been identified (Figure 2.15) a more scale-integrated approach is required to validate these suggestions. Further, in any geomorphological investigation it is almost impossible to isolate the impacts of the cutoff programme from the impacts of other engineering modifications to the fluvial system.

v) Levees and floodways

Figure 2.10 illustrates the temporal increase in levee heights between 1844 and 1978. Heights were gradually raised to 8 metres by 1928, 10 metres by the mid 1940s and 12 metres following the 1973 flood (Smith and Winkley, 1996). The confinement of water between the levees at flood stages has led to an increase in stage for a specific high discharge (Winkley, 1994). This is likely to have had a significant impact on channel hydraulics and hence, interactions between channel process and channel

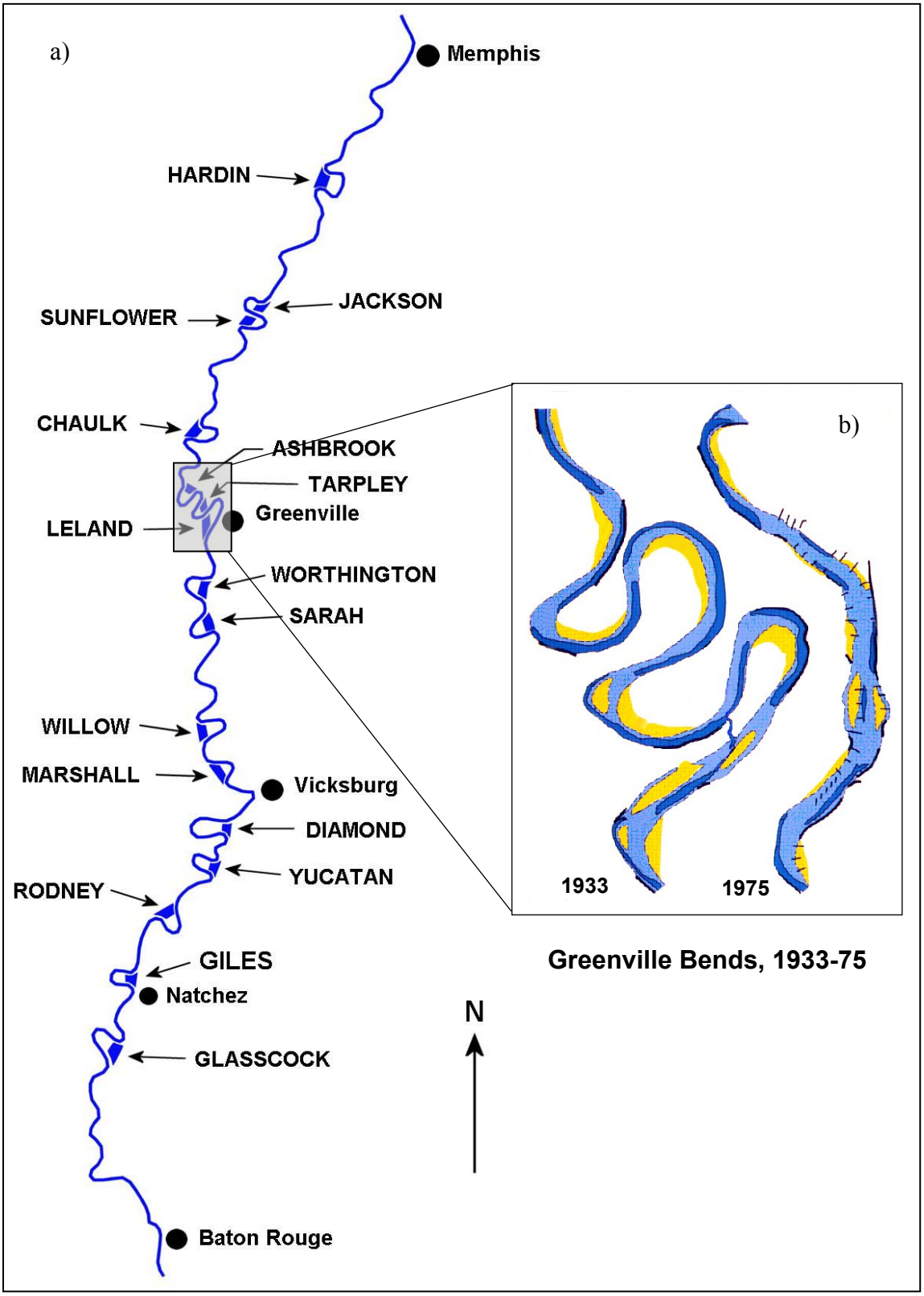

Figure 2.9 Cutoffs on the Lower Mississippi River between 1929 and 1942: a) adapted from Stanley Consultants (1990) and; b) adapted from Winkley (1977).

form. The levee system now confines flow in a floodplain varying from 2 to 24 kilometres (Smith and Winkley, 1996).

To reduce the potential for high flow stages and consequently relieve pressure on the levee system, the Jadwin plan also included the construction of three emergency floodway outlets on the Lower Mississippi River. These have been used during extreme high stages: the Birds Point to New Madrid floodway was used during the flood of 1937; the Morganza floodway was used during the flood of 1973; and the Bonnet Carre Spillway has been opened four times since its completion in 1936 (Moore, 1972).

vi) Revetments, dikes and dredging

The artificial cutoff programme significantly increased valley slope and hence, initiated a period of instability in the fluvial system. Over a certain timescale, a river would expect to regain its original length and hence, channel slope following a cutoff, a process which Winkley (1977) estimates would take between 30 and 80 years on the Lower Mississippi River. Hence, to maintain the cutoff alignment, attention focused on preventing planform migration by extensive stabilisation works in unstable reaches, usually at meander bends. Stabilisation has been achieved by lining susceptible banks with an articulated concrete mattress (Figure 2.11a) to form a strong and impermeable barrier to lateral erosion tendencies (Moore, 1972). Figure 2.12 shows that rates of bank stabilisation were highest in the period immediately following the artificial cutoff programme, between 1940 and 1960. However, many local problems of channel alignment resulted from not being able to stabilise long reaches in a short enough time period. Indeed, Smith and Winkley (1996) reported that by 1989, the Lower Mississippi River was only 160 kilometres shorter than it was in 1930, even though up to 330 kilometres had been eliminated by cutoffs and chute development. Geomorphologically, bank stabilisation is important because it essentially restricts morphological response to two dimensions. The planform morphology is effectively fixed and thus, the river can only adjust its sinuosity, and therefore slope, within the confines of the channel boundaries.

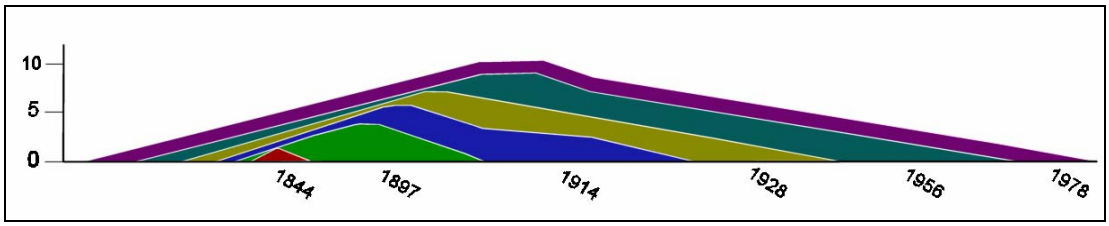

Figure 2.10 Increase in levee heights 1844-1978 (modified from Smith and Winkley, 1996).

a) b)

Figure 2.11 a) Application of an articulated concrete mattress to aid bank stabilisation and b) a stone dike field (Biedenharn, 2000).

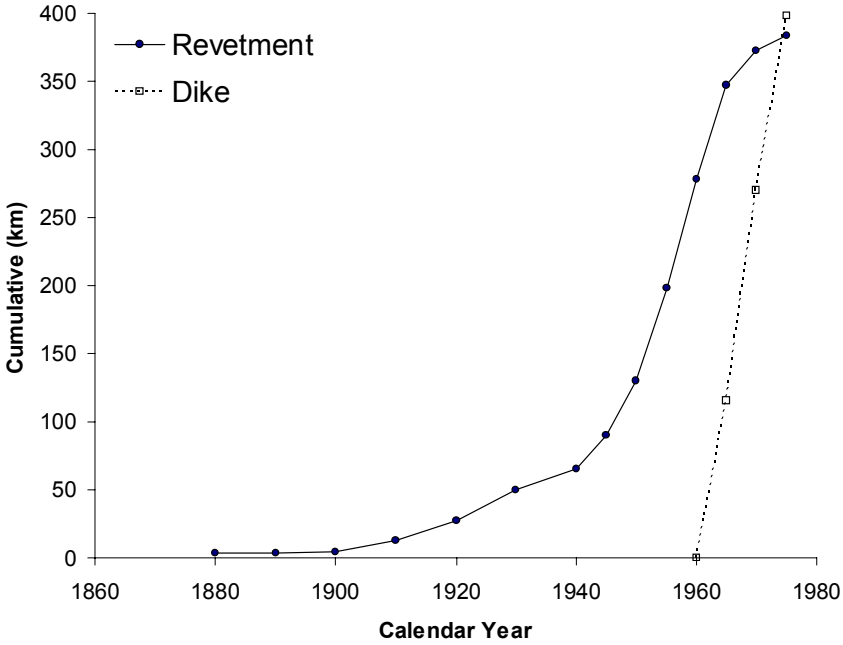

Figure 2.12 Bank revetment and dike field construction in the USACE Vicksburg District (confluence of Arkansas River to Old River distributary) in the period 1860-1980 (Winkley, 1977).

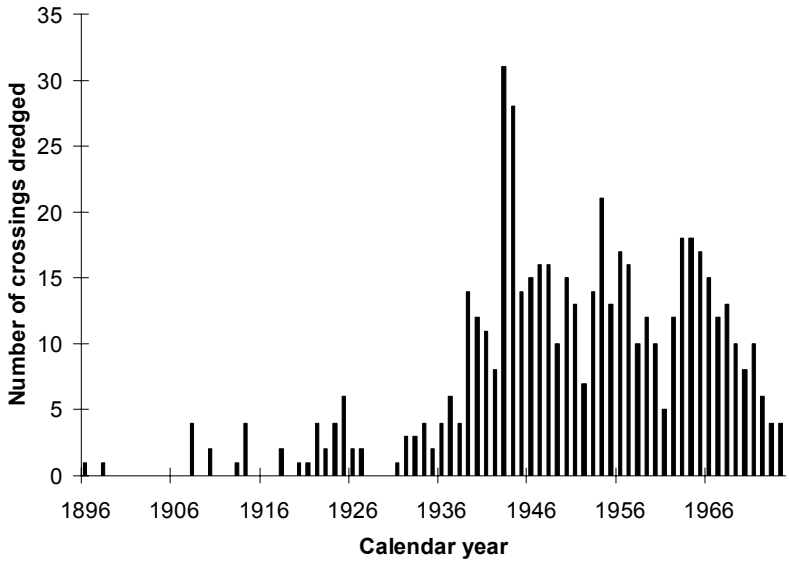

Figure 2.13 Number of crossings dredged in the USACE Vicksburg District (confluence of Arkansas River to Old River distributary) in the period 1896-1975 (Winkley, 1977).

In reaches where widening and sedimentation were being experienced after the cutoff programme, extensive dredging and the construction of dike fields (since 1956) have been used to maintain a navigation channel 2.75 m in depth. During, and in the decade immediately following the period of cutoff construction, over 1.3 billion cubic metres of sediment were dredged in an effort to maintain this depth (Winkley, 1977). Rates of dredging remained high until the late 1960s and early 1970s (Figure 2.13). Both permeable and impermeable stone dikes (Figure 2.11b) have been installed at various angles with respect to the primary flow thread of the channel, encouraging sedimentation either upstream or downstream (Smith and Winkley, 1996). Between 1956 and 1972, 83 dike systems were constructed on the Lower Mississippi River between Cairo, Illinois and Old River, Louisiana (Moore, 1972).

vii) Wider basin-scale changes

In addition to the channel modifications to the Lower Mississippi River, appreciating channel and catchment changes in the wider tributary basins is important to gaining an understanding of the complex geomorphology of the system.

Extensive dam building in the tributary basins and associated reservoir storage has had the cumulative effect of reducing maximum flow stages and augmented low flows on the Lower Mississippi River (Smith and Winkley, 1996). Flooding on the Missouri River is significantly reduced by six dams that control runoff from 715 000 square kilometres of the Upper Missouri River Basin. Meanwhile, on the Upper Mississippi River, 29 major lock and dam systems were built in the 1930s between St. Louis and Minneapolis to allow operation of commercial traffic (Koellner, 1996). In the Ohio River Basin, 74 dam-formed lakes impound the Ohio River's tributary waters, including those associated with the work of the Tennessee Valley Authority.

As well as dam structures, the flows in the major tributary basins have been confined by levees and other channelisation structures. Approximately 20 500 kilometres of levees exist in the Upper Mississippi and Missouri Basin (Koellner, 1996). Hence, without the opposing effects of dams, the isolating of channel and floodplain processes in the major tributary basins would increase the rate of delivery of flow and sediment to the Lower Mississippi River system (Wright, 1996).

2.6.3 Environmental approaches (late 1960s to present)

Although bank stabilisation works and dike field construction has continued, the general rate of new engineering construction as part of the MR & T Project has gradually declined since the late 1960s. This reflects the increasing near completion of the programme and the general transfer of resources from construction towards the continued monitoring and maintenance of existing engineering features.

Official appraisal reports published by the Mississippi River Commission and the U.S. Army Corps of Engineers reflect the view that:

> *'The flood control and navigation project within the Lower Mississippi Valley is a great accomplishment and is now actually a reality, not an idea in the planning stage' (Ferringa, 1952; 25).*

This is supported by the publication of favourable benefit-to-cost ratios. For example, by taking account of the elimination of flood loss to crops and infrastructure, and the savings to navigation, Moore (1972) calculated the ratio to be approximately six to one. Moore (1972) goes further to state that more effective flood control has brought many other intangible benefits to the region and the nation.

Unquestionably, the MR & T project has delivered a multitude of socio-economic benefits, but it has not been without its critics and the true success of the project remains a matter of public debate. This debate has intensified over the last 30 years as geomorphologists have exerted increasing control on river basin management, a field traditionally dominated by engineers (Black, 1987). During the 1960s, the ability of geomorphology to explain river behaviour improved through a series of influential publications, perhaps most notably by Leopold *et al*. (1964). Since then, research programmes have diversified and the true complexity and integrated nature of the fluvial systems has become more apparent (Graf, 1992). On the Lower Mississippi River, increasing recognition of continuity in the fluvial system has led researchers such as Kesel (1988, 1989) to relate accelerated rates of land loss in the Mississippi River delta in Louisiana to rates of sediment supply from the Lower Mississippi River. Researchers have attributed the decline in sediment loads to a variety of factors including increasingly conservation minded land management

practices throughout the Mississippi Basin, increasing reservoir storage relating to dam construction, and a reduction in the rate of bank caving because of improved bank stabilisation (Keown *et al*., 1981; Dardeau and Causey, 1990).

A second criticism is that the project has failed to totally eliminate severe flooding. The 1973 flood inundated approximately 16.5 million hectares of land although it was not all confined to the Lower Mississippi alluvial valley. In response, engineers did estimate that flood control works in 1973 successfully prevented a further 14.5 million acres from inundation. More recently, the catastrophic flood of 1993 has further exacerbated the general concern of placing such a reliance on hard engineering structures as a successful flood alleviation strategy (Tickell, 1993). Although the 1993 flood did not lead to abnormally high stages on the Lower Mississippi River, the flooding of over 20 million acres of land in the Upper Mississippi and Missouri Basins resulted from frequent breaches of the extensive system of levees which had been built to a specific design standard. Researchers such as Denning (1994) have since suggested that by confining flow, levee systems cause flow levels to rise to abnormally high levels, leading to catastrophic flooding in the event of failure. In response to the flooding, Leopold (1994) has called for a broader consideration of utilising the natural storage function of floodplains to decrease downstream flow magnitude, in conjunction with engineering works such as levees and dams. Other authors have investigated the contributory hydrological impact of wetland destruction over the last 200 years. However, Pitlick (1997) concluded that the cumulative loss of storage was too small to have prevented the levee system from overtopping.

The continuing critique of the MR & T project is replicated on a national scale by the changing nature of river channel management projects. Since the peak in dam building in 1968 (Graf, 2001), there has been a general reduction in the number of new channel engineering projects. Several researchers (Brookes, 1988; Newson, 1992; Tickell, 1993; Graf, 2001, Haltiner *et al*., 1996) have attributed this shift to increasing recognition of the adverse environmental impacts of land drainage and large-scale river channelisation works and the catastrophic failure of some high profile engineering schemes such as the Teton Dam failure (Worster, 1985). At a policy making level, the increasing environmental awareness was represented by a

series of legislatory acts in the late 1960s. Most significantly, the National Environmental Act of 1969 necessitated an environmental impact assessment to be included within any proposals stipulating an engineering modification to a river (Brookes, 1988; Moore, 1972). More recently, the benefits of restoring or at least rehabilitating rivers has increasingly been shown. This more radical change in philosophy is perhaps most famously epitomised in the U.S. by the Kissimmee River Restoration Project in south central Florida, created out of the 1992 Water Resources Development Act. This represented one of the world's largest restoration projects and aimed to re-establish natural hydrogeomorphic processes while maintaining existing flood protection to over 100 square kilometres of river and floodplain ecosystem, including reinstating 69 kilometres of meandering river from a straight drainage canal (Toth, 1996).

Despite the increasing environmental awareness in river channel and wider drainage basin management, future trends are still likely to be governed by issues of flood alleviation and water supply. Worster (1985; 326) states how:

> *'The party of preservation since the 1970s has had more success in stopping the expansion of the hydraulic society than in dismantling it.'*

General interest in public policy for river management increased ever since the 1950s when rapid economic expansion began to press the limits of available water resources particularly in the western United States (Graf, 1992). Worster (1985) claims that between 1900 and 1975 demand for water increased by a factor of ten even though the population only tripled in size. In 1971, the Bureau of Reclamation released a plan to transfer water resources by diverting a proportion of the flow from the Lower Mississippi River to the high plains of West Texas and New Mexico to help sustain the irrigation dependent local agricultural economy (Moore, 1972). Although the plan was later shelved because the cost-benefit ratio was deemed unfavourable (Moore, 1972), the possibility of such a scheme in the twenty first century remains because water resources problems are more severe than ever before. Indeed, the plan acts as a reminder that, in the present era of rapid technological evolution, there remains the possibility of further dramatic (and potentially presently unforeseen) engineering modifications to the Lower Mississippi River.

2.6.4 Geomorphological implications

The modern engineering history of the Lower Mississippi River may represent a magnitude of disturbance greater than any experienced during the entire Quaternary period and has therefore, complicated an already complex fluvial system. In hydrological terms, the combined effect of engineering modifications in the tributary basins has been a reduction in maximum flows and an augmentation of low flows. The likely reduction in the frequency and magnitude of extreme flood events in particular has hydraulic and related geomorphological implications through changes to sediment dynamics. This pattern is enhanced by the floodway structures but further complicated by the levees which raise flow levels for a given discharge. Meanwhile, extensive bank stabilisation has effectively confined any morphological response to two dimensions. In essence, the contemporary geomorphology of the Lower Mississippi River remains a product of the spatio-temporal and scale-dependent process-form dynamics but is conditioned by the engineering history of the river channel and wider drainage basin. Hence, the Lower Mississippi River is a 'complex geographical space' (Graf, 2001), both physically and histiographically.

The operation of each physical and human-induced controlling variable in the time-space domain is summarised conceptually by Figure 2.14. All parts of the system are responding to basin scale variables which are geologically and climatically driven over long timescales and land use and engineering intervention driven at shorter timescales. Superimposed on these changes, different parts of the system are responding to both regional and more local-scale variables acting over a range of timescales. These external variables control the discharge and sediment process regime and constrain the nature of internal morphological adjustments (Figures 1.1 and 1.2).

2.7 Geomorphological understanding

Previous studies of large-scale and long-term geomorphological behaviour on the Lower Mississippi River have adopted a functionalist approach by primarily using long-term process-based data sets to infer average changes in the relationship between form and process. The following discussion classifies previous studies into three of the approaches outlined by Richards (1982) to monitor system-scale

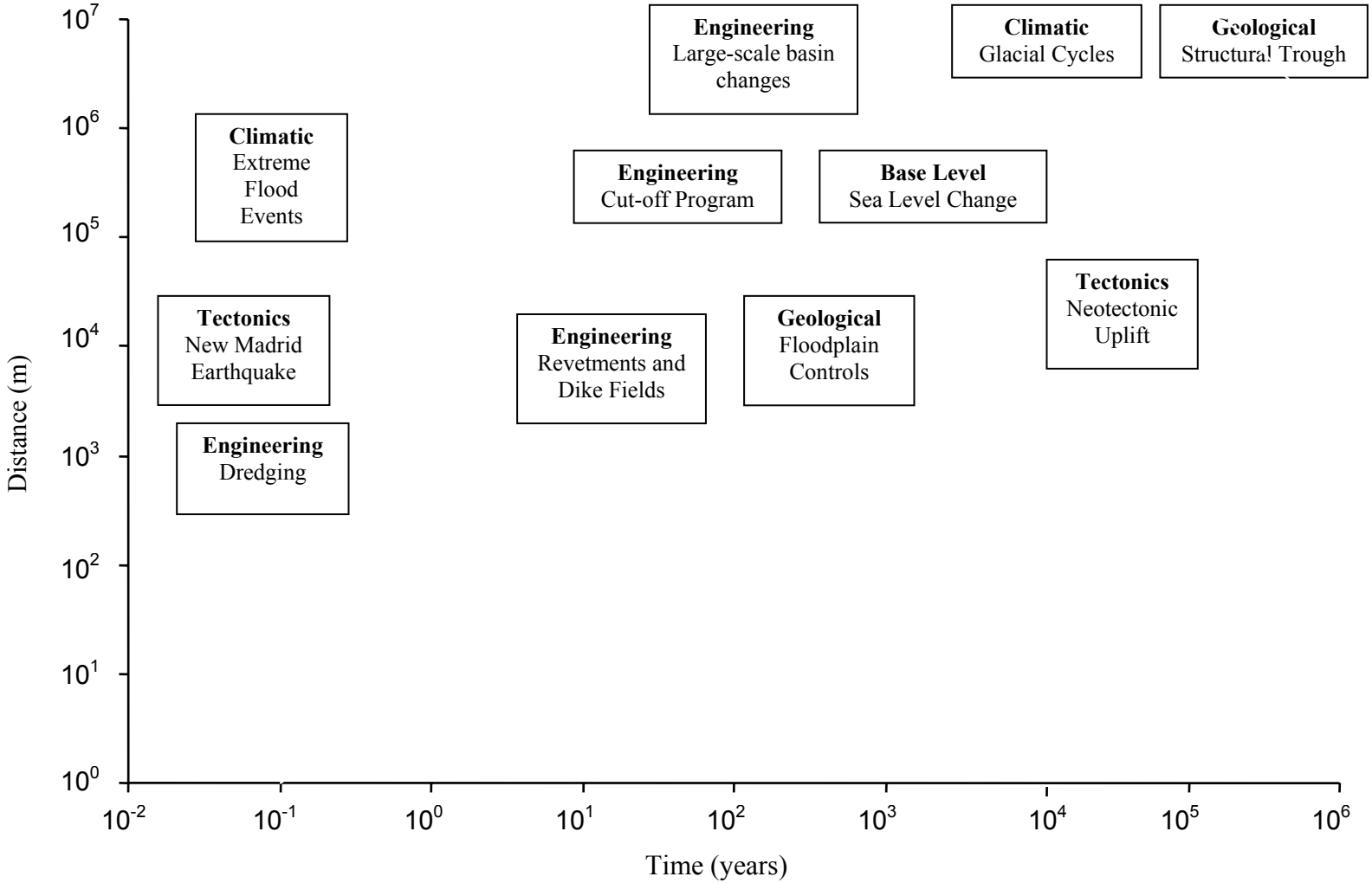

Figure 2.14 The space-time domain of each controlling variable.

stability; those concerned with change in the behaviour of channel form, those concerned with change in sediment transport, and those concerned with change in channel efficiency. These approaches are then integrated to consider the current state of understanding of large-scale and long-term geomorphological behaviour.

2.7.1 Investigation of spatial and temporal variation in channel form

Studies of large-scale channel form changes on the Lower Mississippi River can be divided into those investigating variation in channel planform, and those investigating variation in longitudinal profile.

i) Planform variation

Prior to extensive modification as part of the MR & T Project, the major available data sets illustrating morphological dynamics are historic maps of channel planform. Planform changes in the pre-modification period can therefore be used as a basis to examine the spatial and temporal variation in channel stability in the pre-modification period. This understanding is crucial because it provides an idea of the nature of geomorphological behaviour prior to extensive engineering modification, which may condition geomorphological response in the post-modification period. Despite this need, previous studies of planform variability on the Lower Mississippi River have typically been either entirely qualitative, or if quantitative, been weak in their mutual consideration of spatial and temporal variation.

One of the earliest accounts of planform variation is provided by Friedkin's (1945) qualitative discussion of meandering on the Lower Mississippi River following pioneering flume experiments. Friedkin (1945) was the first author to observe the apparent geomorphological paradox that the meandering process is more rapid in the downstream part of the alluvial valley, despite the presence of more easily erodible sediments in the upper valley. Friedkin (1945) explained this paradox by observing that cross-sections tended to be wider and shallower in the upper valley and hence, there was greater energy loss to channel resistance. In a more rigorous quantitative investigation, Hudson and Kesel (2000) observed a similar pattern of spatial planform stability by investigating historic rates of channel migration and patterns of

meander bend curvature. However, in contrast to the earlier thoughts of Friedkin (1945), Hudson and Kesel (2000) explain this pattern in terms of geological variations in the floodplain deposits, particularly the presence of cohesive clay plug deposits. Although the importance of geological influences on the pre-modification planform is supported by several other authors (Fisk, 1944; Saucier, 1994) this later study may be criticised by its reliance on planform data sets over a relatively short time period. Only two sets of planform data from the periods 1879-89 and 1911-21 were used in the analysis, allowing a maximum time interval of just 42 years. Considering the meander bend cutoff cycle on large alluvial rivers is likely to take at least one hundred years, the ideas from Hudson and Kesel (2000) should be considered only preliminary.

A longer-term planform investigation, incorporating four planform surveys and extending back to 1765, is provided by Walters and Simons (1977). However, this is limited by the spatial averaging of parameters and hence, only reveals general trends in the alluvial valley. Nonetheless, net increases in channel width, meander length, meander amplitude and sinuosity were observed over the total period although decreases in meander wavelength, meander amplitude and sinuosity were reported between 1820 and 1874. Walters and Simons attribute this decrease to a sudden increase in the number of meander cutoffs following the series of New Madrid earthquakes in 1811-1812.

ii) Longitudinal profile variation

Following extensive bank stabilisation, regional-scale geomorphological response to the series of engineering modifications is confined to adjustments to the longitudinal profile. Previous researchers have inferred adjustments from temporal variations in specific gauge records at key gauging stations. Specific gauge records are plots of flow stage through time for a specific discharge. The discharge chosen is usually near bank-full because this has been shown to consistently approximate the dominant discharge (Wolman and Miller, 1960; Hey, 1982). Winkley (1977) concludes from this form of analysis that the Lower Mississippi River was a stable system between Cairo, Illinois and Natchez, Mississippi in the pre-cutoff period. Subsequent analysis of specific gauge records between 1950 and 1994 in the cutoff reach has been used to

propose a pattern of regional-scale response in the longitudinal profile (Biedenharn and Watson, 1997; Figure 2.15).

Upstream from Arkansas City, specific gauge records suggest a degradational trend whilst downstream from Vicksburg the records suggest an aggradational trend. In the reach between Arkansas City and Vicksburg, the absence of a significant trend has been used to propose a zone of relative stability. Hence, this model presents evidence to suggest that at the regional-scale, the river is responding to restore an equilibrium condition in the same manner as the morphological response to a single cutoff outlined by Lane (1947). Such sub-reach slope adjustments have more recently been used by Biedenharn *et al*. (2000) to suggest that the river presently has a much greater stream power than prior to the cutoffs. This is perhaps not surprising considering bank stabilisation has effectively aligned the river at a steeper slope. Most significantly, the largest increases have occurred in approximately the reach reported as undergoing degradation although increases in slope and stream power upstream and downstream have also occurred. Hence, it is proposed that excess stream power in the reaches directly affected by cutoffs resulted in scour that consequently increased bed material load and increased rates of aggradation downstream (Biedenharn *et al*., 2000).

The proposed model of response is attractive because of its conceptual simplicity. However, it can be criticised on a number of grounds. Most importantly, using regression analysis to identify spatio-temporal trends over relatively long (> 100 km) reaches of river ignores potentially important changes at smaller spatial scales. In addition to the reach-scale changes identified by Biedenharn and Watson (1997), an increase in the amplitude and/or decrease in the frequency of the pool-crossing undulations in the longitudinal profile would be consistent with the idea that the river has responded to artificial channel steepening and planform stabilisation by adjusting its longitudinal profile in order to exert greater form resistance. If this has been the case, higher rates of bed material transport may not necessarily be experienced in the post-modification channel because *additional* energy would be expended in overcoming *additional* form resistance and hence, the energy available for bed material transport may remain relatively unchanged. If the pool-crossing configuration has adjusted to exert a greater form resistance, this poses a second,

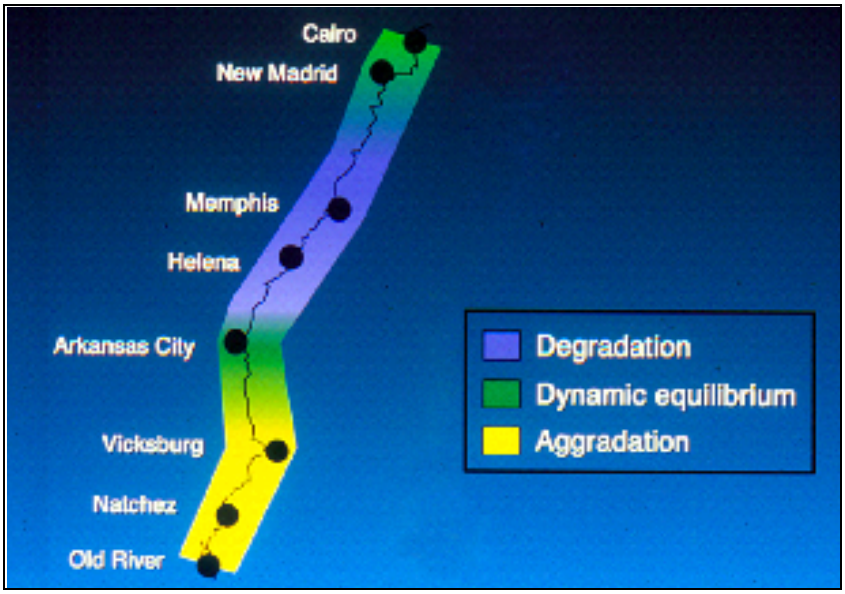

Figure 2.15 Regional-scale adjustments to the longitudinal profile in the period 1950-94, as proposed by Biedenharn and Watson (1997).

related problem with inferring morphological changes directly from specific gauge records. This is because observed vertical changes in flow stage may reflect changes in velocity, driven by changes in flow resistance, rather than vertical aggradation or degradation tendencies in the channel bed.

A third problem is that the conceptual model is based on analysis of specific gauge records at only six gauging stations along an 800 kilometre reach of the river from New Madrid to Natchez and therefore, the chance of inclusion of a systematic sampling bias should be considered. The importance of sampling bias has been demonstrated over the time interval of a single flood event by Lane and Borland (1953) but not over longer time intervals. A fourth issue concerns *explaining how* the construction of sixteen individual cutoffs can produce a consistent pattern of morphological response at the regional-scale. The idea that degradation is occurring as much as 320 channel kilometres downstream from a zone of cutoffs implies a spatial memory or high degree of connectivity in the fluvial system. However, according to Richards (1999; 5):

> *'The river has no knowledge of any condition to which it should restore itself.'*

Hence, if such a pattern does exist at the regional-scale, it is unclear how it could be formed and maintained by form-process interactions at much smaller spatial and temporal scales.

The issue of explanation introduces the fundamental question of whether the Lower Mississippi River acts as a highly connected system which displays a system-wide or regional geomorphological response signal, or whether response is fragmented throughout the system, and therefore, more difficult to detect. This has been partly addressed by Biedenharn and Thorne (1994) who have suggested that, in the post-cutoff period (1950-1982), the elevation of mid-channel bars have become adjusted to a single 'dominant' discharge of approximately 30 000 m^3s^{-1}. Similar results have been obtained from other large alluvial rivers (e.g. Thorne *et al*., 1993); thereby supporting the classical functionalist tenant that average channel form can be directly related to the prevailing process regime in large alluvial rivers. Conversely, other authors have attempted to illustrate the morphological *diversity* of the Lower Mississippi River. Schumm *et al*. (1994) use a qualitative methodology to identify

twenty four 'morphological reaches' on the pre-modification 1765-1930 river between Cairo and Old River. These were based on planform variability as well as geological, tectonic and tributary influences. Orlowski and Schumm (1995) undertake a more rigorous quantitative analysis of the pre-modification 1880-1915 river based on the variables width, depth, width-depth ratio and cross-sectional area. Although the computed reach boundaries are significantly different to those identified by Schumm *et al*. (1994) both techniques do suggest that considerable reach-scale variation may exist.

2.7.2 Investigation of spatial and temporal patterns of sediment transport

On the Lower Mississippi River, researchers comparing recent continuous measured sediment transport records to older and more intermittent historical records have all reported a large decrease in sediment loads at selected monitoring stations over the last 70 to 150 years. Based on the Tarbert Landing record, Keown *et al.* (1981) suggests that the total annual suspended sediment load declined from 427 million tonnes prior to 1963 to 251 million tonnes by 1981. Meanwhile Robbins (1977) compared measured suspended sediment records for the periods 1921 to 1931 and 1967 to 1974 and found that total suspended sediment loads had decreased since 1931 by roughly 40 percent at both Arkansas City and Vicksburg. Extending the historical analysis further by using data from the Humphreys and Abbot (1861) report, Kesel (1988, 1989) suggests that total suspended sediment loads on the Lower Mississippi River have declined by approximately 80 percent in the period 1851 to 1982. The decline in total suspended load since the pre-cutoff period has been associated with more conservation minded land practice in the tributary basins (Keown et al., 1981) and the construction of large dams in the tributary basins, particularly the Missouri and Arkansas basins, and the largest contributors of sediment load (Keown *et al*., 1981; Kesel, 1989). However, from a geomorphological standpoint, the results are only for total measured suspended load, of which approximately 70 percent is wash load (Biedenharn *et al*., 2000). Consequently, the results do not provide a direct indication of how the more geomorphologically significant bed material load may have changed.

Recent studies of the temporal trends in the composition of the bed material have generally noted either no trend or a slight fining trend since 1932 (Robbins, 1977; Keown *et al*., 1981). In perhaps the most thorough study, Nordin and Queen (1992) analysed changes in bed material gradations by comparing a 1932 survey of the channel thalweg with a replicate a survey of the channel thalweg in 1989. In each survey, bed material samples were collected every 1.6 km (one mile) between Cairo, Illinois and Head of Passes, Louisiana. From this investigation, the 1989 bed material was found to contain marginally less coarse sand and gravel than the 1932 bed material, suggesting a slight fining trend. Nordin and Queen (1992) attribute the observed decrease in coarser bed material to bank stabilisation works which prevent the river from gaining access to coarse material deposits in the floodplain, rather than a decrease in coarse material supplied from the tributary basins.

2.7.3 Investigation of the spatial and temporal variation of the efficiency of channel form (flow resistance)

Stanley Consultants (1990) conducted a detailed assessment of flow resistance in the Vicksburg District for the period 1950 to 1988 using a series of eight hydrographic surveys. The results of that study showed that, when computed water surfaces were fitted to known stage-discharge relationships, no discernable spatial or temporal trend in average Manning's n values was noted within the Vicksburg District. However, when water surfaces were computed to match measured water surfaces, a slight increase in Mannings n from 0.026 to 0.029 with distance upstream in the Vicksburg district was noted. In a less comprehensive investigation, Robbins (1977) also reported no discernable trend in channel resistance for this reach of river. However, the use of mean Manning's n values to represent large reaches of river for a specific discharge can be somewhat misleading. As both reports have suggested, channel resistance varies with discharge and planform as well as with form and skin roughness controlled by bedform development and grain size respectively. Hence, to explain spatial and temporal variations in Manning's n, the relative contribution of each of these components and their associated spatio-temporal dynamics needs to be further investigated.

2.7.4 Understanding of regional-scale geomorphological response to engineering intervention

Biedenharn *et al*. (2000) have noted that applying the results of previous investigations of regional-scale geomorphological response to Lane's (1955) short term equilibrium model of channel behaviour reveals a geomorphological paradox. The model specifies that the water discharge (Q_w) and channel slope (S) covary with the sediment discharge (Q_s) and the median particle size (d_{50}):

$$Q_w S \sim Q_s d_{50} \tag{2.1}$$

On the Lower Mississippi River the reported increase in stream power (Biedenharn *et al*., 2000) along with no discernable trend in channel resistance (Stanley Consultants, 1990) provides greater energy for sediment entrainment and transport and hence, would be expected to yield either (or both) an increase in bed material load, or an increase in the median size of the bed material. However, authors have reported a decrease in total suspended sediment loads (Robbins, 1977, Keown *et al*., 1981, Kesel; 1988) and either no trend or a slight fining of bed material (Robbins, 1977; Nordin and Queen, 1992). In response to this paradox, Biedenharn *et al*. (2000) suggests that the reduction in total load primarily represents changes in wash load and thus, the decrease may in fact mask an increase in bed material load. This is supported by Winkley (1977) who proposes that the movement of coarse sediments is more pronounced on the steeper slopes of the cutoff reach because the bars offer only a short temporary storage location whilst the levee system has effectively removed the opportunity for long-term over-bank storage. These sediments are consequently transported downstream to the flatter slopes of the lower alluvial valley below the artificial cutoff reach where the reduction in stream power favours deposition. Although this theory would support the downstream aggradation tendency inferred by Biedenharn and Watson (1997), the problems of defining and measuring trends in bed material load has prohibited further investigation.

The inconsistent findings discussed above provide the basis for the examination of the key research questions posed in section 1.1. To improve understanding of large-scale geomorphological behaviour within the context of response to engineering intervention, there is a critical need to:

1) *Undertake a more comprehensive examination of the pre-modification planform dynamics in order to provide the longer term 'top-down' context to geomorphological response.*

2) *Readdress the conceptual model proposed by Biedenharn and Watson (1997) of adjustment to the longitudinal profile using by analysing reach and sub-reach scale morphological adjustments. This will also reveal changes in large-scale form resistance.*

3) *Re-examine Biedenharn and Thorne's (1994) assertion that the mid-channel bars, or crossing reaches, have systematically aggraded in the post-cutoff period and hence, represent the active contemporary morphological feature of the Lower Mississippi River.*

4) *Improve understanding of sub-reach scale form-process interactions in order to assess the value of 'bottom-up' explanatory power to observed larger-scale and longer-term behaviour.*

These objectives arising from previous research are investigated using the range of data sets outlined in the following discussion. A discussion of the methodological framework and analytical techniques is presented in chapter 3.

2.8 Available data sets

A summary of the key data sets available to this study is presented in Table 3.2. Data sets resulting from direct observations extend as far back as Lieutenant Ross's planform map of the Lower Mississippi River published in 1765. This is supplemented by a reconstructed dataset of the distribution of abandoned channels at a Late Holocene timescale.

Data sets can be divided into those monitoring morphological change of the river channel and the wider alluvial valley, and those monitoring change in hydraulic and hydrological processes within the river channel. Morphological data sets range in timescale from hourly surveys (10^{-2} years) to Late Holocene maps of abandoned channels (10^{3} years). Process-based data sets range from detailed measurements of instantaneous velocity to discharge, flow stage and sediment transport records

extending as far back as the 1930s. Each data set can be classified on the basis of both total coverage and resolution in space and time (Figure 2.2).

2.8.1 Data set coverage and resolution

In terms of temporal coverage, most of the data sets postdate the introduction of the Mississippi River and Tributaries Project in 1928 although historic planform maps and early hydrographic surveys do extend to the period before extensive modification. Since 1928, a more coordinated programme of data collection and monitoring has been established including continuous flow stage and discharge measurements, aerial surveys and more detailed mapping of the alluvial valley. In the last 10 years, technological innovation has revolutionised data collection and enabled the collection of morphological and process data sets at significantly smaller spatio-temporal scales.

The spatial coverage of the data sets together reflects the institutional history of engineering and management of the Lower Mississippi River. Early data sets, such as the first hydrographic surveys, were undertaken by the then powerful Mississippi River Commission along the entire reach of the Lower River Mississippi River from the Cairo to the Gulf of Mexico. However, since the 1950s, the Mississippi River Commission has become largely synonymous with USACE (Moore, 1972). Consequently, the responsibility for data collection has increasingly been devolved to the three USACE Districts within the Lower Mississippi Valley; Memphis, Vicksburg and New Orleans. Although all are directed by the USACE Lower Division Office based in Vicksburg, Mississippi, coordinated monitoring and sampling programmes and the adoption of similar data processing and reporting procedures is difficult because each District manages its own data collection programmes. As a consequence, annual hydrographic surveys have only been undertaken by the Vicksburg District and weekly thalweg surveys have only been undertaken by the New Orleans District. Similarly, the most recent series of decadal scale hydrographic surveys were undertaken three years apart, by the Vicksburg District in 1988-89 and New Orleans District in 1992. Both the coverage and resolution of each data set available to this study are listed in Table 2.4.

Base Data Sets		Method of Collection	Time Interval	Spatial Resolution	Spatial Coverage
10^3	Abandoned channel maps	From Saucier (1994)	Floodplain features are mostly late Holocene age	Continuous coverage	Cairo to Baton Rouge
	Planform Maps	Scanned images from Elliot (1932)	Planform maps from 1765, 1821, 1861, 1880, and 1917 and 1930	Continuous coverage	Cairo to Baton Rouge
	Decadal Hydrographic Surveys	Lead lines pre 1964, single-beam echo-sounding post 1964	Surveys undertaken over the following periods: 1879-93, 1911-21, 1937-38, 1948-51, 1962-64, 1973-75, 1988-89, 1994	Cross-sections at 250 – 400 metre intervals 15 – 50 elevation points per cross-section	Cairo to the Head of Passes
Morphological (years)	Annual Hydrographic Surveys	Single-beam sonar	Hardcopy, mid 1960s to present Digital, 1992 – 2001 excluding 1998	Cross-sections at 300 to 400 metre intervals with 15 – 50 points per cross-section	Vicksburg District
	Weekly Surveys	Single-beam sonar	Every 1-4 weeks from 1998 to 2002	Weekly surveys along the channel thalweg	Selected crossing reaches within the New Orleans District
	Hourly Surveys	Multi-beam Sonar	7-8 March 2001, 13 surveys over a 24 hour period	Spatially Distributed	Selected crossing reaches within the New Orleans District
10^{-2}	Aerial Photography	Light Aircraft	November 1999	Continuous	Vicksburg District
10^2	Discharge	Pre mid 1990s: Velocity-area method Post mid 1990s: ADCP† method	Computed daily records from the 1930s to 2002 Selected, infrequent measured records	Gauging stations at approximately 240 km intervals	Cairo to Head of Passes
Process (years)	Stage	Flow stage surveyed to NGVD* 1929	From 1930s to 2002 Measured daily	Gauging stations at approximately 80 km intervals	Cairo to Head of Passes
10^{-2}	Velocity	ADCP† methods	Up to 4 surveys between January and May 2002	Cross-sections at 50 – 200 metre intervals Approximately 7 000 – 10 000 velocity measurements per cross-section	Selected crossing reaches within the New Orleans District

*National Geodetic Vertical Datum
†Acoustic Doppler Current Profiler

Table 2.4 Base data sets available to the study.

2.8.2 Reliability of data sets

An important issue regarding any secondary data sources is reliability. This is especially the case in this study considering the long timescale over which data collection has been conducted. Uncertainty arises from both primary and secondary data acquisition errors. Primary errors are caused by both the measurement technique adopted and the skill of the observer undertaking the measurement. Tables 2.5 and 2.6 demonstrate the range of techniques that have been used to monitor in-channel morphology both vertically and horizontally. In general, measurement techniques have become both more accurate and more precise through time and consequently, data reliability has improved. Perhaps more importantly, due to improvements in data processing, data storage and metadata recording, more is known about the relative reliability of data sets collected over the last 20 years. Secondary data acquisition errors resulting from data processing are also a particular concern for older data sets that have been digitised. Therefore, geomorphological interpretations from the older data sets must be viewed with reasonable caution. The series of analytical techniques (see section 3.2) applied to the data sets in each results chapter have been chosen with the reliability of the initial data sources in mind.

2.8.3 Historic maps of river planform

Six historic maps of river planform are available to study the sequences of planform change on the Lower Mississippi River prior to the period of sustained channel engineering (Table 2.7). Mapping has been undertaken by four different organisations and the final maps published at a range of scales. The three most recent maps can be assumed to be the most accurate because they were initially published at significantly larger scales than previous maps and by a single unitary organisation, the Mississippi River Commission. However, all maps, especially the earlier versions, may have only been developed using relatively rough methods in comparison to current cartographic standards. Hence, long-term interpretations of channel planform change must be treated with a degree of caution because the reliability of each map, particularly those produced prior to 1881, is largely unknown.

Method	Period	Description	Uncertainties	Resolution	Reliability
Lead Line	1880 – mid 1960s	**Mechanical Measurement** • Heavy lead weight attached to a suitable length of stretch resistant cord. • Weight is lowered into the water and depth measured from gradations marked on the cord.	• At high velocities, sounding line will not hang vertically, causing overmeasurement[1] • At depths greater than 5 metres, accuracy significantly degrades[1]	Manual collection	1.8 m in depths of 30 metres[2]
Single-beam sonar (Echo-sounding)	Mid 1960s to present	**Acoustic Measurement** • Depth can be calculated by timing the interval between the transmission of a pulse of sound energy from the boat and its reception after reflection at the channel bed. • Relies on knowing the velocity of sound.	• Uncertainty increases as transducer beam width, bed irregularity and slope of channel bed increases[1] • Vessel heave, pitch and roll motions[3] • Variations of the velocity of sound in water due to water temperature and suspended sediment[1] • Dependent on accuracy of initial calibration	Permits the collection of depth data at 5-20 soundings per second	Precision will degrade as a function of water depth: 0.03 m plus 0.1 % to 0.5 % of the depth[1]
Multi-beam sonar	Late 1990s to present	**Acoustic Measurement** • Same principle as single-beam except that a single, or pair of transducers, continually transmits numerous sonar beams in a swath or fan-shaped signal pattern.	• Outer beams subject to greater uncertainty • Dataset degrades at depths less than 5 metres[1] • Time delay between the positioning system, sonar measurement and the heave-pitch and roll sensor of boat motion must be accurately known in the processing of the dataset	Number of beams range from 30 to 120, permitting 2 000 to 3 000 elevations per second to be measured[1]	Precision will degrade as a function of water depth: 0.03 m plus 0.1 % to 0.5 % of the depth[1]

[1]U.S. Army Corps of Engineers (2002)
[2]Bannister *et al*. (1988)
[3]Hart and Downing (1977)

Table 2.5 Techniques used to measure depth on the Lower Mississippi River.

Method	Period of Use	Description	Uncertainties	Reliability
Visual Positioning	Pre 1950	Visually aligning survey boats between range markers located on the river banks	Increases with distance between range markers	Approx. ± 30 m[1]
Sextant Positioning	Pre 1950	Simultaneous observation horizontal angles between survey boat and two surveyed locations on the channel bank	• Precision of sextant angles • Observer synchronisation • Plotting errors • Velocity of vessel	Accuracy of ± 10 m at best[1]
Tag Line Methods	Approximately 1950s-70s	• Fixing a wire rope line between the bank to the survey boat to measure horizontal distance • Distances marked at a desired interval, usually every 7.5 metres[1]	• Tag Line direction may not be perpendicular to the channel alignment in the presence of strong currents • Dependent on power of boat to maintain a taut line over a given distance	Approx. ± 5 to 10 m but dependent on distance from river bank[1]
Range-azimuth methods	Approximately 1970s and 1980s	• Positioning by various types of electronic distance measurement (EDM) devices. • Based on the intersection of an angular a distance observation • Automated data acquisition possible	• Periodic calibration necessary • Reliability decreases with distance from the EDM device	In the order of ± 5 m but significantly greater over longer distances[1]
Range-range methods	Early 1980s to 1994	• Accomplished by determining the coordinates of the intersection of two or more measured ranges from known control points. Possible over greater distances than range-azimuth method • Automated data acquisition possible	• Dependent on tracking accuracy and geometric strength of the alignment[1]	Accuracy of ± 5 m possible but dependent on distance of EDM to survey boat[1]
Real time kinematic DGPS	Since 1994	• Used to position a point relative to a reference station whose precise location is known • Does not require time consuming calibrations and not so dependent on geometrical and distance considerations[1]	Errors caused by atmospheric delay at each station effectively cancel each other out	Capable of ± 0.1 m on a moving survey boat[1]

[1]U.S. Army Corps of Engineers (2002)

Table 2.6 Techniques to measure horizontal position on the Lower Mississippi River.

Elliot (1932) reconciled the scale issues associated with comparing between the historic maps by overlaying them onto a single sheet at a common scale and projection. The final sheet is published in eight plates extending from Cairo to the Gulf of Mexico, providing a resource on which to base a study of planform change. However, the methodology used in this procedure in not documented and so it represents a further source of unknown spatial error.

2.8.4 Late Holocene maps of abandoned channels

Maps of abandoned channels provide a longer-term indication of the relationship between the Lower Mississippi River and its alluvial floodplain. Maps have been reconstructed using evidence from several sources. Aerial photography provides the best means of landform identification and delineation because of the large size of most landforms in the alluvial valley (Saucier, 1994). The first complete coverage was obtained by the U.S. Soil Conservation Service in the late 1930s and subsequently, aerial photography has been undertaken at approximately decadal intervals at scales of up to 1:20 000. Through these multiple coverages, it has been possible to observe abandoned channels using a range of different vegetation and soil moisture conditions, enabling reliable geomorphological interpretation (Figure 2.16a). Topographic information, soils maps and field reconnaissance have been used to provide verification where necessary. According to Saucier (1994), more than 90 percent of abandoned channels are identifiable from aerial photographs, in the field, or on maps because of their characteristic drainage, topography, soils and configuration.

Where surface evidence is ambiguous, the presence of all, or a remnant, of a buried abandoned channel has been detected by borings that encountered a large thick mass of fine grained deposits interpreted as a clay plug (Saucier, 1994). Since the early 1930s, the undertaking of over 250 000 subsurface borings has provided an opportunity to locate abandoned channels not evident from the surface investigation (Figure 2.16b). Pioneering surface and subsurface investigations by Fisk (1944) led to the compilation of the first maps of Holocene deposits in the alluvial valley. These have been redrafted following a systematic large-scale (1: 62 500) mapping

Period Undertaken/ Date Published	Organisation	Scale Initially Published
Published 1765	Expedition led by Lieutenant Ross (Elliot, 1932)	1 inch: 14 miles (Elliot, 1932) (Approximately 1:10 million)
1821 – 1830	Expedition led by Captain Young, U.S Army Corps of Engineers	1 inch:1 mile (Elliot, 1932) (Approximately 1:750 000)
Published 1861	Humphrey's and Abbot (1861) investigation	Unknown
1881 – 1893	Mississippi River Commission	Ranging from 1:20 000 to 1:63 360
1913 – 1921		
1930 – 1932		

Table 2.7 Historic planform maps of the Lower Mississippi River, published in the period 1765-1932.

Figure 2.16 a) Aerial photograph mosaic of the 'Cat-Fish Point' bend reach of the Lower Mississippi River, collected by the USACE Vicksburg District in 1999 at an original scale of 1:20 000. b) A team undertaking subsurface borings in the alluvial valley (Moore, 1972).

programme from the early 1960s to the mid-1980s of geomorphological surfaces in the alluvial valley. The large-scale maps have been reproduced by Saucier (1994) as a series of eleven sheets at a scale of 1:250 000. This most recent compilation provides a sufficiently detailed set to use within this thesis.

Surprisingly, no attempt has been made to date abandoned channels despite extensive radiocarbon dating in the alluvial valley and deltaic plain. Determining the approximate date of a meander cutoff is problematic because it is characteristically followed by a long period of gradual infilling (Bravard and Bethemont, 1989). However, such an investigation would provide a long-term chronology of planform dynamics. In the absence of a chronology, the abrupt shifting of meander belts through the Holocene period provides a long-term temporal control. Thus, the cutoffs of abandoned channels within the most recent meander belt have occurred within approximately the last 2 000 years (Saucier, 1994).

2.8.5 Hydrographic survey data sets

At the decadal timescale, the most complete record of Lower Mississippi River channel morphology and its change through time is provided by a series of approximately decadal-interval hydrographic surveys of the entire Lower Mississippi River, dating back to 1879. The earliest two surveys were commissioned by the Mississippi River Commission and collected over a period of years prior to the introduction of the MR & T Project. However, these surveys, undertaken between 1879 and 1894, and 1911 and 1914 in the Vicksburg and Memphis Districts, and between 1921 and 1924 in the New Orleans District, have not been referenced to a consistent vertical datum and therefore, are not used to evaluate morphological changes in this thesis. Later hydrographic surveys, undertaken between, 1949 and 1951, between 1962 and 1964, in 1975 and, between 1988 and 1989, are consistently referenced to the National Geodetic Vertical Datum (NGVD) of 1929 and hence, together provide information on river channel morphology at increasing stages of engineering intervention.

Each decadal hydrographic survey was originally published as a series of sheets within a survey book, at a scale of 1: 20 000. However, over the last decade, the USACE Districts have undertaken the task of digitising the hydrographic surveys. Although this procedure introduces a further source of positional error, for the first time it allows rigorous analysis of the entire dataset, rather than basing studies on only selective measurements. The digitisation has been accompanied by the storage of each survey as a catalogue of digital images, each representing a single mapping sheet. Thus, it is now possible to cross-reference the digitised data sets with the original map images on a standard personal computer (Figure 2.17). The decadal-interval surveys are complemented by annual hydrographic surveys of the 434-kilometre reach of the Lower Mississippi River lying within the jurisdiction of the Vicksburg District. These surveys do extend back to the mid 1960s but are available in a digital format only between 1992 and 2001. Consequently, only this later period is available to this thesis.

The decadal and annual hydrographic surveys represent an important dataset at the regional-scale because the spatial resolution of measured elevations is extremely high in relation to data coverage, and furthermore, the resolution does not degrade with time. This is a tribute to the early days of the Mississippi River Commission when conducting hydrographic surveys was a highly ambitious task considering the limitations imposed by available technology and communication infrastructure. Since these early days, the method of data collection has involved surveying channel depths at 30 – 40 metre intervals along pre-determined range lines. These lines are positioned approximately perpendicular to the channel centreline and are therefore analogous to cross-sections. Longitudinally, range lines are spaced at 250 – 400 metre intervals along the entire Lower Mississippi River, creating a total series of approximately 5 000 cross-sections for each survey. Each cross-section is marked by riverbank posts that have been positioned using precise land surveying methods (Moore, 1972).

Despite consistency in methodology, there have been significant changes in the technology used to measure vertical depth and horizontal position (Tables 3.3 and 3.4). Consequently the *reliability* of these surveys has improved markedly through time. In terms of vertical measurement, the introduction of acoustic single-beam

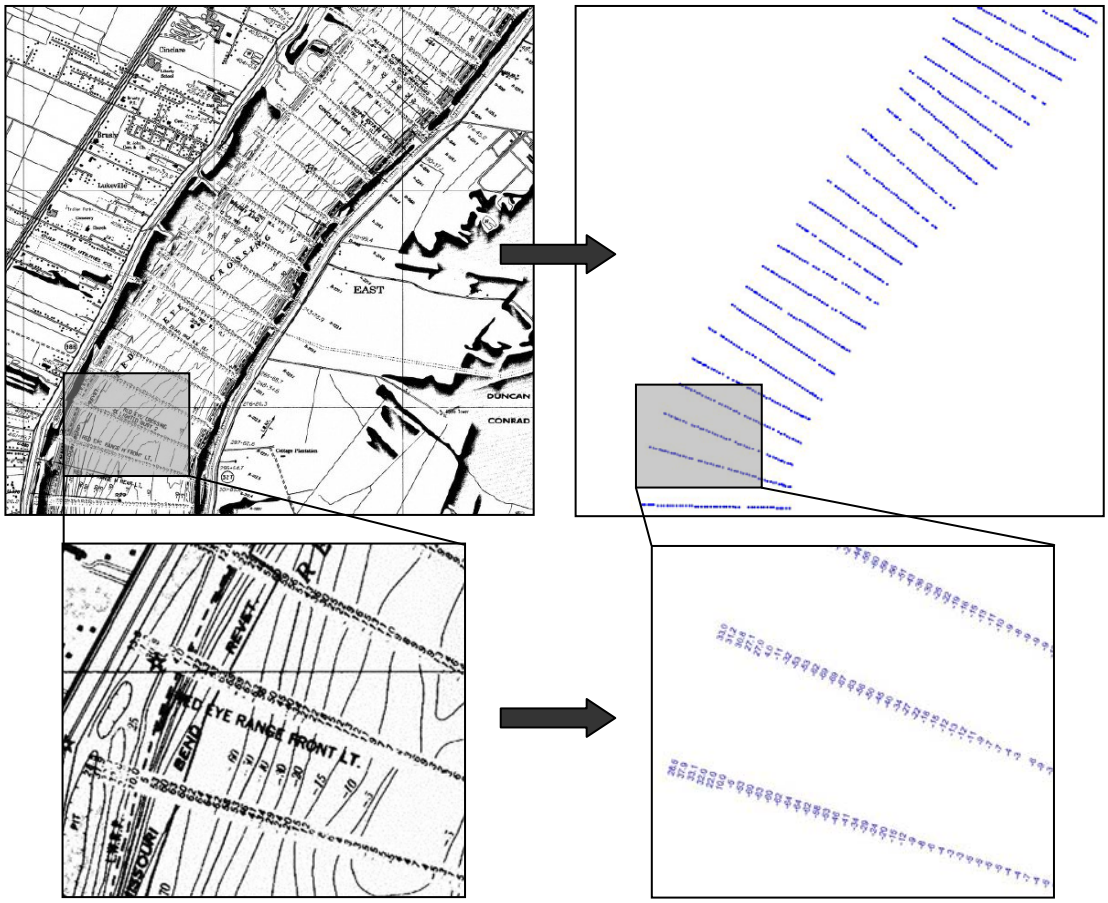

Figure 2.17 The relation between the original USACE decadal-interval hydrographic survey maps and the digitised data. The area shown is the Red Eye Crossing reach, immediately downstream from Baton Rouge in the New Orleans District.

sonar equipment prior to the 1962-4 survey is likely to have increased the vertical reliability by up to an order of magnitude. This instrument can measure depth to a precision of 0.03 m ± 0.5 percent of the depth (U.S Army Corps of Engineers, 2002). So, using the 1988-89 hydrographic survey data, the mean channel depth of approximately 8.5 m (at a discharge of 17 500 m^3s^{-1}) would be precise to approximately ± 0.07 m. Prior to 1964, the use of mechanical lead line equipment was considered precise to ± 1.8 metres in depths of 30 metres which covers almost all but the deepest pools (U.S. Army Corps of Engineers, 2002). Fortunately this error, representing approximately six percent of the total depth, is likely to significantly overestimate the mean error associated with lead line technology because precision degrades significantly with depth.

In terms of horizontal positional reliability, a range of techniques have been used since 1879 but their specific use, particularly for the earlier surveys, has been poorly documented. In general, positional reliability prior to 1950 ranges from ± 10 to 30 metres whereas since 1950, reliabilities in the region of ± 5 metres have been obtained. These positional error bands appear large but they must be viewed within the context of the physical scale of the Lower Mississippi River. At a low flow stage of just 10 000 m^3s^{-1} the average width is over 1.3 km and hence, a maximum positional error of 30 metres represents an error band of only approximately 2.5 percent of the total width.

A further source of uncertainty is associated with the temporal period over which the surveys have been conducted. This was particularly a problem with the earlier decadal-interval surveys where, because of the limited depth and positioning technology available, early measurements required relatively large survey teams and were therefore collected over a period of up to several years. More recent decadal-interval surveys have typically spanned just one or two low water seasons, but the survey period may still have been several months in duration because of the spatial scale of data collection involved.

2.8.6 Flow stage and discharge data sets

Long-term and regional-scale trends in the process regime can be reconstructed by examining historical flow stage and discharge records extending back to the 1930s and 1940s. Daily discharge has been calculated from approximately fortnightly measured records at recording stations spaced at intervals of approximately 150 kilometres. Over the same period, flow stages have been recorded at the seven principal discharge recording stations and intermediate stations spaced at approximately sixty kilometre intervals along the Lower Mississippi River.

Flow stage is measured daily by reading the height of water against a series of stage boards at each recording station. The zero level on each stage board is surveyed to the National Geodetic Vertical Datum (NGVD) of 1929. Until the mid-1990s, the standard method for calculating discharge on the Lower Mississippi River was the velocity-area method. As for the hydrographic surveys, depth measurements were determined by using either weighted lead line or single-beam sonar technology. Velocity measurements were taken at 40 percent of the depth, using a standard Price current meter. Since then, both the USACE New Orleans and Vicksburg Districts have adopted the Acoustic Doppler Current Profiler (ADCP) method. The ADCP instrument measures the Doppler shift in the original frequency of four acoustic pulses transmitted along beams that are positioned ninety degrees apart horizontally and directed downward into the water column at an angle of 30 degrees from the vertical (Simpson and Oltmann, 1993). By using simple trigonometric methods, frequency shifts are converted into water speeds and the three dimensional components of velocity can be resolved. Depths can be simultaneously measured by utilising a bottom tracking feature. Pratt (1995) suggests that the ADCP method has at least doubled the precision of discharge measurement on large rivers.

2.8.7 Sub-reach scale data sets

Sub-reach scale morphological and process data sets are available of the Red-Eye crossing and downstream Missouri Bend (Figure 2.18). The sub-reach is located approximately 16 km downstream from Baton Rouge in the New Orleans District.

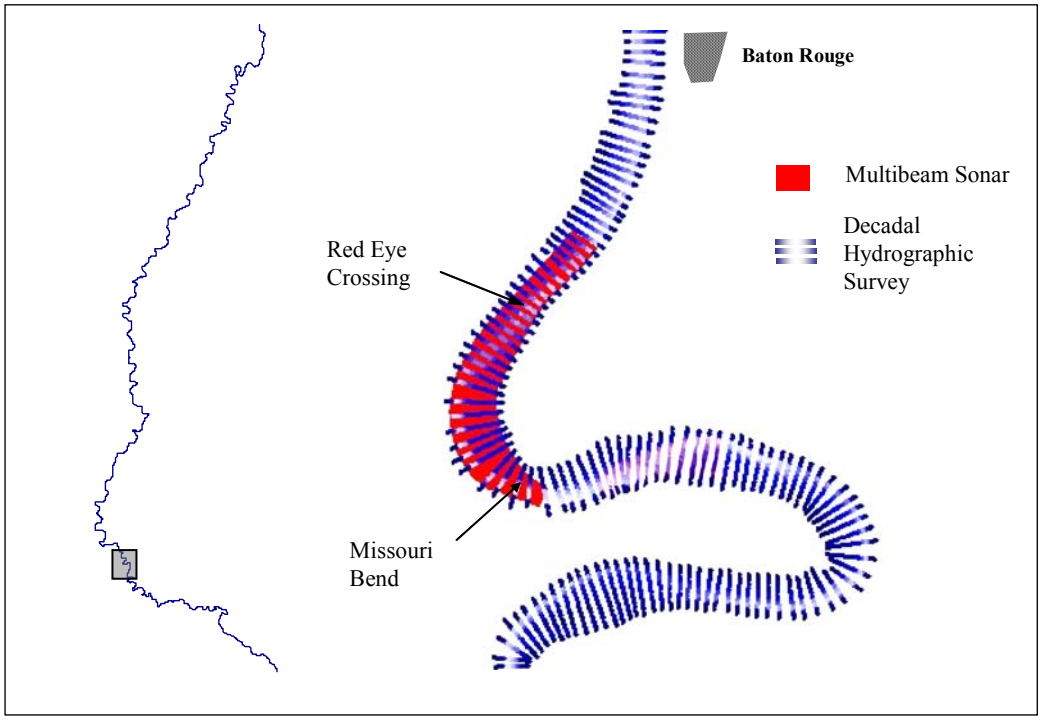

Figure 2.18 The location of Red Eye crossing and Missouri Bend sub-reach.

To reduce the need for maintenance dredging, dike fields were constructed in Red Eye crossing between September 1993 to July 1994 (U.S. Army Corps of Engineers, 1997).

Three key data sets are available to study the complexity of process-form interrelations. First, at weekly or fortnightly intervals, single-beam sonar surveys of the channel thalweg have been undertaken in a series of crossing reaches since 1998. These surveys involve sampling the channel thalweg longitudinally along five parallel range lines so that the District can determine whether the required navigation depth is being maintained and consequently, manage its dredging operations more efficiently. Single-beam sonar surveys are supplemented by a single multi-beam sonar survey of the whole channel, and repeated multi-beam sonar surveys of the channel thalweg. By utilising multiple acoustic beams and a high sampling frequency, multi-beam sonar surveys can deliver a vastly improved spatial resolution of approximately 0.12 observations m^{-2} over significantly reduced time intervals. Table 2.8 shows that this resolution is actually comparable to those obtained from similar case-intensive investigations of much smaller rivers. Multi-beam sonar surveys were undertaken by driving the survey boat along the channel thalweg to obtain a two dimensional, but localised, coverage. Near complete coverage for the whole channel survey was obtained by repeating this manoeuvre at regular increments of the channel width parallel to the channel centreline. Repeated surveys of the channel thalweg were undertaken at approximately hourly intervals over a 24-hour period.

Single-beam and multi-beam morphological surveys are accompanied by ADCP velocity surveys of the sub-reach. ADCP technology provides a spatial resolution of observations at least an order of magnitude greater than those that can be obtained on smaller rivers using the electromagnetic current meter method. Within each reach, ADCP surveys have been undertaken at a range of discharges at up to 36 consistent flow monitoring cross-sections that are positioned approximately perpendicular to the channel centreline. Each cross-section contain up to 400 sampling verticals and up to 10 000 velocity observations (Figure 2.19).

Study	River	Reach Length (m)	No. of cross-sections	Mean cross-section spacing (channel widths)	Point Density (No. m^{-2})
Ferguson and Ashworth (1992)	River Feshie	80	6	0.47	0.08
Goff and Ashmore (1994)	Sunwapta River	60	7	0.28	0.12
Lane *et al*. (1994)	Haut' D'Arolla	18	Spatially Distributed	Spatially Distributed	1.0-7.4
Martin and Church (1995)	Vedder River	8 000	49	0.91	<0.006
Milne and Sear (1997)	Kingledoors Burn	325	60 (1976) 70 (1994)	0.93 (1976) 1.02 (1994)	0.31
Weekly single-beam sonar	*Lower Mississippi River*	*4 000*	*Longitudinal survey*	*Longitudinal survey*	*0.001*
Multi-beam sonar		*8 000*	*Spatially Distributed*	*Spatially Distributed*	*0.12*

Table 2.8 The sub-reach scale morphological data sets in relation to data sets employed in other recent case-intensive investigations.

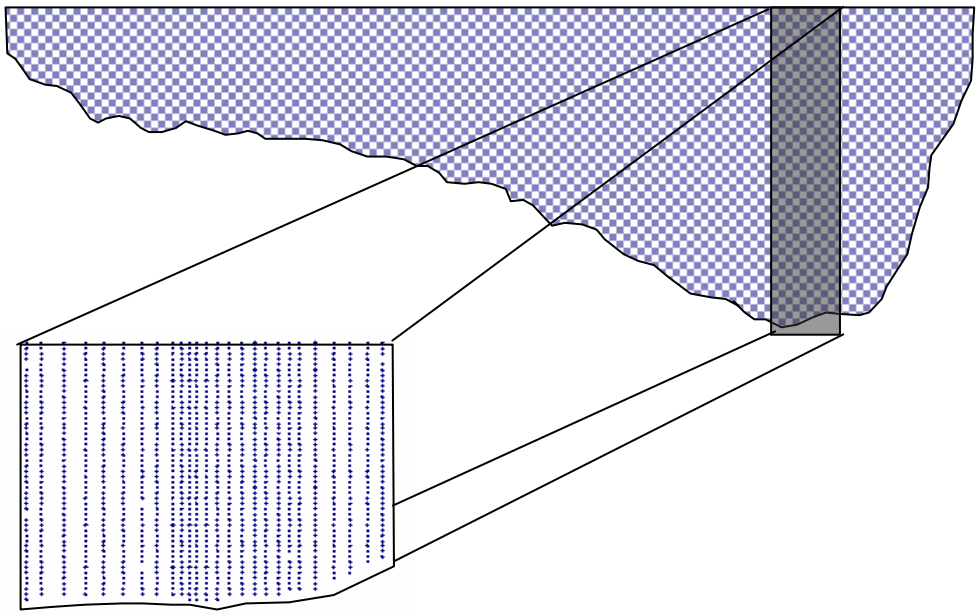

Figure 2.19 The density of observed velocities in each flow cross-section.

The range and association between available sub-reach scale data sets is summarised in Figure 2.20. In 2.20a, the flow monitoring cross-sections are superimposed upon the underlying channel morphology. The morphology is depicted by colour-coding each observation within the multi-beam sonar whole channel survey based on bed elevation. The high density of observations (total number for the reach shown exceeds 1 million) gives the visual impression of a continuous morphological surface. In 2.20b and 2.20c, the weekly-interval single-beam sonar and the hourly-interval multi-beam sonar surveys of the crossing thalweg are displayed respectively.

In the results and analysis sections of this thesis (chapters 4-7), the data sets introduced in this section are used on a selective basis to satisfy the research design outlined in section 2.2. The following chapter discusses the methodological framework and accompanying analytical techniques employed throughout the thesis.

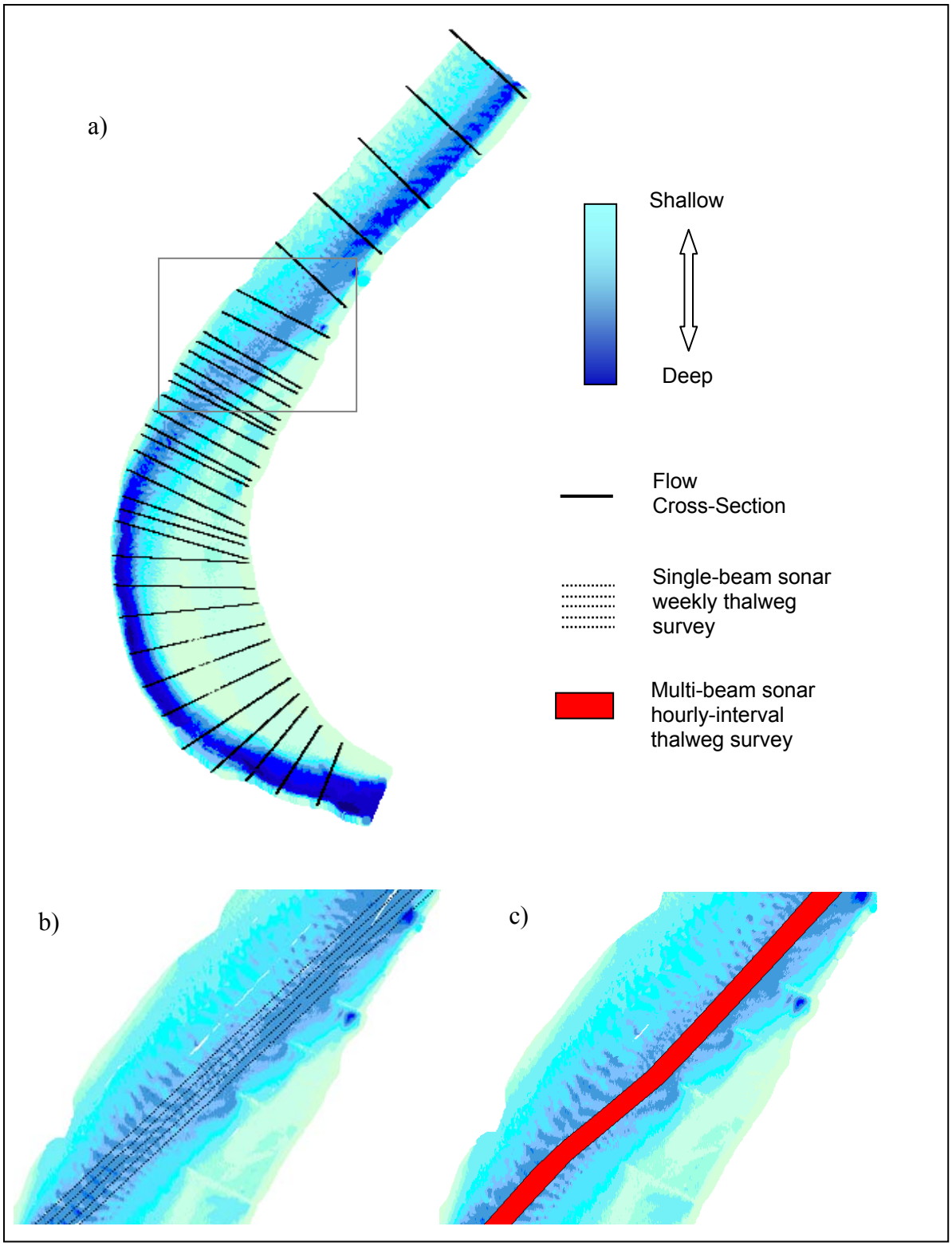

Figure 2.20 The morphology of the Red Eye crossing and Missouri bend sub-reach. Measurements have been colour coded according to elevation to emphasise morphological variation. In: a) velocity cross-sections are overlaid; in b) the crossing is enlarged to show the single-beam sonar longitudinal surveys along range lines around the channel thalweg and; in c) the crossing is enlarged to show the hourly multi-beam-sonar surveys of the channel thalweg.

CHAPTER 3. METHODOLOGICAL FRAMEWORK AND ANALYTICAL TECHNIQUES

3.1 Methodological framework

Two principal methodological approaches are adopted in the thesis. At the regional and reach-scales, the historic planform maps and hydrographic survey data sets are analysed by the application of a variety of novel and more traditional analytical techniques to identify the major morphological characteristics of the Lower Mississippi River. By investigating how these characteristics change through space and time in both the pre-modification and post-modification periods, new insights are revealed regarding how the Lower Mississippi River functions as a large fluvial system. This 'functionalist' approach (Chorley, 1962) is complemented by the local-scale research which uses high resolution data sets of a small number of case-study reaches to explore interrelationships between morphology and process in a 'realist' framework (Richards, 1990).

3.2 Regional-scale and reach-scale methods and techniques

Regional and reach-scale analysis is based upon the application of a series of statistical techniques applied to one dimensional sequences of data. A one dimensional approach was chosen in preference to a two dimensional approach because the latter would have been computationally very demanding at such a large scale. Reducing to one dimension is also advantageous because it reduces the level of uncertainty associated with data quality. This is discussed in the proceeding paragraphs. Following initial data generation and processing, the analytical methods can be divided into two groups. First, a variety of one-dimensional serial techniques are applied to provide a powerful and potentially objective statistical characterisation. Second, a variety of feature extraction and analysis techniques are applied which, despite being less objective, have a greater physical rationale.

3.2.1 One-dimensional parameterisation

i) Planform research

One-dimensional analysis of the channel centreline, rather than two-dimensional analysis based on the channel bank lines, was deemed more appropriate because of the uncertainty regarding both, the spatial accuracy of the bank lines on the historic planform maps, and the spatial accuracy of the reconstructed abandoned channels (see sections 2.8.3 and 2.8.4).

The processing procedure to generate a one-dimensional planform series for each of the six overlain historic planform maps and each abandoned channel is summarised in Figure 3.1. Following initial digital import, each of the eight plates from Elliot (1932) and eleven sheets from Saucier (1994) were tiled to form single digital images using *Jasc Paint Shop Pro Version 7* image editing software. The final two images were then imported into *ESRI Arc View Version 3.3* GIS software to enable on-screen digitising of channel centre-lines. This was undertaken at an approximate point spacing of 0.5 – 1.0 channel widths, as recommended by Hooke and Redmond (1989). Within the abandoned channel series, each discrete channel was uniquely referenced by applying a customised procedure based on the distance and angle between consecutive points. The final stage of the processing procedure for both series involved the interpolation of regularly spaced points from the original digitised points.

Following digitising, a sensitivity analysis was undertaken to quantify the magnitude of error associated with the digitising process. Errors associated with on-screen digitising have been well explored in the GIS community (Dunn *et al*., 1990; Jones, 1997). The magnitude and distribution of digitising error was tested by repeated digitisation of the same channel centreline outlined by Gurnell *et al*. (1994). This was performed using the 1765 bank lines of the reach illustrated in plate *f* from Elliot (1932). This reach, extending approximately 100 channel kilometres upstream and downstream from Vicksburg, was selected because visual comparison between the 8 plates suggested this reach was highly dynamic. The 1765 channel boundary was selected because it is overlain by all later channel boundaries and hence, digitisation of this centre line is susceptible to the greatest error. Following each digitisation, the

total channel length and total number of number of points were recorded. The procedure was repeated thirty times to enable the average positioned error of the line to be estimated. For every 1 km digitised, 95 percent (2 standard deviations) of the digitised centrelines varied in length by less than 1 percent, representing a distance of 10 metres. Considering the initial level of uncertainty, this additional error was therefore deemed insignificant.

Figure 3.2 illustrates the processing procedure for the historic maps of planform from Elliot (1932). In 3.2a, a section of the original plate for the reach of the Lower Mississippi River immediately upstream from Vicksburg is shown. The digitised channel centre-lines for each of the six years have been overlain in Figure 3.2b. A smaller reach has then been enlarged and the digitised points overlain in Figures 3.2c and 3.2d. From the spatial series of digitised points, a customised routine was applied to interpolate points at regular intervals (see Figure 3.1). The same procedure applied to the maps of abandoned channels is presented in Figure 3.3. From a section of the original map (3.3a), the abandoned channels have been emphasised and the centre-lines digitised in 3.3b. The digitised points have been generated in 3.3c. In addition to the generation of regularly spaced points, a further customised routine was then applied to delineate each abandoned channel.

ii) Longitudinal profile research

With respect to the longitudinal profile, a one-dimensional approach was preferred to a two-dimensional surface-based approach because it eliminates problems introduced when the surveyed channel area is not contiguous between sequential hydrographic surveys which are adjacent in time. This can be caused by both planform migration and differences between the flow stage at which each survey in conducted. These problems are illustrated in Figure 3.4. Although bank stabilisation has effectively prohibited planform migration from the contemporary Lower Mississippi River, planform migration was experienced between the 1949-51 hydrographic survey and the 1962-64 hydrographic survey as an immediate response to the artificial cutoff programme (3.4a). Figure 3.4b shows that the 1974-75 hydrographic survey was undertaken at a significantly lower flow stage than both the 1962-64 and 1949-51

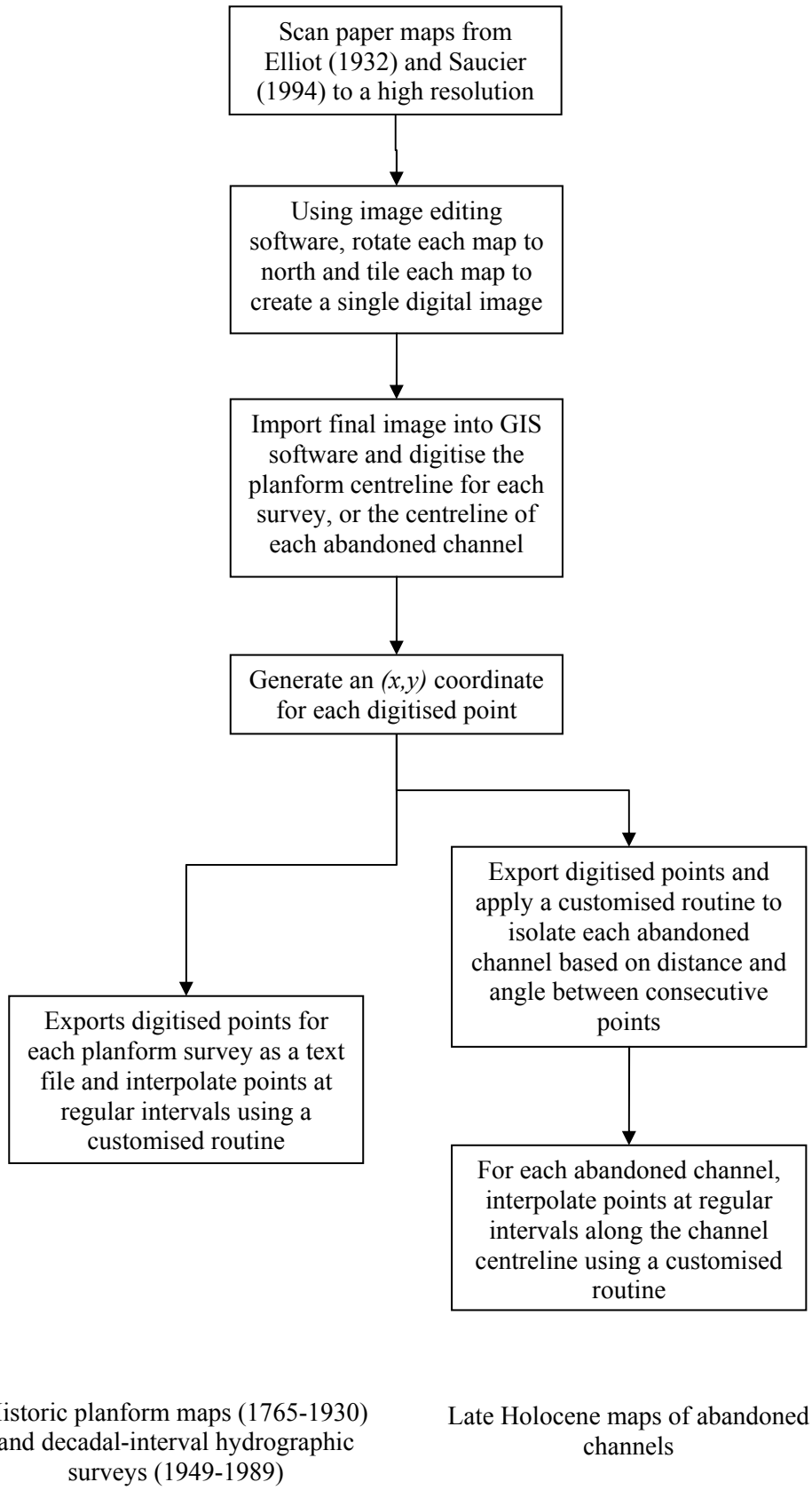

Figure 3.1 Summary of initial processing to allow quantitative analysis of planform.

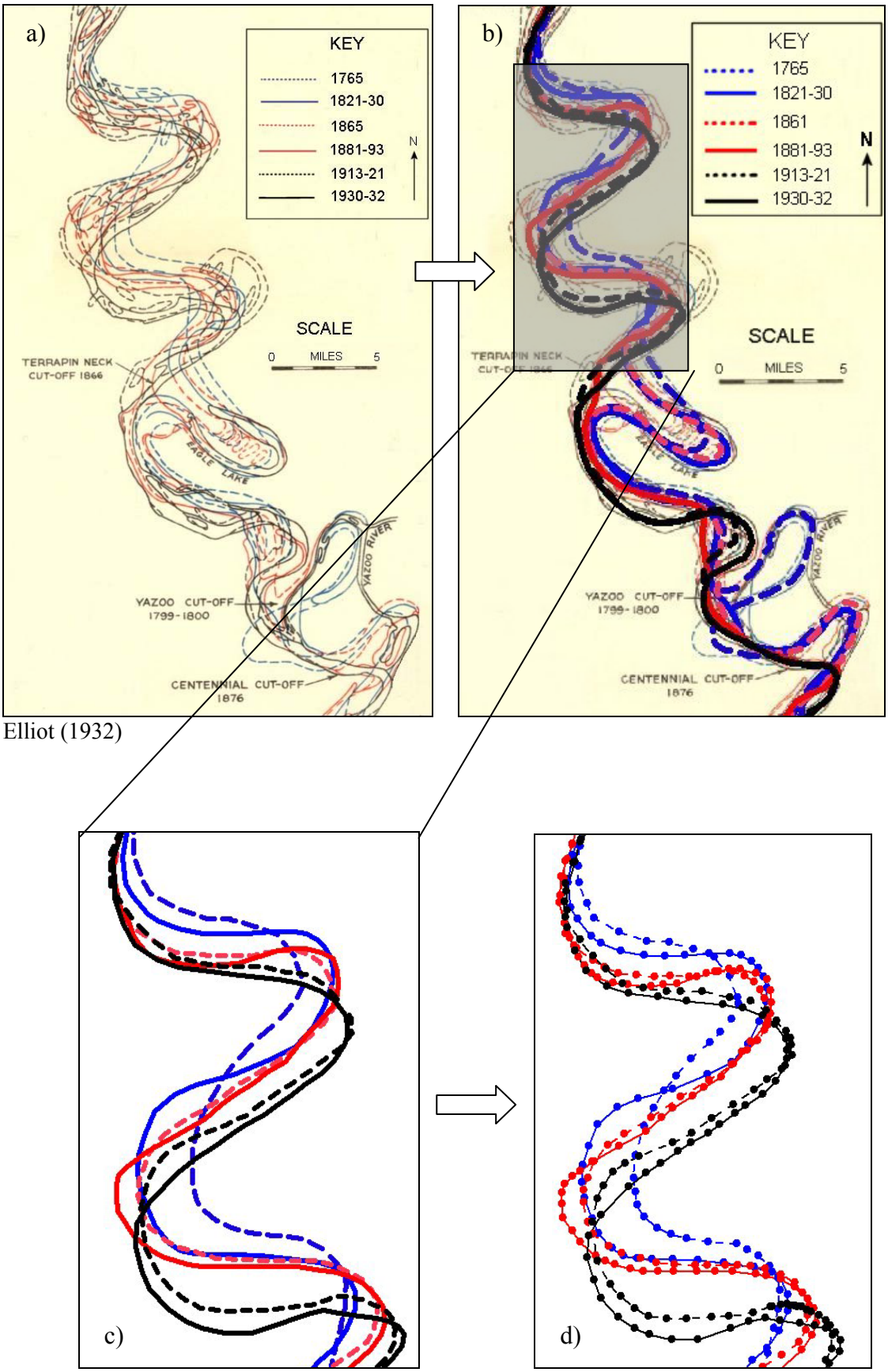

Elliot (1932)

Figure 3.2 Digitising and initial data processing from historic planform maps.

a)

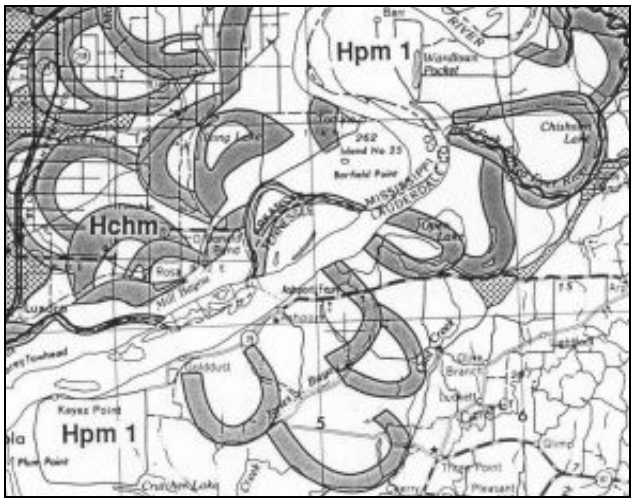

Saucier (1994)

b)

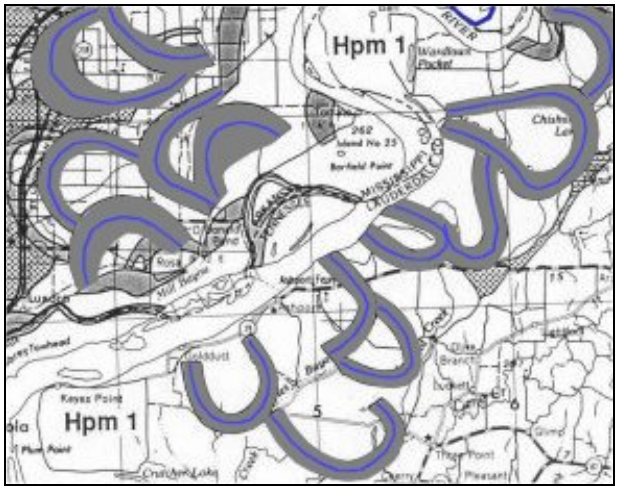

c)

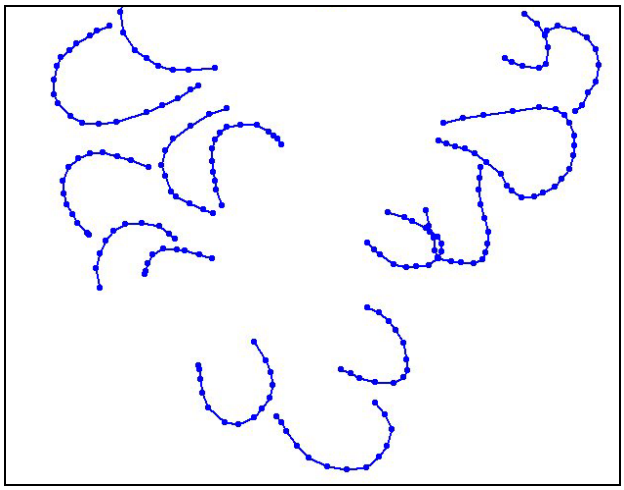

Figure 3.3 Digitising and initial data processing from abandoned channel maps.

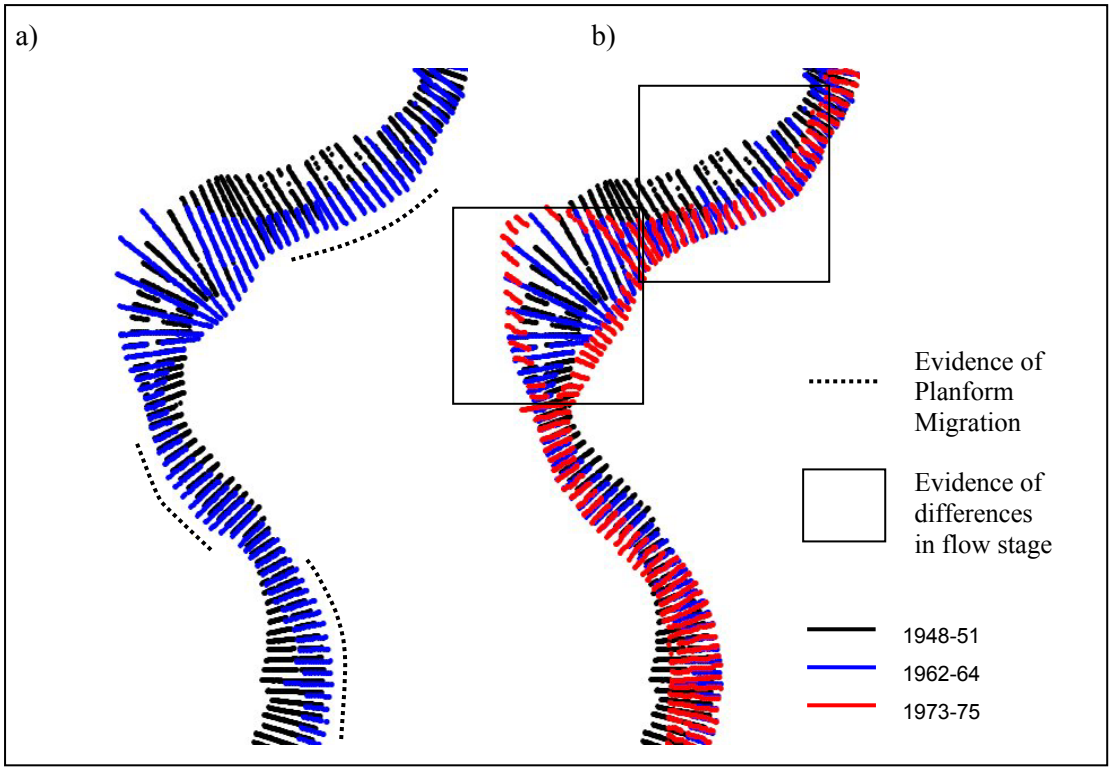

Figure 3.4 Hydrographic survey data sets following removal of 'problem' cross-sections. In a), 1962-64 survey overlays the 1949-51 survey and in b), the 1974-75 overlays the 1962-64 and 1949-51 surveys.

hydrographic surveys. As a consequence, the extent of morphological information at the channel margins is variable between surveys.

Reducing the hydrographic survey data sets to one dimensional spatial series was performed by extracting each cross-section and generating a series of parameters to describe its morphological characteristics. Extracting each cross-section involved developing an automated procedure capable of sorting the tabulated series of *(x,y,z)* coordinates within each hydrographic survey data file into a standard structure which delineated between cross-sections. A structure was chosen in which every observation could be located first, by its relative position within a cross-section from the right bank looking downstream, and second, by the position of each cross-section within the series of cross-sections extending from upstream to downstream. Each observation could therefore, be referenced by a unique combination of a cross-section identifier and a cross-stream identifier. The total routine involved two stages; first, a procedure was performed to delineate the data set into a series of cross-sections, and then a series of shorter procedures were performed to sort the cross-sectional data into the standard structured format.

Prior to the application of the delineation routine, cross-sections which did not lie perpendicular to the channel centreline were manually removed from each survey. These 'problem' cross-sections intersected other cross-sections and hence, would have generated errors in the processing procedure. The initial delineation procedure is summarised in Figure 3.5. Delineation is based on calculating the distance and angle between consecutive observations in the unstructured table of *(x, y, z)* coordinates. If consecutive observations have both a distance and angle less than 2.5 degrees and 65 metres respectively, they are incorporated within the same cross-section. Where a series of consecutive observations have been grouped into a single cross-section, but the next consecutive observation exceeds both the distance and angle thresholds, all of the other observations in the table are searched. A further observation is added to the cross-section only if it satisfies both the distance and angle thresholds, and also if linear regression analysis of the new cross-section generates a coefficient of determination (R^2) value which exceeds 0.95.

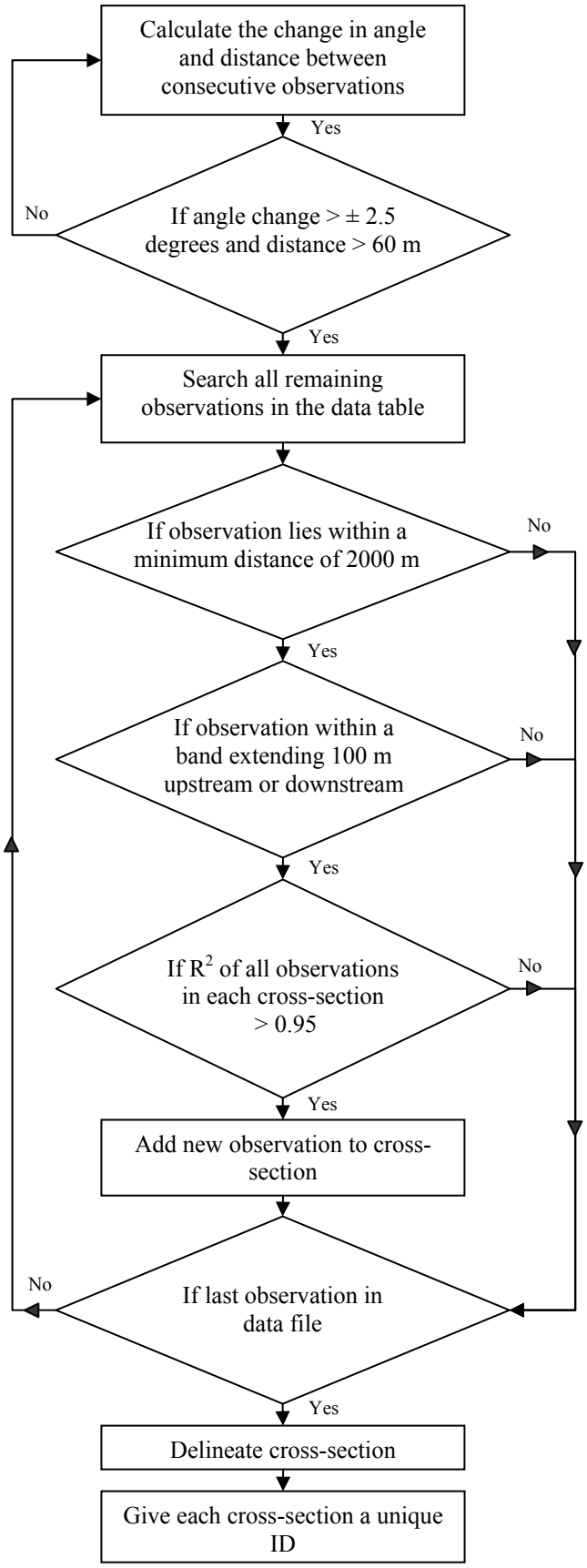

Figure 3.5 Summary of the automated data processing procedure developed to sort an unstructured table of *(x,y,z)* coordinates into delineated cross-sections.

Following application of the delineation routine, two more data quality checks were performed as a method of further validation: calculation of the maximum distance between any two observations in each cross-section and the calculation of the standard deviation of the distances between observations in each cross-section. Errors identified at this final stage of the data quality checking procedures were manually corrected.

The following automated steps were used to sort the cross-sections into a consistent downstream and cross-stream order:

1) *Find the centre-point and the nearest left and right bank observations of each cross-section.*
2) *Sort the centre-points so that they are ordered in a downstream direction.*
3) *Use the ordered centre-points to sort cross-sections into the correct downstream order.*
4) *Sort the observations within each cross-section so that they are ordered from the right bank to the left bank in the downstream direction.*
5) *Give each cross-section a unique ID.*

A final visual inspection was performed following application of the sorting routines. This involved displaying the computed centre-point and identified left and right bank coordinates for each cross-section in a GIS layer at a level above the original observations. Figure 3.6 compares the structured data in this final check to the original data files.

3.2.2 Serial analysis

i) Background

Serial analysis has been widely employed by geomorphologists to characterise large-scale variability in both the channel planform (Ferguson, 1975; 1977) and longitudinal profile (Richards, 1976b; Clifford, 1993). It is based on the premise that any spatial or temporal sequence of discrete and regularly spaced observations can be described in terms of an underlying systematic pattern plus a random error component. If a series can be predicted exactly, it is described as being deterministic; however, if a series can only be described through probabilistic laws, it

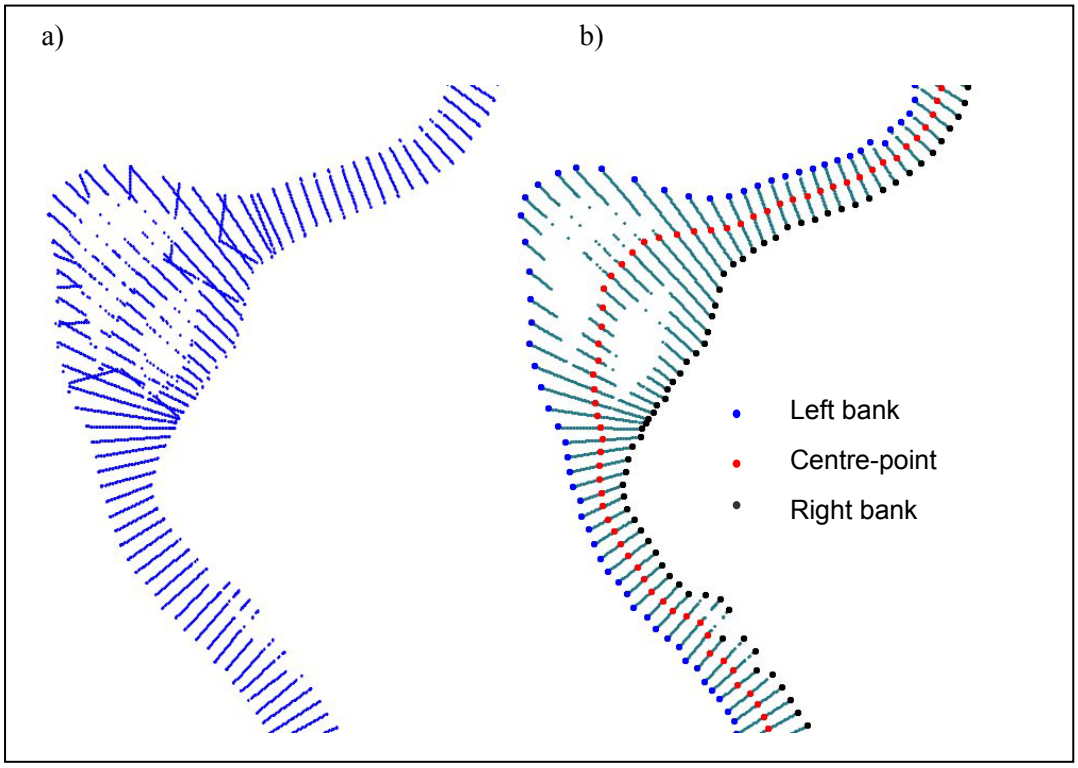

Figure 3.6 Initial data processing performed on the hydrographic survey data sets. In a), the original cross-sections are plotted in ESRI Arc View GIS and in b), processed cross-sections are plotted following removal of 'problem' cross-sections and application of automated routines.

is described as being stochastic (Chatfield, 1989). Most environmental series, including both river planform and river longitudinal profile cannot be described by solely deterministic relations and are therefore, assumed to be realisations of probabilistic processes (Richards, 1979). In this thesis, a range of serial techniques are used to reveal the underlying systematic patterns within the regional-scale data sets. The geomorphological significance of these patterns is then examined.

The primary objective of serial analysis is to decompose the total variation in an observed series into a series of deterministic and stochastic components which can be explained by known physical processes. This procedure is performed by sequentially removing trends from the series which can be physically explained, and searching for trends in remaining residual series which cannot be explained. In any series, up to three types of trend contribute to the total variance. The remaining variance is a residual error component (Richards, 1979):

$$V_T = V_R + V_C + V_S + V_E \qquad (3.1)$$

where:

V_T = the total variance

V_R = a deterministic 'long term' regression component

V_C = a deterministic periodic component

V_S = a stochastic component

V_E = a residual error component

Each of these components are illustrated using a hypothetical data series in Figure 3.7.

Within each regional-scale data series a variety of techniques are used to decompose the total variation. First, long-term trends in each series are identified using a combination of zonation and regression techniques. In practice, trend removal is a subjective process because there is no generally accepted and satisfactory definition of what is meant by a trend (Granger, 1969). Zonation provides a statistical method of identifying boundaries in river morphology at a scale which is intermediate between the local scale, representing a single meander wavelength or pool-crossing undulation, and the regional-scale, representing the entire dataset. The identification

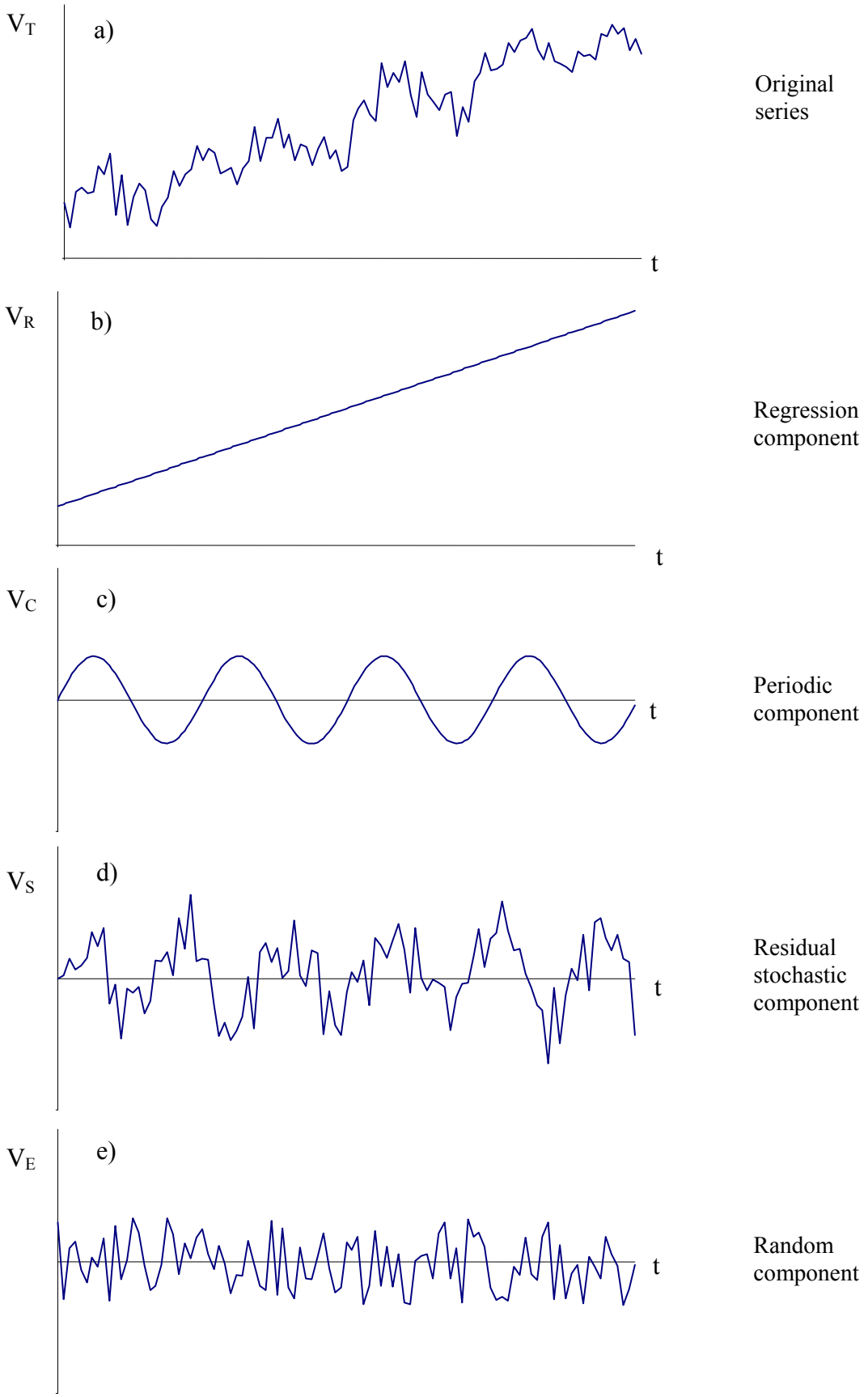

Figure 3.7 The decomposition of a series into its constituent components (adapted from Richards, 1979).

of morphological reaches and assessment of their temporal stability is then used to characterise the functioning of the Lower Mississippi River as a large fluvial system. Regression analysis examines the degree to which linear and low order polynomial trends can be fitted between the identified discontinuities. This provides a method of examining the extent to which the morphology of the Lower Mississippi River is consistent with a range of recognised empirical relationships that specify average behaviour. In a statistical sense, long-term trend removal is a necessary to generate a stationary series, a pre-requisite for most examinations of serial periodicity.

Second, although the removal of a deterministic, periodic trend is not justified because there is no *a priori* reason to assume a regular wavelength or amplitude of oscillation within either the planform or longitudinal profile series (Richards, 1979), the *degree* of periodicity within each data series is examined by applying a range of techniques derived from the analysis of persistence. This reveals the degree of *regularity* within the meander bend and pool-crossing series. Three principal serial techniques are used: autocorrelation and partial autocorrelation, which measure aspects of spatial dependency; and spectral techniques, which measure the distribution of variation in the frequency domain. Using these techniques in parallel provides the opportunity to identify consistent statistical trends which may have a physical significance.

Third, autoregressive modelling is used as a method of identifying stochastic behaviour within each dataset. Previous studies have shown that meandering planform series and riffle-pool sequences in the longitudinal profile exhibit psuedo-periodic behaviour (Richards, 1976b; Clifford, 1993): this statistical behaviour means that there is a periodic tendency, but the period of oscillation is disturbed by random shocks so that the period and phase are constantly changing due to the influence of a random component (Richards, 1979). Autoregressive modelling is used in this thesis to examine whether pseudo-periodic behaviour can be identified. Attention is specifically focused on the fitting of a second order autoregressive process (spatial dependence over 2 lag intervals) because this is the stochastic generating process for which a realisation will exhibit pseudo-periodic behaviour. Following successful identification, geomorphological explanations for pseudo-periodicity are explored.

ii) *Zonation*

Zonation is performing using local boundary hunting and global zonation procedures. These are outlined below.

a) Local boundary hunting

Local boundary hunting procedures are based on the principle of moving a window of constant dimensions through the data series and applying a function to identify breaks in morphological characteristics. The function applied can be adapted to identify specific types of morphological variation. The number of data points included in the boundary hunting procedure can also be adjusted by altering the dimensions of the window. This increases or decreases the sensitivity of the technique to variations in the data. Local boundary hunting procedures have been used in the environmental sciences for the analysis of soil transect data (Webster, 1973). However, they have not been widely applied within geomorphological research. In this thesis, a range of functions and window sizes are used to examine the extent to which morphological 'boundaries' can be identified in the planform and longitudinal profile series at scales larger than individual meander bends or pool-crossing units respectively.

b) Global zonation

Global zonation procedures differ from local boundary hunting procedures because the entire sequence is considered at one time instead of just the portion within the window. By considering the entire sequence, global zonation, attempts to divide the sequence into a number of zones which are as internally homogenous as possible and as distinct as possible from adjacent zones. This provides an objective identification of zones. The global zonation procedure used in this thesis is based on the iterative analysis of variance algorithm first developed by Beghtol (1958) and since used by Gill (1970), and Hawkins and Merriman (1973, 1974), as a method of automatically zoning digitised well logs. The algorithm involves dividing the sequence into zones based on the computation of two estimates of variance, the within zones variance (SS_E) and the total variance (SS_T):

$$SS_T = \sum_{i=1} [\sum_{j=1} (x_{ij} - M)] \qquad (3.2)$$

$$SS_E = \sum_{i=1} [\sum_{i=1} (x_{ij} - Mi)] \qquad (3.3)$$

where:

SS_T is the total variance (total sum of squares

SS_E is the within zone variance (error sum of squares)

x_{ij} is the jth point within segment i

M_i is the mean of the ith segment

M is the grand mean

Computationally, the procedure begins with moving a partition through the sequence and recomputing the two quantities, SS_T and SS_E at each position in the sequence. For every possible position of the boundary, the variation explained, denoted by the ratio R, is computed where:

$$R = (SS_T - SS_E) / SS_T \tag{3.4}$$

Where R is maximised, a boundary is inserted. Next the two zones are themselves portioned by repeating the process to insert an additional boundary which again maximises R. The statistical significance of the additional variation explained by the incorporation of a new boundary is examined by calculating the error variance (M_{SE}) and then performing an analysis of variance (F-test) based upon:

$$M_{SE} = S_{SE} / (N\text{-}m) \tag{3.5}$$

and

$$F = \textit{change in } S_{SE} / M_{SE} \tag{3.6}$$

where:

N = total number of observations

m = total number of zones

The zonation can be repeatedly run until the entire sequence is divided into the specified number of zones, or until the additional variation explained by further zonation is no longer significant. The zonation process is illustrated by the hypothetical series in Figure 3.8. The procedure has been set to identify the four most significant boundaries in the original series. Visual validation shows that these boundaries coincide with the distances at which there is greatest relative change in elevation on the y-axis. Together these boundaries demarcate the two peaks in the distribution.

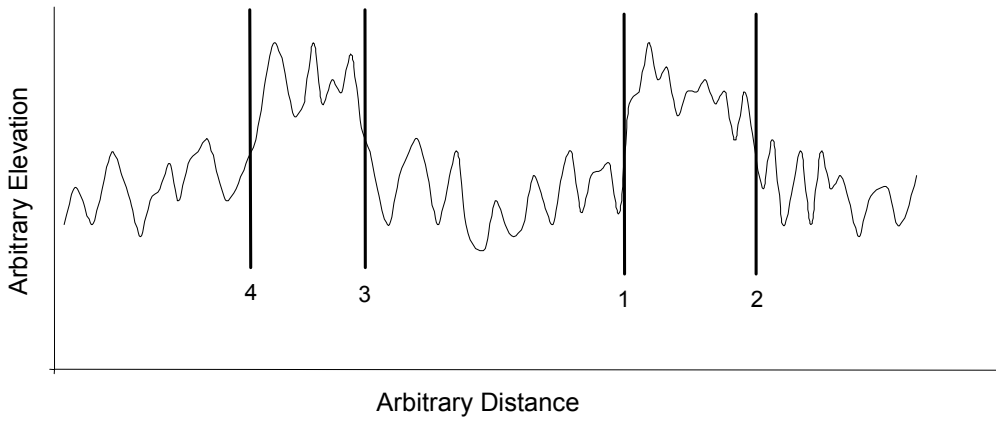

Figure 3.8 Hypothetical boundaries identified using the global zonation method. Boundaries are labelled according to the order in which they are identified.

iii) Autocorrelation and partial autocorrelation

Autocorrelation had been widely used in geomorphology to assess the degree of self-similarity in a series. The autocorrelation function (ACF) describes the covariance between observations in a series at regular lag intervals and so represents a measure of spatial dependence. The partial autocorrelation function (PACF) describes the excess covariance between successive observations which has not been accounted for by the first order autocorrelation. Readers are referred to Chatfield (1989) and Harvey (1993) for a mathematical description of the autocorrelation and partial autocorrelation functions. In this thesis, the interpretation of the ACF and PACF is used as an additional method to identify periodic tendencies in the planform and longitudinal profile data series, and to investigate underlying stochastic trends.

If a series displays periodic behaviour, the ACF is characterised by an oscillating tendency because the series moves in and out of phase with itself when lagged at increasing increments. If only short term correlation exists, the ACF will display relatively large values of autocorrelation at smaller lags, but at longer lags, autocorrelation will tend towards zero. Meanwhile, if a series is random, the ACF will be close to zero at all non-zero lag intervals (Chatfield, 1989). If the series is a realisation of a stochastic process (contains an underlying stochastic trend), the PACF provides an indication of the order of the most appropriate stochastic model. If the generating process is *AR (p)*, the value of the partial autocorrelation function at lag $p+1$ will be approximately zero because there is no residual excess correlation to be accounted for by this next higher order process (Chatfield, 1989). Partial autocorrelations are tested for significance at the 95 percent confidence level by examining whether they approximate to random and normally distributed variables with standard error (Richards, 1979):

$$S.E. = 1 / (\sqrt{N}) \qquad (3.7)$$

In this thesis, autocorrelation and partial autocorrelation analysis is conducted using *SPSS Software Version 11 for Windows.*

iv) Spectral analysis

Spectral analysis has become well established in geomorphology as a technique for identifying the dominant frequency or wavelength groupings present in both meander series (Speight, 1965; Thakur and Scheidegger, 1970; Chang and Toebes, 1970; Ferguson, 1975, 1977) and longitudinal profile series (Richards, 1976a, 1976b, Clifford, 1993). Spectral analysis represents the harmonic transformation of the autocovariance function (Chatfield, 1989). It involves identifying those frequencies which contribute most of the variance to the series (Richards, 1979). Any series can be considered the sum of sinusoidal waves at a range of frequencies and amplitudes. Therefore, by fitting a series of sine and cosine waves, the original series can be decomposed into its constituent waveforms. The contribution of each frequency to the total variance of the series is plotted as a spectral density plot. This can be smoothed by using a windowing routine to remove irregular variation. The shape of the spectral density plot reveals the regularity of the initial series. A single dominant peak is indicative of narrow range of wavelengths accounting for a large proportion of series variance. In this study, this would suggest a well-defined, and regular, planform or longitudinal profile pattern. Conversely, a number of nearly equal peaks over a range of frequencies would indicate a highly irregular pattern.

Unless otherwise specified, the spectral density plots presented in this thesis have been smoothed using weights based on the Tukey-Hanning filter applied over five lags intervals. Spectral analysis is conducted using *SPSS Software Version 11 for Windows* using the methods outlined by Chatfield (1989) and Davis (2002).

v) Second-order autoregressive modelling

Autoregressive modelling involves identifying and estimating the most appropriate statistical model to describe the inhomogeneity within a stochastic series (Chatfield, 1989). It represents a dynamic method of characterising a physically determined series operating in the presence of one or many noise sources (Clifford, 1993). Hence, it has wide application within the environmental and physical sciences.

In studies of fluvial morphology, pseudo-periodic tendencies have been noted in both the planform (Ferguson, 1976) and the longitudinal profile (Richards, 1976b;

Clifford, 1993) by the fitting of a second order autoregressive model, a particular type of autoregressive model of the form:

$$X_t = Ø_1 X_{t-1} + Ø_2 X_{t-2} + e_t \qquad (3.8)$$

Where X_t is the value of the series at time t, $Ø_1$ and $Ø_2$ are coefficients of directional change at a given lags 1 and 2 respectively and e_t is random error term. If the series is to be considered a realisation of a second order autoregressive process, the coefficients must satisfy the following stationarity constraints (Harvey, 1993):

$$\begin{aligned} &Ø_1 + Ø_2 < 1 \\ &-Ø_1 + Ø_2 < 1 \\ &Ø_2 > -1 \end{aligned} \qquad (3.9)$$

If the stationarity requirements are met and both parameters are positive, the series will be characterised by long successive runs of the same sign. This is because cumulating the effects of two previous shocks will demand a larger input random 'shock' to derive negative values (Richards, 1979). If however, $Ø_1$ is positive and $Ø_2$ is negative, the process will tend to exhibit marked variability between being positive and negative because cumulating $Ø_1$ and $Ø_2$ will produce a small value which can easily change sign with the addition of random shock value. Specifically, if the following inequality is satisfied:

$$Ø_1^2 + 4Ø_2 < 0 \qquad (3.10)$$

The series is a realisation of a pseudo-periodic process that oscillates as a damped sinusoidal function (Box and Jenkins, 1970).

The mean frequency, f, of the deterministic periodic component of the process can be calculated from:

$$cos2\pi f = Ø_1 / (2\sqrt{} - Ø_2) \qquad (3.11)$$

Autoregressive modelling is used to examine possible pseudo-periodic tendencies in both the pre-modification period (between 1765 and 1930) and through following modification (between 1880 and 1975). In each case, the applicability of fitting a second order autoregressive process is assessed by using the three-stage stochastic modelling framework developed by Box and Jenkins (1976). First, the

autocorrelation properties of each series are examined different stochastic models have characteristic patterns (Richards, 1979). An oscillating tendency within the autocovariance function and a significant partial autocorrelation at the first and second lags only are diagnostic of a second order autoregressive process. Following this model identification stage, the coefficients of the model are estimated. The final stage of the framework is the diagnostic checking of the modelling process. The residuals from the fitted process are tested to ascertain that they behave as a white noise, a random series where autocorrelations for all lags up to the maximum lag are close to zero. This is achieved by observing lags 1 and 2 to see if they are significantly different from zero using 95 percent confidence intervals based on standard error (Chatfield, 1989). The appropriateness of fitting a second order autoregressive model is then tested by calculating coefficient of determination (R^2), representing the percentage of the total variation explained by the model. Autoregressive modelling is conducted using *SPSS Software Version 11 for Windows.*

3.2.3 Morphological feature extraction and analysis

Morphological feature extraction provides a second method of exploring large scale and long term morphological dynamics. The method is used to first, examine the extent to which meander bends and pool-riffle sequences can be objectively identified in the planform and longitudinal profile series respectively, and second, examine their changing distributions in time and space. Because feature extraction is based on the identification of *characterisitic landform morphologies* which may be indicative of particular process regimes, the method has greater underlying physical basis than serial analysis. However, owing to the problems associated with initial landform identification, the method is less objective.

The techniques used to identify meander bends and pool-crossing sequences are discussed in section 3.3.2. Following feature extraction, each feature is assigned a spatial location within a one dimensional spatial series and parameters are generated to describe its morphology. In the planform investigation, identified meander bends are classified according to their amplitude, wavelength, and radius of curvature. In

the longitudinal profile investigation, pool-crossing sequences are classified according to their amplitude, wavelength, and spacing.

i) Meander bend identification and parameterisation

The most widely used method to delineate meander bends from a digitised planform series is based on the objective identification of points of inflexion. These are identified by calculating the change in angle (curvature) between consecutive points and identifying turning points, representing a change in the direction of curvature, in the resulting series. This method provides an objective procedure that can also be easily automated. However, identification of points of inflexion does not answer the basic problem of deciphering when a curve in the planform can be defined as a distinct meander bend (Hooke, 1984). This has been confronted by several researchers. Hickin (1977) applied a line filtering algorithm developed by Douglas and Peucker (1973) to filter frequency wavelengths most attributable to 'wobble' within the digitising procedure (Hooke, 1984). Meanwhile, Hooke (1977b) and Carson and Lapointe (1983) identify 'meander bends' as those exceeding specific minimum meander length and curvature criterion. In this thesis, to ensure that single inconsistencies in the digitising did not generate false inflexion points, a customised buffering algorithm is developed which removes inflexion points which do not involve a change in direction of at least 2 or more consecutive observations.

Ferguson (1977) suggests that meander bends can be classified according to three planimetric properties: the scale or size of the bend, the shape, and the degree of irregularity. In this thesis, the degree of irregularity is examined using the one dimensional serial techniques. The well established parameters of meander wavelength, amplitude and radius of curvature are used to examine the changing size and shape characteristics of meander bends (Brice, 1964; Lewin, 1977; Hooke, 1984).

ii) Pool and crossing identification and parameterisation

The objective identification of pools and crossing has rarely, if at all, been performed on long reaches of river such as is examined in this thesis. However, even over short

river reaches, a truly objective pool-riffle classification has remained elusive (Clifford, 1993). Previous research has generally adopted one of two principal techniques. Richards (1976a) and Milne (1982) have used a regression-based technique to classify pools and crossings as positive and negative residuals respectively from linear or low order polynomial trends fitted to the longitudinal profile. The pool-crossing characteristics identified by this technique are highly dependent on the ability of the chosen function to model the variation in the profile. Over short reaches of river, it is possible to obtain relatively good model fits but this becomes increasingly problematic over longer reaches because a single regression model cannot handle large scale variability than pool-crossing variation in the longitudinal profile. Over long reaches such as the entire Lower Mississippi River, this limitation of the regression technique can be partly overcome by using a series of regression models based on smaller-scale reaches which have been initially identified through zonation techniques. However, by following this approach, there is a consequent loss of objectivity as pools and crossings are classified according to regression equations which vary on a reach by reach basis.

As a result of these concerns, an alternative technique known as bedform differencing may be applied. This technique identifies pools and crossings based on relative elevation changes along the longitudinal profile series (O'Neill and Abrahams, 1984). New bedforms are identified if the cumulative elevation change since the last identified bedform exceeds a tolerance value, based on the standard deviation of the bed elevation series. The chosen value of tolerance can vary between sites based on the sampling interval and the amplitude of the bedforms. By visual interpretation of the bedforms identified for tolerance values ranging from 0.5 – 1.5 standard deviations, O'Neill and Abrahams (1984) concluded that a tolerance value of 0.75 standard deviations generated the most realistic set of results. However, the research was based on the longitudinal profile for a small creek with a catchment area of 5.15 km^2. Therefore, an appropriate tolerance value for the Lower Mississippi River longitudinal profile is further explored before spatial and temporal analysis is undertaken.

The differencing technique assumes that the first upstream observation of the longitudinal profile is a significant bedform. The next significant bedform is

denoted when the cumulative elevation change between consecutive bed elevations has exceeded the chosen tolerance and the bed elevation has reached a maximum (crossing) or minimum (pool). This is illustrated in Figure 3.9. If A is assumed to be a significant crossing, the procedure searches for the next significant downstream pool. B is identified as a pool because the cumulative elevation change has exceeded the tolerance value, *T*. However, C does not exceed *T* and so cannot be classified as a crossing. Following C, D is a deeper pool than B and is followed by a new exceedance of *T* to denote E as a crossing. Hence, D replaces B as a significant crossing. B and C are therefore, classified as a local minimum and a local maximum respectively.

3.3 Sub-reach scale methods and techniques

The sub-reach scale methodology involves coupling 1-D feature extraction techniques with 2-D surface based techniques to analyse the changing spatial and temporal distributions of key morphological and flow parameters. Following initial data processing, the analytical method can be divided into morphological and flow analysis.

3.3.1 Initial data processing

Each weekly interval single beam sonar survey comprised 5 parallel surveys of the channel thalweg region. Because the exact location of observations is not consistent between surveys, each survey was re-sampled by generating a 2-D morphological surface and extracting a consistent one dimensional profile, sampled at regular intervals. This enabled more objective comparison between surveys.

Initial data processing for the flow analysis involved the computation of resolved downstream and resolved cross-stream velocity. At each cross-section, the *downstream* direction is defined according to the direction angle of the channel centreline. The simplest method of determining centreline direction is to use the angle which is perpendicular to the angle of each cross-section. However, this assumes that the cross-section is located *exactly* perpendicular to the channel

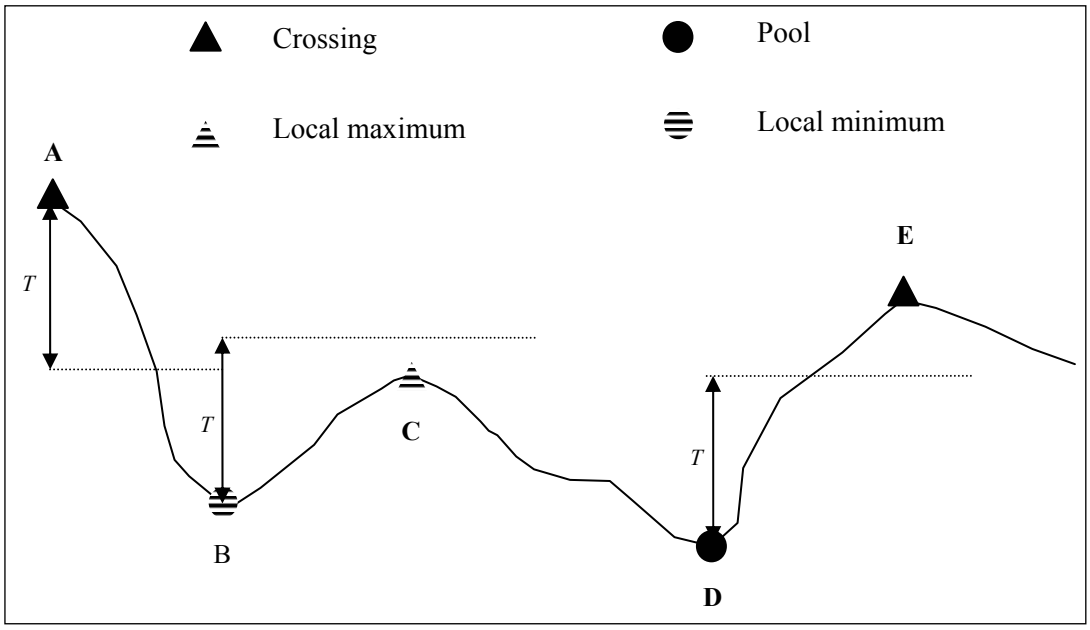

Figure 3.9 Identification of pool and riffle bedforms based on the bedform differencing technique (modified from Robinson, 2003). Features A, B, C ad D are defined based on the application of tolerance value *T*. See text for further description.

centreline. Instead, a method is used that involves the identification of the channel centreline by joining adjacent cross-section centre points. This computed centreline is displayed in Figure 3.10. At each cross-section, the centreline direction is defined as the average of the direction chords adjoining the centre-point with the centre-points of both the nearest upstream and downstream cross-sections. The velocity component in the resulting downstream direction is then computed from the easting and northing components of velocity for each observation in the cross-section.

3.3.2 Morphological analysis

The seasonal variability of morphology is examined using a select number of weekly interval single beam sonar surveys for each reach. Surveys are selected which individually, are close to short-term minima or maxima in flow stage, and together are characteristic of the hydrograph in any single water year. The variation is examined temporally, in a single reach, and spatially, between reaches, to investigate the predictability of observed behaviour. Two specific sets of relationships are examined:

- *Dune amplitude and wavelength with flow stage*
- *Mean sedimentation or scour with flow stage*

This provides a characterisation of the seasonal changes in channel morphology at two spatial scales. At a shorter timescale, the variability of morphology is examined using selected multi-beam sonar surveys of the channel thalweg over a 24 hour period. Although such short term dynamics are likely to be insignificant at annual and decadal scales, the spatial and temporal resolution is fine enough to offer an indication of *how* bed material is transported on the Lower Mississippi River.

Whole-channel multi-beam sonar data are used to reveal the variability of within-reach morphology through the generation of a range of 2-D surface maps. 1-D profiles are extracted from these surfaces to investigate the additional morphological information provided by the finer resolution multi-beam sonar surveys in comparison to the weekly-interval single-beam sonar surveys. This is important because it reveals a finer scale of morphological change which cannot be observed from single beam sonar surveys.

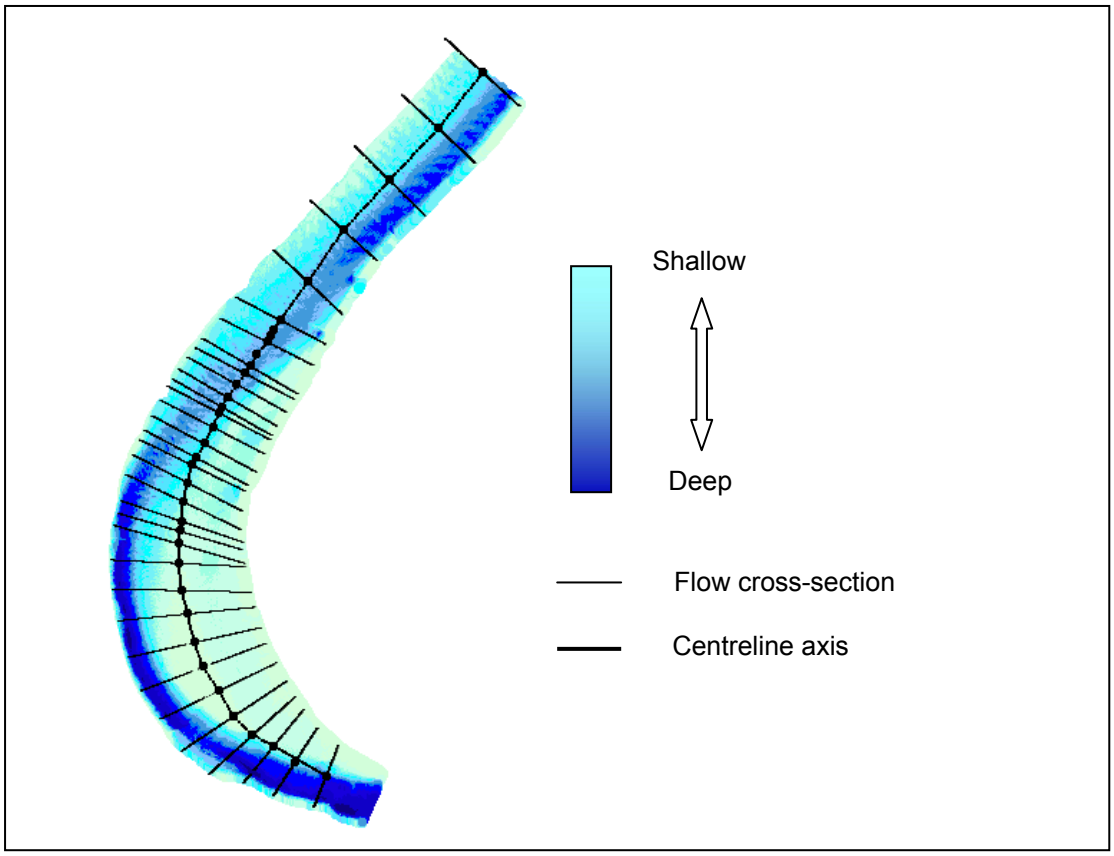

Figure 3.10 Computation of the channel centreline using the flow cross-sections. Flow cross-sections are superimposed onto the multi-beam sonar data set which is colour coded according to elevation.

3.3.3 Flow analysis

Flow analysis is performed using a select number of cross-sections from the series available for each reach. Cross-sections are selected which individually have a morphological significance (i.e. crossing mid-point) and together, are representative of the morphological variation within each reach. Selections are made based using s 2-D topographic surface of whole channel morphology and an interpolated 1-D thalweg profile.

Following cross-section selection, differences in the magnitude and distribution of resolved downstream and cross-stream velocity are analysed, both between selected cross-sections and at high and low flow stage. Analysis of velocity magnitude utilises visual analysis from 2-D topographic surfaces and computation of near-bed velocities. Two parameters are used to describe the distribution of the velocity field in each flow cross-section. The asymmetry ratio, *a*, relates the mean flow velocity on one side of the cross-section to that on the other (Knighton, 1998):

$$a = (V_L - V_R) / V \qquad (3.12)$$

where:

V_L = Mean velocity in the left half of the cross-section

V_R = Mean velocity in the right half of the cross-section

V = Mean cross-sectional velocity

The alpha coefficient, α, describes the variation of velocity in relation to channel area (Chow, 1959):

$$\alpha = [(V_1^3.A_1) + (V_2^3.A_2) + \ldots\ldots + (V_i^3.A_i) / (V^3 .A)] \qquad (3.13)$$

where:

V = mean cross-sectional velocity

A = total area of cross-section

V_1 = mean velocity in sector *1*

A_1 = mean area of sector *1*

V_i = mean velocity in sector *i*

A_i = mean area of sector *i*

The asymmetry ratio is simply calculated by dividing the channel into two halves at the cross-section centre-point. Values close to zero indicate a symmetrical velocity distribution whereas values close to ± 1 indicate an asymmetrical distribution. The alpha coefficient is calculated by divided each cross-section into a series of sectors based on equal increments of channel width. The effect of varying the number of sectors on the calculated coefficient is examined and an optimum number of sectors selected. Values nearing unity indicate a uniform velocity distribution. Progressively higher values are associated with increasing lateral diversity in the velocity field. The velocity distribution coefficient (α) for each cross-section was computed by inputting the channel area and average velocity between each consecutive vertical in the cross-section into equation 3.13.

The techniques described above are used in varying combinations in the following chapters, beginning with planform dynamics. All of the raw and processed data sets are stored on the accompanying CD-ROM. This is described in Appendix A.

CHAPTER 4. PLANFORM DYNAMICS

4.1 Chapter synopsis

The ability to interpret long-term and large-scale geomorphological response to engineering modification is in part dependent on understanding system-scale dynamics in the pre-modification period. Analysis of channel length, width and a variety of parameters describing bend size and shape in the 1765-1975 period show that the artificial cutoff programme dramatically shortened the river (increased slope) and removed form resistance exerted by the most sinuous bends at a time of relatively low stream power per unit width and high sediment loads. Prior to the MR & T project, the Lower Mississippi River adjusted its planform to satisfy regional-scale form resistance requirements through multiple adjustments of channel length, width and curvature characteristics. However, it is difficult to recognise characteristic behaviour because some reaches demonstrated relatively little gemorphological change whilst others were more responsive. The type of behaviour in each reach is shown to be closely related to the distribution of longer-term geological and neotectonic controls within the alluvial valley. This supports the idea that spatially distributed feedbacks between form and process do operate at larger spatial and longer temporal scales.

4.2 Quantifying planform variation

4.2.1 Scales of planform variation

At the regional-scale, variation in planform can be decomposed into two principal components: a component which is *imposed* by valley topographic influences; and a second component created by the *active* internal geomorphological dynamics of the fluvial system (Meuller, 1968). These components can be isolated by representing planform variation by a series of direction or direction change angles that are computed between consecutive regularly spaced observations (section 3.2.1). This is illustrated for the 1880 planform survey in Figure 4.1: the only data set that predates the artificial cutoff programme and is available for the entire Lower Mississippi

River from Cairo to the Head of Passes. Regional-scale trends in the direction angle series have been emphasised by applying a low pass filter moving average to remove variation associated with individual meander bends. The five broad zones or 'direction reaches' identified in the smoothed direction series (4.1a) relate to large scale topographic trends in the valley-axis (4.1b).

At the longest 2 000 year timescale considered in this chapter, the Lower Mississippi River has occupied its contemporary meander belt and therefore, observed planform changes are independent of longer term valley topographic variation. Hence, this chapter is principally concerned with analysing and explaining planform variation after regional-scale valley topographic effects have been removed. This is achieved by differencing each series to generate direction change series. The differenced series is presented for the 1880 planform alongside the original direction series at three scales in Figures 4.2 and 4.3. Differencing represents a type of high pass filter that removes low-frequency variation (Chatfield, 1989) and generates a series that is stationary with respect to the mean value. The direction and direction change series of the enlarged reach (4.2b and 4.2c) shows that differencing retains similar periodic properties to the original direction series. The variance of the differenced series therefore provides a measure of planform variability independent of 'imposed' regional-scale valley topographic effects. Figures 4.3a and 4.3b illustrate the variability of the direction change series for two reaches of contrasting sinuosity: the highly sinuous Greenville bend reach; and the relatively straight reach immediately downstream from New Orleans.

4.2.2 Determination of a suitable sampling interval

Series of direction change are sensitive to the chosen sampling interval. A long sampling interval reduces the potential for shorter wavelength meander bends to be identified because they are progressively removed by smoothing. This is illustrated in Figure 4.4 where the effect of varying the sampling interval within the range 0.5 – 4 km is examined in terms of both planform representation (4.4a) and the resulting direction change series (4.4b). Figure 4.4a suggests that there is only negligible loss of information when the sampling interval is increased from 0.5 km to 2 km.

a)

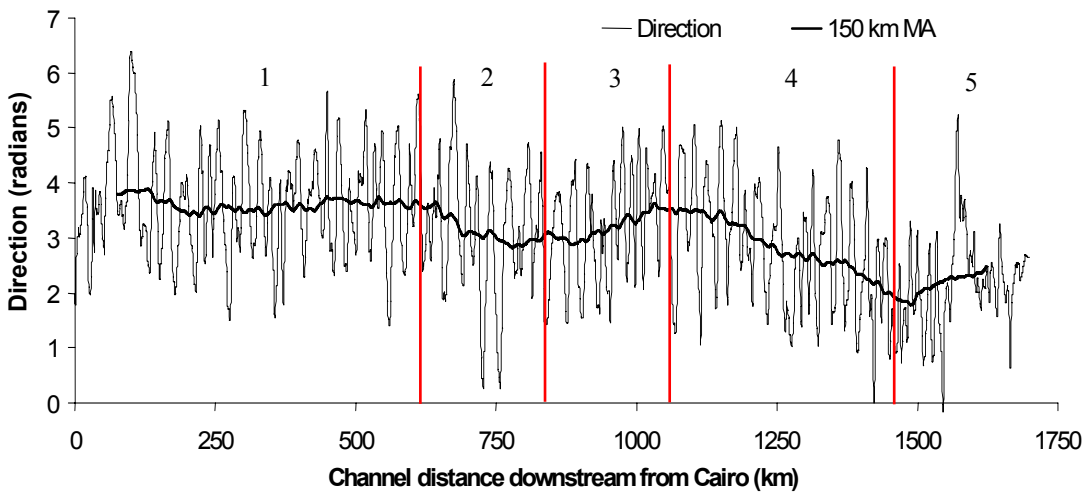

b)

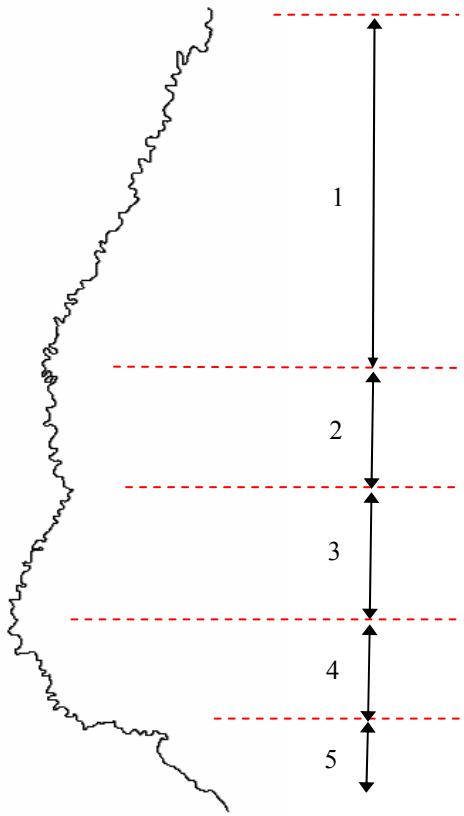

Figure 4.1 a) The direction series for the 1880 planform of the Lower Mississippi River between Cairo and the Head of Passes, based on a sampling interval of 2 km. A 150 km moving average has been fitted to emphasise regional-scale trends. b) The corresponding planform with the five 'direction reaches' identified.

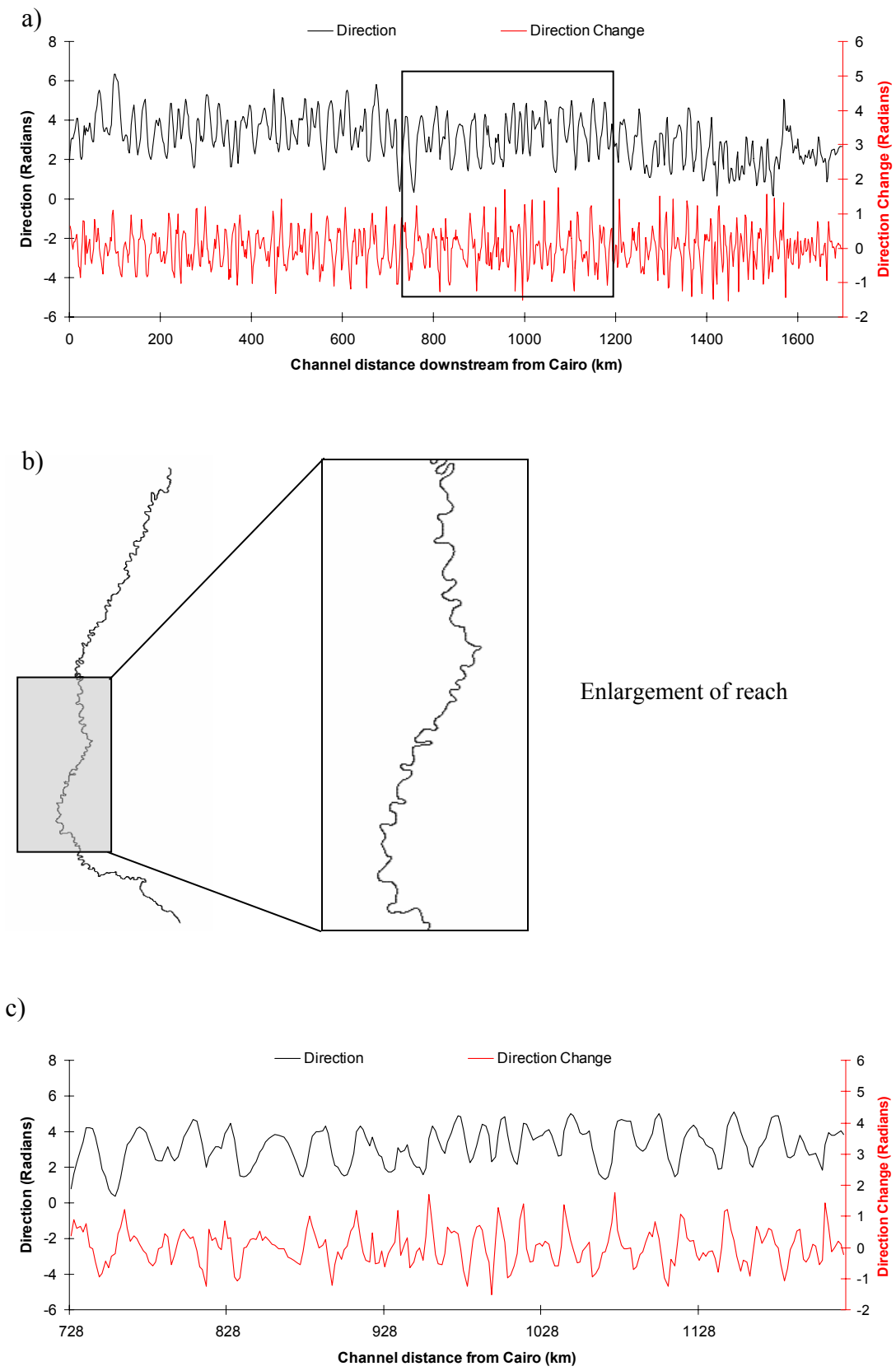

Figure 4.2 a) Direction and direction change series from Cairo to the Head of Passes for the 1880 planform series; b) the selected reach from 730-1200 km and; c) the selected series. Based on a sampling interval of 2 km.

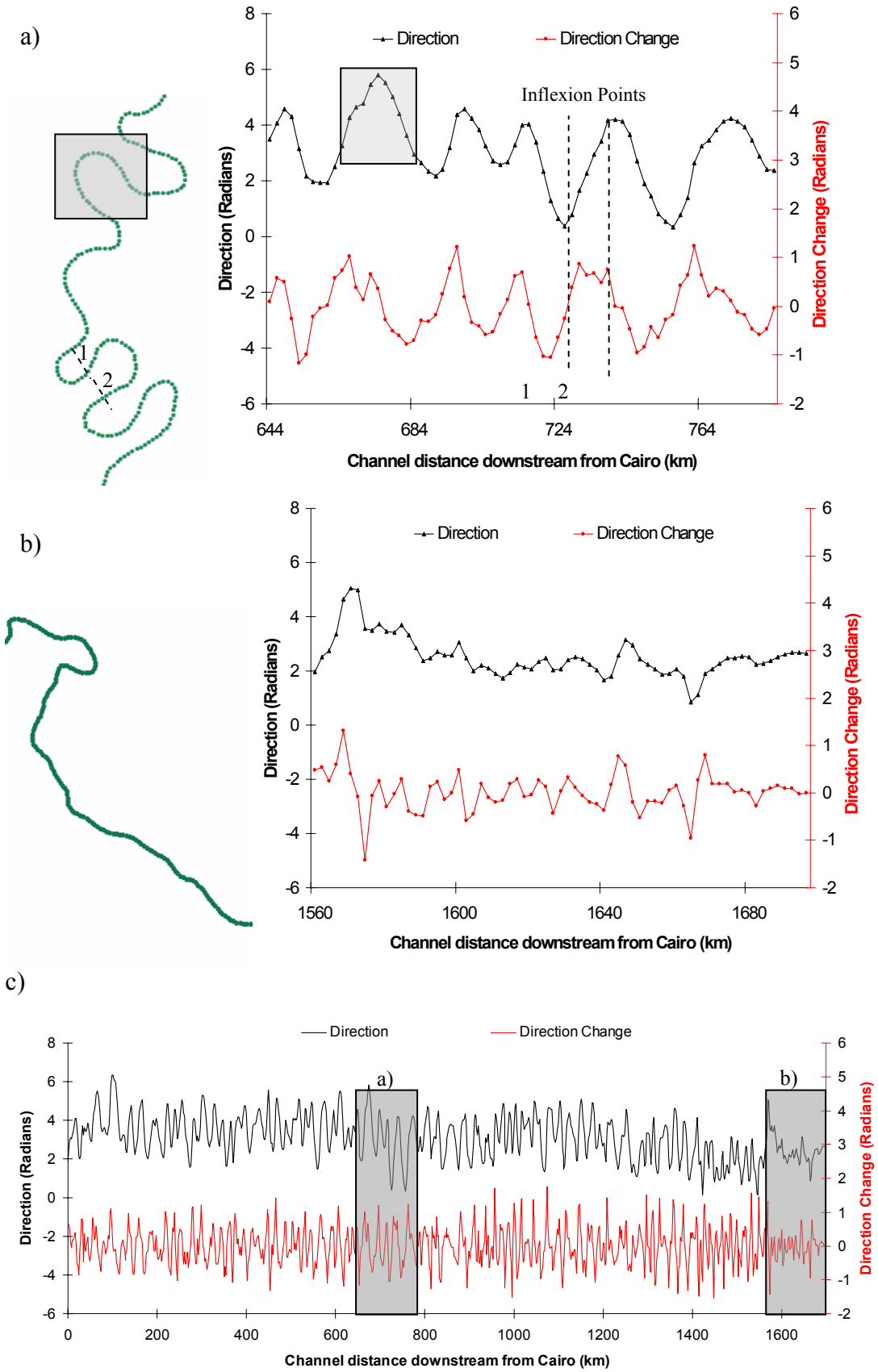

Figure 4.3 The direction and direction change series for reaches: a) in the vicinity of the Greenville bends and; b) immediately downstream from New Orleans. Based on a sampling interval of 2 km.

However, at a longer sampling interval of 4 km, considerable smoothing of meander bends is evident. For example, sub-reach i) in Figure 4.4b is characterised by two peaks of direction change at sampling intervals less than, or equal to, 2 km but at sampling interval of 4 km, only a single peak is recorded. Similarly, in sub-reach ii) a single sharp peak in direction change at a 4 km sampling interval is represented by two peaks in direction change at shorter sampling intervals. Meanwhile, a series sampled at very short intervals is sensitive to high frequency, low amplitude variations, which may simply represent 'wobble' in the digitising process (Ferguson, 1975). This is demonstrated by the increasing level of local-scale noise as sampling interval is reduced in Figure 4.4b. Given these problems, a compromise sampling interval was required that was short enough to prevent important information loss whilst being long enough to prevent the introduction of unhelpful local-scale noise.

Progressive information loss by smoothing over longer sampling intervals is termed aliasing (Davis, 2002). Nyquist (1928) suggests that for periodic functions, a sampling interval equal to half the wavelength of the signal of interest (0.5 λ) is the minimum permissible that might ensure information is not lost by aliasing. Robinson (2003) showed more recently that by using a sampling interval of 0.5 λ, topographic undulations can be completely removed if the initial measurement falls equidistant between crests and troughs (in a regular, periodic function). Robinson therefore recommends using a sampling interval not greater than 0.25 λ. Determining a suitable sampling interval to prevent aliasing requires identification of the wavelength frequency of principle interest and hence, an assessment of the variability of the record. Previous planform studies have typically measured meander wavelength based on a multiple of bankfull width because of its association with the dominant or 'channel forming' discharge (Wolman and Miller, 1960). Conventionally, average meander wavelength is considered to fall within the interval of 10-14 bankfull widths (Leopold and Wolman, 1957). Taking the lower limit of 10 channel widths, the maximum sampling interval before the onset of aliasing is equal to 2.5 bankfull widths. Winkley (1977; see section 4.5) reports the reach-averaged minimum top-bank width on the Lower Mississippi River in the 1765-1975 period to be 0.8 km. Based on this value therefore, aliasing is only likely at sampling intervals in excess of 2 km.

Given the negligible loss of information as sampling interval is increased in the range 0.5 – 2.0 km (Figure 4.4a), and the decline in local sensitivity within the resulting direction change series (Figure 4.4b), a sampling interval of 2 km is used as a standard throughout this chapter. This is supported by both second-order autoregressive modelling and spectral analysis of the 1930 planform series in Table 4.1 and Figure 4.5 respectively. Table 4.1 reveals that the inequality for pseudo-periodicity is only satisfied when sampling at intervals in excess of 1 km. This is because at shorter intervals, local-scale noise in the direction change series obscures the presence of larger-scale meander bends. Meanwhile, at longer sampling intervals, the proportion of variation explained by the model (denoted by the R^2 value) declines as shorter wavelength meander bends are removed by aliasing. The spectral density plots in Figure 4.5 indicate that only a very small proportion of total variance is accounted for by waveforms of a wavelength lower than 10 km. This supports the 2 km sampling interval because it suggests that, to adequately, characterise series variance, a sampling interval shorter than 2.5 km is required.

4.3 Identification of planform reaches

4.3.1 Development of zonation methodology using the 1880 direction change series

The variability of planform independent of valley-axis effects is highlighted by moving a standard deviation window through the direction change series. This is illustrated in Figure 4.6 for the 1880 series using three window sizes in the range 40-120 km. Regional-scale trends are clearly identifiable, with broad peaks in standard deviation at approximately 1 000 km and 1 400 km and low standard deviation between 0 and 200 km and over 1 600 km.

Given the variability highlighted visually, zonation algorithms are employed as a method of objectively identifying statistically significant reach boundaries within the standard deviation series of direction change. In addition to searching for boundaries which have physical significance, zonation provides a means of dividing each data series into reaches which have direction change series that are homoscedastic (stationary in variance) as well stationary in the mean. These stationarity properties

a)

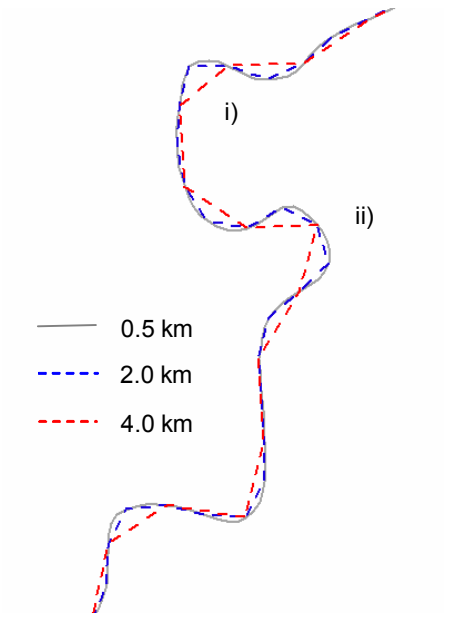

b)

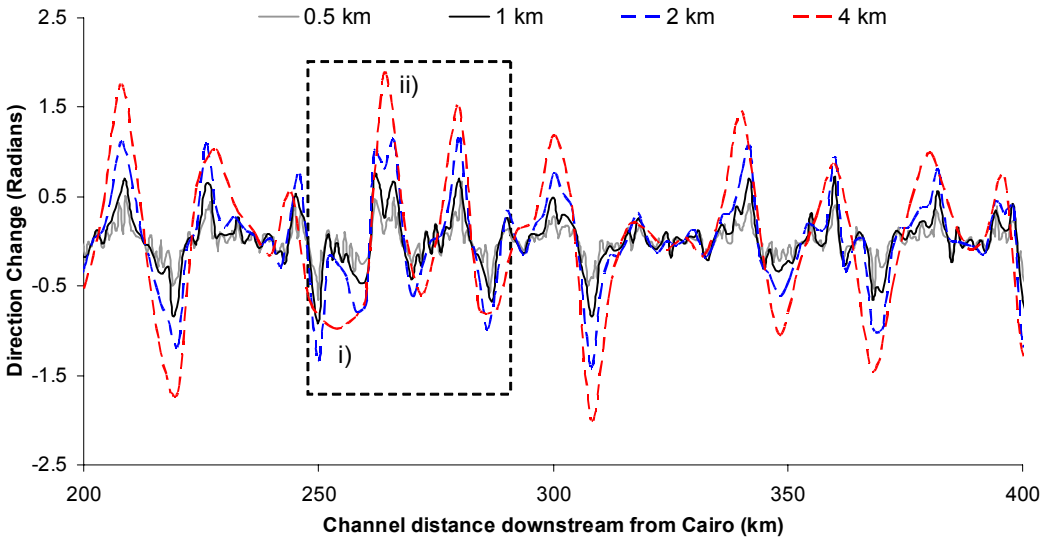

Figure 4.4 Experimenting with sampling intervals in the range 0.5-4 km: a) direction change series for the reach 200-400 km downstream from Cairo and b) representation of planform for the selected reach 250-290 km downstream from Cairo.

Sampling Interval (km)	**0.5**	**1**	**1.5**	**2**	**2.5**	**3**	**3.5**	**4**
$Ø_1$	0.556	0.795	0.842	0.832	0.787	0.701	0.579	0.262
$Ø_2$	0.153	-0.113	-0.25	-0.364	-0.46	-0.53	-0.572	-0.444
Stationary?	Yes	Yes	Yes	Yes	Yes	Yes	Yes	Yes
R^2	0.445	0.517	0.486	0.454	0.44	0.431	0.414	0.223
$Ø_1^2 < -4Ø_2$?	0.92	0.18	-0.29	-0.76	-1.22	-1.63	-1.95	-1.71
Pseudo-periodic?	No	No	Yes	Yes	Yes	Yes	Yes	Yes
Wavelength (km)	---	---	16.54	15.52	16.50	17.64	18.67	19.31

Table 4.1 Second-order autoregressive coefficients, R^2, and estimated mean wavelength based on fitting second-order autoregressive models to direction change series with sampling intervals in the range 0.5-4.0 km. Based on the 1930 planform series.

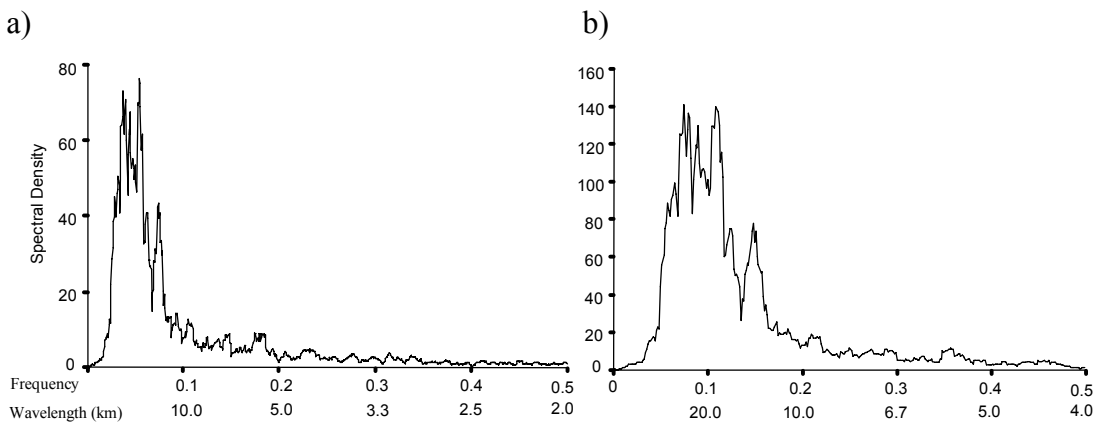

Figure 4.5 Spectral density plots for the 1930 planform series at sampling intervals of a) 1 km and b) 2 km.

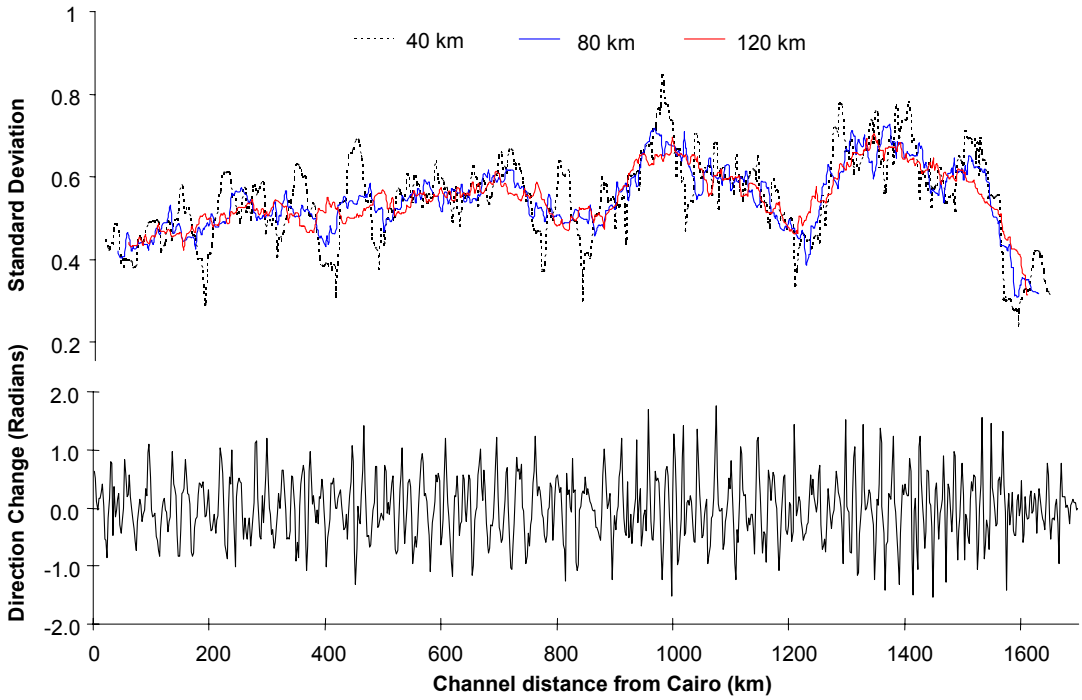

Figure 4.6 Direction change and moving standard deviation for the 1880 planform series. Moving standard deviation has been calculated using window sizes of 40 km, 80 km and 120 km.

are required in order to apply serial techniques (autocorrelation, autoregressive modelling and spectral analysis) to examine trends in meander wavelength and amplitude characteristics. The integrity of data analysis using these techniques is compromised by trends within the data sets.

Figure 4.7 shows initial application of zonation to the 1880 data series. A window size of 80 km has been used to compute the moving standard deviation. The first five boundaries are labelled and located by a solid red line and five further boundaries are located by a broken red line. This convention is followed throughout this section. The first five boundaries explain 69.4 percent of the total variance within the standard deviation series and the identification of five further boundaries explains an additional 13.1 percent of the variance. Figure 4.8 presents a boxplot of the distribution of standard deviation within each reach for five boundaries (six reaches) and superimposes the identified reach boundaries on the initial planform. Close inspection reveals that identified boundaries do delineate reaches into varying degrees of sinuosity. For example, the high standard deviation for reaches 3 and 5 of the six reach delineation in Figure 4.8a correspond with highly sinuous reaches in Figure 4.8b. Conversely, low standard deviations in reaches 4 and 6 correspond with relatively straighter reaches of the Lower Mississippi River.

Initial zonation therefore indicates that the technique is capable of identifying reach-scale planform variability. However, before applying the technique to multiple direction change series in the period 1765-1975, two related issues must be clarified: the degree to which the technique is sensitive to the initial size of window used to compute the moving standard deviation and; the degree to which the variation explained increases with number of boundaries identified. Clarification of these issues is critical to being able to select the most appropriate window size for the computing the moving standard deviation and the most appropriate number of boundaries to identify.

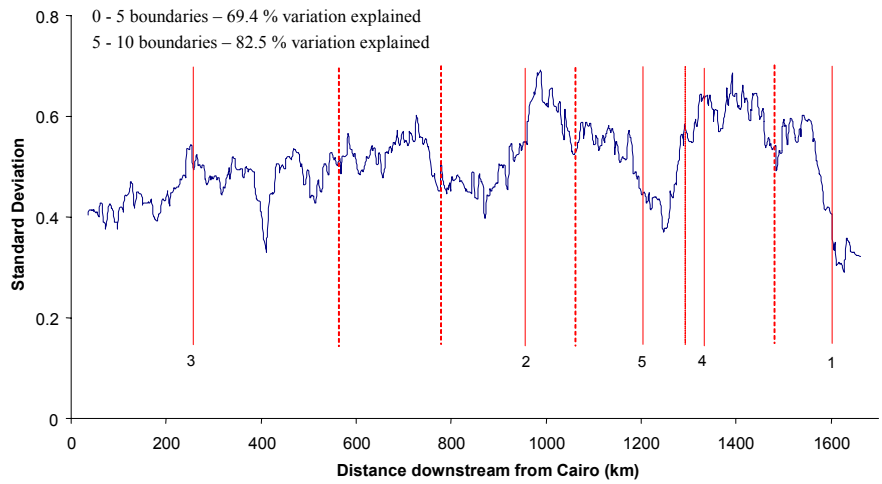

Figure 4.7 Boundaries identified in the 1880 standard deviation series generated using a window size of 80 channel km. See text for further explanation. Solid red lines show boundaries 1-5 and broken red lines show boundaries 6-10 identified in the series.

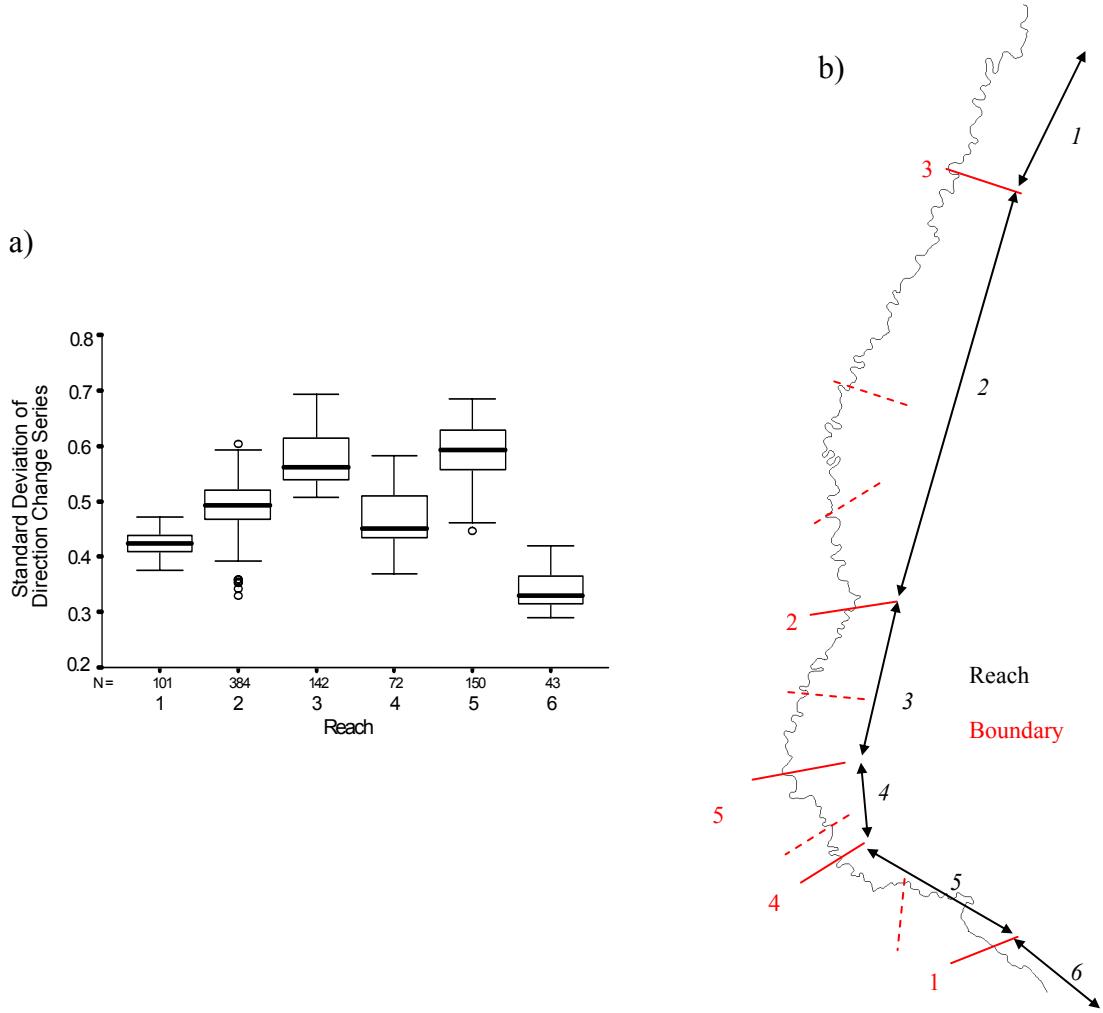

Figure 4.8 a) A box plot illustrating the distribution of standard deviation within the six reaches (identified by five boundaries) and b) identified boundaries superimposed on the 1880 planform. Solid red lines show boundaries 1-5 and broken red lines show boundaries 6-10 identified in the series.

4.3.2 Determining the most appropriate window size and number of boundaries

The addition of each new boundary can be considered by its additional contribution to the proportion of the total variation explained (equivalent to R^2). A sensitivity analysis was therefore performed by examining the relationship between the proportion of total variation explained and the number of boundaries for window sizes in the range 20-120 km. For the 1765 and 1930 data series, the nature of this relationship is revealed by the plots in Figure 4.9. Generally, the curves are asymptotic, confirming that the additional proportion of the total variation explained by adding a new boundary declines as the number of boundaries already identified increases. However, the rate of decline increases as the initial size of the window used to compute the standard deviation increases. This is not surprising because the window size is itself akin to a filtering process, with a larger window subduing the effect of smaller-scale variation in the original direction change series.

The 20 km window size demonstrates a near-linear relationship between variation explained and number of boundaries. Based on Winkley's (1977) average channel top-bank width in the period 1830-1975 of approximately 1.5 km, this window size falls within the range of 10-14 channel widths which is well established as corresponding to a single meander wavelength (Leopold and Wolman, 1957). Hence, zone boundaries using this window size are most likely to reflect variation at the scale of the individual meander bend rather than larger reach-scale trends. Indeed, the near-linear form of the relationship indicates that each meander bend contributes an approximately equal magnitude of additional variation explained. As window size is increased beyond 60 km the form of the relationship becomes increasingly asymptotic because the identification of a small number of boundaries contributes a relatively high proportion of additional variation explained. This is suggestive of considerable variation in planform characteristics at the larger reach-scale.

For the 1930 series, the first ten boundaries identified for each of the standard deviation series corresponding to window sizes of 60 km, 80 km and 100 km are presented in Figure 4.10. Boundary locations are highly consistent between window

a)

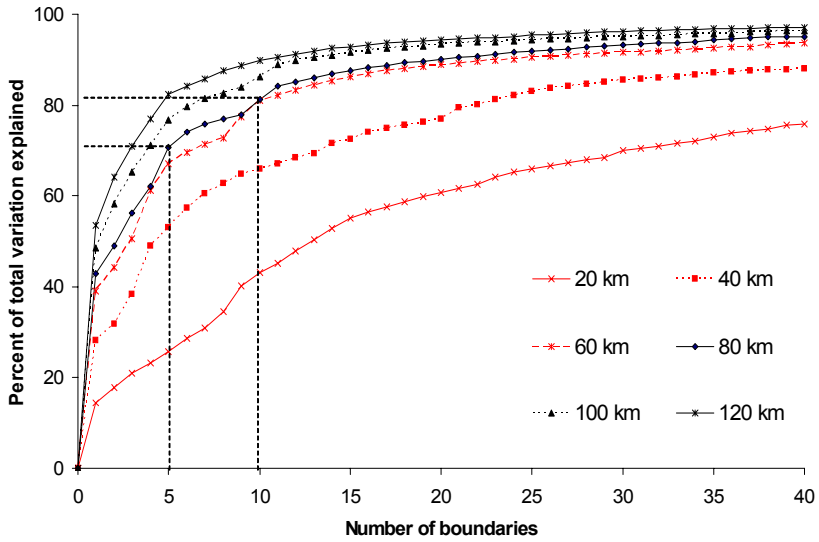

b)

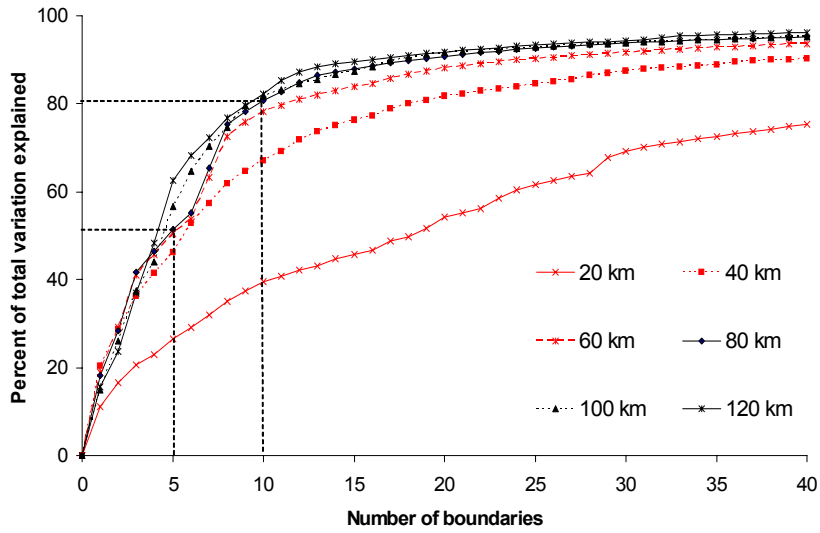

Figure 4.9 Percentage of total variation explained against number of zonation boundaries for the a) 1765 and b) 1930 planform series.

sizes of 60 km and 80 km but are less consistent between window sizes of 80 km and 100 km. This pattern is reflected by the nature of the relationships in Figure 4.9b. For window sizes of 60 and 80 km, the percentage of total variation explained by between either 5 or 10 boundaries is very similar. However, there is an increase in percentage variation explained for a window size of 100 km, particularly between 0 and 5 boundaries. This suggests that the degree of curve similarity in Figure 4.9 is indicative of boundary consistency. To compute a standard deviation series appropriate to identify planform reaches, a window size is required that is both long enough to generate a standard deviation not skewed by individual meander bends, and short enough to identify planform reaches which may exist at a scale greater than an individual meander bend. Based on the above analysis, a window size of 80 km was chosen.

To perform zonation, a number of boundaries is required that represents a compromise between maximising the proportion of variation explained, whilst limiting the number of boundaries identified. This latter constraint is imposed first, to allow straightforward analysis of the temporal stability of reach boundaries through time and second, to maintain reaches that are of a sufficient length to not degrade the integrity of serial techniques performed in section 4.9. At the chosen window size of 80 km, relatively few boundaries are required to explain a high proportion of the total variation. For the 1765 series, 67 percent of the variability is explained by the identification of 5 boundaries, 80 percent is explained by the identification of 10 boundaries, and 88 percent is explained by the identification of 20 boundaries. Based on these figures and similar figures for 1930, zonation is performed by identifying the five and ten most prominent boundaries in the standard deviation series.

4.3.3 Planform reach dynamics

Figure 4.11 shows the first ten boundaries within each planform series in the period 1765-1975. Boundaries that are consistent between surveys adjacent in time are highlighted by a connecting black dotted line. By comparing the temporal stability of identified reaches, an assessment can be made of the extent to which reaches are: first, either permanent or ephemeral; and second, either natural or engineered.

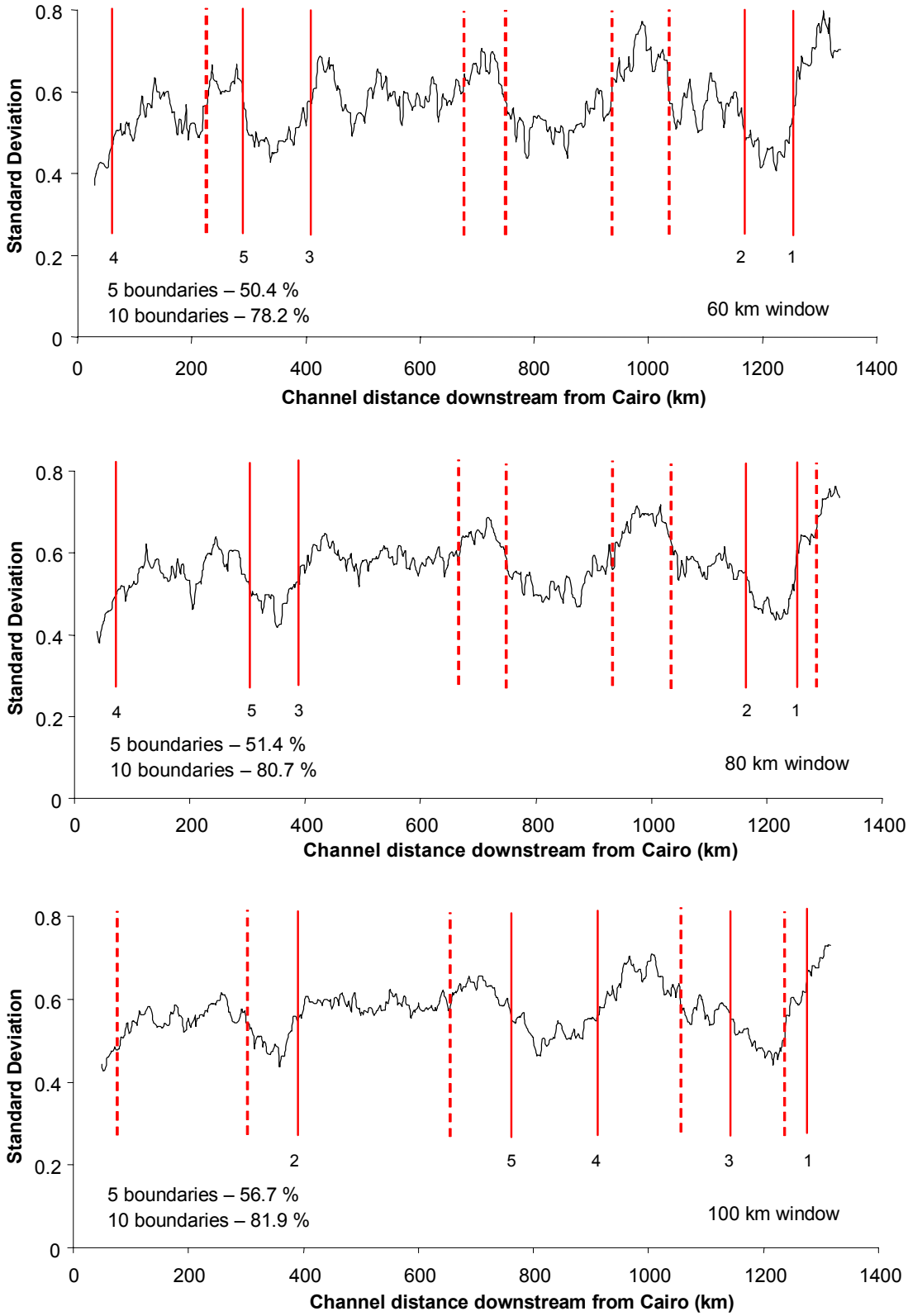

Figure 4.10 Boundaries identified in the 1930 standard deviation series for window sizes of 60 km, 80 km and 100 km.

Analysis of temporal variability must be treated with a degree of caution because zonation is performed by considering each series as a whole and is therefore affected by relative changes within each series. This is exemplified by considering the relatively straight reach delineated by boundaries 4 and 5 in 1765. The same reach can be traced in 1830 and 1930 (between boundaries 5 and 3) but is not identified in 1887. Closer inspection of planform behaviour in the reach, during the period 1765-1930, reveals very little change. Hence, in 1887, the reach is not bounded because of planform changes outside the reach which preferentially generate reach boundaries.

The observed pattern of reach consistency can be examined in relation to the timeframe of major disturbances to the fluvial system over the 1765-1975 period. The poor consistency between 1830 and 1880, when only four consistent boundaries can be identified, may be interpreted as a delayed planform response to the New Madrid earthquakes in 1811-1812. This level of consistency is not surprising given that this period records the largest reach length change in the pre-cutoff period (1765-1930). There appears to be better consistency during the period of artificial cutoffs (1930-1975) although only two out of the six consistent boundaries are located within the artificial cutoff reach. In the period immediately preceding the artificial cutoff programme (1887-1930), reach consistency is not only higher than during the cutoff period, but five out of the seven consistent boundaries are located within the reach of artificial cutoffs. Hence, the artificial cutoff programme is directly associated with the loss of three consistent reach boundaries. Over the entire 1765-1975 period, reach consistency is highest between 1765 and 1830 when eight out of the ten boundaries are consistent. This is not so surprising because this earliest period records the smallest net change in total reach length in comparison to the other time periods.

Only one boundary is consistent between all the surveys. This boundary, located immediately downstream of the modern Old River control structure, represents the most significant (first) boundary to be identified in both the 1930 and 1975 planform. Hence, observations from the 1765-1930 period indicate that reaches are generally ephemeral features which persist on average for less than approximately 120 years. Despite this temporal variability, six temporally consistent reaches are identified

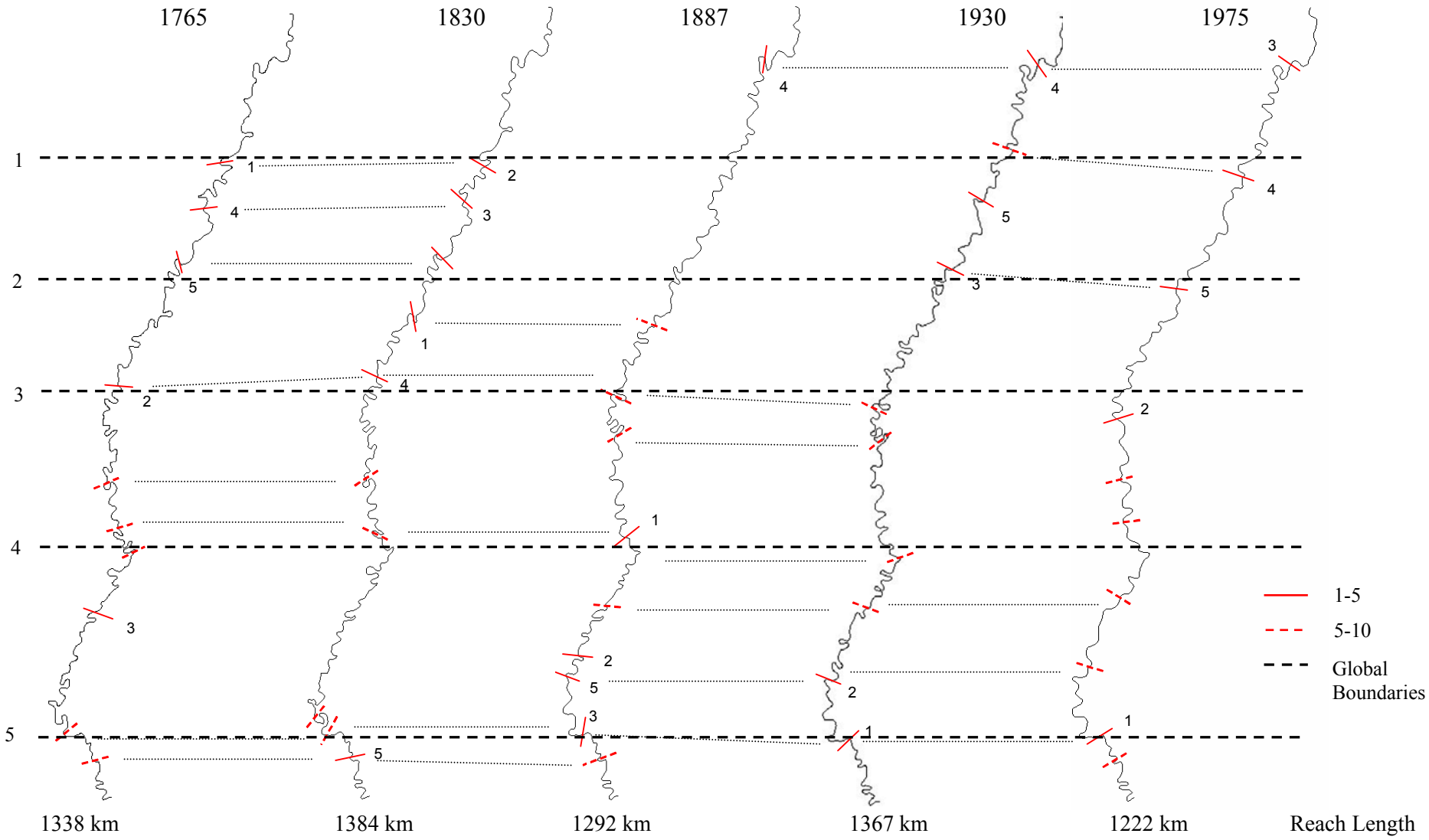

Figure 4.11 Boundaries identified by applying the zonation procedure to the moving standard deviation of direction change series in the period 1765-1975.

using the single consistent boundary, and a further four based on boundaries that are consistent within at least three out of the five planform series. This part consistency is deemed appropriate in view of the problems previously identified regarding making temporal comparisons. Interestingly, reach boundaries 2-5 correspond approximately with tributary junctions on the Lower Mississippi River: the St Francis River; the Arkansas River; the Yazoo River and Old River respectively. This may suggest that planform behaviour changes between tributary junctions and hence, such junctions exert a planform control. The dynamic nature of planform about these six reaches is explored in subsequent sections.

4.3.4 The statistical significance of identified boundaries

In addition to allowing an examination of the spatio-temporal dynamics of identified planform reaches, zonation can be used to inform the most appropriate unit size with which to view planform changes. This is assessed by considering the statistical significance of the additional proportional of total variation explained by each boundary through an F-test (see section 3.2.2). The change in p-value is plotted against the boundary number in Figure 4.12 for the 1930 series. Statistical significance is plotted on a linear (4.12a) and logarithmic (4.12b) scale to highlight the magnitude of change.

The maximum p-value obtained is approximately 0.007, confirming that all reach boundaries up to the 120th boundary are statistically significant at the 99 percent confidence level (corresponding to a p-value of 0.01). However, there is a discontinuity in the relationship at approximately 30 boundaries. At fewer boundaries than the discontinuity, the p-value increases by an order of magnitude with the addition of each new boundary, and at a greater number of boundaries the p-value increases by a power function. This pattern relates back to the asymptotic pattern of additional variation explained with the addition of each further boundary identified in Figure 4.9. Hence, the existence of a relatively low number of highly significant reach boundaries further supports the existence of 'planform reaches' at a spatial scale greater than a single meander bend. Very similar trends in statistical significance are noted for initial window sizes of 40 km and 120 km (Figure 4.13).

Hence, this observation is relatively insensitive to the initial size of window size used to compute the moving standard deviation series.

A further method of assessing zonation is to examine the changing distribution of reach lengths as the number of boundaries is increased. This is presented as a series of histograms in Figure 4.14 based on an initial window size of 80 km. As the number of boundaries identified increases, the larger reaches are sub-divided and the mean and median reach length consequently decline. However, more interestingly, with a higher number of boundaries, the overall distribution becomes less negatively skewed, and consequently more normally distributed, as the mean and the median converge towards 12 km. At boundary numbers greater than 40, the modal reach length is maintained in the range 8-12 km. Moreover, with 40 boundaries identified, 27.5% of reaches have a length in range 8-16 km. This increases to 47 percent when 100 boundaries are identified. Viewed in conjunction with the rate of increase in statistical significance at high number of boundaries (Figure 4.12), these observed ranges may suggest that once sub-reaches have been identified, zonation increasingly divides the Lower Mississippi River into individual meander bends. Hence, although considerable reach-scale variability does exist, zonation may suggest that each meander bend can also be considered a unique entity with unique morphological properties.

4.4 Variation of channel length

Variation in channel length is investigated in the 1765-1975 period to highlight more dynamic and less dynamic reaches and time periods. Geomorphologically, variation in channel length is important because valley slope can be assumed constant at this timescale and therefore it provide a direct indication of variation in channel slope.

4.4.1 Method

In the period 1765-1975, the variation of channel length was analysed in two ways. First, a customised routine was developed to compute the channel length for each of the six global reaches identified in Figure 4.11 for each of the five survey years. A

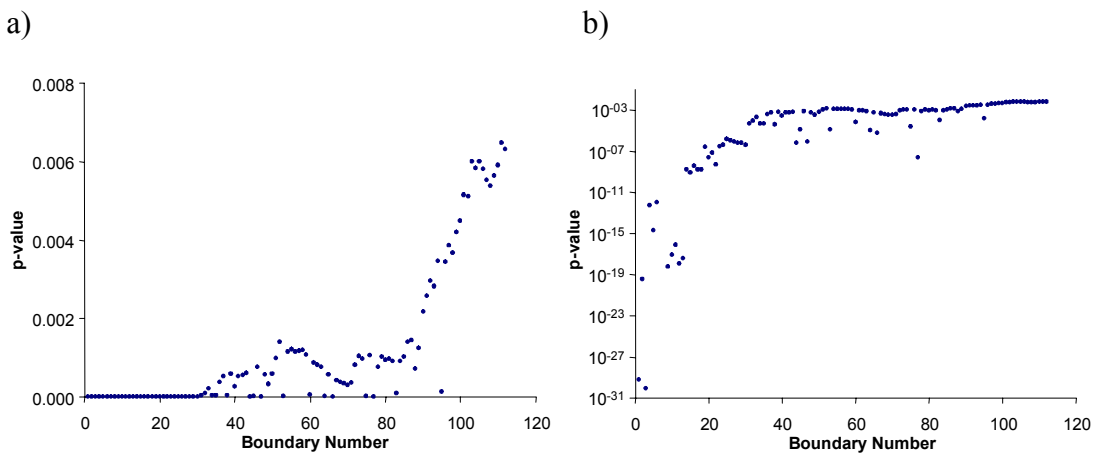

Figure 4.12 Statistical significance (denoted by p-value) of adding additional boundaries to the 80 km moving standard deviation of the 1930 direction change series. In a) the p-value is plotted on a linear y-axis and in b) a logarithmic y-axis is used.

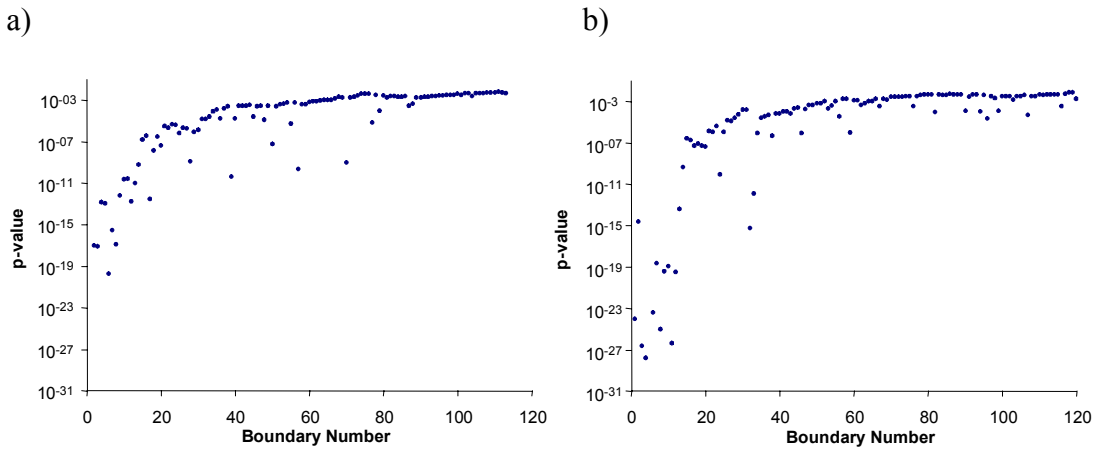

Figure 4.13 Statistical significance (denoted by p-value) of adding additional boundaries to the: a) 40 km and; b) 120 km moving standard deviation of the 1930 direction change series. Logarithmic y-axes are used.

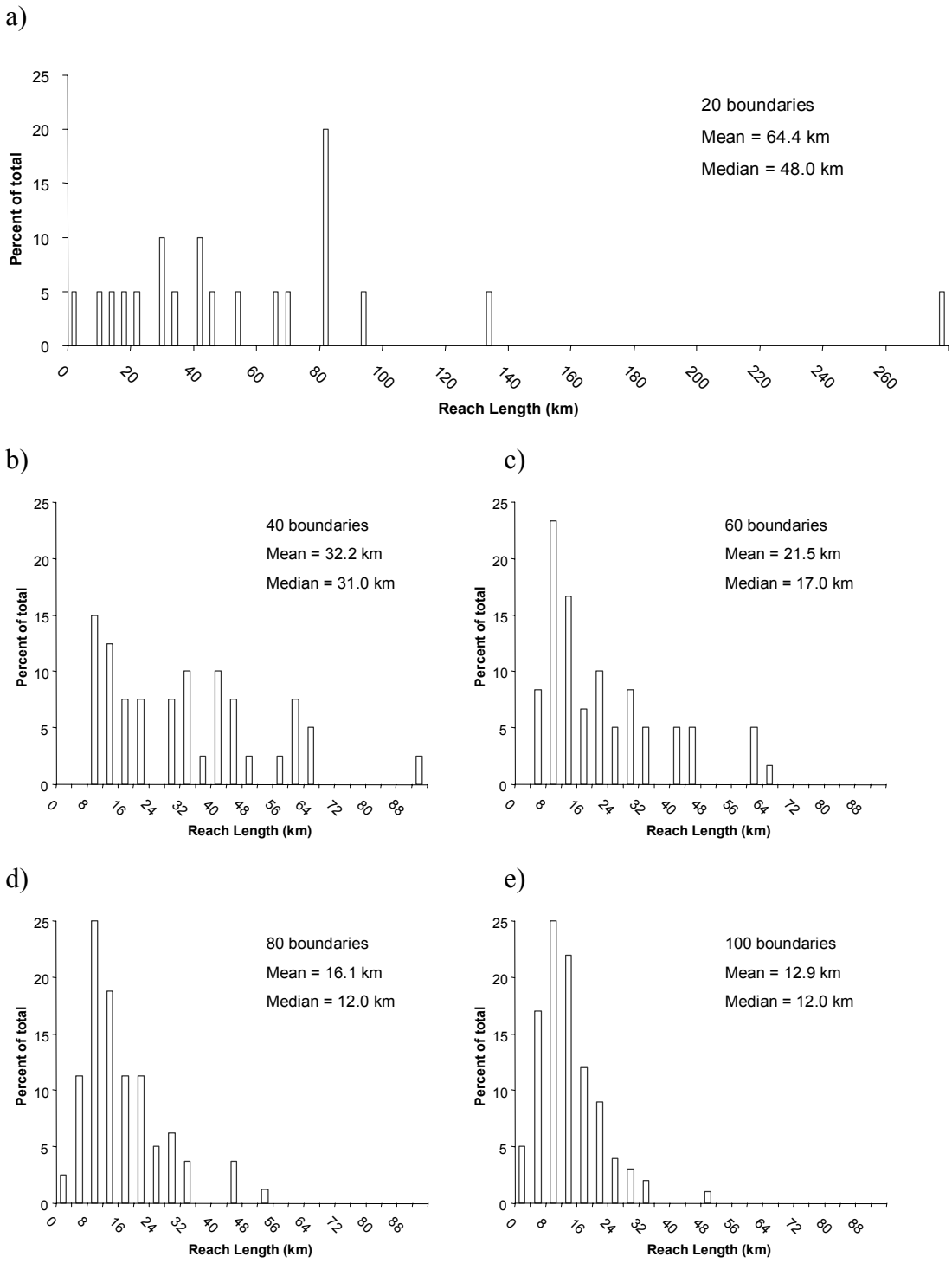

Figure 4.14 Histograms of the distribution of reach length for: a) 20; b) 40; c) 60; d) 80; and; e) 100 boundaries.

second parallel technique was developed to highlight the variation of channel length at a smaller-scale based on reaches of equal valley distance.

The second technique involved dividing the Lower Mississippi River between Cairo and Baton Rouge into two hundred sub-reaches of equal *valley* length. Valley sub-reach delineation was based on a valley axis that was digitised on-screen by identifying key points relating to regional-scale change in direction within the planform (see Figure 4.1). Following identification of regularly spaced boundaries along the valley axis, a customised routine was then developed to identify a corresponding boundary in each of the planform series. For each valley axis boundary, this was achieved by finding the *(x,y)* coordinate of the point in each planform series which intersects a line drawn perpendicular to the direction of the valley axis. In the event of identification of multiple intersections for a single planform series (caused by tortuous meandering for example) a further customised routine was developed to find the closest set of intersections for all planform series. The resulting two hundred coordinate pairs for each planform series were then visually validated by overlaying on top of the original planform in a GIS (Figure 4.15).

4.4.2 Analysis of results

Length changes classified on the basis of the six planform reaches identified in Figure 4.11 are presented in 4.16a. These are expressed as percentage rates of change in 4.16b, removing the bias associated both with reaches of varying length and with surveys undertaken at different time periods. The channel shortening as a consequence of the artificial cutoff programme is clearly emphasised. Total channel length decreased by 146 km in the period 1930-1975 but increases in reaches 1 and 6 mask a greater actual loss of 182 km, or 21 percent of original length, in reaches 3, 4 and 5 where the cutoffs were imposed. In relation to previous studies, these figures may underestimate the magnitude of channel shortening. For example, Smith (1996) reports that total channel length for the longer period 1930-1989 declined by 160 km, 14 km greater than in Figure 4.16a. Smith also reports however, that this value masks a greater level of dynamics, with a period of more dramatic shortening

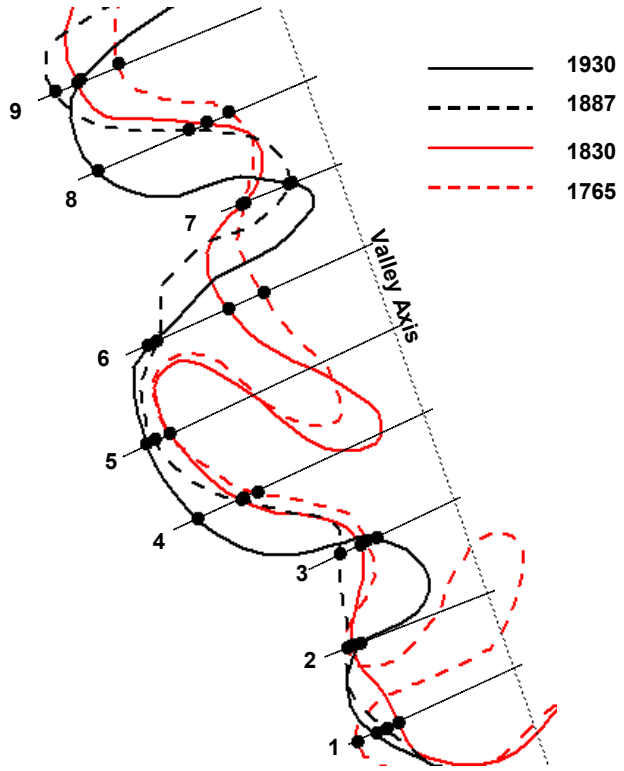

Figure 4.15 A summary of the processing routine used to delineate sub-reaches based on equal valley distance. The reach shown is immediately upstream from Vicksburg.

caused by the artificial cutoff programme and associated chute cutoff development (up to 330 km, see section 2.6.2), being followed by a period of post-cutoff net lengthening. This lengthening phase is likely to have been most dramatic in the 1940s prior to extensive bank stabilisation (see section 2.6.2). Net increases in channel length in the period 1930-1975 in reaches 1 and 6 may suggest that net lengthening was experienced regionally and not just confined to the artificial cutoff reaches. However, given the uncertainty regarding total length changes, further investigation is required of channel length changes during, and following, the artificial cutoff programme. The latter is returned to in section 6.2 where length changes are considered over the 1949-89 period.

In the pre-cutoff period between 1765 and 1930, Figure 4.16 reveals that relatively large spatial and temporal fluctuations in channel length were observed. These fluctuations are illustrated at a finer spatial resolution (200 valley zones) in Figure 4.17. Immediately prior to the artificial cutoff programme in the period 1887-1930, total channel length increased by 75 km. This period corresponds with the 'no cutoff policy' adopted by the Mississippi River Commission between 1879 and 1930, and thus, this observed lengthening may be interpreted as 'managed lengthening.' Interestingly, 4.16b and 4.17c show that reaches three, four, and five experienced considerably greater rates of net lengthening over this period than reaches one, two and six. This is important geomorphologically because it suggests that, by 1930, the cutoff reaches may have become artificially over-lengthened through the prevention of neck and chute cutoff formation. Hence, in a natural scenario, a degree of channel shortening through cutoff formation would have been expected in the following decades and therefore, this may have dampened the geomorphological effects of the artificial cutoff programme.

The trend of systematic lengthening followed by dramatic shortening in the period 1887-1975 was experienced, albeit to a lesser extent, in the preceding period 1765-1887. In this earlier period, total channel lengthening of 46 km between 1765 and 1830 was followed by a large decline of 92 km in the period to 1887. This channel shortening may be interpreted as a geomorphological response to the series of earthquakes at New Madrid in the period 1811-12. Narrative reports suggest that the earthquakes triggered widespread landsliding and bank caving and consequently led

to a sudden large input of coarse-grained sediment into the channel (Jibson *et al.*, 1988). The likely geomorphological response to an increase in sediment load and calibre is an increase in stream power per unit width, achievable through any one or a combination of an increase in channel gradient, a decrease in channel width, or an increase in discharge (Lane, 1955). Hence, channel steepening through the increased incidence of both neck and chute cutoff development throughout the alluvial valley is a likely geomorphological response to the New Madrid earthquakes. Mutual variations in channel width and discharge are considered in sections 4.5 and 4.6.

The dramatic shortening of the river between 1830 and 1887 may also be partly explained by land clearance for agriculture and timber clearcutting. These activities were commonplace in the alluvial valley during the nineteenth century (Saucier, 1994). The important stabilising role of vegetation in river banks has been demonstrated by Thorne (1990) and hence, at the scale of the Lower Mississippi River, systematic removal of vegetation is likely to have led to significant increases in rates of bank erosion. Saucier (1994) estimates that rates of erosion in the alluvial valley increased by several orders of magnitude in relation to the rates from the preceding several thousand years. Figure 4.17 reveals that cutoffs in the period 1830-1887 appear to be distributed throughout the Lower Mississippi River, thereby supporting the theory that increased instability is attributable to the dramatic sediment input into the river at New Madrid following the 1811-12 earthquakes in combination with systematic removal of riparian vegetation.

The reach-scale dynamics in the pre-modification period (1765-1930) illustrated in Figure 4.16 and 4.17 are plotted as gross and net changes in Figure 4.18. For each reach, the total length change has been divided by the length of each reach in 1765 to standardise reach length. In terms of gross changes, 4.18a reveals that Reach 5 (from the confluence of the Yazoo River at Vicksburg to just downstream from the confluence of Old River) was clearly the most dynamic reach prior to the cutoff programme. Furthermore, reaches 2, 3 and 4 were more dynamic than the most upstream and most downstream reaches (1 and 6). In terms of net changes (4.18b), the pattern is reversed: the greatest net change in channel length is recorded in those reaches which are less dynamic reaches (1 and 6) and conversely, only slight changes are recorded in the more dynamic reaches (4 and 5). Thus, from a geomorphological

a)

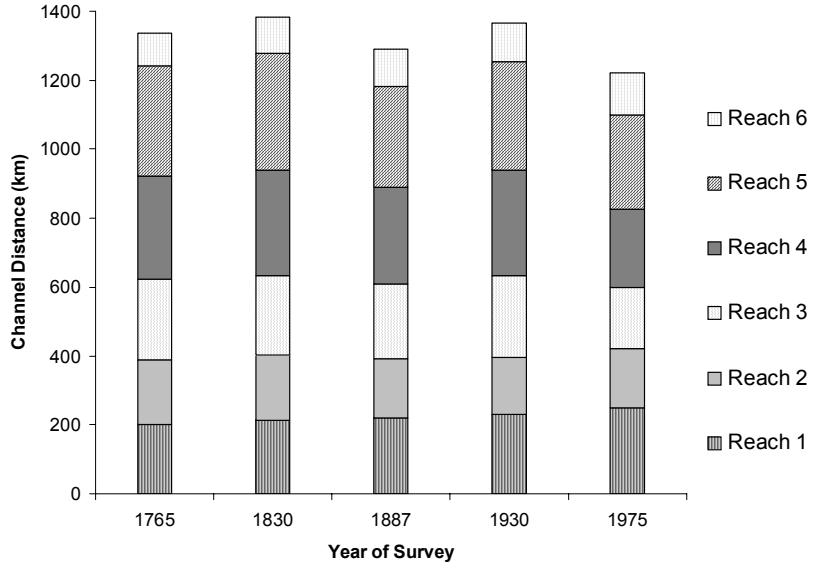

b)

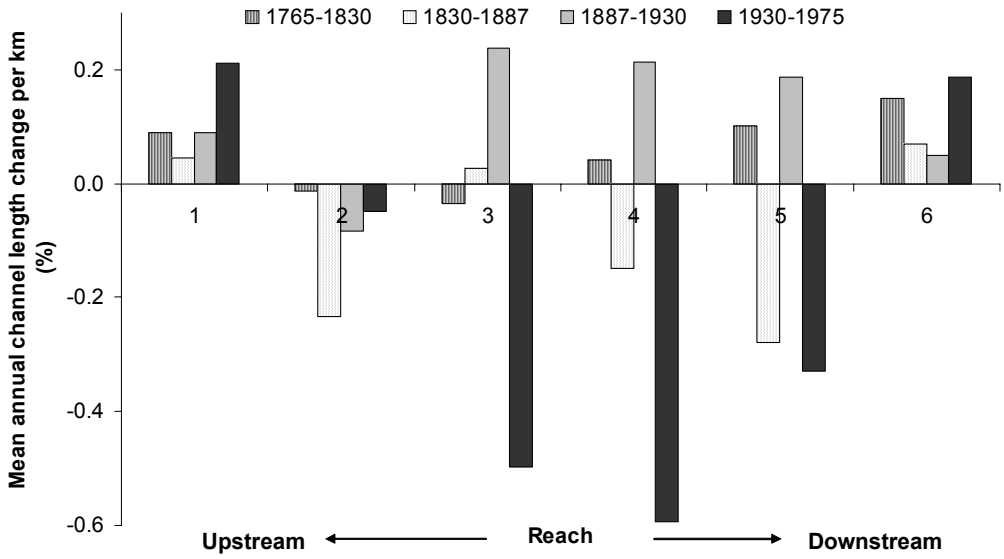

Figure 4.16 Channel length changes between Cairo and Baton Rouge in the period 1765 1975: a) total length change; b) percentage mean annual rates of channel length change. Reaches correspond to those identified in Figure 4.11.

a) 1765-1830

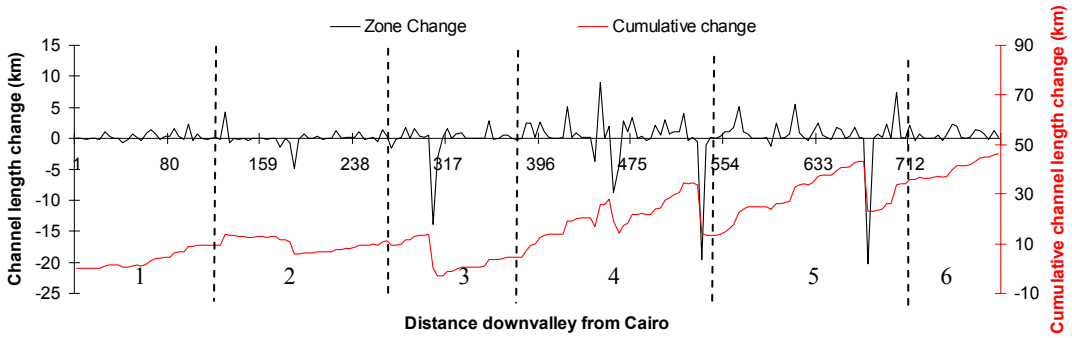

b) 1830-1887

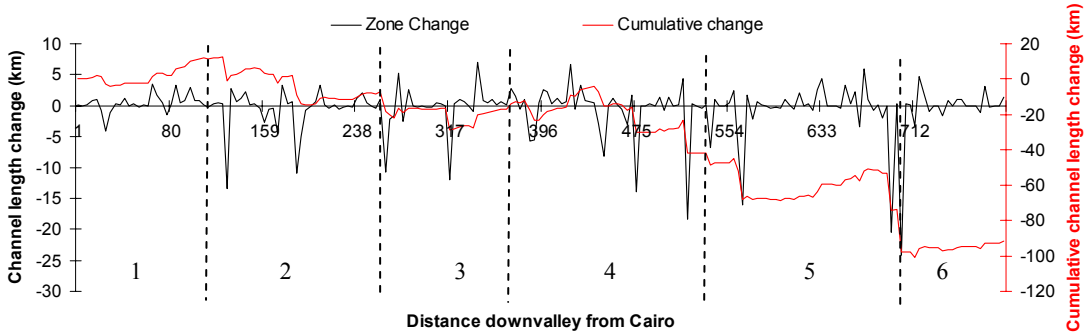

c) 1887-1930

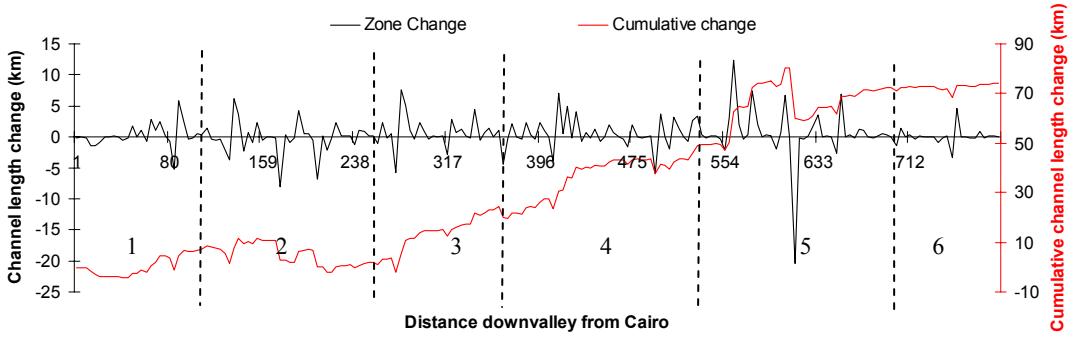

Figure 4.17 Channel length changes in the period 1765-1930 based on division of the valley axis into 200 sub-reaches of equal length. Labelled reaches correspond to those identified in Figure 4.11.

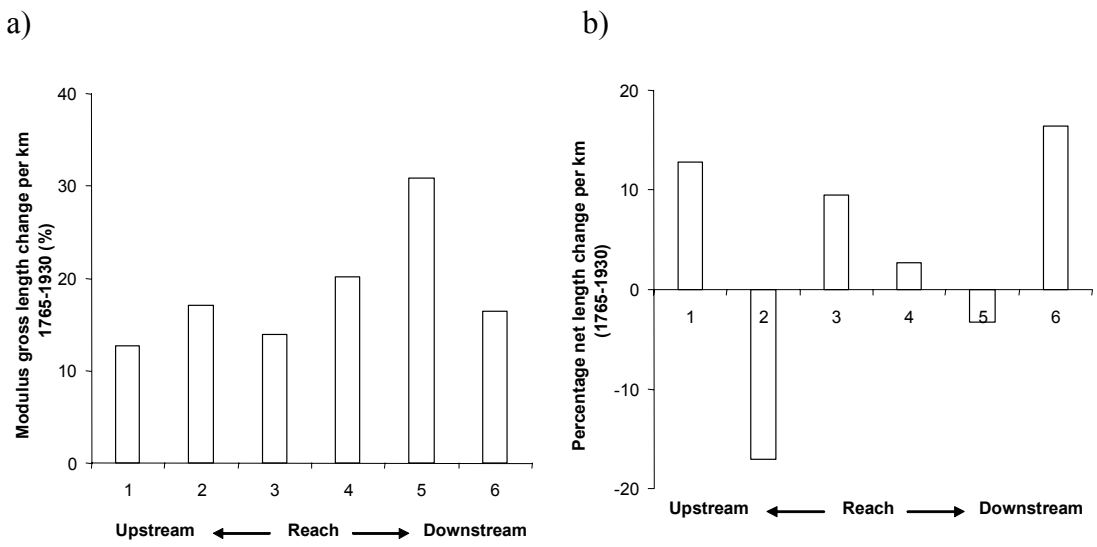

Figure 4.18 Average percentage rates of length change per km for the pre-cutoff period 1765-1930. Rates in a) are presented as a modulus of gross length changes whereas rates in b) are presented as net changes over the period.

perspective, it is possible to differentiate a group of reaches that demonstrate consistent little planform behaviour from a group of reaches that are relatively sensitive to disturbances. In the pre-modification period, the temporal dynamics within reaches 4 and 5 (from the confluence of the Arkansas River to just downstream from the confluence of Old River) in particular drive the changes which are observed at the regional-scale. Physical explanations for these apparent trends in planform dynamics are explored in section 4.9.

4.5 Variation of channel width

Winkley (1977) reports trends in the mean top-bank width in the period 1830-1975 for four reaches of the Lower Mississippi River: Cairo to the St Francis River; St Francis River to the Arkansas River, the Arkansas River to Vicksburg and Vicksburg to Red River. In relation to Figure 4.11, the first reach therefore encompasses reaches 1 and 2, and the remaining three reaches approximately correspond to reaches 3, 4 and 5 respectively. The earlier measurements for the period 1830-1930 were made from original copies of historic planform maps whilst measurements for the more recent 1950-1975 period were made from decadal hydrographic surveys. Owing to issues of data reliability (see section 2.8.2), top-bank widths are only reported to the nearest 100 feet (30.5 m). In Figure 4.19, top-bank widths have been converted to SI units and plotted to decipher both temporal and inter-reach variation.

Top-bank widths have increased dramatically in the period 1830-1975 in all reaches. The greatest increases were observed during the period 1830-1887 when annual rates of percentage increase averaged nearly 1.4 percent, representing an average total increase of 0.65 km. This increase coincides with the net channel shortening noted in section 4.4. Dramatic increases in channel width during this period are most likely attributable to the reduction in bank stability following extensive riparian vegetation clearance throughout the nineteenth century (Saucier, 1994). Of further interest geomorphologically is the observation that reaches 4 and 5 (from the confluence of the Arkansas River to just downstream from Old River) display both the highest rates of width increase, and the highest rates of channel shortening over the period (Figure 4.16). This indicates a close coupling between length and width parameters, and

hence suggests that morphological response to disturbance involves the mutual adjustment between multiple degrees of freedom. In the later period 1887-1930, marginal increases in channel width were observed in all reaches with the exception of reach three. Thus, by 1930, the mean length of the Lower Mississippi River was similar to that in 1830, but the top-bank width had approximately doubled. In the most recent period 1950-1975, considerable further increases were observed in all reaches with the exception of the upstream reaches 1+2. These changes are discussed further within the context of unit stream power in section 4.7.

4.6 Variation of the process regime

When considering geomorphological behaviour, morphological changes such as channel length and channel width variability cannot be divorced from flow and sediment transport process variability. Available records of computed daily discharge on the Lower Mississippi River extend back to the 1930s and 1940s and thus, do not cover the pre-modification period (see section 2.8.6). However, a record of mean annual discharge for the longer period 1817-1975 is reported by Winkley (1977). Although it is the effective discharge and not the mean annual discharge which has the greatest importance geomorphologically (Wolman and Miller, 1960), the mean annual discharge record at least provides an indication of possible longer-term trends. In the original format, the record is published as a histogram where the mean annual discharge for each calendar year is labelled and categorised into classes of 500 cfs (cubic feet per second) for the range 250-1000 cfs. By assuming the mean annual discharge in any survey year is the discharge representing the mid-point of the class range, it is possible to reconstruct the temporal trend. This is presented in Figure 4.20. Mean annual discharge has been converted to standard SI units (m^3s^{-1}). The reliability of the more recent 1937-1975 record has been validated by comparing to computed mean annual discharge using daily records available to this study. However, a degree of caution because must be asserted when interpreting the pre-1874 record because the procedure and equipment used to measure discharge during this early period is not documented (Winkley, 1977).

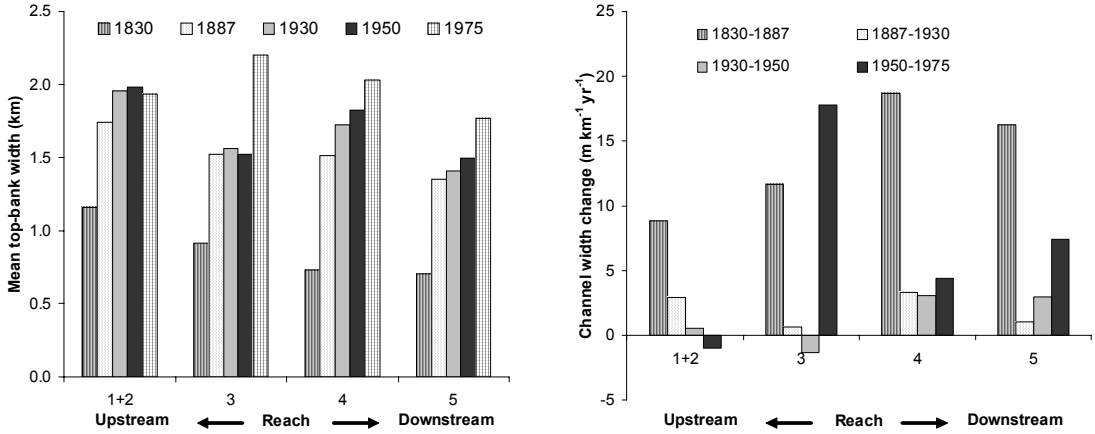

Figure 4.19 a) Mean top-bank channel width and b) standardised rates of top-bank channel width change in the period 1830-1975 (based on data collected by Winkley, 1977). Reaches correspond to those identified in Figure 4.11.

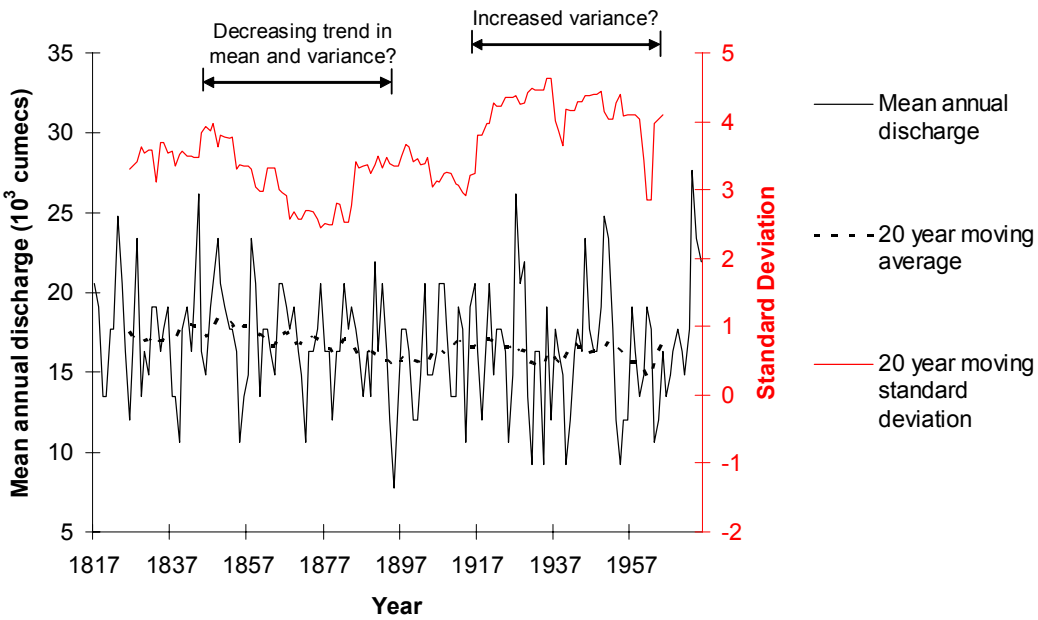

Figure 4.20 Trends in mean annual discharge in the period 1817-1975 based on data from Winkley (1977). Data is for calendar year at Vicksburg. See text for further description.

A 20 km moving average and moving standard deviation have been fitted to the record to emphasise temporal trends in the mean and variance respectively. The record reveals that it is difficult to decipher a long term trend in mean annual discharge because of significant shorter term variability at decadal and sub-decadal timescales. However, if anything, the record is suggestive of a declining trend during the second half of the nineteenth century with an approximately stable trend both prior to this period and thereafter. The record may also indicate that the variability of mean annual discharge declined between approximately 1840 and 1880 but then increased between 1880 and 1930 to a high level of variability thereafter. This high level of variability coincides with the period of artificial cutoff construction between 1932 and 1942.

Trends within measured sediment transport records are discussed in section 2.7.2 and are therefore not repeated here except to state the widely accepted belief that suspended sediment loads on the Lower Mississippi River have declined sharply over the last 70-150 years (Keown *et al.*, 1981; Robbins, 1977; Kesel, 1988, 1989). Thus, the shorter post-cutoff channel transports less sediment in suspension than the longer pre-cutoff channel. However, what has remained very difficult to establish is how measured sediment loads in the pre-modification period, on which almost all of the reported decreases are ultimately based, compare to the mean sediment loads over the much longer timescale of the Holocene period. Saucier (1994) reports that the suspended sediment loads throughout the nineteenth and early twentieth centuries were almost certainly elevated by soil erosion induced by land clearance for agriculture and settlement throughout the alluvial valley and wider drainage basin. This is best exemplified by the 'dustbowl' effect experienced throughout the interior plains in the western portion of the Mississippi River drainage basin during the 1930s.

It is therefore reasonable to suggest that although the post-cutoff suspended sediment loads on the Lower Mississippi River are significantly lower than during the immediate pre-cutoff period, they may well be of a comparable magnitude to mean suspended sediment loads throughout most of the Holocene period. In relation to trends in other parameters, enhanced sediment loads throughout the nineteenth and early twentieth centuries correspond with relatively rapid increases in channel width,

an initial decrease and later increase in channel length and perhaps a slight decrease and then increase of discharge. These mutual changes are considered in the next section in the context of variations of unit stream power.

4.7 Integrating morphological and process variation: unit stream power

Variations in both morphological parameters and the prevailing process regime determine, and are determined by, variations in unit stream power and unit stream power expenditure. If variations in channel length are considered in terms of channel gradient, then length, width, and channel discharge determine unit stream power (ω), a measure of the total energy of flow per unit bed area, and hence, the total energy available for hydraulic and geomorphological processes.

$$\Omega = (\gamma Q s) / w \qquad (4.1)$$

where: γ = bulk unit weight of water (constant)

Q = discharge

s = channel slope (inversely proportional to channel length)

w = channel width

The relationship between channel length and channel width in the stream power equation is considered in Figure 4.21, assuming a constant valley slope and no long term trend in discharge. Unit stream power can remain constant if channel length and channel width vary by exactly inverse proportions. For example, if the length of a meandering channel through a reach halves following dramatic cutoff development, this corresponds to an effective doubling of channel slope. Hence, for unit stream power to remain at unity, channel width must also double. This is shown by the line of constant unit stream power in Figure 4.21. Unity can also be achieved when an increase in channel length is effectively balanced by a proportional decrease in channel width. This concept can be related to the variation of channel length and width of the Lower Mississippi River shown in Figure 4.22.

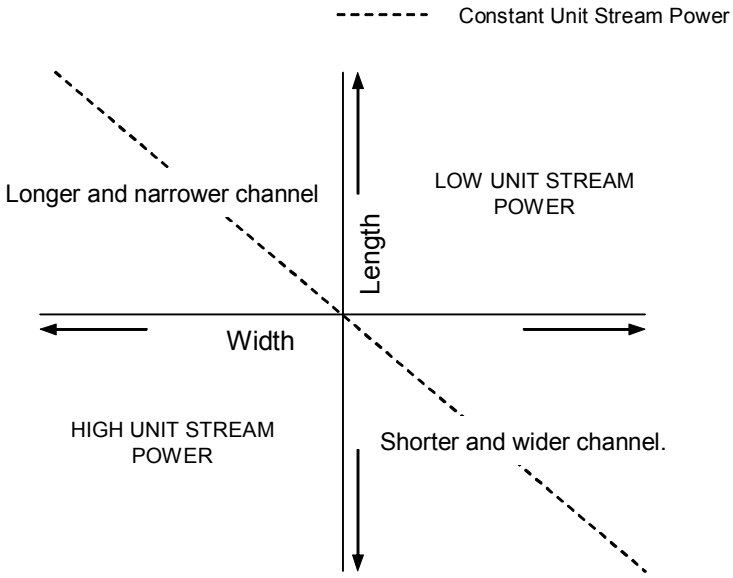

Figure 4.21 The implications of channel length and width variability for unit stream power.

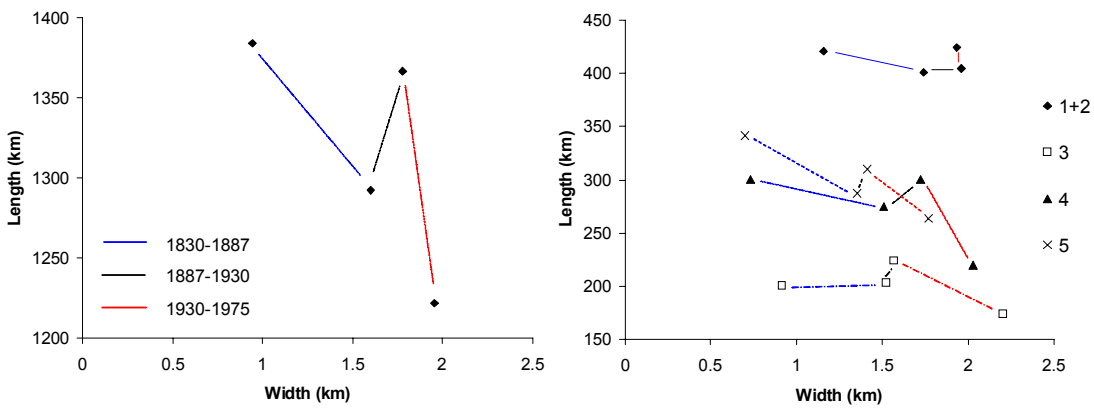

Figure 4.22 Plots of average length against width in the period 1830-1975 for: a) the Lower Mississippi River from Cairo to Old River (reaches 1-5) and; b) the individual planform reaches identified in Figure 4.11 (with reaches 1 and 2 amalgamated).

Figure 4.22a displays the reach-averaged changes in channel length against corresponding changes in channel width. If no long term trend in discharge is assumed once again, there has been a general decrease in unit stream power in the 1830-1975 period because, whilst width has more than doubled, total channel length has shortened by only ten percent. However, this observation assumes reliability of the top-bank width for 1830, reported by Winkley (1977). If this is removed from the analysis and variation in channel length and width are considered from 1887, net lengthening in combination with slight net widening is suggestive of a decline in unit stream power in the period 1887-1930. In the latter 1930-1975 period however (incorporating the period of artificial cutoff construction), a decline of channel length by approximately ten percent, in combination with an increase in channel width of approximately ten percent, is suggestive of very little or no change in unit stream power. This latter finding suggests that the assertion made by Biedenharn *et al*. (2000), that the contemporary, post-cutoff, Lower Mississippi River has a much larger stream power than prior to the cutoffs, may be misleading because it is based solely on stream power per unit length of channel, not unit stream power and thus, does not consider simultaneous variations in channel width.

In Figure 4.22b, the regional-scale changes in channel length and channel width observed in Figure 4.22a are decomposed to the reach-scale. Observed regional-scale changes mask the considerable inter-reach variation highlighted in sections 4.4 and 4.5. Most evidently, the upstream reaches 1 and 2 demonstrate considerably different behaviour in the period 1887-1975 to the artificial cutoff reaches (3-5). This reveals that it may be misleading to consider changes in unit stream power at only the regional-scale.

If the variation in the process regime noted in section 4.6 is factored into the above discussion, the geomorphological significance of the artificial cutoff programme is further reinforced. Immediately prior to the artificial cutoff programme in 1930, the Lower Mississippi River had lengthened and widened in all reaches between Cairo and Old River over the previous 43 years. Although discharge may have slightly increased over the same period, unit stream power is likely to have been considerably lower in 1930 than in 1887. Published records indicate that measured suspended sediment loads were high in 1930 and hence, there was most likely, an imbalance

between available stream power per unit width and available sediment load. In the 1930-1975 period, the artificial cutoff programme dramatically reduced channel length although simultaneous increases in channel width indicate that stream power per unit width may have remained approximately constant. However, bank stabilisation, together with improved land use practices, reduced rates of sediment supply and consequently, measured suspended sediment load. Biedenharn *et al*. (2000) propose that excess stream power alongside declining suspended sediment loads in the post-cutoff period must be balanced by an increase in bed material transport. However, stream power per unit width cannot be simply related to rates of sediment transport because energy is first lost in overcoming flow resistance. Spatial and temporal variations of flow resistance therefore require investigation before variations in unit stream power can be related to sediment transport processes.

Resistance to flow is comprised of several different components (Leopold et al., 1964; see section 1.5). At the regional-scale, bend size and shape is a major source frictional resistance (Richards, 1982). This induces internal energy losses within eddies and vortices within the flow field and therefore exerts a strong control on total flow resistance. Flow resistance increases as bend tightness increases. However, the relationship between channel curvature and flow resistance is more complicated because tighter meander bends are associated with a longer channel length (lower channel slope) and therefore, the rate of energy loss per unit length may be reduced, particularly as energy is dissipated more efficiently in a meandering channel (Davies and Sutherland, 1980; Yang, 1971). In the following two sections, two complementary techniques are together used to inform variations in flow resistance: spatio-temporal trends in radius of curvature is first examined to highlight changes in bend tightness; and then bend wavelength and amplitude are examined to highlight changes in bend size and shape.

4.8 Variation of radius of curvature

A radius of curvature series was computed from each planform series using the method outlined in Figure 4.23. For each regularly spaced observation, the radius of curvature was defined as the intersection of lines drawn perpendicular to the mid-

point of the upstream and downstream chords. The median radius of curvature is plotted for each reach, and for each survey year in Figure 4.24. The median is used as a measure of central tendency in preference to the mean in this case because radius of curvature decreases as a logarithmic function as direction change, and hence, bend tightness increases (Brice, 1983). Thus, straight reaches (very low direction change) are characterised by extremely high radii of curvatures.

In general, the spatial and temporal variation of radius of curvature follows a similar pattern to the variation of channel length noted in section 4.4. This is not surprising, because the variation of channel length, if considered over a timescale in which there are no significant changes in the orientation of the valley axis, is a direct indicator of variation in sinuosity. Sinuosity and radius of curvature are different measures of the degree of meandering in a river channel. Generally, an increase in sinuosity would be expected to be accompanied by a decrease in radius of curvature as meandering become more tortuous and vice versa. This association is demonstrated by observing the inter-reach variability in radius of curvature in the pre-modification (1765-1930) period. Reaches 1 and 6 are generally characterised by both a higher average radius of curvature and lower overall variability than reaches 2-5. Thus, the more dynamic reaches in the pre-modification period were the reaches demonstrating more tortuous meandering. This observation is consistent with Figure 4.18a which shows that the reaches 2-5 displayed the highest rates of gross length change per km over the same period. The association between length and radius of curvature variability can also be demonstrated temporally. In the artificial cutoff period (1930-1975), the considerable increase in radius of curvature in reaches 3-5 is consistent with the elimination of the most sinuous bends and hence, the net reduction in length (see Figure 4.16b). Similarly, the increase in curvature in reaches 2-4 in the 1830-1887 period is consistent with the large number of cutoffs at this time. Conversely, in the period 1765-1830, the decrease in curvature in the lower reaches (4-6) is consistent with observed net lengthening.

This general trend discussed above is illustrated by the broad inverse linear relationship between radius of curvature and sinuosity in Figure 4.25. However, the plot also reveals a considerable degree of scatter about the trend. This is confirmed by a coefficient of determination (R^2) value of just 0.49 between the two variables

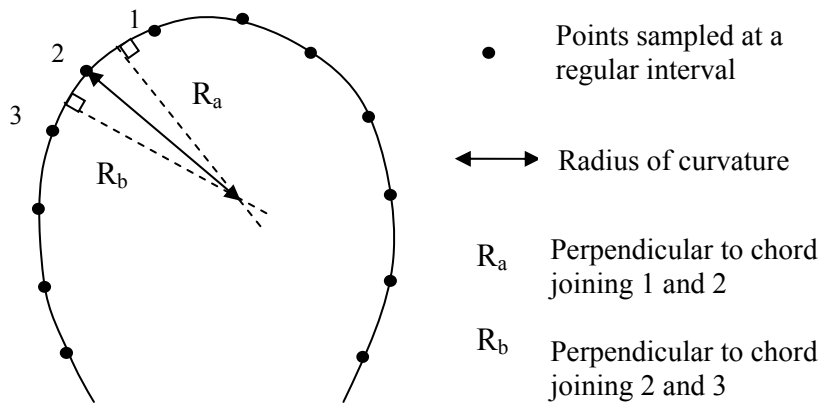

Figure 4.23 Determination of radius of curvature at each sampling point.

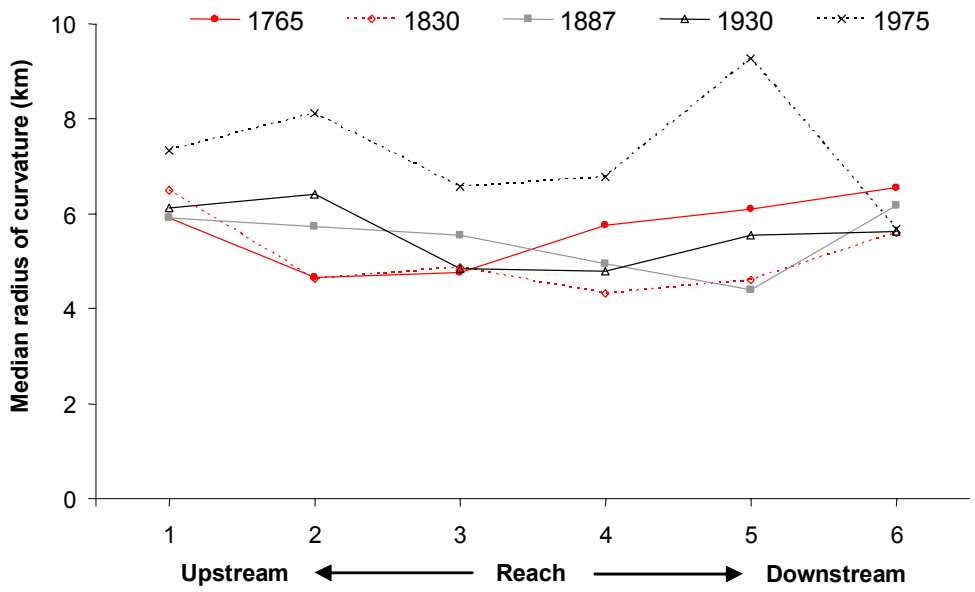

Figure 4.24 Median radius of curvature in relation to survey reach and survey year.

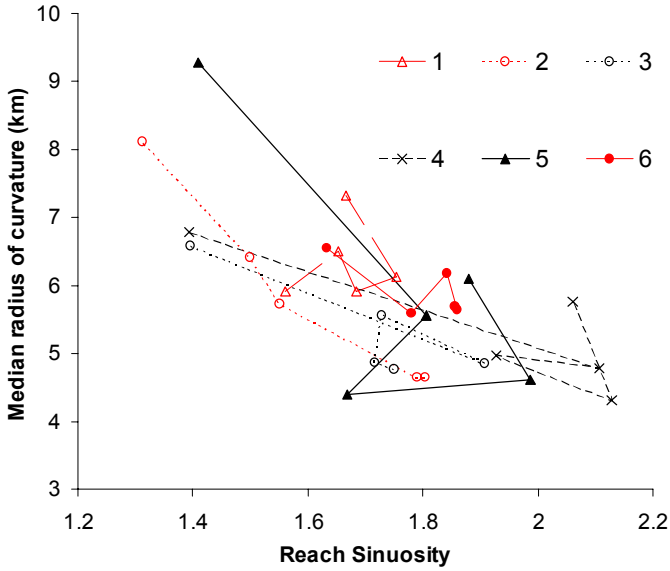

Reach	R^2
1	0.01
2	0.96
3	0.79
4	0.74
5	0.57
6	0.53
All	0.49

Figure 4.25 Median radius of curvature against reach sinuosity for each reach and planform survey in the period 1765-1975. Data points in each reach are connected to illustrate temporal changes. R^2 values are presented for each individual reach and for all reaches.

when all reaches are considered. Scatter in the relationship is important to consider because it provides an indication of spatial and temporal variations in bend size and shape and hence, flow resistance. If the rate of decrease of radius of curvature is greater than the rate of increase of sinuosity, meander bends are likely to have become tighter per unit length and flow resistance is therefore likely to have increased. Conversely, if the rate of decrease of radius of curvature is less than the rate of increase of sinuosity, meander bend tightness, and consequently flow resistance, are likely to have decreased. The strength of the relationship (denoted by the R^2 values) between radius and curvature and sinuosity in each reach is dependent on the magnitude of both channel length (sinuosity) variation and bend size and shape variation over the 1765-1975 period. R^2 values for each reach are therefore highest in the midstream reaches 2 to 5 which were considerably more dynamic in terms of channel length changes than both the upstream and downstream reaches (1 and 6).

Scatter about the broad inverse-linear trend can be explained by considering the relative sensitivity of radius of curvature and sinuosity variables to changes in bend size and shape. These are explored through analysis of two well established parameters: meander wavelength and meander amplitude (see Figure 4.29). Radius of curvature is more sensitive to variations in meander wavelength and amplitude than sinuosity. This is conceptualised in Figure 4.26 by considering translations of a series of regular sinusoidal waves. Although changes in sinuosity are obtained through most changes in meander wavelength and/or meander amplitude, it is possible for sinuosity to be stable if changes in wavelength and amplitude counteract each other. For example, the regular waveforms in quadrants b) and c) of Figure 4.26 have the same sinuosity because wavelength and amplitude have increased by the same proportion. This scenario is indicative of an increase in bend size but maintenance of bend shape. Recording a change in bend size is important because flow resistance decreases in larger bends as radius of curvature increases (Figure 4.27). Thus, simply analysing variations in sinuosity is not a reliable method to understand changes in flow resistance because variations in bend size are not adequately accounted for.

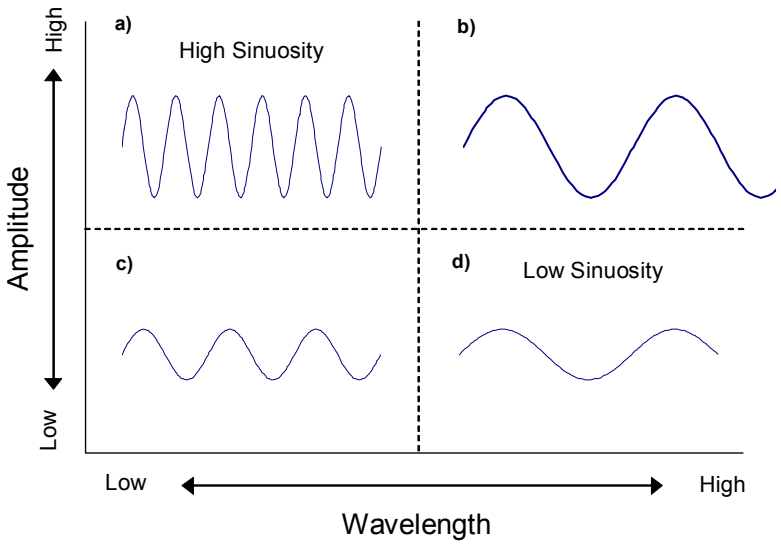

Figure 4.26 The relationship between meander wavelength, meander amplitude and sinuosity.

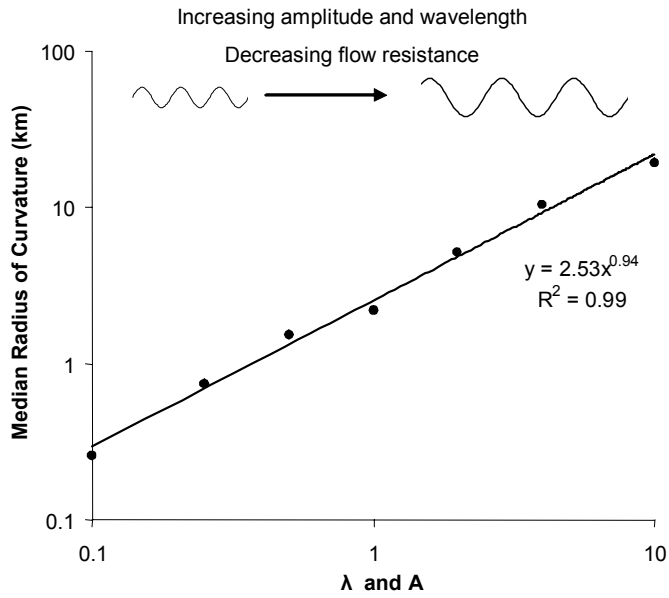

Figure 4.27 Median radius of curvature against the relative size of meander bends, measured by proportional increases in both wavelength *and* amplitude.

Previous attempts to relate radius of curvature directly to flow resistance have standardised radius of curvature by expressing in terms of multiples of channel width. The dimensionless ratio (R_c/w) is then independent of scale effects. Following measurement of meander wavelength, width and radius of curvature for meander bends at a range of scales and in a range of fluvial environments, Leopold and Wolman (1957) derived the following empirical relationship to describe the average tightness of meander bends:

$$R_c / w = 2.3 \qquad (4.2)$$

This is supported by the large dataset compiled by Williams (1986) in which 42 percent of radius of curvature-width values were in the range of 2 to 3. Bagnold (1960) related this window directly to flow resistance by showing that the rate of increase in flow resistance with increasing curvature is minimised within this range of values and hence it represents the most efficient hydraulic shape (and hence, the most effective geomorphologically).

Observed R_c / w ratios on the Lower Mississippi River are compared to this window in Figure 4.28. During the 1887-1975 period, the regional-scale and reach-scale ratios are in the range 3-4 and 2.5-5.5 respectively. Ratios for the 1830 planform are considerably greater, supporting suspicions raised in section 4.5 that the earliest channel widths reported by Winkley (1977) may be unreliable. Together, results suggest that the most efficient hydraulic shape, according to Bagnold's (1960) theory, is not being achieved. It is difficult however to isolate the extent to which this may merely be a methodological artefact or alternatively, a finding which has physical significance. This is because the radius of curvature in Figure 4.28 represents regional-scale and reach-scale averages whereas the empirical relationship derived by Leopold and Wolman (1957) was formulated by subjectively identifying the characteristics of 'representative' meander bends (Brice, 1983).

To counteract this difference, the median radius of curvature is also calculated for individual meander bends with a sinuosity in excess of 1.5 in Figure 4.28. These were identified by the inflexion point technique described in section 4.9.4. Although the sinuosity threshold is arbitrary, the R_c / w ratio in the 1887-1975 period is lowered to approximately three. This is closer empirically to the conventional

window but is still not directly comparable to Leopold and Wolman's (1957) relationship because it is based on computation of a median measure of central tendency in the bend distribution, as recommended by Brice (1983), rather than a mean value. An alternative approach is to measure the minimum radius of curvature in each bend rather than the median radius of curvature. However, R_c / w ratios decrease dramatically to a range of 1-1.5 in the 1887-1975 period.

The problem of parameter definition exposes a fundamental limitation with basing flow resistance estimates on radius of curvature. Although Figure 4.27 revealed that median radius of curvature is strong diagnostic tool for recording changes in bend size, it is unclear exactly how it varies with changes in bend shape. This is exemplified by considering a simple increase in bend amplitude, but maintenance of bend wavelength, such as moving from quadrant c) to a) in Figure 4.26. In terms of median radius of curvature, the development of more tortuous bends is equalised by the development of longer, straighter reaches. However, total flow resistance is likely to be greater in bends of higher amplitude because of the greater reach length. This suggests therefore that radius of curvature is also inadequate alone to resolve changes in flow resistance.

In summary to the above discussion, there are problems with relating radius of curvature and sinuosity parameters directly to flow resistance, especially when considering changes over longer river reaches. Taken together, the two techniques are more powerful because they can inform changes in both bend size and bend shape and hence, suggest changes in flow resistance. An alternative, more direct technique, is to consider changes in bend size and shape parameters explicitly. This is considered in the following section by examining changes in meander wavelength and meander amplitude.

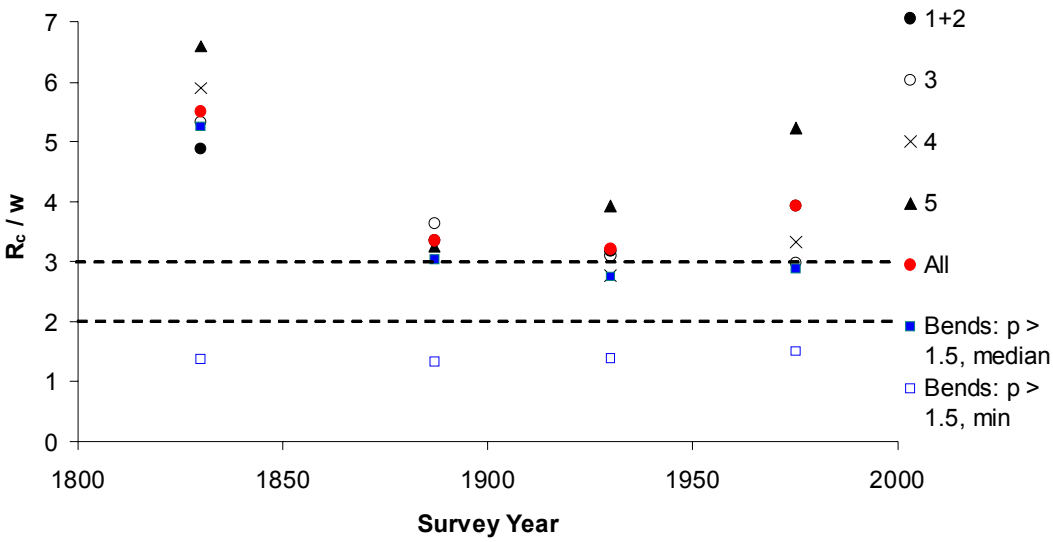

Figure 4.28 Spatial and temporal variability of the median radius of curvature/width (R_c/w) relationship. Broken lines indicate the conventional window of (R_c/w) values in the range 2-3. Results are plotted i) as a regional-scale average for the Lower Mississippi River from Cairo to Old River; ii) as averages for the planform reaches identified in Figure 4.11 and; iii) as an average of the median and minimum (R_c/w) for individual bends with a bend sinuosity greater than 1.5. Bends are defined using the inflexion point techniques introduced in section 4.9.4.

4.9 Variation of meander wavelength and amplitude

In early work by Inglis (1947) and Leopold and Wolman (1960) meander wavelength and amplitude parameters were measured by computing statistics for each individual meander bend. Meander wavelength was defined as the tangential distance between the meander peaks or two meander inflexion points, and meander amplitude was defined as the tangential distance between subsequent meander peaks and troughs (Figure 4.29). More recent work has utilised a range of alternative serial techniques to generate these parameters (Speight, 1965; Ferguson, 1975, 1977; Hooke, 1977; Lewin, 1977). In this section, the results of both bend statistic and serial methods (incorporating autocorrelation, second-order autoregressive modelling, spectral analysis) are critically evaluated in order to infer spatio-temporal changes in wavelength and amplitude parameters.

4.9.1 Autocorrelation and partial autocorrelation

The ACF and PACF for the entire 1930 direction change series are presented in Figure 4.30. The ACF is clearly characterised by an oscillating tendency indicative of a type of periodic behaviour (see section 3.2.2*iii*). The high significance of second coefficient in the PACF suggests that the periodic behaviour in the series is likely to be explained by fitting a second order stochastic model. The PACF also clearly shows that subsequent coefficients are significant, or near significant, negative coefficients up to a lag distance of approximately 20 km. This is highlighted by a red box in Figure 4.30b. Occasional significant values at high lags would not be a major concern because even in a randomly generated series, one significant value at the 95 percent confidence level can be expected in every 20 lag intervals (Chatfield, 1989). However, a group of significant coefficients at relatively low lag distances in the PACF does suggest that variability exists beyond that which can be explained by a second-order stochastic process alone.

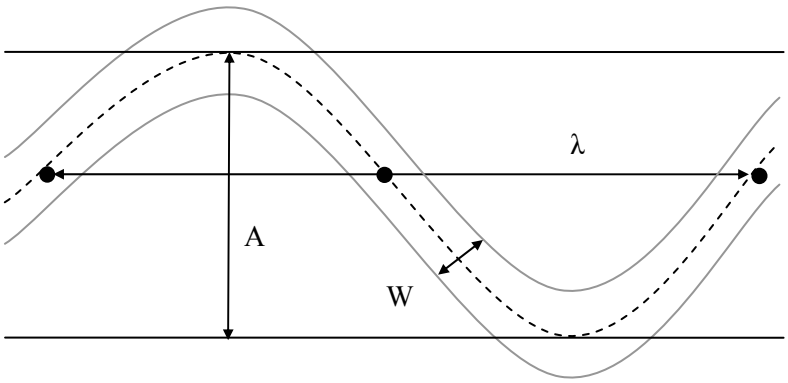

λ = Meander wavelength
A = Meander amplitude
W = Channel width

Figure 4.29 The definition of meander amplitude and wavelength parameters according to Inglis (1947) and Leopold and Wolman (1960).

In Figure 4.31, the 1930 PACF is segmented into separate PACFs for each of the six reaches identified in Figure 4.11. In each of the reaches, the first and second order coefficients are statistically significant and there is a tendency for negative partial autocorrelation up to a lag distance of approximately 20 km. However, the magnitude of the second-order coefficient in relation to the magnitude of coefficients up to a lag distance of 20 km is lower in the most upstream and most downstream reaches (1 and 6) than the midstream reaches 2 to 5. The resulting assertion, that reaches 2 to 5 are better modelled by a second-order stochastic model, is examined in the next section.

4.9.2 Second-order autoregressive modelling

The autoregressive statistics for second-order modelling of each planform series in the period 1765-1975 are presented in Table 4.2. Most interestingly, each series satisfies the inequality for pseudo-periodicity. The identification of a pseudo-periodic component in each survey year reveals that the meander bend oscillations in the planform are adequately described by a periodic component which varies in both wavelength and amplitude according to a random element (Ferguson, 1976). This therefore supports the concept of meandering as a product of a regular hydrodynamic oscillation disturbed at the local-scale by environmental influences such as neotectonic controls and variation in bank material and riparian vegetation.

Year	1765	1830	1887	1930	1975
$Ø_1$	0.854	0.79	0.812	0.832	0.865
$Ø_2$	-0.442	-0.395	-0.402	-0.364	-0.386
Stationary?	Yes	Yes	Yes	Yes	Yes
R^2	0.476	0.426	0.443	0.454	0.481
$Ø_1^2 < -4Ø_2$?	-1.04	-0.96	-0.95	-0.76	-0.80
Pseudo-periodic?	Yes	Yes	Yes	Yes	Yes
Wavelength (km)	13.12	12.86	13.09	15.52	14.31

Table 4.2 Detection of pseudo-periodicity and mean wavelength estimation using second-order autoregressive models for the Lower Mississippi River between Cairo and Baton Rouge.

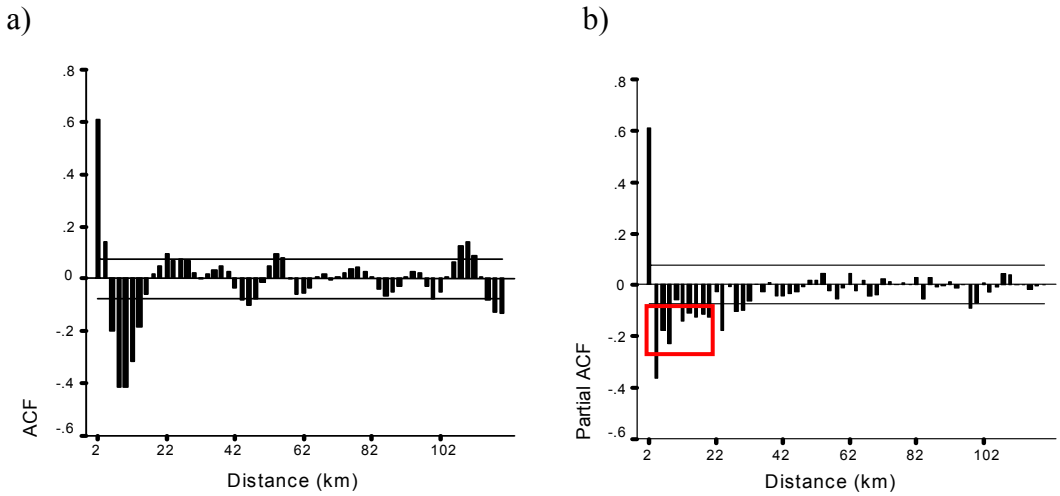

Figure 4.30 a) The ACF and b) the PACF for the Lower Mississippi River between Cairo and Baton Rouge in 1930.

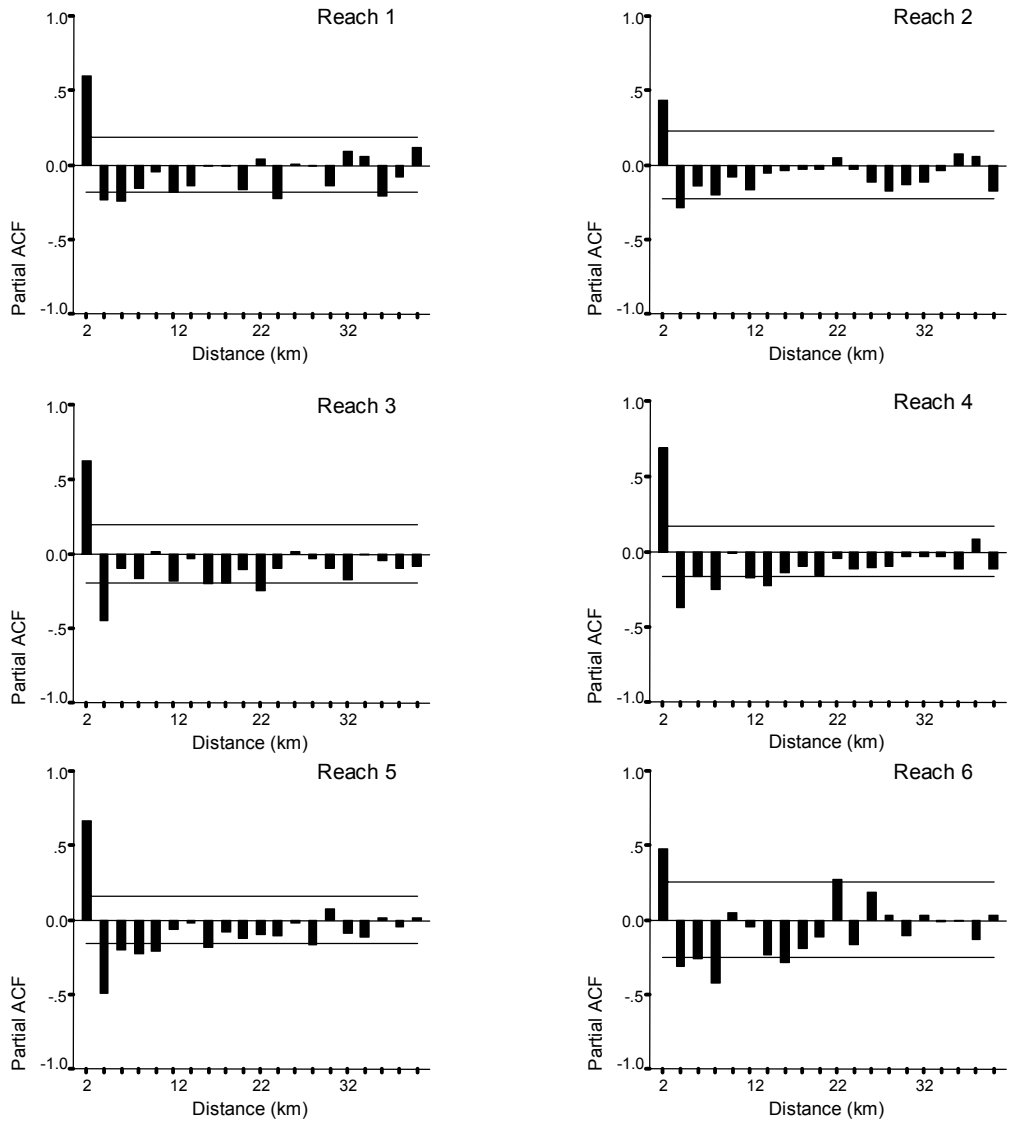

Figure 4.31 PACFs of the 1930 direction change series for the reaches identified in Figure 4.11.

Values of R^2 in the range 0.4-0.5 indicate that less than half of the total variance is explained by the model. However, closer inspection of the association between modelled and observed behaviour (Figure 4.32) reveals that the periodicity of the observed series is retained by the model. In Figure 4.33, the unexplained variance is explored further by plotting modelled (predicted) direction change against observed direction change. The data points are clustered in the top-right and bottom-left quadrants, reinforcing the good association noted in Figure 4.32. Linear regression of the two variables gives a regression equation with a gradient of 0.49. Hence, the predicted direction change underestimates the observed direction change. Further inspection of Figure 4.32 suggests that this underestimation is manifest at the peaks and troughs in the direction change series.

To explore the spatial and temporal dynamics further, second-order autoregressive modelling was performed for each of the six planform reaches identified in Figure 4.11. Autoregressive statistics for each reach and for each survey year are presented in Table 4.3. Each reach satisfies the stationarity assumptions and the inequality for pseudo-periodicity in all survey years. This latter finding is perhaps surprising following the significance of higher order coefficients noted in the PACFs for reaches 1 and 6 (see Figure 4.31). Interestingly though, it reveals that the Lower Mississippi River has maintained a level of order in the planform morphology that is consistent with the maintenance of a regional-scale hydrodynamic control in all reaches over the temporal period considered. This is important because it indicates that despite the dramatic length and width variability in some reaches documented in sections 4.3 and 4.4, the same hydrodynamic control operates in all reaches.

The temporal variability of the mean wavelength in each reach is illustrated by Figure 4.34. In 4.34a, the mean wavelengths are plotted for both survey year and reach. These are separated in 4.34b and 4.34c, with error bars (±1 standard deviation) used to denote the corresponding temporal or spatial variability. Figures 4.34a and 4.34c show that the highest mean wavelengths (approximately 17.5 km) are found in reaches one and four. Conversely, reach six records the lowest mean wavelength (approximately 13.5 km). Temporally, there is little variation in mean wavelength in the period 1765-1887 and a slight increase thereafter. This is interesting because the broad stable temporal pattern masks the spatio-temporal

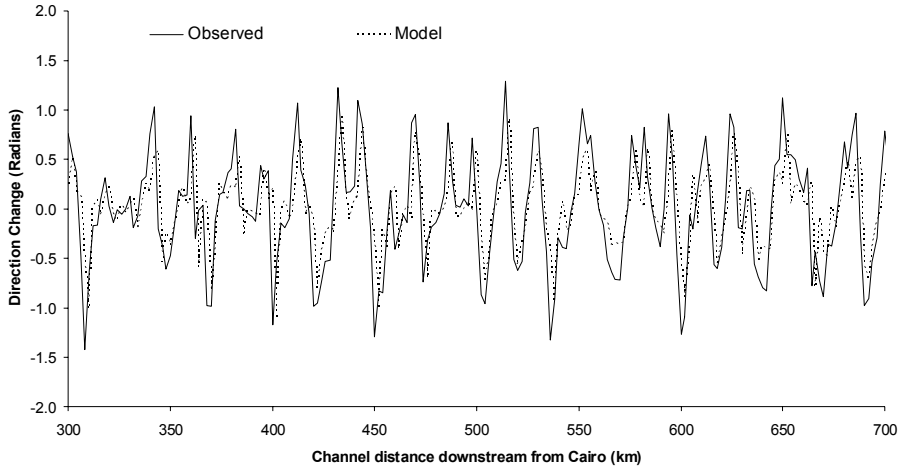

Figure 4.32 Modelled direction change in relation to observed direction change for the 1930 planform series.

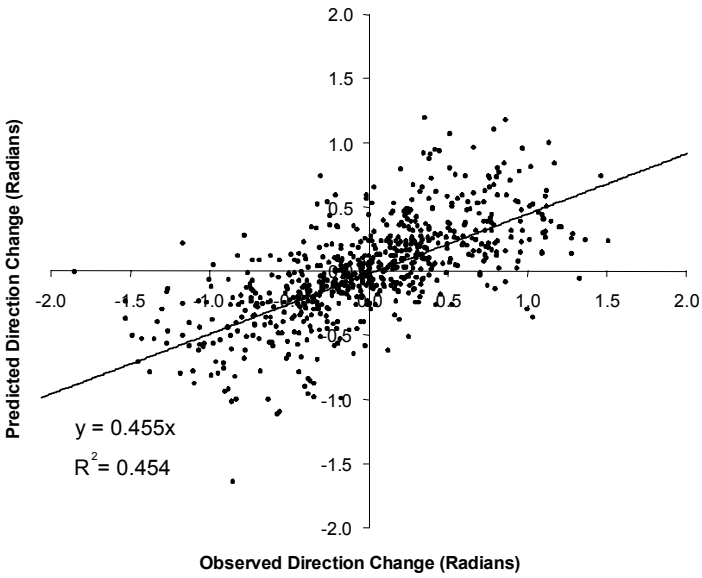

Figure 4.33 Predicted direction change against observed direction change for the 1930 planform series.

	1	2	3	4	5	6
1765						
$Ø_1$	0.920	0.809	0.903	0.963	0.809	0.642
$Ø_2$	-0.421	-0.405	-0.444	-0.522	-0.415	-0.435
Stationary?	Yes	Yes	Yes	Yes	Yes	Yes
R^2	0.509	0.446	0.492	0.55	0.426	0.355
$Ø_1^2 < -4Ø_2$?	-0.84	-0.97	-0.96	-1.16	-1.01	-1.33
Pseudo-periodic?	Yes	Yes	Yes	Yes	Yes	Yes
Wavelength (km)	16.06	14.25	15.21	14.94	14.09	11.83
1830						
$Ø_1$	0.907	0.971	0.975	0.902	0.716	0.579
$Ø_2$	-0.385	-0.520	-0.523	-0.450	-0.422	-0.348
Stationary?	Yes	Yes	Yes	Yes	Yes	Yes
R^2	0.500	0.573	0.554	0.484	0.392	0.292
$Ø_1^2 < -4Ø_2$?	-0.72	-1.14	-1.14	-0.99	-1.18	-1.06
Pseudo-periodic?	Yes	Yes	Yes	Yes	Yes	Yes
Wavelength (km)	16.73	15.10	15.12	15.08	12.73	11.88
1887						
$Ø_1$	0.831	0.886	1.022	0.900	0.717	0.618
$Ø_2$	-0.398	-0.462	-0.558	-0.350	-0.422	-0.349
Stationary?	Yes	Yes	Yes	Yes	Yes	Yes
R^2	0.453	0.505	0.613	0.511	0.392	0.305
$Ø_1^2 < -4Ø_2$?	-0.90	-1.06	-1.19	-0.59	-1.17	-1.01
Pseudo-periodic?	Yes	Yes	Yes	Yes	Yes	Yes
Wavelength (km)	14.75	14.60	15.37	17.79	12.74	12.32
1930						
$Ø_1$	0.759	0.578	0.919	0.953	0.992	0.630
$Ø_2$	-0.250	-0.307	-0.471	-0.376	-0.496	-0.312
Stationary?	Yes	Yes	Yes	Yes	Yes	Yes
R^2	0.522	0.388	0.508	0.497	0.458	0.488
$Ø_1^2 < -4Ø_2$?	-0.42	-0.89	-1.04	-0.60	-1.00	-0.85
Pseudo-periodic?	Yes	Yes	Yes	Yes	Yes	Yes
Wavelength (km)	17.73	12.30	15.01	18.46	15.92	12.93

Table 4.3 Detection of pseudo-periodicity and mean wavelength estimation by fitting second order autoregressive models to each reach. All values are given to three decimal places except the inequality for pseudo-periodicity and wavelength calculations which are given to two decimal places.

1975						
$Ø_1$	0.898	0.744	0.895	0.882	0.824	0.863
$Ø_2$	-0.321	-0.342	-0.482	-0.381	-0.343	-0.443
Stationary?	Yes	Yes	Yes	Yes	Yes	Yes
R^2	0.522	0.388	0.508	0.497	0.458	0.488
$Ø_1^2 < -4Ø_2$?	-0.48	-0.81	-1.13	-0.75	-0.69	-1.03
Pseudo-periodic?	Yes	Yes	Yes	Yes	Yes	Yes
Wavelength (km)	19.16	14.26	14.44	16.22	15.90	14.52

Table 4.3 (cont).

a)

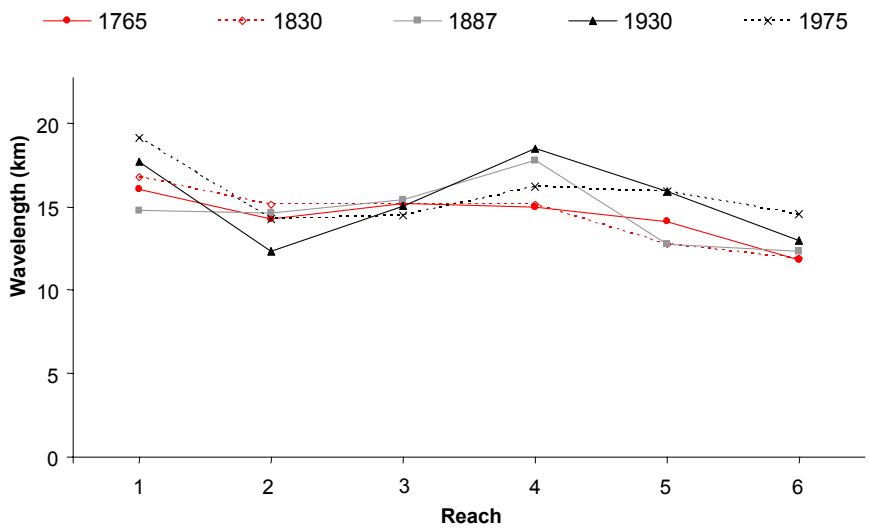

b)

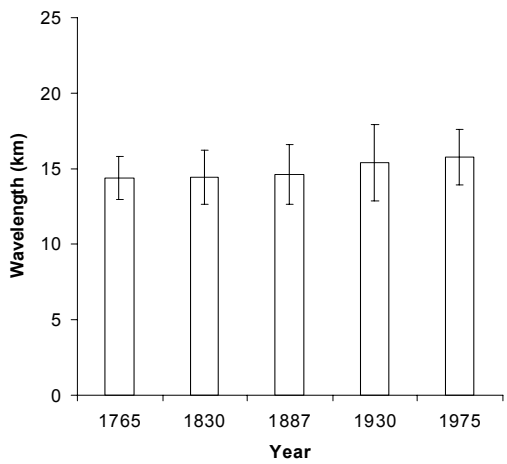

c)

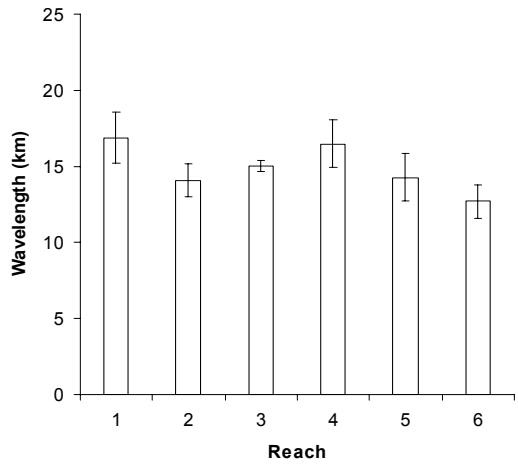

Figure 4.34 a) Mean wavelength classified by both reach and survey year; b) mean wavelength for each survey year and; c) mean wavelength for each reach. Error bars in b) and c) illustrate ± 1 SD (standard deviation) of the variability by reach and by survey year respectively.

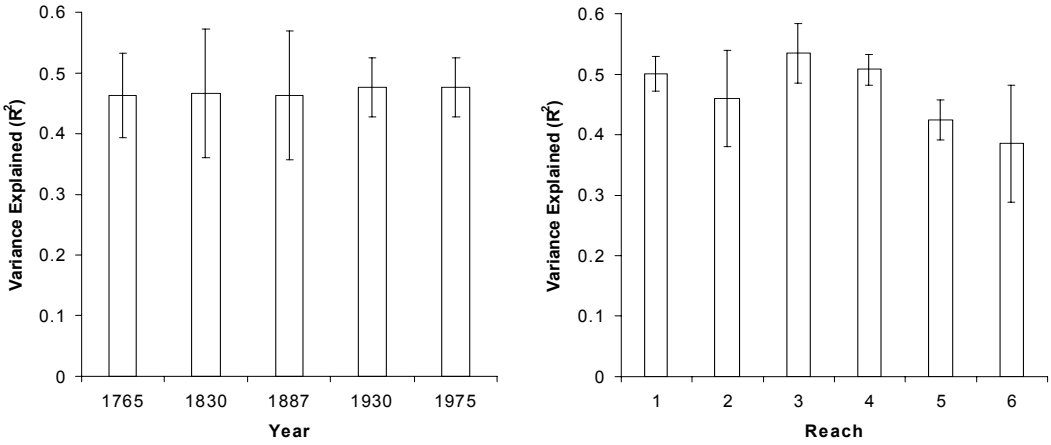

Figure 4.35 Variation explained (R^2) against: a) survey year; and b) reach. Error bars illustrate ± 1 SD (standard deviation) of the variability by reach and by survey year respectively.

variability revealed by Figure 4.34a. These findings imply therefore, that increases in mean wavelength in particular reaches are compensated for by decreases in mean wavelength in other reaches. Figure 4.35 explores the spatial and temporal variability of variation explained (R^2) by second order autoregressive modelling. The lowest proportion of variation explained is in reach six; this is consistent with the observation of significant coefficients at a higher order than two in the PACF for this reach (Figure 4.31). Once again, the inter-reach variability exceeds the temporal variability if the entire reach is considered. This indicates that autoregressive modelling becomes unsuitable as a diagnostic technique over sufficiently long reach lengths because any trend is obscured by inter-reach trends.

4.9.3 Spectral analysis

Plots of spectral density against frequency and channel wavelength are presented for the 1930 and 1975 planform surveys of the Lower Mississippi River between Cairo and Baton Rouge in Figure 4.36. By visually comparing the two plots, it is evident that there has been a lowering of peak spectral density, which is indicative of a lowering of bend amplitude, and a marginal shift of the peak spectral density to a shorter wavelength. These observations are therefore consistent with the elimination of larger bends by the artificial cutoff programme (see section 3.2.2*iv*).

A clearer analysis of series change is provided by examining the same temporal change at a finer spatial resolution, based on the six planform reaches identified in Figure 4.11. Most of the spectra are characterised by a broad single peaks, indicating that a high proportion of total series variance can be explained by fitting waveforms over a range of wavelength bands. This is consistent with a pseudo-periodic tendency and therefore provides further support for the assertion that environmental irregularities distort an underlying hydrodynamic process to give a planform that combines both regular and random components. Broad, single peak spectra were also identified by Ferguson (1975) in most of 19 British rivers surveyed. Hence, it suggests that the planform of the Lower Mississippi River, both before and after the artificial cutoff programme and extensive bank stabilisation, demonstrated variance properties similar to other alluvial river systems.

The greatest changes in the form of spectra are notable in reaches, three, four and five. This is not surprising because all sixteen of the artificial cutoffs are located within these three reaches (see Figure 2.9). In reach three, the 1930 peak in spectral density at a wavelength of approximately 25 km is not present in 1975. This elimination of longer wavelengths is consistent with the elimination of large bends. Meanwhile, the lowering of the peak spectral density in reaches 4 and 5 is indicative of declining bend amplitude. Both upstream and downstream of the artificial cutoff reach, in reaches 1, 2, and 6, there are no significant changes in the form of the spectral density plot. This provides further evidence that the changes observed in reaches 3, 4 and 5 are directly attributable to the artificial cutoff programme.

To extend the analysis temporally, additional spectral density plots were generated for each reach for the period 1765-1887. The dominant wavelength and associated peak density were recorded following visual inspection. In Figure 4.38, variations in spectral density are plotted against variations in peak wavelength for each global reach. The points are joined in order to highlight the trajectory of each spectral density-wavelength relationship in the period 1765-1975. Most significantly, visual comparison of reach trajectories indicates a general absence of inter-reach consistency, suggesting that the planform dynamics of each reach was unique over the period of analysis. This is particularly interesting when viewed in conjunction with Figure 4.39 which illustrates regional-scale temporal trends in both parameters. There is no discernable regional-scale temporal trend in meander wavelength and similarly, with the exception of the artificial cutoff period 1930-1975 (as noted in Figure 4.37), there is no discernable trend in spectral density. Thus, in the pre-cutoff period at least, although planform characteristics are inconsistent at the reach-scale, relatively stable 'average' planform characteristics are maintained at the regional-scale.

The magnitude of inter-reach planform dynamics is indicated by the total length of each trajectory in Figure 4.33. The data points in reaches one, six, and to a lesser extent reach two, are clustered into a specific segment of the plot and thus, total trajectories are relatively short in comparison to the remaining reaches where data

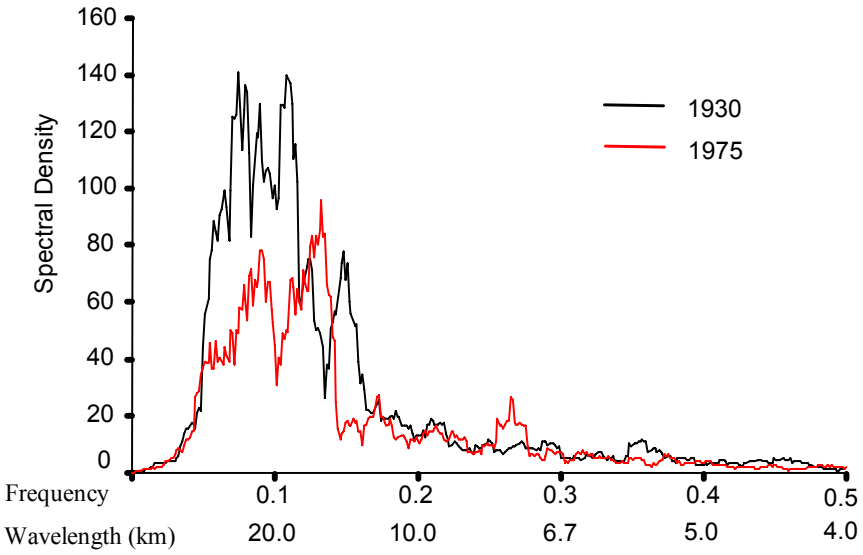

Figure 4.36 Spectral density plots for the Lower Mississippi River between Cairo and Baton Rouge, in 1930 and 1975. A Tukey-Hanning filter of nine intervals has been used to smooth the series. Based on direction change series sampled a regular 2 km intervals.

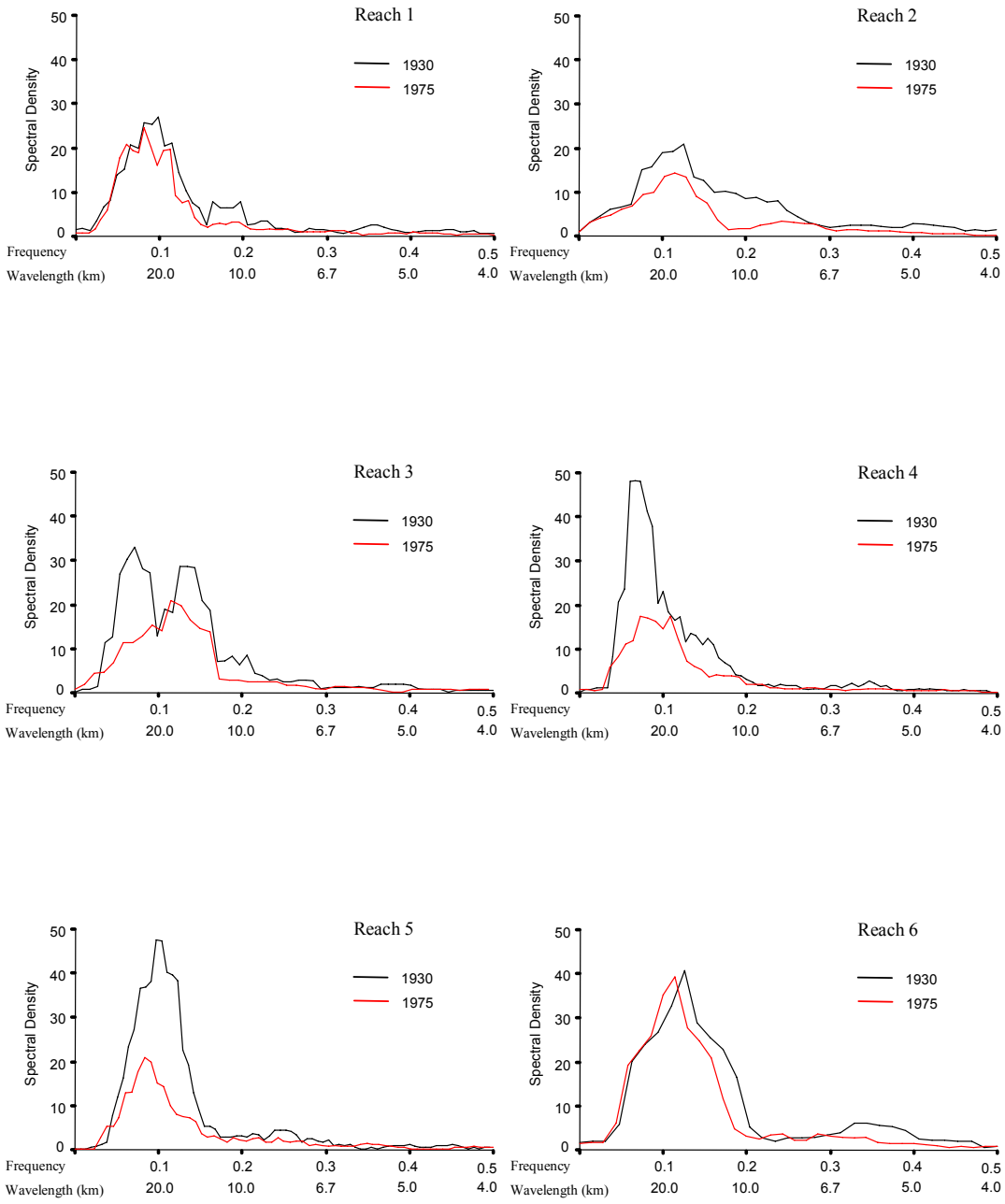

Figure 4.37 Spectral density plots for the six planform reaches of the Lower Mississippi River from Cairo to Baton Rouge (Figure 4.11) for the 1930 and 1975 planform series.

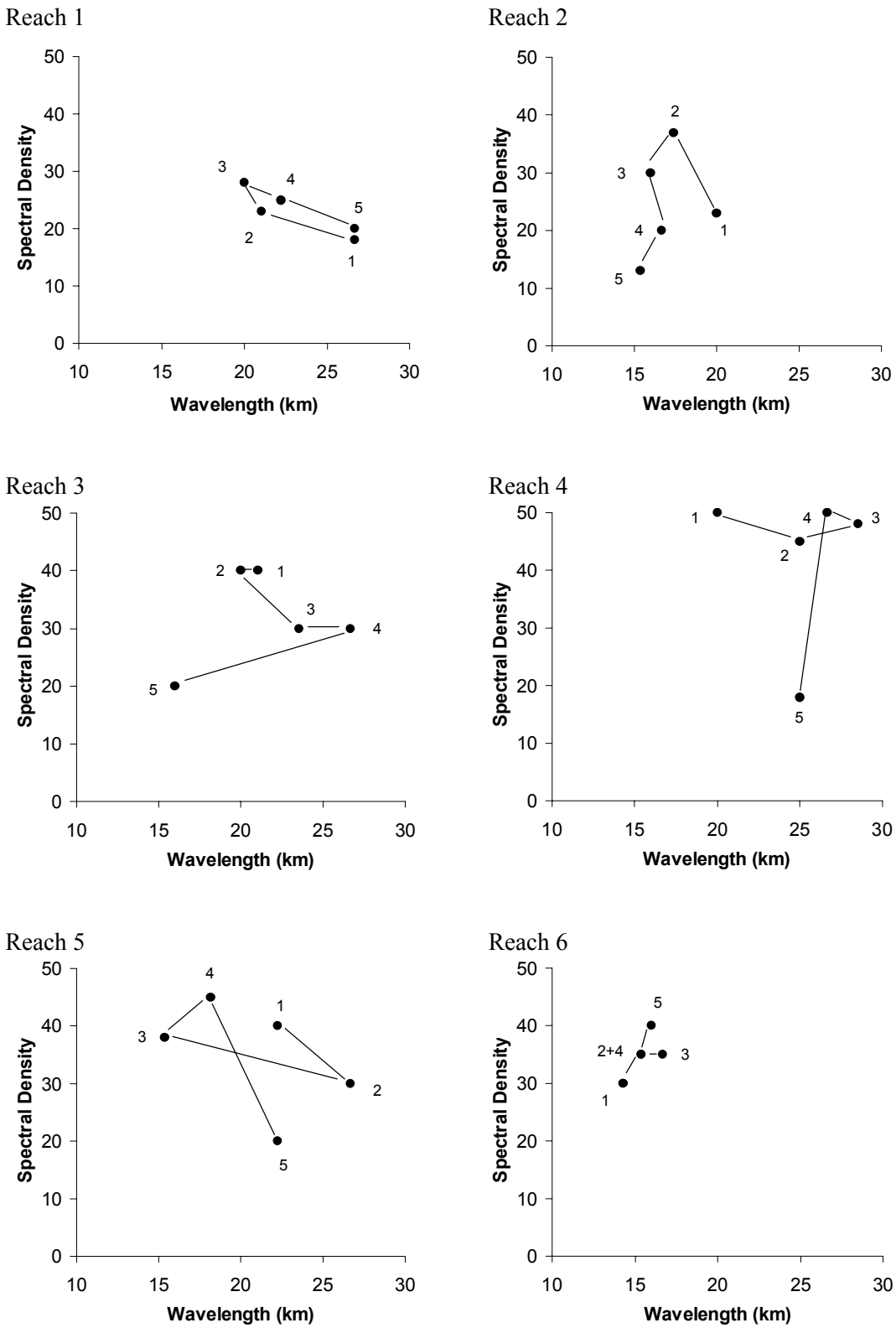

Figure 4.38 Plots of peak spectral density against wavelength for the six global reaches identified in Figure 4.11. Each point is labelled in the range 1-5 where:
1 = 1765; 2 = 1830; 3 = 1887; 4 = 1930; and 5 = 1975.

a) b)

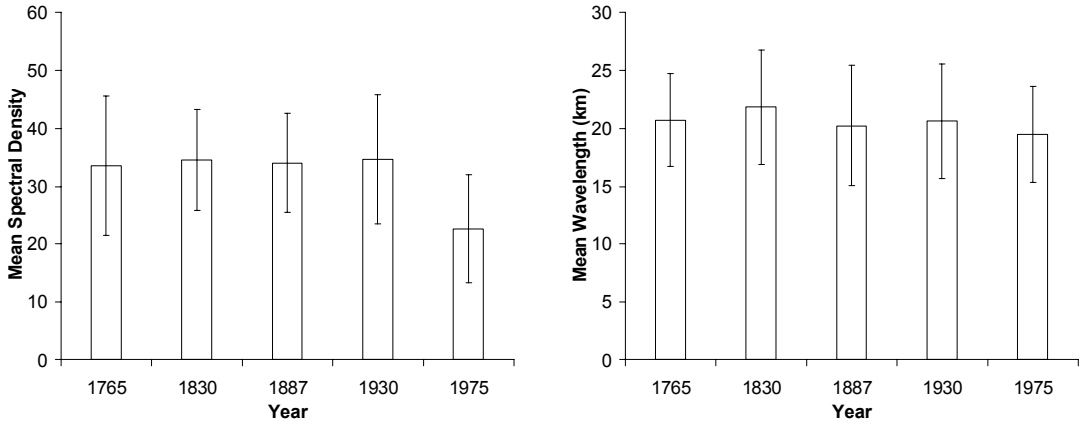

Figure 4.39 a) Peak spectral density and b) peak wavelength for each survey year for the Lower Mississippi River between Cairo and Baton Rouge. Error bars illustrate ± 1 SD (standard deviation) of the variability by reach or by survey year respectively.

points are more widely scattered. Hence, there is greater stability of amplitude-wavelength characteristics over the period in these reaches. This observation is consistent with the greater stability of these reaches in terms of length and width variation in relation to the artificial cutoff reaches (sections 4.4 and 4.5).

4.9.4 Meander bend statistics

i) Identification of inflexion points

Planform inflexion points are located at turning points in the direction series, where direction change is equal to zero. A customised routine was developed to identify such turning points in each of the five planform surveys of the Lower Mississippi River. The number of identified points of inflexions is dependent on the sampling interval; particularly at relatively short intervals (Hooke, 1984). This is illustrated by the asymptotic nature of the relationship in Figure 4.40.

The object of identifying inflexion points is to divide each planform into a series of meander bends which have a physical significance. This is a subjective task because it involves confronting the basic problem of when does a curve in the planform become a meander bend (Hooke, 1984). For example, the high number of inflexion points at sampling intervals shorter than 0.5 km in Figure 4.34 is most likely associated with high frequency 'wobble' in the digitising process (Hooke, 1984) in addition to the presence of larger meander bends. As the sampling interval increases, the number of inflexion points decline and hence, high frequency 'wobble' is removed. However, at larger sampling intervals there is a concurrent loss in the potential accuracy of meander bend definition. Given this trade-off, a compromise sampling interval of one kilometre was selected to identify inflexion points. This is half the standard sampling interval used throughout this chapter (section 4.2).

Following determination of a basic sampling interval, distance-based and curvature-based tolerances were applied to filter identified inflexion points which were not deemed to have physical significance. The distance-based tolerance specified a minimum distance between consecutive inflexion points. This is explored using three tolerance values in Figure 4.41. Fourteen inflexion points are identified using a tolerance value of zero kilometres (i.e. no tolerance value). This identifies every

turning point in the direction series irrespective of the magnitude of total distance between inflexion points. Using a tolerance value of one kilometre (i.e. one sampling interval), only ten of the original inflexion points are identified; this reduces further to just six inflexion points when a tolerance value of two kilometres (i.e. two sampling intervals) is applied. If these points are superimposed on the original planform, the original fourteen inflexion points delineates two very short reaches, between points one and two, and nine and ten. Meanwhile, using a tolerance value of two kilometres does not divide the reach between inflexion points labelled seven and twelve into two discrete meander bends. Given these observations, a minimum distance tolerance value of one kilometre was applied.

A curvature-based tolerance specified a minimum angle change between consecutive inflexion points. This was explored using tolerance values in the range 0.1-0.5 radians. The most realistic set of inflexion points were obtained using tolerances in the narrower range of 0.2-0.3 radians. These are illustrated in Figure 4.42a and 4.42b. A tolerance value of 0.2 radians does not filter the inflexion points symbolised by crosses in Figure 4.42a. These define a very short straight reach which may be considered part of the larger meander bend, defined by the filled circles immediately upstream and downstream from the crosses. Meanwhile, if the tolerance value is increases to 0.3 radians, the inflexions points symbolised by unfilled circles in Figure 4.42b are removed. This leaves a large bend defined by the upstream and downstream filled circles when in fact the reach is relatively straight. Hence, a minimum curvature tolerance of 0.25 radians was applied alongside the minimum distance tolerance in the identification of inflexion points.

The set of identified inflexion points using the final procedure (including the distance and curvature tolerances) is displayed for the reaches immediately upstream and immediately downstream from Vicksburg in Figures 4.43a and 4.43b. Visual inspection does reveal that the procedure identifies an appropriate set of meander bends from which parameters can be estimated and analysed. The term 'appropriate' is used loosely because the developmental procedure discussed in the preceding paragraphs may be criticised on the grounds of subjectivity. This problem has been experienced by previous researchers: Hooke (1984) states that there is a lack of standardisation in the choice of points between which to make measurements when

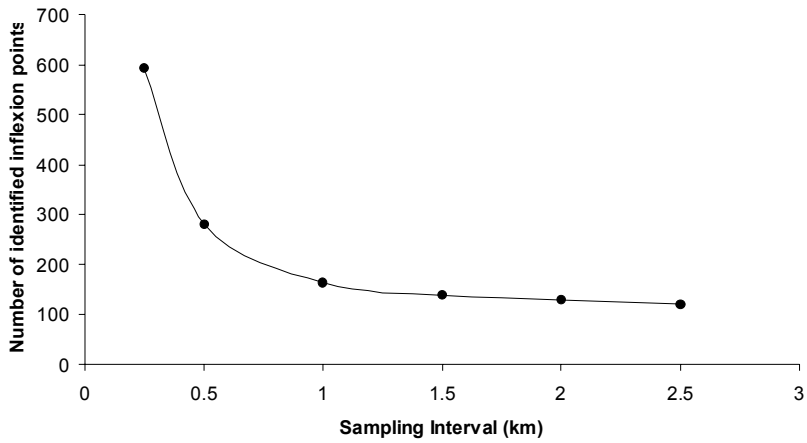

Figure 4.40 Number of identified inflexion points against original sampling interval for the 1930 planform survey.

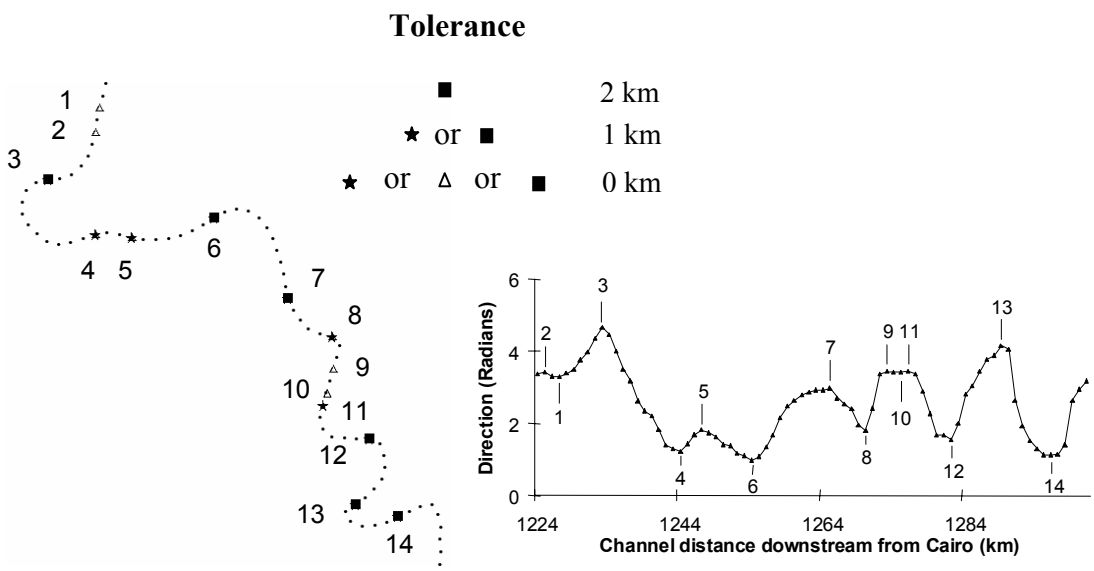

Figure 4.41 Identification of inflexion points in the 1930 planform survey by applying a tolerance value specifying a minimum distance between inflexion points. The reach shown is located approximately 1225-1300 km downstream from Cairo (downstream from Baton Rouge).

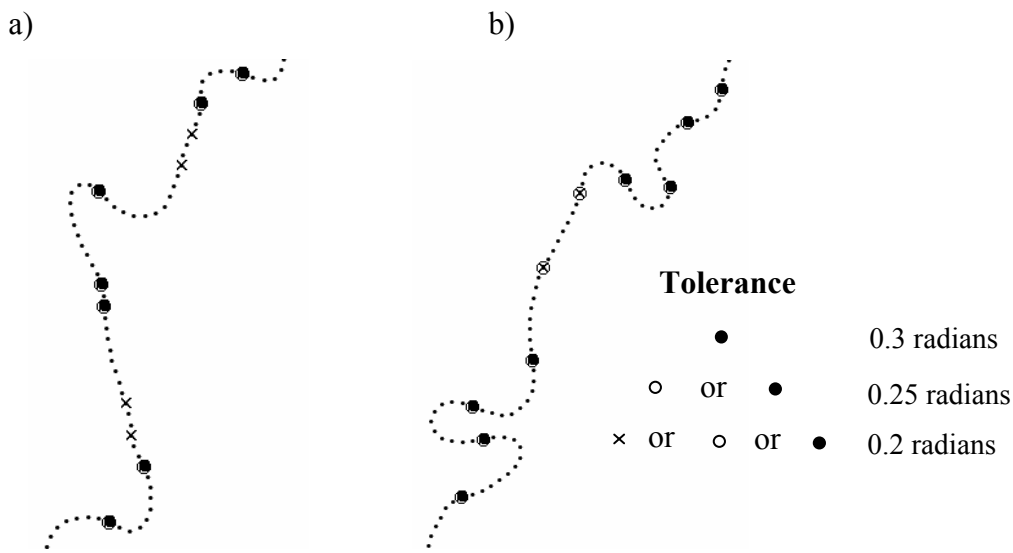

Figure 4.42 Identification of inflexion points in the 1930 planform survey by specifying an additional tolerance based on angle change.

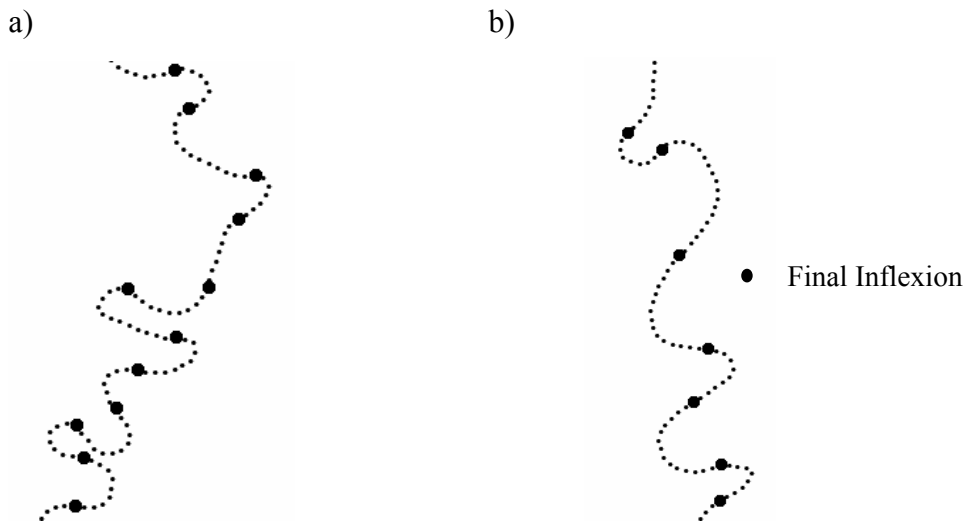

Figure 4.43 The final set of identified inflexion generated by specifying a minimum distance tolerance of 1 km and an angle change tolerance value of 0.25 radians.

estimating meander bend parameters and Lewin (1977; 171) states more generally that it is *'notoriously difficult'* to achieve a measure of objectivity in assessing meander wavelength in tortuous or irregular channels by sampling individual meander bends. Parameter replicability is explored in relation to parameters estimated from serial techniques in section 4.9.5.

ii) Meander bend parameterisation and analysis

In a regular meander form, the meander wavelength, as defined by Inglis (1947) and Leopold and Wolman (1960), is the wavelength of two consecutive and symmetrical meander loops. In meander planforms of most natural rivers, this definition is problematic to apply because adjacent meander loops vary widely in size. However, over sufficiently long river reaches, the average wavelength would be expected to be approximately twice the average wavelength measured between consecutive points of inflexion. Bend parameters were therefore calculated between identified inflexion points, as illustrated in Figure 4.44.

In Figure 4.45, bend amplitude is plotted against bend wavelength for the six global reaches identified in Figure 4.11. The temporal trajectory within each reach is very different to that revealed using spectral techniques in Figure 4.38. This apparent lack of association is discussed in greater detail in section 4.9.5. Despite this however, the same relative trends are apparent. The most upstream and downstream reaches (1 and 6) are generally less dynamic in terms of bend amplitude-wavelength variation than reaches 2-5. The period of artificial cutoff construction was characterised by a considerable increase in bend wavelength in reaches 2-5, and a decrease in bend amplitude in the artificial cutoff reach (3-5). Surprisingly, the two periods of net lengthening (1765-1830 and 1887-1930) demonstrate very different characteristics: the earlier period is characterised by decreases in both amplitude and wavelength in all reaches except reach 1, and the latter period is characterised by increases in both amplitude and wavelength in reaches 3-5. This is important because, referring back to section 4.8, it demonstrates that bend size declined in the earlier period (and consequently, large-scale form resistance probably increased), whereas channel lengthening probably had the opposite effect during the latter period. These responses are consistent with the likely elevation of sediment loads during the late nineteenth and twentieth centuries by a range of anthropogenic causes (section 4.6)

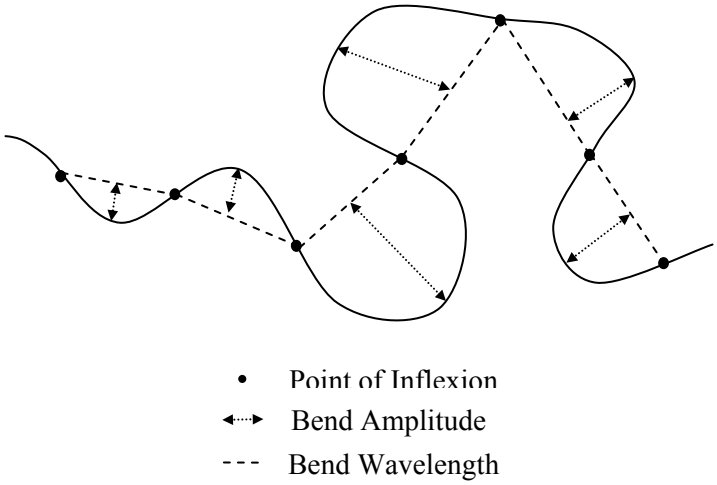

Figure 4.44 Identifying parameters from ‘unpaired’ meander bends (after Brice, 1983).

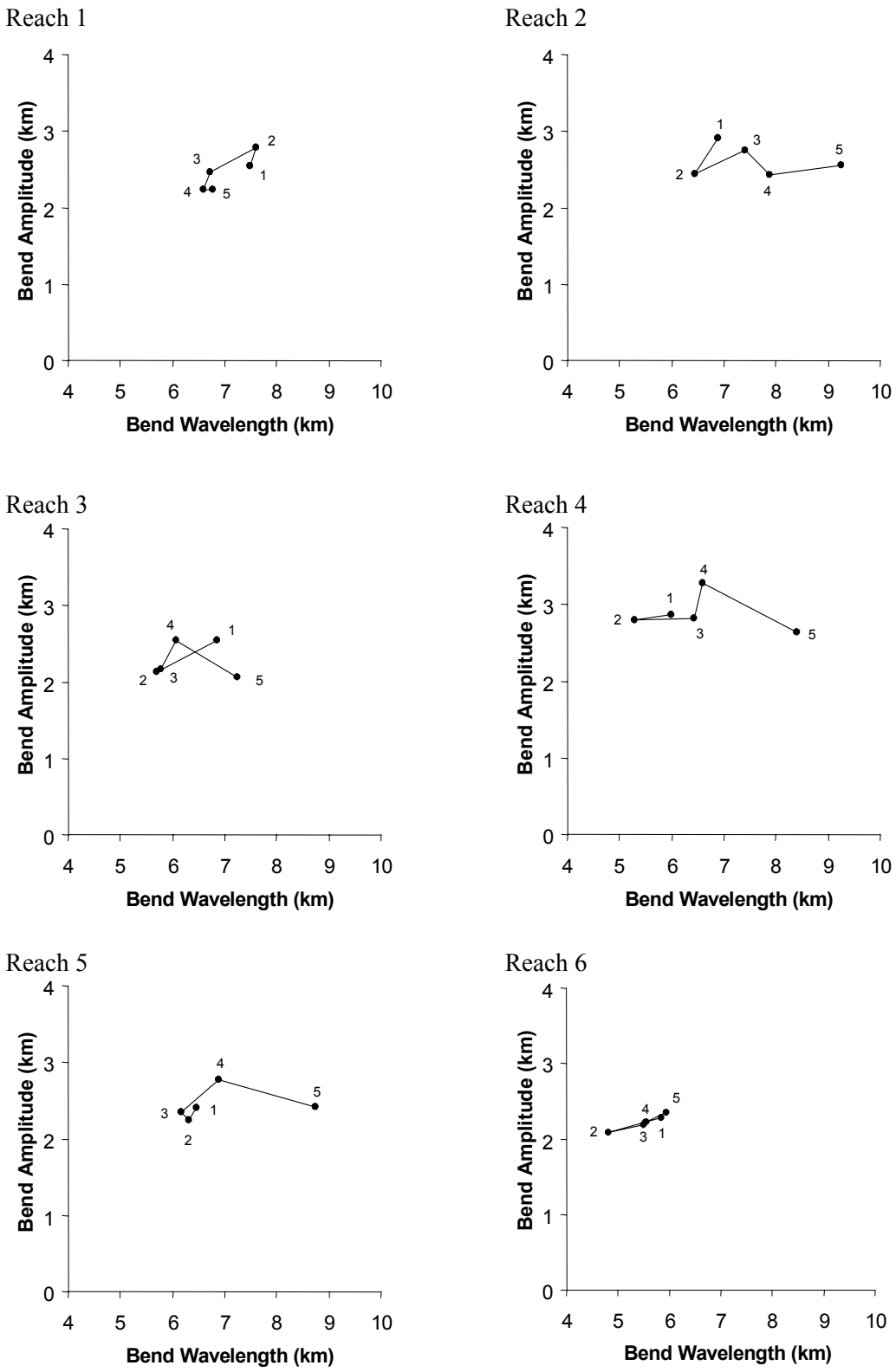

Figure 4.45 Plots of mean bend amplitude against mean bend wavelength for the six reaches identified in Figure 4.11. Each point is labelled in the range 1-5 where:
1 = 1765; 2 = 1830; 3 = 1887; 4 = 1930; and 5 = 1975.

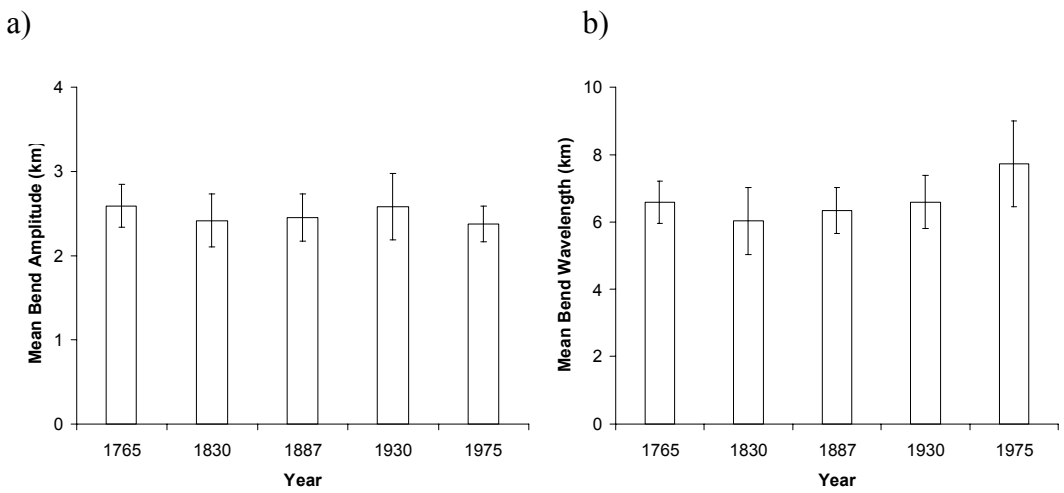

Figure 4.46 a) Mean bend amplitude and b) mean bend wavelength for each survey year for the Lower Mississippi River between Cairo and Baton Rouge. Error bars illustrate ± 1 SD (standard deviation) of the variability by reach or by survey year respectively.

because higher sediment loads provide a form of flow resistance and thus, reduce the requirement for flow resistance to be increased through morphological changes.

Figure 4.46 reveals that at the regional-scale, relatively stable characteristics are maintained in bend amplitude throughout the 1765-1975 period, and in bend wavelength at least in the pre-modification period. These trends are explored in relation to the trends from other techniques in the next section.

4.9.5 Meander wavelength estimation: comparability between techniques

The three techniques used to estimate meander wavelength are compared by survey year and by reach in Figure 4.47. At first glance, these plots reveal considerable differences between estimates from each technique, classified by both reach and survey year. The highest wavelengths are generally generated using spectral analysis, followed by autoregressive modelling and then the inflexion point technique. This order reflects the different methods of wavelength estimation. By estimating wavelength from the dominant peak in direction change spectra, spectral analysis records the wavelength of the waveform that explains the highest proportion of the total variance of the series. However, the wavelength estimated from autoregressive modelling represents the mean wavelength of the pseudo-periodic model fitted to the data series. Although these two estimates represent different measures of wavelength within the spatial frequency domain, they are complementary because they describe different properties of a single wavelength distribution. The difference between the two estimates can be explored with reference to a hypothetical spectral density plot (Figure 4.48). The difference between spectral and autoregressive estimates of wavelength estimates is greater when the spectra is characterised by a sharp peak at a long wavelength rather than a broad peak at a short wavelength because the distribution of variance associated with fitting a range of waveforms is less skewed. In Figure 4.47a, this is demonstrated by the greater difference between wavelengths estimated from spectral and autoregressive techniques in 1830 and 1930 than the other survey years. This is also evident in Figure 4.47b by the greater differences in reaches three, four and five than reaches two and six.

a)

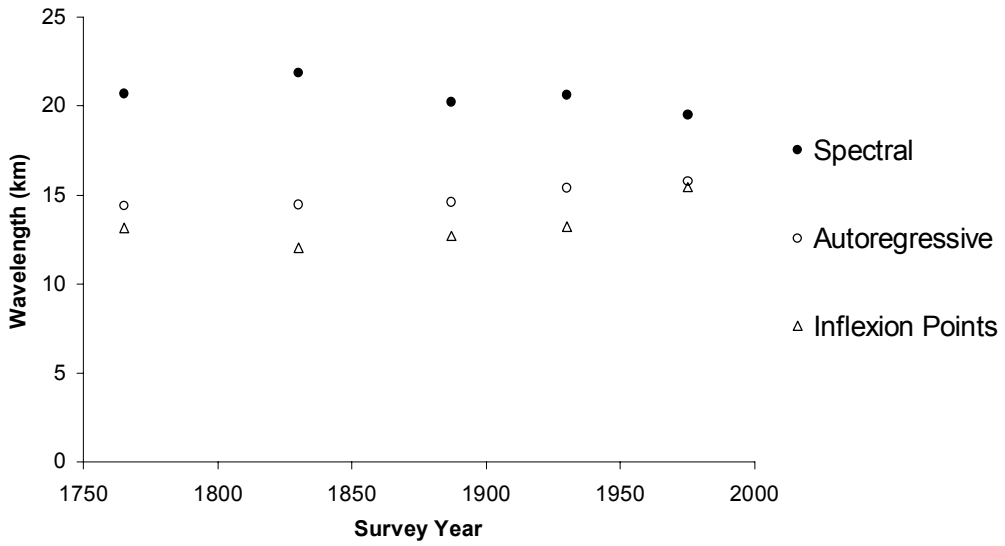

b)

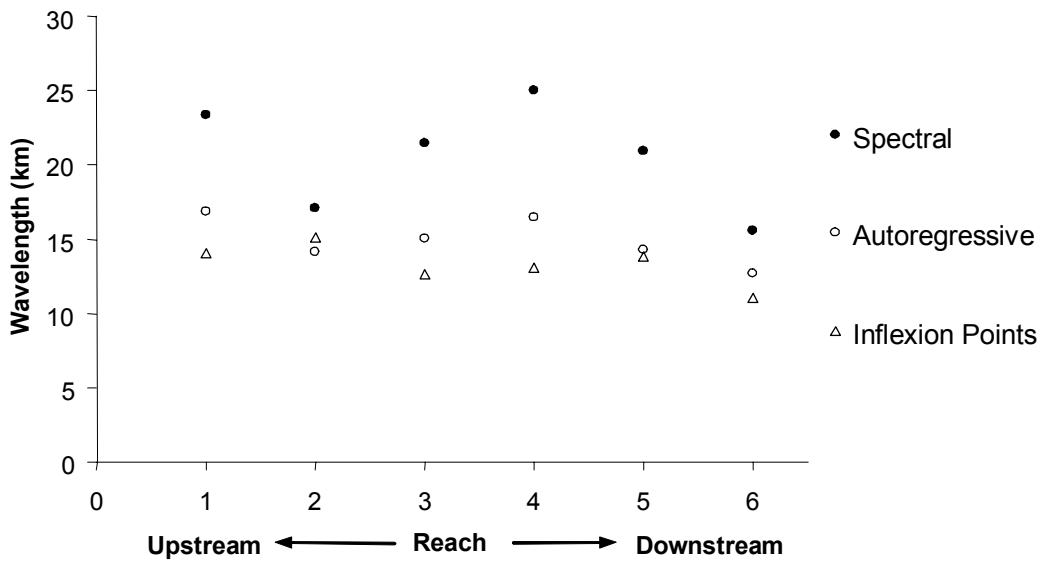

Figure 4.47 Comparison of meander wavelengths estimated by spectral, second-order autoregressive and inflexion point techniques. In a) the average wavelength for the Lower Mississippi River from Cairo to Baton Rouge (regional-scale) is plotted against the corresponding survey year. In b) the time averaged (1765-1975) wavelength is plotted against the corresponding survey reach. Reaches correspond to those identified in Figure 4.11.

Wavelengths estimated by the inflexion point technique are consistently lower than estimates from both spectral and autoregressive techniques. This observation can be explained by considering the representativeness of identified points of inflexion in relation to true planform variability. Viewed individually, bends in a meandering river represent a range of geometric forms including regular sine generated curves (Langbein and Leopold, 1966) or circular arcs (Brice, 1973) and more irregular forms. This diversity is highlighted on the Lower Mississippi River by the wide scatter in the bend amplitude-wavelength relationship (Figure 4.49).

However, this wide diversity only provides a partial insight into the true variation because, over longer reaches of river, planform is the product of the juxtaposition of bends of a range of different sizes and shapes (Furbish, 1991) in which small and simple meanders are superimposed on more complex meanders and larger scale undulations. This diversity of meander bend morphology has been noted by several previous researchers. In particular Brice (1974) required 4 major categories and 16 form types to be able to adequately classify meander bends from 125 alluvial stream reaches and Hooke and Harvey (1983) have noted a wide range of meander bend behaviours on the River Dane in the UK. Given this diversity, applying the inflexion point technique is problematic because it is only able to define meander bends at the smallest spatial scale. Therefore, it cannot account for compound meander bend features that contain more than one inflexion point (Carson and Lapointe, 1983). Figure 4.50 illustrates this problem. Three meander bends (numbered 2, 3 and 4) have been defined by the identification of four points of inflexion, however, total planform variation is not adequately accounted for because these three bends are contained within a much larger meander bend (numbered 1) whose wavelength is ignored by the procedure.

Stolum (1996) has advanced this idea of nested meander bends by showing that the planform of the meandering Juará River in the Amazon basin can be decomposed into a hierarchy of multiple scales of meander forms. Viewed in this way, wavelengths estimated between identified inflexion points in the original planform series represent only the first order of variability. Scales of planform variability on the Lower Mississippi River were explored further using the inverse renormalisation procedure outlined by Stolum (1996). Inflexion points identified from the original

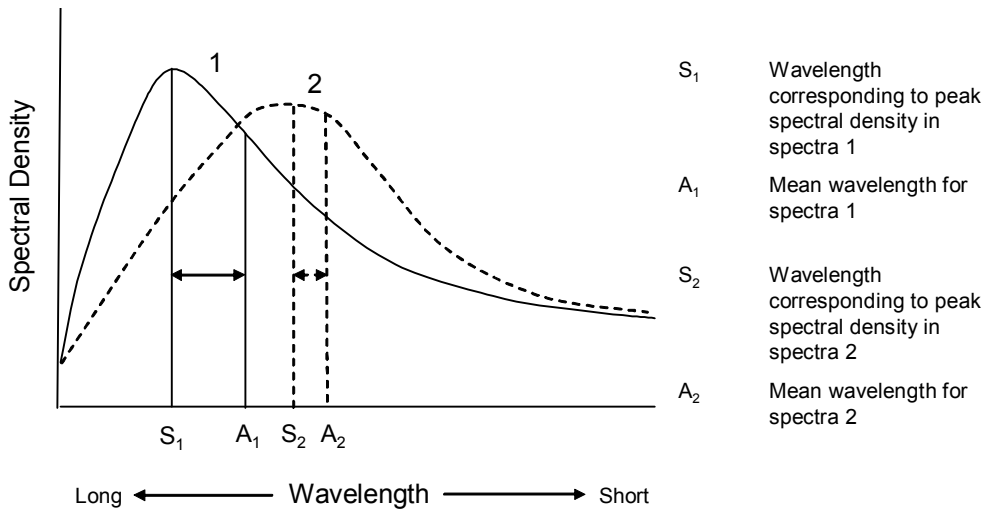

Figure 4.48 Hypothetical direction change spectra showing that as the dominant peak spectral density broadens, the distribution becomes less skewed and the dominant wavelength therefore approaches the mean value.

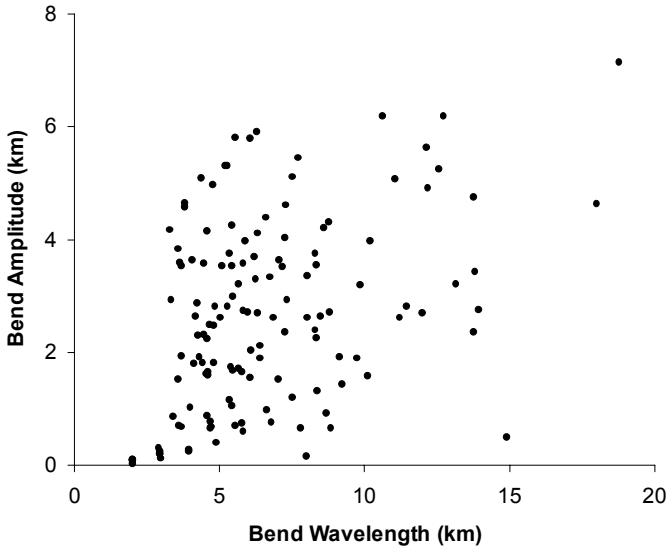

Figure 4.49 The relationship between bend amplitude and bend wavelength for first order points of inflexion identified from the 1930 planform series.

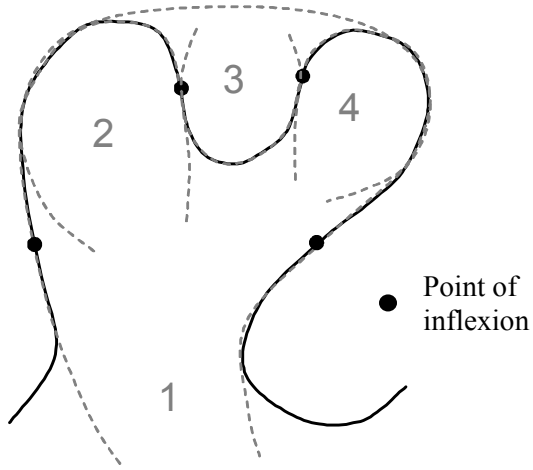

Figure 4.50 Hypothetical superimposition of meander bends

planform series were defined as first-order inflexion points. These inflexion points were then connected to form a new meandering course that defines the next hierarchical level of the planform. Second-order inflexion points were identified using the same method as applied to the first-order planform. This process was repeated to generate the four scales of planform illustrated in Figure 4.51. In Figure 4.52, the second-order wavelengths are plotted as a histogram alongside the first-order wavelengths. Although the modal wavelength of the two distributions falls in the class 5-10 km, the second order wavelength distribution is strongly negatively skewed. Consequently, the mean second-order wavelength of 30.1 km is considerable greater than the mean first-order wavelength of 5.8 km. This comparison therefore shows that estimates of meander wavelength using a point of inflexion technique (first-order) are incapable of accounting for longer wavelengths in the distribution and thus, average estimates of meander wavelength are significantly underestimated.

Given the differences in the three techniques noted above, it is important to evaluate the extent to which each technique can be used to inform spatial and temporal variations in flow resistance. Energy expenditure through a reach is determined by the total curvature in relation to reach length. Energy expenditure is increased as large bends deform into compound bends of the type shown in Figure 4.50 to create additional flow resistance. It is the average wavelength of all bend forms, irrespective of the extent to which bends can be considered part of a larger compound form, which is of principal interest. This is a first-order measure of wavelength, obtained from the inflexion point technique. The wavelength that explains the greatest proportion of variation obtained from spectral analysis cannot alone be directly related to form resistance. However, it is complementary to the first-order measure of wavelength because the difference between the spectral wavelength and the average inflexion point wavelength provides an estimation of the proportion of meander bends that could be classified as existing within a larger compound bend form. This difference therefore is diagnostic of the extent to which the river has had to increase energy expenditure by developing complex, compound bend forms.

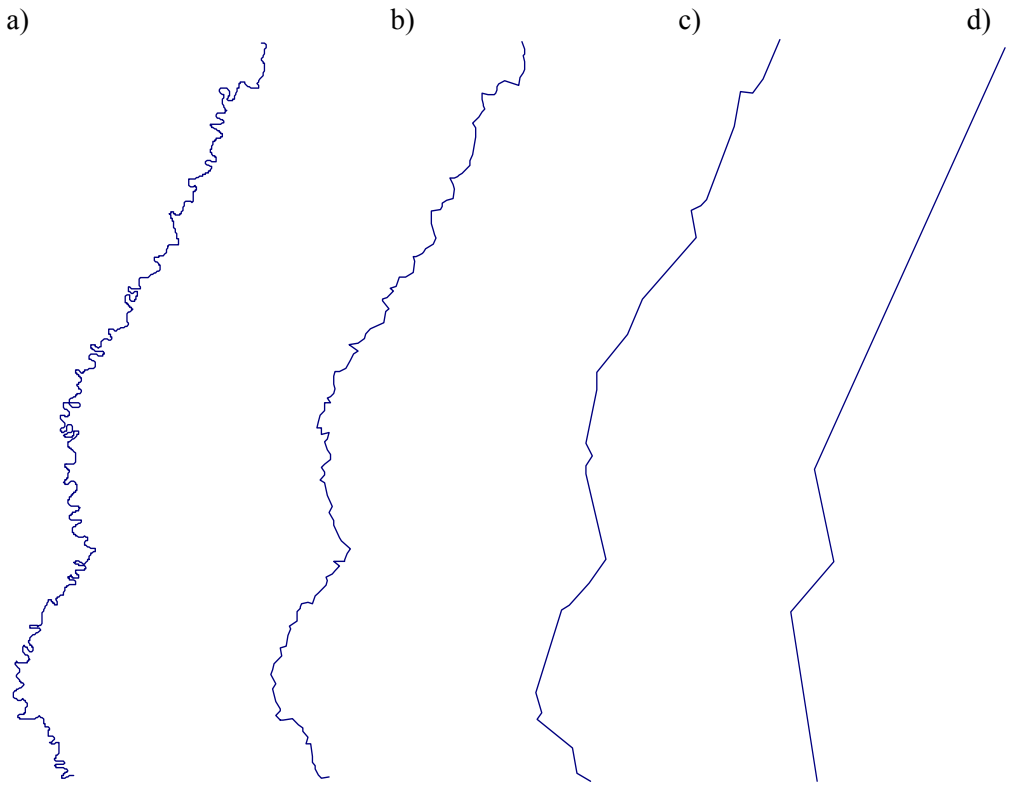

Figure 4.51 Generation of a hierarchy of meanders and higher order undulations in the 1930 planform series by the inverse renormalisation method: a) First-order; b) second-order; c) third-order and d) fourth-order. See text for further description.

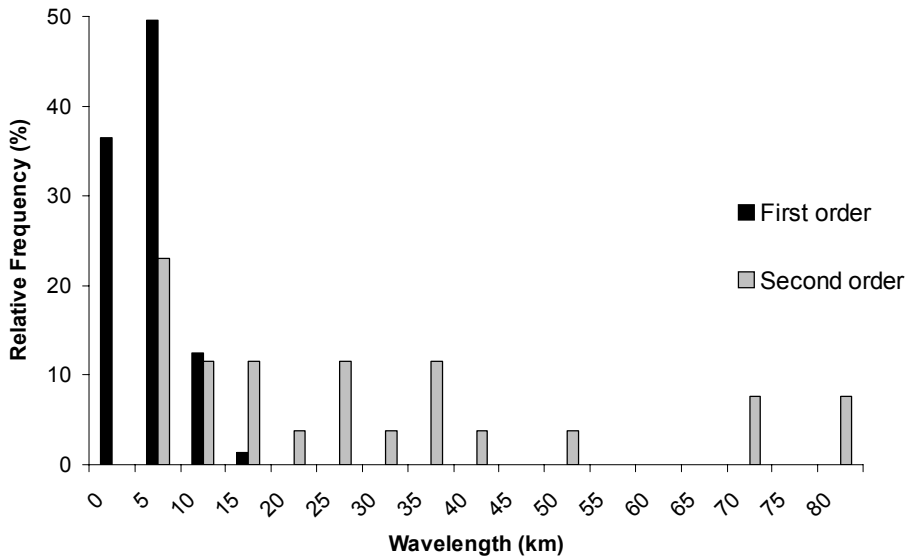

Figure 4.52 The distribution of wavelengths computed between identified points of inflexion in the first and second-order hierarchy for the 1930 planform series.

The differences in the inflexion-point wavelength estimation and the spectral wavelength estimation revealed in Figure 4.47 must be viewed within the context of variations in channel length (Figure 4.16) and radius of curvature (Figure 4.24). Regional-scale temporal variations in Figure 4.47a reveal that the two periods of net lengthening exhibit considerably different behaviours in terms of planform dynamics. In the 1765-1830 period, the increase in the difference between the two wavelength estimations indicates that meanders developed into more complex, compound forms to increase energy expenditure. Meanwhile in the 1887-1930 period, a shorter period experiencing greater total lengthening, there is very little change between the two estimates of wavelength. Hence, on average, more compound meander forms probably did not develop. This difference is supported by changes in radius of curvature: median radius of curvature declined over the earlier period (bends became tighter) but there is very little change in the latter period. This difference in planform behaviour is consistent with the idea that sediment loads increased throughout the nineteenth and early twentieth centuries and thus, a greater proportion of total energy expenditure was required to perform sediment transport processes in the latter period. As a consequence, there was not the requirement to increase large-scale form resistance by developing tighter bends.

Figure 4.47a also reveals that by 1975, the difference between inflexion point and spectral wavelength estimations is lower than at any other survey date in the previous 210 years. Removing the most sinuous bends by the artificial cutoff programme therefore reduced the form resistance offered by the planform configuration in addition to steepening the long profile. Spatial pattern of differences in wavelength estimation (Figure 4.47b) reveals that over the total time period, complex, compound meander bend forms were more commonly found in the artificial cutoff reaches (3-5). This is consistent with spatial patterns of both length changes and radius of curvature changes. Physical explanations for this observation are offered in section 4.10.

Although the difference between wavelength estimates can be used as an important diagnostic tool, it is evident that the actual change in estimated wavelength is strongly dependent on the technique selected. This is exemplified by the change in wavelength when a reach is straightened such as during the period of artificial cutoff

construction (1930-1975). Figure 4.47a shows that spectral analysis records a decrease in wavelength whereas the bend inflexion technique records a considerable increase in bend wavelength. This apparent inconsistency can be explained by considering how a regular waveform of varying amplitude and wavelength can produce a low sinuosity indicative of a straighter reach. Referring back to Figure 4.26, this can be achieved by some combination of two translations of a regular waveform: by increasing wavelength whilst maintaining amplitude as constant; or by decreasing amplitude whilst maintaining wavelength as constant. This concept is emphasised if wavelength distributions between identified points of inflexion are categorised according to an arbitrary sinuosity value such as 1.5 (Figure 4.53). Although the average characteristics of each distribution are comparable (denoted by either mean, mode or median), straighter reaches (i.e. where sinuosity < 1.5) demonstrate a greater range of wavelengths and therefore, show a tendency to be both longer, and shorter than more sinuous bends. Thus, it is possible that the opposing tendencies in meander wavelength recorded by spectral and bend inflexion techniques are both consistent with declines in sinuosity.

Greater consistency can be achieved however if variations in amplitude are considered alongside wavelength. Although the amplitude-wavelengths plots for spectral analysis and inflexion point techniques (Figures 4.38 and 4.45 respectively) are inconsistent in terms of the actual variations within each reach, both Figures do reveal that the relationship is more dynamic in the midstream reaches 2-5 than the most upstream and downstream reaches (1 and 6). This is consistent with the variation in channel length, width, and radius of curvature noted in sections 4.4, 4.5 and 4.8. Moreover, the regional-scale changes in meander wavelength and amplitude are not inconsistent with variations in sinuosity. This can be demonstrated using the example of the abrupt changes in the artificial cutoff period (1930-1975). At the regional-scale (all reaches), spectral analysis revealed a larger decrease in amplitude than wavelength (Figure 4.39). Referring back to Figure 4.26, these simultaneous changes are consistent with a decrease in total sinuosity and hence, net straightening. Meanwhile, inflexion point analysis estimated a considerably larger increase in wavelength than amplitude which is also consistent with a net decrease in sinuosity. From these observations, it can be concluded that although inter-technique

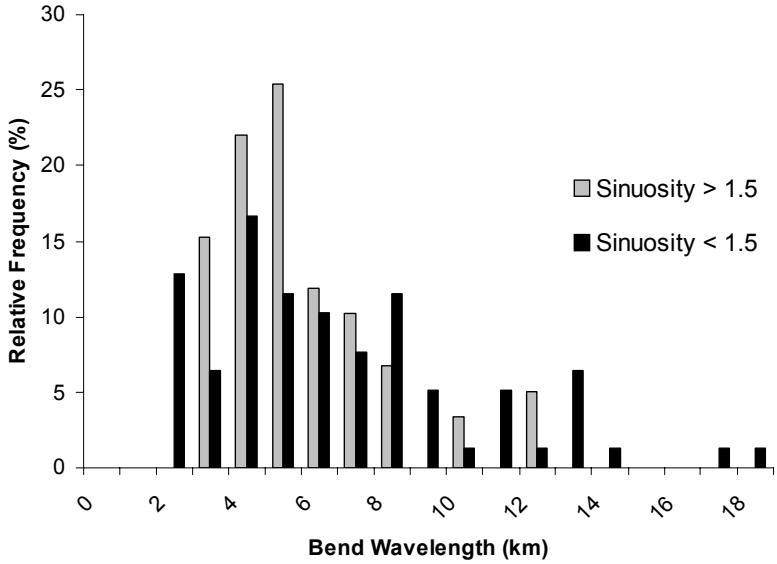

Figure 4.53 The distribution of wavelengths for bends with a sinuosity greater than 1.5 in comparison to all bends for the 1930 planform series.

consistency is not apparent in terms of recording absolute variation, the relative changes recorded by each technique are consistent.

4.9.6 Empirical relations between meander wavelength, channel width and channel discharge

Comparing the changes in meander wavelength discussed above with respect to recognised empirical relationships provides a method of evaluating the extent to which the planform dynamics of the Lower Mississippi River exhibit similar properties to those of other alluvial rivers. The suitability of two sets of empirical relations, developed at a range of scales and in a range of fluvial environments, is explored: between meander wavelength and channel width; and between meander wavelength and channel discharge.

i) Meander wavelength and channel width

The most widely quoted relationship between meander wavelength (λ) and channel width (w) is presented by Leopold and Wolman (1957, 1960) who identified consistent power-law regression relation where:

$$\lambda = 10.9\, w^{1.01} \qquad (4.3)$$

Because these relationships transcend scales, at any one scale, the nature of the reported relationships are more variable. For example, the upper bound and lower bound wavelength-width relations noted by Leopold and Wolman (1957, 1960) in the formulation of the above relationship are presented in Table 4.4 along with earlier empirical relations reported by Inglis (1947).

Source	**λ**
Leopold and Wolman (1957, 1960) – lower limit	$7.32\ w^{1.1}$
Leopold and Wolman (1957, 1960) – upper limit	$12.13\ w^{1.09}$
Inglis (1947), based on data from Jefferson (1902)	$6.6\ w^{0.99}$
Inglis (1947), based on data from Bates (1939)	$10.9\ w^{1.04}$

Table 4.4 Published meander wavelength-width relationships.

Hence, the range of coefficients indicates there is considerable variation within wavelength-width relations (Thorne, 1997). The exponents are all close to unity and hence, a linear relation of wavelength-width ratio in a window of between 10 and 14 is often quoted (Knighton, 1998). This is supported by Richard's (1982) subsequent reanalysis of Leopold and Wolman's (1957, 1960) data which showed that a linear regression function defined by:

$$\lambda = 12.34\, w \qquad (4.4)$$

is equally acceptable (Richards, 1982).

In Figure 4.54a, the meander wavelength-width relationship is explored with respect to the three techniques used to generate meander wavelength parameters. For each survey year in the period 1830-1975, the regional-scale average from each technique is plotted in relation to the window of 10-14 channel widths. In the 1887-1975 period, estimates based on spectral analysis fall within the window whereas estimates from autoregressive and bend inflexion techniques are less than ten channel widths. Hence, the nature of the reported relationship is sensitive to the initial technique of parameter calculation. This sensitivity is interesting because, as Hooke (1984) states, there is no rigorous standardisation in the definition of parameters used in empirical relationships. Figure 4.54b shows that the regional-scale mean values also masks greater inter-reach variability: typically, only two out of the four identified reaches fall within the window of 10-14 channel widths.

Although inter-reach variation appears considerable, it must be remembered that the empirical relations were originally developed using datasets which transcend multiple spatial scales. The importance of this is demonstrated in Figure 4.55, where wavelength-width ratios for each reach are plotted onto the regression relationship identified by Leopold and Wolman (1957). Despite the variation noted in Figure 4.54, the data point cloud for the Lower Mississippi River is consistent with the regression relationship when wavelength is identified by both spectral and inflexion point techniques. This shows therefore that, by developing empirical relations that transcend scale boundaries, the problem of parameter classification is essentially removed because the level of variation between scales is far greater than the level of variation at any one scale.

a)

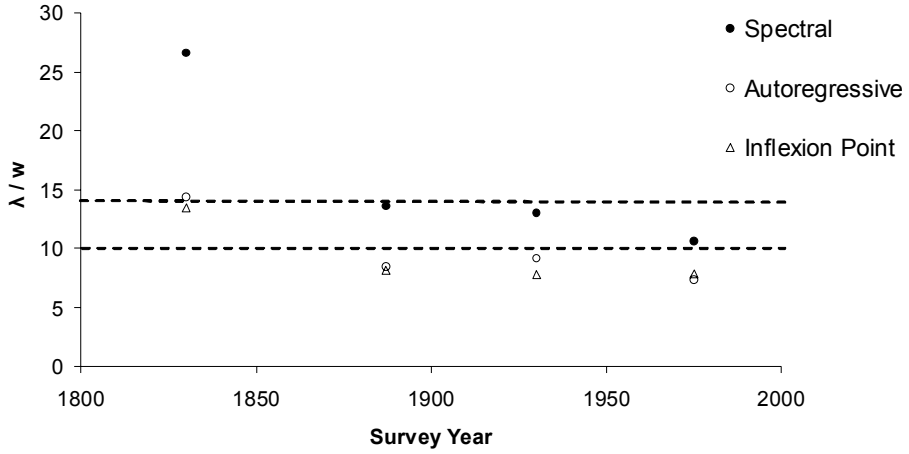

b)

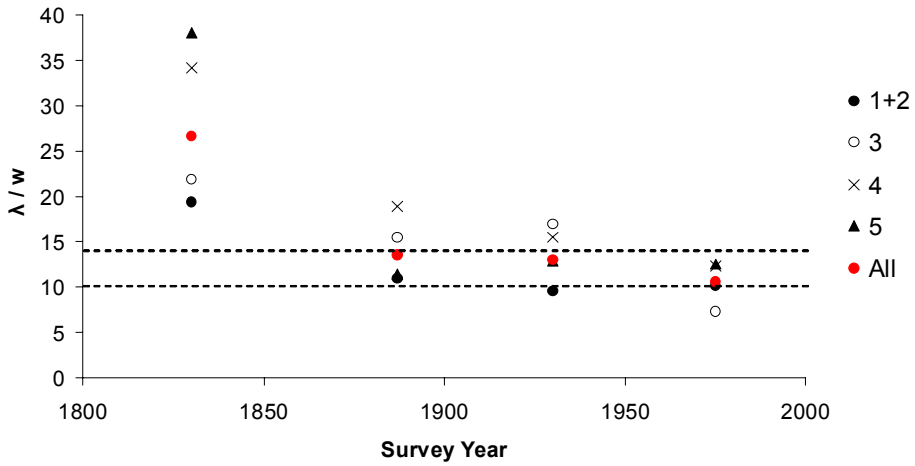

Figure 4.54 Spatial and temporal variability of the channel wavelength/width (λ/w) relationship for: a) each technique (results are a regional-scale average) and; b) each reach and a regional-scale average (denoted by *All*) using wavelengths derived from spectral analysis. Broken lines indicate the widely quoted window of 10-14 channel widths. Individual reaches are identified in Figure 4.11 (with reaches 1 and 2 amalgamated).

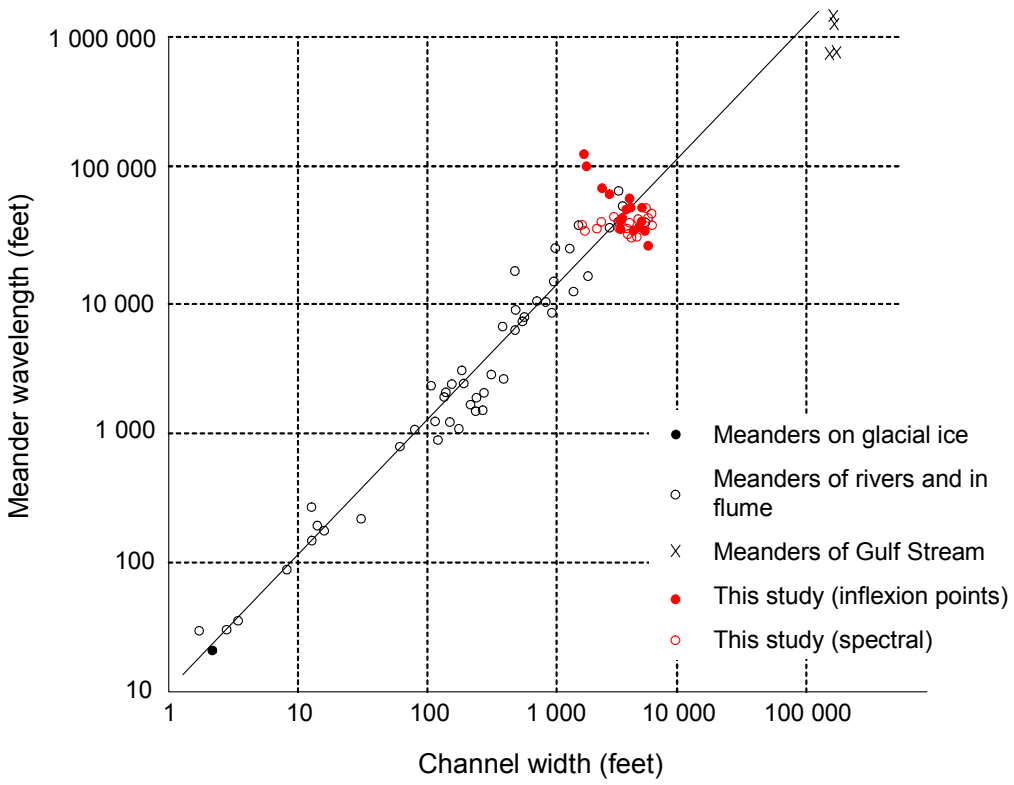

Figure 4.55 Wavelength-width ratios for each reach identified by spectral and inflexion point techniques plotted onto the regression relationship identified by Leopold and Wolman (1957). *Conversion to SI units: 1 foot = 0.3048 m.*

ii) Meander wavelength and channel discharge

An empirical relation between meander wavelength and discharge has been established by a variety of authors. This is linked to the other relations because width is approximately proportional to the square root of discharge (Inglis, 1949; Leopold and Maddock, 1953). In Table 4.5, meander wavelength is calculated from these relations using daily discharge data at the Vicksburg gauge for the period 1937-2001.

Discharge	Source	Relationship	λ (km)
Mean annual discharge	Allen (1970)	$\lambda = 168\ Q_a^{0.46}$	14.74
Mean annual flood discharge	Dury (1956)	$\lambda = 54.3\ Q_{ma}^{0.5}$	10.64
Constant bankfull discharge	Ackers and Charlton (1970)	$\lambda = 62\ Q_b^{0.47}$	7.88
Dominant discharge exceeded 1 percent of time (from spectral analysis)	Ferguson (1975)	$\lambda = 57\ Q_d^{0.58}$	28.91

Table 4.5 Calculation of meander wavelength according to published meander wavelength-discharge relationships

Computed wavelengths vary considerably depending on the relationship applied. The relationship identified by Ferguson (1975), which relates a measure of discharge to meander wavelengths estimated by spectral techniques, generates a considerably longer meander wavelength than other relations. This is therefore consistent with the pattern identified in section 4.4.6. However, the computed estimate of 28.9 km (1.d.p) significantly overestimates the mean regional-scale spectral wavelength of approximately 21 km in the 1765-1975 period. Out of the remaining three relationships, Allen's (1970) relation, based on mean annual discharge provides the closest estimate of the mean regional-scale inflexion point wavelength of approximately 14 km over the same period. However, dominant discharge studies have indicated that mean annual discharge has little or no geomorphological significance (Wolman and Miller, 1960; Ackers and Charlton, 1970). These results therefore support Knighton's (1998) claim that meander wavelength is not related to any single measure of discharge but to a range of discharges. At a more fundamental level, simplistic relationships of this nature could never provide a good approximation because they do not account for the variability of bank materials. On

the Lower Mississippi River, the importance of bank materials to rates of planform dynamics has been documented by both Fisk (1944) and Saucier (1994).

In summary to this section, there is at least some degree of association between recognised empirical relations and meander wavelength behaviour on the Lower Mississippi River. Analysis of the wavelength-width relationship has shown that scatter at any one scale can be reduced when results are collectively considered across multiple scale of analysis. Meanwhile, analysis of wavelength-discharge relationships has shown that the degree of association is sensitive to the empirical relationship selected. Assuming that a regional-scale hydrodynamic control does exist, results presented so far in this chapter indicate that scatter about empirical relationships is a product of a combination of methodological inconsistencies in parameter definition and physical disturbances at the reach and sub-reach scales. In the following section, physical disturbances are considered further by examining the importance of longer-term controls on planform morphology.

4.10 Reach History: The importance of longer-term controls

The longer-term significance of changes in the 1765-1975 period can only really be evaluated by considering the range of planform patterns previously adopted by the Lower Mississippi River over longer time intervals, and the rate of change between these patterns.

4.10.1 Magnitude and rates of planform changes during the Holocene period

Prior to 9.8 kA BP (thousand years before present), the Lower Mississippi River flowed in a wide, and probably relatively shallow, braided channel pattern throughout the alluvial valley. This pattern, indicative of high energy expenditure, was necessary to balance a high stream power provided by the combination of a high discharge flowing on a valley slope that was considerably steeper than present. Teller (1990) estimates that the average long-term discharge between 14 kA BP and 8 kA BP exceeded the present long-term discharge by a factor of up to five. This difference may be far greater if peak discharges are compared because the late

Wisconsin period was characterised by extremely large magnitude flood events caused by sudden outbursts from pro-glacial lakes Agassiz and Superior (Porter and Guccione, 1994). Valley slope was considerably steeper than the present valley slope owing to sea-level rise and alluvial valley aggradation during the early and mid-Holocene. Braided stream patterns are characteristic of high rates of sediment transport, particularly coarse bed load transport. These coarse fractions are preserved in the northern third of the alluvial valley as valley train deposits of coarse sands and gravels (Fisk, 1944; Saucier, 1994).

In contrast, since approximately 9.8 ka BP, the Lower Mississippi River has maintained a meandering course throughout the alluvial valley whilst switching between a series of meander belts. Stream power has been significantly lower than in the late-Wisconsin period because of the lower long-term discharge and reduced channel gradient in relation to valley gradient (caused by meandering). Moreover, Saucier (1994) presents evidence which may suggest that, for much of the Holocene period, the Lower Mississippi River has not flowed in a single meandering channel, but rather as an anastomosing river in two or more meandering anabranches, for up to several hundreds of kilometres. This assertion was reached following examination of the relative size and number of cutoffs associated with each identified meander belt, suggesting that only three of the six meander belts carried the full discharge of the Lower Mississippi River, and only two of these for a significant time period. Anabranching is a method of obtaining a higher total sinuosity (and therefore lower total gradient), than can be obtaining in a single thread meandering channel. Hence, it is a relatively stable channel pattern indicative of low energy expenditure (Thorne, 1997).

The tendency to switch between single-thread meandering, multi-thread meandering, and multi-thread braided channel patterns in response to variations in flow and sediment regime over the last 15 kA demonstrates that the Lower Mississippi River exhibits dynamic planform properties characteristic of a classic alluvial river. Rather than representing discrete morphologies, these three types of channel pattern can be considered as part of a wider continuum of channel patterns. Schumm (1985) recognises 14 channel patterns including the three conventional types noted by Leopold and Wolman (1957), plus anastomosing patterns (Thorne, 1997), and broad

range of transitional patterns of varying total sinuosity and stability (Figure 4.56). In terms of energy expenditure, the present single thread meandering channel can therefore be considering somewhere intermediate between the two extremes of energy expenditure: a low energy, anastomosing planform (pattern 14 in Figure 4.56) and a high energy braided planform (pattern 5 in Figure 4.56). This is important considering that, although significantly controlled by human modifications, the magnitude of flow and sediment transport processes in the 1765-1975 period are more likely to be closer to long-term mean levels during the Holocene period than the late-Wisconsin period. Given this, the present single thread meandering channel throughout the alluvial valley can be considered a less sinuous (in terms of total sinuosity) and therefore, higher energy expenditure channel, than has persisted throughout much of the Holocene period.

In terms of rates of channel pattern changes, abrupt changes of channel morphology on the Lower Mississippi River have not been uncommon over the Holocene period. According to Saucier (1994), the transition between a braided and a meandering channel planform throughout the alluvial valley around 9.8 ka BP may have lasted for as little as 100 years. Throughout the Holocene period, Saucier (1994) also reports that the abandonment of channel courses, defined as being greater than a single meander bend and up to hundreds of kilometres long, and the diversion or avulsion to a new course (and possibly meander belt) has operated over relatively short time intervals, between decades and centuries (10^2-10^3 years). Thus, the Lower Mississippi River is not only capable of adopting a wide range of channel patterns, but relatively rapid changes in planform through the adjustment of multiple degrees of freedom have been observed throughout the Holocene period. This is important when considering recent geomorphological response to engineering intervention associated with the MR & T project because it shows that the Lower Mississippi River can adjust relatively rapidly to high magnitude disturbances and significant changes in channel morphology are possible.

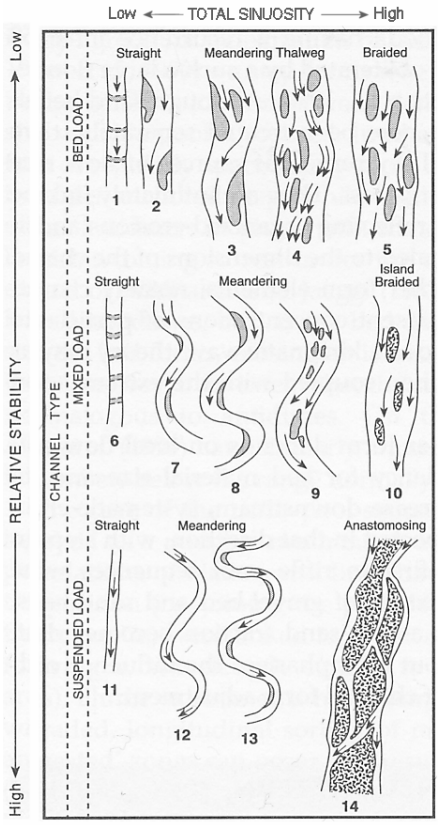

Figure 4.56 The classification of channel pattern based on sediment load, total sinuosity and relative stability (modified from Schumm, 1985).

4.10.2 Planform dynamics at the 2000 year timescale

The Lower Mississippi River has flowed in its modern meander belt for at least the last 2000 years (Saucier, 1994). Investigating the spatial distribution of abandoned channels within this meander belt provides a method of identifying spatial variations in planform stability at this timescale. This section explores the association between the spatial distribution of abandoned channels and regional-scale geological, neotectonic and tributary controls.

i) Method

Following the data processing routine outlined in section 3.2.1, a data quality procedure was applied to the data set to ensure that that each abandoned channel satisfied the same geometric definition. For each digitised bend, the 'abandoned channel' was defined as the longest channel length between any points of inflexion identified in the direction change series. The procedure processed each individual meander bend according to the following rules: where no points of inflexion were identified, the existing bend was defined as the abandoned channel; where a single inflexion point was identified, the longest segment was defined as the abandoned channel; and, where two or more inflexion points were identified, the bend was defined as the greatest distance between any two inflexion points.

To analyse the relative distribution of abandoned channels along the present course of the Lower Mississippi River, a method of reducing the two dimensional distribution of abandoned channels into a one dimensional sequence was developed. This method involved two stages of data processing and is summarised in Figure 4.57. First, each abandoned channel was reduced to a single point observation by finding the maximum and minimum x and y coordinates and computing a centre point. The additional positional error introduced by this procedure is deemed insignificant in relation to the physical scale being considered. Second, a method to transform the centre-point of each abandoned channel, located at varying distances away from the present river channel, onto a one dimensional valley axis was required. The valley axis was created by on-screen digitising of key directional change points in the regional-scale planform. Each abandoned channel was

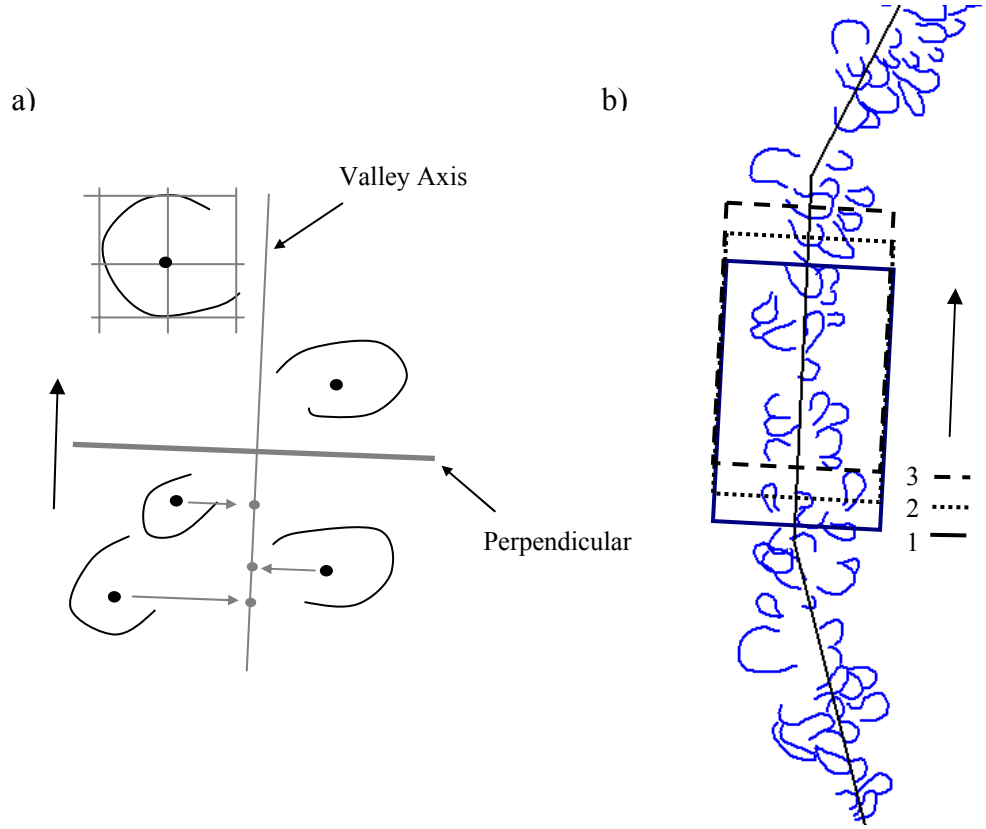

Figure 4.57 Abandoned channel data processing and analysis routine. In a), each abandoned channel is positioned on the valley axis by reducing to a centre-point and then snapping to the valley axis at the angle of the perpendicular. In b), the distribution is analysed by counting the number of channels in a moving window.

referenced to the valley axis at the angle of the perpendicular. The new location of each abandoned channel on the valley axis was measured by the valley distance from Cairo.

To analyse the one-dimensional distribution of abandoned channels, the valley axis was divided onto 100 zones of equal distance and a windowing routine was applied, moving through successive zones in the down valley direction. This provided a strong diagnostic technique with which to detect changes in the distribution of abandoned channels within the alluvial valley. At each location, the number of abandoned channels distributed within the limits imposed by the window was counted. Three sizes of window were applied, representing 5, 10, and 20 zones. These zone numbers correspond to valley distances of approximately 37.5 km, 75 km and 150 km respectively. The distribution of abandoned channels is illustrated in Figures 4.58 in relation to regional-scale geological changes, neotectonic activity, and tributary influences. The distribution peaks at approximately 360 valley km downstream from Cairo and in general there is a gradual decline thereafter. Broad peaks also exist at 100-150 valley km and 440-510 valley km.

The distribution of abandoned channels is examined to determine whether characteristic signatures could be identified from each of three sets of physical controlling variables; geological, neotectonic, and tributary inputs.

ii) Regional geological controls

Regional geological variation within the alluvial valley is of primary importance to planform stability through its influence on rates of bank erosion. As introduced in section 2.5.1, geological variations exist in the alluvial valley at a range of spatial scales. From the distribution of abandoned channels (Fig. 4.58a), two regional geological influences are evident. First, the general down valley decline in the number of abandoned channels from approximately 400 km most likely reflects a fining of Holocene sediment moving towards the deltaic plain. These more cohesive sediments are well-known to restrict rates of meander migration (Fisk, 1947; Kolb, 1963).

a)

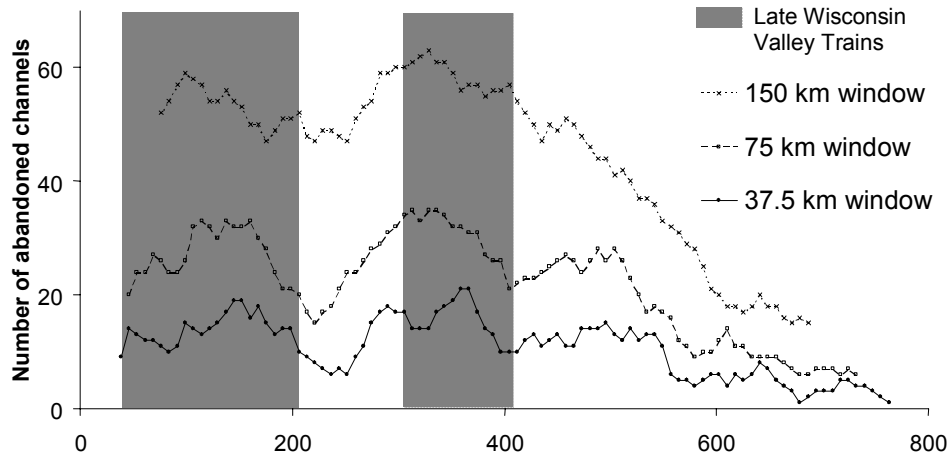

b)

c)

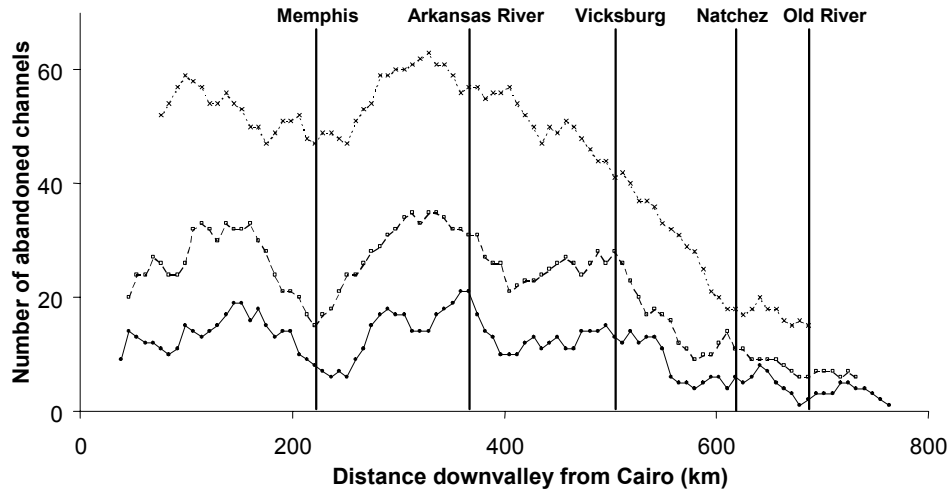

Figure 4.58 The distribution of abandoned channels in the alluvial valley in relation to: a) the broad distribution of Late Wisconsin valley train deposits; b) two areas of active neotectonic uplift and; c) tributary inputs and major settlements.

Second, in the northern or upstream half of the alluvial valley, the distribution of relict Late Wisconsin 'valley train' (Fisk, 1944; Saucier, 1994) deposits coincides with peaks in the number of abandoned channels. Late Wisconsin deposits consist of relatively shallow and unconsolidated masses of coarse sands and gravels. These are more easily susceptible to bank erosion than the generally cohesive mix of fine sands, silts and clays which compose the Holocene deposits. Several authors have used observations over much shorter (10^2 year) timescales to suggest a causal link between regional-scale planform stability and the distribution of Late Wisconsin deposits (Schumm *et al*., 1994; Smith, 1996; Hudson and Kesel, 2000). However, isolating the difference has proved difficult due to the significant influence of local geological controls over such short timescales. At longer late Holocene timescales, visual observations led Saucier (1994) to suggest an association between the distribution of zones of abundant abandoned channels and Late Wisconsin deposits. However, this association has never previously been quantified. Figure 4.58a shows that deposits impinge upon the present meander belt of the Lower Mississippi River in two reaches. In the most upstream area, from Cairo to approximately 200 valley km, the present meander belt is confined to the eastern side of the alluvial valley and dissects a broad valley of Late Wisconsin deposits mainly to the west (Smith, 1996). This region coincides with a relatively peak in the number of abandoned channels at approximately 140 valley km. The downstream zone, extending from approximately 300 to 400 valley km from Cairo coincides with a peak in abandoned channels at around 360 km. These findings therefore support Saucier (1994) earlier observations.

Between the reaches of impinging Late Wisconsin deposits, is a short reach characterised by relatively few abandoned channels. The meander belt within this reach impinges upon extensive backswamp deposits to the west of the present course, around the latitude of the city of Memphis. Because of their high clay content, backswamp deposits are relatively cohesive in relation to other types of Holocene deposit (Saucier, 1994) and therefore, constrain rates of planform migration. Extensive regions of backswamp deposits are also found along both sides of the present meander belt between Lake Providence and Vicksburg, and extend upstream to the Arkansas River confluence on the western side of the present course.

iii) Neotectonic controls

Areas of active neotectonic uplift features are of importance to planform stability primarily through their control on local valley slope (Schumm and Khan, 1972). On the downstream side of regions of active uplift, valley slope will increase locally. This may increase the energy available for sediment transport and consequently result in a less stable channel (Burnett and Schumm, 1983). Conversely, on the upstream side, the reverse is likely to be true, thereby supporting a more stable channel form.

The importance of the two regions of active neotectonic uplift in the alluvial valley to the historic planform dynamics of the Lower Mississippi River has been documented by Schumm *et al*. (1994). However, no previous researchers have investigated this association over longer timescales by analysing the spatial distribution of abandoned channels. The Lake County uplift feature in southeast Missouri traverses the valley axis for approximately 35 km whereas the larger Monroe uplift extends for approximately 120 km through south eastern Arkansas and west central Mississippi (see Figure 2.7). The 37.5 km moving window output shows a significant increase in the number of abandoned channels in the alluvial valley for up to 70-80 valley km downstream from the Lake County Uplift feature (Figure 4.58b). Meanwhile, according to both the 37.5 km and 75 km moving window outputs, the geographic location of the Monroe Uplift might coincide with a stabilisation of the general decline in the number of abandoned channels. Together, these observations are therefore suggestive of some association between regions of instability in the alluvial valley and active regions of neotectonic activity.

iv) Tributary inputs

Flow and sediment inputs from tributary basins may represent an important control on planform stability at this timescale because they can cause sudden changes to the flow and sediment regime of the main river downstream from the confluence. The effect of tributary inputs on the Lower Mississippi River has not previously been considered over a 2000 year timescale. However, at the much shorter 165 year timescale, Schumm *et al*. (1994) propose that an increase in the range of sinuosity downstream from the junction of the Arkansas River is the result of an introduction

of large quantities of medium sand and increased discharge from the Arkansas River basin. Over longer timescales, Ray (1964) has interpreted the presence of a large alluvial fan just downstream from Cairo as evidence of the higher sediment concentrations upstream from Cairo on the Middle Mississippi River as opposed to immediately downstream.

In terms of discharge and sediment load input, the major tributaries draining into the Lower Mississippi River over the last 2000 years have been the Arkansas and White Rivers at approximately 372 valley km and, prior to the completion of the Old River Diversion Project, the Red River at approximately 689 valley km. Over the last 250 years, the Atchafalaya distributary, immediately downstream from the Red River confluence, has transported an increasing proportion of the total discharge. However, this is not considered significant over a Late Holocene timescale. Examination of Figure 4.58c suggests that no dominant signal from tributary inputs can be identified. Indeed, downstream from the Arkansas/White and Red River confluences, there is a decrease in the number of abandoned channels. This observation is the reverse of conventional geomorphological theory which would predict greater planform instability downstream from tributaries which contribute relatively high and/or coarse, sediment loads in relation to their discharge. This perhaps highlights the greater relative importance of the geological controls noted above in these reaches. More generally, this emphasises the problem of linking cause and effect in observed data series. As Renwick (1992) suggests, geomorphic systems may exhibit several types of instabilities simultaneously; separating them is certainly difficult and perhaps impossible.

4.10.3 Linking the 2 000 year and 165 year timescales

Figure 4.59 compares the distribution of abandoned channels in the Late Holocene period to the spatial pattern of planform dynamics estimated from historic maps in the period 1765-1930. The latter is based on division of the alluvial valley into 200 zones of equal valley distance (see section 4.4). In each zone, planform dynamics are measured by calculating the maximum range of channel length over the period.

A 24 km moving average has been applied to the resulting series to smooth the resulting local variability and hence, emphasise regional-scale trends.

At the 165 year timescale, there is considerable local variation with several reaches demonstrating a very dynamic planform whilst immediately adjacent reaches appear relatively stable. Schumm *et al*. (1994) attribute such variation to isolated geological controls in the channel bed and banks which constrain the planform development of some meander bends. For example, the highly sinuous Greenville Bends on the pre-cutoff river were caused by the compression of meander against highly resistant Tertiary clays on the upstream flank of the Monroe Uplift. Despite these local-scale controls, a general trend can be identified of planform becoming more dynamic with distance downvalley from approximately 250 valley km to approximately 720 valley km. Over the same reach, there is a general reduction in the number of abandoned channels. This supports Smith's (1996) assertion that the reaches of the Lower Mississippi River which were previously much more active are less so today than vice versa. The association between the two timescales suggests that clay plug deposits, resulting from the filling of abandoned channels with fine, cohesive sediments, were the major control on regional-scale planform dynamics on the pre-modification Lower Mississippi River. This is perhaps surprising given the downstream fining of bank material in the alluvial valley reported by Fisk (1947). In a study of rates of meander bend migration over a shorter time period 1878-1924, Hudson and Kesel (2000) reported a similar general pattern of increasing planform instability downstream in the alluvial valley and identified a distinct change in the magnitude of instability in the vicinity of Lake Providence (approximately 460 valley km). Figure 4.59 reveals a gradual increase in planform instability downvalley and hence, the identification of this boundary is not clearly supported.

Although clay plug deposits control the pre-modification planform dynamics in much of the alluvial valley, at least three further associations of geomorphological interest can be identified. The three corresponding reaches are shaded grey in Figure 4.59 and labelled from a) – c). Region a) is situated in the upper alluvial valley (0 – 56 valley km) and defines a reach that has been relatively stable at both the Late Holocene and 165 year timescales. Schumm *et al*. (1994) explain this relative stability by the presence of the Charleston alluvial fan which lies immediately to the

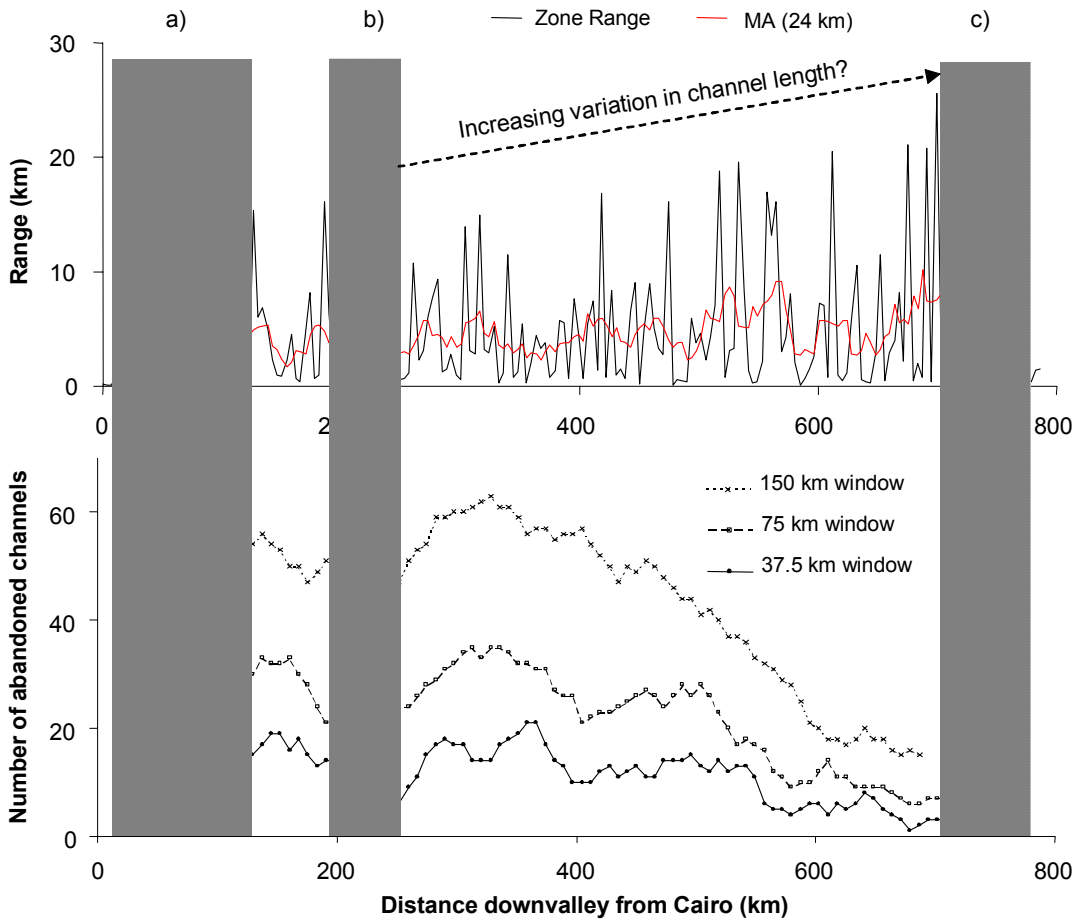

Figure 4.59 The range of channel length experienced in each of the 200 valley reaches in the pre-cutoff (1765-1930) period in relation to the distribution of Late Holocene abandoned channels. A 24 km moving average (MA) has been fitted to emphasise regional-scale trends. Highlighted reaches a), b) and c) are characterised by relative stability in the pre-cutoff period and relatively few abandoned channels. These are discussed further in the text.

west of the present course. The alluvial fan is body of medium and coarse sands approximately 380 square kilometres in area and at least eight metres in thickness. Detailed studies by Ray (1964) and more recently, by Porter and Guccione (1994) interpret this feature as a remnant large-magnitude flood deposit formed around 10.9 kA BP when pro-glacial lakes Agassiz and Superior discharged their meltwater into the Mississippi River. This explanation is consistent with the location of the fan immediately downvalley from Thebes Gap, a constriction in the bluff lines where the Middle Mississippi River enters the head of the alluvial valley. On entering the alluvial valley, there is a sudden decline in valley gradient (Schumm *et al.*, 1994) and hence, the consequent sudden dissipation of energy during flood events is consistent with the observed deposition. Throughout the Holocene, the Lower Mississippi River has flowed in a single meander belt throughout this reach between the Charleston alluvial fan to the west and the loess bluff line to the east. Thus, the presence of the Charleston alluvial fan has effectively prohibited sustained active meandering in this reach.

Region b) defines a relatively stable reach at both timescales in the vicinity of the city of Memphis (193 – 256 valley km). Here, relatively resistant backswamp deposits have limited planform migration to the western side of the meander belt. This reach also coincides with an absence of erodible valley train deposits which border the meander belt both upstream and downstream of the reach (see Figure 2.7). Finally, region c) identifies a stable reach at approximately 720 valley km where the general trend of increasing planform dynamics downstream ends abruptly. This distance is approximately 20 valley km downstream from Old River and hence, may be interpreted as the boundary between the alluvial valley and the deltaic plain. Hudson and Kesel (2000) noted that at this boundary, the mean rate of meander migration declined by an order of magnitude, from 59.1 m yr^{-1} to 15 m yr^{-1}. In relation to Schumm's (1977) division of the fluvial system into zones of sediment erosion, transport and deposition, there is therefore, a clear regional division between the alluvial valley, primarily a zone of sediment transport, and the deltaic plain, primarily a zone of sediment deposition.

4.11 Discussion

The following discussion draws together the results and analysis presented above to summarise how it informs understanding of large-scale and long-term geomorphological behaviour of the Lower Mississippi River.

Results presented throughout this chapter have revealed that the planform of the Lower Mississippi River was highly dynamic over the 1765-1975 time period. Because tighter meander bends exert a greater form resistance (Richards, 1982), planform dynamics can be interpreted in the context of a need to balance total energy expenditure against the energy available for hydraulic and gemorphological processes, denoted by stream power per unit width. At the regional-scale, analysis of channel length, radius of curvature, and meander wavelength and amplitude parameters has revealed that form resistance exerted by the planform was probably greatest in 1830 when total channel length in the 1765-1975 period was at a maximum and channel curvature, denoted by the median radius of curvature and the number of complex, compound bend forms was at a maximum. Following a period of net channel lengthening, the planform in 1930 was of a similar length but both curvature and the number of complex bend forms was lower. This difference is consistent with the idea that sediment load increased considerably between the two surveys, caused by both a lagged response from the New Madrid earthquake in combination with changes in land use practices within the alluvial valley and more generally, the wider drainage basin (Saucier, 1994; Prince, 1997). Therefore, a greater proportion of total energy was expended in performing sediment transport by 1930, and hence, a lower proportion of energy was available to overcome form resistance.

Interestingly, the regional-scale temporal behaviour highlighted above masks considerable inter-reach differences. Application of zonation algorithms to direction change series revealed that it is possible to divide the Lower Mississippi River into a series of reaches based on planform characteristics. However, such reaches are typically transient features that generally persist for only up to approximately 120 years. This shows that prior to engineering modification, a series of straight and sinuous reaches were continually formed, and modified, through intrinsic planform

adjustments (the natural meander bend growth and cutoff cycle) on the Lower Mississippi River. On the post-modification river, this aspect of natural dynamics has been removed by effectively fixing to a constant planform alignment through bank stabilisation.

Despite the temporal variation of planform reaches on the pre-modification river, application of zonation routines provides some evidence that tributary junctions provide a longer term reach control. Multi-parameter analysis of six planform reaches defined by tributary junctions reveals a consistent spatial pattern in terms of the magnitude of dynamics: the upstream and downstream reaches 1 and 6 demonstrate relatively consistent geomorphological behaviour whereas the midstream reaches 2 to 5 demonstrate more dynamic behaviour. It is particularly important to note that, in the pre-modification period, the artificial cutoff reach (downstream from Memphis to just upstream from the Old River distributary) exhibited the greatest rates of length changes, the lowest median radius of curvature and generally more complex compound meander bend forms than other reaches. This suggests that the engineers designing the cutoff programme may have had a prior understanding of the planform dynamics of the Lower Mississippi River because constructing artificial cutoffs in this reach not only increased slope (and hence, stream power per unit width), but also minimised the total form resistance exerted by the planform.

If inter-reach and downstream differences are considered alongside regional-scale changes, it is apparent that, although different reaches respond in different ways and at different timescales, they do so in such a way that regional-scale requirements for energy expenditure are met. The raises the issue of why there is such diversity in reach-scale and sub-reach scale behaviour. Analysis of longer-term controls has supported the close association between rates of planform migration in the pre-modification (1765-1930) time period, and the distribution of resistant clay plug deposits within the contemporary meander belt, identified by Hudson and Kesel (2000). Further analysis has shown that the distribution of these deposits in turn correlates strongly with neotectonic activity and extensive areas of coarse glacial outwash deposits in the alluvial valley. This therefore resonates with Schumm and Lichty's (1965) assertion that the status of explanatory variables and the nature of

their interrelationships change with the time and space scale adopted. However, there are exceptions to this rule with some reaches demonstrating consistent behaviour over longer timeframes. This also supports the idea that spatially-distributed feedbacks between form and process do operate at larger spatial scale and longer temporal scales than those envisaged by Lane and Richards (1997). As a result, understanding the often complex morphological configurations of individual reaches is critical to explaining contemporary dynamics as a constant interplay between immanent and configurational elements of the fluvial system (Simpson, 1963).

In addition to informing the complex spatial and temporal patterns of planform changes on the Lower Mississippi River, the results presented in this chapter highlight some of the more general problems associated with capturing and explaining the dynamics of alluvial river channels. Capturing the full range of dynamics is vital if coherent explanations of river channel changes are to be developed, but this is reliant on being able to reliably detect changes in both stream power per unit width, and total energy expenditure. Most quantitative studies of planform changes rely on the computation of the standard morphological parameters examined in this chapter. Dynamics can only be reconstructed by integrated measurement obtained from several complementary parameters because reliance on individual parameters can often generate misleading results. At least two reasons for this are demonstrated in this chapter. First, there is a danger of miss-association (Mackin, 1963). For example, it has been shown that an increase in the sinuosity of a specific river reach is not necessarily indicative of the formation of tighter bends that exert a greater form resistance. Second, parameters obtained are often highly sensitive to the method of computation. This has been shown with meander wavelength: the three techniques used measure different wavelength properties and as a consequence, generate different spatial patterns. Thus, reliance on only a single technique can lead to the generation of only partial, or worse, mistaken conclusions.

In terms of the adequacy of existing theories to explain dynamics, by focusing on spatial and temporal diversity in geomorphological behaviour, this chapter has demonstrated both the relative merits and limitations of traditional functionalist approaches (introduced in section 1.6). Importantly, both empirical relations and

autoregressive modelling have shown that the planform of the Lower Mississippi River exhibits planform properties similar to other large alluvial rivers. Such association between scales is suggestive of a common hydrodynamic forcing mechanism. However, this approach is not particularly helpful with regard to exploring dynamics in space and time and at any one particular scale.

An alternative mode of explanation is provided by the theory self-organisation based on the central tenant that there is no single state to which a system is trying to adjust towards, but rather, flow resistance requirements can be satisfied by multiple states and thus, multiple modes of adjustment are possible (Phillips, 1991). Hooke (2003) has interpreted periods of long term planform stability on the River Bollin in the UK, interspersed with relatively short periods of cutoff development, in terms of the perpetual desire to self organise towards a *critical state*. This is defined as a balance between two states: a *supercritical state*, in which small inputs to the system cause clusters of changes to migrate or avalanche through the whole system; and a *subcritical state* in which small inputs to the system have a negligible impact on system properties or cause only small-scale system changes (Bak and Chen, 1991). Length changes on the Lower Mississippi River are consistent with this theory: the more dynamic reaches 2 to 5 displaying properties of a system close to the critical state, with periods of sudden net shortening through cutoff development (avalanching in the supercritical state) inter-dispersed with periods of net lengthening (stability in the sub-critical state). The less dynamic reaches 1 and 6 can be classified as existing in sub-critical state due to contingent influences.

This approach may provide a useful conceptualisation within which to view past changes and possibly predict the likelihood of future changes but a fundamental criticism is that it does not provide any physical basis for explaining such dynamics. Richards (1982; Figure 1.1) provides a more realist interpretation by highlighting the complex array of interrelationships between a wide range of morphological and process parameters in the fluvial system. This interpretation can accommodate the central principle of functionalist relationships: that form adjusts to process, but also shows how process can adjust to form. Most importantly, it can also accommodate the idea of that rivers can respond to changes in stream power per unit width through adjustments to a series of different parameters. However, by focusing on measured

parameters, it is necessarily selective. For example, meander wavelength is included without consideration of meander amplitude even though both parameters together describe the shape of a meander bend. This approach can also be criticised on the grounds that by focusing on measured parameters, it does not clearly illustrate the *real* adjustments within the fluvial system.

Channel adjustments are better interpreted as mutual adjustments between energy availability and energy expenditure, each of which can be measured by a series of parameters. Total energy expenditure is a product of form resistance, skin resistance and sediment transport processes (Figure 2.1). This chapter has assessed the relationship between stream power changes and form resistance exerted by the planform over a 210 year time period. At this timescale, this is acceptable because historically the planform has been the most dynamic degree of freedom. However, an examination of downstream changes in the long profile and cross-sectional form is also critical because it not only provides an additional element of form resistance through the pool-crossing undulations, but it also determines the channel slope and hence stream power per unit width. These are considered in the next two chapters.

CHAPTER 5. THE REGIONAL-SCALE LONG PROFILE

5.1 Chapter synopsis

In this chapter, the analytical techniques introduced in Chapters 3 and 4 are used to examine spatial trends in the downstream configuration of the long profile from Cairo to the Head of Passes. This is based upon three independent hydrographic surveys of the river in 1974-75 by the U.S. Army Corps of Engineers (USACE). Results presented show that the regional-scale concave long profile can be considered as partly inherited from past geomorphological conditions; partly continually adjusting to other long-term physical controlling variables; and partly a direct product of engineering modification during the twentieth century. Hence, the present concavity is more of a collective outcome of a set of disparate controls than a direct product of the prevailing process regime. At the smaller sub-reach scale, pool-crossing sequences are shown to be spaced pseudo-periodically and are closely associated with the spacing of meander bends in the planform. Analytical techniques reveal that the difference of pool-crossing amplitude and wavelength characteristics between the alluvial valley and deltaic plain cannot easily be related to changes in stream power per unit width. Hence, the morphology at this smaller-spatial scale cannot completely be considered as adjusted to the prevailing process regime either, at least not in conventional engineering terms.

5.2 Obtaining a consistent data series

Examining downstream trends within the long profile relies upon obtaining a data series, sampled at regular intervals, that accurately characterises the variation in bed topography. An adequate resolution must be found which maintains the variation which is of interest whilst being appropriate in view of the resolution of original data collection.

The 1974-75 hydrographic survey was undertaken over a period of 20 months between April 1974 and November 1975, and comprises a total of 4 515 cross-sections. However, the survey was undertaken independently by the three USACE

Districts (Memphis, Vicksburg and New Orleans) and, although, the same data collection methodology was used (see section 2.8.5), the mean sampling spacing and level of variation about the mean differs between the Districts (Table 5.1). The mean sampling spacing ranges from 0.3 km in the New Orleans District to almost 0.4 km in the Memphis District. Figure 5.1 shows that systematic changes in variance are closely related to the boundaries between adjacent USACE Districts, with the Memphis District demonstrating the highest variance and the neighbouring Vicksburg District the lowest variance. The significance of these changes is examined by performing multi-way ANOVA using USACE District as the fixed factor. The proportion of the total variance attributed to variance 'between groups' is highly significant (p value = 0.000 to 3.d.p); indicating at the very least that one of the means is significantly different from the other two.

Regular sampling is a requirement for the application of the analytical techniques introduced in chapters 3 and 4. Based upon the widespread observation of two pool-crossing units in a single meander bend, a sampling interval of 1 km is used throughout this chapter to be consistent with the interval of 2 km used in chapter 4. The loss of original series variance associated with interpolating at this interval is examined in Figures 5.2. 5.2a and 5.2b show the reduction in series variance as the sampling interval is increased and local sensitivity is inevitably reduced. 5.2c shows that an interval of 0.25 km demonstrates a close association with the original series. The importance of this loss of variance is examined by inspecting the change in the form of spectral density plots at sampling intervals in the range 0.25-1.0 km (Figure 5.3). Only a negligible proportion of total variance is provided by wavelengths less than approximately 4 km. This therefore suggests that sampling at a 1 km interval does not remove important variation within the series.

A 1 km interval is also low enough to prevent errors being introduced through aliasing. This was established by considering the wavelength of the pool-to-pool and crossing-to-crossing spacing and then estimating the maximum sampling interval permissible to prevent aliasing. Although the mean pool-to-pool and crossing-to-

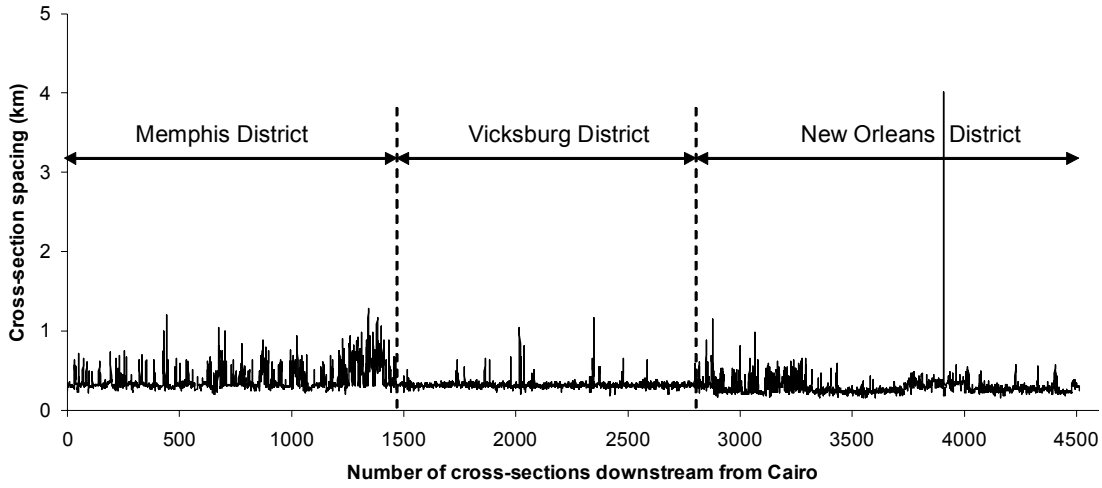

Figure 5.1 The variability of cross-sectional spacing in the 1974-75 hydrographic survey from Cairo to the Head of Passes.

	Memphis	Vicksburg	New Orleans
Start Date	April 74	August 75	July 74
End Date	February 75	November 75	November 75
Duration (Months)	10	3	16
Number of cross-sections	1467	1288	1760
Mean spacing (km)	0.393	0.326	0.300
Median spacing (km)	0.328	0.320	0.274

Table 5.1 Differences in data collection between the three USACE Districts for the 1974-1975 hydrographic survey. The Memphis District extends from Cairo downstream to the Arkansas River confluence; the Vicksburg District extends from the Arkansas River confluence to 8 km upstream from Old River and; the New Orleans District extends from 8 km upstream from Old River to Head of Passes. Mean and median cross-sectional spacing is given to three decimal places.

		Sum of Squares	Degrees Freedom	Mean Square	*F*	*p*
Factor	Between Groups	6.929×10^6	2	3.464×10^6	239	0.000
Error	Within Groups	6.534×10^7	4510	1.449×10^4		
Total		5.861×10^8	4513			

Table 5.2 Comparing the variation in sampling spacing between the three USACE Districts using ANOVA. Values are given to three decimal places where appropriate.

a)

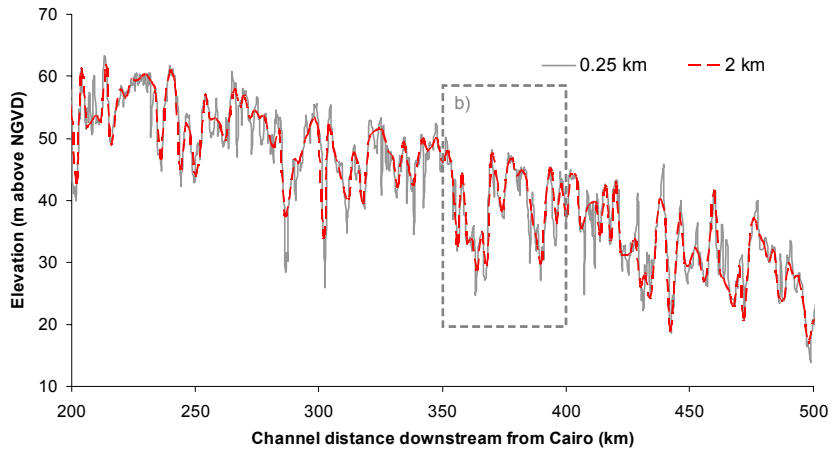

b)

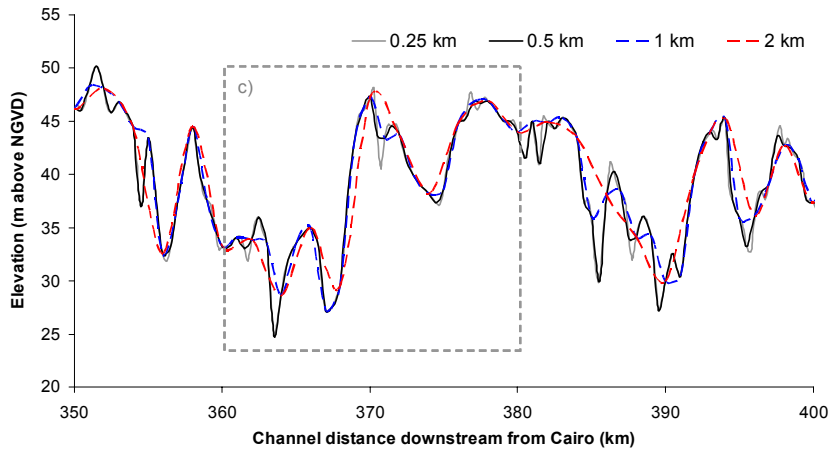

c)

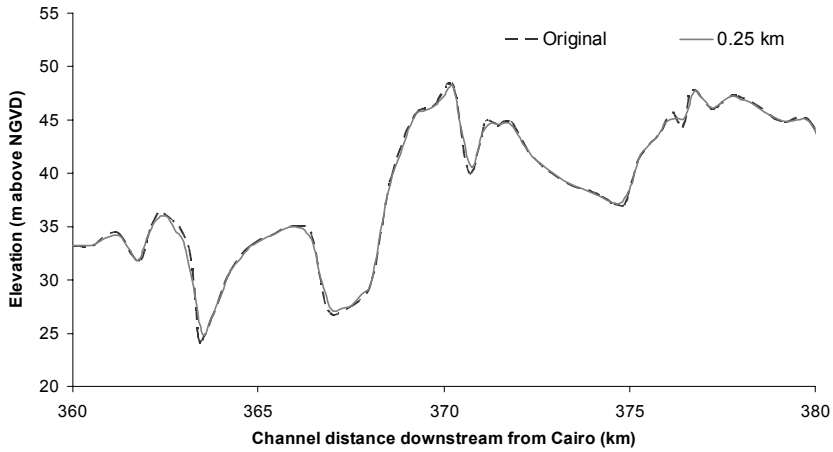

Figure 5.2 Representation of the 1974-75 long profile using a variety of sampling intervals: a) The reach between 200 and 500 km downstream from Cairo (within the USACE Memphis District) is sampled using intervals of 0.25 km and 2 km; b) a selected 50 km reach is sampled at four intervals in the range 0.25-2 km and; c) sampling at an interval of 0.25 km is compared to the original series for a selected 20 km reach.

a)

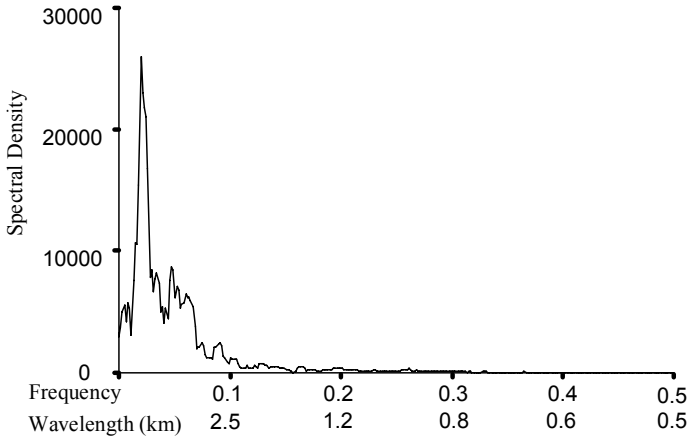

b)

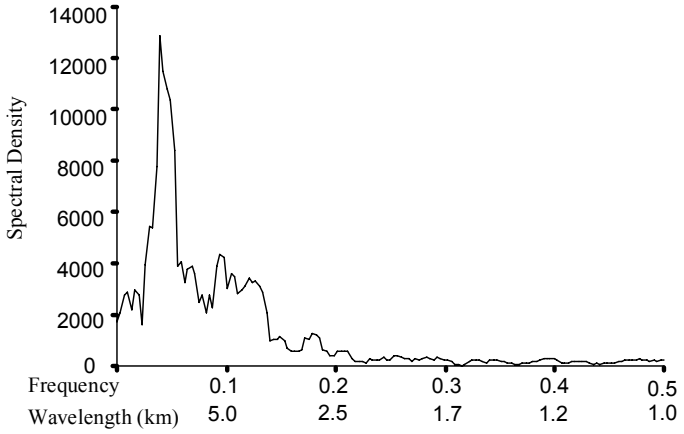

c)

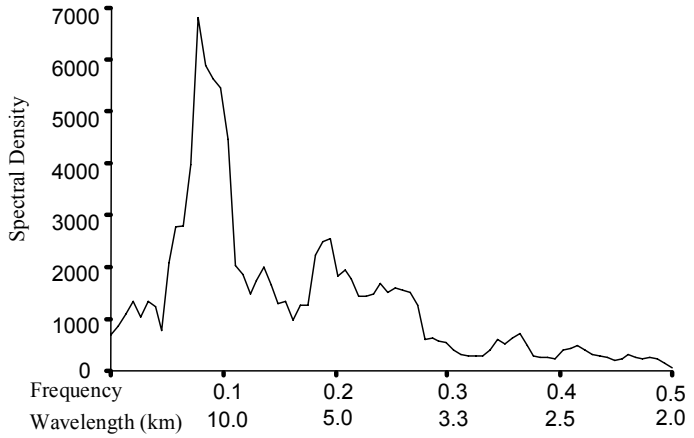

Figure 5.3 Spectral plots for the detrended long profile in reach 7 at sampling intervals of: a) 1.0 km; b) 0.5 km and; c) 0.25 km. Each series has been detrended by removal of the second-order polynomial regression function.

crossing spacing is widely quoted as being in the interval 5-7 wB (bankfull widths), studies on a variety of river systems suggest that the modal wavelength of pools and crossings is closer to 3 wB (Keller and Melhorn, 1978; Milne, 1982; Clifford, 1993). Assuming the modal wavelength on the Lower Mississippi is close to 3 wB, the minimum permissible sampling interval required to prevent aliasing is equal to 0.75 wB. Application of a 1-D step-backwater model to the 1988-89 hydrographic survey in the reach between the confluence of the Arkansas and White Rivers to just upstream from the Old River distributary suggests a mean width of 1.65 km at a discharge of 30 000 m^3s^{-1} (section 6.7). Biedenharn and Thorne (1994) state that this is close to bankfull discharge on the Lower Mississippi River. Hence, assuming this computed mean bankfull width is typical along the entire Lower Mississippi River, the maximum permissible sampling interval to prevent aliasing is approximately 1.25 km.

In addition to satisfying variance and aliasing criteria, a sampling interval of 1 km is considerably greater than the largest original mean sampling spacing in the USACE Districts. As a result, the likelihood of the statistically significant variation in original sampling spacing between the three USACE Districts (Figure 5.1) being important is reduced.

5.3 Detecting variation in profile slope at the regional, reach, and sub-reach scales

At the regional-scale, linear and second-order polynomial regression functions are fitted to the long profile to assess the degree of regularity of profile slope. Two further techniques are applied at the shorter reach-scale: moving averages and zonation algorithms. Moving averages are used as low pass filters to smooth local-scale pool and crossing undulations and therefore, emphasise trends at the larger reach-scale. Zonation algorithms are used to detect subtle and abrupt changes in the mean and variance of the series. These are based on a split window procedure where characteristics identified in first half of the window are compared to those identified in the second half of the window. Variation in the mean of the series is examined by squaring the difference in mean elevation between the two halves of the window (equation 5.1).

$$A = (X_1 - X_2)^2 \qquad (5.1)$$

where:

X_1 = mean elevation in window 1

X_2 = mean elevation in window 2

Peaks in the plot of coefficient *A* with distance downstream are indicative of abrupt changes in the characteristics of the profile. Trends over longer distances are indicative of more subtle changes. To investigate downstream trends in series variation, a similar zonation procedure is applied based on the standard deviation of the series. However, because series variance is sensitive to changes in the series mean at larger scales, trends in the mean are first removed by differencing the series. Variation is then examined by squaring the difference in the standard deviation between the two halves of the window (equation 5.2).

$$B = (\sigma_1 - \sigma_2)^2 \qquad (5.2)$$

where:

σ_1 = standard deviation of the differenced series in window 1

σ_2 = standard deviation of the differenced series in window 2

5.4 Variation in profile slope at the regional-scale

The long profile based on the channel thalweg from Cairo (0 km) to Head of Passes (1522 km) is presented in Figure 5.4. At the regional-scale, the profile generally declines in slope with distance downstream. Thus, the shape of the profile is concave. A single second-order polynomial function explains a high proportion of the total variance of the series (R^2 = 0.960), indicating that the reduction is well approximated by a parabolic curve. Most of the remaining variation can be explained by the pool and crossing undulations that are superimposed on the concave trend. However, fitting multiple linear trends by regression reveals that the reach of the Lower Mississippi River within the alluvial valley, from Cairo to the Old River distributary (1028 km), can be almost equally adequately modelled by a single linear function (R^2 = 0.956) with a gradient of 8.8 cm km^{-1} (representing a ratio of 8.8×10^{-5}). In the reach downstream from the Old River distributary, channel gradient

declines by more than a factor of four. The relatively low coefficient of determination (R^2 = 0.071) in this reach is a product of the lower reach slope and shorter reach length which together cause an increasing proportion of total variation to be explained by the pool crossing undulations.

The observation of concavity in the long profile is consistent with the findings of early researchers who identified profile concavity at a variety of spatial scales and in a variety of fluvial environments (Gilbert, 1877; Yatsu, 1955; Hack, 1957; Leopold *et al.*, 1964). However, explaining this observation has proved problematic. Mackin's (1948, 471) definition of graded state in which:

> *'slope is delicately adjusted to provide, with the available discharge and prevailing channel characteristics, just the velocity required for the transportation of the load supplied from the drainage basin.'*

focused attention on downstream trends in discharge and sediment regime. Thus, in a graded system, increases in discharge downstream through tributary input, allows sediment load to be transported on progressively lower slopes even if it remains constant in size and quantity (Richards, 1982). Similarly, the fining of bed material downstream reduces flow resistance and therefore allows the same sediment load to be transported on progressively lower slopes (Leopold *et al.*, 1964). These controls on channel slope are represented in Figure 1.1 by the connecting arrows from bed material and discharge. In the following paragraphs, these two factors are explored in relation to the long profile of the Lower Mississippi River.

Between Cairo and the Head of Passes, the Lower Mississippi River can be divided into three reaches of near-constant mean discharge (see Table 2.2). First, from Cairo downstream to the confluence of the Arkansas and White Rivers (591 km), mean discharge in the 1983-1997 water year period was approximately 16 000 m^3s^{-1}. The Arkansas and White Rivers contributed an average additional 2 000 m^3s^{-1} to the Lower Mississippi River in the second reach downstream to the Old River distributary (1025 km). In the most downstream reach, mean discharge declines by an average of approximately 3 000 m^3s^{-1} over the same period as up to 30 percent of the flow is diverted into the Atchafalaya distributary. Gauging stations within these three reaches are colour coded in Figure 5.5 to highlight the magnitude of discharge

variation both within and between the three reaches. Relating these trends to the long profile concavity identified in Figure 5.5 reveals that the reach of lowest discharge, downstream from the Old River distributary, flows on the lowest slope. Downstream discharge trends alone are therefore incapable of explaining profile concavity.

Discharge trends are more meaningful in relation to profile concavity if they are studied alongside variations in channel width because it is the stream power per unit width that determines the total energy to perform hydraulic and geomorphoological processes, not simply the channel discharge. This is rather implicitly suggested by Mackin's (1948) concept of grade through the notion of 'prevailing channel characteristics.' Analysis of reported top-bank widths by Winkley (1977) in section 4.5 provides evidence general decline in channel width downstream from Cairo to Old River (Figure 4.19a). Because this reach is well modelled by a linear trend, and discharge increases slightly through the reach, this is indicative of an increase in unit stream power with distance downstream in the alluvial valley. In addition to a reduction in the number of clay plug deposits, this therefore provides a second reason why the planform was shown to be more dynamic further downstream in the alluvial valley: bank erosion represents one possible mechanism of dissipating excess energy.

An insight into downstream trends of bed material size on the Lower Mississippi River is provided by comparison of bed material obtained from the channel thalweg in 1989 with that obtained in 1932 (Nordin and Queen, 1992). Figure 5.6a confirms that there is a general decrease in bed material size with distance downstream. Between Cairo and Memphis, in the upper reaches of the alluvial valley, approaching 50 percent of each sample was typically coarser than 0.5 mm. Downstream from Baton Rouge, the same size material typically contributed to less than 5 percent of the total distribution. The fining of bed material is consistent with the reduction in channel gradient because sediment transport can be maintained on lower slopes. The relationship is more complex however, because superimposed on this general trend is an abrupt coarsening of bed material in the vicinity of the confluence of the Arkansas and White rivers. This supports the assertion that the Arkansas River is a

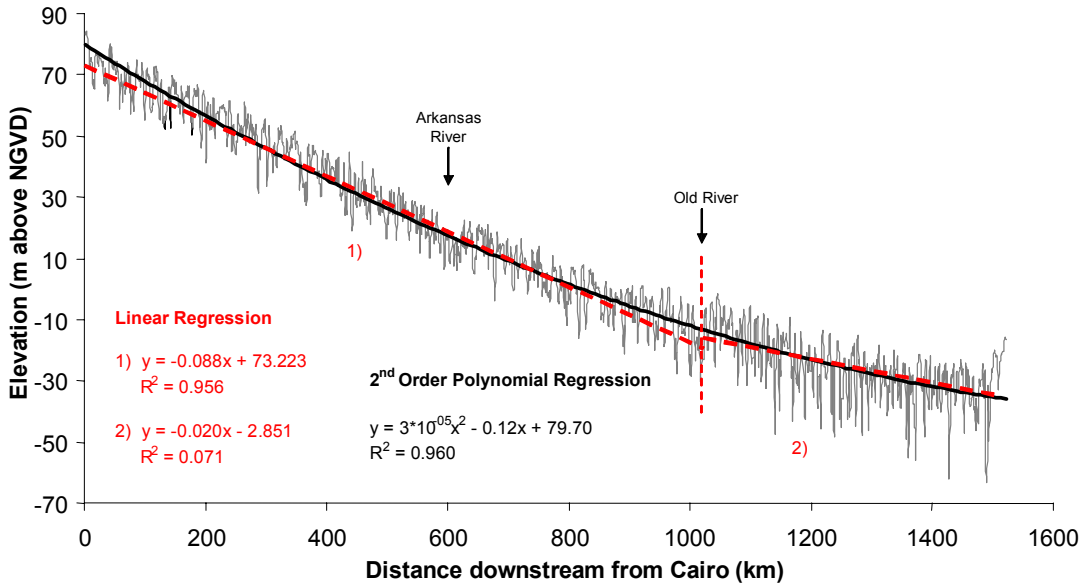

Figure 5.4 The fitting of a second-order polynomial trend and linear trends to the 1974-5 long profile of the channel thalweg. Elevations have been interpolated from the original data series at 1 km intervals.

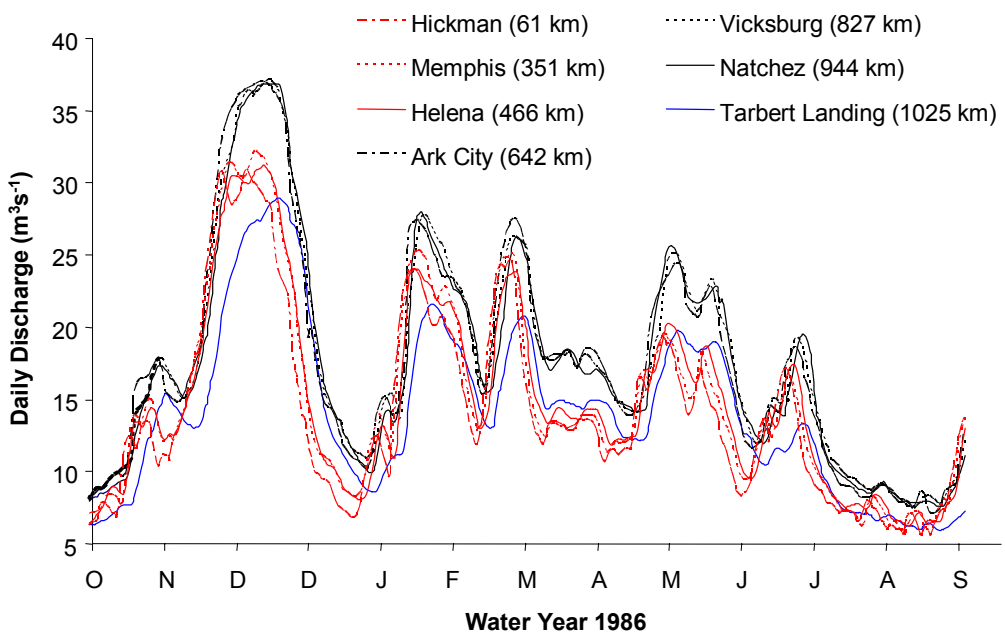

Figure 5.5 Daily discharge trends for seven gauging stations in the 1986 water year. Gauging stations are colour coded based on the following reaches (see text):

1) Red – Cairo to confluence of Arkansas and White Rivers
2) Black – Confluence of Arkansas and White Rivers to Old River distributary
3) Blue – Old River distributary to Head of Passes

key supplier of relatively coarse material to the Lower Mississippi River system (Hudson and Kesel, 2000).

Figure 5.6b indicates that reach-scale variation in bed material size was generally much greater in 1932 (pre major modification) than in 1989 in the Lower Mississippi River upstream from Vicksburg. Whilst this may be suggestive of a change in unit stream power between the two survey dates and thus, a change in system behaviour, it may equally be explained by changes in tributary sediment supply or changes in channel management activities. Regarding the former, the reduction in sediment load has been well documented by previous authors (section 2.7.2) although no study has explicitly focused on the delivery of coarser material to the alluvial valley. In terms of channel management activities, the introduction of concrete bank revetment has dramatically reduced the potential for bank erosion and hence, preventing the river from moving laterally into historic deposits of coarse material. Furthermore, extensive gravel mining, particularly in the upper part of the alluvial valley has decreased the quantity of coarse material in the Lower Mississippi River (Queen, 1994). This demonstrates the general difficultly of isolating changes in the internal geomorphological dynamics of the Lower Mississippi River behaviour from changes that are imposed on the system by either natural or anthropogenic causes.

In addition to resolving this difficultly, explaining changes in bed material size with respect to channel gradient is problematic because the variables are not strictly independent of each other (Richards, 1982). Thus, although bed material size influences channel slope through consideration of flow resistance, slope profile also conditions bed material size because coarser particles are deposited when they cannot be transported over lower gradients. An even more fundamental problem with attempting to explain profile slope in terms of bed material is that it only allows for one component (skin resistance) of total flow resistance to be considered. Changes to the morphology of the channel probably provide a much greater proportion of total resistance via *form* resistance (Carey and Keller, 1957; see Figure 2.1). Chapter 4 demonstrated that before effective bank stabilisation, the Lower Mississippi River was able to change form resistance by adjusting its planform morphology. The following sections of this chapter examine downstream morphological changes in the long profile at the reach and sub-reach scales.

a)

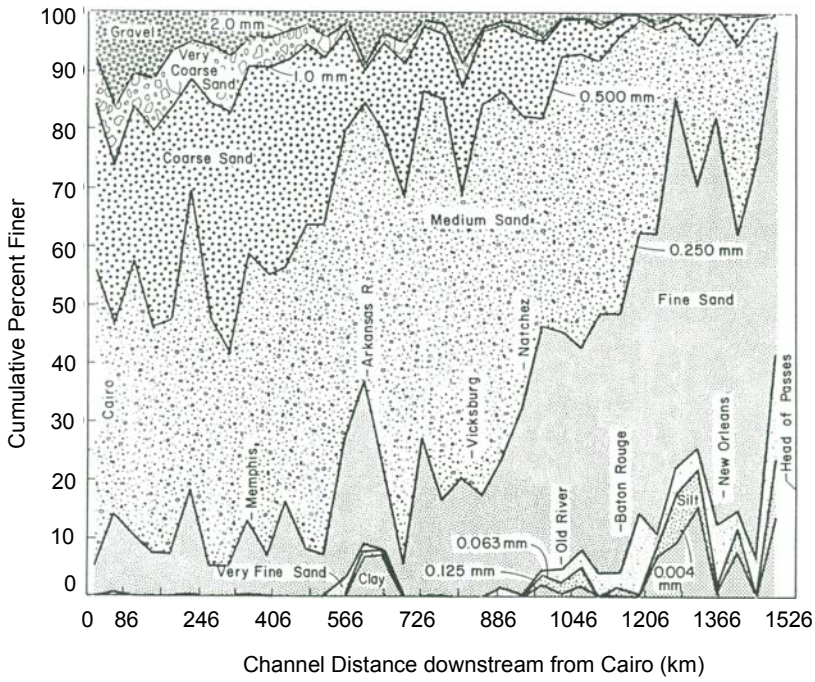

b)

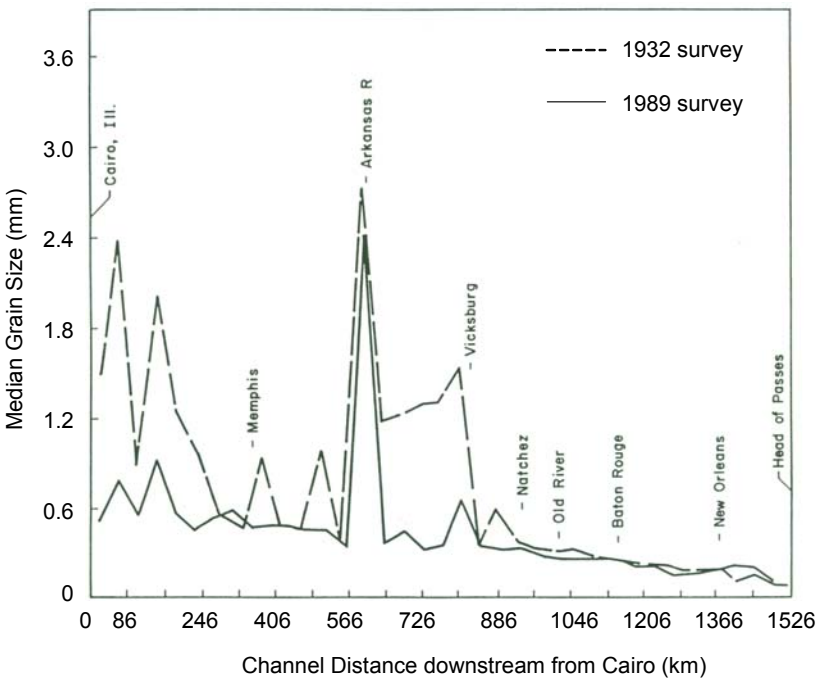

Figure 5.6 a) Composition of bed material in 1989 thalweg survey and b) comparison of median grain diameters for the 1989 and 1932 thalweg surveys. Both plots are averaged over 40 km reaches and modified from Queen (1994). Channel distance downstream from Cairo is converted from USACE 1962 river miles upstream from Head of Passes.

5.5 Variation in profile slope at the reach-scale

Reach-scale trends in the long profile are examined using moving average smoothing filters and the mean elevation difference coefficient (equation 5.1). In Figure 5.7a, a 40 km moving average has been fitted to the longitudinal thalweg profile. This interval was selected as an initial window size by estimating the likely mean wavelength of pool-crossing units and hence, the minimum moving average window required to effectively dampen this scale of undulation by smoothing. Based on a bankfull channel width (w_B) of 1.65 km (see section 6.7) and assuming that pool-to-pool spacing is within the conventional interval of 5-7 w_B, a 40 km window incorporates at least four pool-crossing units. If a modal spacing of 3 w_B is assumed meanwhile, a 40 km window incorporates at least eight pool-crossing units. Hence, this interval effectively dampens the pool-crossing scale of variation. To examine larger reach-scale trends, an 80 km moving average smoothing filter is plotted against distance downstream in Figure 5.7b. Downstream trends are difficult to detect visually and so coefficient *A* is plotted alongside the moving average to detect remaining downstream variation. This is generated by moving a 160 km split window through the series and applying equation 5.1. A window size of 160 km was selected because each half-window is 80 km in diameter. This is therefore, directly comparable with the size of the moving average window.

Figure 5.7a reveals considerable variation at a scale intermediate between sub reach-scale sequences of pools and crossings, and regional-scale profile concavity. This supports Leopold *et al*.'s (1964) assertion that long profiles are rarely smooth curves, or composites of smooth curves. At least two reaches are evident where the elevation of the moving average increases, rather than decreases downstream. This suggests that the Lower Mississippi River has sufficient stream power to maintain 'uphill' flow over short reaches. At the larger reach-scale in Figure 5.7b, these reaches are still evident despite further smoothing. Downstream trends within coefficient *A* are used to propose a tripartite division of the Lower Mississippi River. First, from Cairo to approximately 550 km downstream, an increasing trend of *A* is indicative of an increase in the magnitude of difference between the two halves of the window and hence, profile convexity (Reach *a*). From approximately 700 km to

1 000 km, no increasing or decreasing trend of coefficient *A* is indicative of the maintenance of a consistent profile gradient and therefore, a linear profile (Reach *b*). Finally, from approximately 1100 to approximately 1450 km, a decreasing trend of coefficient *A* is indicative of a decrease in the magnitude of difference between the two halves of the window and hence, profile concavity (Reach *c*). Such a tripartite division may indicate that the long profile is more appropriately considered in physical causative terms as the product of three profiles instead of a single profile. This is considered further in the discussion section at the end of this chapter. In the following paragraphs, the downstream reach-scale trends in profile slope noted above are discussed in relation to geological, neotectonic, tributary, and engineering controls.

5.5.1 Geological controls

The form of the 1974-75 long profile at the reach-scale in Figure 5.7b reflects at least two geological controls that have been 'inherited' from past geomorphological conditions. First, the slight convexity of the longitudinal thalweg profile within the upper alluvial valley is most likely attributable to high rates of localised aggradation in the late Wisconsin and early Holocene periods in the reach immediately downstream from Cairo. This is supported by three lines of evidence. First, during the drainage of proglacial lakes Agassiz and Superior, discharge through the Mississippi River system was at least an order of magnitude greater than today (Teller, 1990). The coarse sand and gravel bedload transported by the Lower Mississippi River during this period is preserved as coarse valley train deposits in the upstream third of the alluvial valley. These deposits are discussed in the context of implications for rates of planform migration in section 4.10.2. Second, more localised evidence of aggradation in this reach is provided by the Charleston alluvial fan deposit, formed around 10.9 kA BP (Porter and Guccione, 1994; see section 4.10.3). Finally, evidence of coarser bed material in the reach immediately downstream from Cairo is provided by the 1932 median grain size (Figure 5.6b).

Second, profile concavity in the downstream reach is a product of high rates of deltaic sedimentation, especially during the late-Holocene period (Saucier, 1994). The degree of present-day concavity is unique because the modern 'Plaquemines'

a)

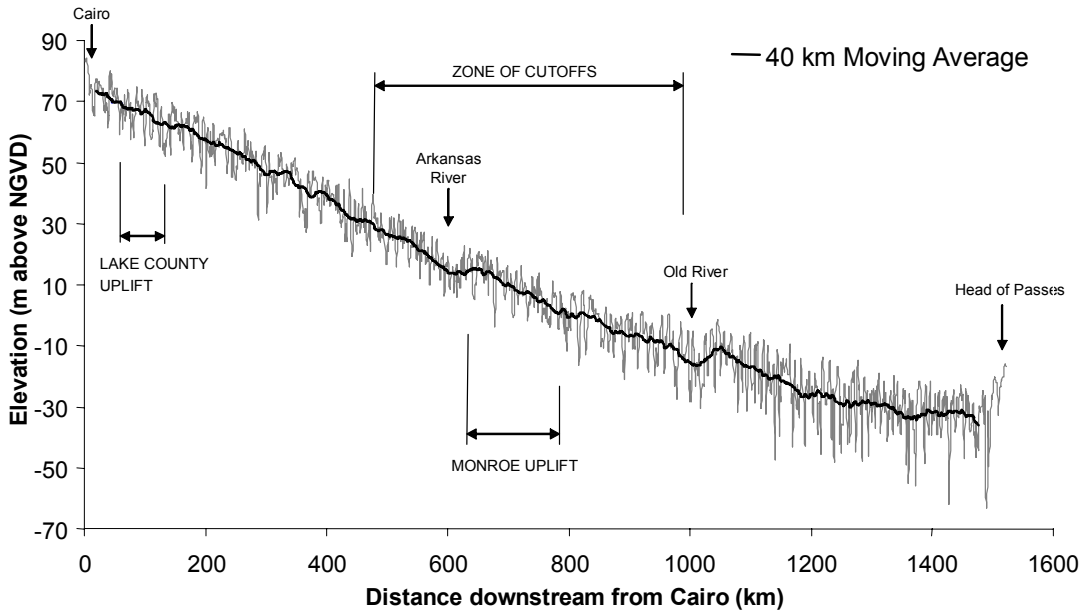

b)

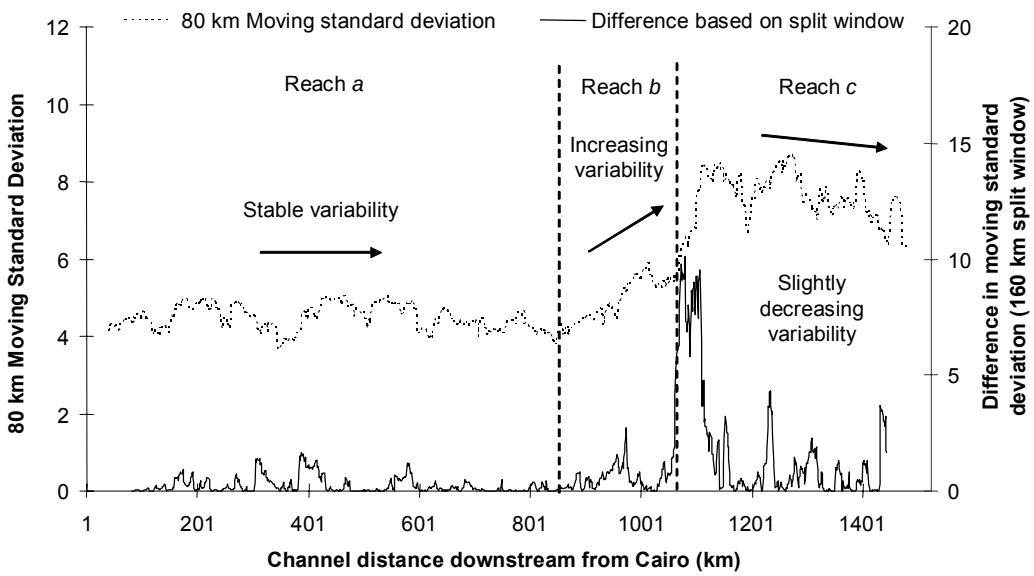

Figure 5.7 a) Smoothing the 1974-5 long profile using a 40 km moving average. b) An 80 km moving average applied to the long profile plotted alongside the coefficient obtained by applying equation 5.2 using a 160 km split windowing procedure.

delta is the only complex of those formed in the Holocene period which has prograded to the edge of the continental shelf (Figure 5.8). This suggests that the downstream reach of the 1974-5 long profile may be longer and flatter (and therefore, more concave) than at any other time during the Holocene period. This concavity is also at least partially a product of engineering modification and is discussed further in section 5.5.4.

5.5.2 Tributary controls

The two reaches of apparent 'uphill flow' in Figure 5.7a are both located immediately downstream from major tributary and distributary junctions: the confluence of the White and Arkansas Rivers; and the Old River distributary. This is perhaps suggestive of localised aggradation downstream from both junctions. Downstream from the confluence of the Arkansas and White Rivers, localised aggradation would be most likely caused by deposition of the coarser fractions of the bedload supplied by the Arkansas River. This hypothesis is consistent with the relatively coarse median bed material size in this reach, sampled in both 1932 and 1989 (Figure 5.6b). Meanwhile, downstream from Old River distributary, localised aggradation is possible if the abrupt decline in discharge is accompanied by no change in channel width because this would result in a reduction in stream power per unit width.

5.5.3 Neotectonic controls

A second explanation of apparent 'uphill flow' downstream from the confluence of the Arkansas and White rivers in Figure 5.7a is provided by considering the pattern of surface deformation caused by the Monroe Uplift (see Figure 2.7). Neotectonic uplift produces a physical control in a river system by reducing slope and stream power upstream from the axis of uplift and increasing them further downstream (Richards, 1987). Figure 5.7a shows that the upstream flank of the Monroe Uplift coincides with the apparent increase in elevation. Gregory and Schumm (1987) suggest that in this reach, Tertiary bedrock has been uplifted by neotectonic activity and now forms a resistant, non-alluvial, hard point in the channel bed. On the

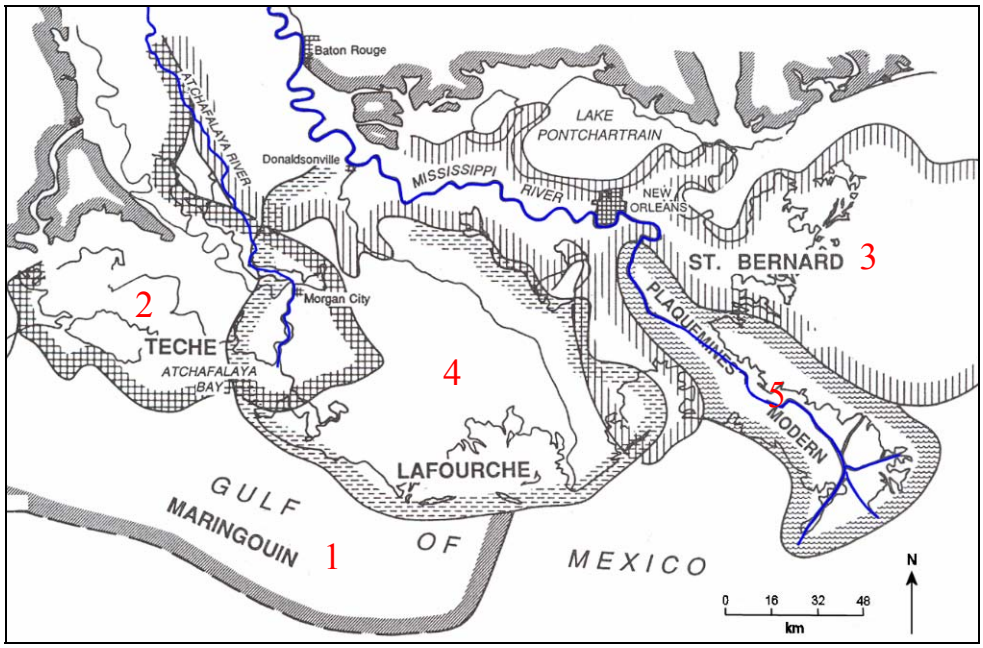

Figure 5.8 The five Holocene delta complexes recognised in the most recent interpretation of delta chronology (modified from Frazier, 1967; in Saucier, 1994): 1 = oldest complex; 5 = most recent complex.

downstream flank of the Monroe Uplift, profile steepening is difficult to detect, especially as recent profile steepening in this reach is most likely attributable to the artificial cutoff programme.

In the upper alluvial valley, Gregory and Schumm (1987) report surface uplift in the Lake County neotectonic zone as much as ten metres above the general level of the Lower Mississippi River. However, the 40 km long profile moving average does not provide clear evidence of any significant surface deformation in the Lake County Uplift zone. This suggests that any uplift is of a magnitude considerably less than that suggested by Gregory and Schumm (1987), and is probably only of limited importance to reach-scale processes.

5.5.4 Engineering controls

During the twentieth century, engineering modifications have influenced the long profile in two major ways. First, the opening of the Old River control structure in 1956 at the confluence of the Old River distributary has regulated the distributary outflow of the Lower Mississippi River and prevented the avulsion of the entire flow into the Atchafalaya River. Without the operation of the Old River control structure, Hardin (1956) anticipated that total avulsion would have occurred sometime between 1968 and 1985. The channel distance to the Gulf of Mexico from the Old River distributary is 275 km shorter down the Atchafalaya River than the present course of the Lower Mississippi River (Figure 5.8). Therefore, if the river had been allowed to naturally drain into the Atchafalaya River, the long profile through the delta would be much steeper. Referring back to Figure 5.4, it is reasonable to argue that the whole profile may have approximated a single linear function. Second, the apparent linear trend in the middle reach of the long profile must also be viewed in the context of engineering modification. This reach has been oversteepened first, by dramatic channel shortening caused by the artificial cutoff programme, and second, by forcing a fixed planform alignment through bank stabilisation.

Since valley slope can be assumed constant at the 200-year timescale, variation in channel sinuosity between fixed locations in the valley is indicative of variation in

channel slope. Exploring temporal variations in channel sinuosity in the 1965-1975 period therefore provides a method of situating the magnitude of steepening associated with engineering modification within the context of observed pre-modification adjustments. This does assume no long-term vertical degradation or aggradation in the river throughout the 1765-1975 period. In the pre-cutoff (1765-1930) period, this assumption is supported by Beidenharn *et al*. (2000) based on specific gauge records. Although the conceptual model of morphological response advocated by Biedenharn and Watson (1997; see Figure 2.15) is suggestive of a spatial trend of vertical changes in the post-cutoff period (1930-1975), the importance of vertical change is considered small in relation to changes in channel length.

In Figure 5.9a, the 1974-75 longitudinal thalweg profile is segmented into eight reaches with the sinuosity of each reach labelled. The first six reaches correspond to the six reaches identified in Figure 4.11 between Cairo and Baton Rouge. The remaining channel between Baton Rouge and Head of Passes has been divided into two further reaches of approximately equal channel length. The boundary between reaches 7 and 8, at 1375 km downstream from Cairo, is located at approximately the city of New Orleans (see Figure 2.3). Sinuosity is highest in reaches 1 and 6 but consistently lower in the artificial cutoff reaches (reaches 3, 4 and 5). However, during the pre-cutoff 1765-1930 period, sinuosity was consistently higher in the artificial cutoff reaches, especially in reach 4 (Figure 5.10b). Relating back to the 1974-75 long profile, this indicates that prior to the artificial cutoff programme, the upstream reaches 1 and 2 would have been steeper than the midstream reaches 3, 4 and 5 and hence; the long profile downstream through the alluvial valley would have been more concave. The present near-linear profile through the alluvial valley (Figure 5.4) is therefore, at least partially, a product of engineering modification. A concave profile in the pre-cutoff period is more consistent with the increase in discharge downstream from the confluence of the Arkansas and White Rivers (Figure 5.5) at the boundary of reaches 3 and 4.

a)

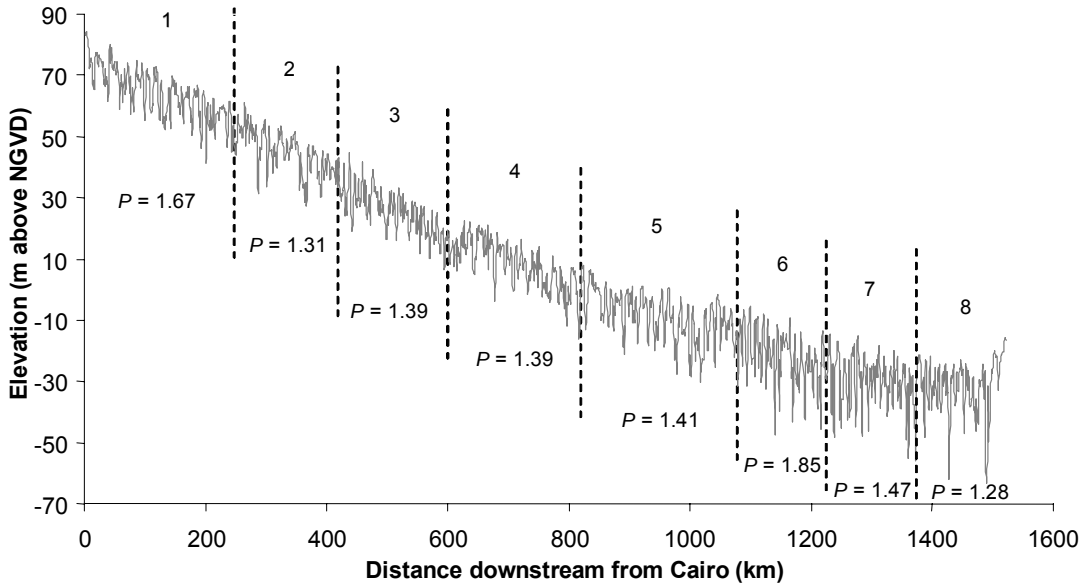

b)

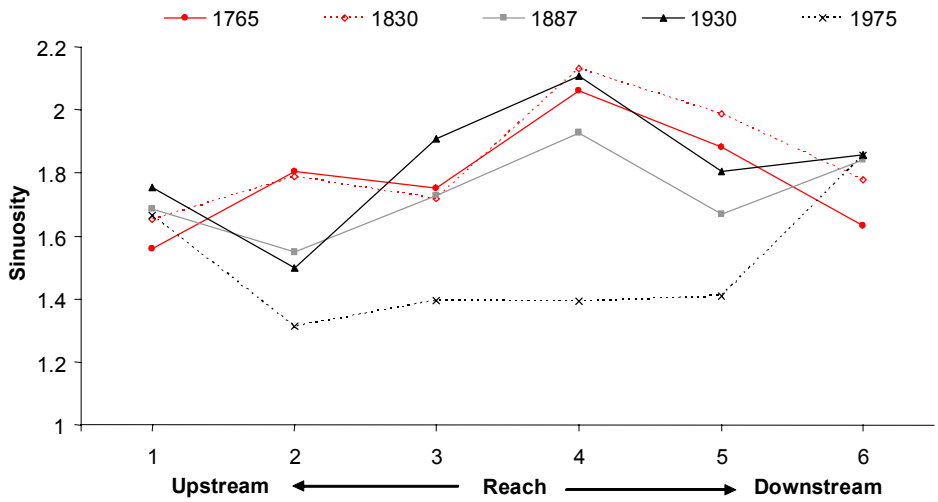

Figure 5.9 a) Reach sinuosity in relation to the 1974-75 long profile and; b) temporal trends in reach sinuosity (reaches 1-6) in the period 1765-1975.

5.6 Variation in profile slope at the sub-reach scale

In Figure 5.10, an 80 km moving standard deviation of the longitudinal thalweg profile is plotted alongside the mean standard deviation difference coefficient (*B*, equation 5.2). Three reaches have been identified based on trends within the variance of the series. Reach *a*, extending from 0 km (Cairo) to approximately 850 km downstream (between Vicksburg and Natchez) is characterised by a stable level of variation, indicated by both stability in the moving standard deviation and coefficient *B*. Reach *b* extends from approximately 850 km to 1050 km (approximately 20 km downstream from Old River distributary) and is characterised by increasing variation with distance downstream. This is illustrated by a steady upward trend in the standard deviation. At approximately 1050 km, an abrupt peak in coefficient *B* is indicative of a dramatic increase in the level of variation. Further downstream (Reach *c*), variation is maintained at this high level before marginally decreasing towards the Head of Passes (1525 km).

This abrupt increase in sub-reach scale variance downstream from Old River is consistent with the geological boundary between the alluvial valley and the deltaic plain. However, the gradual increase in variation from approximately 850 km suggests that this boundary does not represent a sharp division between geological units but rather a gradual transition as median bed material size declines with distance downstream within the alluvial valley (Figure 5.6b). It is important to note however, that these trends based on standard deviation do not reveal how the *type* of variation changes downstream. For example, increases in series variance could be caused by an increase in pool and/or crossing amplitude and/or a decrease in wavelength. Figure 5.9a suggests that bedform amplitude does increase in the downstream direction but it is difficult to visually identify differences in the relative behaviour of pools and crossings. Moreover, no impression can be gained of changes in bedform wavelength. In the next section, serial techniques are used alongside pool and crossing classification techniques to reconcile the downstream variation in pool-crossing amplitude and wavelength.

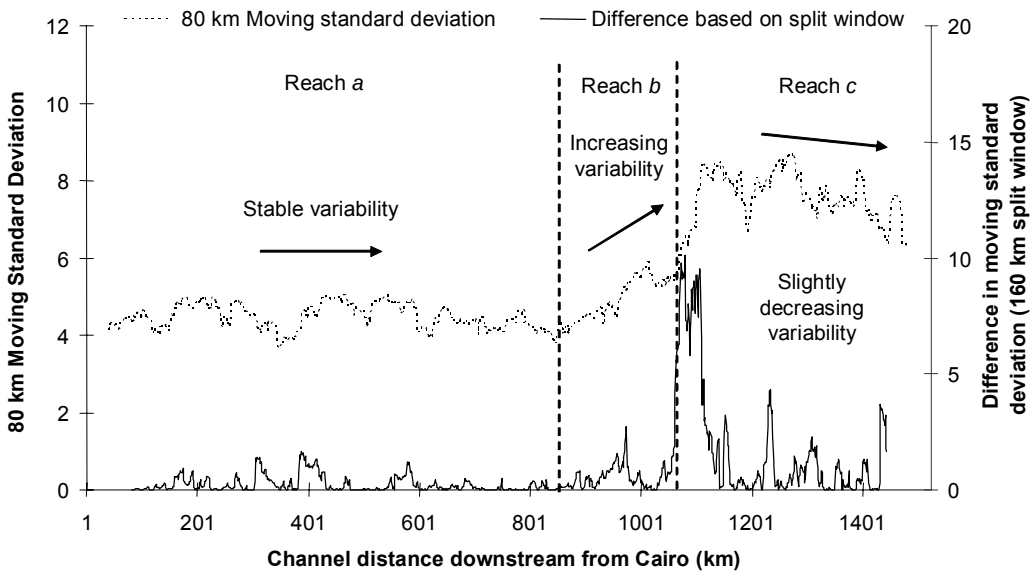

Figure 5.10 Moving standard deviation plotted alongside the coefficient obtained by applying equation 5.2 using a 160 km split windowing procedure.

5.7 Variation in pool and crossing amplitude and wavelength

Variation in pool and crossing amplitude and wavelength is examined between the eight reaches (six planform reaches and two further reaches) extending from Cairo to the Head of Passes (see Figure 5.9). Parametisation of wavelength and amplitude is achieved by the same set of serial techniques applied to the planform series in Chapter 4, in conjunction with regression and bedform differencing techniques. The latter two techniques are used to consistently classify pools and crossings in order to isolate relative differences in their downstream wavelength and amplitude characteristics. Definitions of the key parameters used throughout this section are given in Figure 5.11. Definitions are generally synonymous with definitions of meander bend parameters (see Figure 4.29). This is considered appropriate since pool-crossing undulations in the long profile have been deemed analogous with meandering in the vertical dimension (Keller and Melhorn, 1978).

5.7.1 Downstream trend removal by regression

Because interest is in elevation changes about the larger-scale mean, downstream trends in profile gradient were removed by fitting regression functions to the original profile (Table 5.3). Pool and crossing undulations are preserved in the unstandardised residuals.

The fitting of second-order polynomial functions generate consistently higher R^2 values than linear functions. Hence, second-order polynomials were used to detrend all of the profiles. This was deemed an appropriate method of achieving stationarity since, with respect to spectral analysis, Granger and Hatanaka (1964; 136) argue that:

> *'Polynomial regression and subtraction does not affect to any worthwhile extent the spectral estimates of frequency bands other than the band centred on zero frequency, which it effectively removes'*

R^2 values tend to decrease with distance downstream, particularly downstream from reach 4. This may support the increasing amplitude of pools and crossings in downstream reaches although this trend may also be explained by the reduction in

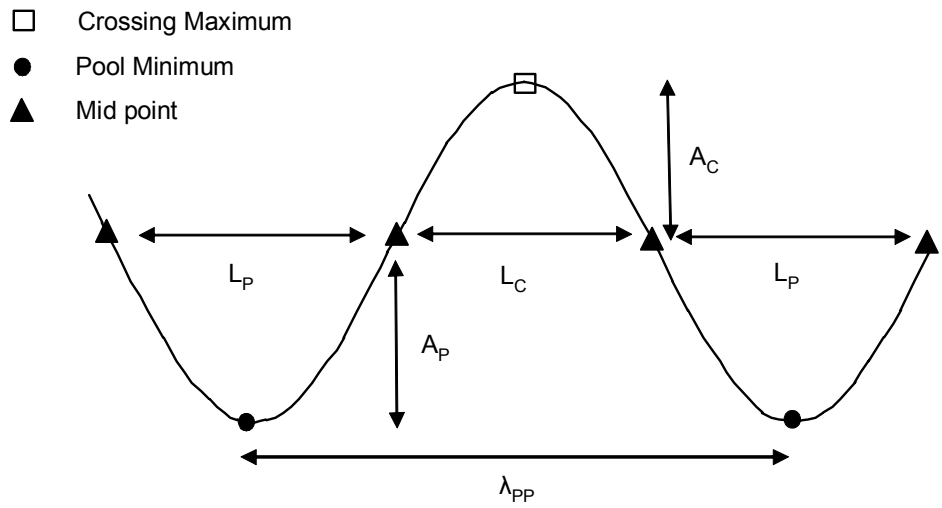

where:

λ_{PP} = pool-to-pool wavelength

L_P = length of pool

L_C = length of crossing

A_P = pool amplitude

A_C = crossing amplitude

Figure 5.11 Definition of pool and crossing amplitude, length and spacing (pool-to-pool wavelength) based on a regular sine wave.

profile slope. The skewness ratio is a measure of the distribution of the residuals in relation to the regression line. All of the residuals from second-order polynomial regression are negatively skewed, indicating that crossings are generally longer but lower in amplitude (above the regression line) than pools.

5.7.2 Second-order autoregressive modelling

For all reaches except reaches 4 and 6, the autocorrelation function demonstrates an oscillatory tendency and the second-order coefficient is significant at the 95 percent confidence level in the PACF (Figure 5.12). All of the reaches except reach 4 satisfy the equation for pseudo-periodicity. Although R^2 values are typically low (less than 0.5) this is most likely attributable to the inability of the second-order autoregressive model to replicate the relatively high amplitude of pools and crossings, especially in the downstream reaches (see Figures 4.32 and 4.33).

The identification of a pseudo-periodic component in the majority of reaches reveals that the pool-crossing oscillation in the long profile is adequately described by a periodic component which varies in both wavelength and amplitude according to a random element. Pseudo-periodic trends have been noted in the long profile in a variety of fluvial systems (Nordin and Algert, 1966; Richards, 1976b; Clifford, 1993). The identification of pseudo-periodicity within the long profile of the Lower Mississippi River is therefore important because it indicates that despite extensive engineering modification, the river has maintained sub-reach scale longitudinal properties typical of natural systems.

5.7.3 Spectral analysis

The spectral plots for the eight reaches are presented in Figure 5.13. The spectra for reaches 2, 6 and 7 are characterised by single, relatively sharp peaks, indicative of dominance of a regular, periodic form of undulation. In the other reaches, more than one peak dominate the spectra, indicating that the variance is distributed over a wider range of wavelength scales. Spectral estimates of wavelength range from 5.3 km in reach 2 to 30.3 km, also in reach 2. These are more variable than autoregressive

a)

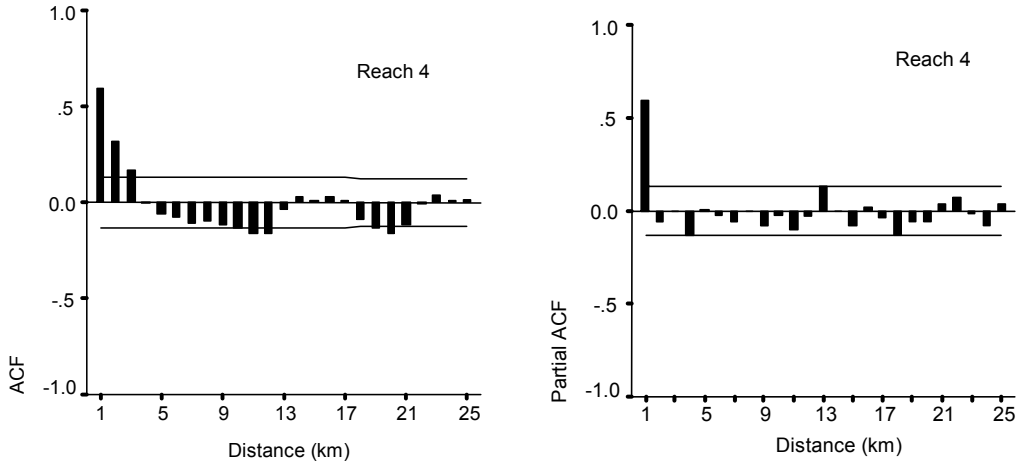

b)

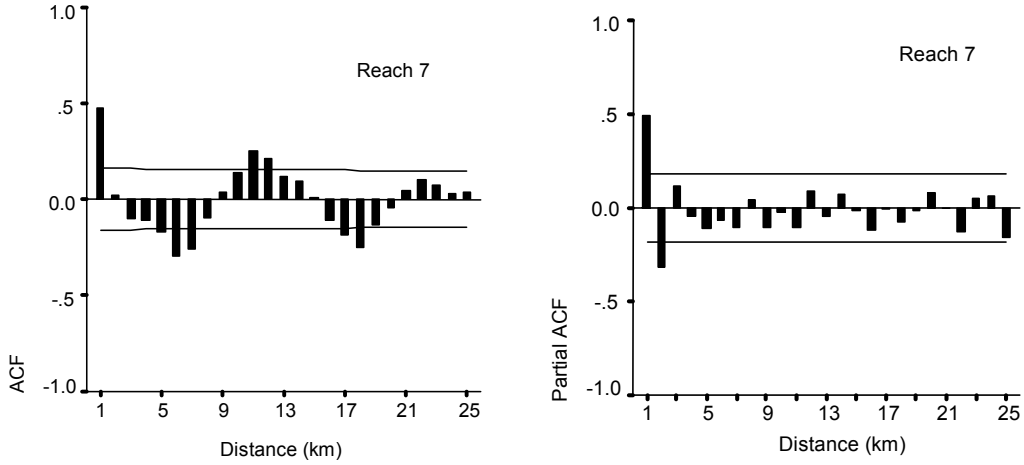

Figure 5.12 Comparison of the ACFs and PACFs for: a) reach 4 (confluence of Arkansas River to confluence of Yazoo River at Vicksburg) and; b) reach 7 (Baton Rouge to New Orleans).

		Regression			Second-order autoregressive modelling						
	Reach	**Linear R^2**	**Polynomial† R^2**	**Skewness ratio**	**$Ø_1$**	**$Ø_2$**	**R^2**	**$Ø_1^2 < -4Ø_2$?**	**Pseudo-periodic?**	**Sig. 2nd coef. in PACF?**	**Wavelength (km)**
Upstream	1	0.637	**0.640**	-0.555	0.763	-0.202	0.424	-0.226	Yes	Yes	11.28
	2	0.369	**0.373**	-0.943	0.836	-0.251	0.473	-0.305	Yes	Yes	10.76
	3	0.503	**0.527**	-0.095	0.613	-0.146	0.302	-0.208	Yes	Yes	9.82
	4	0.510	**0.528**	-0.422	0.658	-0.079	0.37	0.117	No	No	---
	5	0.325	**0.343**	-0.647	0.865	-0.209	0.51	-0.088	Yes	Yes	19.04
	6	0.201	**0.204**	-0.676	0.519	-0.128	0.224	-0.243	Yes	No	8.28
	7	0.096	**0.114**	-0.732	0.608	-0.274	0.283	-0.726	Yes	Yes	6.61
Downstream	8	0.076	**0.085**	-1.252	0.653	-0.316	0.324	-0.838	Yes	Yes	6.61

† Second-order

Table 5.3 Removing the trend from the longitudinal thalweg profile of each reach by linear and second-order polynomial regression and detection of pseudo-periodicity by second-order autoregressive modelling.

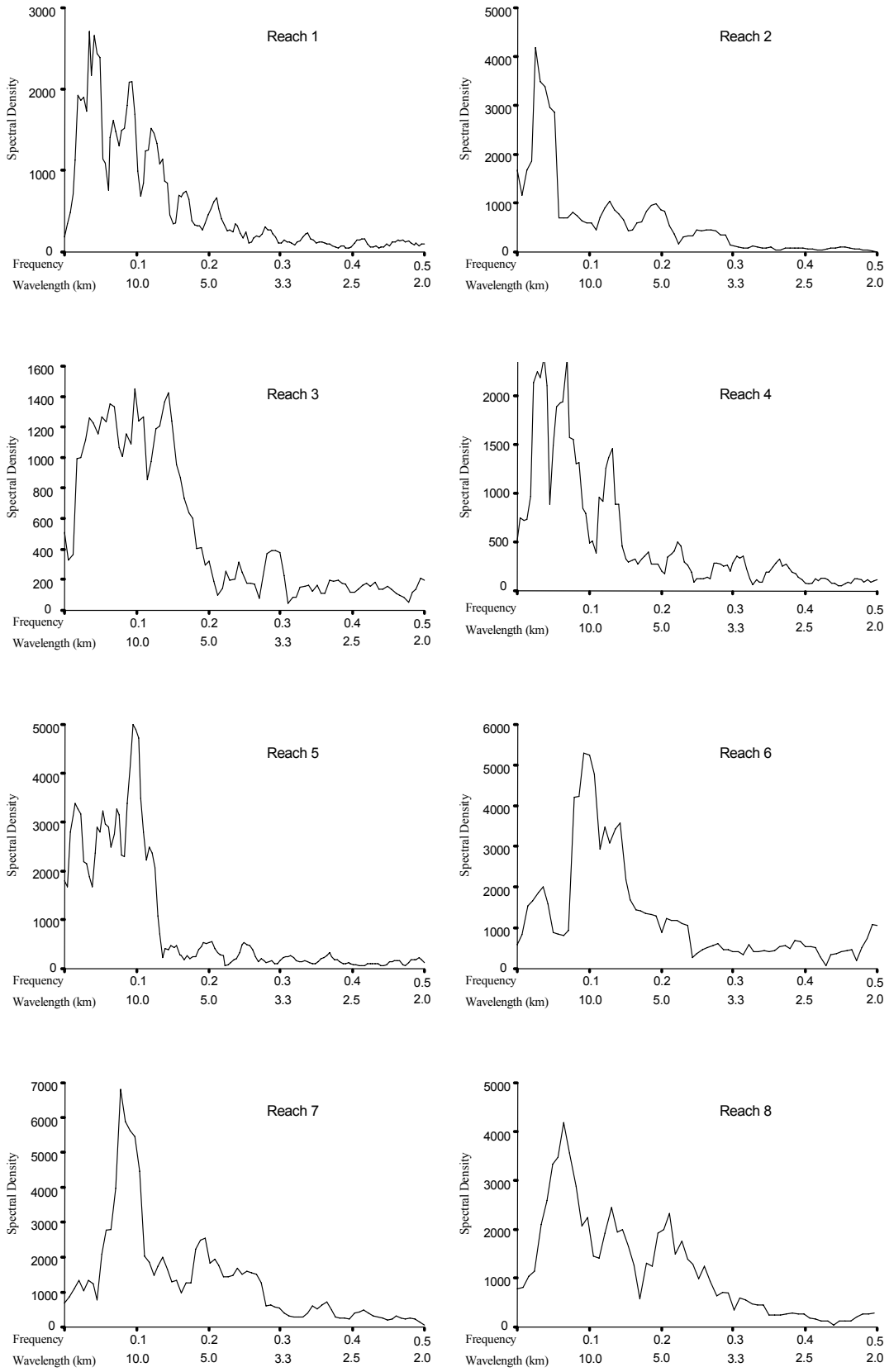

Figure 5.13 Spectral plots of the detrended long profile in each of the eight reaches.

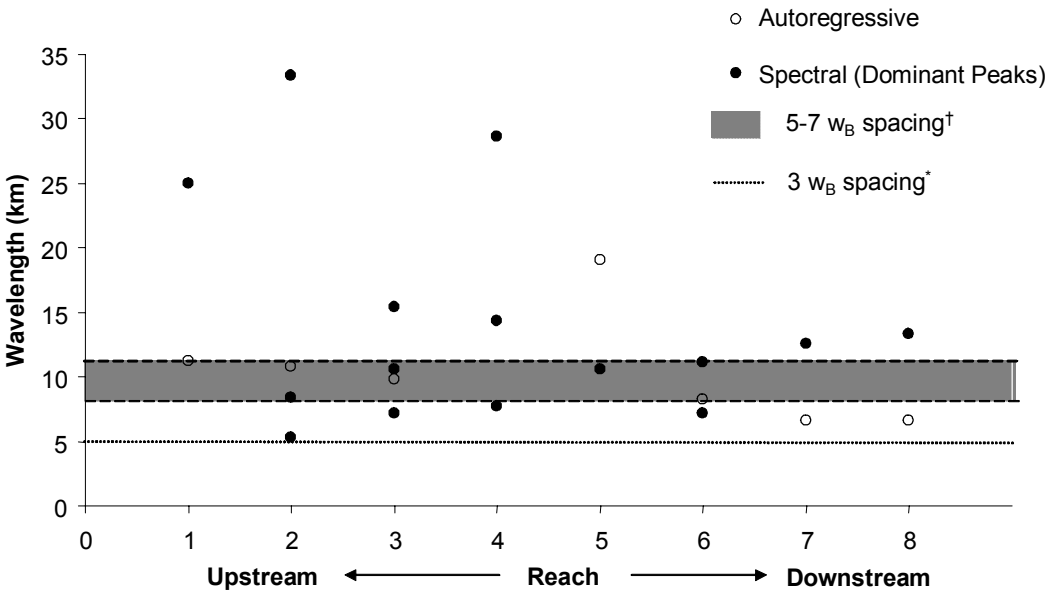

Figure 5.14 Variation in wavelength downstream estimated by second-order autoregressive and spectral techniques. †Expected average spacing in the range 5-7 bankfull widths and *expected modal spacing at $3w_B$. The estimate of bankfull width is based on the 1988-89 flow model estimate for a discharge of 30 000 m^3s^{-1} (see section 6.7.4).

estimates which range from a maximum of 19.2 km in reach 5, to a minimum of 6.6 km in reaches 7 and 8 (Table 5.3). Despite different levels of variability, both spectral and autoregressive estimates are suggestive of a decline in wavelength with distance downstream (Figure 5.14). Spectral analysis reveals a tendency of very long wavelengths in the upstream reaches 1-4 with considerably lower wavelengths downstream. With the exception of reach 5, second-order autoregressive estimates indicate a near-linear decline in downstream wavelength.

Based on a computed bankfull channel width of approximately 1.65 km (see section 6.7.4), these wavelength estimates are compared to the 'expected' spacing of pools and crossings in the conventional interval of 5-7 w_B and the reported modal spacing at approximately 3 w_B. Autoregressive estimates of wavelength are close to the former interval range except in reach 5 whereas wavelengths obtained from spectral techniques tend to deviate more widely. All estimates lie above the expected modal wavelength estimate.

5.7.4 Pool and crossing parameterisation by regression

i) Determination of the most appropriate sampling interval

Regression analysis utilises best-fit regression functions to define the pool-crossing mid-point (Figure 5.11) and hence classify pools and crossings (see section 3.2.3). Robinson's (2003) classification of bedforms on the Clyne River in Wales by regression analysis revealed a high sensitivity to the initial sampling interval. Doubling the sampling interval increased the number of bedforms by an average of 50 percent. Therefore, prior to analysing downstream trends in pool and crossing parameters, the sensitivity of the technique to sampling interval was examined. In Figure 5.15, the reach-averaged pool-to-pool wavelength is plotted against reach number at sampling intervals of 0.25, 0.5 and 1.0 km. A sampling interval of 1.0 km was the maximum interval examined because this is the maximum permissible interval to prevent aliasing (see section 5.1). Increasing the sampling interval from 0.25 to 0.5 km increases the pool-to-pool wavelength by an average of 20 percent and further increasing the sampling interval to 1.0 km increases this by a further average of 30 percent. Mean wavelength estimates from the fitting of second-order autoregressive models are plotted to provide inter-technique comparability. A

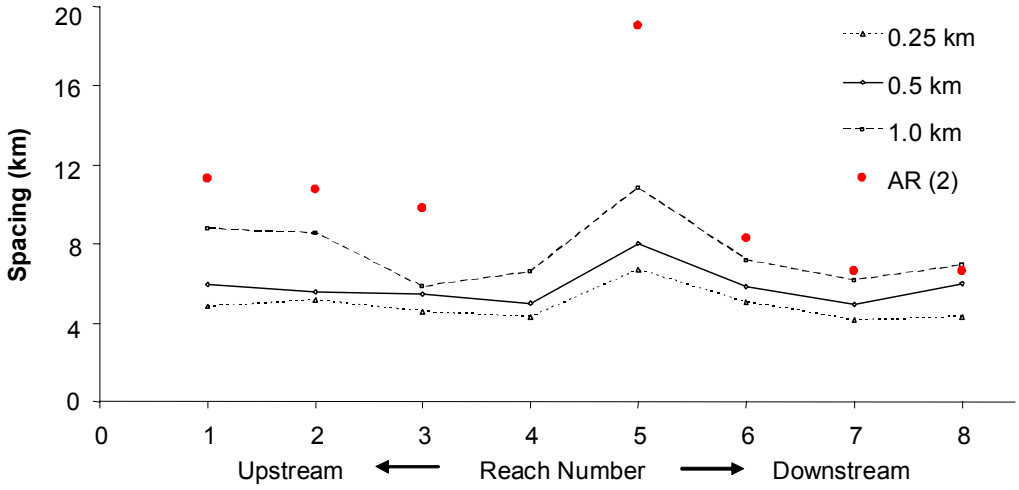

Figure 5.15 Downstream trends in reach-averaged pool-to-pool wavelength using the regression techniques at three sampling intervals: 0.25; 0.5 and; 1.0 km. Wavelength estimates are compared to those obtained from second-order autoregressive modelling.

sampling interval of 1 km provides estimates of wavelength which are empirically closest to those provided by second-order autoregressive modelling. Hence, this sampling interval is maintained in the subsequent analysis.

ii) Downstream analysis of amplitude and length characteristics

Downstream reach-averaged trends in pool and crossing amplitude, length and amplitude/length ratio are presented in Figure 5.16. Most notably, reaches on the deltaic plain (reaches 6-8) are characterised by higher amplitude and shorter length pools and crossing reaches than reaches in the alluvial valley (reaches 1-5). This change is more marked for pools than crossings, especially with respect to amplitude. For example the mean amplitude of pools in reach 6 (downstream from the Old River distributary to Baton Rouge) is over twice the mean amplitude of those in reach 4 (confluence of the Arkansas and White Rivers to the confluence of the Yazoo River at Vicksburg).

To highlight upstream and downstream variations in bedform amplitude, downstream changes in the frequency distributions of the residuals from second-order polynomial functions are presented in Figure 5.17. The combined distribution for the five upstream reaches within the alluvial valley is compared to the combined distribution for the downstream three reaches on the deltaic plain. The modal frequency is approximately stable but there is clearly enhanced variability of both extremes, indicative of both higher crossings and deeper pools on the deltaic plain. This is important, because it suggests that there is a relatively abrupt increase in large-scale bedform resistance associated with pool and crossing undulations at the boundary between the alluvial valley and the deltaic plain. This is interesting when related to both profile slope and planform characteristics. In relation to slope, the reaches flowing on the steepest slopes in the alluvial valley are characterised by lower large-scale bedform resistance than on the flatter slopes in the deltaic plain. In relation to planform characteristics, the enhanced variability coincides with a decline in the sinuosity and curvature of the river on the deltaic plain in comparison to the alluvial valley. This finding refutes Langbein and Leopold's (1966) assertion that a meandering river has larger variations in bed elevation than an otherwise straight reach.

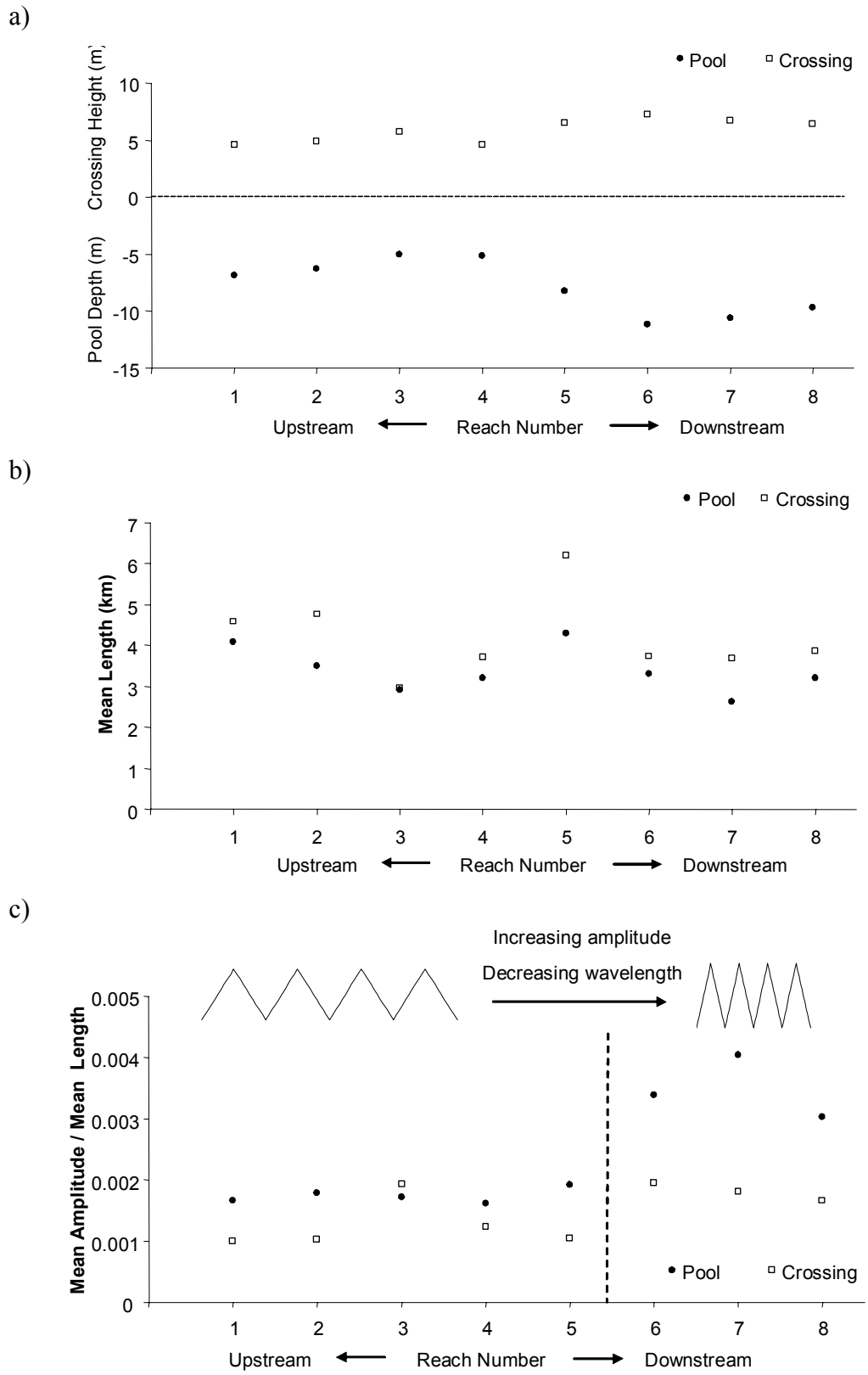

Figure 5.16 Downstream trends in reach-averaged: a) amplitude; b) length and; c) amplitude/length ratio; as identified by regression for the eight reaches of the Lower Mississippi River in 1974-75. In a), crossing amplitude is positive and pool amplitude is negative to illustrate their respective positions above and below the regression line.

In a graded river of approximately constant downstream discharge, bed material size, and width (constant unit stream power and skin resistance) it would be intuitive to expect larger and/or more frequent bedforms on the steeper slopes in order to expend the excess energy that the steeper slope provides. If the downstream variations in discharge, bed material size (section 5.4), and width are taken into account on the Lower Mississippi River, it would therefore be intuitive to expect the largest and/or most frequent bedforms where unit stream power is highest (in the midstream reaches 4-5), and the smallest and/or less frequent bedforms where unit stream power is probably at its lowest (in the deltaic plain reaches 6-8). The opposing trend noted in Figure 5.16 therefore presents an apparent paradox.

Wohl *et al.* (1993) explained a pattern of increasing wavelength and amplitude (and therefore, size) of pools and riffles, with distance downstream in three small drainage basins, in terms of changing modes of energy expenditure. This involved the idea that in higher gradient reaches, a greater proportion of total energy is expended overcoming boundary and internal resistance, and therefore, a smaller proportion of total energy can be directed towards channel bed scour. Hence, the pool riffle sequence is better developed further downstream because the river can mobilise a higher proportion of its bed and bank material. This theory can at least be partially related to the Lower Mississippi River because prior to bank stabilisation, the river throughout the alluvial valley expended a proportion of total energy by bank erosion and related sinuosity changes. At this time therefore, it can be hypothesised that, despite a low median radius of curvature, the continual migration of planform effectively prohibited the development of very deep pool features because a greater proportion of total energy at high flow was expended eroding the banks rather than scouring the bed.

Conversely, deep pools in the deltaic plain may be interpreted as a direct consequence of low rates of bank erosion (see Figure 4.59) owing to the low erodibility of the fine, cohesive bank sediments. As a result, excess energy at high discharges on the deltaic plain is expended by scouring the channel bed rather than eroding banks. This principle has been demonstrated in pioneering flume experiments by Friedkin (1945). Because this process may have occurred over a long time period, deep pools on the deltaic plain may represent an inherited, instead

of an active, geomorphological feature. Advancing this reasoning further, a similar trend of pool deepening may result from bank stabilisation in the alluvial valley. This idea is returned to in chapter 6 when temporal changes in the sub-reach scale characteristics of the long profile are considered between 1949 and 1989.

Given the downstream trends in bedform wavelength and amplitude, an important issue remains identifying the configuration which gives optimal flow resistance. Johnson (1944) approached this problem by conceptualising flow resistance over cubes at three different spacings in a flume. If blocks are spaced very close together (Figure 5.17a), flow distortion is minimised because the blocks form a relatively smooth, flat surface. Similarly, if the blocks are spaced widely apart, the total effect of individual distortions provides only a negligible resistance because most of the flow is across a flat surface (5.17b). Johnson proposes that the maximum roughness, and hence flow resistance, is provided by surface blocks with an amplitude: block spacing ratio of 0.07-0.1 (ratio *a/c* in 5.17d) and an amplitude: block length ratio in the interval 0.25-0.8 (ratio *a/b* in 5.17d). If these two ratios are combined, a maximum resistance can be achieved with an amplitude/total spacing ratio within the interval of approximately 0.055-0.09 (ratio *a/d* in 5.17d). These finding were at least partially supported in more complex flume experiments by Sayre and Albertson (1961) whose results suggested that the amplitude/total spacing ratio for maximum flow resistance lies at approximately 0.1 but is dependent on both the material and shape of the roughness elements.

Relating these ratios to amplitude/length ratios on the Lower Mississippi River indicates that maximum resistance is not being achieved by any configuration by at least an order of magnitude. However, it is unclear how relevant small-scale flume experiments are to considering the flow resistance offered by pool-crossing undulations in a large river such as the Lower Mississippi. The results from the flume experiments discussed above demonstrate a clear association with much smaller-scale dune bedforms that have an average amplitude/length of 0.06 and a maximum of 0.1 (Yalin, 1977). Dune bedforms have been shown to be related to macroturbulent flow structures that scale with flow depth (Yalin, 1992). However, pools-riffle sequences are more clearly related to macroturbulent flow structures that scale on channel width (Keller and Melhorn, 1978). Furthermore, because they are

spaced at approximately half the wavelength of meander bends, maximum large-scale bedform resistance is contolled to a certain extent by planform properties. As a result of these differences, the optimum flow resistance spacing of roughness elements is re-examined in the context of smaller-scale dune feature on the Lower Mississippi River in chapter 7. In terms of pool-crossing spacing and flow resistance, it can be assumed that the larger amplitude and lower frequency pool-crossing undulations on the deltaic plain do offer a greater resistance to flow that those in the alluvial valley.

In addition to revealing downstream trends, Figures 5.16 and 5.17 together reveal systematic differences in the shape of pools and crossings. The reach-averaged residual frequency distributions presented in Figure 5.17 are negatively skewed, indicating that pools deviate further from the regression function than crossings. Hence, on average, pools are deeper than crossings are high. Viewed in conjunction with Figure 5.16b, crossings are also generally longer features than pools. In relation to Robinson's (2003) qualitative classification of bedform shapes (Figure 5.19), these results suggest that pools and crossings on the Lower Mississippi River typically demonstrate a 'dome-up' morphology. This tendency may become more marked with distance downstream (Figure 5.16c).

Consideration of bedform shape is to some extent paradoxical because, whilst being informative on the one hand, it also reveals a flaw in the use of the regression technique to objectively identify pools and crossings. Bedform shape conditions the initial regression trend and therefore, directly influences the pool and crossing lengths and amplitudes which are subsequently derived. If pools and crossings are regular triangular features, the regression line is midway between the crossing maximum amplitude and the pool minimum amplitude. Hence, the skewness ratio is zero and the residuals from regression are normally distributed. However, in a distribution of dome-up pools and crossings, which predominate in this study, the regression line is biased towards the crossings. These are therefore subsequently interpreted as lower amplitude forms in relation to pools. The opposite situation arises in a distribution of dome-down bedforms. Because the shape of pools and crossing is variable within each reach and more critically, between each reach, the

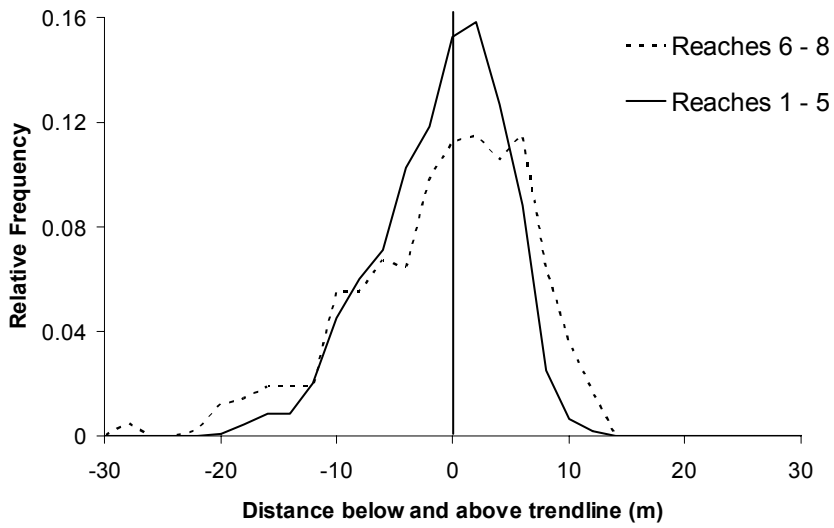

Figure 5.17 Variation in bedform shape between the upstream (reaches 1-5) and downstream reaches (reaches 6-8) of the Lower Mississippi River in 1974-75.

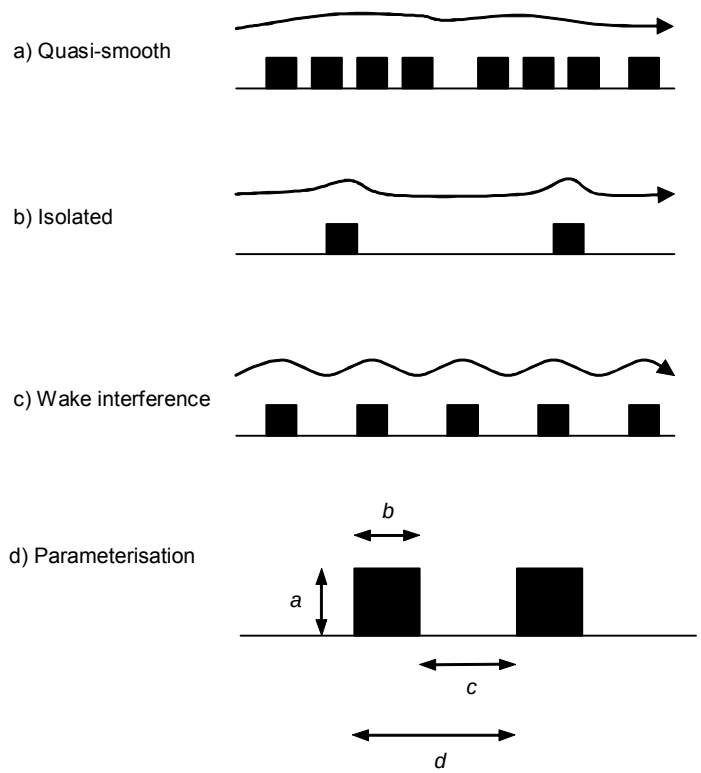

Figure 5.18 Roughness due to triangular blocks on a plane bed (modified from Richards, 1982).

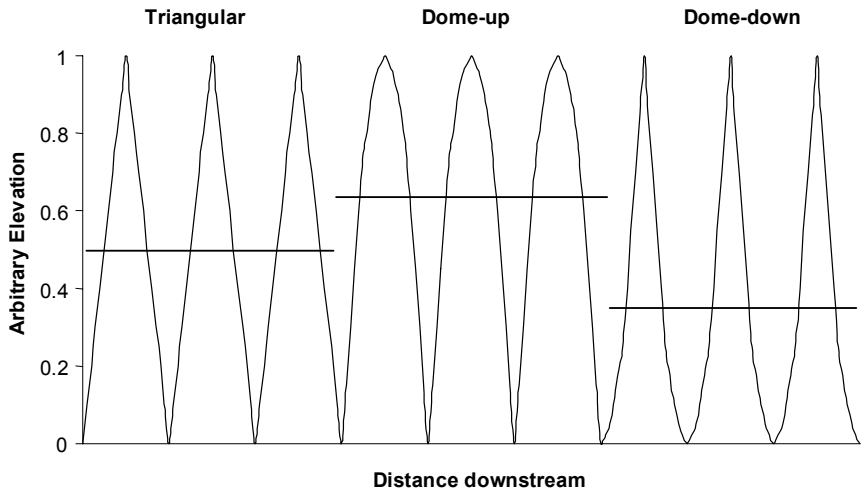

Figure 5.19 Contrasting bedform shapes and their implications for removal of regression trends (modified from Robinson, 2003).

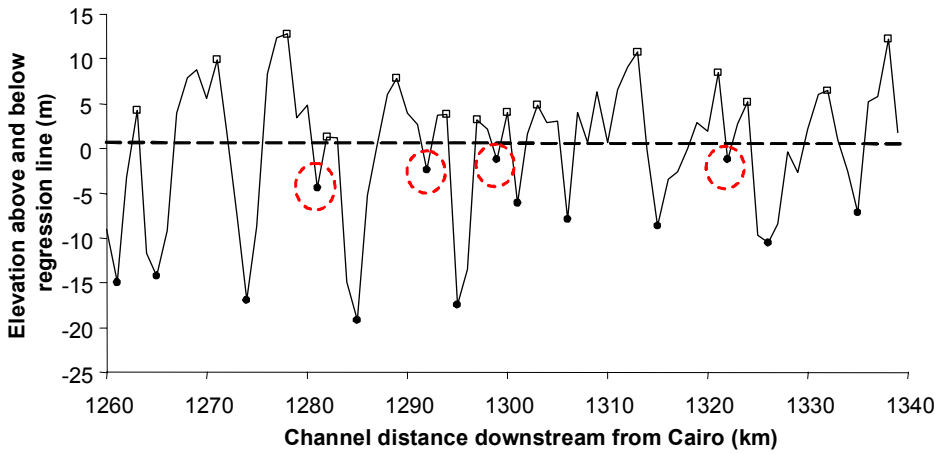

Figure 5.20 Identification of both significant and insignificant bedforms in the reach 1260-1340 km downstream from Cairo (reach 7). Pools deemed insignificant are highlighted by broken red circles.

physical significance of downstream trends in pool and crossing morphological characteristics must be viewed with an appropriate degree of caution.

A further weakness of the regression technique is that it is inevitable that 'insignificant' bedforms are incorrectly identified as being significant. This problem is illustrated in Figure 5.20 where four local-scale undulations are inappropriately classified as pools. Amplitude and wavelength tolerance values can be applied to counteract this problem but in a series of 'dome-up' bedforms, the application of such tolerances is biased towards the prior removal of crossings. In view of these problems, characteristics identified by regression classification are compared with those observed through application of the cumulative elevation change technique in the next section.

5.7.5 Pool and crossing parameterisation by the cumulative elevation change technique

Classifying pools and crossings based on cumulative elevation change between consecutive bedforms avoids the identification of 'insignificant' small amplitude pools and crossings which is inevitable if classification is based on fitted regression trends. An introduction to this technique is provided in section 3.2.3

i) Adaptations from the original 'bedform differencing' technique

For the purposes of this research, the bedform differencing technique is renamed the cumulative elevation change technique because it is adapted in several ways. Most importantly, O'Neill and Abraham (1984) apply a tolerance value based on multiples of the standard deviation of the series. However, this method of obtaining tolerance values is not applied in this study for two reasons. First, the standard deviation is not consistent between reaches and therefore, applying a tolerance value based on a multiple of the standard deviation in each reach would compromise the downstream comparability of recorded trends. In the eight identified reaches, standard deviations of the detrended long profiles range from a minimum of 4.79 to a maximum of 7.79 (Table 5.4).

	Reach	Standard Deviation
Upstream	1	5.05
	2	5.21
	3	4.79
	4	4.85
	5	6.38
	6	7.54
	7	7.79
Downstream	8	7.21

Table 5.4 The standard deviation of the detrended long profile in each reach

Second, the standard deviation measure implicitly incorporates variation in wavelength as well as amplitude within the series. Thus, it is not deemed an appropriate method of specifying a threshold for defining pools and crossing based solely on cumulative elevation changes, a measure of amplitude variation. In recognition of these two problems, tolerance values applied in this study are based on increments of amplitude change (representing elevation change) rather than the standard deviation of the series.

In addition to the method of tolerance determination, the bedform differencing technique is adapted in two further respects. First, to allow comparability with regression-based analysis of amplitude and wavelength, the technique is performed using a sampling interval of 1 km. Based on a bankfull width equal to 1.65 km (see section 6.7.4), this is a shorter sampling interval than the 1 w_B recommended by O'Neill and Abrahams (1984), although it is closer to the 0.5 w_B more recently recommended by Robinson (2003). Sampling at the original 1 w_B is not recommended here because it may lead to aliasing (see section 5.1). Second, O'Neill and Abraham (1984) apply bedform differencing to the original long profile. However, in this study, bedform differencing is undertaken on the detrended data series (section 5.7.1). This is deemed preferable because it allows comparison of pool and crossing amplitudes in disparate upstream and downstream reaches which may vary significantly in reach-scale slope.

ii) Analysis of amplitude-based tolerance

Figure 5.21 shows the application of tolerance values in the range 2-8 m to the detrended series between 1220 and 1320 km downstream from Cairo (reach 7). Applying a tolerance value of 2 m defines almost all undulations in the thalweg profile as pools and crossings. As tolerance is increased toward 8 m, fewer undulations exceed the critical tolerance and a more 'realistic' definition of pools and crossings is obtained. Over this range of tolerance values, both the mean wavelength, defined by the mean pool-to-pool distance, and the mean number of identified pools and crossings, decline by approximately 50 percent. It is particularly interesting to note, however, that all pools and crossings removed by increasing the tolerance are within the reach 1265-1320 km downstream from Cairo. The upstream portion of the reach shown in Figure 5.20 is therefore insensitive to tolerance in the range 2-8 m and hence, is characterised by higher amplitude variation. This observation is important because it reveals that, by incrementally increasing the value of tolerance, the adapted bedform differencing technique provides a powerful diagnostic tool to examine the relative sensitivity of reaches to variation in tolerance, and hence, to characterise the changing nature of variation downstream.

In Figure 5.22, mean pool-to-pool spacing is plotted against tolerance values in the range 1-8 m. At very low tolerance values of 1-2 m, the mean pool-to-pool spacing is comparable between reaches, indicating that the wavelength of local-scale undulations is consistent downstream. However, at tolerance values in excess of 3 m, a spatial trend is clearly evident with the upstream and midstream reaches (1-5) demonstrating higher rates of increase in mean pool-to-pool spacing than the downstream reaches (6-8). This is indicative of lower amplitude variation in reaches within the alluvial valley in comparison to reaches within the deltaic plain. The exception to this trend is reach 3 which demonstrates a trend more typical of the deltaic plain reaches than those in the alluvial valley.

All of the relationships between wavelength and tolerance are close to being linear. This is interesting to note because it indicates that as the tolerance value is increased at equal increments, a consistent number of undulations are deemed of insignificant amplitude and hence, no longer identified as either pools or crossings. This in turn suggests therefore that the Lower Mississippi River is not characterised by pool and

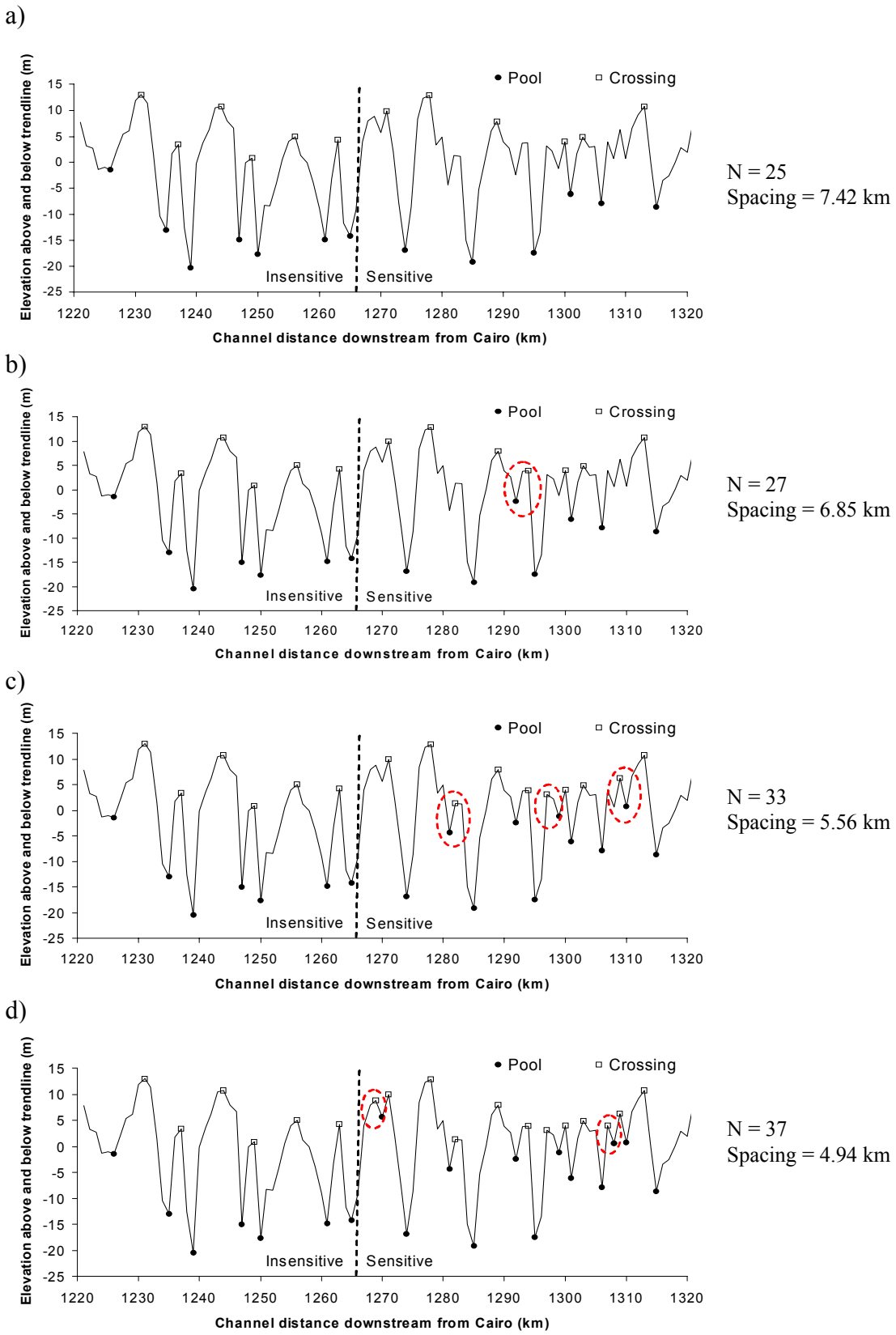

Figure 5.21 The identification of pools and crossings between 1220 and 1320 km downstream from Cairo (reach 7) using tolerance values of: a) 8 m; b) 6 m; c) 4 m and; d) 2 m. Dashed red circles indicate the identification of new pools and crossings as tolerance declines. At each tolerance level, the number of identified pools and crossings (N) and the mean pool-to-pool spacing is given.

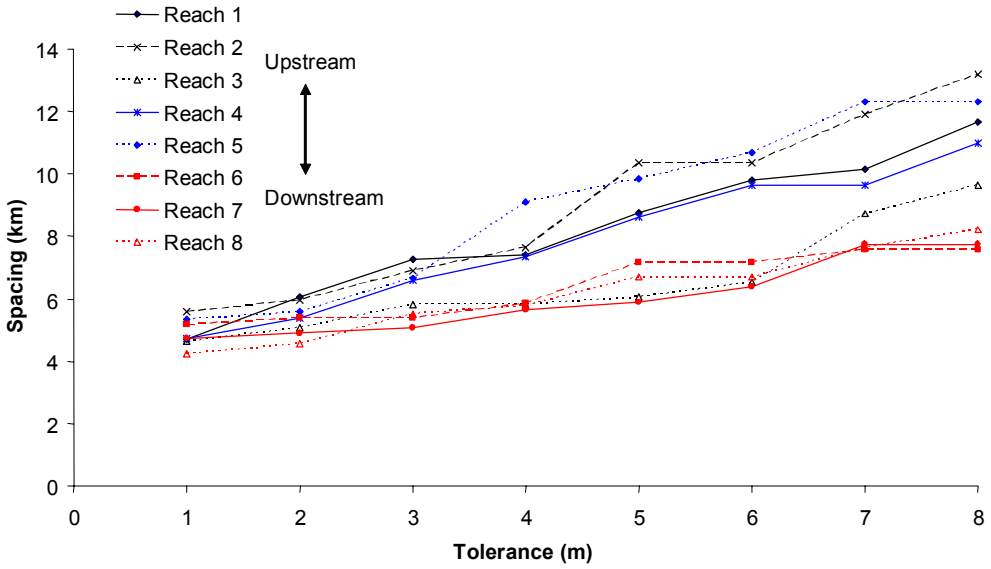

Figure 5.22 The increase in mean pool-to-pool spacing as tolerance value is increased for each reach. Upstream reaches (1-3) are colour coded black, midstream reaches (4-5) are colour coded blue, and downstream reaches (6-8) are colour coded red.

crossing sequences in the long profile at any single scale of variation but rather, at multiple scales of variation. In terms of geomorphological response, this is important because it demonstrates that bedform resistance associated with undulations in the long profile cannot be classified at discrete scales but rather transcend a multitude of scales. Section 5.7.4ii showed that these scales cannot easily be related to flow resistance although relative roughness must increase with the number of scales of variation observed.

iii) Downstream analysis of amplitude and length characteristics

In order to compare pool and crossing length and amplitude characteristics, the cumulative elevation change technique was performed using an amplitude tolerance value of 6 m. This was selected because it generates a pool-to-pool spacing which is most comparable with mean estimates from second-order autoregressive modelling (Figure 5.23). The procedure used to quantify the length and amplitude characteristics of pools and crossings is more complex than the regression technique because classification cannot be based on the application of a definitive function. Instead, the limits of pools and crossings were identified by computing the distance and elevation at which half of the pool/crossing elevation difference was exceeded. Where insignificant bedforms were identified (i.e. those of a lower amplitude than the tolerance threshold), classifying pools and crossings based on the mid-point elevation becomes unreliable and so the procedure was modified to compute a start and end elevation for each pool or crossing. This rectification is illustrated in Figure 5.24. In 5.24a, pool and crossing classification is simply based on the exceedance of the mid-point elevation value. Where insignificant bedforms are identified, classified pools and crossing are longer than if these are first removed by the rectification procedure (5.24b).

Reach-averaged downstream trends in amplitude, length and amplitude: length ratios are presented in Figure 5.25. Measures of amplitude are based on the elevation difference between consecutively defined pools and crossings. Because pool depths are conditioned by the previous crossing height and vice versa, consecutive amplitude values are not independent. For example, a deep pool upstream will increase the relative elevation of a crossing immediately downstream. As a result,

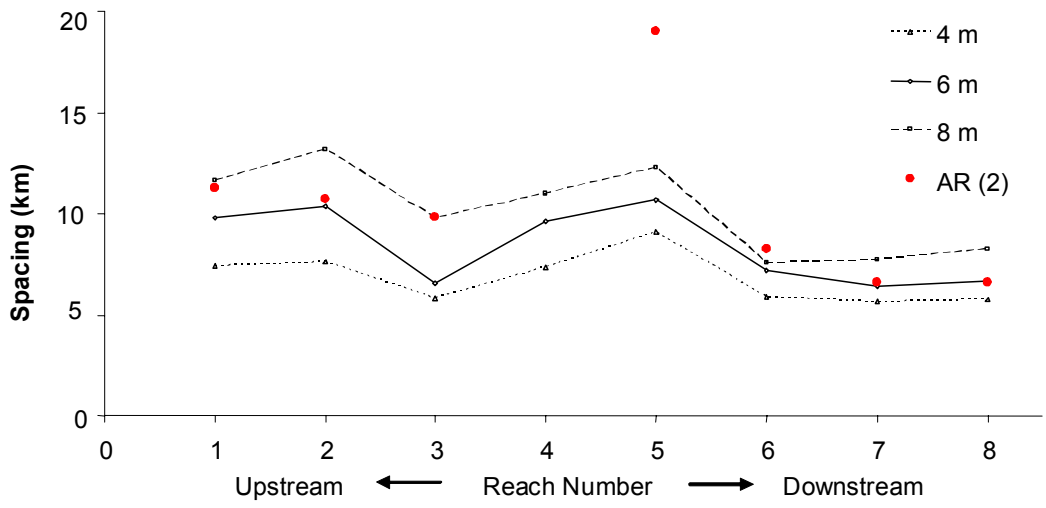

Figure 5.23 Comparison of wavelengths estimated from second-order autoregressive modelling with mean pool-to-pool spacing at tolerances of 4 m, 6 m and 8 m using the cumulative elevation change technique.

a)

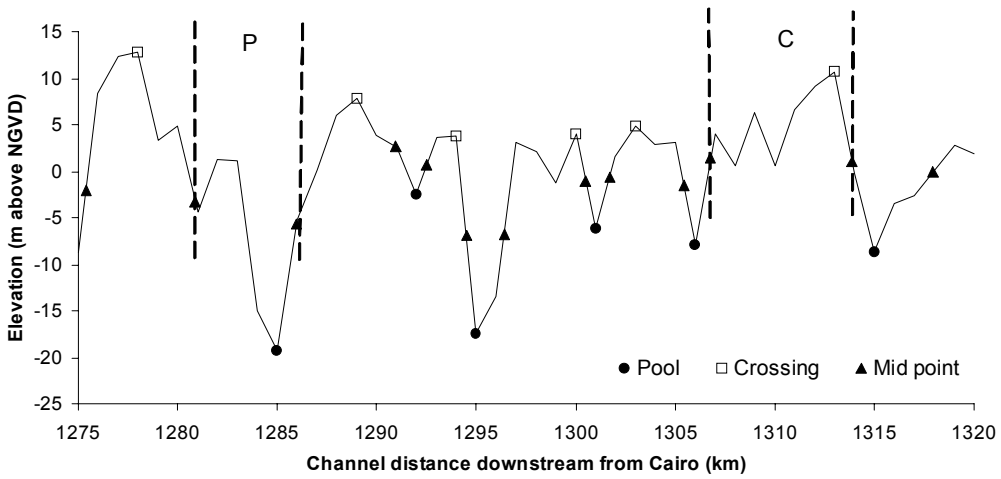

b)

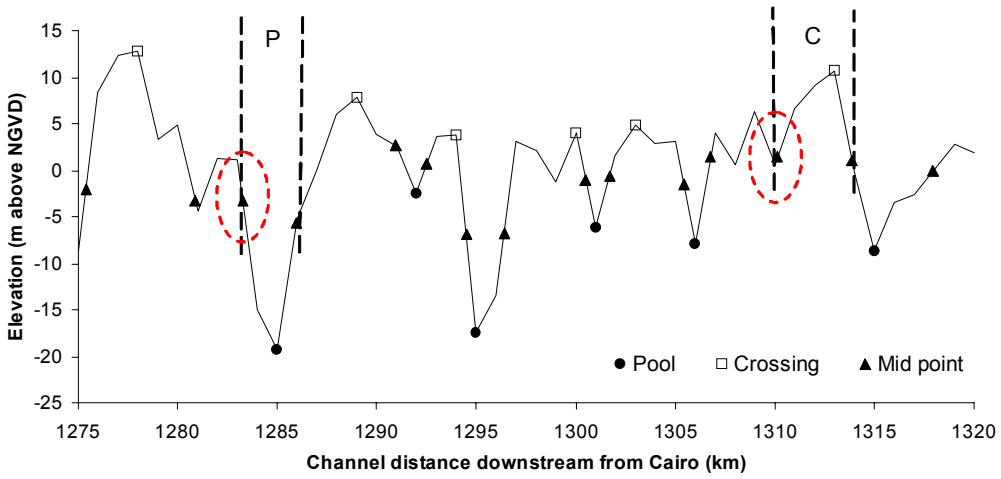

Figure 5.24 Defining the length of a pool and crossing using mid-point elevations. A mid-point elevation is mid-way between the maximum crossing elevation and the minimum pool elevation. In a), the mid point elevation is simply used to define pools and crossings. A refined definition is presented in b) where the start and end mid-point elevation of each pool and crossing is defined.

a)

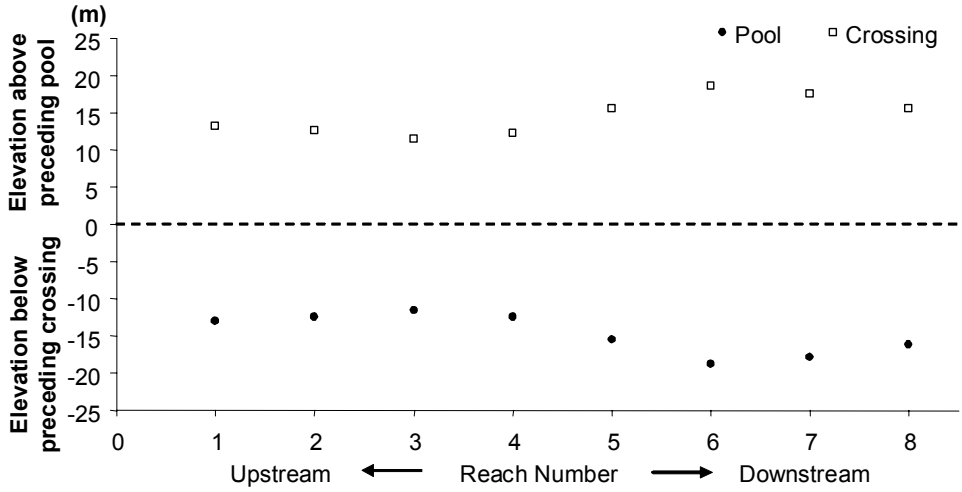

b)

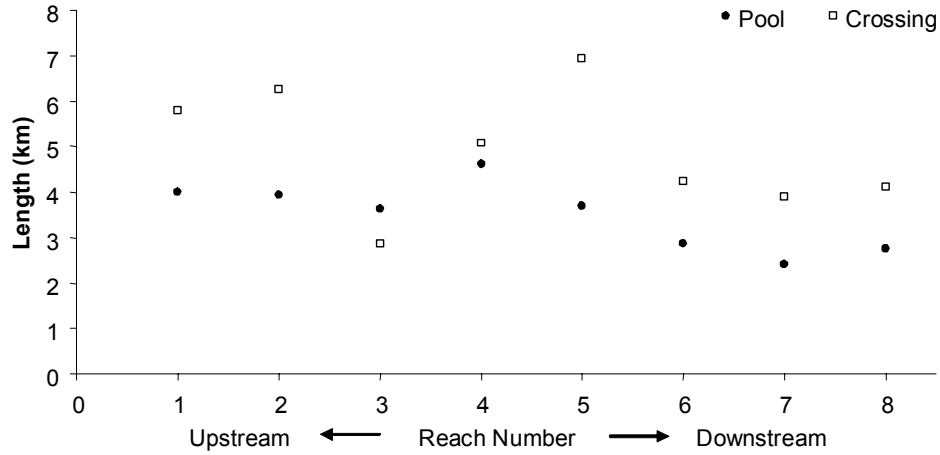

c)

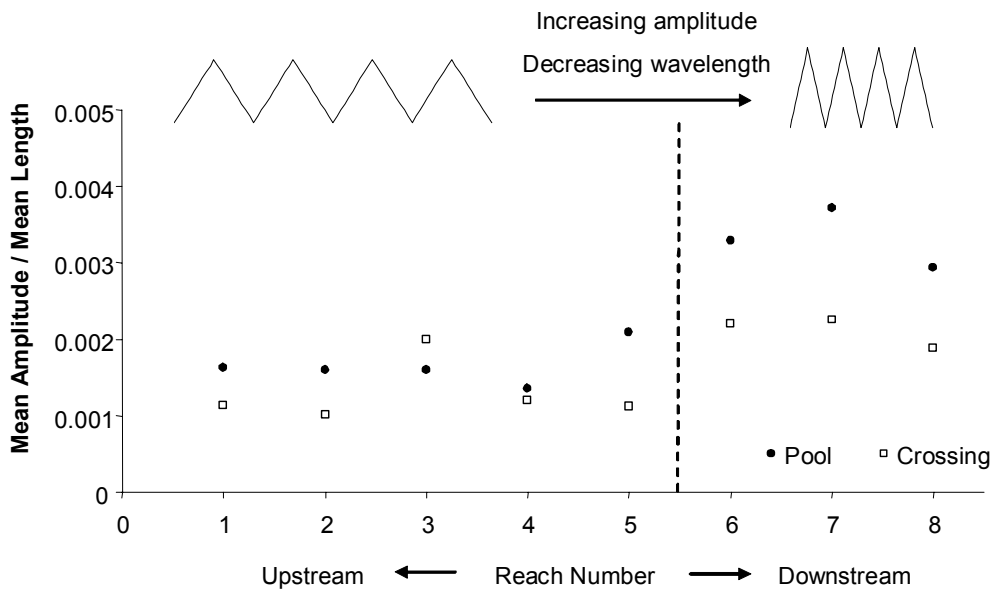

Figure 5.25 Trends in pool and crossing: a) amplitude; b) length and; c) amplitude/length ratio for the eight reaches of the Lower Mississippi River. In c), the value of amplitude used in the ratio calculation has been halved to reflect the elevation above or below the mid-point elevation.

obtained heights are not directly comparable with amplitudes identified by regression-based classification. Despite this inconsistency however, downstream trends in amplitude, wavelength and amplitude: wavelength ratios revealed by cumulative elevation change are consistent with those identified by regression-based classification in Figure 5.16. This is important because it inspires confidence that the identified trends have a physical significance.

5.7.6 Pool and crossing classification: comparability of regression and the cumulative elevation change technique in relation to meander length spacing

A clear association between the spacing of pool-riffle (crossing) undulations in the long profile and the wavelength of meander bends in the channel planform has been widely documented in river channels (Leopold and Wolman, 1960; Harvey, 1975; Lewin, 1976; Richards, 1976a, 1976b). Comparing the distribution of pool-to-pool spacing estimated by both classification techniques with the distribution of meander length spacing, as identified by consecutive points of inflexion in the planform (see section 4.9.4) may therefore, provide a method of evaluating the relative reliability of each classification technique.

Histograms for the three distributions are presented in Figure 5.26. All three distributions are positively skewed and are similar in overall shape. The meander bend length distribution is more comparable in terms of mean and modal length, skewness ratio and total frequency (*N*) to the pool-to-pool spacing identified by cumulative elevation change. The lower mean and modal pool-to-pool wavelength and more positive skewness ratio estimated by the regression technique, reflect the identification of short-wavelength, low amplitude 'insignificant' bedforms which lie just above or just below the regression line (see Figure 5.20). This suggests that, in terms of wavelength calculation, cumulative elevation change offers a more reliable technique of pool and crossing classification than regression.

Based on a mean bankfull channel width (w_B) of 1.65 km (section 6.7.4), the mean pool-to-pool wavelength, identified by the cumulative elevation change technique, falls within the conventional interval of 5-7 w_B, and the modal wavelength is close to the 3 w_B modal average based on previous analysis of other river systems (Leopold

a)

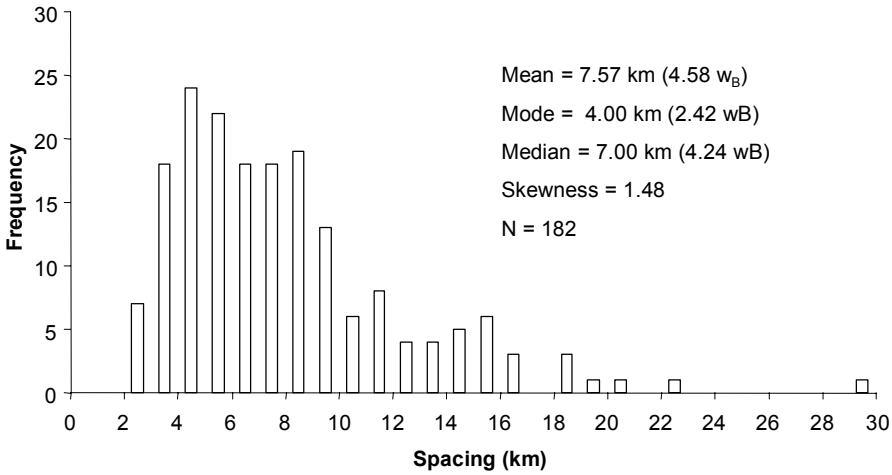

b)

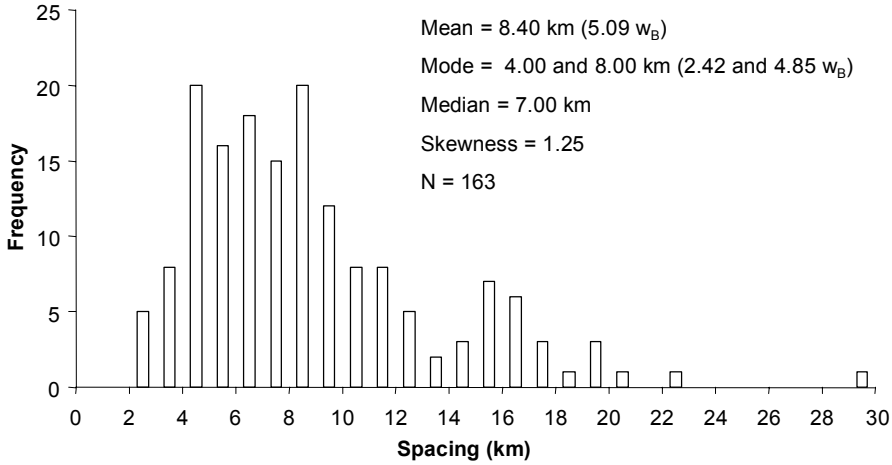

c)

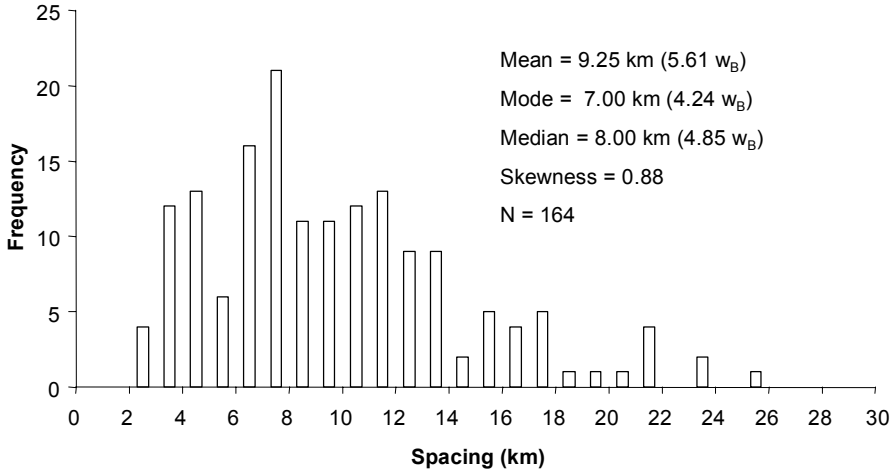

Figure 5.26 The distribution of pool-to-pool wavelength obtained by: a) regression classification and; b) the cumulative elevation change technique in relation to c) the distribution of meander bend lengths defined by points of inflexion. Wavelengths are combined for all reaches (1-8). Descriptive statistics of each distribution are given to two decimal places.

et al., 1964, Keller and Melhorn, 1978; Clifford, 1993). This is important because it shows that despite its size, the pool-to-pool wavelength distribution on the Lower Mississippi River is similar to those identified in previous studies, undertaken in a range of environments and at a range of scales.

The relationship between mean meander bend spacing and mean pool-to-pool spacing is explored on a reach-by-reach basis in Figure 5.27. A close association between the two measures is indicated by the points lying close to the line of equality, in all but two of the eight defined reaches. This association is especially interesting because the relationship is developed in reaches of varying sinuosities. This supports the idea that the secondary circulation flow structure, which is widely believed to operate in meandering streams, is also present in straighter reaches (Keller, 1972; Hey, 1976). It is also interesting to note that, with the exception of reach 3, there is evidence that both average meander bend spacing and average pool-to-pool spacing is lower on the deltaic plain (reaches 6-8) than in the alluvial valley (reaches 1-5).

This second finding is interesting academically because previous research has exposed uncertainty regarding the nature of the relationship between the resistance of materials forming the channel perimeter and meander wavelength. Following research by Hack (1965) and Tinkler (1971) in mixed bedrock and alluvial channels, Kennedy (1972) proposed that meander wavelength is a function of both discharge and perimeter material. Abrahams (1983) uses this reasoning to suggest that meander wavelength should increase with rock hardness as the return interval of channel forming discharge increases. However, Figure 5.27 illustrates the reverse relationship: a decline in meander wavelength as material cohesivity (and hence, strength) increases from the alluvial valley to the deltaic plain. Brauun (1983) found the same reverse relationship in a study of bedrock meander dimensions in the headwater areas of the Appalachian Valley and Ridge Province. Brauun (1985) offers an explanation based on the relationship between material strength and channel shape: as the cohesiveness, and therefore material strength, of the channel boundary increases, the channel should get narrower and deeper, rather than becoming wider and shallower. This is consistent with the deepening of pools from

the alluvial valley to the deltaic plain evident in Figures 5.16a and 5.25a and is suggestive of a decline in average channel width.

Association between longitudinal and planimetric planes of adjustment is further analysed in Figure 5.28 where cross-correlograms of the detrended thalweg elevation and direction change series, computed at an interval of 1 km, are presented for reaches 4 and 7. The greatest negative correlation at a shorter lag spacing in reach 7 provides further evidence of the deeper pools and shorter pool-to-pool spacing on the deltaic plain. Interestingly, the negative lag distance to peak correlation in both reaches reveals that the peak in the detrended thalweg elevation series typically occurs downstream from peaks in the direction change series. Hence, pools are typically located just downstream from the meander bend apex. This distance is greater in reach 4 (2 km) than reach 7 (1 km) although this most likely reflects the shorter pool-to-pool spacing in reach 7.

The above associations are diagnostic of a close coupling between the morphology of the meander bend sequence and pool-crossing sequence. Historically, the Lower Mississippi River has modified the rate and distribution of energy loss at the reach-scale to balance flow resistance requirements by mutual adjustments of these two degrees of freedom. Because the potential for planform adjustments has effectively been removed through bank stabilisation, changes to flow resistance requirements must now be met through adjustments to the sequence of pools and crossings. This is examined in the post-modification period (1948-88) in chapter 6.

5.9 Discussion

5.9.1 Explaining the concave long profile

The 1974-75 long profile of the Lower Mississippi River from Cairo to the Head of Passes demonstrates a clear concave trend. At this regional-scale, this trend cannot be simply related to downstream trends in discharge or bed material size. However, a more thorough investigation of reach-scale variability offers at least a degree of explanation.

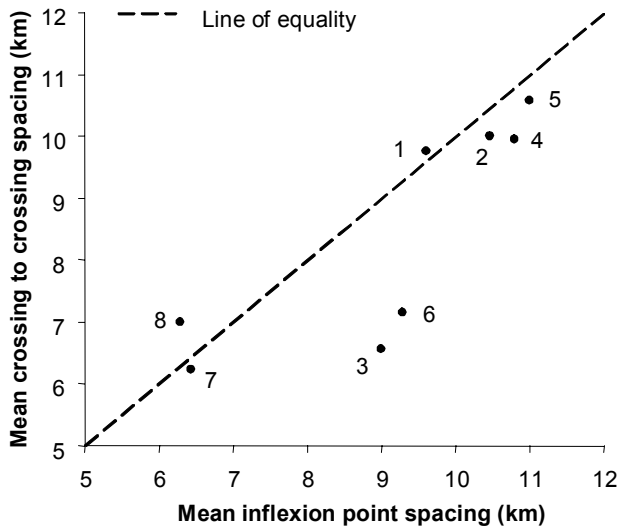

Figure 5.27 Mean crossing-to-crossing spacing against mean distance between identified points of inflexion (indicative of meander wavelength) for the eight reaches of the Lower Mississippi River.

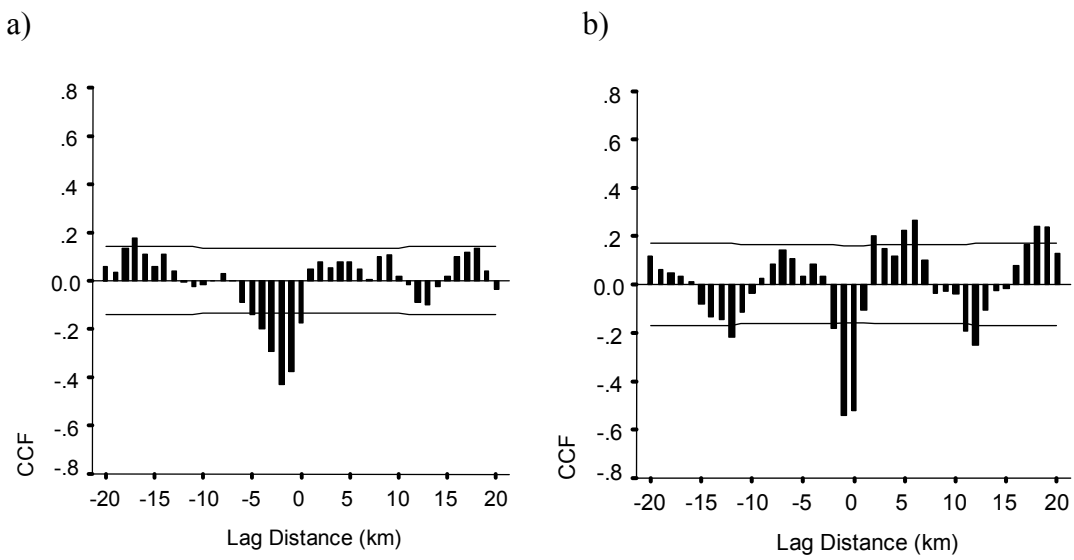

Figure 5.28 Cross-correlation of detrended thalweg elevation with the modulus of direction change for: a) reach 4 and; b) reach 7.

Closer examination reveals that regional-scale concavity disguises considerable variation at the reach-scale. It is proposed that slight convexity in the upper alluvial valley and strong concavity downstream from Old River distributary within the contemporary long profile are features reflecting the late Wisconsin and Holocene geological history of the Lower Mississippi River. Because coarse sediments are no longer being delivered into the upper alluvial valley in such vast quantities, and the delta front of the modern Plaquemine complex is no longer prograding, these features can be considered inherited from past geomorphological conditions. At a shorter reach-scale, discontinuities in the long profile are also recognised, reflecting both continual warping of the alluvial valley surface by neotectonic activity and abrupt changes to the flow and sediment regime at tributary and distributary junctions. In addition to these natural controls, the contemporary long profile of the Lower Mississippi River is strongly influenced by engineering modifications. Through the central alluvial valley, the long profile has been oversteepened by the artificial cutoff programme and further downstream, the regulation of distributary outflow has prevented distributary avulsion and consequently maintained the very low valley slope associated with the modern Plaqumines delta complex.

As a result of these findings, the 1974-75 long profile can be considered as partly inherited from past geomorphological conditions; partly continually adjusting to long-term natural controlling variables; and partly a direct product of engineering modification during the twentieth century. The occurrence of regional-scale concave long profile is therefore the consequence of processes operating in a range of physical (geological, tectonic, fluvial) and anthropogenic domains over a range of space and timescales. Although a regional-scale concave trend fitted through the observed long profile provides a good-fit statistically, the concave trend is not, therefore, diagnostic of a system which is adjusted to the prevailing process regime at the regional-scale (i.e. not graded at the regional-scale). Indeed it is more appropriately described as the collective outcome of a series of physical processes and engineering modifications.

5.9.2 Downstream trends in large-scale bedform resistance

At the sub-reach scale, downstream trends in pool and crossing amplitude and wavelength are an important indicator of large-scale bedform resistance. Although the average spacing of pools and crossings is consistent with those identified on other rivers, results from regression and cumulative elevation change techniques do suggest that pool and crossing characteristics vary between the alluvial valley and the downstream deltaic plain. Average pool-crossing spacing is shorter and average pool depth is considerable greater on the deltaic plain. These changes are therefore consistent with an increase in the form resistance exerted by the large-scale bedform configuration downstream.

This observation must be placed in the context of changes in stream power per unit width downstream. Both average slope and discharge are lower on the deltaic plain. However, the reduction in the average spacing of first-order meander wavelengths is suggestive of a decline in channel width downstream because meander wavelength is known to scale with channel width. These mutual changes therefore indicate that it is not easy (even qualitatively) to reconcile morphology with the downstream variation in stream power per unit width. Instead, it has been shown that first-order meander wavelengths and pool-to-pool spacing are clearly correlated in most reaches and therefore, given the decline in meander wavelength on the deltaic plain, it is not surprising that pool-to-pool spacing should decrease. This characteristic change between the alluvial valley and the deltaic plain is most likely to be related to the increase in bank material strength, as proposed by Braun (1983). It is unclear however, the extent to which deeper pools on the deltaic plain increase large-scale bedform resistance because they may only be actively scoured during periods of high flow and therefore, for most flows, it is possible that their presence may exert only a negligible addition.

Although downstream trends in the morphological characteristics of the pool-crossing configuration have been noted in this chapter, an unresolved issue remains the timescale over which the identified pool-crossing configuration persists. This is especially important given that characteristics identified in this chapter are based on

hydrographic surveys of the river in 1974-75, and hence, may have recently adjusted as part of a geomorphological response to engineering intervention. Temporal changes in the post-modification pool-crossing configuration are therefore examined in chapter 6.

CHAPTER 6. REACH-SCALE LONG PROFILE DYNAMICS

6.1 Chapter synopsis

Following extensive bank stabilisation, the geomorphological response to the artificial cutoff programme was effectively confined to adjustments to the long profile. Results obtained through application of a range of analytical techniques in this chapter reveal two principal scales of geomorphological response: at the reach-scale, the river has adjusted through vertical changes in the channel bed; and at the sub-reach scale, the river has adjusted the longitudinal and cross-section form characteristics of pools and crossings. 1-D step-backwater modelling based on average stage-discharge relationships is used to show that these changes are consistent with an increase in flow resistance, and consequently, the changes in the water surface elevation reported by Biedenharn and Watson (1997). In terms of geomorphological response, it is evident that, at the shorter (40-year) timescale, morphological dynamics are not as conditioned by reach history as observed in chapters 4 and 5, but rather by process-form behaviour in upstream and downstream reaches and at larger spatial scales.

6.2 Obtaining representative data series

Temporal variations in the long profile are studied between 1949 and 1989 using four consecutive hydrographic surveys for the reach extending from the confluence of the Arkansas and White Rivers to 8 km upstream from Old River distributary. In relation to the eight defined reaches, this incorporates all of reach 4 (confluence of the Arkansas and White Rivers to confluence of Yazoo River at Vicksburg) and most of reach 5 (confluence of Yazoo River at Vicksburg to Old River distributary). Critically, the period of study follows the programme of artificial cutoffs (1929-1942) and covers the period of extensive bank stabilisation and dike field construction.

The time period of data collection together with the cross-section spacing characteristics for each hydrographic survey are presented in Table 6.1. The two

earlier hydrographic surveys (1949-51 and 1962-64) were collected over a period in excess of two years whereas the later hydrographic surveys (1975 and 1988-89) were collected in less than one year. Thus, interpretation from the earlier hydrographic surveys must be treated with an additional degree of caution. The mean and median cross-sectional spacing is comparable between surveys, both ranging by just 0.014 km. However, the variability of cross-sectional spacing (indicated by the standard deviation) is considerable higher in the earliest two hydrographic surveys. Referring back to section 5.2 though, this level of variation is lower than that within the USACE Memphis and New Orleans Districts 1974-1975 hydrographic surveys (see Table 5.1). Therefore, given this higher level of variation was shown to be acceptable, the range of cross-sectional spacing within the data sets used in this chapter is not deemed significant. To be consistent chapter 5, analysis is performed on observations linearly interpolated at regular 1 km intervals from the original series.

Consideration of channel length variations in Table 5.1 reveals a range of just 5.5 km over the 1949-1989 period. Because this covers part of the artificial cutoff reach, this temporal stability over the period casts severe doubt on the 171 km of post-cutoff net channel lengthening reported by Smith (1996). Channel length changes associated with, and following, the artificial cutoff programme therefore require further investigation (see sections 2.6.2 and 4.4.2).

6.3 Discharge variation in relation to the data collection

In addition to recording large-scale geomorphological response, hydrographic survey data sets may record shorter-term changes in channel morphology associated with variations in discharge. Figure 6.1 compares discharge records for the two year and ten-year period before each hydrographic survey was undertaken and Figure 6.2 plots the percent of time exceeding discharges of 17 000 m^3s^{-1} and 30 000 m^3s^{-1} in the post-cutoff period. 6.1a shows that discharge was unusually high in the two years prior to the 1975 hydrographic survey in comparison to the two years prior to the other hydrographic surveys. During the 1973-75 water year period, the dominant discharge of 30 000 m^3s^{-1} (Biedenharn and Thorne, 1994) was exceeded over 36

percent of the time. Over the longer ten-year interval prior to 1975 however (6.1b), discharge trends are comparable to the ten-year periods in two out of three of the other hydrographic surveys. Thus, prior to the 1973 and 1974 high discharge years, discharge was relatively low (Figure 6.2). Prior to the 1949-51 hydrographic survey, the frequency of discharge events in excess of 30 000 m^3s^{-1} was high when considered over both the previous ten-years and two years. However, over the shorter two-year period, discharges were not as high as those prior to the 1975 hydrographic survey.

	1949-51	**1962-64**	**1975**	**1988-89**
Start Date	January 1949	February 1962	August 1975	April 1988
End Date	April 1951	April 1964	November 1975	January 1989
Duration (Months)	28	27	4	10
Number of cross-sections	1397	1383	1348	1369
Mean spacing (km)	0.313	0.317	0.327	0.318
Median spacing (km)	0.307	0.308	0.321	0.320
Standard deviation	0.085	0.993	0.058	0.043
Channel length (km)	437.3	438.4	440.8	435.3
Mean elevations per cross-section	32.30	29.62	21.80	46.08
Mean elevation spacing per cross-section (m)	48.99	48.17	54.78	36.86
Mean left bank to right bank distance (m)	1545	1412	1191	1711

Table 6.1 Differences in data collection between the 1949-51, 1962-64, 1975 and 1988-89 hydrographic surveys in the USACE Vicksburg District (reaches 4 and 5). The mean, median and standard deviation of spacing between cross-section is given to three decimal places and the mean elevation and mean elevation spacing within each cross-section is given to two decimal places.

In contrast to both of these hydrographic surveys, the 1962-64 hydrographic survey was collected during a prolonged period of relatively low flow, when considered over either a two-year or ten-year time interval. Prior to the 1988-89 hydrographic survey, the frequency of discharges in excess of 30 000 m^3s^{-1} was very low although over a ten-year period, discharge trends are comparable to prior to the 1949-51 and 1975 hydrographic surveys.

6.4 Referencing long profiles to a common channel distance

To analyse the temporal variation in reach-scale long profile slope, a procedure was developed to reference each cross-section within each hydrographic survey to a standardised channel distance downstream from Cairo. If referenced individually, variation in channel length may result in the same distance downstream from Cairo, on consecutive surveys, corresponding to different reaches. A standardised distance measure therefore allowed direct comparability between hydrographic surveys. The standardised measure of channel distance selected was based on the USACE standard measure: river miles above Head of Passes in 1962. River mile markers are spaced at one mile (1.6 km) intervals and define the channel centreline in 1962 from the Head of Passes to Cairo. Each cross-section within each hydrographic survey was given a unique river mile reference by computing the intersection of the line adjoining the left-bank and right bank coordinates of each cross-section with the chord adjoining the nearest river mile markers. To maintain consistency with previous analysis, this distance was then converted from a river mile distance upstream from the Head of Passes to a river kilometre distance downstream from Cairo.

Based on this referencing system, the upstream limit of the reach is located at 574 km, and the downstream limit at 1017 km, downstream from Cairo. The boundary between reaches 4 and 5 (the confluence of the Yazoo River at Vicksburg) is located at 828 km. In Figure 6.3, long profiles for the four hydrographic surveys are plotted against the standardised channel distance downstream from Cairo. Elevations within each profile have been linearly interpolated at 1 km intervals based on the standardised distance.

a)

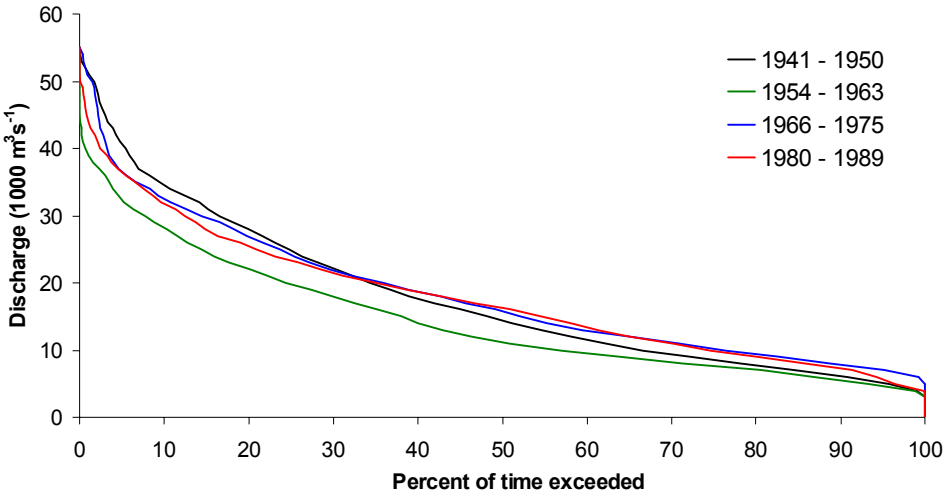

b)

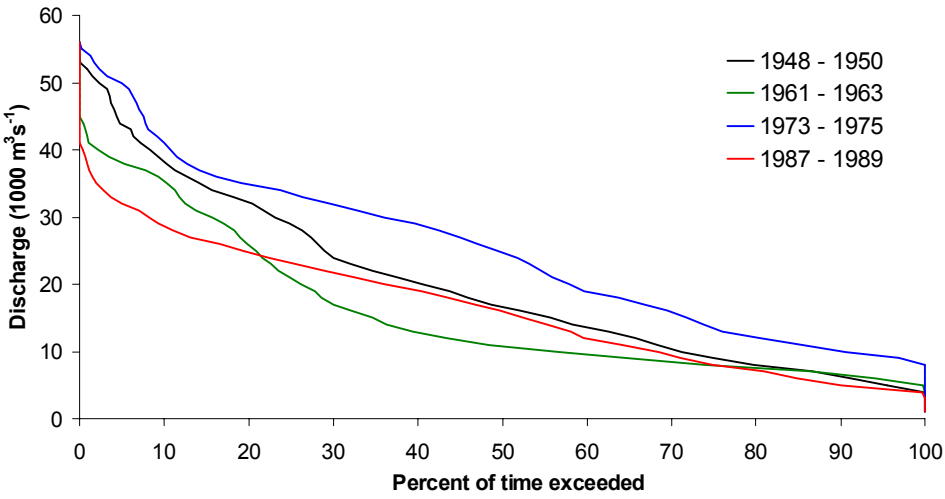

Figure 6.1 Discharge against percent of time exceeded at the Vicksburg gauge for two timescales: a) ten water years prior to each hydrographic survey and; b) two water years prior to each hydrographic survey.

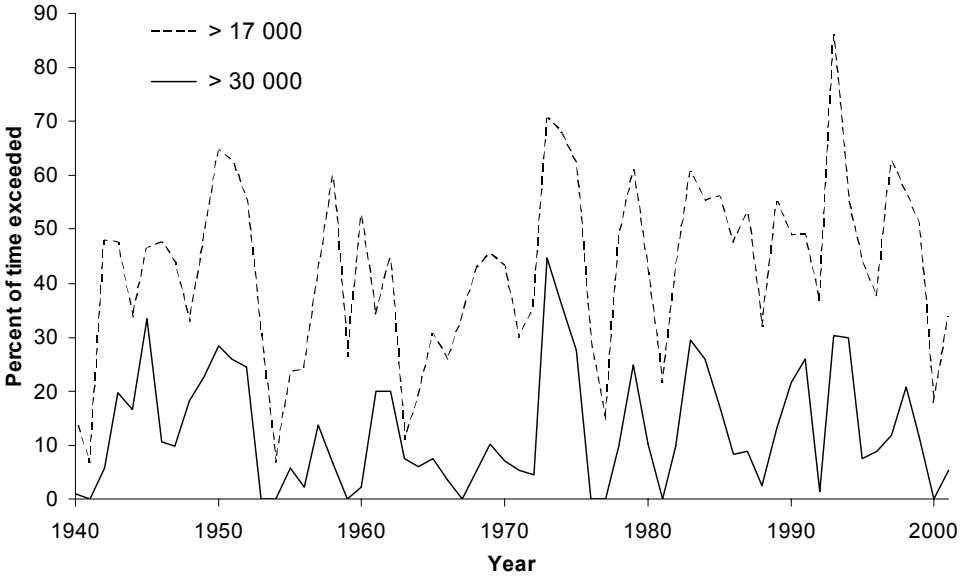

Figure 6.2 Percent of time exceeding 17 000 m^3s^{-1} and 30 000 m^3s^{-1} in each water year during the 1940-2001 period. 17 000 m^3s^{-1} is the mean discharge for this period and 30 000 m^3s^{-1} represents the dominant discharge according to Biedenharn and Thorne (1994).

Visual inspection of Figure 6.3 reveals that the regional-scale location of pools and crossings has remained remarkably consistent throughout the 1949-1989 period. This observation is consistent with the lack of significant change noted by Dury (1970) in a comparison of pool and riffle locations on the Hawkesbury River in the period 1870-1969. However, despite this stability, at more localised scales the general form of some isolated pools and crossings has changed considerably whilst others have remained relatively stable. In an attempt to capture the broad range of local-scale pool and crossing behaviour, nine sub-reaches, each demonstrating particular types of behaviour, have been selected from Figure 6.3. These are shaded grey and labelled from *a*) to *i*). The behaviour identified within each sub-reach is described in Table 6.2.

Within sub-reaches *a*), *b*), and *i*), the dominant pool and crossing undulations in the thalweg profile are maintained throughout the 1949-1989 period and hence, these represent areas of relative stability. Sub-reaches *b*) and *i*) are deep pools at the apex of highly sinuous bends, indicating the importance of sinuosity when explaining pool and crossing stability (Figure 6.4). Other sub-reaches are characterised by a range of behaviours including: the development of multiple pools and crossings in a sub-reach initially dominated by a single crossing reach (*c* and *d*; Figure 6.5); the infilling of a pool and hence, the merging of adjacent crossing units (*f*); changes in pool or crossing amplitude (*e* and *h*); and more complex behaviour (*g*).

This qualitative approach is useful for demonstrating the variation in the types of pool and crossing behaviour. However, it is difficult to detect visually evidence of changes which are consistent at the larger reach-scale and hence, have wider geomorphological significance. In the following two sections, such changes are investigated using similar analytical techniques to those applied in chapters 4 and 5.

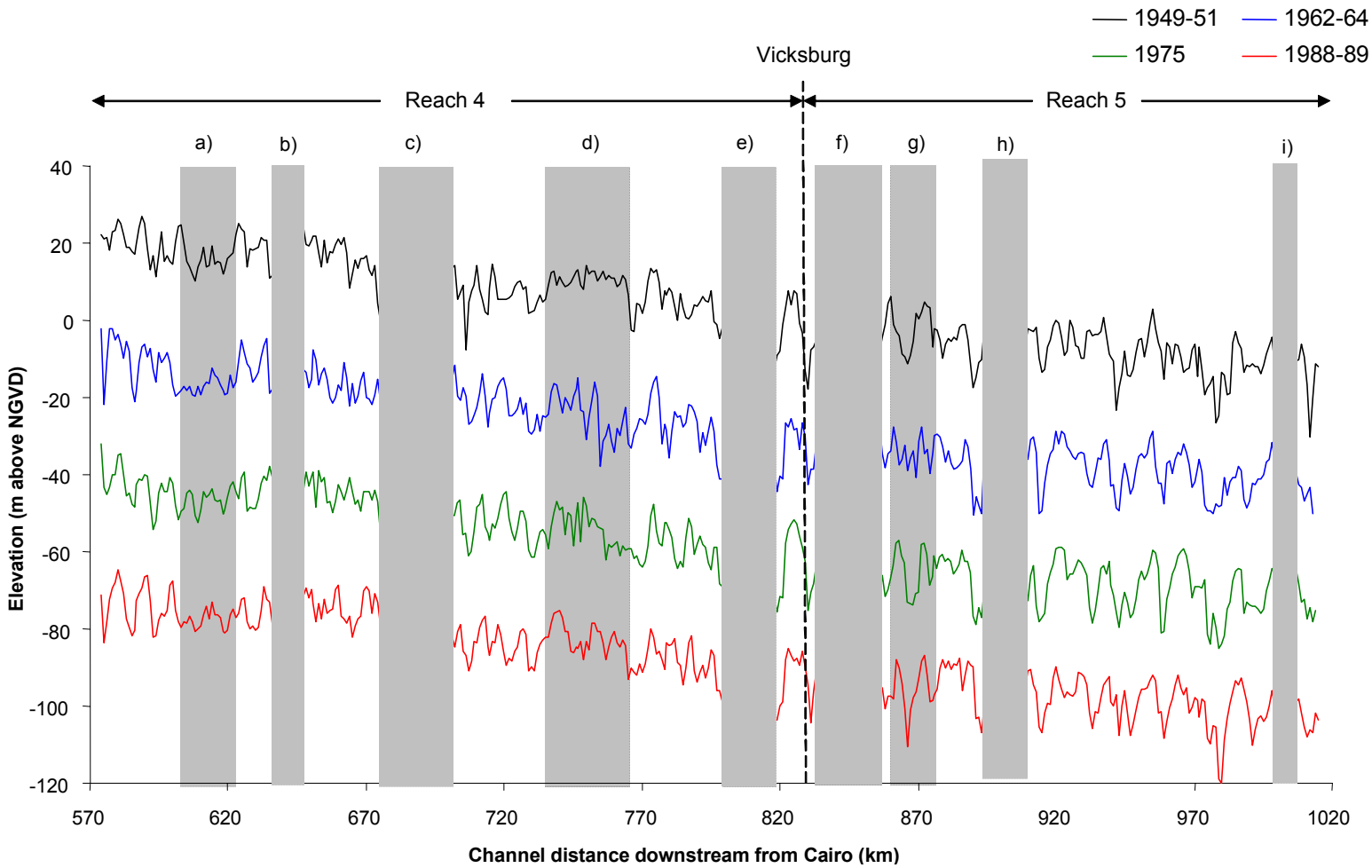

Figure 6.3 Long thalweg profiles for the four hydrographic surveys in the 1949-89 period. Each profile is referenced to a standard channel distance downstream from Cairo. To aid visual comparison between profiles, profiles consecutive in time are separated by an arbitrary interval of 20 m on the y-axis. Shaded areas identify sub-reaches which together demonstrate a range of temporal behaviours.

Sub-reach label	Channel distance downstream from Cairo (km)	Comment
a)	603 – 623	Maintenance of low amplitude pools and crossings throughout the period.
b)	635 – 645	Maintenance of deep pool throughout the period (see Figure 6.4a).
c)	675 – 700	Development of moderate amplitude pools and crossings by 1989 from a single crossing reach in 1949. The reach is located immediately downstream from the Greenville Bend artificial cutoffs (see Figures 2.9 and 6.5).
d)	735 – 765	Development of multiple pools and crossings by 1989 from a single crossing reach in 1948.
e)	800 – 820	Increase in the amplitude of crossing in the period 1949 – 1964.
f)	835 – 860	Infilling of a pool and consequent merging of two crossing reaches in the period 1962-1975.
g)	860 - 875	Infilling of pool in the period 1949 – 1964 and then redevelopment in the period 1962 – 1989.
h)	895 – 910	Gradual deepening of pool throughout the period.
i)	1000 - 1010	Maintenance of deep pool throughout the period (see Figure 6.4a).

Table 6.2 The behaviour of selected pool/crossing reaches within the 1949-1989 period.

a) b)

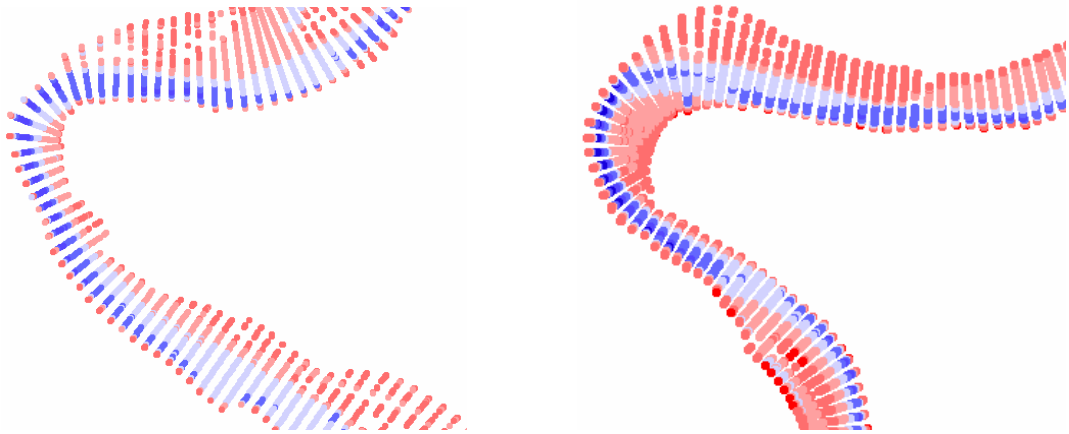

Figure 6.4 Deep pools at the apex of highly sinuous bends represent stable sub-reaches in the 1949-1989 period: a) corresponds to sub-reach *b*) in Figure 6.3 and is located 635 – 645 km downstream from Cairo; b) corresponds to sub-reach *i*) in Figure 6.3 and is located 1000 – 1010 km downstream from Cairo. In each image, the processed hydrographic survey data has been detrended by second-order polynomial regression (based on the long thalweg profile) and colour coded according to deviation from the mean elevation. See Figure 6.5 for key.

a) 1949 - 1951 b) 1988-89

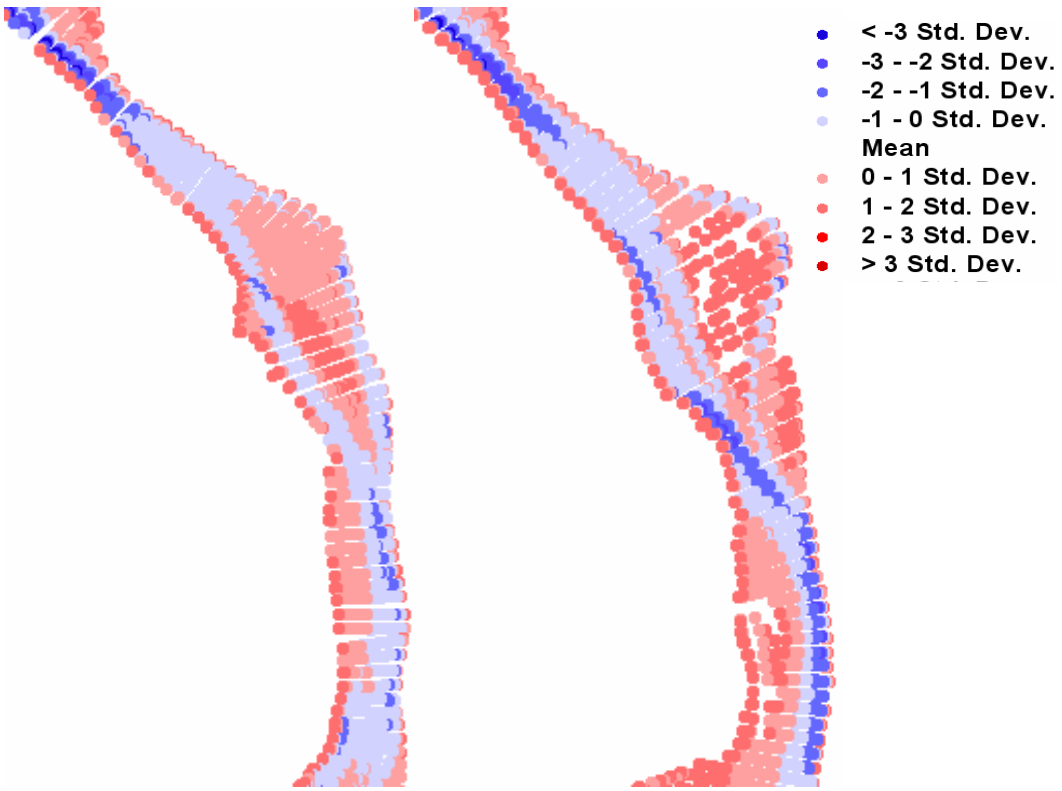

Figure 6.5 The development of pools in the sub-reach labelled *c)* in Figure 6.3. This sub-reach is located 675 – 700 km downstream from Cairo, immediately downstream from the Greenville Bends.

6.5 Temporal variation in long profile slope at the reach- scale

Temporal variation at the reach-scale is explored through regression, moving average, and cumulative elevation difference techniques. These are applied to the standardised long profile series of net change, created by subtracting consecutive standardised long profiles.

Over the whole 1949-89 period, the downstream net change in thalweg elevation during the period 1949-1989 is presented in Figure 6.6. If a linear function is applied to the series, the slope coefficient of -0.009 equates to a reach-averaged net degradational trend of 9 cm for every 10 km in the downstream direction. However, this does not reveal where within the reach, and when within the time period, the highest rates of degradation were occurring. The nature of this change is explored further in Figure 6.7a by plotting elevation change between 1949 and 1989 cumulatively from upstream to downstream. This reveals a clear difference between the observed trend upstream and downstream from Vicksburg. Upstream (reach 4), a consistent rate of decline of cumulative elevation change is suggestive of a consistent magnitude of degradation throughout the reach. Downstream meanwhile (reach 5), there is no clear trend in cumulative elevation change with localised increases being negated by localised decreases. This difference in reach-scale response supports the location of the boundary between reach 4 and reach 5 and indicates that the single linear function fitted to the elevation change series in Figure 6.6 would be more appropriately replaced by two linear trends with a break at Vicksburg.

In Figure 6.7b, the net cumulative elevation change noted over the 1949-1989 period is decomposed to a finer temporal resolution based on the intervening hydrographic surveys. Observed trends are classified in Table 6.3 based on the rate of change. The behaviour noted in Figure 6.7a masks both higher and lower rates of change over shorter time periods. In particular, upstream from Vicksburg (reach 4), the rate of net degradation was considerably greater in the earlier 1949-51 – 1962-64 period than the later 1975-1988-89 period. This is important because it suggests that following the period of artificial cutoff construction (1929-1942; see section 2.6.2), rates of degradation were high for up to approximately twenty years and declined

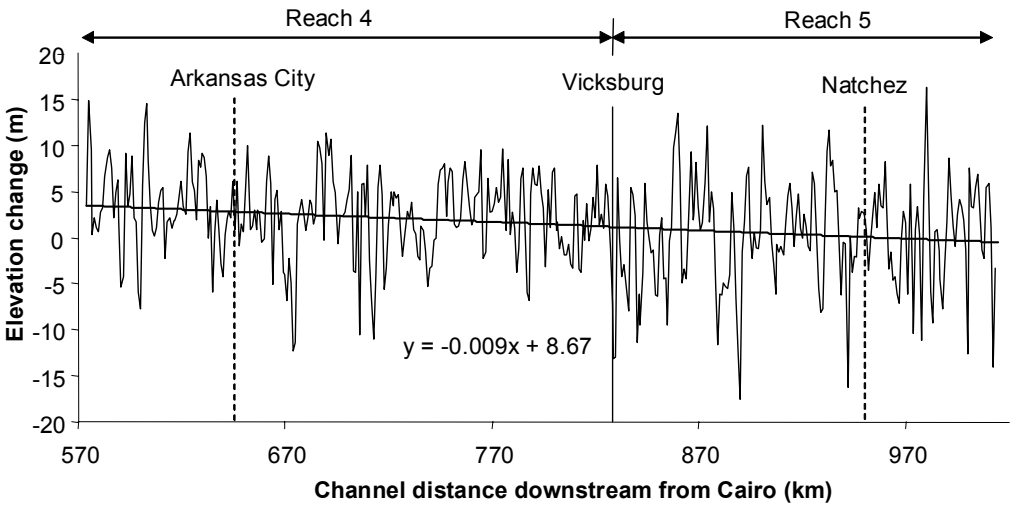

Figure 6.6 Linear regression of downstream elevation change in the period 1949 - 1989 within the reach 570 – 1020 km downstream from Cairo.

a)

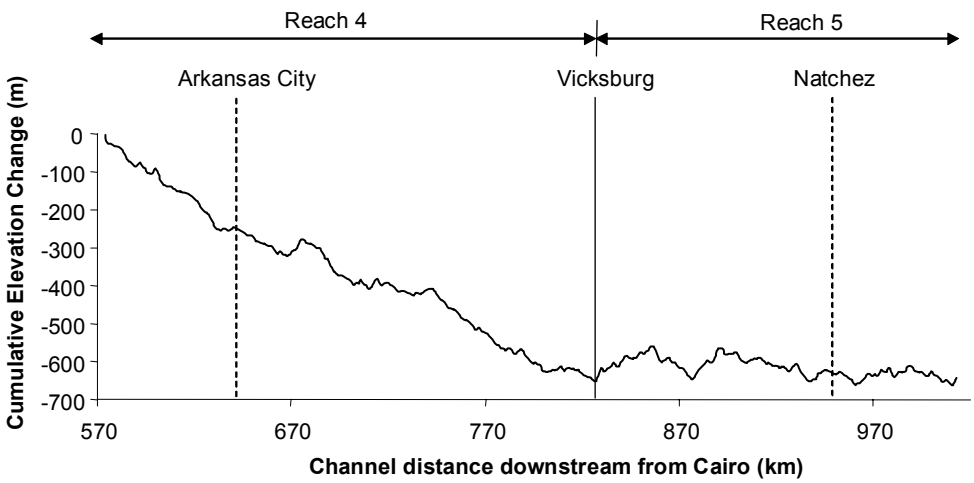

b)

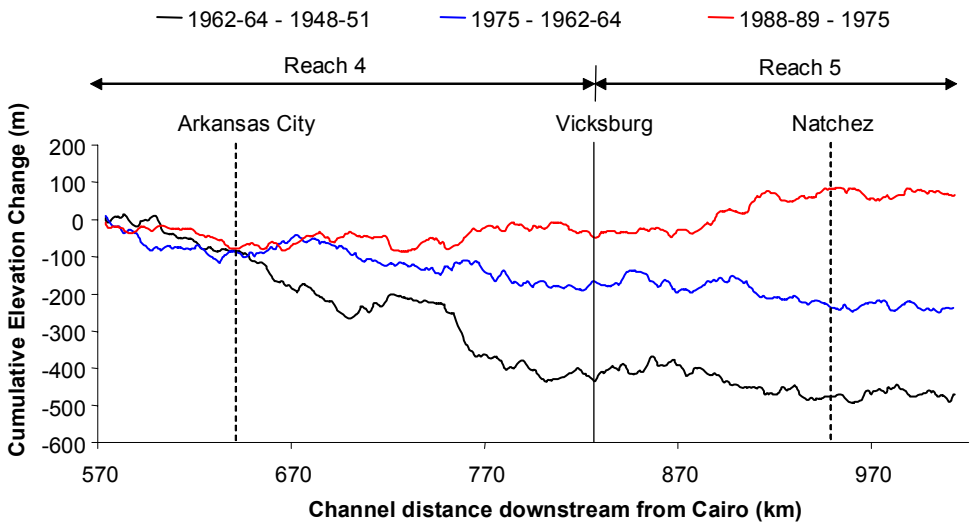

Figure 6.7 a) Cumulative elevation change from 570 km downstream from Cairo in the period 1949-1989; and b) cumulative elevation change within three sub-periods dictated by the dates of intermediate hydrographic surveys.

Period	Reach 4†	Reach 5*
1949-51 – 1962-64	Degradation	Slight degradation
1962-64 – 1975	Slight degradation	Slight degradation
1975 – 1988-89	Negligible change	Aggradation

†Confluence of Arkansas and White Rivers to confluence of Yazoo River at Vicksburg
*Confluence of Yazoo River at Vicksburg to Old River distributary

Table 6.3 Vertical trends in long profile gradient in the period 1949 – 1989.

considerably thereafter. After approximately 33-48 years (corresponding to 1975 – 1989), the absence of a net trend indicates a return to a stable condition. The high rate of degradation in the 1949-1964 period is consistent with the increase in stream power per unit width following the shortening associated with artificial cutoff construction. Given the absence of a trend in discharge over the period of record (1949-1989), the decline in the rate of degradation indicates that total sediment transport into, and out of, the reach are closer to being in balance. Thus, either, sediment transport out of the reach has declined, or sediment input into the reach has increased. These scenarios may be further complicated by flow resistance changes within the reach, caused by adjustments to the bedform configuration. Flow resistance changes are examined in the next section by assessing temporal changes to the wavelength and amplitude characteristics of pools and crossings.

Downstream from Vicksburg (reach 5), the absence of a clear trend in Figure 6.7a masks a trend of slight degradation up until 1975 and then aggradation thereafter. Conceptually, observed spatial and temporal trends of cumulative elevation changes in reaches 4 and 5 are consistent with a knickpoint migrating upstream through time. However, further analysis of the thalweg profile upstream from the confluence of the Arkansas and White River is required to verify whether the zone of degradation extends further upstream.

Relative reach-scale temporal trends noted by plotting cumulative elevation change are consistent with those identified by series smoothing using a low pass moving average filter (Figure 6.8). Smoothing is undertaken in order to remove the sub-reach (pool-crossing) scale of variation and hence, emphasise larger reach-scale trends that may not be apparent in the original data series. The use of moving averages is complementary to considering cumulative changes because, although relative rates of changes are more difficult to detect, moving averages retain absolute changes within the series. Three additional characteristics of reach-scale temporal changes are revealed by Figure 6.8. First, in the vicinity Vicksburg, profile slope has remained relatively consistent over the 1949-89 period. This is no a priori physical reason to suspect temporal stability in this area. Thus, it may simply reflect the equalisation of contrasting behaviours upstream in reach 4 and downstream in reach 5. Second, at the upstream limit of the total reach, the plot suggests that the zone of

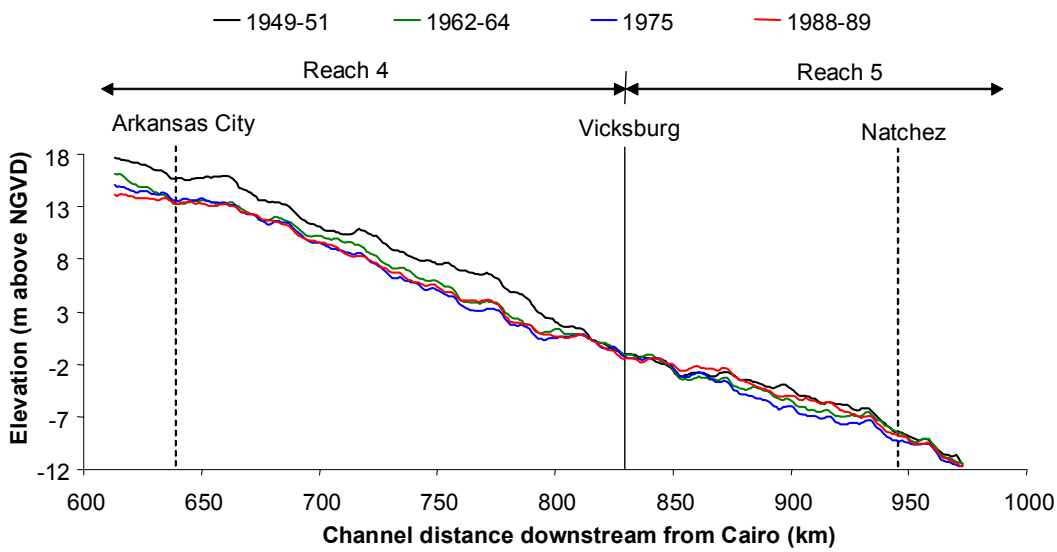

Figure 6.8 Comparing long profiles in the 1949-89 period that have been smoothed by applying an 80 km moving average. This window size is sufficient to remove the sub-reach scale (pool-crossing) scale of variation and hence, emphasise reach-scale trends.

degradation during the 1949-1964 period probably extended further upstream than the confluence of the Arkansas and White Rivers. Third, and conversely, at the downstream limit of the total reach, the merging of each smoothed long profile may suggest that the reach-scale slope of the long profile is stable in the vicinity of Old River distributary.

The temporal trends revealed by Figures 6.7 and 6.8 are at least partially consistent with the model of morphological response proposed by Biedenharn and Watson (1997; Figure 2.15). From examination of specific gauge records for the period 1950-1994, Biedenharn and Watson (1997) report a condition of 'dynamic equilibrium' or stability in the reach between Arkansas City and Vicksburg and aggradation in the reach between Vicksburg and Natchez. These trends are consistent with thalweg profile changes in the 1975 – 1989 period but not the earlier period. The apparent lag of morphological trends behind trends in specific gauge records (representing changes in the water surface slope) may indicate that morphological changes have been accompanied by an increase in flow resistance. For example, the degradation of channel bed can occur with no change in water surface elevation *if* degradation is accompanied by an increase in the amplitude and/or the frequency of pools and crossings because this will increase large-scale bedform resistance, decrease flow velocity and hence, increase flow stage. By the same reasoning, an increase in water surface elevation may result from reach-scale stability of the channel bed *if* it is accompanied by an increase in the amplitude and/or frequency of pools and crossings. Temporal variation in the amplitude and wavelength of pools and crossings is therefore explored in the next section.

In addition to issues of flow resistance, the identification of systematic morphological response at the reach-scale raises important questions regarding the causal mechanisms of morphological change. First, sustained vertical changes imply a high degree of connectivity at the sub-reach (pool-crossing) and possibly at the reach-scale in which geomorphological changes migrate through the system through a series of positive feedback mechanisms. This raises the question of whether such feedback mechanisms can be identified and how they are sustained. Such sub-reach scale dynamics are explored in detail in chapter 7. Second, but related to the first, the identification of reach-scale morphological response does not necessarily imply

that all parts of the channel are changing in the same manner. For example, Biedenharn and Thorne (1994) concluded from dominant discharge analysis that mid-channel bars (crossings) represent the contemporary active morphological feature of the Lower Mississippi River. This assertion is assessed following examination of the relative temporal behaviour of pools and crossings.

6.6 Temporal variation in the amplitude and wavelength of pools and crossings

The temporal behaviour of pools and crossing is explored using the unstandardised long profile data series for downstream distance because the process of distance standardisation (section 6.4) would introduce error and therefore degrade the reliability of wavelength estimates. In the following sections amplitude and wavelength is estimated using serial techniques alongside regression classification and the cumulative elevation change technique (see Figure 5.11 for a definition of pool and crossing wavelength, amplitude, and length parameters).

6.6.1 Removal of regression trends

Each hydrographic survey was divided into two reaches, corresponding to reaches 4 and 5. Within each reach, downstream trends were removed by fitting regression functions to the original profile (Table 6.4). The fitting of second-order polynomial functions generate consistently higher R^2 values than linear functions. Hence, second-order polynomials were used to detrend all of the long profiles.

6.6.2 Serial Analysis

Second-order autoregressive modelling performed on each reach reveals contrasting behaviour between the reaches in each hydrographic survey. In reach 4, each hydrographic survey satisfies the equation for pseudo-periodicity with the exception of the first survey in 1948-49. This suggests that immediately following the artificial cutoff programme (1932-1942), pool and crossing undulations in the long profile of this reach may not have been ordered in a statistically determinate manner that is

consistent with other river systems. However, over a longer time period of response, physical processes have adjusted the long profile to create a level of order consistent with pseudo-periodic pool and crossing spacing at the regional-scale. Meanwhile, in reach 5, each hydrographic survey satisfies the equation for pseudo-periodicity with the exception of the survey in 1975. This may indicate that the flood event in 1973-74 caused relatively dramatic changes to the wavelength and amplitude characteristics of pools and crossings, destroying the 'ordered' bed topography that had developed previously. Pseudo-periodicity is again evident in the 1988-89 survey. Hence, the short-term removal of pseudo-periodicity in 1975 indicates that pools and crossings on the Lower Mississippi River are adjusting at sub-decadal intervals as well as over longer time intervals. This is explored further in chapter 7.

Spectral density plots for each reach are presented in Figure 6.9. Each spectra is characterised by either a broad peak or multiple peaks, reflecting the presence of two or more dominant wavelengths. Because a pseudo-periodic process is represented by a broad peak spectrum these characteristics are at least partially consistent with results from second-order autoregressive modelling. In reach 4, there is a tendency for the dominant peak in the distribution to shift further to the right through the period 1949-89. This is diagnostic of a shortening of wavelength over the period. This trend however, is not consistent with mean wavelengths estimated by second-order autoregressive modelling in series that satisfy the equation for pseudo-periodicity. In reach 5, there is no clear tendency of change in the distribution of spectral peaks through time whereas second-order autoregressive modelling is suggestive of a decline in mean wavelength in this reach. The inconsistencies between the two serial techniques therefore preclude any clear spatial or temporal change in wavelength to be identified. In the following section, these characteristics are examined using regression classification and the cumulative elevation change technique.

6.6.3 Pool and crossing parameterisation by regression

Spatial and temporal trends in reach-averaged amplitude, length, and amplitude: length ratio identified by the regression classification technique are presented in

	Regression			Second-order autoregressive modelling						
Year	**Linear (R^2)**	**2nd Poly. (R^2)**	**Skewness Ratio**	**$Ø_1$**	**$Ø_2$**	**R^2**	**$Ø_1^2 < -4Ø_2$?**	**Pseudo-periodic?**	**Sig. 2nd coef. in PACF?**	**Wavelength (km)**
Reach 4										
1949-51	0.576	0.581	-0.697	0.800	-0.143	0.501	0.068	No	Yes	---
1962-64	0.558	0.560	-0.244	0.734	-0.217	0.376	-0.329	Yes	Yes	9.471
1975	0.544	0.554	-0.429	0.745	-0.168	0.410	-0.117	Yes	Yes	14.601
1988-89	0.539	0.571	-0.385	0.844	-0.224	0.490	-0.184	Yes	Yes	13.375
Reach 5										
1949-51	0.374	0.395	-0.500	0.783	-0.192	0.442	-0.155	Yes	Yes	13.491
1962-64	0.367	0.371	-0.716	0.759	-0.210	0.418	-0.264	Yes	Yes	10.561
1975	0.310	0.312	-0.604	0.758	-0.139	0.457	0.019	No	No	---
1988-89	0.418	0.422	-0.860	0.845	-0.274	0.483	-0.382	Yes	Yes	9.951

Table 6.4 Removing the trend from the long thalweg profile in reaches 4 and 5 by linear and second-order polynomial regression and detection of pseudo-periodicity by second-order autoregressive modelling.

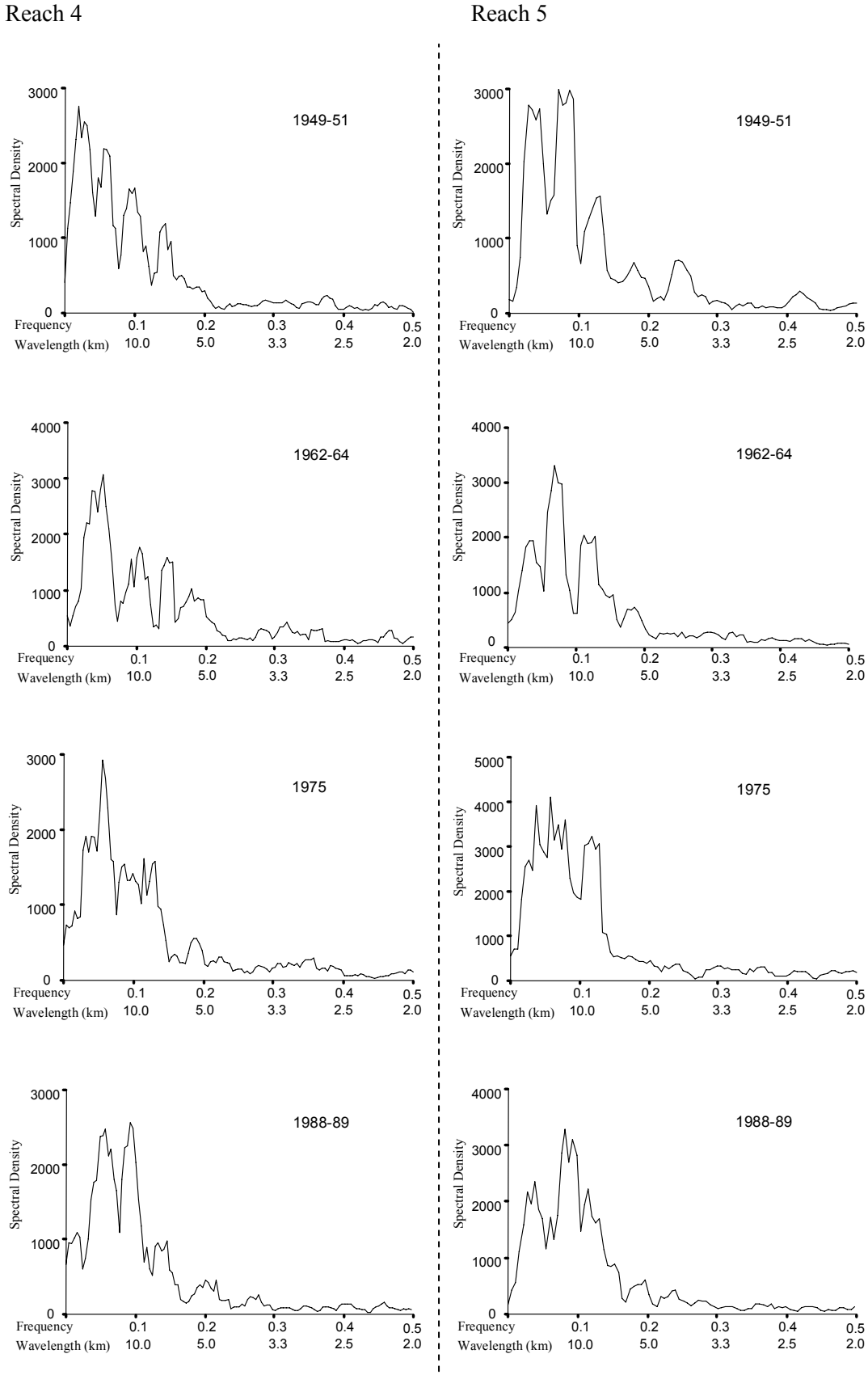

Figure 6.9 Spectral plots in the period 1948-1988 for reaches 4 and 5.

Figure 6.10. These trends generally support the contrasting temporal trends noted in reaches 4 and 5 by serial techniques.

Temporal reach-averaged trends in amplitude: length ratios within reach 4 are particularly interesting because, although there is no clear change in pools, crossings demonstrate a dramatic increasing ratio from 1949-51 to 1962-64, a slight decreasing ratio from 1962-64 to 1975, and a stable ratio from 1975 to 1988-89. Figures 6.10a and 6.10b indicate that the dramatic increase in crossing amplitude: length ratio in the early period was caused by an increase in crossing amplitude and a decrease in crossing wavelength. This finding must be treated with a degree of caution however, because, as noted in section 5.7.4, apparent changes recorded by regression classification can simply reflect changes in the shape of pools in relation to the shape of crossings.

Relative bedform shape changes can be assessed by examining temporal trends in the skewness ratio of the residuals following initial removal of the polynomial trend. Throughout the 1949-89 period, the residuals remain negatively skewed, indicating that crossings are generally longer and lower amplitude features than pools. Therefore, in terms of Robinson's (2003) bedform shape classification, bedforms are maintained as 'dome-up' features (see Figure 5.19). However, during the 1949-1964 period, the skewness ratio increases considerably (becomes less negatively skewed). This is indicative of a move towards more triangular bedforms and hence, a relative increase in crossing amplitude and decrease in pool depth. Because a reach-averaged increase in crossing amplitude in the 1949-64 period was not accompanied by a reach-averaged decrease in pool depth, this suggests again that the increase in crossing amplitude: length ratio is physically significant. Therefore, the high rate of degradation at this time was accompanied by an increase in form resistance exerted by the pool-crossing configuration. This is indicative of a negative feedback response whereby the system has attempted to increase form resistance in order to expend additional energy and hence, restore bed stability.

In reach 5, there is no clear temporal trend in reach-averaged amplitude: length ratio, suggesting that that the longitudinal component of flow resistance has remained approximately constant through time. This is consistent with the much slighter

trends in slope profile in reach 5, noted in section 6.3. However, Figures 6.10a and 6.10b do reveal that this has been achieved through complementary adjustments to both amplitude and wavelength, both increasing in the period 1949-1975 and both decreasing thereafter. Temporal trends in the skewness ratio in reach 5 (see Table 6.4) are not consistent with length and amplitude changes and thus, there is no reason to believe that changes in the relative shape of pools and crossings has influenced these temporal trends. Furthermore, the abrupt change in the amplitude and wavelength of pools and crossings in the 1975 hydrographic survey is consistent with the abrupt change in the level of pseudo-periodicity in reach 5 at this time. These changes may represent a signature of the high discharge experienced in the 1973 and 1974 water years, immediately prior to collection of the hydrographic survey (section 6.3).

6.6.4 Pool and crossing parameterisation by the cumulative elevation change technique

Section 5.7.5 showed that the cumulative elevation change technique gives a more reliable estimate of pool-to-pool spacing and pool and crossing lengths than regression classification but is unable to distinguish relative differences between changes in pool and crossing amplitude. Hence, temporal trends in amplitude are not considered here.

Figure 6.11 plots the relationship between observed pool-to-pool spacing and tolerance value applied to the cumulative elevation change technique for each hydrographic survey in the period 1949-89. This is informative for three reasons. First, the 1949-51 relationship in reach 4 is characterised by an abrupt increase in pool-to-pool spacing at tolerances in excess of 5 m. This is consistent with the longer length of pools and crossings noted by the regression classification technique in this reach and at this time. Second, in both reaches, the rate of increase of pool-to-pool spacing with increasing tolerance in excess of 5 m is relatively low in 1962-64. This is therefore indicative of a marked increase in the number of pools and crossings in the period 1949-64 in reach 4 and at least a slight increase in reach 5. Third, the line connecting points plotted for the 1988-89 survey is positioned at a consistently higher pool-to-pool spacing than the line connecting points for the 1962-

a)

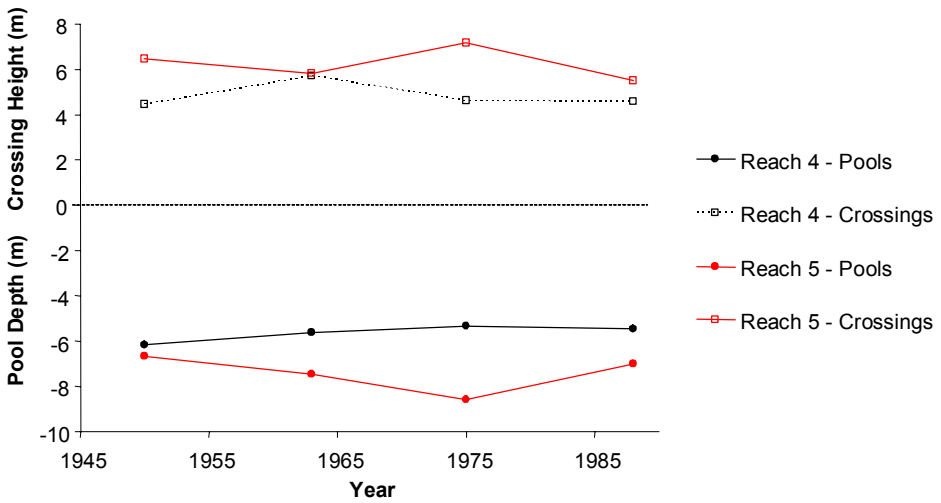

b)

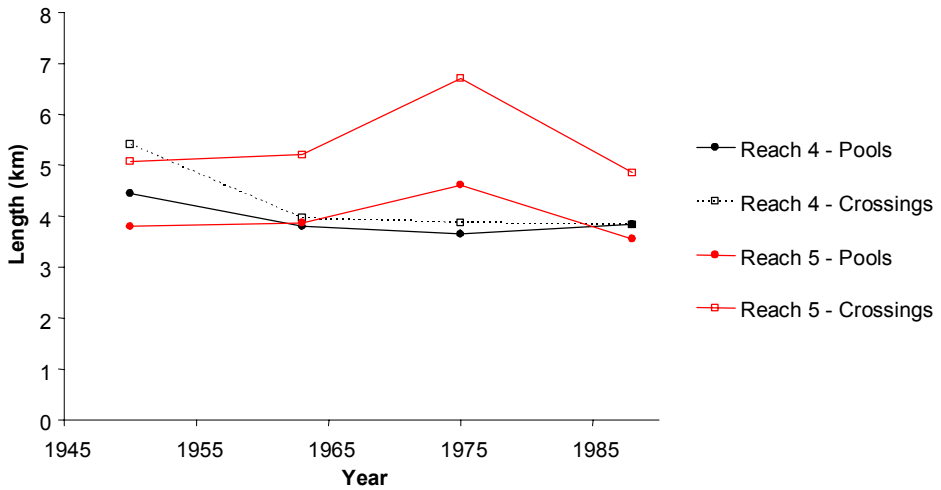

c)

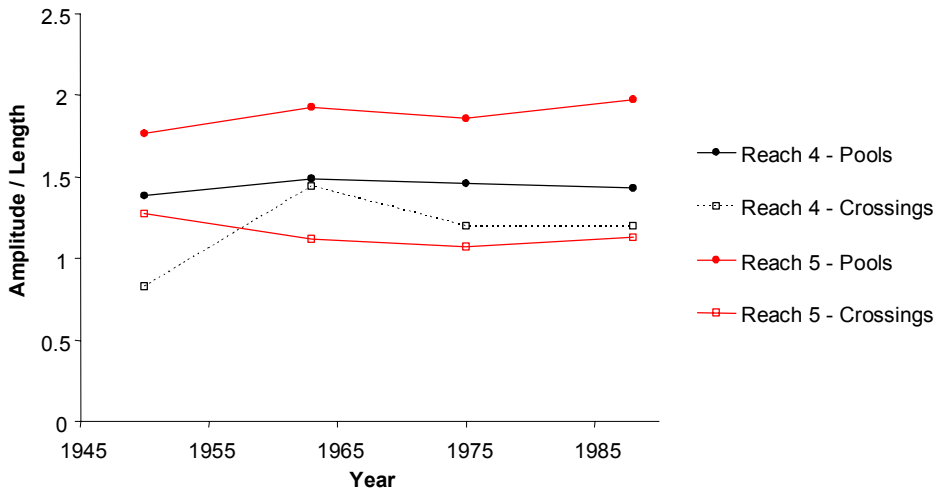

Figure 6.10 Temporal trends in reach-averaged: a) amplitude; b) length and c) amplitude/length ratio as identified by regression for the four hydrographic surveys in the period 1949-1989. In a) crossing amplitude is positive and pool amplitude is negative to illustrate their respective positions above and below the regression line.

a) Reach 4 (confluence of Arkansas and White Rivers to the confluence of the Yazoo River at Vicksburg).

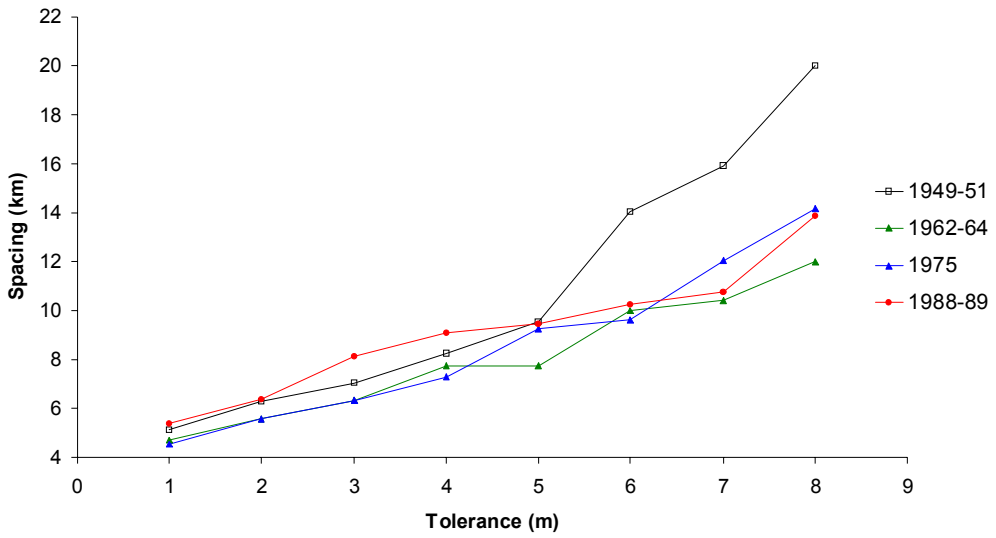

b) Reach 5 (confluence of Yazoo River at Vicksburg to 8 km upstream from Old River).

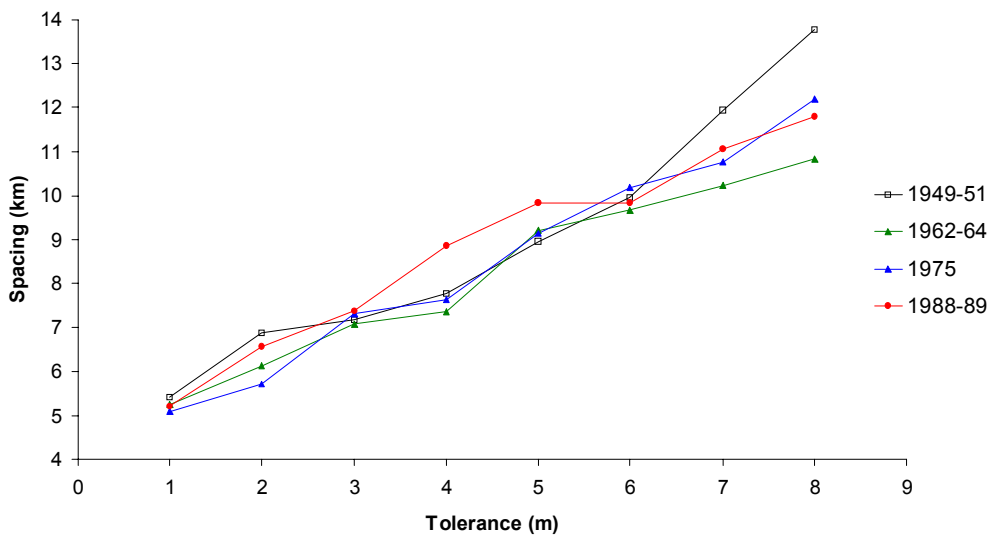

Figure 6.11 The increase in average pool-to-pool spacing as tolerance value is increased for the four hydrographic surveys in the period 1949-1989.

64 survey. This is indicative of a decrease in the number of pools and crossings in the 1962-89 period in both reaches 4 and 5, but not to the number noted in the 1949-51 hydrographic survey.

The decrease in pool-to-pool spacing in the period 1949-64 is examined further in Figure 6.12a by considering the change in the average length of pools and crossings. The sharp decline in reach-averaged crossing length, together with the absence of a discernable trend in reach-averaged pool length, provides further support for the move from a dominant 'dome-up' bedform shape towards a more triangular form. Pool and crossing length in reach 5 is considerably more stable when estimated by the cumulative elevation change technique than regression classification, although the slight increase in crossing spacing in 1975 is still maintained. Figure 6.12b relates bedform changes to planform attributes by considering the relative planform direction change through a pool or crossing identified by the cumulative elevation change technique. The decrease in reach-averaged crossing direction change in the 1949-64 period in reach 4 demonstrates that new crossings tended to form in straighter reaches of the river (Figure 6.5). Given that most of the sinuous bends on the Lower Mississippi River were removed by the artificial cutoff programme, this most likely reflects the formation of pool and crossing topography in the straightened reaches. Reach 5 displays a contrasting trend, with reach-averaged direction change of both pool and crossings increasing in the period 1949-75 and then decreasing thereafter.

6.6.5 Relating changes in the pool-crossing configuration to changes in profile slope

Results obtained from regression classification and cumulative elevation change techniques suggest that the sub-reach scale pool-crossing configuration on the Lower Mississippi River has adjusted to larger reach-scale changes in profile slope. In reach 4, the development of pools and crossing oscillations in the 1949-64 period, particularly in the straightened reaches where the artificial cutoffs had been constructed, is suggestive of an increase in form resistance exerted by the bedform configuration. This change is diagnostic of a river attempting to dampen the degradational trend identified in this reach at this time by expending energy in ways

a)

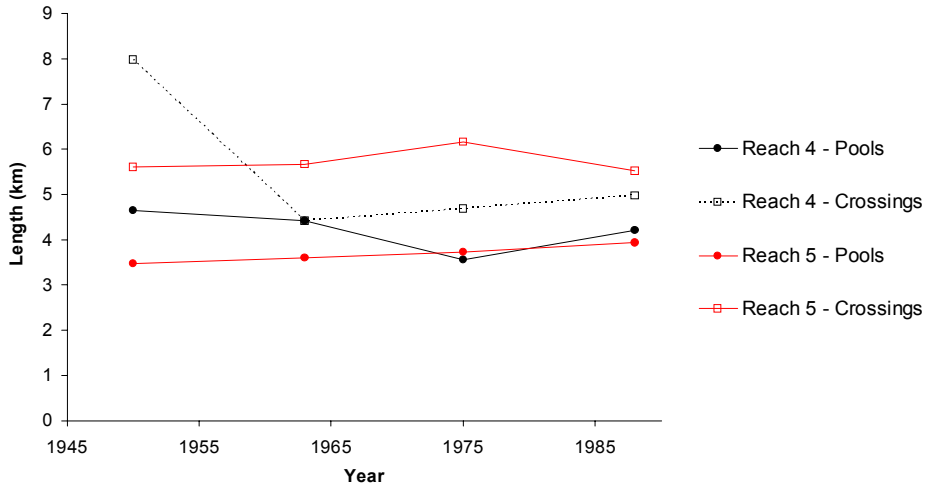

b)

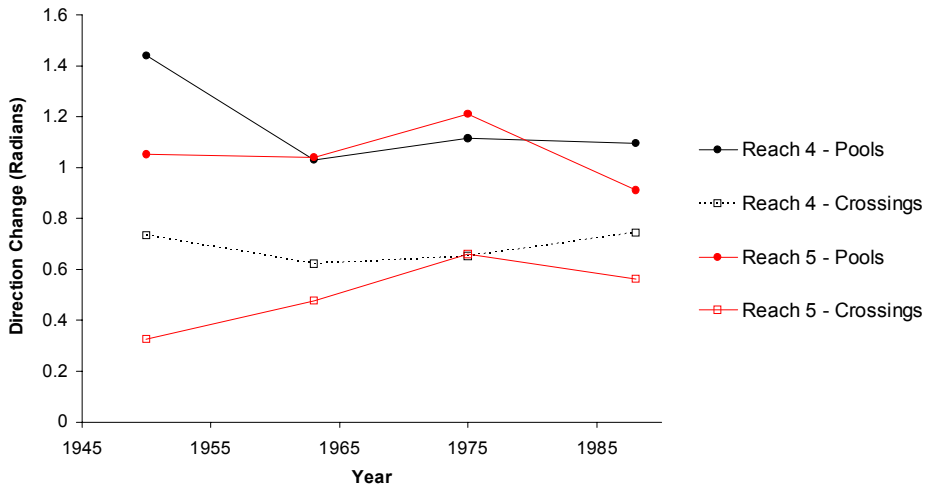

Figure 6.12 Temporal trends in reach-averaged: a) length and; b) direction change as identified by the cumulative elevation change technique for the 1949-89 period. To maintain consistency with section 5.7.4, a tolerance value of 6 km has been applied. Direction change is defined as the difference between the direction angle of the digitised channel centreline at the upstream entrance and downstream exit of each pool or crossing. Thus, low values of direction change and indicative of straight reaches and vice versa.

other than performing sediment transport. In reach 5, no consistent temporal change in large-scale bedform resistance are evident over the 1949-1989 time period. This is consistent with the much smaller magnitude changes in reach-scale bed slope in comparison to reach 4. However, despite this longer-term stability, the increase in the size of pools and crossings in 1975 in relation to other survey years suggests that the pool-crossing configuration in reach 5 is more sensitive to disturbance by large magnitude flood events.

These changes in bedform configuration are at least partially helpful to resolving the apparent paradox between bed surface slope and water surface slope changes noted in section 6.5. In reach 4, the suggested increase in form resistance following the artificial cutoff programme is likely to have acted to reduce flow velocity and consequently increase flow stage. This increase in flow stage may offset the reduction in flow stage caused by net degradation and hence, explain the absence of a discernable temporal trend in water surface elevation in the 1950-1994 time period whilst the channel thalweg was degrading. This assertion is examined further in section 6.7 by analysis of changes in flow velocity. In reach 5, the apparent reach-scale stability of the channel bed whilst the water surface increased in elevation for the same discharge cannot be explained in terms of longitudinal large-scale bedform resistance changes.

These identified changes only partially support Biedenharn and Thorne's (1994) assertion that the crossing sub-reaches represent the geomorphologically active feature of the contemporary Lower Mississippi River. Both regression classification and cumulative elevation change techniques indicate that average changes to the length of crossings is most apparent in the 1949-64 period within reach 4. Aside from this period however, it is not evident that the magnitude of changes in crossings was greater than those in pools. This is also important in relation to chapter 5 because it does not support the hypothesis that pools may represent more stable and hence, possibly relict geomorphological features. However, reaches 4 and 5 are both situated in the alluvial valley (between the confluence of the Arkansas River and Old River distributary) and therefore, identified temporal patterns cannot necessarily be used to inform the behaviour of deep pools on the deltaic plain.

6.7 Spatio-temporal variation in cross-section morphological and process parameters

In addition to adjusting their long profiles, alluvial rivers can adjust their cross-sectional morphology in response to imposed discharge events and sediment waves. In this section, spatio-temporal variations in cross-sectional size, shape, velocity, and value of Mannings *n* roughness coefficient are explored in the 1949-89 time period. This is achieved following the process of obtaining a reliable water surface profile.

6.7.1 Obtaining a water surface profile

A water surface profile was generated by applying a 1-D step-backwater model as outlined by Chow (1959). A condition of gradually varied flow is assumed in which flow is steady but not uniform because depth varies gradually along the length of the channel. Gradually varied flow is based on the Bernoulli equation which defines total head (*H*) as:

$$H = z + d + (\alpha V^2 / 2g) \qquad (6.1)$$

where:

z = the vertical distance of the channel bed above datum

d = depth of flow

θ = channel slope angle

α = velocity distribution coefficient

V = mean velocity of flow

Between two cross-sections, the total head at a downstream cross-section is equal to the total head at the upstream cross-section plus the head loss (h_L) between the two cross-sections. This is illustrated in Figure 6.13. The bed slope gradient is steeper than the water surface gradient and so the depth of flow increases between the two cross-sections. To compensate for this change, the velocity head decreases between the two cross-sections. This is shown by a steep energy gradient slope in comparison to both the bed slope and the water surface slope and is indicative of flow deceleration. The reduction in velocity head reflects losses caused by both flow resistance and sediment transport (Richards, 1982).

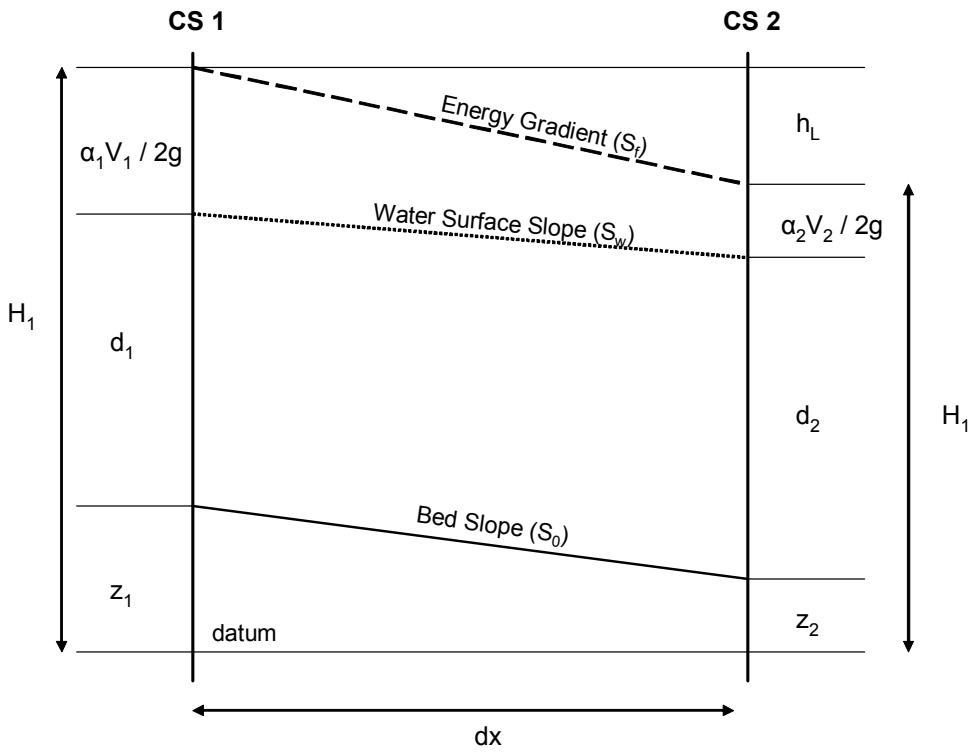

Figure 6.13 Derivation of the equation for gradually varied flow (after Richards, 1982).

The change in total head between the two cross-sections is described by the energy balance equation:

$$z_1 + d_1 + (\alpha_1 V^2_1 / 2g) = z_2 + d_2 + (\alpha_2 V^2_2 / 2g) + h_L \qquad (6.2)$$

In differential form, this can be written:

$$dH/dx = dz/dx + dd/dx + [d(\alpha v^2/ 2g) / dx] \qquad (6.3)$$

In Figure 6.13, if the head loss over the reach (dH/dx) = -sin S_f = -S_f for small slopes and similarly the change in elevation above the datum (dz/dx) = -sinS_0 = -S_0 then, the energy balance equation may be expressed as (Richards, 1982):

$$dd/dx = (S_0 - S_f) / [1 + d(\alpha v^2/ 2g) / dd] \qquad (6.4)$$

If dd/dx is positive, the water surface diverges from the bed, whereas if dd/dx is negative, the water surface draws down towards the bed. The water surface profile was generated using the iterative standard step-backwater procedure outlined by Chow (1959). In addition to cross-sectional data, this procedure required a single flow discharge, a downstream water surface elevation, a value for the (Manning's) roughness coefficient (n), and a value for the velocity distribution coefficient (α), to be specified. The latter two parameters allow flow resistance losses caused by skin, form and internal distortions (eddy motions) to be accounted for in the computation of the water surface profile.

Step-backwater modelling was performed on the 1949-51 and 1988-89 hydrographic survey data sets for the reach of the Lower Mississippi River from the confluence of the Arkansas and White rivers (574 km) downstream to approximately 8 km upstream from Old River. These surveys were undertaken over time periods long enough to incorporate considerable variation in flow stage (see Table 6.1) and hence some cross-sections may have been surveyed at relatively high flow stages and others at relatively low flow stages. Therefore, to maximise the number of cross-sections included within the analysis of morphological parameters, 1-D step-backwater modelling was performed at a low flow stage of 10 000 m^3s^{-1}. Figure 2.4 shows that this discharge was exceeded approximately 70 percent of the time at the Vicksburg gauging station in the 1938-2001 water year period. The 1962-64 and 1975 hydrographic survey data sets were not used in the analysis because they were

collected at a lower flow stage than the 1949-51 and 1988-89 surveys and hence, a higher proportion of cross-sections were removed. This is reflected in Table 6.1 by the lower mean left-bank to right-bank distance in relation to the earlier (1949-51) and later (1988-89) hydrographic surveys.

Water surfaces computed by 1-D step-backwater modelling were calibrated using known water surface elevations at flow gauging stations throughout the reach. Long-term (1940-2001) flow stage and discharge records exist at Arkansas City; Vicksburg; and Natchez. At each of these three gauging stations, the mean flow stage elevation for a discharge of 10 000 m^3s^{-1} was estimated from the relationship between flow stage and discharge (Figure 6.14a). Relationships were developed for each hydrographic survey using data for a ten-year period: five years before and five years following the mid-date of the survey period. Thus, calibration of the computed water surface profile for the 1949-51 and 1988-89 surveys used stage and discharge records for the 1945-1955 period 1983-93 water year periods respectively. A ten-year period was selected because it was considered long enough to incorporate sufficient data to estimate a reliable mean which is not biased by known hysterisis effects (Simons *et al.*, 1973) whilst not being too long to incorporate long-term trends noted in specific gauge records (Biedenharn, 1995; Biedenharn and Watson, 1997).

At three further intermediate stations in the reach: Greenville; Lake Providence; and St Joseph, additional long-term records (1940-2001) of flow stage have been collected but without corresponding discharge measurements. At each of these stations, a long-term discharge record was constructed by distance-weighted linear interpolation. This used the nearest upstream and nearest downstream discharge recording station and an appropriate time lag to allow for the transport of flow between gauging stations. In each case, the appropriate time lag interval was chosen based on cross-correlation of the upstream and downstream discharge records. Hence, in total, relationships of flow stage against discharge at six gauging stations were used to calibrate the computed water surface profile.

The most downstream cross-section within each survey (approximately 8 km upstream from Old River) does not correspond directly with a gauging station.

Therefore, the downstream water surface elevation, required as an initial input into the step-backwater model was determined by distance-weighted linear interpolation. This used the average flow stage corresponding to a discharge of 10 000 m^3s^{-1} at the nearest upstream and downstream gauging station. The nearest upstream gauging station is Natchez which has long-term records of both flow stage and discharge. Meanwhile, the nearest downstream gauging station with a long-term (1940-2001) flow stage record is Tarbert Landing (1028 km downstream from Cairo). However, this is located immediately downstream from the Old River distributary which diverts up to 30 percent of the discharge during periods of high flow. Hence, use of this gauging station as a downstream control would violate the assumption of steady flow. Instead, an intermittent record was used at Coochie, a discontinued sediment sampling station which is located immediately upstream from the Old River distributary (1025 km downstream from Cairo). A single plot of stage against discharge was developed using measured records at approximately 2-4 week intervals between May 1967 and December 1998. Although this relies on considerably fewer observations than records at other gauging stations, Figure 6.14b shows that there are still a sufficient number of observations to compute a reliable average flow stage for a discharge of 10 000 m^3s^{-1}.

The calibration procedure involved maintaining the velocity distribution coefficient (α) constant whilst varying the value of the roughness coefficient (n) through a process of trial and error until the computed water surface at each gauging station was within the error band of ± 0.1 metre of the ten-year average flow stage. The roughness coefficient and the velocity distribution coefficient are both diagnostic of flow resistance so an increase or decrease in computed water surface elevation can be achieved through adjustments to only one parameter. Based on the computation of the α in a single pool-crossing sub-reach on the Lower Mississippi River (see section 7.4), a value of 1.1 was specified as the constant value. Because, the reliability of the computed water surface could only be calibrated at gauging stations, constant values of n were specified between gauging stations. This maintained necessary control in the calibration process. The ten-year average flow stage at each gauging station and the specified value of n for the reach to the next gauging station upstream are listed in Table 6.5 for both the 1949-51 and 1988-89 hydrographic surveys. The calibrated water surface profile for the reach in 1988-89 is plotted alongside the channel

a)

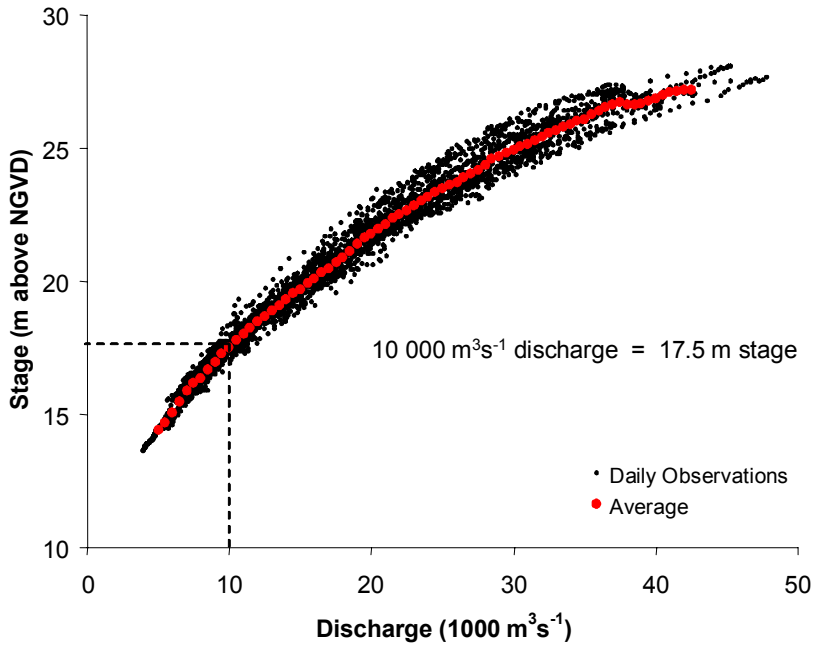

b)

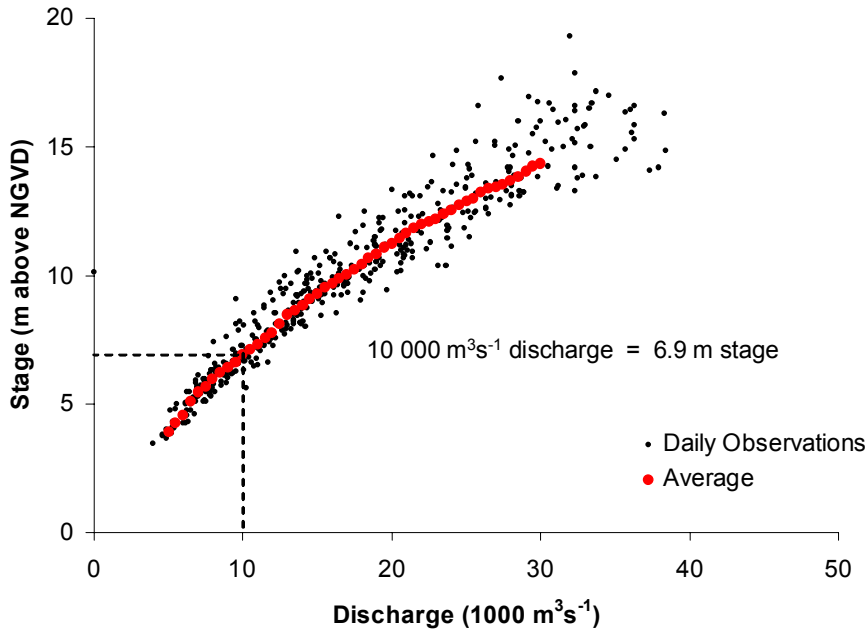

Figure 6.14 Stage against discharge relationships: a) Flow stage against computed daily discharge for the Vicksburg gauge in the period 1983 – 1993 and; b) flow stage against discharge measured intermittently in the period 1967-1998. The average flow stage (filled red circles) for each 500 m^3s^{-1} increment of discharge has been computed using the method outlined in the accompanying text.

thalweg in Figure 6.15 with the location of gauging stations clearly marked.

6.7.2 Variation of the roughness coefficient (*n*)

The roughness coefficient required to calibrate the computed water surface is a reach-averaged indicator of total flow resistance. Thus, examining its variation can be used as a technique to further inform spatial and temporal trends in flow resistance.

Table 6.5 shows that the specified roughness coefficients in the 1949-51 hydrographic survey are consistently lower than those in the 1988-89 hydrographic survey. The magnitude of difference ranges from a minimum of 22 percent (0.005) in the reach from Vicksburg to Lake Providence to a maximum of 39 percent (0.0085) in the reach from the downstream limit to Natchez. The consistent increase in required roughness coefficient is consistent with the general increase in form resistance exerted by the bedforms in reach 4 (section 6.6). In reach 5, the relative stability of the bedforms despite the increase in required roughness coefficient may suggest that total flow resistance has been increased by changes other than adjustments to the pool-crossing sequence. Because morphological adjustments in the planform have effectively been prohibited by bank stabilisation, an increase in form resistance is most likely to be accomplished through adjustments to the cross-sectional configuration of the reach. This is examined in section 6.7.5.

Downstream trends in the required roughness coefficient are consistent with the higher combined amplitude: length ratio of pools and crossings in reach 5 in comparison to those in reach 4 (see Figure 6.10c). This suggests that total flow resistance increases downstream within the reach. In Figure 6.16, the roughness coefficient required to calibrate the computed water surface for the 1988-89 hydrographic survey is plotted against distance downstream for discharges in the range 10 000-30 000 m^3s^{-1}. This reveals that as discharge increases, the roughness coefficient required decreases. This observation is expected, given that, at higher discharges, the hydraulic radius increases and therefore large-scale bedform resistance declines. The magnitude of downstream variation in required roughness

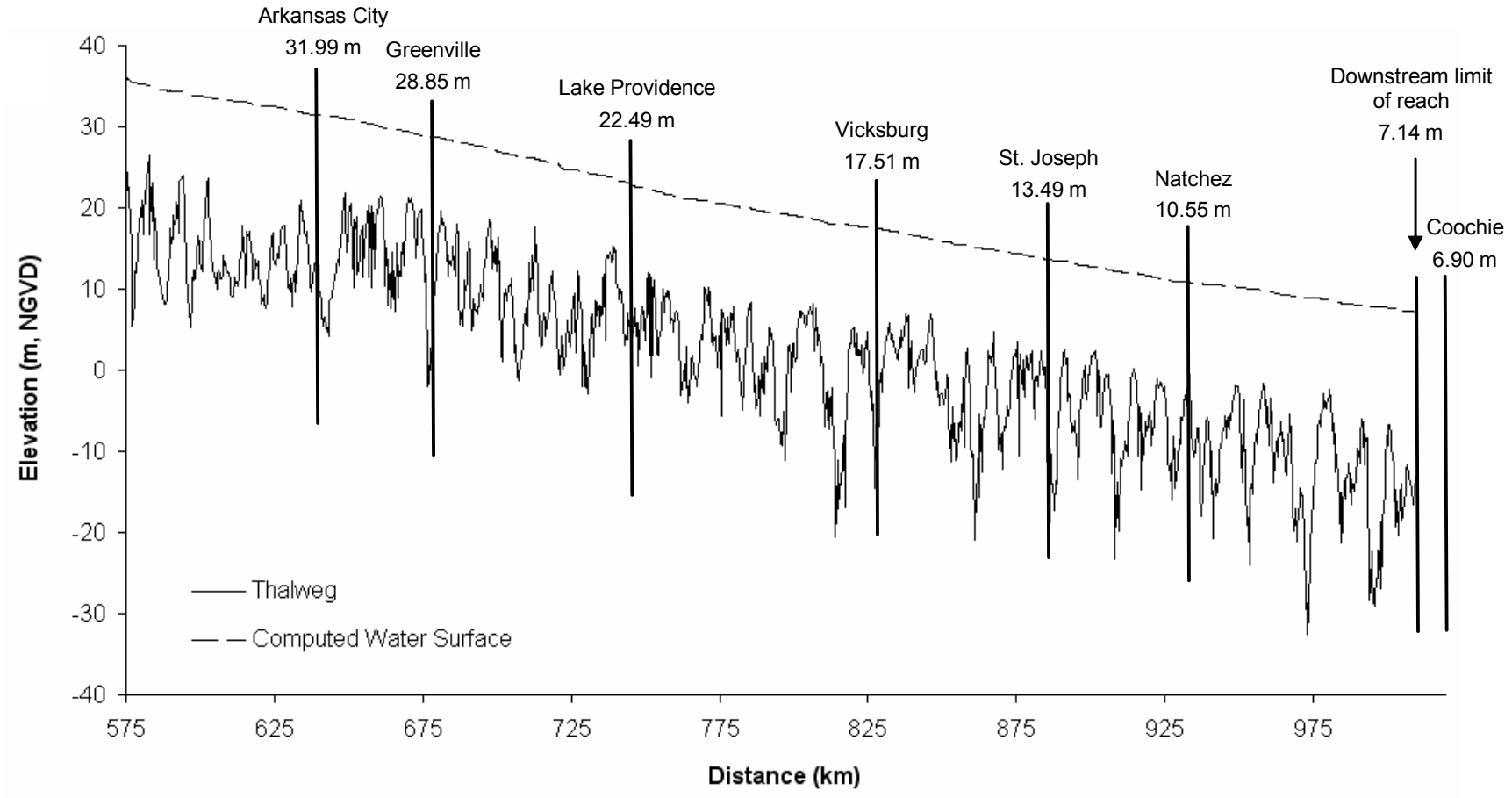

Figure 6.15 Long thalweg profile and computed water surface profile for a discharge of 10 000 m^3s^{-1}. The reach extends from the confluence of the Arkansas and White Rivers (575 km) to 8 km upstream from Old River (1018 km). The computed water surface profile is precise to within 0.1 m of the mean flow stage at available gauging stations (referenced to metres above NGVD).

Gauge	Distance downstream from Cairo (km)	1949-51		1988-89	
		Stage†	n*	Stage†	n*
Coochie	1025	6.90		6.90	
Downstream limit of reach[Δ]	1018	7.07	0.0220	7.14	0.0305
Natchez	951	9.81	0.0245	10.55	0.0305
St. Joseph	898	12.84	0.0235	13.49	0.0290
Vicksburg	835	17.02	0.0225	17.51	0.0275
Lake Providence	752	22.62	0.0225	22.49	0.0285
Greenville	682	28.95	0.0215	28.85	0.0270
Arkansas City	645	32.01	0.0215	31.99	0.0270

[Δ]Downstream flow stage obtained by distance-weighted linear interpolation using nearest downstream (Coochie) and nearest upstream (Natchez) records.
†Flow stage computed from the stage-discharge relationship over a ten-year period, given as metres above NGVD.
*Roughness coefficient for each cross-section in reach from current gauging location to next upstream gauging location.

Table 6.5 Gauge locations, flow stage and values of roughness coefficient (n) used in the flow model computation.

coefficient also declines with increasing discharge because the importance of the downstream increase in the amplitude of bedforms (Figure 6.10a) to total flow resistance decreases.

Despite both downstream and temporal trends in roughness coefficient being at least partially consistent with observed morphological changes, it is interesting to note that they are inconsistent with previous investigations of reach-averaged values of Mannings *n*. outlined in section 2.6.3. These generally report no discernible downstream or temporal trends (Robbins, 1977; Stanley Consultants, 1990). Given that the investigation by Stanley Consultants involved the same analytical procedure to calculate the roughness coefficient (calibrating water surfaces generated by 1-D step-backwater modelling against measured water surfaces), this is especially surprising. To resolve this inconsistency, it is recommended that step-backwater modelling is undertaken using further hydrographic survey data sets. This could include the annual-interval surveys used in chapter 7.

6.7.3 Computation of morphological parameters

Following computation of a water surface, a series of morphological and process parameters were computed for cross-sections within each hydrographic survey. This enabled a more comprehensive analysis of geomorphological behaviour in the 1949-89 period.

To maintain data quality, parameters were only computed for cross-sections whose outer left and outer right bank elevations exceeded the elevation of the computed water surface. Because a low discharge of 10 000 m^3s^{-1} was selected to perform 1-D step-backwater modelling, less than 15 percent of the total number of cross-sections were removed from either the 1949-51 or the 1988-89 hydrographic survey at this stage in the analysis. The range of parameters computed for remaining cross-sections within each hydrographic survey is listed in Table 6.6. Standard morphological parameters were used to measure variation in channel size and channel shape. Hydraulic changes were estimated based on trends within mean cross-sectional velocity.

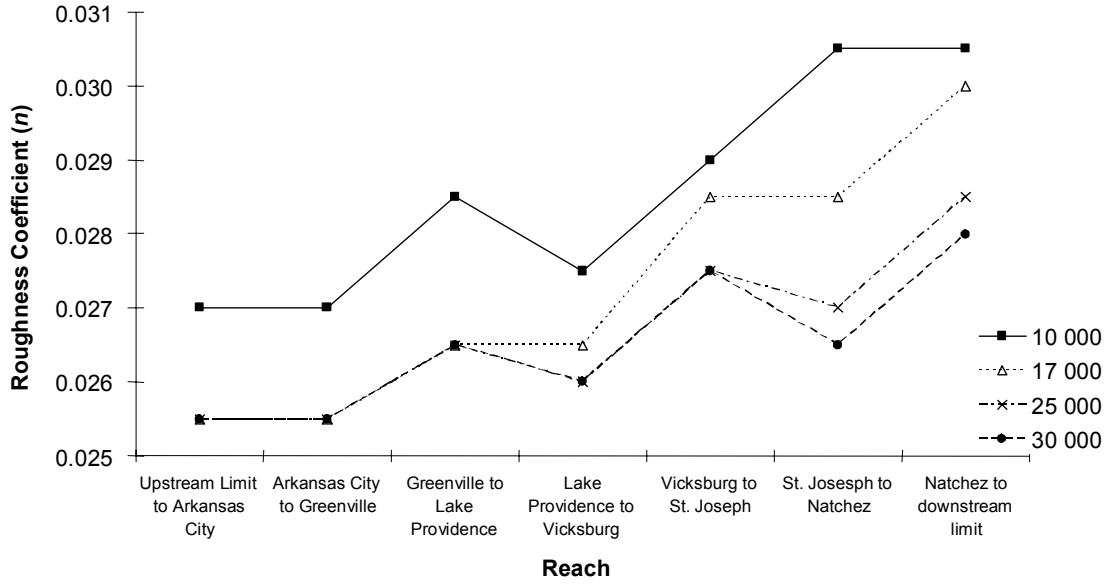

Figure 6.16 The roughness coefficient (n) entered into the 1-D step-backwater model in order to calibrate the computed water surface with average flow stages at each gauging station. The roughness coefficient is varied between gauging stations and according to the specified discharge. Based on the 1988-89 hydrographic survey and flow data sets.

Channel Morphology		**Channel Process**
Channel size	**Channel shape**	
Width (w)	Width : depth ratio (w/d)	Mean Velocity (Q/A)
Average Depth (d)	Asymmetry (a)	
Maximum Depth (d_{max})		
Area (w x d)		
Wetted Perimeter (P)		
Hydraulic Radius (A / P)		

Table 6.6 Standard morphological and process parameters.

a)

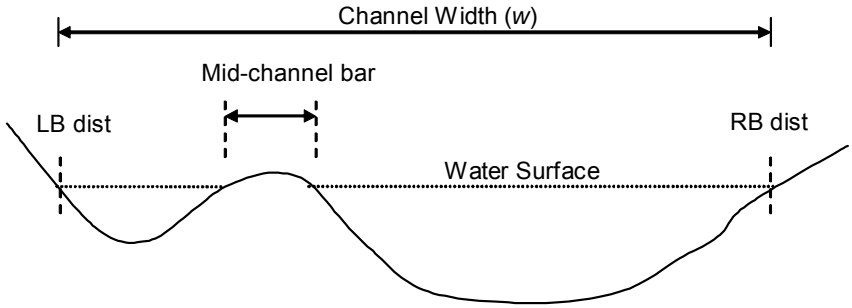

$$w = LB\ dist - RB\ dist \qquad (6.5)$$

Where:

LBdist = distance from start of cross-section to left bank
RBdist = distance from start of cross-section to right bank

b)

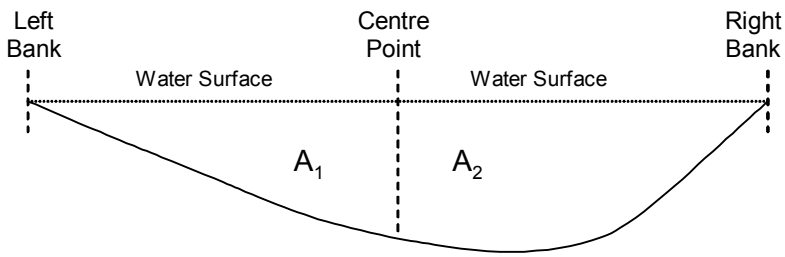

$$a = (A_2 - A_1) / A \qquad (6.6)$$

Where:

a = asymmetry ratio

A_2 = area of left half of the channel

A_1 = area of the right half of the channel

A = total area

Figure 6.17 Determination of: a) channel width (w) and; b) the asymmetry ratio (a) parameters.

a)

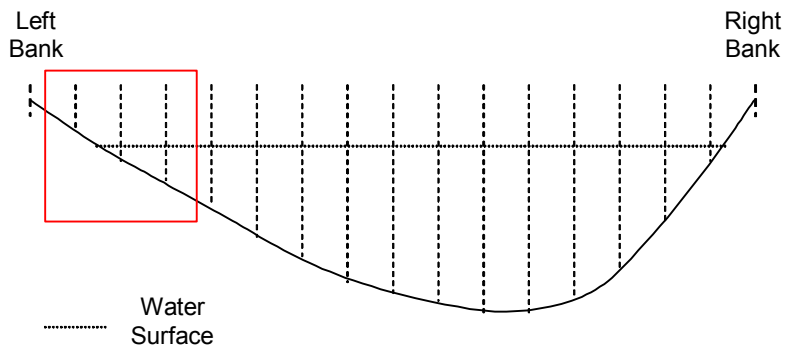

b)

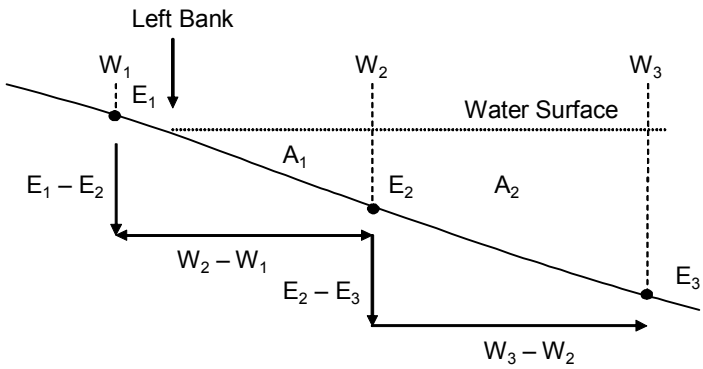

$$A_1 = [(E_2 \text{ x } W_2\text{-}LBdist) / 2] \quad (6.7)$$

$$A_2 = [(WSE\text{-}E_2) \text{ x } (W_3\text{-}W_2)] + [(E_2\text{-}E_3) \text{ x } (W_3\text{-}W_2) / 2] \quad (6.8)$$

Where:

W = distance from start of cross-section

E = elevation above datum

A = area of segment

WSE = water surface elevation

Figure 6.18 Determination of channel area based on verticals of equal channel width. The area highlighted in a) is enlarged in b) to show the computational procedure for each vertical.

The analysis presented in section 6.7.5 involves all the parameters listed above with the exception of wetted perimeter and hydraulic radius. This is because large alluvial river such as the Lower Mississippi River are characterised by high width: depth ratios and, as consequence, they are sensitive to variations in single parameters: the wetted perimeter (*P*) is strongly related to variations in channel width and the hydraulic radius is strongly related to variations in average depth (*d*). The computational procedure used to determine channel width, the asymmetry ratio and channel area are described in Figures 6.17 and 6.18.

6.7.4 Comparability of computed bankfull width to measured bankfull width

1-D step-backwater modelling performed at a discharge regarded to approximate bankfull discharge can be used to compute an estimate of the average bankfull width of the Lower Mississippi River in reaches 4 and 5. In this section, computed average bankfull width is compared to widths measured from aerial photographic surveys of the river in March 1999. This provides an indication of the degree of downstream variation masked by the use of an average bankfull width value and hence, an indication of the validity of exploring parameter relationships such as meander wavelength, meander radius of curvature, or pool-to-pool spacing, scaled to a single channel width value. More generally, the use of a second data set to measure channel width provides a check on the general reliability of the computational procedure described in sections 6.7.1 and 6.7.3 for determining not only channel width, but also other standard morphological parameters.

i) Computation of average bankfull width

Computation of bankfull width is reliant upon there being sufficient cross-sections with left and right bank elevations above the computed water surface to gain a reliable estimation. Because the average left bank to right bank distance is greater in the 1988-89 hydrographic survey, analysis of bankfull width was performed using this survey in preference to the earlier 1949-51 survey (see Table 6.1). On the Lower Mississippi River, Biedenharn and Thorne (1994) have showed that there is no single discharge which represents bank-top elevations that can vary by up to three metres or more. Instead, following examination of flow stage-discharge relationships at key

gauging stations along the Lower Mississippi River, Biedenharn and Thorne (1994) suggest that bankfull discharge lies within the range 30 000 – 42 000 m^3s^{-1}. The lower limit of the range represents the dominant discharge which is widely equated with bankfull discharge in temperate rivers (Hey, 1975).

Table 6.7 displays the increase in computed average channel width as discharge is increased from 10 000 to 30 000 m^3s^{-1}. The number of cross-sections used in the computation declines considerably at discharges higher than 17 000 m^3s^{-1} (mean discharge in the period 1937-2001). Based on a conservative estimate of bankfull discharge of 30 000 m^3s^{-1}, the computed average bankfull channel width is 1.65 km to one decimal place This estimate is based upon 458 cross-sections, or 33 percent of the number of original cross-sections. At discharges higher than 30 000 m^3s^{-1}, the number of cross-sections declines dramatically and therefore, the reliability of the computed bankfull width becomes a greater issue.

ii) Determination of top-bank channel width from aerial photographs

An alternative measure of top-bank channel width was obtained from 12 digital aerial photographs of the Lower Mississippi River from the confluence of the Arkansas River to Old River distributary (reaches 4 and 5). These photographs, obtained from U.S. Army Corps of Engineer archives, show the river in November 1999 when the computed daily discharge was 6 000 m^3s^{-1}. At this low discharge, a high proportion of mid channel bars and alternate bars are exposed. Because these bars appear as near-white features on greyscale photography, this enabled clearer definition of the left and right bank lines.

To record downstream variations in top-bank channel width, a methodology was devised to measure top-bank width at regular intervals based on chords drawn perpendicular to the channel centreline. This required digitisation of the left and right top-bank lines in addition to the channel centreline. Determining top-bank lines from aerial photographs is necessarily subjective and therefore, to create a reliable width series, it was essential that a consistent definition was maintained throughout the digitisation process. Channel banks appear as darker features on greyscale aerial photographs because of their steeper gradient. Therefore the top-bank was

Discharge (m^3s^{-1})	Percent exceeded†	Mean Width (m)	Number of cross-sections*
10 000	75	1328	1236
17 000	50	1467	1157
25 000	24	1568	836
30 000	14	1646	458

†at the Vicksburg gauge 1937-2001 water years

*used to calculate mean width. Cross-sections removed from the computation if the both the left and right bank elevations do not exceed the computed water surface elevation

Table 6.7 Percent of time exceeded, mean channel width, and number of cross-sections where the measured elevation extends beyond the computed left and right banks in the 1988-89 hydrographic survey. A discharge of 30 000 m^3s^{-1} corresponds to the dominant discharge of the Lower Mississippi River and provides a conservative estimate of bankfull discharge (Biedenharn and Thorne, 1994).

consistently defined as the outer limit of the darker channel bank, beyond the interface of exposed channel bed sediment and the lower bank line. Digitisation was undertaken using ESRI Arc View version 3.3 GIS software. An example of the digitised bank lines for the sub-reach just upstream from Vicksburg (reach 4) is presented in Figure 6.19a. The scale of each digital aerial photograph was determined by comparing the on-screen straight-line distance between two features on the ground surface with the straight-line distance between the same features on the 1988-89 hydrographic survey which is mapped to a known scale. This was performed five times for each digital image. Because there is a ten-year interval between the two sources, it was important to measure distance along static features such as roads and levee tops. A scaling factor to apply to the measured distances was obtained from linear regression of all distances obtained from the hydrographic survey with those obtained from the 1999 aerial photographs.

Following creation of the left and right bank lines, a channel centreline was digitised. A customised routine was then developed to first, interpolate sample points at regular intervals down the channel centreline and second, measure the distance between the intersections of the left and right bank lines from the chord positioned perpendicular to the channel centre line. A 2 km sampling interval was chosen to be consistent with the interval used in the study of planform dynamics (chapter 4). Measured top-bank channel widths were then converted to kilometre units based on the scaling factor.

Although the methods used to both identify bank lines and rectify scale are relatively crude, they were deemed appropriate to assess the relative variability of channel width and comment upon the reliability of the computed average channel width. The measured top-bank width series is presented in Figure 6.20. The average top-bank channel width in both reaches 4 and 5 are lower than the computed average top-bank channel width of 1.65 km. Indeed, an independent-samples t-test applied to the two distributions shows that the average computed and average measured channel widths are significantly different. Using the 1975 hydrographic survey, Winkley (1977) estimates the average top-bank width of the Lower Mississippi River to be 2.02 km from the confluence of the Arkansas River to the confluence of the Yazoo River at Vicksburg (reach 4) and 1.77 km from the confluence of the Yazoo River to the Old

a)

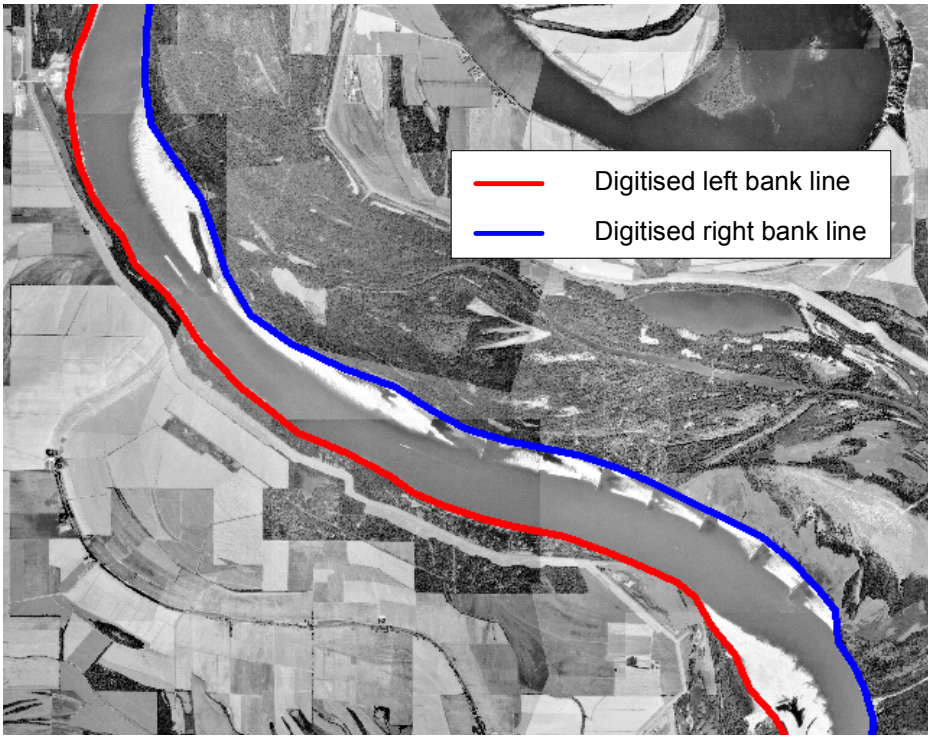

b)

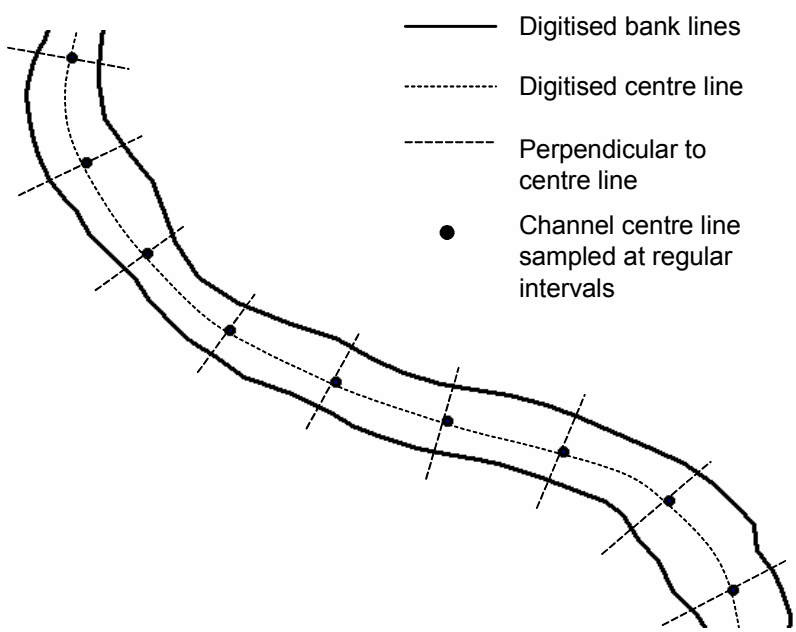

Figure 6.19 Obtaining a channel width series. In a) the top-banks are digitised from aerial photographs of the river in 1999 and in b) a centre-line is digitised based on these bank lines. Width is measurements at points interpolated at regular 2 km intervals along the centre line. At each point, width is the distance between the bank lines that is perpendicular to the channel centre line.

River distributary (reach 5). These estimates are closer to the computed average channel width. This indicates therefore that the estimation obtained from aerial photographs may have systematically underestimated the true top-bank width.

Despite the differences in means, the variance of the computed and measured channel width distributions are not significantly different (Figure 6.21). Variation within the computed channel width series therefore provides a good representation of true variation of channel width despite being based on only 33 percent of the original cross-sections. When considered alongside the apparent reliability of the computed mean bankfull channel width, this finding suggests that computed estimates of channel width are realistic. This has general significance because it implies that the computational procedure adopted does provide a reliable method of generating morphological parameters.

Figure 6.20 shows that channel width is highly variable at the sub-reach scale. This may be correlated with the pool-crossing sequence, as noted more generally in alluvial rivers by Richards (1976a). At the larger reach-scale, mean channel width values presented by Winkley (1977), together with the series presented in Figure 6.20, are both suggestive of a declining trend downstream. This implies that it may be inappropriate to scale morphological parameters, such as radius of curvature, meander wavelength and pool-to-pool spacing, to measures of channel width averaged over long reaches of river. This issue is confounded further because the distributions of channel width in Figure 6.21 are positively skewed. Therefore average bankfull channel width used as a scaling parameter does not necessarily have any physical significance.

6.7.5 Analysis of morphological and hydraulic relations in the 1949-89 time period

Results presented so far in this chapter have emphasised that the Lower Mississippi River is dynamic in terms of adjustments to its long profile at both the sub-reach and larger reach-scales. Both of these scales are therefore considered in the analysis of morphological and hydraulic relations. At the sub-reach scale, the parameters described in section 6.7.3 are presented as averages for each pool and crossing, as

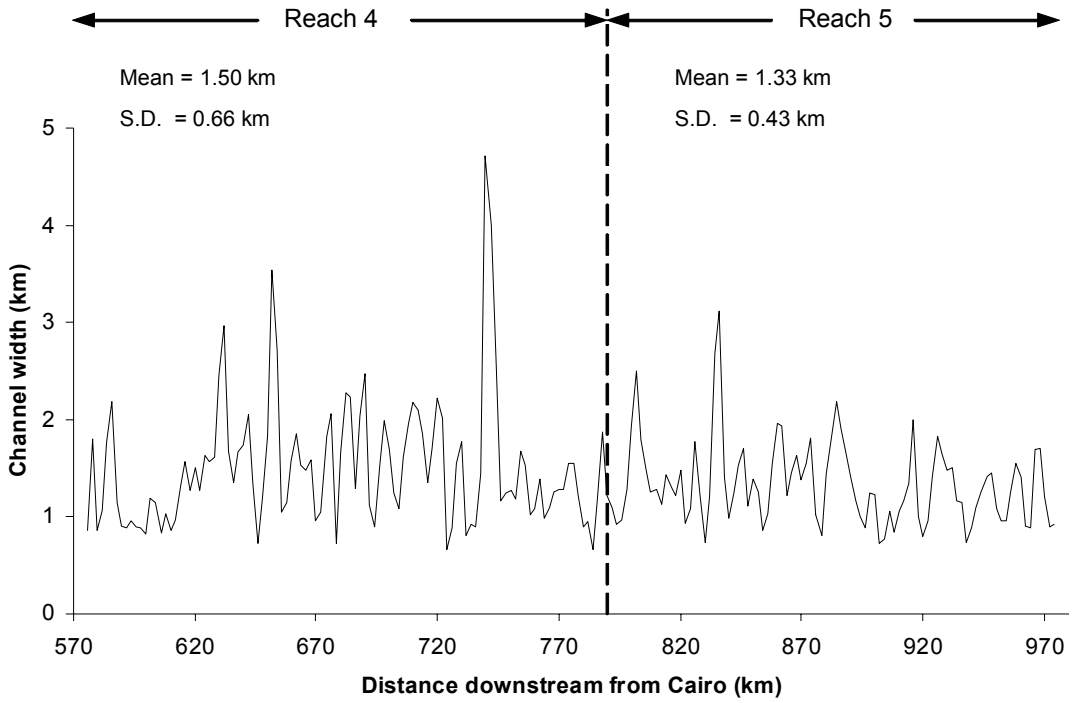

Figure 6.20 Variation in channel width with distance downstream.

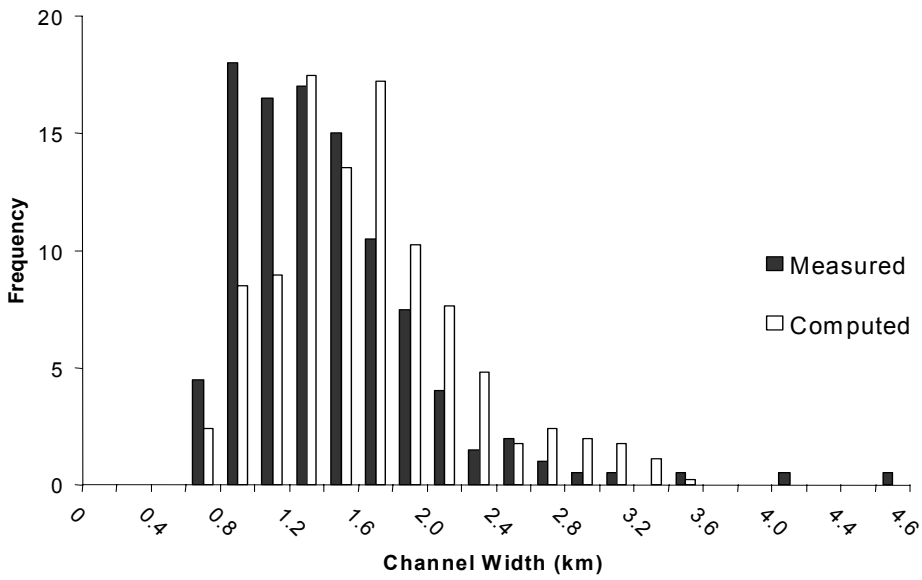

Figure 6.21 Histogram of channel widths: i) measured from aerial photographs and; ii) computed using the 1-D step-backwater model. An independent samples t-test demonstrates that the measured and computed means are significantly different (t statistic = -4.728, degrees of freedom = 656 and corresponding p-value = 0.000 to 3.d.p). However, equal variances must be assumed (F = 0.484 and corresponding p-value = 0.487 to 3.d.p).

defined by the cumulative elevation technique. To assess the importance of variations in curvature on pool and crossing characteristics, each pool and crossing is classified as 'straight' or 'curved' based on exceedance of an arbitrary planform direction change angle of 0.78 radians (45 degrees) between the pool or crossing entrance and exit. In order to examine differences in larger reach-scale behaviour, cross-sectional based analysis of pools and crossing behaviour in reach 4 is isolated from that in the downstream reach 5.

In Figures 6.22 and 6.23, average depth of each pool or crossing is plotted against width for both the 1949-51 survey and the 1988-89 survey in reaches 4 and 5 respectively. Corresponding width-depth ratios are labelled on each plot because as width-depth ratio increases, the hydraulic radius decreases and therefore, it provides a strong indicator of the form resistance exerted by the cross-section configuration. Plots of average depth against width are also diagnostic of changes in cross-sectional-area. On each plot, solid lines representing constant cross-sectional area are used to specify the upper and lower bound areas of pool and crossing sub-reaches.

Figures 6.22 and 6.23 reveal two important temporal changes. First, there is a clearer difference in the width-depth ratio of pools and crossings in the 1949-51 survey than the 1988-89 survey in both reaches 4 and 5. In the earlier survey, a width-depth ratio of around 100 divides pools with usually a smaller ratio, from crossing reaches with usually a larger ratio. This clear division is expected because crossings are known to be both wider and shallower morphological features (and hence, offer a greater form resistance) than pools (Richards, 1976a). By 1988-89 however, the division is much more blurred, reflecting a temporal 'equalisation' of form characteristics at the sub-reach scale. The results from independent t-tests of mean width and mean average depth parameters demonstrate that these changes are statistically significant (Table 6.8). In 1949-51, pools and crossings are significantly different at the 95 percent confidence level with respect to both parameters but by 1988-89, there is no significant difference between pools and crossing with respect to either parameter.

Interestingly, close examination of both plots reveals that the equalisation of form is not the combined result of an increase in the width-depth ratio of pools, and decrease

in width-depth ratio of the crossings, but rather almost entirely a result of an increase in the width-depth ratio of pools. Less than half the total number of pools in 1988-89 have a width-depth ratio less than 100, and some have developed width-depth ratios in excess of 200. The nature of this change is important because the increasing width-depth ratio of pools, whilst stability of crossings, is indicative of an increase in the component of form resistance exerted by the cross-sectional configuration. Examination of inter-reach differences reveals that the average width-depth ratio of pools increased by 70-80 percent in both reaches. This consistent rate of increase however masks a real difference in width-depth ratios: the average width-depth ratio of pools and crossings is between 30 and 50 percent higher in both the 1949-51 and 1988-89 surveys in reach 4 in comparison to reach 5. When viewed alongside the long profile changes in Figure 6.10, this finding is particularly significant because it suggests that the greater form resistance offered by the longer wavelength and higher amplitude pool-crossing undulations in the long profile in reach 5, in relation to reach 4, may be balanced by the lower form resistance offered by the cross-sectional configuration in this reach.

Comparison between the longitudinal and cross-section configurations is also interesting because it reveals differences in the nature of sub-reach scale dynamics. The apparent dynamism of pools in terms of variation in width-depth ratio is intriguing because it contrasts with results presented in section 6.6 showing that longitudinally, it is generally the crossing reaches which have displayed the greatest dynamism over the same period of time. Taken together, this therefore indicates that despite movement in the planform being effectively prohibited by bank stabilisation, the engineered channel is still capable of adjusting its morphology to balance flow resistance requirements through mutual adjustments to several degrees of freedom. In relation to previous research, the dynamics of pools in the cross-sectional domain suggests that Biedenharn and Thorne's (1994) assertion, that the mid-channel bars (crossings) are the dynamic morphological feature of the post-cutoff Lower Mississippi River is slightly misleading. This emphasises the danger of relying on investigation of changes in a single dimension (longitudinal) to represent behaviour that is fully three dimensional in form.

a) Reach 4: 1949-51

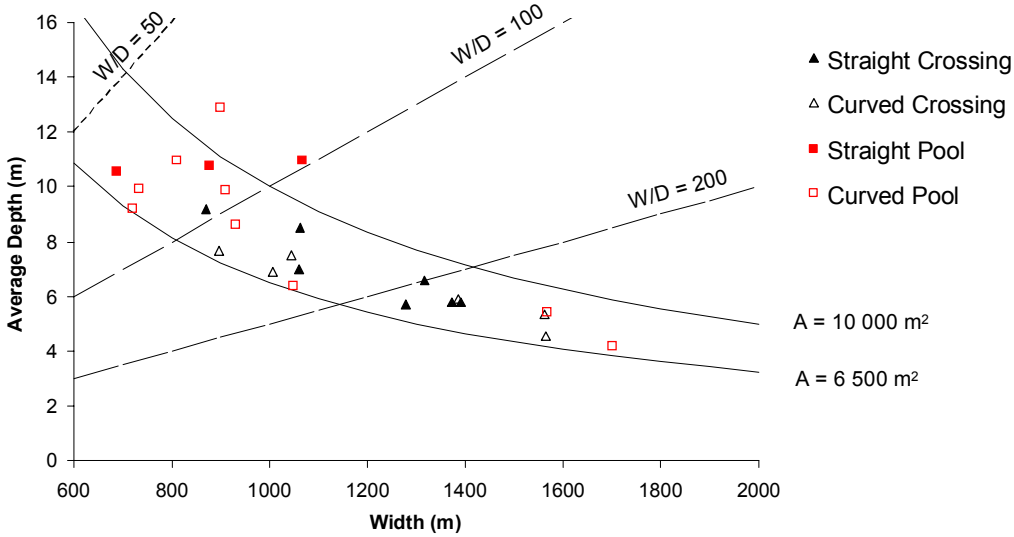

a) Reach 4: 1988-89

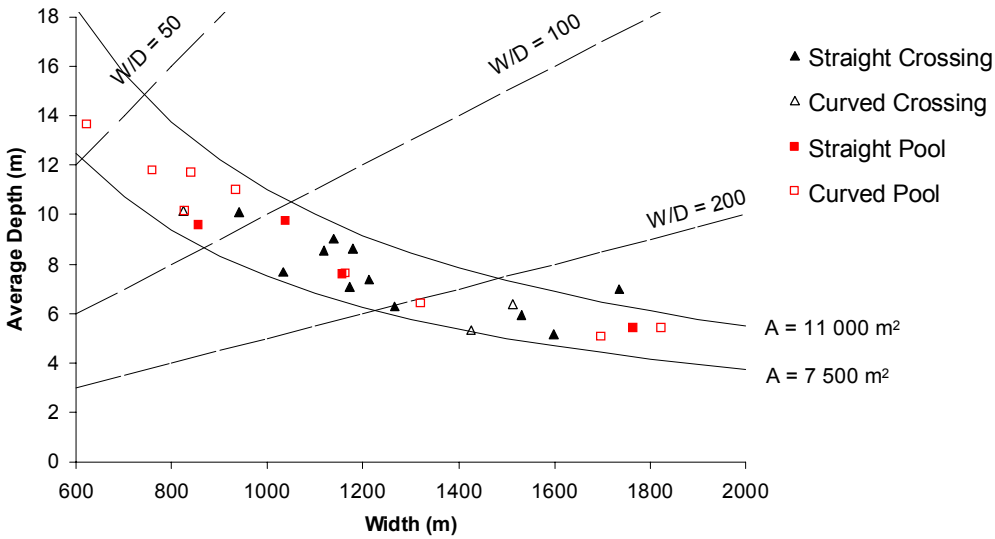

Figure 6.22 Average depth against width for pools and crossings in reach 4. Solid lines represent the upper and lower bound area between which the points are distributed. Dashed lines represent constant width-depth ratios (W/D).

a) Reach 5: 1949-51

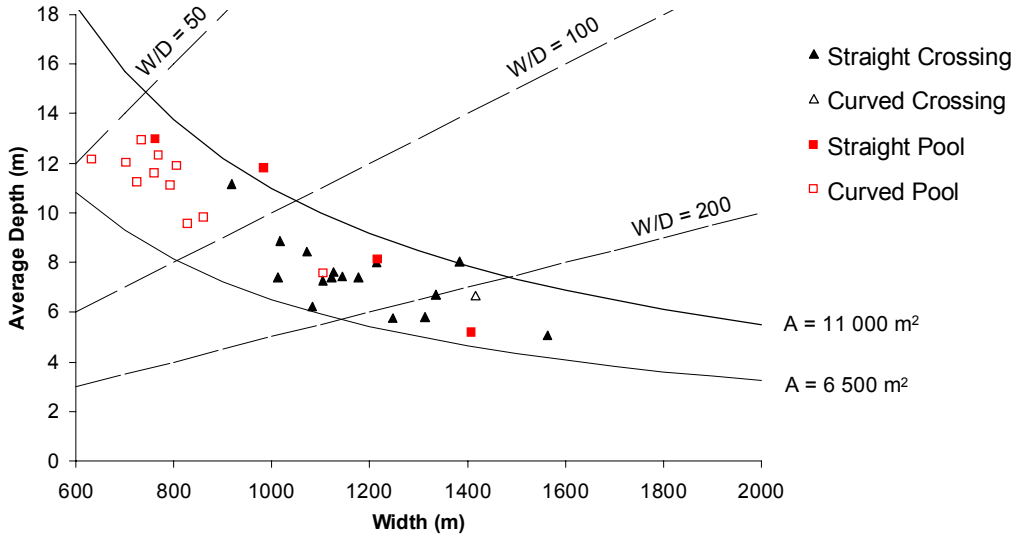

b) Reach 5: 1988-89

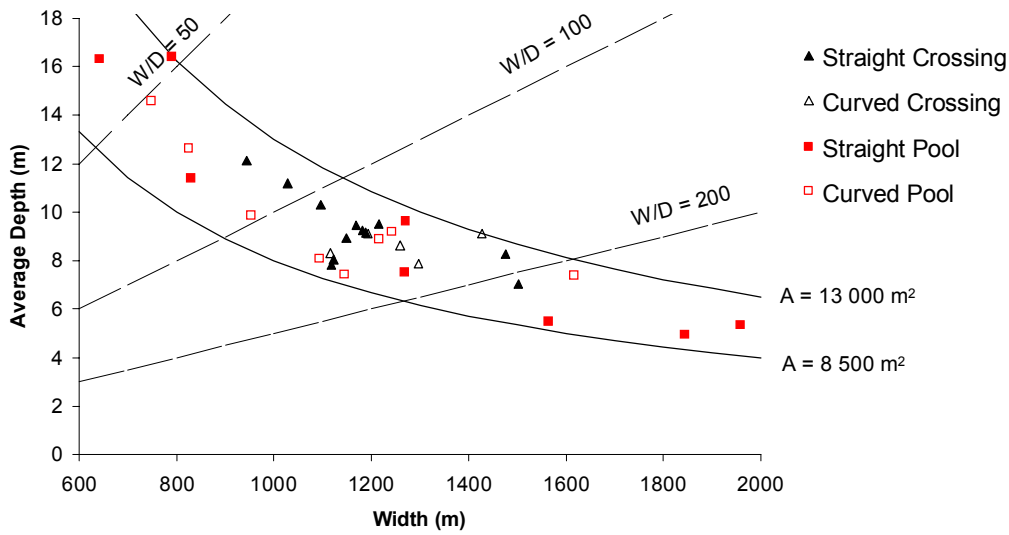

Figure 6.23 Average depth against width for pools and crossings in reach 5. Solid lines represent the upper and lower bound area between which the points are distributed. Dashed lines represent constant width-depth ratios (W/D).

Parameter	1949-51						1988-89					
	Pools	**Crossings**	**t**	**DF**	***p***	**Sig. at 95% level?**	**Pools**	**Crossings**	**t**	**DF**	***p***	**Sig. at 95% level?**
Reach 4												
Width	971	1347	-2.36	23	0.03	Yes	1444	1451	-0.26	33	0.98	No
Average Depth	9.44	6.28	3.34	23	0.00	Yes	8.23	7.02	1.35	23.56	0.19	No
Maximum Depth	20.64	12.51	7.03	23	0.00	Yes	21.97	14.00	9.02	33	0.00	Yes
Asymmetry Ratio	0.50	0.38	2.09	23	0.05	Yes	0.53	0.33	4.01	33	0.00	Yes
Velocity	1.30	1.41	-1.46	23	0.16	No	1.19	1.15	0.96	33	0.35	No
Reach 5												
Width	847	1192	-4.61	28	0.00	Yes	1255	1237	0.13	18.29	0.90	No
Average Depth	11.31	7.37	4.04	28	0.00	Yes	9.40	8.89	0.46	17.68	0.65	No
Maximum Depth	23.26	14.68	7.14	28	0.00	Yes	24.03	15.55	6.02	29	0.00	Yes
Asymmetry Ratio	0.48	0.38	1.91	28	0.07	No	0.52	0.24	5.66	29	0.00	Yes
Velocity	1.18	1.26	-1.11	28	0.23	No	1.06	1.00	2.24	29	0.03	No

Table 6.8 Comparison of morphological and hydraulic characteristics of pools and crossings in reaches 4 and 5 based on independent samples t-tests. Where appropriate, values are given to two decimal places.

The second temporal change regards variation in channel area. At the sub-reach scale, despite their different form characteristics in the earlier 1949-51 hydrographic survey, there is no evidence that there is any systematic difference between the area of pools and the area of crossings. However, at the larger reach-scale, movement of the upper and lower limits to the distribution in both reaches 4 and 5 provides some evidence that channel area increased between the two surveys. The increase is more apparent in reach 5 where in 1949-51, all pools and crossings, with the exception of one pool, have an average area in the range 6 500-11 000 m^2. By the time of the hydrographic survey in 1988-89, the lower and upper limits of this range had increased to 8 500 – 13 000 m^2. A temporal increase in the cross-sectional area required to transport a constant flow of 10 000 m^3s^{-1} is important because it indicates that the computed average velocity has decreased between the two surveys. This is evident in both reaches in Table 6.8. It is interesting to note however, that the average velocity in crossings declined by almost double the rate of decline in pools. Given adjustments to crossing reaches have been shown to be greater in the longitudinal than the cross-section dimension, this may suggest that the changes observed in the sub-reach scale long profile are more important in terms of their contribution to total form resistance than adjustments to the cross-sectional configuration.

Spatial and temporal changes in the cross-sectional form are examined further by plotting average depth against the asymmetry ratio in Figures 6.24 and 6.25. The asymmetry ratio provides a measure of the distribution of flow cross-section area within the channel (see Figure 6.17b). Comparing between the 1949-51 survey and the 1988-89 survey in both reaches clearly reveals that the cross-section morphology has become more ordered with respect to asymmetry, with pools developing more asymmetric cross-sections, and crossings developing more symmetrical cross-sections. This change is demonstrated statistically in Table 6.8: there is no significant difference at the 95 percent confidence level between the asymmetry ratio of pools and crossings in both reaches in the earlier 1949-51 survey, but a significant difference is obtained in the later 1988-89 survey. These changes are consistent with the idea that the river has attempted to achieve the maximum curvature possible, and hence, maximum form resistance exerted by the planform, within the confines of the stabilised bank lines.

a) Reach 4: 1949-51

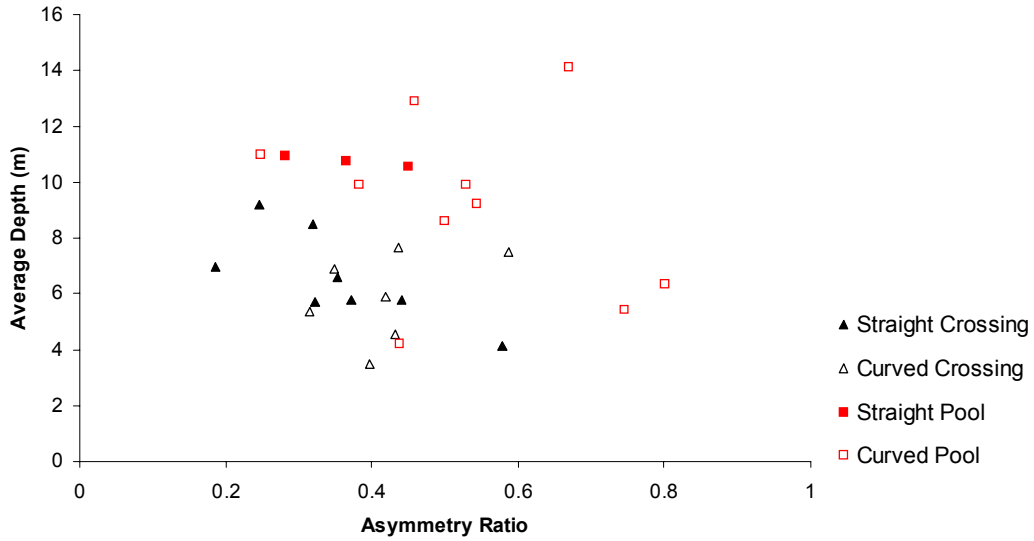

b) Reach 4: 1988-89

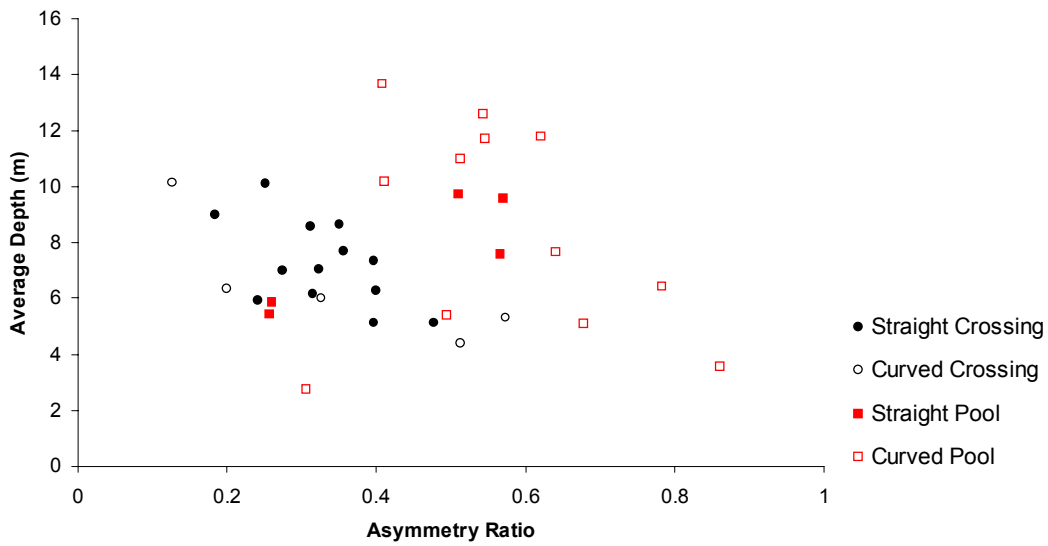

Figure 6.24 Average depth against asymmetry ratio for pools and crossings in reach 4.

c) Reach 5: 1949-51

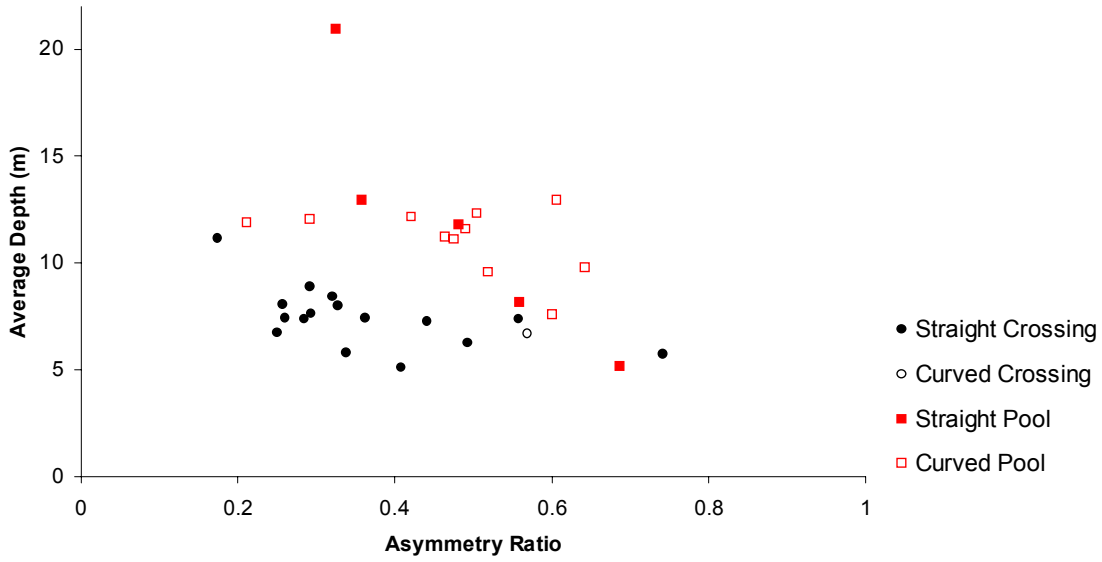

b) Reach 5: 1988-89

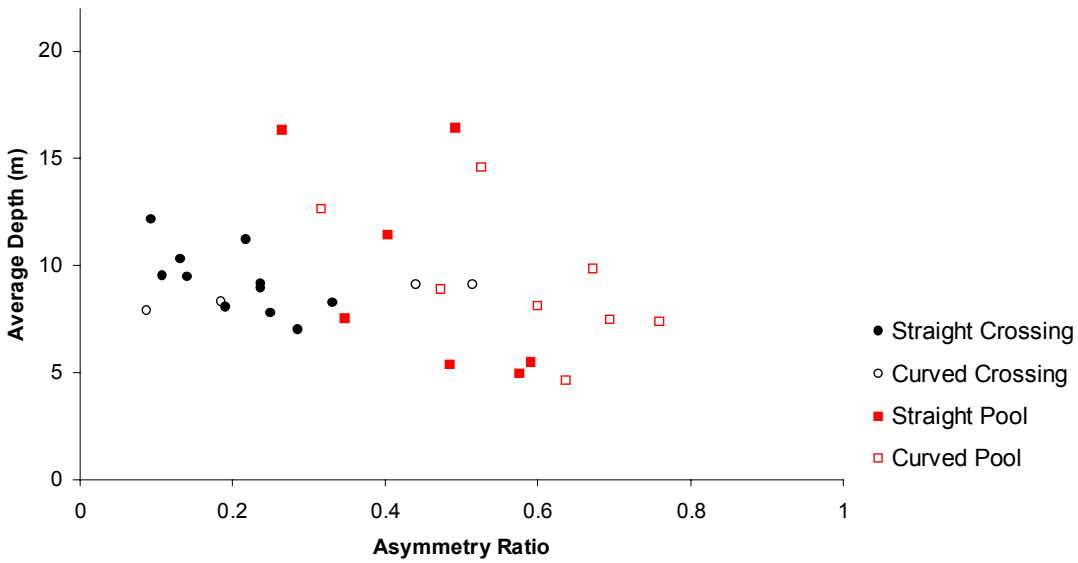

Figure 6.25 Average depth against asymmetry ratio for pools and crossings in reach 5.

6.8 Discussion

The following discussion focuses on three issues drawn from the results and analysis within this chapter: the complex nature of geomorphological response; the importance of undertaking a number of parallel investigations in being able to detect the identified response; and finally, the adequacy of existing conceptual models in explaining the identified response.

First, the Lower Mississippi River has responded to engineering and management imposed during the twentieth century by a complex suite of morphological adjustments at different scales and through multiple degrees of freedom. Since planform adjustments have been effectively prevented by bank stabilisation, the river has been forced to adjust its longitudinal and cross-section characteristics at the reach and sub-reach scales to balance total energy expenditure (flow resistance and sediment transport) against available stream power per unit width.

From a reach-scale longitudinal perspective, analysis of vertical changes in the thalweg profile reveal a spatial and temporal pattern of morphological response. Following the artificial steepening of channel slope and the removal of form resistance exerted by the most sinuous bends, the channel bed degraded along the entire reach from the confluence of the Arkansas River to Old River distributary. Rates of degradation were highest from the confluence of the Arkansas River to the confluence of the Yazoo River at Vicksburg. Through time, the rate of degradation has declined throughout the reach to the extent that in the downstream reach (reach 5), a slight aggrading trend is observed between 1975 and 1989.

At the sub-reach scale, longitudinal changes demonstrate that the pool-crossing configuration has adjusted to larger reach-scale changes in profile slope. In reach 4, the development of more frequent pools and crossing oscillations in the 1949-64 period (particularly in the straightened reaches where the artificial cutoffs had been constructed) is diagnostic of a river attempting to dampen the degradational trend identified in this reach at this time by expending energy in ways other than performing sediment transport. Meanwhile, in reach 5, the relative temporal stability of pool and crossing characteristics over the 1949-1989 time period is consistent with

the much smaller changes in reach-scale bed slope. Despite the pool-crossing configuration in reach 4 being more dynamic (particularly during the 1949-64 period), downstream trends in the roughness coefficient indicate that total flow resistance is actually higher downstream in reach 5. This suggests that the higher amplitude and longer wavelength characteristics of pools and crossings in reach 5 is more important in terms of total form resistance than the difference in cross-sectional configuration between the two reaches: the average width-depth ratio is consistently higher in reach 4 than in reach 5.

Two scales of geomorphological response can therefore be identified. The river is adjusting both at the reach-scale, as imagined by Biedenharn and Watson (1997) and at the sub-reach scale, as imagined by Carey and Keller (1957) in order to satisfy regional-scale flow resistance requirements. Together, these changes are indicative of a 'top-down' scale linkage with smaller spatial scales responding to changes at larger spatial scales. In chapters 4 and 5, it is shown that the contemporary regional-scale planform and long profile is a product more of the geological and tectonic history of the reach than the contemporary process regime. However, at the shorter, 40-year, timescale examined in this chapter, it is evident that morphological dynamics at the sub-reach scale are not so conditioned by reach history, but rather by behaviour in upstream and downstream reaches and at larger spatial scales.

The second major finding is that a thorough understanding of the complexity of geomorphological response can only be gained by undertaking a number of parallel investigations (Thorne, 2002). This is apparent when considering the results presented in this chapter in relation to past research. The qualitative tripartite model of morphological response, advocated by Biedenharn and Watson (1997), is misleading because changes in the water surface elevation reflect changes in flow resistance as well as vertical changes in the channel bed. Furthermore, changes identified during the 1950-1994 time period from specific gauge records mask considerable variation in the rates of vertical changes over that time period. A second example concerns Biedenharn and Thorne's (1994) assertion that mid-channel bars (crossing sub-reaches) represent the dominant morphological expression of the post modification Lower Mississippi River. Whilst results presented in this chapter support this assertion longitudinally, cross-sectional

analysis has revealed that the pools have actually been more dynamic than the crossings with respect to changes in the width-depth ratio. This shows that the temporal dynamics observed at a single scale may differ considerably depending upon the domain or dimension in which they are viewed (Renwick, 1992). Thus, relying on one technique to inform geomorphological response can be misleading and even, dangerous if it is used as a basis to develop future channel management strategies, or to approach geomorphological 'explanation.'

The final issue concerns the manner in which the longitudinal and cross-section changes discussed in this chapter can be used to provide a critique of the two conceptual models of the fluvial system presented in chapter 1. Richards's (1982) flow chart of interconnected morphological and process parameters (Figure 1.1) provides an indication of how parameters are related, and hence, why particular adjustments occur. For example, in the context of morphological changes presented in this chapter, it shows that changes in the bedform configuration, friction factor and ultimately velocity field are interrelated with changes in stream power per unit width. A criticism however, is that it is difficult to relate Figure 1.1 directly to considerations of geomorphological response because it does not explicitly consider either spatial or temporal scales of morphological adjustment. The concept of situating changes within a spatial and temporal framework is explicit in Knighton's (1998) hierarchy of morphological adjustments (Figure 1.2) but no indication there is provided of the interrelationships between variables, and hence, explanation of why adjustments occur. Hence, because the models display different characteristics of the fluvial system, an improved model might incorporate *both* scale and interrelationships. This idea is returned to in the conclusion of this study.

Although fluvial morphology may be at least partially conditioned from the top-down, it represents the cumulative product of interrelationships between the existing morphology and the prevailing process (flow and sediment) regime at small spatial and temporal scales. Therefore, being able to adequately *explain* longer-term and larger-scale morphological changes relies upon understanding the interrelationships between form and process at all scales. In Chapter 7, morphological changes are examined using a range of annual and sub-annual interval morphological and process

data sets at the sub-reach scale. This completes analysis of the morphological hierarchy of data sets identified in the research design in Figure 2.2.

CHAPTER 7. SUB-REACH SCALE DYNAMICS

7.1 Chapter synopsis

In this chapter, annual-interval hydrographic surveys at the reach-scale are coupled with a series of high resolution data sets at the sub-reach scale to explore whether changes in the morphological configuration can be identified that are consistent with the longer-term and larger-scale changes identified in chapter 6. Examination of annual hydrographic surveys reveals that although extreme high or low discharge events are associated with the greatest morphological changes, the magnitude, order and location of changes over relatively long reaches of the Lower Mississippi River are very difficult to predict. Improving explanation of larger-scale and longer-term behaviour therefore requires an understanding of how bed material is transported through pools and crossings and how this is related to temporal variations in flow stage.

Detailed observations of morphological changes in a single sub-reach suggest that bed material is transported through a pool-crossing unit as a wave of sediment which moves according to variations in flow stage. Bedform waves are shown to be the largest bedform of a complex configuration including smaller-scale dunes and micro-dunes. Recognition of morphological diversity at the sub-reach scale poses problems for the reliable estimation of rates of bedload movement because bed material is transported in different ways in different parts of the channel. Analysis of velocity field dynamics suggests that process-form relations governing the movement of sediment waves are more complex than simple hypotheses based on the reversal of section-averaged velocity suggest. Indeed, morphological changes are more closely related to changes in the distribution of near-bed velocities between pools and crossings with variations in flow stage.

7.2 Pool-crossing dynamics at annual timescales

Annual dynamics were studied using hydrographic surveys of an 88 km reach of the Lower Mississippi River upstream and downstream from the confluence of the Arkansas River (Figure 7.1a). The surveys used were undertaken between December 1991 and February 2001 at low water season (November to February). Surveys were not available for the 1993-1994 or the 1997-1998 low water seasons so seven hydrographic surveys in total were available for analysis. The cross-sectional spacing and sample spacing within each cross-section are consistent with the decadal-interval hydrographic surveys analysed in chapter 6. The series of pre-processing routines applied to the datasets are those described in section 3.3.1.

7.2.1 Method of standardising channel distance

To allow direct comparability between annual hydrographic surveys, a procedure was developed to reference each cross-section to a standardised channel distance. This was similar to the procedure developed in section 6.4 using the decadal hydrographic surveys. A channel centreline was first digitised for the entire reach. Each cross-section within each survey was then given a unique distance by computing the intersection of the line adjoining the left-bank and right bank points and the digitised centre line. To maintain consistency with previous analysis, this distance was then converted to a river kilometre distance downstream from Cairo. Based on this referencing system, the upstream limit of the reach is located at 534 km, and the downstream limit is located at 622 km downstream from Cairo. The confluence of the Arkansas and White Rivers is located at 590 km downstream from Cairo.

7.2.2 Thalweg elevation changes between December 1991 and February 2001

Net changes in the thalweg profile from December 1991 to February 2001 are presented in Figure 7.1b. The reach encompasses eight pool and crossing sub-reaches that have maintained their relative location over the nine year period. However, the plot of cumulative elevation change shows that ordered changes have

occurred, with a general degrading trend upstream from 575 km, and a general aggrading trend downstream. This masks a range of stabilities at the sub-reach scale: sub-reaches 1, 2 and 8 are particularly stable over the period; the crossing in sub-reach 3 has been scoured and moved slightly upstream; whilst the crossings in sub-reaches 5, 6 and 7 have all aggraded. Over the time period, there is no apparent trend in discharge although high discharge years such as water years 1993 and 1994 are interspersed with much lower discharge years in water years 1992 and 2000. This therefore raises the issue of why and how has the apparent change developed has developed and critically, whether the trend has any physical significance.

7.2.3 Thalweg elevation changes at 1-2 year intervals

In Figure 7.2, the net cumulative elevation change plotted in Figure 7.1 is disaggregated at approximately 1-2 year intervals. At this shorter timescale, considerable variation in behaviour is revealed. Marked degradation and aggradation generally correspond with periods of relatively high and low discharge respectively. For example, the highest rate of degradation experienced over the entire period, between November 1992 and November 1994, corresponds to a period when the long-term (1937-2001) mean discharge of 17 000 m^3s^{-1} was exceeded for 70 percent of the time, and the dominant discharge of 30 000 m^3s^{-1} was exceeded for 30 percent of the time. Meanwhile, the highest rate of aggradation over the period, from February 2000 to February 2001, corresponds with a low discharge year in which a discharge of 30 000 m^3s^{-1} was never exceeded.

Rates of degradation and aggradation cannot be explained solely in terms of discharge however. For example, the period from November 1996 to December 1998 exhibited a higher discharge in relation to most other periods but there is no clear trend in terms of cumulative elevation change. Also, despite very similar hydrographs in the 1991 and 2000 water years, rates of aggradation were considerably higher during the latter period. In addition to discharge, morphological changes in alluvial rivers are driven by rates of sediment supply. Thus, it is the relative timing of discharge and sediment supply processes that is critical in

a)

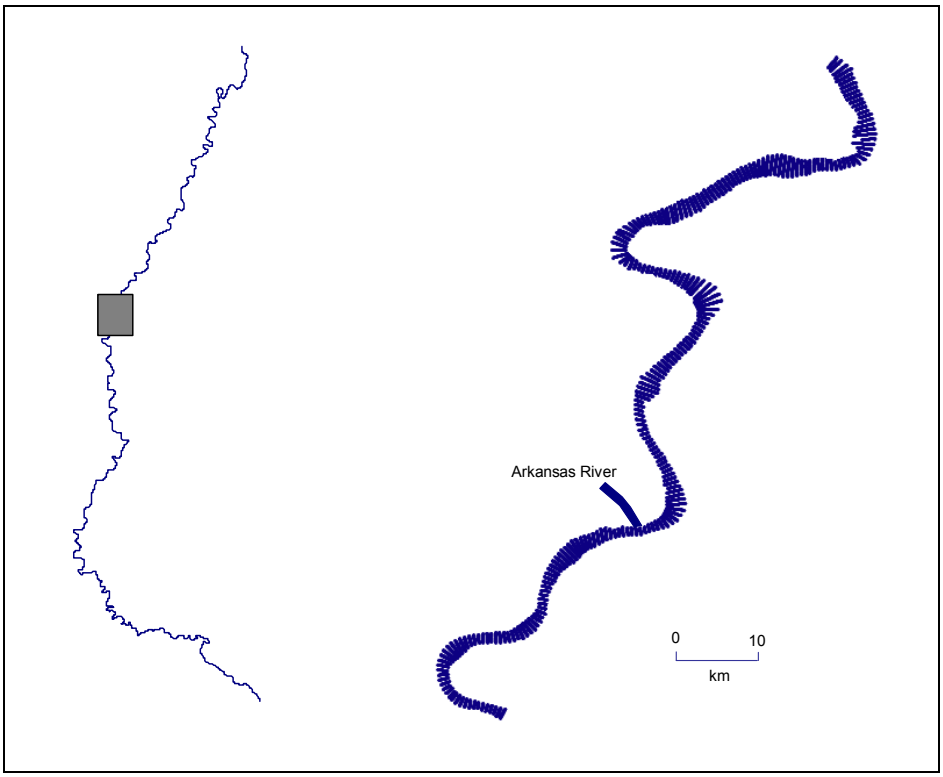

b)

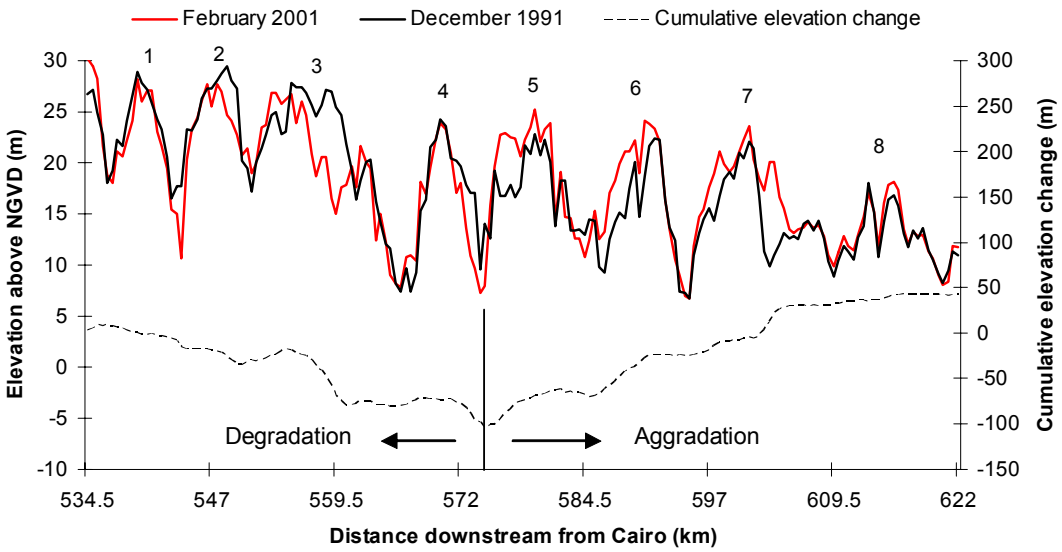

Figure 7.1 a) The location of the annual dynamics study reach of the Lower Mississippi River from 534 to 622 km downstream from Cairo and b) thalweg elevation against distance downstream in December 1991 and February 2001. Cumulative elevation change is plotted to emphasise the reach trend over the time period.

a)

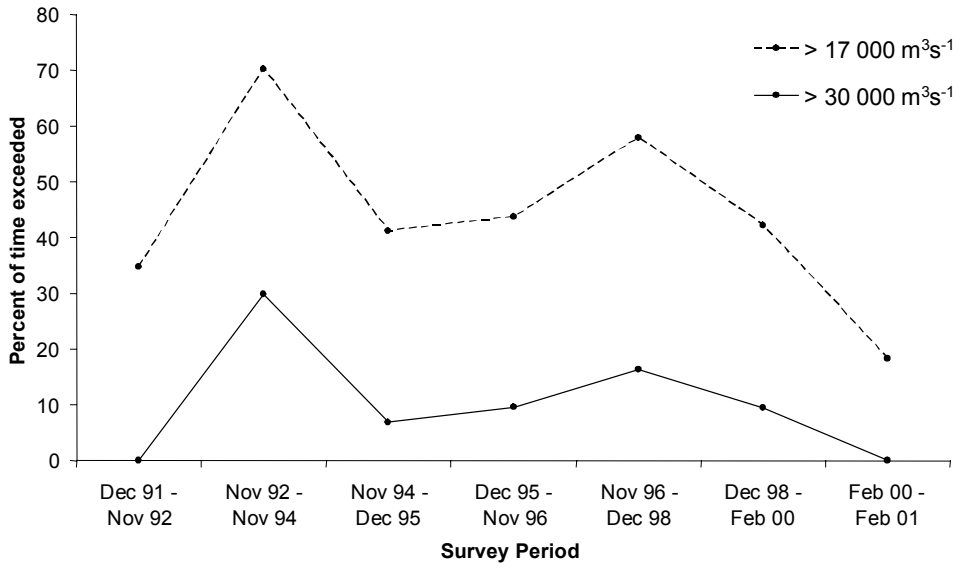

b)

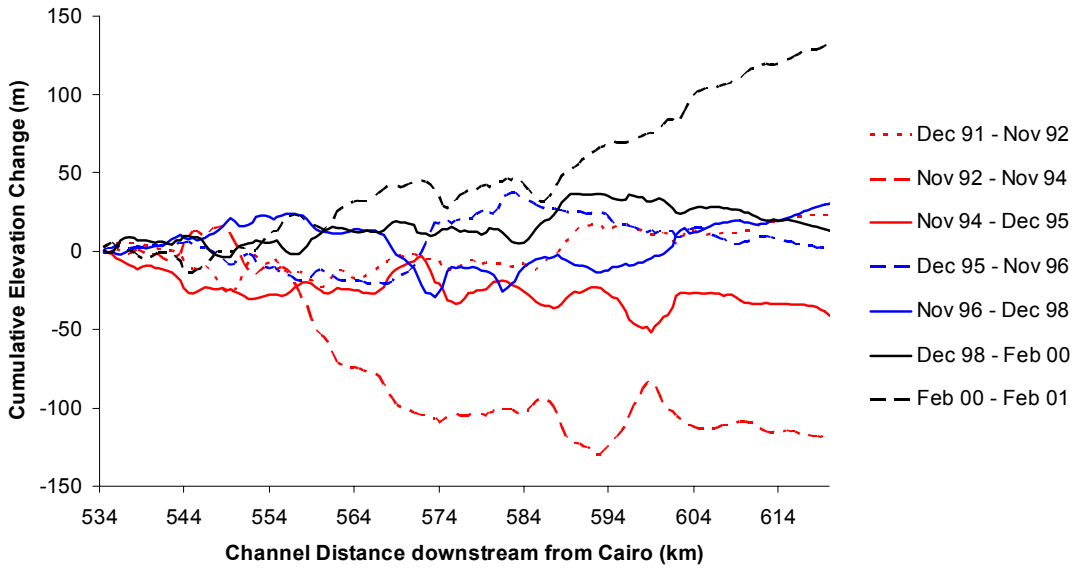

Figure 7.2 Changes in thalweg elevation in relation to variation in discharge for seven sub-periods between December 1991 and February 2001. In a) the percentage of days in each sub-period with a discharge exceeding 17 000 m^3s^{-1} (mean discharge in the period 1937-2001) and 30 000 m^3s^{-1} (dominant discharge) is presented. In b), cumulative thalweg elevation change from 534 km downstream from Cairo is plotted for each sub-period.

determining the nature of morphological change (Lane *et al.*, 1996). Focusing on sediment supply (particularly bed material supply) as well as discharge implies that morphological changes in any one sub-reach must be conditioned by both the behaviour of upstream sub-reaches and the previous behaviour of the sub-reach in time.

To examine these spatial and temporal feedbacks, thalweg profile changes were examined before, during and after the high discharge period from November 1992 to November 1994. Figure 7.3 compares elevation changes at the time of the relatively low discharge water year of 1992 with the following two higher discharge years. At this timescale, it is clearly possible to distinguish between two groups of dynamic sub-reaches (2-3 and 6-7) and the remaining relatively stable sub-reaches (1, 4-5 and 8). Within the dynamic reaches, there is some evidence of spatial and temporal feedbacks operating. Temporally for example, a tendency for reversal of behaviour is apparent, with filling, or scour in the earlier period often being followed by scour, or degradation, in the latter period, and vice versa. In either time period, thalweg elevation changes between adjacent sub-reaches suggest a high degree of connectivity in terms of bed material transport. For example, scour is evident on the upstream side of sub-reach 6 and fill on the upstream side of crossing 7 during the period of high discharge (November 1992 – November 1994).

In Figure 7.4, changes between during the high discharge period are compared to those in the following two years, between November 1994 and November 1996. In this period, sub-reaches 4 and 5 are no longer stable, with filling on the two crossing reaches. Following the degradation of sub-reaches 2 and 3 in the high discharge period, this observation is consistent with Cary and Keller's (1957) assertion that material is transported downstream as a series of sand waves. Spatial and temporal trends in cumulative elevation change are supportive of migration further downstream in subsequent years. For example, between November 1996 and December 1998, degradation in sub-reach 4 (566-572 km) is accompanied by a broad aggrading trend downstream. Meanwhile, from December 1998 to February 2000, there is no apparent trend in cumulative elevation change, with the exception of aggradation in the pool at 582-890 km.

a)

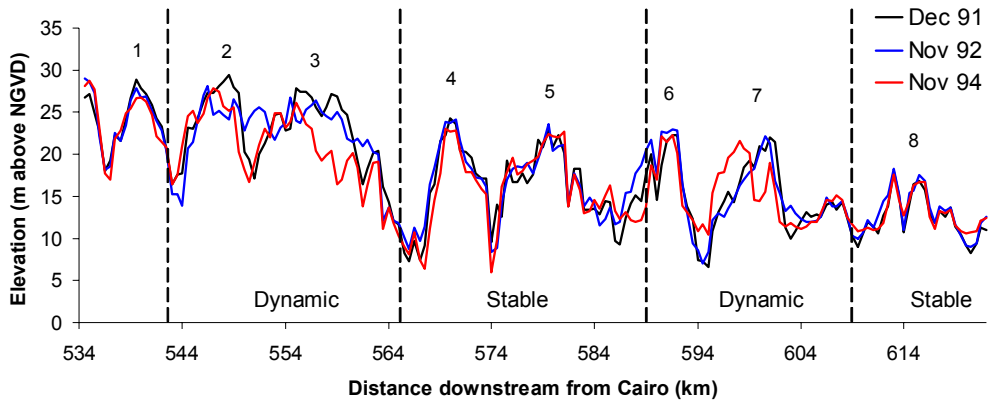

b)

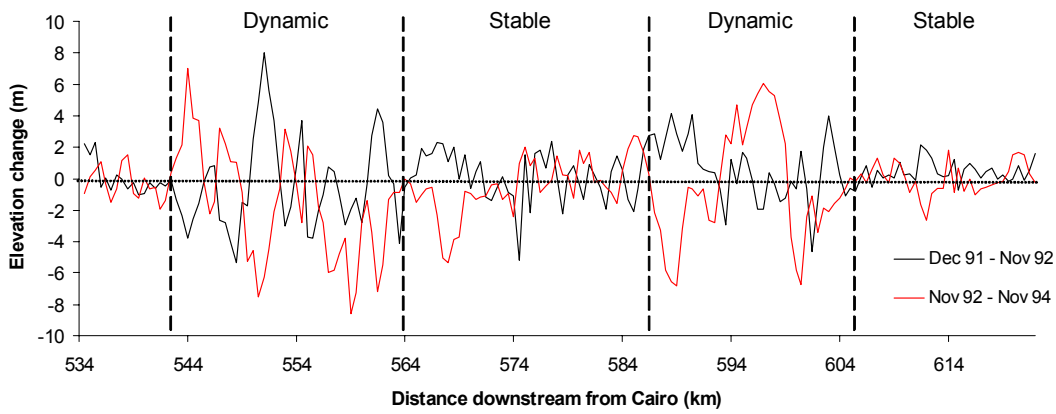

c)

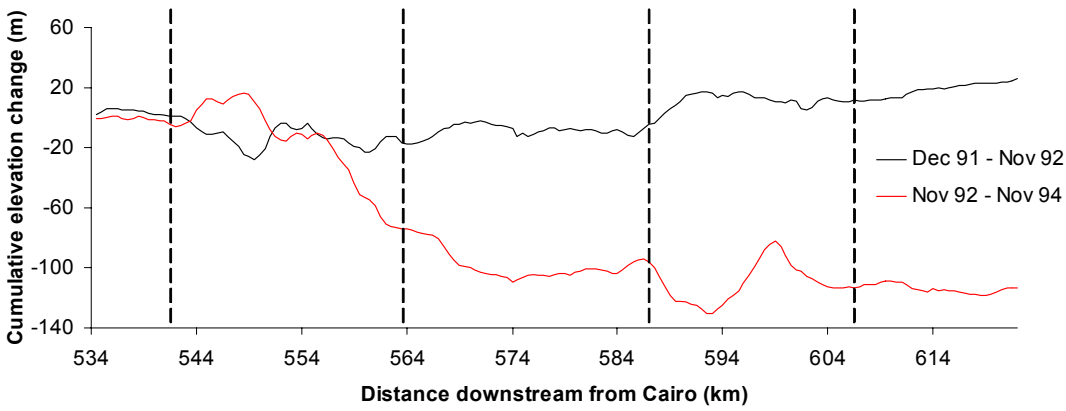

Figure 7.3 Thalweg dynamics between December 1991 and November 1994. In a) thalweg elevation is plotted against distance downstream. In b) elevation change with distance downstream for a high a period of high flow stage (Nov. 92 – Nov. 94) is compared to a period of low flow stage (Dec. 91 – Nov. 92). In c) cumulative elevation change is plotted to emphasise reach-scale trends.

a)

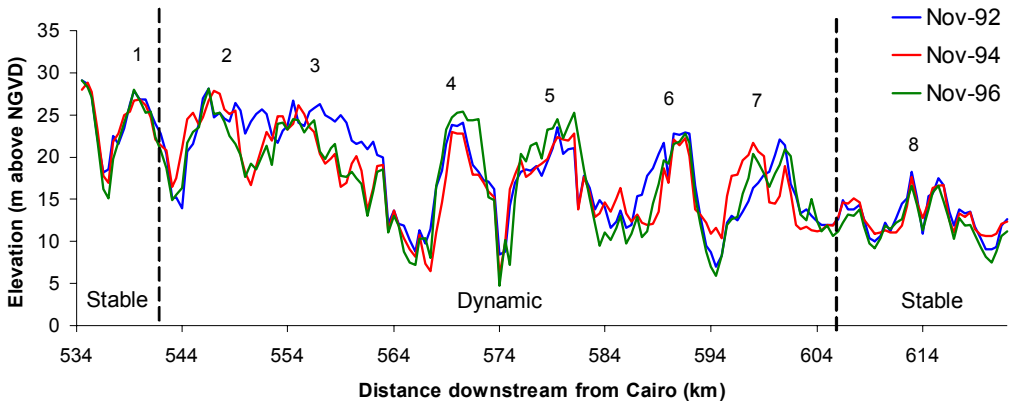

b)

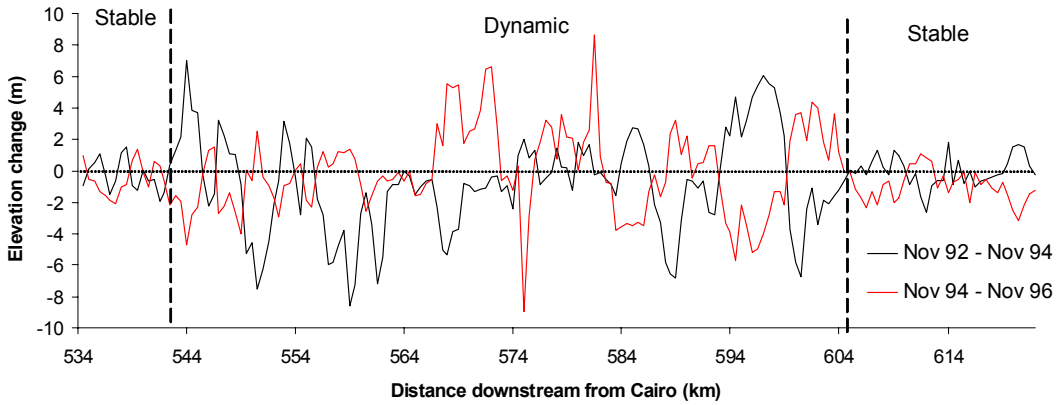

c)

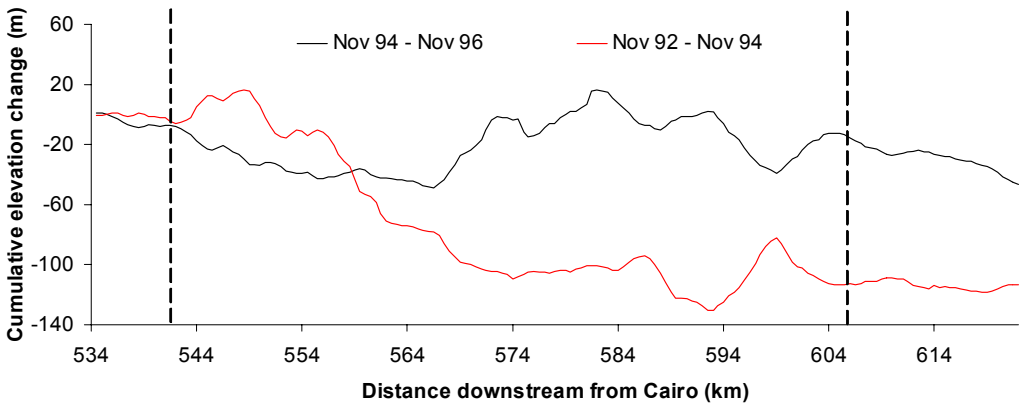

Figure 7.4 Thalweg dynamics between November 1992 and November 1996. In a) thalweg elevation is plotted against distance downstream. In b) elevation change with distance downstream is for a period of high flow stage (Nov. 92 – Nov. 94) is compared to a period of low flow stage (Nov. 94 – Nov. 96). In c) cumulative elevation change is plotted to emphasise reach-scale trends.

7.2.3 Significance for longer-term and larger-scale dynamics

The spatial and temporal feedbacks between form and process noted above have implications for understanding the longer-term and larger-scale dynamics of pools and crossings. First, analysis of annual-interval hydrographic surveys reveals that the observed pattern of reach-scale aggradation or degradation over an approximately nine year interval (December 1991 – February 2001; Figure 7.1) is strongly controlled by the sequence of extreme high or low flow events. Two periods are particularly important in determining the observed pattern: most of degradation experienced upstream from 575 km actually occurred between November 1992 and November 1994; whilst most of the aggradation in the downstream reach occurred between February 2000 and February 2001. These events therefore leave a characteristic signature which is preserved in the channel morphology for up to a period of several years. In relation to the decadal-interval morphological changes (chapter 6), this therefore suggests that the large flood event in 1973-1974 was almost certainly capable of causing the changes noted in pool-crossing configuration experienced between the confluence of the Yazoo River and Old River distributary (reach 5) between the 1962-64 and the 1975 hydrographic surveys. Hence, the stability of the characteristic pool-crossing morphology (characteristic forms) of the Lower Mississippi River is dependent on the magnitude, frequency and distribution (recurrence interval) of extreme flow events through time (Wolman and Miller, 1960; Brunsden and Thornes, 1979).

Second, more detailed analysis suggest that although broad trends can be identified, observed morphological changes in any sub-reach are very difficult to explain because they represent the collective result of a range of feedbacks between adjacent pool-crossing units. Thus, although extreme discharge events can be associated with greatest morphological change, the magnitude, order and location of changes over relatively long reaches of the Lower Mississippi River is very difficult to predict. Further research is therefore required to explore how sequences of changes at relatively short time and space scales combine to create the reach-scale changes noted in chapter 6. As a first step, improving explanation requires a better understanding of the nature of bed material movement through pools and crossings

and associated form-process interrelationships. These issues are explored in the remainder of this chapter.

7.3 Bed material movement at sub-annual timescales

7.3.1 Studies of bed material movement on smaller-scale alluvial rivers

Previous studies on alluvial rivers have demonstrated that the rate of bed material movement is related to variations in discharge and bed material supply, but the nature of these relationships is dependent on location within the channel.

At the timescale of the individual flood event, it has been observed that the channel bed is usually scoured (degrades) at high discharges on the rising stage and usually fills (aggrades) to near the pre-flood event level on the falling stage (Leopold *et al*., 1964; Leopold and Emmett, 1983). However, the spatial pattern of bed material movement is almost certainly more variable than this simple relationship suggests. On a large alluvial river, this has been demonstrated most effectively by Lane and Borland (1953). They showed that along a 160 mile (256 km) reach of the middle Rio Grande River in New Mexico the above relationship was flawed because the average annual volume of material deposited into the reservoir downstream was an order of magnitude lower than the volume predicted if the whole reach had scoured and filled during the passage of each flood event. Lane and Borland therefore proposed that bed material was only transported a short distance downstream, between narrow sections which scoured, and wider sections which filled as discharge increased.

Similar patterns of bed material movement have been noted on the smaller East Fork River in Wyoming. Along a relatively short reach (430 m) reach, Andrews (1979) suggests that patterns of short-term scour and fill are related to relative changes in the levels of form resistance offered by pool and riffle-like (i.e. crossing) sections. At a low discharge, the pool sections had larger dune bed forms than the riffle sections, but as discharge increased, the dune fields washed out (and hence, form roughness declined) so that scour dominated by the time of the flood crest. Meanwhile, the height of dunes (and therefore, form resistance) increased in riffle

sections as sand accumulated on the bed during a rise in flow stage. Over a longer reach of the same river, direct observations made by Meade (1985) are consistent with the idea that bed material is moving downstream as a series of discrete waves. During a typical runoff season, pulses of bed material are moved downstream from storage at low flow in a pool-section, to storage at the next low flow in the next pool section downstream. This is consistent with Andrew's earlier work, because bed material must move over the intervening riffle section at higher flow stages. The mean distance between pool sections therefore corresponds approximately with the mean annual distance of bed material transport. This has implications for measurement because:

> *'Changes in bed configuration observed from one day to the next during runoff season are at least an order of magnitude greater than the changes observed from one year to the next during low-water season' (Meade, 1981, 227).*

Thus, during the season of active bed material transport, bed configuration, (and therefore, flow resistance) changes day-to-day but there is very little change in bedform resistance between one low water season and the consecutive low water season. This idea of translational bed material waves which move according to variations in flow stage is also consistent with other observations on smaller alluvial rivers and in laboratory flumes (Gomez *et al.*, 1989, Hoey and Sutherland, 1991).

Despite the obvious difference in drainage basin size, the annual hydrograph of the East Fork River is similar in general form to the hydrograph of the Lower Mississippi River because it is dominated by a strong seasonal component caused by regular snowmelt runoff. Hence, it is not unreasonable to expect similar spatial and temporal dynamics of bed material movement on the two rivers. Crossing aggradation and degradation on the Lower Mississippi River with the rise and fall of flow stage respectively has been well documented by previous researchers (Carey and Keller, 1957; Winkley, 1977; Harbor, 1998). This therefore implies that the adjustments noted in Figures 7.3 and 7.4 from annual-interval hydrographic surveys may mask a much greater intra-annual variation in pool-crossing morphology.

Carey and Keller also report that any pool-crossing scale patterns of bed material movement in the form of waves is further complicated on the Lower Mississippi

River by the existence of multiple scales of bedforms. Irregularly spaced 'sand waves' on the river bed, which range in maximum height from 3.0 – 9.1 m (10 – 30 ft) at high flow stage to 0 – 1.2 m (0 – 4 ft) at low flow stage, are identified alongside smaller-scale secondary and tertiary wave systems. However, two issues remain unclear: the relative importance of each scale of bedform role in relation to both form resistance and rates of bed material transport; and how this complex bedform configuration varies through both space and time with changes in the velocity field.

7.3.2 Method

Morphological dynamics at sub-annual timescales were studied using selective single-beam sonar surveys of the crossing thalweg and selective multi-beam sonar surveys of the Red Eye Crossing and downstream Missouri Bend sub-reach. These data sets were introduced in section 2.8.7.

Single-beam sonar crossing surveys were selected to allow comparison of morphological changes during the relatively low discharge 2000 water year (Oct. 1999 – Sept. 2000) with those in the higher discharge 2001 water year (Oct 2000 – Sept. 2001). 1-D analysis utilised the selected weekly-interval longitudinal single-beam sonar surveys of the crossing thalweg (Figure 2.20b). Because surveyed range lines were not consistent between consecutive surveys, elevations were surveyed at regular intervals along a constant profile from a TIN (triangulated irregular network) topographic surface of each selected survey. TIN surfaces were created based upon the Delaunay method of triangulation. Along the surveyed range lines, elevation points were sampled at regular 50 ft (15.1 m intervals). To minimise loss of variance, elevations were linearly interpolated from each TIN surface at regular 5 m intervals.

2-D surface analysis utilised the approximately monthly-interval single-beam sonar surveys of specific cross-sections in the pool-crossing sub-reach. Morphological changes between selected surveys were visualised by generating surfaces of difference. In the last decade, this GIS-based technique has been widely applied in studies of reach and sub-reach scale morphological change (Goff and Ashmore, 1992; Lane *et al*., 1994; Milne and Sear, 1997). Surfaces of difference can only be

generated for areas of the channel that are contiguous to all surveys. In this case, surfaces of difference were limited to the channel banklines for the lowest flow being compared. These low flow bank lines were therefore digitised as a polygon and used as break line for surface generation. Surfaces of difference are generated by subtracting corresponding nodes in gridded surfaces that have the same origin and spacing (Lane, 1998). However, instead of generating grids directly, initial surfaces were created as TINs and then converted to grids because interpolation errors are minimised (Milne and Sear, 1997; Jones, 1997).

The complete multi-beam sonar survey of the sub-reach was performed on the 8th March 2001 at a flow stage of 10.68 m above NGVD (see Figure 7.7). This is close to the peak flow stage reached in the 2001 water year, and therefore the data set offered the opportunity to undertake a more detailed examination of bedform configuration at a high flow stage. Analysis involved the extraction of the 1-D thalweg profile from a TIN surface of the sub-reach, and visualisation of bedform diversity through the generation of 2-D surfaces. All data processing was accomplished using a combination of standardised and customised routines in ESRI Arc View version 3.3 software.

7.3.3 Bed material movement: multiple scales of dynamics

i) General observations from single beam sonar

Plots showing changes in thalweg elevation in Red Eye crossing at sub-annual intervals are presented in Figure 7.5 and corresponding trends in flow stage are presented in Figure 7.6. Together these plots show that as flow stage increases, aggradation in the crossing reach is combined with an increase in the amplitude and wavelength of dune bedforms. In the both the 2000 and 2001 water years, the maximum amplitude dunes develop following the peak flow stage. As flow stage declines, the dunes eventually become washed out as bed material supply from upstream declines. The magnitude of crossing aggradation is higher in the 2001 water year when a higher peak flow stage is reached (Figure 7.6). This identified mechanism demonstrates that the river adjusts its form resistance at sub-annual timescales in accordance with changes in flow stage, by both increasing the amplitude difference between adjacent pools and crossings, *and* developing smaller

dune forms in the crossings. If observed changes at Red Eye crossing are characteristic of those at other crossings, this is very significant because it suggests that, at sub-annual timescales, regional-scale flow resistance requirements are met by multiple adjustments at the sub-reach scale.

ii) Evidence for 'waves' of sediment moving downstream

The movement of material into, and out of, Red Eye crossing with changes in flow stage is consistent with previous observations of bed material movement in other pools and crossings on the Lower Mississippi River (Carey and Keller, 1957; Winkley, 1977; Harbor, 1998). Following a sharp increase in flow stage, the survey on the 13th March 2001 shows an average of over 2 metres of aggradation on the crossing since the 2nd November 2000. However, the magnitude of aggradation declines at distances greater than approximately 1.6 km, suggesting that the wave of sediment has not yet reached the lower crossing region. Conversely, the relatively sharp increase in elevation between 1.25 km and 1.5 km on the 9th July 2001 suggests that, as flow stage declines, and the dune fields become washed out, crossing degradation occurs by a wave of sediment moving from the upper crossing, towards the lower crossing and eventually towards the downstream pool.

The 2-D surfaces of difference presented in Figure 7.7 highlight the spatially-distributed nature of this process. During the period of rising and falling flow stage, solid zones of red and blue respectively do not extend to the bank lines but rather, are focused on the channel thalweg, as it crosses the channel. This is important because it indicates that aggradation and degradation tendencies in the crossing are greatest in the channel thalweg, thereby supporting analysis of the 1-D thalweg profile in Figure 7.5. From a longitudinal perspective, clear patterns of aggradation and degradation are restricted to the crossing. In relation to research on the East Fork River, Andrews (1979) showed that accumulation of material on riffles at higher discharges was accompanied by scour in the pools. However, in Figure 7.7, it is difficult to identify consistent morphological adjustments in the pool reaches. Only in 7.7d is it possible to suggest that crossing aggradation may be accompanied by pool degradation. The lack of clarity with respect to pool behaviour may be because the deepest part of the pool occurs further downstream than the downstream limit of the surfaces of

a) 2000 water year

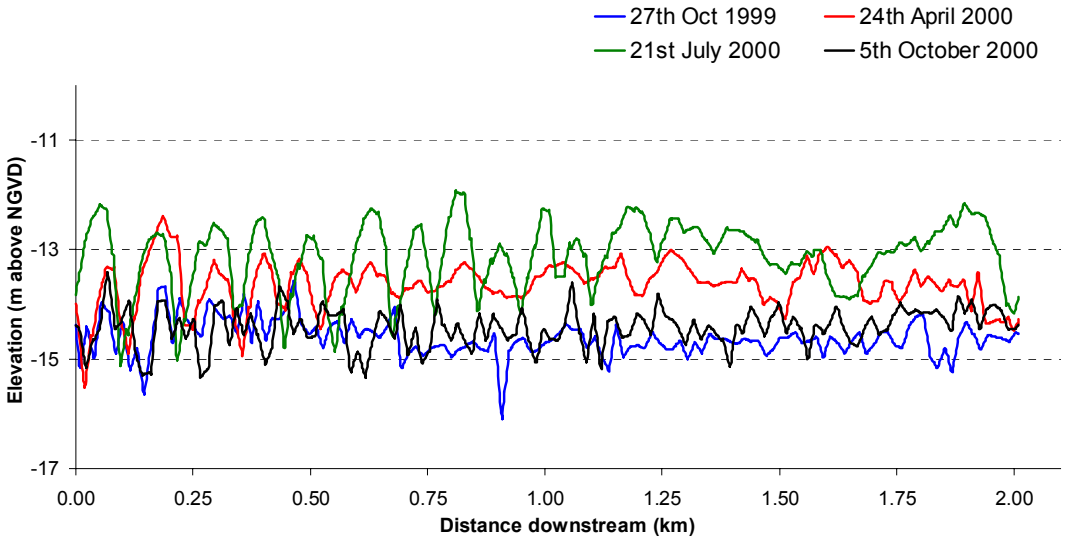

b) 2001 water year

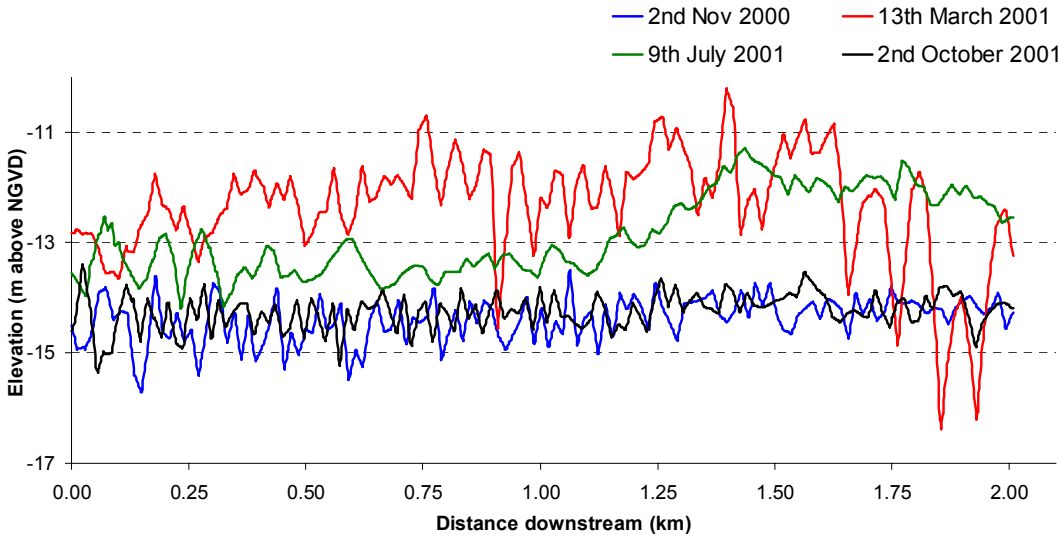

Figure 7.5 Elevation change of the thalweg through Red Eye crossing. Plot a) corresponds approximately with the 2000 water year (October 1999 – September 2000) and plot b) corresponds approximately with the 2001 water year (October 2000 – September 2001).

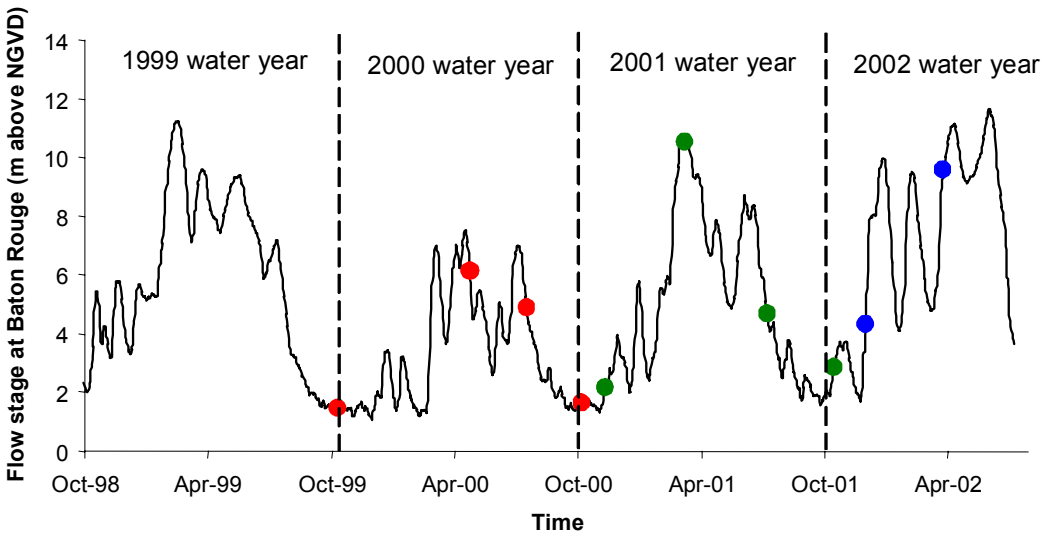

Figure 7.6 Flow stage at Baton Rouge from October 1998 to April 2002. The flow stage for 1-D channel thalweg analysis in Figure 7.6 and velocity field analysis in Figure 7.18 are shown by dots that are coded according to the corresponding water year.

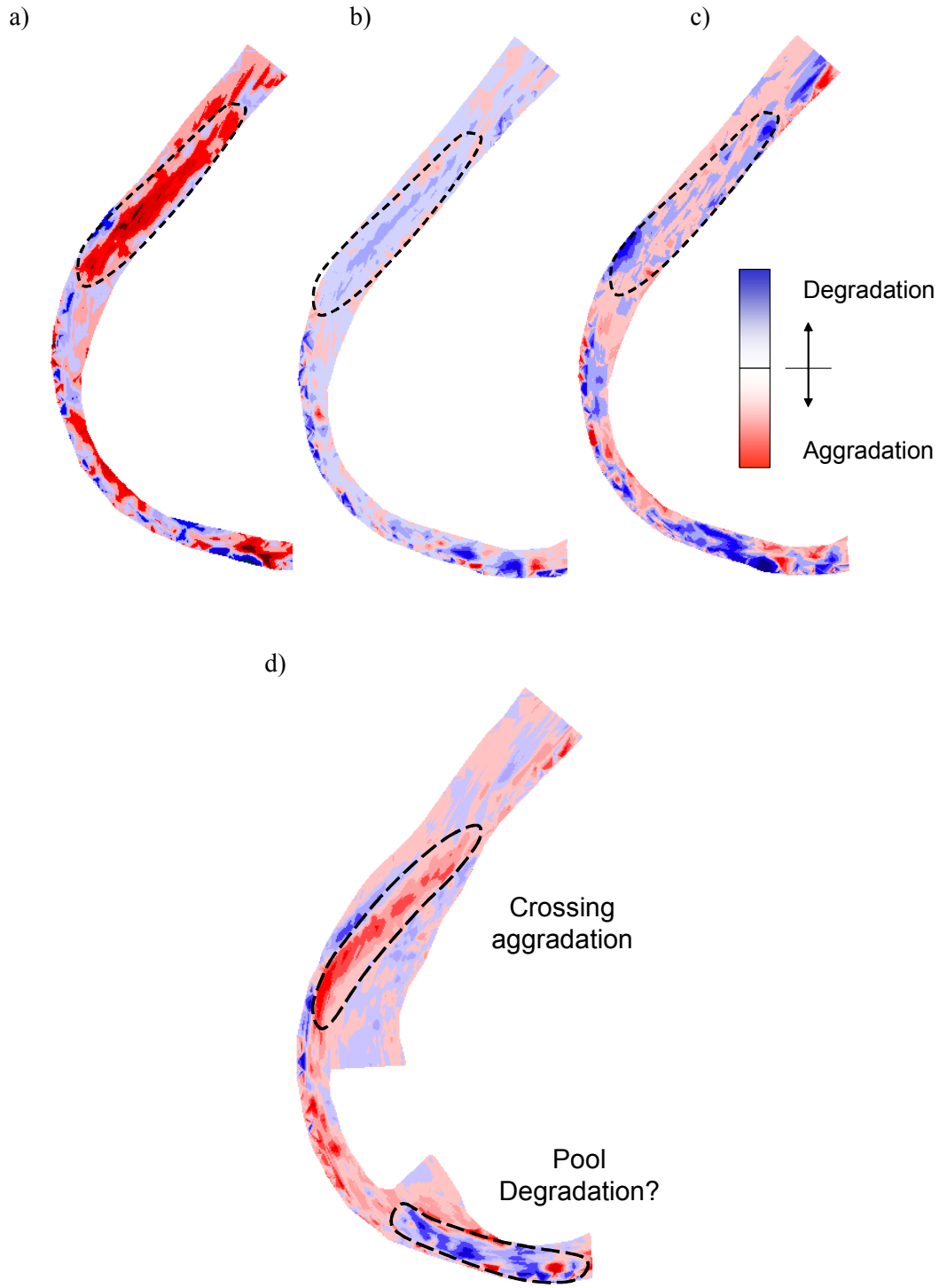

Figure 7.7 Surfaces of difference for four time periods: a) a rise in flow stage of 6.21 m from the 5th October 2000 to the 25th April 2001; b) a fall in flow stage of 4.77 m from the 14th June 2001 to the 7th August 2001; c) a rise in flow stage of 2.07 m from the 5th October 2000 to the 25th October 2001 and; d) a rise in flow stage of 1.79 m from 12th January 1999 to the 22nd July 1999.

difference (see Figure 2.18). Hence, there is a need to modify routinised sampling programmes to improve understanding of sediment wave movement and offer more informed management recommendations.

iii) Dune bedforms and flow stage

The general mechanism identified in the previous section indicates that at the sub-annual and sub-reach spatial and temporal scales, process and form are mutually adjusted to provide the flow resistance required to balance energy availability. However, the relationship between bed configuration and flow stage is complicated because dune bedforms are never fully adjusted to the prevailing flow conditions on large alluvial rivers. This is because although discharge can remain approximately constant for a period of several days over many days, a massive redistribution of sediment is required if a dune bed is to be substantially modified (Allen, 1970). Thus, dunes can continue to grow in height and in wavelength after the peak discharge has passed.

A degree of form lag is evident in Figures 7.8a which shows the trajectories of dune height/length characteristics in the 2000 and 2001 water years. The greatest dune heights (and hence, most developed dune field) is surveyed on the 21st July 2000. This is on the falling limb of the 2000 water year hydrograph and at a flow stage lower than the flow stage for the surveys on the 24th April 2000 and the 13th March 2001. Hence, at the time of these earlier surveys, the bed configuration was probably still adjusting to the prevailing process regime. Figure 7.8a also reveals that dunes can change in a variety of ways with changes in flow stage. In the 2000 water year for example, dunes lengthened before increasing in height, whereas in the 2001 water year, dunes increased in height before lengthening. This observation may reflect the timing of surveys in relation to variations in flow stage: the survey on the 13th March 2001 followed a sustained increase in flow stage over the previous two calendar months whereas the corresponding survey on the 24th April 2000 followed a period of more fluctuating flow stage. However, it may also reflect variations in sediment supply, known to be a critical factor in determining the type of bed formation (Simons and Richardson, 1966). A third trajectory has been noted by Dinehart (2002) on the Lower Sacremento River: mean bedform heights remained similar to

those at lower flow stages but bedform wavelength decreased by a factor of between 2 and 3. Hence, the characteristics of dune development with changes in flow stage are extremely complex.

Figure 7.8b shows a hysterisis effect in the relationship between crossing elevation and flow stage. For a given flow stage, crossing elevation is higher on the falling limb of the hydrograph in comparison to the rising limb. Hence, the maximum form resistance exerted by both crossing aggradation is likely to occur after the peak in flow stage.

iv) Dune bedforms characteristics in relation to existing theoretical and empirical relationships

The generation of dunes and their controlling dynamics is generally poorly understood (Best, 1996). Yalin's (1977) theory that dunes are formed and maintained by macroturbulent eddy structures within the flow has dominated thought for many years. Yalin postulates that the average length of dunes is determined by the average burst path length of macroturbulent eddies which are scaled on flow depth. As a result, dune length (Λ_d) is related to flow depth (d) in the following manner (Yalin, 1977):

$$\Lambda_d = 6d \qquad (7.1)$$

Figure 7.9a shows that the length characteristics at high flow stage (April 2000 and March 2001) show good correlation with Yalin's (1992) relationship but at lower flow stages, dune length is longer in relation to flow depth. This supports Julien and Klaassen's (1995) general finding that Yalin's relationship provides a better fit to measurements of a near-fully developed dune field at high flow stage than at low flow stage. At lower flow stages, the dunes observed are closer to the lower boundary of the dune stability field (transition from ripples to dunes) and hence, average dune length is considerably longer.

The relationship between dune height (H) and flow depth (d) is less clearly defined. Although Yalin (1964) reports that $d/H = 6$, Allen (1970) states that 'most' d/H ratios actually fall within the range 5-10 and Bridge (2003) prefers an even larger window

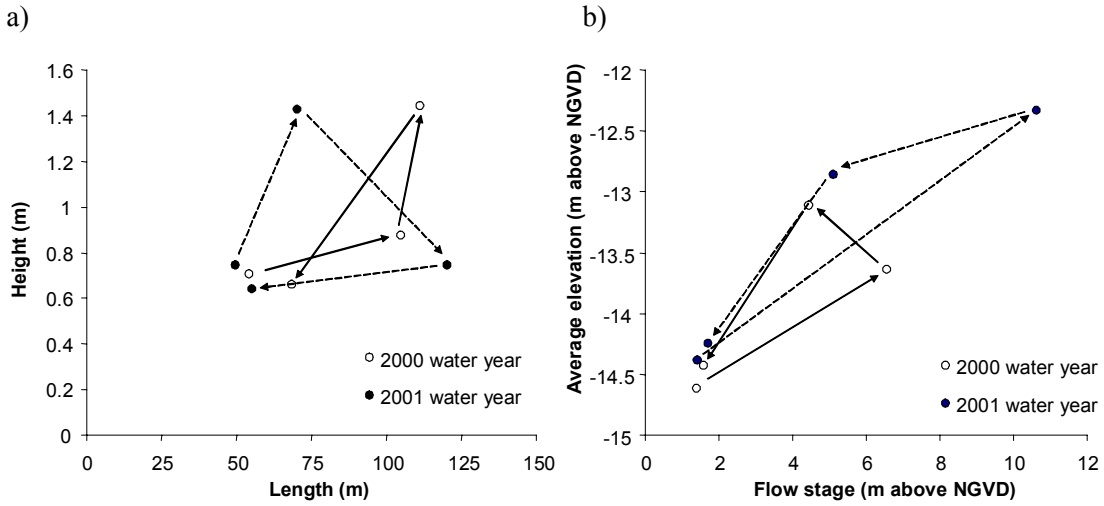

Figure 7.8 a) Dune height and length dynamics identified by the cumulative elevation change technique using a tolerance value of 0.1 m and b) crossing elevation against flow stage at Baton Rouge in the 2000 and 2001 water years.

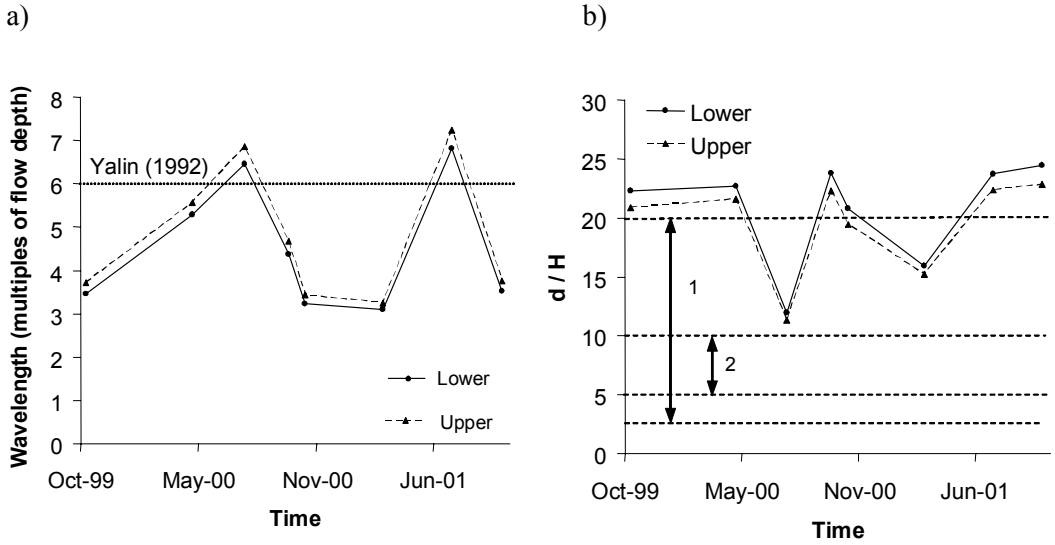

Figure 7.9 Temporal variations in a) dune length as a multiple of flow depth and b) dune height as a percentage of flow depth. In b), label *1* refers to the d/H window identified by Bridge (2003) and label *2* refers to the d/H window identified by Allen (1970). Length and height parameters are determined by the cumulative elevation technique using an amplitude tolerance of 0.1 m. Because the exact water surface elevation at the time of the single-beam sonar surveys is not known, flow depth was estimated as the difference between the flow stage at Baton Rouge (16 km upstream from Red Eye crossing) and the average crossing elevation, with an arbitrary elevation subtracted to allow for the decline in water surface elevation for the distance downstream from the gauging station. Both an upper bound elevation value estimate of 1.34 m and a lower-bound value of 0.34 m were subtracted based on the two linear regression equations describing the regional-scale properties of the longitudinal profile (see Figure 5.4).

in the range 3-20 to capture the degree of variability. Figure 7.9b shows that *d/H* ratios in Red Eye crossing are greater than Yalin and Allen's predictions at all flow stages and fall within Bridge's larger window only at high flow stages (April 2000 and March 2001). The relatively low dune height in relation to flow depth suggests that fully developed dunes are not forming in Red Eye crossing, irrespective of the flow stage. However, an alternative explanation is that the relatively low height of dunes may simply be a product of sampling the channel bed at an interval that is too coarse to detect the characteristic form of such dune fields. This idea is returned to later in the chapter.

v) Identifying further bedform complexity using multi-beam sonar

Examination of higher-resolution multi-beam sonar measurements show that bedform arrangement is more complicated than the arrangement detected by single-beam sonar measurements. In Figure 7.11, a 1-D thalweg profile has been extracted from a TIN topographic surface of the complete channel multi-beam sonar survey of the sub-reach (Figure 7.10a). Three areas are enlarged to show the range of bedforms present within the sub-reach. In enlarged area *A* (Figure 7.12) smaller-scale bedforms are superimposed on both the stoss and less sides of larger-scale dunes. These superimposed bedforms are greater than 0.04 m in height and 0.6 m in length and therefore, according to Allen's (1970) definition, are too large to be classified as ripples. They are therefore referred to as 'micro' dunes. In Figure 7.12b, repeated multi-beam sonar surveys at approximately 4-hour intervals show these micro-dunes migrating across the surface of larger-scale dunes. In enlarged area *B* (Figure 7.13), just downstream from the crossing midpoint, there is no evidence of bedform superimposition, and repeated surveys illustrate the movement of the individual large-scale dunes. Finally, in enlarged area *C* (Figure 7.14), within the pool, there is a more complex range of bedforms because, whilst there is very little superimposition between 6.00 and 6.55 km, there is a relatively abrupt increase in 'micro' dune superimposition downstream from 6.55 km.

Different dune types are linked to different flow and sediment transport characteristics (Kostaschuk and Villard, 1996). Identification of a relatively complex bedform configuration raises the question of whether particular configurations can be

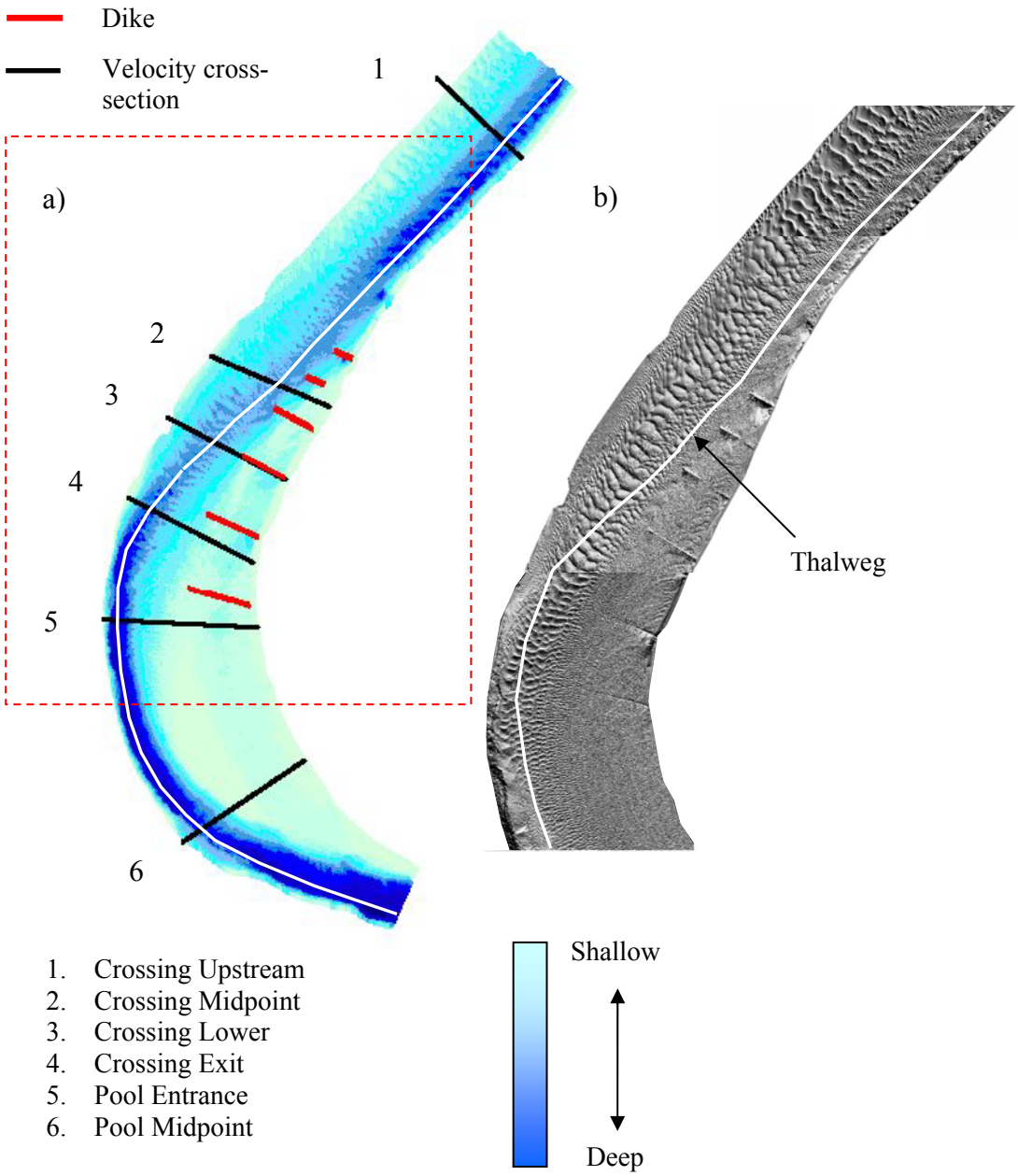

Figure 7.10 a) Multi-beam sonar survey of Red Eye crossing and Missouri Bend on the 8th March 2001. The original points are colour coded according to elevation to give the appearance of a topographic surface. The six labelled cross-sections correspond to selected velocity cross-sections; b) an enlarged area of the channel which has been shaded to emphasise bedform variation through the crossing reach. The light source was computed from a low altitude above the surface and at an azimuth approximately equal to channel direction (25 degrees from north) in order to maximise effectiveness. Shading was performed following TIN and grid generation using ESRI Arc View version 3.3 software.

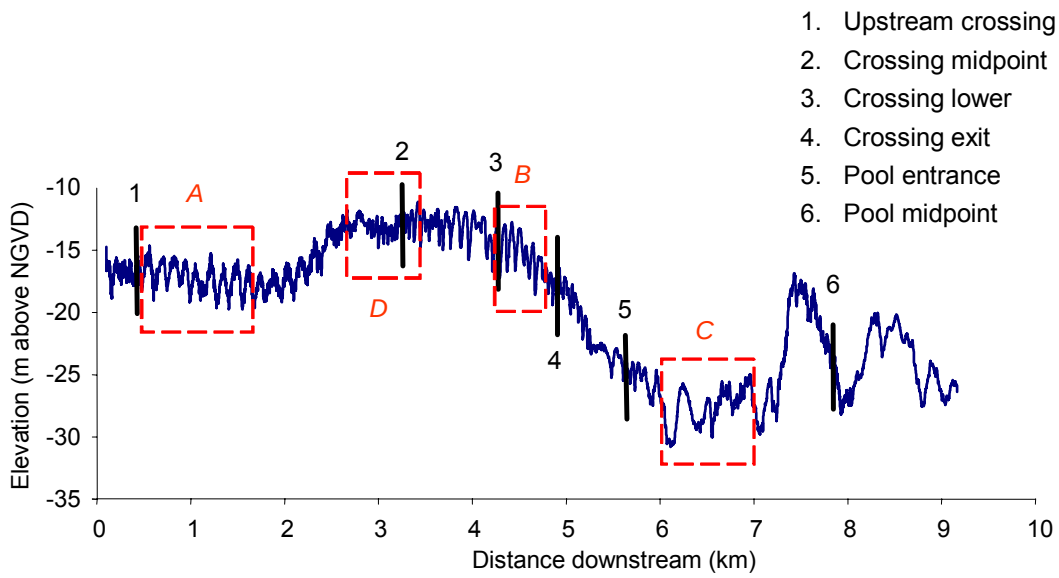

Figure 7.11 1-D profile of the channel thalweg showing the crossing and downstream pool obtained by extracting a thalweg profile from triangulated surfaces of multibeam-sonar data sets and interpolating at 1.5 metre intervals. Selected velocity cross-sections are labelled.

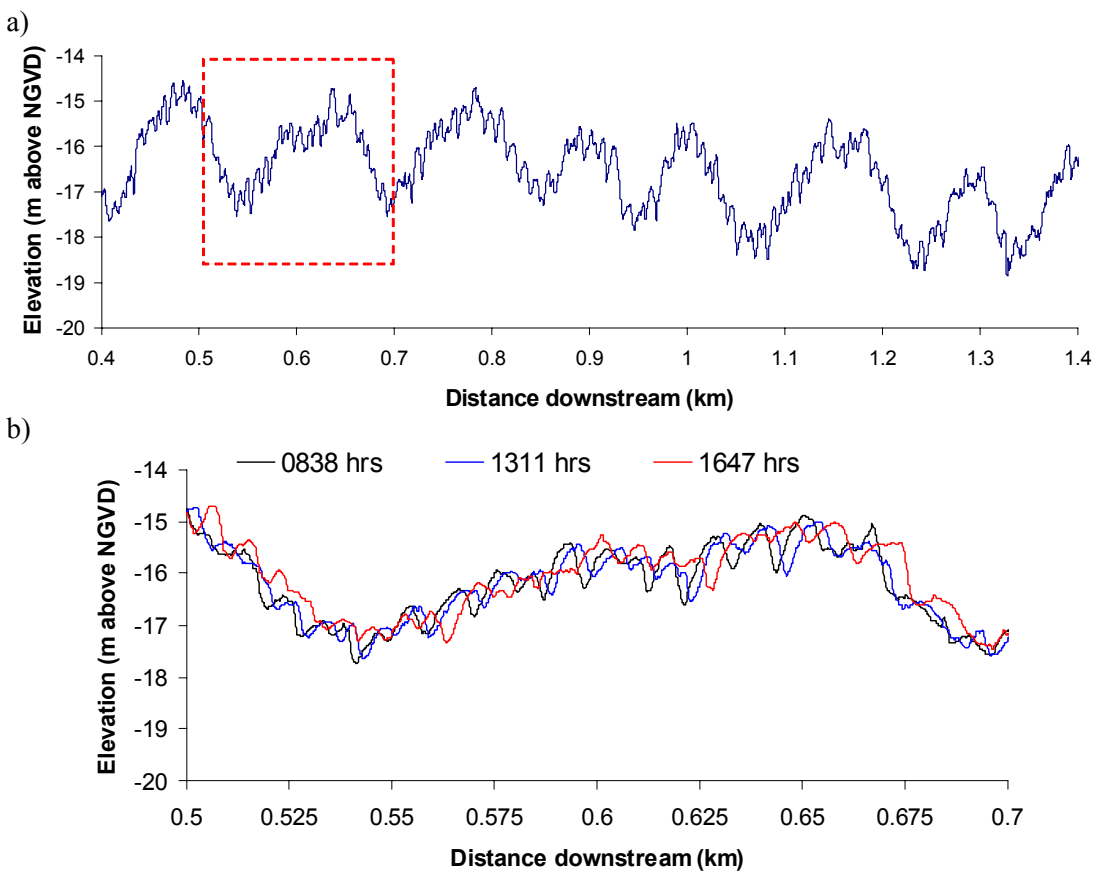

Figure 7.12 a) Area *A* of Figure 7.11 enlarged to show mega-dunes within the crossing reach and; b) an enlarged area of a) showing the migration of smaller-scale dune bedforms over an eight hour period, superimposed upon the larger dune forms.

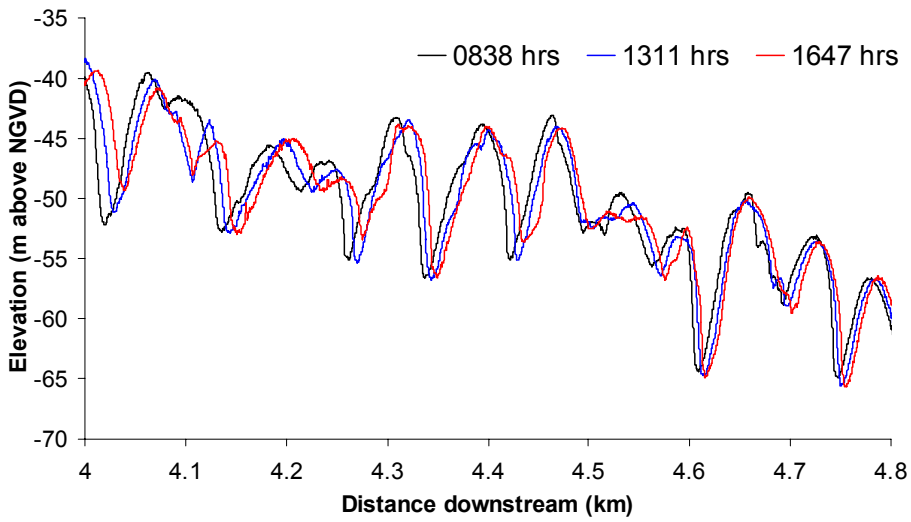

Figure 7.13 Area *B* of Figure 7.11 enlarged to show the movement of dunes over an eight hour period. Superimposition of bedforms is not present in this area of the channel.

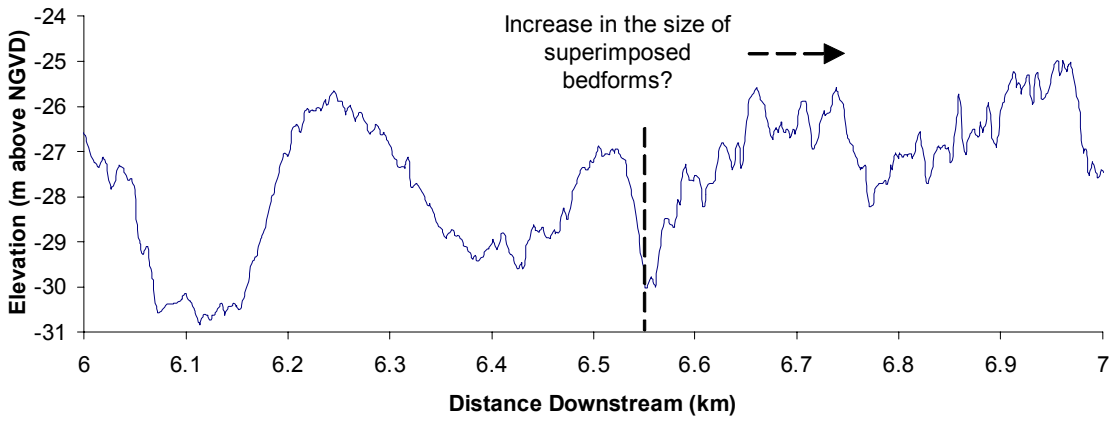

Figure 7.14 Area *C* of Figure 7.11 enlarged to show the variation in bedform superimposition within the pool.

detected in particular parts of the channel, which may in turn, suggest differences in form resistance, rates of bed material movement, and differences in the prevailing flow regime. Figure 7.15 presents a description of the change in bedform characteristics along the thalweg of the sub-reach. Bedform undulations are disaggregated at three scales by specifying varying height tolerance values using the cumulative elevation change technique. To be consistent with geomorphological terminology, these scales are termed micro, meso and macro for height tolerance values of 0.1m, 0.5 m and 2.0 m respectively (Summerfield, 1991). For each value of tolerance, the length (trough to trough) of each individual dune is plotted against its relative location within the profile. Each plot therefore illustrates how: *i)* the length (and hence, frequency) and; *ii)* the degree of variation of length (indicative of dune regularity), varies along the thalweg through the sub-reach. Although downstream trends are different at each of the three scales, four broad configurational 'types' are identified:

1. On the upstream approach to the crossing (0.2 – 2.7 km), micro-dunes are superimposed on the surface of macro-dunes. Both micro and larger-scale dunes are spaced at fairly regular intervals, indicative of a well organised configuration. The enlarged profile in Figure 7.12 is typical of bedforms in this zone.
2. At the crossing midpoint and on its downstream side (2.7 – 5.2 km), superimposed micro-dunes are not evident (shown by the relatively high average length in 7.15d). The average length of meso and macro-dunes are both approximately 0.1 km, indicating that there is only one scale of dune in this zone.
3. Within the downstream pool (5.2 – 8.0 km), the decline in average length in Figure 7.15d in relation to zone 2 is diagnostic of a return of superimposed micro-dunes. However, the degree of variation suggests that superimposition of micro-dunes is variable locally, as illustrated in Figure 7.14. Therefore, the configuration is less well organised than in zone 1. Macro-dunes have a longer average length than at the crossing. The large bedform between approximately 7 and 8 km is considerably larger than the largest-scale dunes noted throughout the crossing.
4. A large bedform with no superimposed micro dunes at the downstream limit of the surveyed reach (8.0 – 9.0 km).

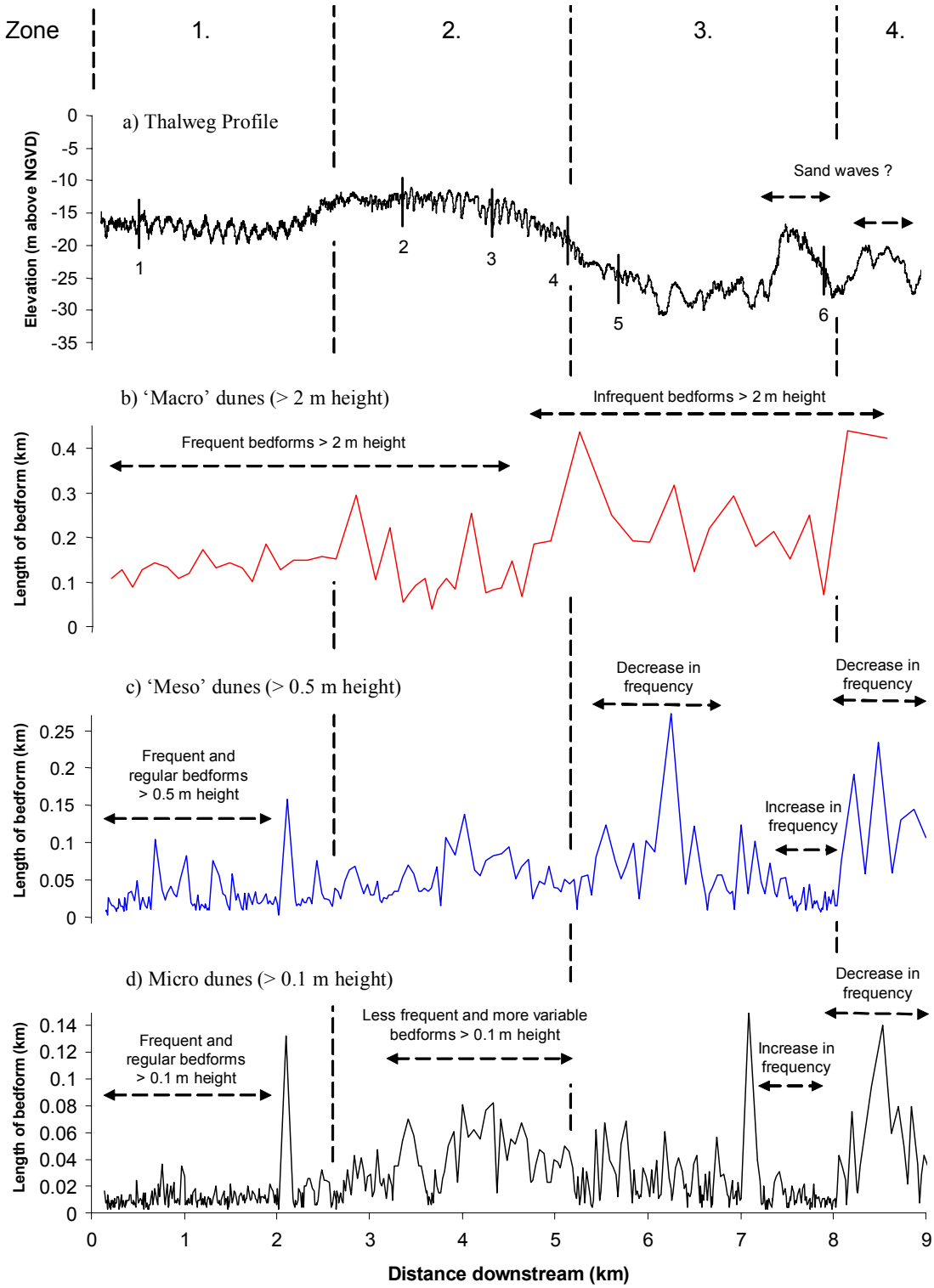

Figure 7.15 The length of bedform undulations in the thalweg profile disaggregated at three scales using the cumulative elevation change technique. Bedform height (amplitude) tolerance values of 2 m, 0.5 m and 0.1 m have been used in plots b), c) and d) respectively. The length of each bedform is the spacing between consecutive troughs. The labels (1-6) in a) show the relative locations of the six velocity cross-sections, as illustrated in Figure 7.11a.

vi) Explaining bedform configurations

Although complex bedform configurations have been noted on other large alluvial rivers (Dinehart, 2002) as well as in tidal environments (Rubin and McCullogh, 1980), accounting for their development, maintenance, and timescale of existence has proved problematic (Dalrymple, 1984; Carling, 2000). Jackson (1975) suggests that each scale of alluvial bedforms has its own characteristic formative process and timescale of existence. Thus, whilst dunes are formed by macroturbulent flow structures that are scaled on channel depth and persist for the timescale of a 'dynamic event,' Jackson proposes that superimposed micro-dunes are formed and maintained by micro-turbulent interactions of flow and bed material and persist for only a shorter period of time. The importance of micro-turbulent interactions in small-scale bedform formation is supported by Jain and Kennedy (1974) and Best (1996).

Within this hierarchy, Jackson envisages that configurations of superimposed bedforms are created because bedforms at different scales have differing sensitivities to changes in the local flow regime. As bedform size increases, sensitivity declines and hence, larger-scale bedforms can become 'stranded' by a change in local flow regime. In relation to the configurations noted in Figure 7.15, the presence of micro-dunes superimposed upon larger-scale dunes on the upstream approach to the crossing, is therefore suggestive of a lower energy flow regime in comparison to the crossing midpoint and its downstream side. This is perhaps not surprising since the crossing represents a local maximum in channel bed elevation and thus, the upstream approach to the crossing must represent an area of greater energy loss in comparison to its downstream side. A second implication of differing bedform sensitivities to changes in local flow regimes is that configurations are likely to become more disorganised as the degree of variation in flow regime increases. Applying this reasoning to the configurations noted in Figure 7.15, it is possible that the relatively distinct bedform configurations are indicative of differences in the consistency of the flow regime through the sub-reach. For example, the greater consistency of the configuration at the crossing suggests that the bed morphology is more adjusted to the prevailing process regime. This would be consistent with the idea that flows through the crossing are more consistent in terms of velocity variation with change in

flow stage than in the pool. ADCP surveys at high and low flow stage are used to explore this hypothesis later in this chapter.

7.3.4 Form resistance at the sub-reach scale

Bedform configurations complicate understanding of form resistance at the sub-reach scale. Although total form resistance is dependent on the size, shape and spacing of all bedforms present, and therefore, cannot easily be predicted (Allen, 1983; Smith and McLean, 1977), the relative form resistance (k_{form}) of bedforms identified can be compared using the function proposed by Van Rijn (1984). This quantifies relative resistance as a function of bedform height (H) and bedform steepness (H/L).

$$k_{form} = 1.1\ H\ (1 - e^{-25(H/L)}) \qquad (7.2)$$

Values of k_{form} for dunes identified by both single-beam and multi-beam sonar are presented in Table 7.1. Single-beam sonar values confirm that form resistance in the crossing does increase with increases in flow stage because dunes become steeper in relation to their height. Regarding bedform superimposition, values of k_{form} from multi-beam sonar reveal that micro-dunes exert a form resistance relative to their height which is less than half that of larger-scale dunes. However, this form resistance is of a comparable magnitude to that exerted by dunes identified by single-beam sonar at, or near, peak flow stage. Because the height of the micro-dunes is approximately five times less than the height of the larger-scale dunes (identified by multi-beam sonar), the total form resistance exerted by micro-dunes is only likely to be approximately one tenth of that exerted by the larger-scale dunes. Hence, the development of superimposed dunes probably does not increase overall form resistance significantly.

In addition to these findings, Table 7.1 reveals a disparity between k_{form} values estimated from multi-beam sonar and single-beam sonar which is suggestive of two different scales of bedforms. This is intriguing, because the single-beam sonar survey on the 13th March 2001 was undertaken just five days after the multi-beam sonar survey and thus, dramatic changes in bed configuration are unlikely. Comparison of dune length values shows that dunes sampled in the lower crossing by

multi-beam sonar have a length consistent with the single-beam sonar survey (approximately 70 m). In the upper crossing region, the larger dunes surveyed by multi-beam sonar have a much longer length although this is upstream from the area surveyed by single-beam sonar so lengths are not directly comparable. Comparison of dune height values meanwhile yields a considerable difference, even in the lower crossing region. Estimates of dune height obtained from multi-beam sonar are more than double those obtained from single beam sonar.

Differences in dune height are explored further in Figure 7.15 where a 1-D profile extracted from a single-beam sonar survey on the 8th March is compared to a 1-D profile extracted from a multi-beam sonar survey on the same date. Single-beam sonar measurements are unable to capture the micro-dunes between 2.6 and 2.7 km and considerably underestimate the height of larger dunes. This finding is important because it indicates that the relatively high average d/H ratios for dunes identified by single-beam sonar (Figure 7.9b) can be attributed, at least partially, to sampling the channel bed at an insufficient spatial resolution. If dune heights were obtained by multi-beam sonar, they would be close to a d/H ratio of 6, as advocated by Yalin (1964) and almost certainly within the 5-10 window suggested by Allen (1970) at high flow stages. This emphasises the danger of drawing misleading conclusions from analysis of data sets collected at a resolution too coarse to adequately represent the variation of the property of interest. Given the underestimation of dune height using single-beam sonar, it is recommended that future studies of bed material movement based on repeated morphological surveys are performed using multi-beam technology.

7.3.5 Estimating bed material movement at the sub-reach scale

Analysis of pool-crossing dynamics at annual timescales revealed that improving understanding of bed material movement at the sub-reach scale is critical to improving understanding of large-scale and longer-term behaviour (section 7.2). Given the complex bed configuration present at this scale, this section considers the potential for obtaining reliable estimates of bed material movement.

	Average Height (m)	Average Length (m)	H/L Ratio	k_{form}
Selected hourly-interval - Multi beam sonar (8 March 2001)				
Upper crossing micro-dunes (Figure 7.13)	0.55	9.30	0.059	0.470
Upper crossing dunes (Figure 7.13)	2.67	131.62	0.020	1.165
Lower crossing dunes (Figure 7.14	2.89	70.32	0.041	2.043
Selected weekly-interval - Single beam sonar (Figure 7.6)				
27 October 1999	0.70	54.42	0.013	0.214
24 April 2000	0.88	104.89	0.008	0.182
21 July 2000	1.44	111.33	0.013	0.438
05 October 2000	0.66	68.57	0.010	0.154
02 November 2000	0.75	49.82	0.015	0.256
13 March 2001	1.42	70.37	0.020	0.623
09 July 2001	0.74	120.25	0.006	0.117
02 October 2001	0.64	55.11	0.012	0.178

Table 7.1 Height, length, H/L ratio and k_{form} characteristics of dunes measured by the weekly-interval single beam sonar and the hourly-interval multi-beam sonar surveys of Red Eye crossing. Dune height and length are determined by the cumulative elevation technique using an amplitude tolerance value of 0.1m.

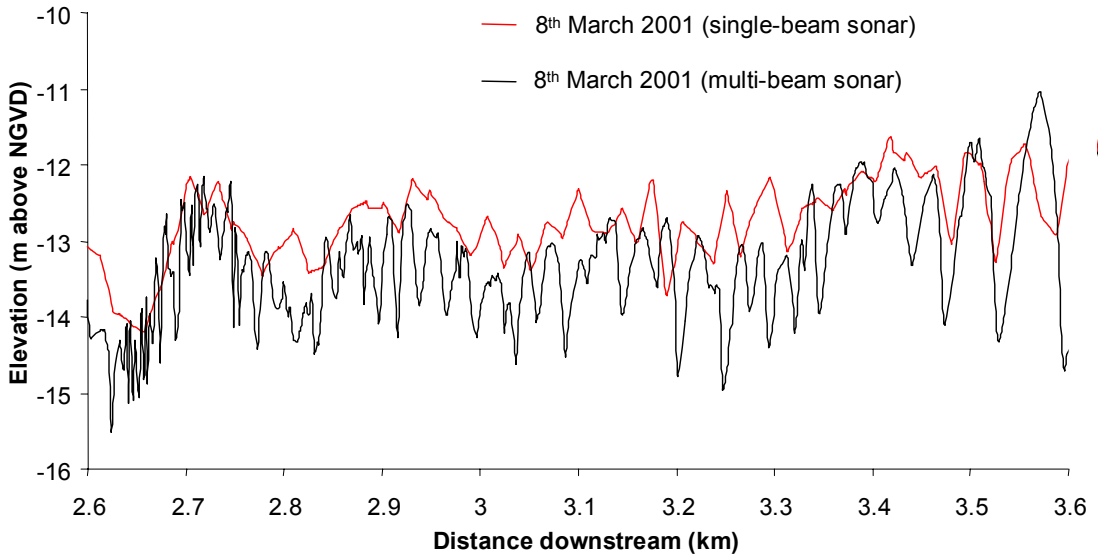

Figure 7.16 Area *D* of Figure 7.11 enlarged to compare dune characteristics obtained from multi-beam sonar with dune characteristics obtained from single beam sonar. Both surveys were undertaken on the 8th March 2001 and are extracted from TIN topographic surfaces at regular 1.5 m intervals.

Repeated bedform surveys have traditionally been used to estimate rates of bed material movement by applying the bedform migration equation based on the height and celerity of bedforms (Simons *et al*., 1965). Reasonable estimates of bed material transport have been obtained using this function by Van den Berg (1987) and Dinehart (2002).

$$Q_{bf} = (H/2)c(1-\lambda_p) \qquad (7.3)$$

where:

Q_{bf} = bedform transport quantity

H = bedform height

λ_p = porosity of bedform sediment (between 0.3 and 0.4 for well sorted sands)

c = bedform celerity or speed of bedform migration

At very local scales, and over very short (sub 24-hour) time periods, Figures 7.12b and 7.13 show that it is possible to track the movement of individual bedforms along the channel bed. Bedform height is easily obtained using the cumulative elevation technique and bedform celerity can be reliably obtained by using cross-correlation to determine an overall correlation lag. The problem with this method is using it to estimate bed material movement at the larger sub-reach scale. Up-scaling introduces complexities because, as the previous discussion has demonstrated, bed material is not only transported at different rates according to variations in flow stage, but it also moves in different ways in different parts of the channel. For instance, when bedforms are superimposed, it is unclear what proportion of total bedload is transported by the migration of smaller-scale dune forms and what proportion is transported by the migration of larger-scale dunes forms.

An alternative technique at the sub-reach scale is to use surfaces of difference, such as those presented in Figure 7.7, to estimate net volumes of erosion and deposition. This approach has been widely to estimate net changes in sediment storage within a reach (Lane *et al*., 1995; Goff and Ashmore, 1994; Martin and Church, 1995). However, translation of this information into reliable estimates of bed material transports is problematic because if bed material transport into and out of a reach are exactly balanced, high rates of bed material transport can occur without there being a noticeable change in reach morphology (Lane, 1998).

Although there are problems with both techniques, they may together be able to supply a reliable estimate of bed material transport if multi-beam sonar surveys are collected at a frequency that is sufficient to adequately capture the spatio-temporal nature of bed material movement. The most suitable sampling strategy requires further research, but it is recommended that 'intense' surveys over the complete channel, collected over a period of days, are repeated at a range of flow stages within a single water year. Importantly, this would allow estimates of bed material movement, derived from bedform tracking in both 1-D and 2-D, to be computed throughout the channel. Hence, understanding would be improved of how superimposed bedforms develop, how stable they are temporally, and their relative contribution to total bed material transport. Crucially though, it would also allow changes in estimates of bed material movement, obtained from bedform tracking, between different flow stage, to be compared to net volumetric changes obtained from surfaces of difference.

In addition to reconstructing rates of bed material movement, it is desirable to improve explanation of how and why different bedform configurations develop in different parts of the channel with variations in flow stage. Repeated morphological surveys implicitly include several forms of bed material transport (rolling sliding and saltation over a range of distances). Explaining the evolution of bedform configurations (and hence sub-reach scale channel roughness) in time and space ultimately requires these different forms to be disentangled. Obtaining direct measurements of bed material transport on large alluvial rivers is not feasible. Thus, it is recommended that in addition to increasing the frequency of repeated morphological surveys, innovative research is undertaken to explore the potential use of modern remote monitoring technologies to isolate components of bed material transport.

7.3.6 A re-appraisal of bed material movement

Results presented so far in this chapter have confirmed Carey and Keller's (1957) proposition that bed material movement on the Lower Mississippi River can be

considered at multiple scales of analysis. What is intriguing however, is not so much that multiple scales of bed material movement exist, but how the scales are related. This is considered below.

At the longest timescale studied (the annual timescale), pool-crossing dynamics revealed that there is usually very little change between consecutive water years at the reach-scale. Even in years of unusual discharge (either extreme high or low), adjustments are generally ordered in such a way that the relative locations of pool and crossings are maintained. If scales are reduced and a single sub-reach is isolated however, it is revealed that annual surveys actually mask a cycle of crossing aggradation and degradation with the rise and fall of flow stage. Considered over a period of several years, this mechanism is consistent with the idea of translational 'waves' of bed material moving downstream between adjacent sub-reaches over the course of a single water year, as identified by Meade (1985) on the smaller East Fork River. Reducing scale again reveals that each wave of material is composed of multiple dunes, whose dimensions, if adjusted to the prevailing flow regime, tend to scale with flow depth. At Red Eye crossing, these dunes are at the lower end of the height range suggested for 'sand waves' by Carey and Keller (1957) and thus, the two types of bedform are possibly synonymous. For example, the *average* height of large-scale dunes (2.7 - 2.9 m; Table 7.1) is not inconsistent with the lower range of the 3.0-9.1 m *maximum* sand wave height in crossing reaches observed by Carey and Keller. Finally, reducing scale a fourth time reveals that some of these dunes are actually the largest dune in a configuration of dunes including smaller, superimposed microdunes.

If this hierarchy is reversed and smallest scales are considered first, it is obvious that it is very difficult to predict much larger-scale behaviour even if understanding at smaller-scales was close to being complete (i.e. determinate). For instance, a complete knowledge of dune formation and development processes would not enable explanation of the movement of translational waves between adjacent pool-crossing units. In this way, fluvial morphology may seem to demonstrate emergent properties (Harrison, 2001). However, observed order in the fluvial morphology at any scale is not simply a cumulative product of 'bottom-up' interactions, it also conditioned by larger-scales and hence, is also a product of 'top-down' interactions. What is

particularly intriguing in the above hierarchy is that, despite variation in bedform configuration over short distances within the channel, and over relatively short timescales, morphological changes at the pool-crossing scale over longer (annual) timescales demonstrate remarkable consistency. Thus, the complexity of the system becomes less *apparent* as the scale of observation is increased. This is consistent with the idea that morphology is adjusted to hydrodynamic processes which act to maintain the pool-crossing configuration. Testing this idea requires examination of feedbacks between form and process at a range of spatial and temporal scales. This is achieved in the following section through analysis of velocity field dynamics based upon repeated ADCP surveys of Red Eye crossing.

7.4 Form-process interrelationships: velocity field dynamics

7.4.1 Method

ADCP surveys were performed at two flow stages between the 19th January 2002 and 7th April 2002, ranging from 4.6 – 10.7 m above NGVD at the Baton Rouge. Six cross-sections were selected for analysis from the 36 available (see Figure 2.20a) by identifying cross-sections from the thalweg profile and the whole channel multi-beam sonar survey that characterised the pool-crossing topography within the sub-reach. These cross-sections are labelled in Figure 7.11a and Figure 7.12.

7.4.2 Evaluation of existing theories of pool-crossing maintenance

On gravel-bed rivers, the most widely accepted account of pool-riffle maintenance is provided by the hydraulic reversal hypothesis, which outlines a reversal in velocity between pools and crossings as discharge rises (Keller, 1971; Lisle, 1979; Clifford and Richards, 1992). Pool-crossing maintenance processes on large alluvial rivers have comparatively been relatively understudied, possibly owing to the scarcity of high resolution data sets.

The classic, and relatively untested, idea of velocity reversal on large alluvial rivers is provided by Lane and Borland (1953). These authors explained the 'reversal' in mean velocity between crossings and deeps (pools) with flow stage by the

characteristic cross-sectional shapes of crossing and pool reaches (Figure 7.17). Because the characteristic crossing shape is rectangular and the characteristic pool shape is triangular, the hypothesis states that the increase in cross-sectional area for a given increase in flow stage will be greater in crossings than in pools, providing that channel width is greater at crossings and both flow resistance and water surface slope are constant. If discharge is assumed constant over the time period of measurement, variations in cross-section area are indicative of variations in section-averaged velocity and hence, this mechanism is therefore able to account for a convergence and possible reversal in mean section velocity as discharge rises.

This hypothesis is examined in Figure 7.18 by plotting the area of each flow cross-section at a low flow stage (19th January 2002) and at a high flow stage (7th April 2002). Rates of increase in cross-section area are greatest at the pool entrance (96 percent) and lowest at the upstream crossing section and crossing midpoint sections (56 and 62 percent respectively). Thus, the observed changes are not only inconsistent with Lane and Borland's hypothesis, if anything they are suggestive of the opposite tendency. This is perhaps not so surprising because each of the three conditions specified by Lane and Borland are not met. First, channel width is actually greater in the pool than in the crossing (Figure 7.18). Second, analysis of morphological changes in section 7.3.3 revealed that flow resistance is far from constant with changes in flow stage because form resistance changes according to patterns of crossing degradation/aggradation and related dune field development. As a result of morphological changes, water surface slope, a third condition, is unlikely to be constant with changes in flow stage.

A further fundamental problem with applying the hypothesis is that morphological adjustments cannot simply be related to measures of section-averaged velocity, but are dependent on the spatial distribution and uniformity of the velocity field at any single cross-section. This is demonstrated in the following two sections by more detailed analysis of spatial and temporal variations of the resolved downstream and resolved cross-stream velocity components.

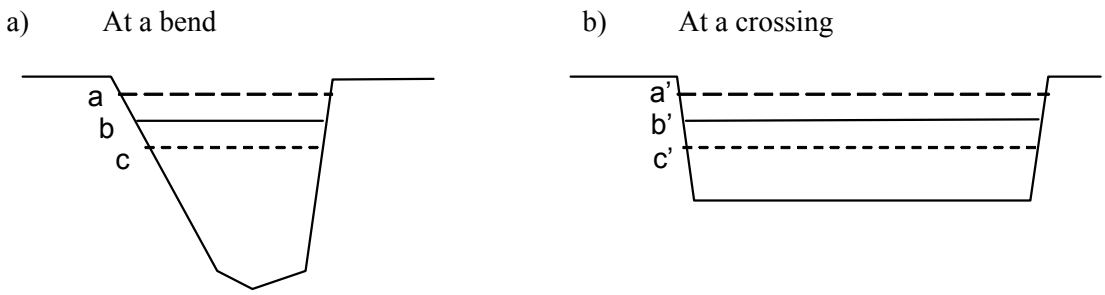

where:

a and *a'*	=	water level at high flow stage
b and *b'*	=	water level at medium flow stage
c and *c'*	=	water level at low flow stage

Figure 7.17 Typical bend and crossing sections in a large alluvial river (modified from Lane and Borland, 1953).

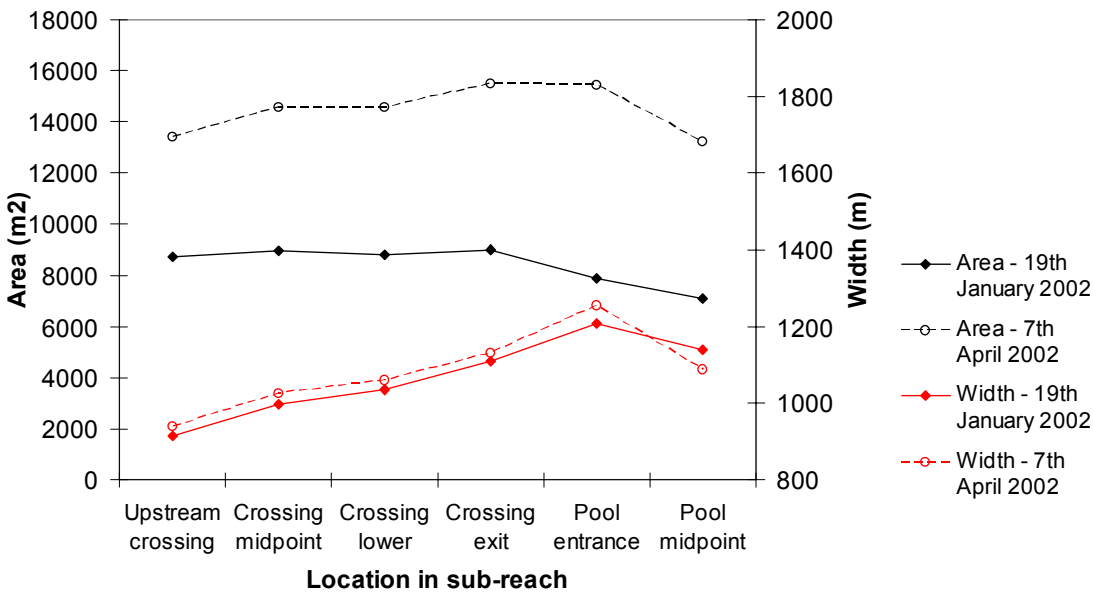

Figure 7.18 Change in area of selected velocity sections through the pool-crossing sub-reach.

7.4.3 Analysis of ADCP velocity data sets

i) Identification of a consistent hydrodynamic structure

Within the sub-reach, a consistent flow structure is maintained at both high and low flow stage. This can be considered the product of a regional-scale hydrodynamic process, being conditioned by the pre-existing morphology and therefore demonstrates the existence of a 'top-down' form-process behaviour. The flow structure is emphasised by presenting the resolved downstream and cross-stream velocity field at each of the selected flow sections as a shaded TIN surface at high and low flow stage (Figures 7.19 - 7.22). At each section, the pattern of resolved downstream velocity is strongly associated with the shape of each cross-section. This is illustrated by considering the asymmetry in the velocity field in relation to the degree of asymmetry in cross-section shape (Figure 7.23). In the upstream crossing section, the core of maximum velocity is aligned adjacent to the right bank where the section is deepest. This migrates towards the channel centre line through the crossing midpoint and the lower crossing sections, and is accompanied by the development of a more symmetrical section shape. Further downstream the section shape becomes more asymmetrical once again and the core of maximum velocity migrates towards the left bank (looking upstream). This is the outer bank around Missouri Bend. As flow stage rises, there is an increase in uniformity (more symmetrical velocity distribution) at most sections.

Cross-stream velocities patterns reinforce this velocity structure (Figures 7.21 and 7.22). The dominant blue region in the crossing midpoint, crossing lower, crossing exit and pool entrance sections are consistent with the core of highest velocity migrating from close to the right bank to the left bank (looking upstream) through the crossing region. At the upstream crossing section, the absence of a dominant colour at low flow in any part of the section indicates that the resultant velocity is close to being parallel to the channel centreline (i.e. downstream). Meanwhile, at the pool midpoint section, the block of red within the pool confirms that the current is being deflected towards the convex right bank (looking upstream) At the upstream crossing section at high flow, there is evidence of secondary circulation where flow along the bed flows towards the convex bank (left bank looking upstream) and flow at the surface flows towards the steeper right bank. Hence, in terms of larger-scale

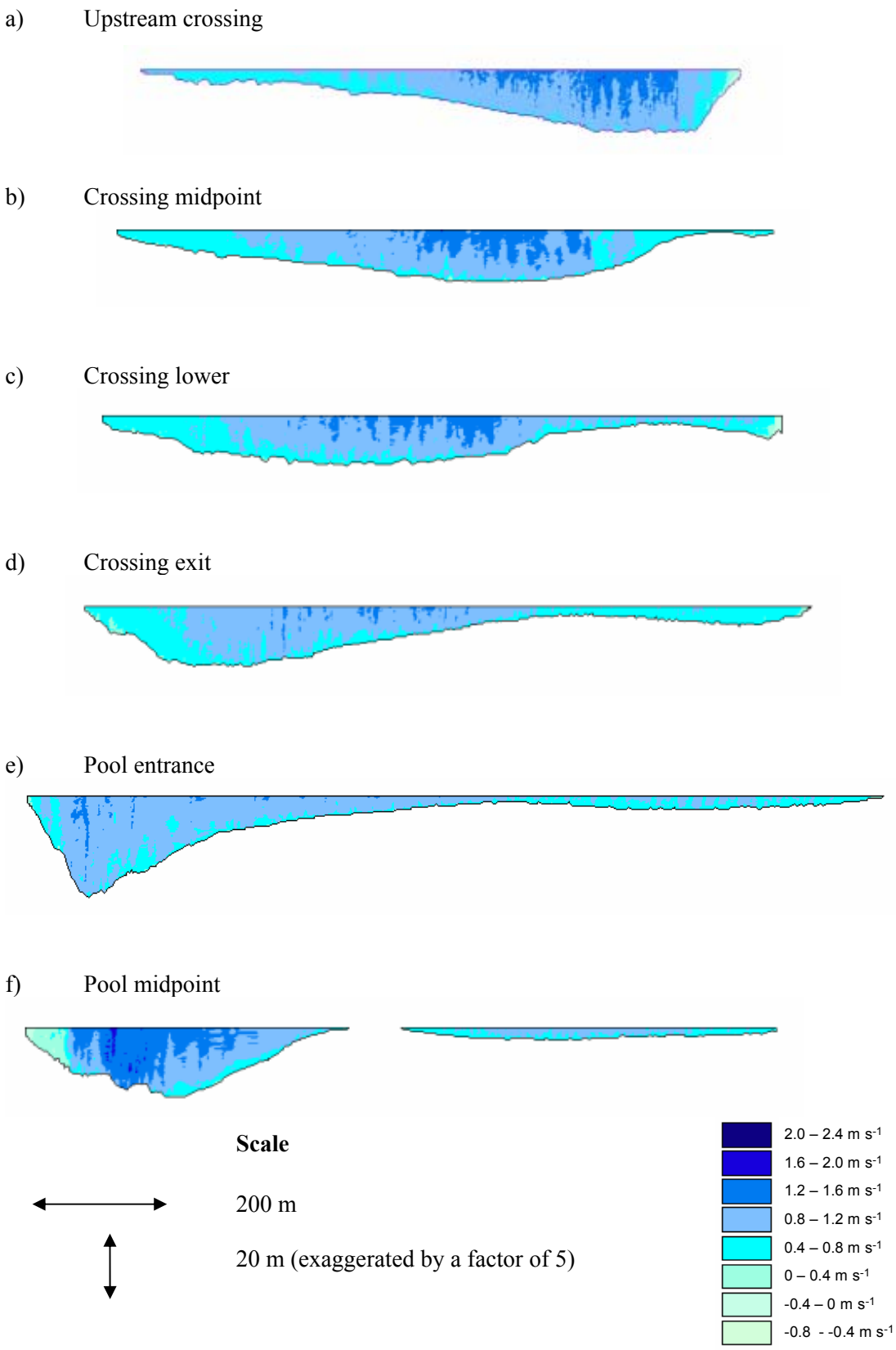

Figure 7.19 TIN surfaces of resolved downstream velocities (parallel to the channel centre-line) at each selected flow cross-section for low flow stage on the 19th January 2002.

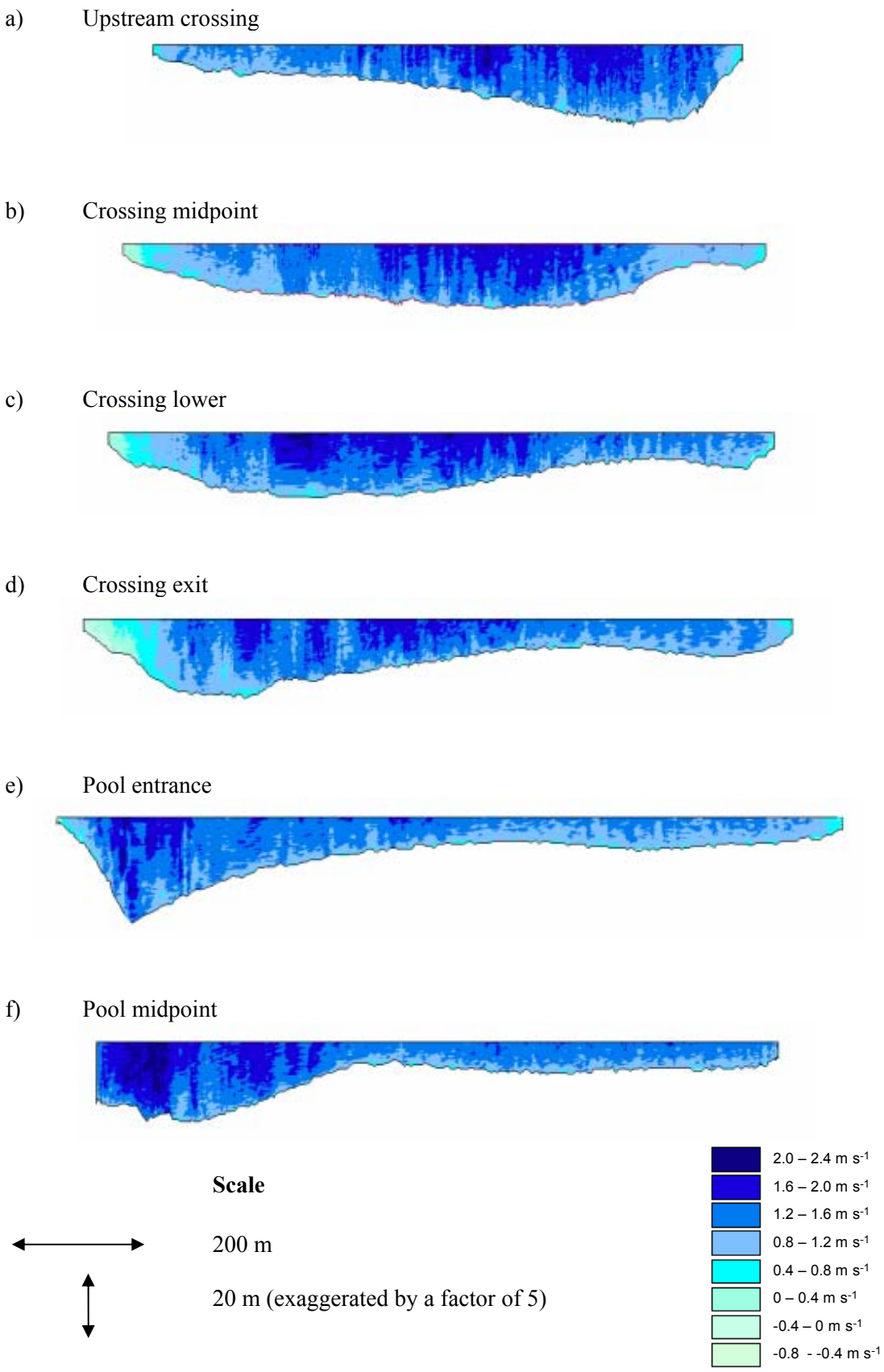

Figure 7.20 TIN surfaces of resolved downstream velocities (parallel to the channel centre-line) at each selected flow cross-section for high flow stage on the 7th April 2002.

a) Upstream crossing

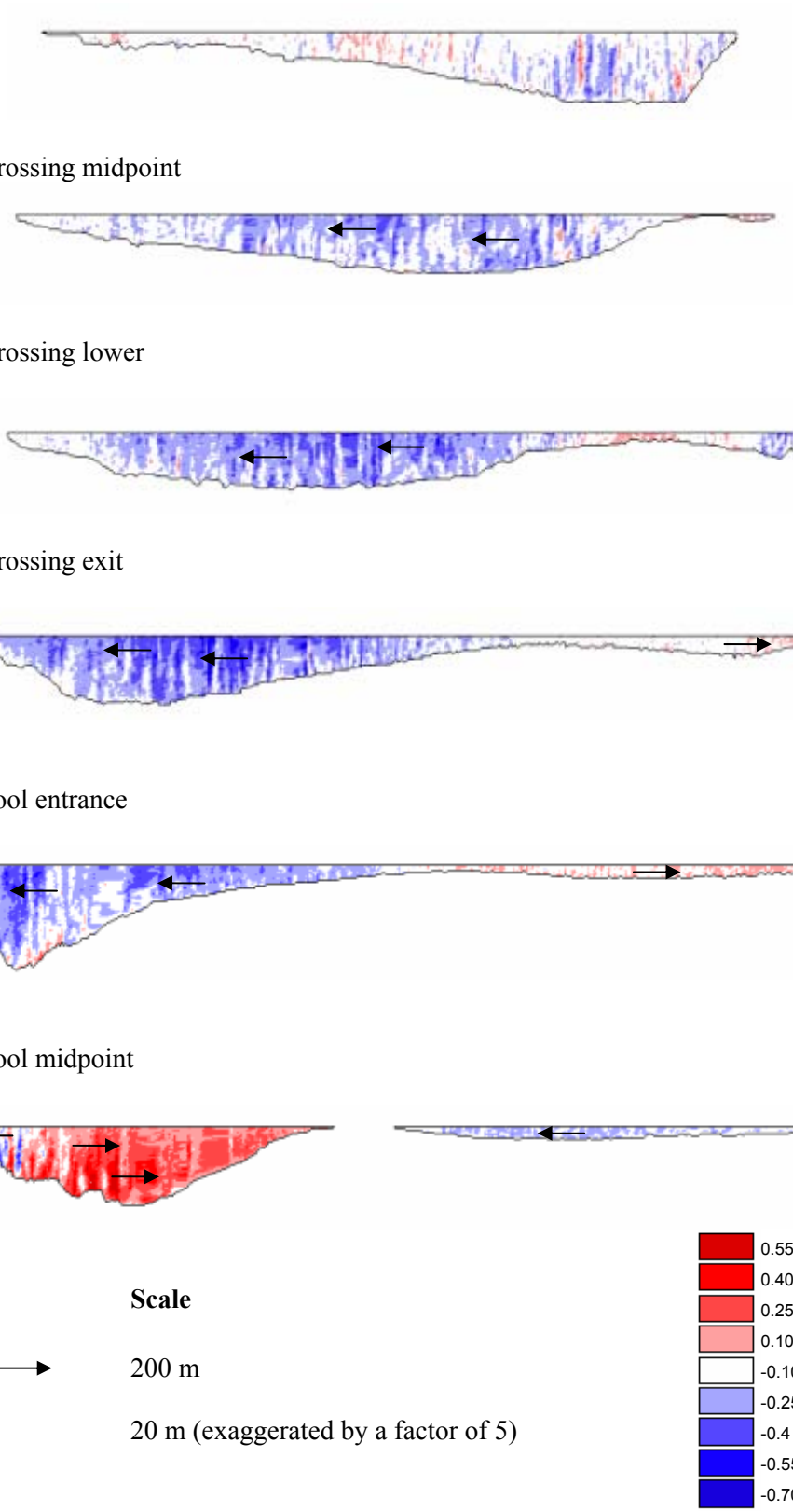

Figure 7.21 TIN surfaces of resolved cross-stream velocities (perpendicular to the channel centre-line) at each selected flow cross-section for low flow stage on the 19th January 2002.

a) Upstream crossing

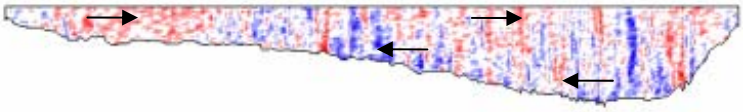

b) Crossing midpoint

c) Crossing lower

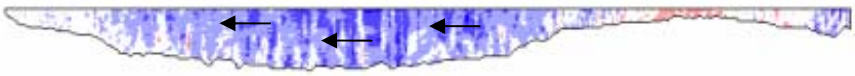

d) Crossing exit

e) Pool entrance

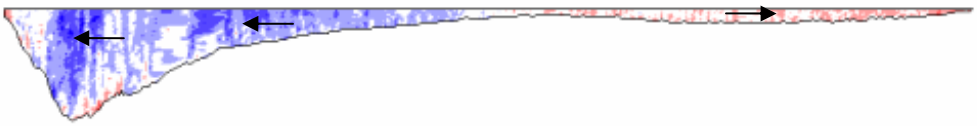

f) Pool midpoint

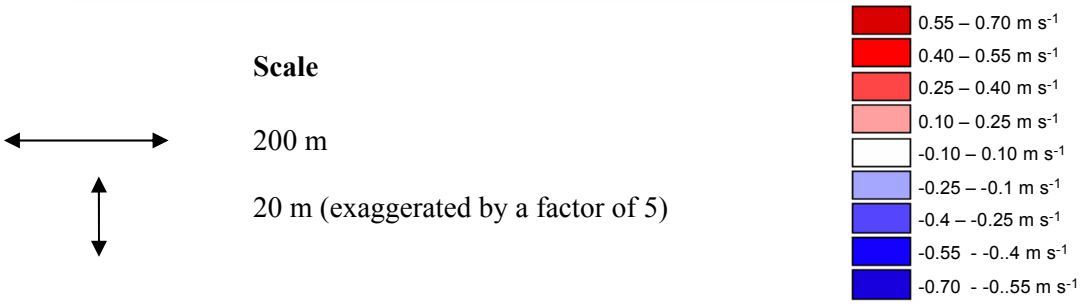

Figure 7.22 TIN surfaces of resolved cross-stream velocities (perpendicular to the channel centre-line) at each selected flow cross-section for high flow stage on the 7th April 2002.

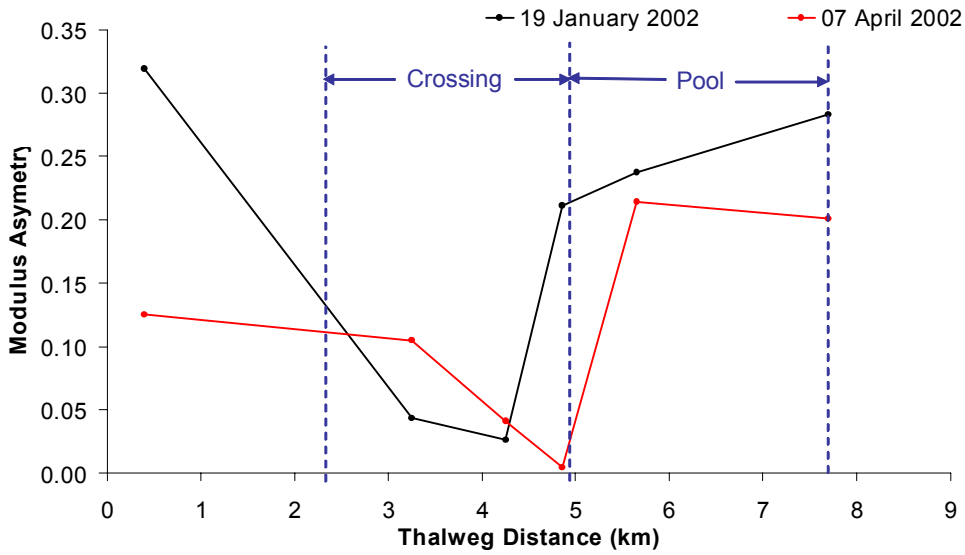

Figure 7.23 Comparison of asymmetry in the resolved downstream velocity distribution between channel locations within the sub-reach: at a low flow stage of 4.6 m above NGVD on 19th January 2002 and; at a higher flow stage of 10.7 m above NGVD on the 7th April 2002.

hydrodynamics, the flow cross-sections can therefore be imagined as being samples from a single cell of helicoidal flow.

ii) Pool-crossing maintenance

In Figure 7.24, the magnitude and distribution of resolved downstream velocities at each section is visualised by plotting the cumulative area of each section that exceeds a range of threshold velocities. In terms of velocity magnitude, the highest point velocities in the sub-reach are located at the pool midpoint section at both low and high flow stage. Meanwhile, the crossing exit exhibits the lowest average point velocities at both low and high flow stage. This velocity pattern is consistent with observed aggradation at the crossing and proposed degradation at the pool as flow stage falls but does not seem intuitively consistent with observed degradation at the crossing and proposed aggradation in the pool as flow stage rises. However, it is the distribution and range of velocities close to the channel bed which is most important in controlling the transport of bed material and hence, determining morphological change.

As flow stage rises, Figure 7.25 reveals that the rate of increase of average near-bed velocity is greater at the pool mid-point section than at the crossing mid-point section. This is consistent with the observed pattern of aggradation and degradation with variations in flow stage. At low flow stage, the point bar on the convex right bank (looking upstream) of the pool midpoint section is only just submerged and therefore, near-bed velocities over a relatively large proportion of the channel wetted perimeter are relatively low (Figure 7.19). Figure 7.26a reveals that although near-bed velocities are highest at the pool midpoint section, a higher near-bed velocity is exerted over a greater wetted perimeter distance at the crossing midpoint section. For example an arbitrary near-bed velocity of 0.6 ms^{-1} is exceeded over 500 m of the wetted perimeter at low flow stage in the crossing midpoint section but just 316 m in the pool midpoint section. Therefore, the distribution of near-bed velocities at low flow stage is not inconsistent with greater scour at the crossing. As flow stage rises, the flow depth over the point bar in the pool midpoint section increases and hence, this is responsible for the significant increase in average near-bed velocity. Scoured material from the pool is deposited at the crossing where the rate of increase of near-

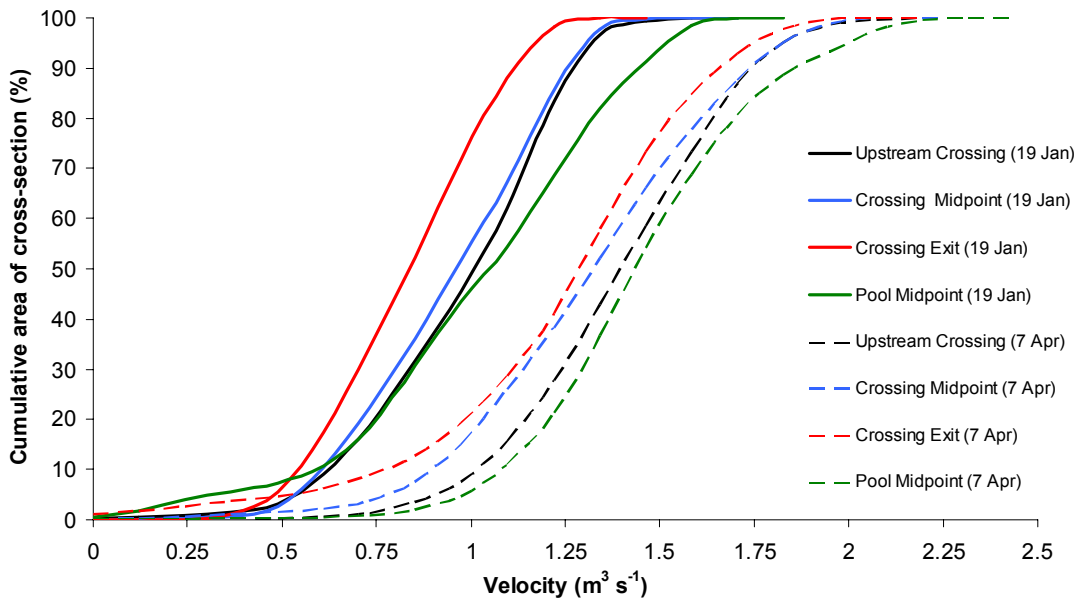

Figure 7.24 Percentage area of cross-section less than a series of threshold velocities for four selected cross-sections at a low flow stage of 4.6 m above NGVD on 19th January 2002 and at a higher flow stage of 10.7 m above NGVD on the 7th April 2002. Flow stages are recorded at Baton Rouge. Area was calculated from a TIN topographic surface of each cross-section at each flow stage.

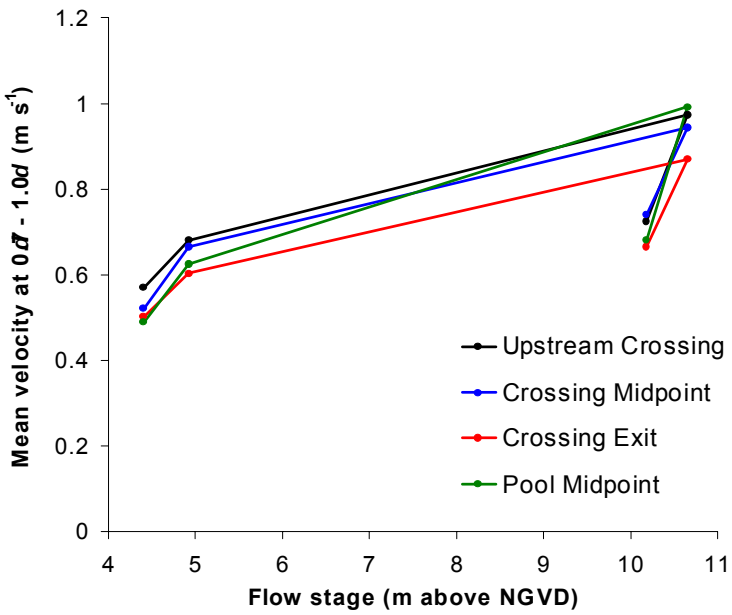

Figure 7.25 Change in mean bed velocity with flow stage, calculated as the average between 0.7 and 1.0 multiples of the depth. Survey dates are the 19th January 2002 (lowest flow stage), 15th March 2002, 7th April 2002 (highest flow stage) and the 22nd April (2002).

a)

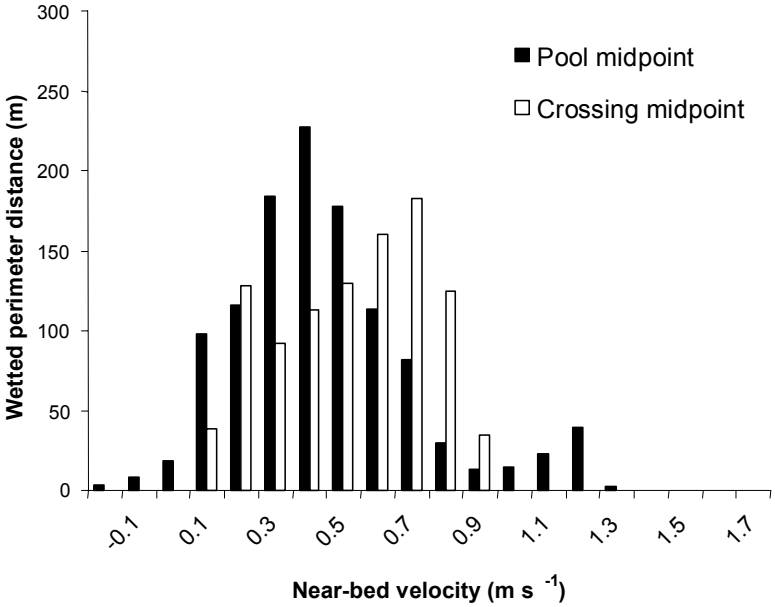

b)

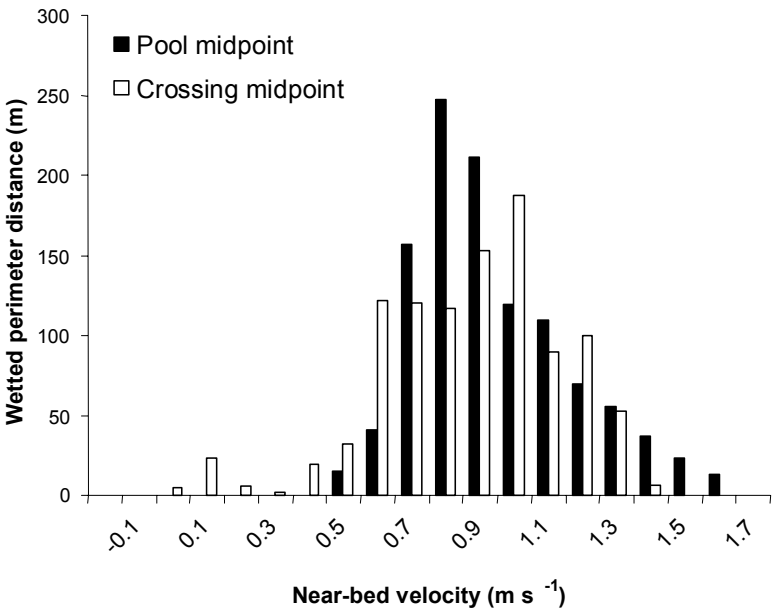

Figure 7.26 The distribution of near-bed velocities over the wetted perimeter a) at low flow stage on the 19th January 2002 and b) at high flow stage on the 7th April 2002. Near bed velocity is the point-averaged velocity for points between 0.7 and 1.0 multiples of the flow depth.

bed velocity with increasing flow stage is suppressed by increasing form resistance caused by dune field development.

In terms of morphological changes, the above mechanism suggests that it may be misleading to identify the pool midpoint section as a zone of net sediment deposition at low flow because most material may be deposited onto the point bar adjacent to the pool. This is difficult to verify through analysis of surfaces of difference because the point bar is frequently exposed at very low flow stages. Hence, the location of the area of active scour and fill within the pool area does demand further research.

iii) Bedform feedbacks

The velocity distribution coefficient (α) provides an alternative measure of distribution by describing the variation in average velocity between channel segments defined by sampling verticals. Calculated values of α in Figure 7.27 are within the range 1.04 – 1.41. These values are at the lower-end of the 1.09 - 2.90 range for natural, regular trapezoidal channels, as reported by Hulsing *et al.*, (1966). This relative uniformity in the distribution of the velocity field is perhaps surprising given that Red Eye crossing contains a dike field (Figure 7.10b). Hence, it may suggest that the effect of the dikes on flow velocity is predominantly only local and does not propagate through the entire cross-section velocity field.

With respect to variation with channel location and flow stage, Figure 7.27 reveals two interrelated findings. First, at both a low and high flow stage, the crossing midpoint and lower crossing have relatively high values of α in relation to the crossing exit and pool entrance. This is surprising given that Clifford and Richards (1992) report lowest α-values at riffle mid-points on the River Quarme at all flow stages surveyed. Examination of Figures 7.19 and 7.20 shows that, in these sections, a series of localised threads or filaments of high magnitude velocity exist across the section. It is reasonable to hypothesise that these complex flow structures are caused by bedform development in the crossing. It is recommended that further research is undertaken to investigate modifications of the velocity field caused by bedform development. If proven to be correct however, this is an example of a 'bottom-up' form of morphological conditioning of the velocity field. Second, velocity does

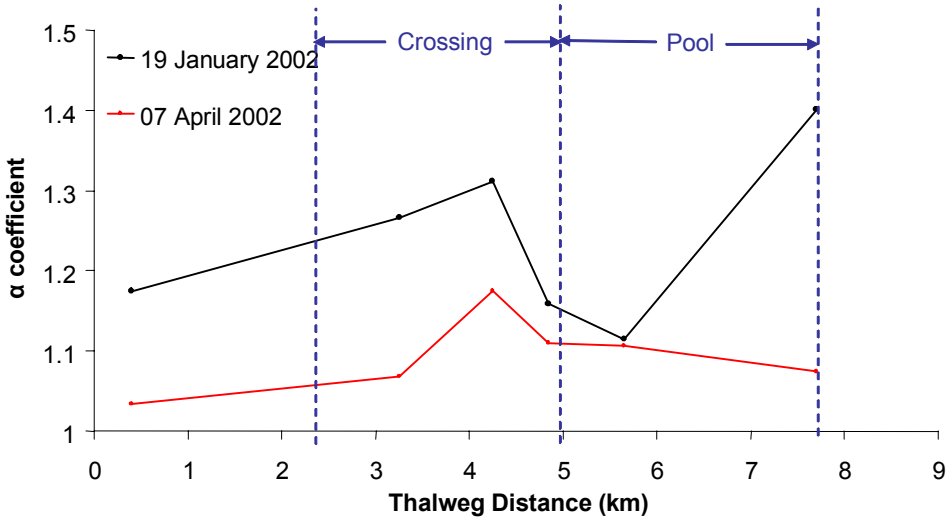

Figure 7.27 Comparison of the velocity distribution coefficient (α) in the resolved downstream velocity distribution between channel locations within the sub-reach: at a low flow stage of 4.6 m above NGVD on 19th January 2002 and; at a higher flow stage of 10.7 m above NGVD on the 7th April 2002.

become more evenly distributed at high flow, therefore, supporting analysis based on flow asymmetry. This is particularly the case in the pool which in fact has a more uniform velocity distribution than the crossing at high flow stage.

7.5 Discussion

In the following discussion, the results and analysis presented in this chapter are integrated to consider the implications for informing larger-scale and longer-term geomorphological behaviour.

7.5.1 Multiple scales of morphological and process dynamics

The multiple scales of morphological and process dynamics identified in this chapter demonstrate the difficulties of explaining larger-scale and longer-term behaviour from 'bottom-up' approaches.

At annual intervals and at the reach-scale, analysis reveals that, although sequences of morphological changes can be traced between adjacent pool-crossing units and over 1-2 year intervals, over a ten-year interval, the magnitude, order and location of observed changes becomes difficult to explain. This is because morphological changes in each pool-crossing unit are not only driven by variations in flow stage, but also by the nature and rate of bed material supply. At sub-annual timescales, analysis of bed material movement in a single pool-crossing unit (Red Eye Crossing and downstream Missouri Bend) suggests that over longer annual timescales, bed material moves downstream as a series of discrete translational waves, as noted on other rivers (Meade, 1985; Gomez *et al*, 1989; Hoey and Sutherland, 1991). Hence, predicting longer-term morphological changes at the reach-scale on the Lower Mississippi River relies upon improving understanding of the variation and nature of bed material wave movement downstream. Although this may sound like a relatively simple future research objective, this is actually very complex because analysis at smaller scales shows that bed material waves move into, and out of, a single pool-crossing unit through the formation and destruction of smaller-scale bedforms.

Reconstructing rates of bed material movement even at the sub-reach scale is therefore difficult because of complex spatio-temporal bedform dynamics.

Explaining geomorphological behaviour from a solely bottom-up approach is partly problematic because fluvial morphology demonstrates some characteristics of an emergent system (Davies, 1987; Johnson, 2001) where properties emerge from bottom-up interactions at larger spatial and temporal scales. For instance, a complete knowledge of dune formation and development processes would not enable explanation of the movement of translational waves between adjacent pool-crossing units. Emergent properties further complicate an already complex system by adding new variables and changing the nature of relationships between existing variables in the system. The presence of a bed material wave for example will modify characteristics of the velocity field, and therefore, change the nature of process-form relations. Thus, even with a sound understanding of fundamental physical dynamics at one scale, it is possible for the system to exhibit unpredictable behaviour at larger spatio-temporal scales.

Multiple scales of dynamics in the alluvial channel system cannot solely be explained in terms of emergent properties however, because order arrives from the 'top-down' as well as the 'bottom-up.' Top-down behaviour can be considered in two respects. First, morphological properties higher up the space-time hierarchy (Figure 1.2) provide the larger-scale boundary conditions within which smaller-scale process-form relations operate. For example, process-form relations in the Red Eye crossing sub-reach are at least partially dependent on the reach-scale slope and planform characteristics. Second, to maintain a level of stability, rivers attempt to adopt a morphological configuration that satisfies regional-scale requirements for flow resistance. Hence, a higher level (top-down) system control does exist which effectively precludes explanations based solely on bottom-up approaches.

Given that scale relations exist from both the bottom-up and top-down, geomorphological behaviour can only be explained with reference to continual spatially distributed feedback mechanisms (Richards, 1990) operating between the velocity field and the morphological configuration at a range of scales. Analysis of

velocity field dynamics revealed two scales of such mechanisms. At the larger reach and regional-scales, the existence of a coherent hydrodynamic flow structure at both low and high flow stages through the Red Eye Crossing and Missouri Bend sub-reach is consistent with the idea that pool-crossing undulations in the long profile are related to the cells of helocoidal flow motion. This hydrodynamic structure is at least partially conditioned by pre-existing cross-section shape. At the sub-reach scale meanwhile, the movement of bed material waves is closely related to the changing spatial distribution of near-bed velocities with variations in flow stage. These changes cannot be explained by any single mechanism, but are rather a product of cross-section shape and smaller-scale bedform development; both of which condition the larger-scale hydrodynamic flow structure.

The complex morphological configuration at the sub-reach scale is therefore conditioned by a large-scale hydrodynamic process but is also adjusted in order to satisfy local flow resistance requirements. Thus, to a certain degree, the fluvial system self-organises through the operation of spatially-distributed form-process feedbacks mechanisms to an optimum, but inherently unpredictable morphological configuration in which cause and effect are very difficult to isolate. From a methodological perspective, the presence of regional-scale and sub-reach scale components in the morphological configuration justifies the use of stochastic techniques such as second-order autoregressive modelling at larger scales in chapters 4, 5 and 6.

7.5.2 Issues of representation

A more general (and perhaps more fundamental) problem involves the degree to which studies of a single reach, or sub-reach, can be considered to be representative of more general dynamics.

Given the reach-scale and temporal variations in planform and long profile noted in chapters 4, 5, and 6, it is possible that the annual-interval pool-crossing dynamics discussed in section 7.2 may not be representative of longer-term, or larger-scale, morphological behaviour. It is therefore recommended that representativeness is

explored by extending analysis further downstream and over a longer time period. The latter can be achieved by digitising existing hardcopy hydrographic survey data sets that extend back to the mid-1960s. Analysing changes in the pool-crossing configuration over this longer period would be particularly interesting because it would allow more detailed understanding to be developed of spatial and temporal large-scale bedform configurational changes associated with the 1973-74 flood event (section 6.3).

At the sub-reach scale, issues of representativeness can be considered in at least three respects. First, given the differences between the characteristics of the pool-crossing configuration in the alluvial valley and the deltaic plain (chapter 5), further research must be undertaken at selected sub-reaches in the alluvial valley to examine the degree of association with observations made at Red Eye Crossing. Second, Harbor (1998) has suggested that differences in the bedform morphology of three sub-reaches in the USACE Vicksburg District (from the confluence of the Arkansas River to 8 km upstream from Old River distributary) can be explained by differences in the planform morphology. This is not surprising, given that the planform is an important control on the spatial patterns, and therefore, the hydraulics of flow. However, additional analysis is required to examine the extent to which sub-annual scale sediment movement varies between sub-reaches with different planform characteristics. Finally, Red Eye is a diked crossing. Dike fields aim to reduce dredging requirements by constraining flow to a narrower channel width, thereby increasing flow velocity and through time, increasing channel depth. Thus, it is not unreasonable to suggest that the presence of the dike field may have reduced the relative differences in flow velocity between Red Eye crossing and downstream Missouri Bend, and consequently, suppressed the movement of bed material waves at sub-annual timescales. According to this reasoning, morphological dynamics at this timescale may therefore be greater elsewhere on the Lower Mississippi River. To test this hypothesis, it is recommended that additional research is performed into form-process relations in sub-reaches that do not contain dike fields.

CHAPTER 8. CONCLUSION

The results and discussion contained within the previous chapters form the basis of a scale-integrated approach within which to characterise geomorphological response to engineering intervention. The concluding discussion considers how this approach advances current understanding of geomorphological response, outlines its wider implications for studying large-scale geomorphological behaviour of rivers, and makes recommendations for further research.

8.1 Understanding of geomorphological response

Results presented in chapters 4 to 6 show that morphology of the Lower Mississippi River was naturally highly dynamic prior to engineering modification with respect to its planform, and since a fixed alignment has been enforced, has retained a dynamic morphology with respect to its long profile and cross-sectional form.

Prior to major engineering modification (chapter 4), the Lower Mississippi River adjusted its morphology to satisfy regional-scale form resistance requirements through changes to its planform. This was achieved through adjustments to channel length, width, and bend size and shape properties. Analysis reveals that reaches of consistent planform characteristics were an entirely natural characteristic of the Lower Mississippi River. These reaches were transient features, typically persisting for up to 120 years. Hence, reaches were continually formed and modified through intrinsic planform adjustments (meander bend growth and cutoff cycle) and consequently, process-form behaviour varied between adjacent reaches and through time. On the post-modification Lower Mississippi River, planform reaches still exist although they have become fixed through bank stabilisation. Thus, geomorphological dynamics must now operate in a constrained channel system.

Despite the temporal variation of planform reaches on the pre-modification river, six temporally-consistent reaches are identified between Cairo and Baton Rouge, defined mainly by tributary confluences. Analysis of planform properties about these six reaches reveals two important findings regarding the location and timing of the artificial cutoff programme on the Lower Mississippi River. In terms of location,

analysis reveals that the artificial cutoff reach (downstream from Memphis to just upstream from the Old River distributary) exhibited the greatest rates of length changes, the lowest median radius of curvature, and generally more complex compound meander bend forms than other reaches. Constructing artificial cutoffs in this reach therefore not only increased slope and hence, stream power, but also maximised the total form resistance loss (exerted by the planform).

Regarding timing, prior to the artificial cutoff programme in 1930, the Lower Mississippi River had widened significantly over the previous 100 years and had lengthened by 75 km since 1887. Net lengthening was at least partially a result of the 'no-cutoff policy' adhered to by the Mississippi River Commission between 1887 and the dramatic flood in 1927 (Moore, 1972). In addition, sediment loads in 1930 may have been elevated by riparian vegetation clearance throughout the alluvial valley and changing land use practices within the wider drainage basin (Winkley, 1977; Prince, 1997). Thus, the artificial cutoff programme was undertaken at a time of relatively low stream power per unit width and relatively high rates of sediment supply. Since channel shortening through the formation of neck and chute cutoffs was observed between 1830 and 1887 following an earlier period of net lengthening between 1765 and 1830, it is likely that, without the artificial cutoff programme, a degree of 'natural' shortening would have been expected in the following decades. Hence, part of the channel shortening caused by the artificial cutoff programme would have been expected without engineering intervention and therefore, this may have contributed to observed longer-term geomorphological response. Thus, the complex spatial and temporal dynamics in the pre-modification period demonstrate that elucidating large-scale alluvial river response is a very difficult task.

In the post-cutoff period (1949-1989), extensive bank stabilisation has effectively restricted morphological adjustments to the long profile. Analysis in chapter 6 shows that, between the confluence of the Arkansas River and Old River distributary, the Lower Mississippi River has adjusted to engineering modification at two principal scales. First, at the reach-scale, the channel thalweg degraded throughout the reach between 1949 and 1964. Rates of degradation were highest from the confluence of the Arkansas River to the confluence of the Yazoo River at Vicksburg (reach 4). Through time, rates of degradation declined, to the extent that in the downstream

reach, from the confluence of the Yazoo River at Vicksburg to Old River distributary (reach 5), a slight aggrading trend was actually observed between 1975 and 1989. Second, at the smaller, sub-reach scale, the longitudinal pool-crossing configuration has adjusted to reach-scale changes in profile slope. In reach 4, the frequency of pool-crossing undulations increased between 1949 and 1964, particularly in the straightened reaches where artificial cutoffs had been constructed. This is consistent with the idea that the high rate of degradation and hence, channel steepening in this reach during this time period is offset by an increase in the bedform resistance. Meanwhile, in reach 5, the greater relative stability of pool and crossing characteristics over the 1949-1989 time period is consistent with the much smaller magnitude changes in reach-scale profile slope.

In relation to Biedenharn and Watson's (1997) conceptual model of response (Figure 2.15), analysis of spatio-temporal variations in the channel thalweg elevation confirm that dynamic reaches of consistent response can be identified on the Lower Mississippi River. However, changes in the channel thalweg elevation show a tendency to lag behind changes in water surface elevation. For example, between Arkansas City and Vicksburg (approximately coincident with reach 4), the reach defined by Biedenharn and Watson as being in 'dynamic equilibrium' is only stable with respect to changes in the thalweg elevation between 1975 and 1989. Prior to this period, a degradational trend is recorded. Furthermore, the reach identified by Biedenharn and Watson as aggrading (reach 5) is only aggrading with respect to changes in thalweg elevation between 1975 and 1989. Both slight degradation and a period of stability are experienced before this time. The apparent lag between reach-scale changes in water surface elevation (from specific gauge records) and reach-scale changes in thalweg elevation is at least partially accounted for by the sub-reach scale changes outlined above. In relation to understanding large-scale geomorphological behaviour, this therefore emphasises the importance of first, taking into account all possible degrees of freedom by adopting a holistic research and second, being careful with appropriate timescales of analysis.

The fitting of a water surface to stage-discharge relations for a relatively low flow (10 000 m^3s^{-1}) using a 1-D step-backwater model demonstrated that the area increased (and hence, flow velocity decreased) in pools and crossings in both reaches

4 and 5 between 1949 and 1989. In reach 4, it is therefore proposed that the increase in the frequency of pools and crossings increased large-scale bedform resistance and therefore, increased flow stage through a reduction in flow velocity. Relating back to Biedenharn and Watson (1997), this increase in flow stage offset the reduction caused by net degradation and hence, explains the absence of a discernable temporal trend in water surface elevation in the 1950-1994 time period when the channel thalweg was degrading. In reach 5 meanwhile, the greater longitudinal stability of pools and crossings is not consistent with the decrease in flow velocity and increase in flow stage between 1949 and 1989. However, analysis of changes in cross-sectional form revealed that longitudinal stability masks a decline in the width-depth ratio of pools over the period. Therefore, it is proposed that the increase in flow stage in reach 5 was driven by adjustments to the cross-sectional form, an additional component of total form resistance.

Changes in form resistance through adjustments at the sub-reach scale also go some way to resolving the geomorphological paradox reported by Biedenharn *et al*. (2000). The steepening of channel slope by the artificial cutoff programme, and consequent increase in stream power, has not necessarily caused an increase in rates of bed material transport and/or coarsening of the bed material, as suggested by Lane's (1955) qualitative relation, because at least some of the additional energy has been expended in overcoming additional form resistance, despite the lack of adjustment in planform.

Although analysis identifies decadal-interval and reach-scale morphological response to engineering intervention, chapter 7 demonstrates problems that remain in explaining this behaviour. At annual timescales, analysis of the channel thalweg changes revealed a strong tendency for pool-crossing maintenance rather than configurational adjustments. Morphological changes that did occur were greatest following very high or very low discharge events. Explaining morphological changes in any single sub-reach is problematic because changes are the collective result of a range of feedbacks between adjacent pool-crossing units. Thus, the order and location of changes over relatively long reaches of the Lower Mississippi River is very difficult to predict.

As a first step, improving understanding of feedback operation requires a better understanding of the nature and rate of bed material movement through pools and crossings and associated form-process interrelationships. Detailed analysis of the morphological dynamics of the Red Eye Crossing and Missouri Bend sub-reach in the deltaic plain have shown that the variations in pool-crossing morphology within a single water year are typically of greater magnitude than variations between consecutive low water seasons. Red Eye crossing aggrades and degrades with the rise and fall of flow stage respectively, and the magnitude of vertical change is related to the magnitude of change in flow stage. Carey and Keller (1957) report that this sub-annual variation is typical of pool-crossing sub-reaches on the Lower Mississippi River and, this is consistent with the idea that bed material moves as a series of translational waves with variations in flow stage (Meade, 1985; Gomez *et al.*, 1989, Hoey and Sutherland, 1991). Aggradation and degradation of the crossing with variation in flow stage is shown to be related to changes in the velocity field, albeit in a more complex manner than is suggested by Lane and Borland (1953). Although the difference in section shape between pools and crossings is important, there is no simple reversal of section-averaged velocity based on changes in cross-sectional area. Rather, aggradation of the crossing as flow stage rises is driven by changes to the near-bed velocity field caused by differences in cross-section shape and complex bedform feedback mechanisms.

These observations have important implications for the way in which geomorphologists view dynamic behaviour between scales. Decadal-interval morphological changes cannot easily be explained by observing annual-interval morphological changes. Similarly, at smaller spatio-temporal scales, seasonal changes in pool-crossing morphology cannot easily be explained by observing dynamics in the process regime. Hence, although shorter timescale and smaller space-scale processes may have implications for longer timescale and larger space scale processes (Lane and Richards, 1997) explaining large-scale and long-term geomorphological behaviour is more complicated than simply scaling from the 'bottom-up'. The process of scaling-up is complicated by three factors: the emergence of properties that are unpredictable from initial conditions; the influence of 'top-down' conditioning behaviour; and the continual operation of spatially-distributed form-process feedbacks which change the boundary conditions imposed

by morphology and hence, continually modify the nature of form-process relations. Therefore the nature of scale relations in geomorphology may be closer to Schumm and Lichty's (1965) early proposition that the nature of physical relationships changes with the space and time scale at which they are observed.

8.2 Significance of geomorphological response

The U.S. Army Corps of Engineers are effectively committed to long-term maintenance of existing engineering structures on the Lower Mississippi and to the design and implementation of future management policies. Two findings from this thesis are potentially significant in informing such policy.

First, it is clear from results presented in chapter 6 that engineering intervention in the twentieth century has not generated a period of prolonged geomorphological instability, despite representing the greatest disturbance to the geomorphology of the Lower Mississippi River, certainly since 1765, and possibly during the occupation of the present meander belt over the last 2000 years (Saucier, 1994). The most dramatic reach-scale and sub-reach scale morphological changes occurred between 1949 and 1964, within 22 years of the end of the artificial cutoff programme. Although some reach-scale changes have occurred after 1964 (particularly in reach 4) the magnitude of these changes was considerably less than in the earlier period. Considering the socio-economic and political benefits of the MR & T Project (chapter 2), the relatively short geomorphological response may support the 'man over nature' philosophy that prevailed in the early and mid twentieth century (Reisner, 1986). However, channel morphological changes within the alluvial valley may not be the most significant geomorphological consequence of the by the MR & T Project. For example, dramatic increases in the rate of land loss in the delta have been attributed to the dramatic decline in sediment loads throughout the twentieth century as well as to global sea-level rise (Kesel, 1988; Kesel and Yodis, 1992). Second, in an era where best practice engineering is considered that which harmonises the natural processes and forms of a river (Thorne *et al.*, 1997), the identification of reach-scale, and relatively short-term temporal (<20 year), variations in geomorphological behaviour is important because it indicates that management strategies will be most

appropriate in different reaches of the Lower Mississippi River over such time periods.

From a physical perspective, it is clear from analysis of planform dynamics in chapter 4 that engineering modification during the twentieth century represents the greatest disturbance to the Lower Mississippi River over the 1765-1975 period. Over a longer-term Holocene and Late-Wisconsin timescale however, the Lower Mississippi River has repeatedly demonstrated the ability to abruptly change its planform between braided, anabranching and single-thread meandering configurations in response to sometimes relatively dramatic changes in discharge and sediment regime (Porter and Guccione, 1994; Teller, 1990). This demonstrates that the actual geomorphological response associated with engineering modification are probably only of physical significance when viewed over a Late-Holocene timescale. Engineering modification may be unique however if it is able to prevent large-scale and relatively abrupt morphological changes in the future, such as meander-belt or distributary avulsion. Because such events are rare over timescales associated with engineering projects, it is possible therefore that the physical significance of engineering intervention has yet to be fully realised.

8.3 Representing dynamic geomorphological behaviour

In addition to informing geomorphological response to engineering intervention, this study has demonstrated the nature of process-form relations at a variety of spatial and temporal scales and emphasised the importance of understanding linkages between scales in order to understand the dynamics observed at any single scale. Existing conceptual models of process-form interrelationships (Figure 1.1) and scales of morphological adjustment (Figure 1.2) do not alone provide adequate representation of the nature of geomorphological behaviour because of their inability to show feedback mechanisms operating at a range of spatial and temporal scales. A revised representation integrates aspects of both models and is presented in Figure 8.1.

This representation recognises four principal spatial scales of morphology: regional-scale; reach-scale; sub-reach scale and bedform scale. Each spatial scale of

morphology is plotted on the space-time axes in Figure 8.1 to represent the magnitude and frequency of major 'formative' changes. At the regional-scale, formative adjustments to the planform and long profile of the Lower Mississippi River probably occur over timescales in the order of 10^4 - 10^5 years in response to climatic and related base-level (sea-level) variations (section 2.4.5). Reach-scale formative adjustments occur at timescales in the order of 10^3 years, by switching between a continuum of channel patterns: braided; anabranching; and meandering (Saucier, 1994). Sub-reach scale formative adjustments fall within the timescale of data sets analysed within this thesis, in the order of 10^1 and 10^2 years. Sub-reach scale adjustments incorporate variations in planform properties (channel length, width, and degree of curvature), long profile properties (magnitude and/or frequency of pool-crossing oscillations) and cross-sectional properties (width/depth ratio and degree of asymmetry). Finally, bedform-scale adjustments occur at shorter sub-annual timescales (10^{-1} – 10^0 years) in response to variations in flow stage.

At small spatial scales, results presented show that it is possible to relate morphological adjustments directly to changes in the process regime. Process signatures may be detected at three scales. First, at the sub-reach scale, comparison of meanders bend and pool-crossing spacing with existing empirical relations, in chapters 4 and 5 respectively, demonstrate possible adjustments to macroturbulent flow structures, scaled on channel width. Second, at a smaller scale, empirical analysis in chapter 7 showed that the spacing of dune bedforms may be related to macroturbulent flow structures scaled on channel depth. Finally, at an even smaller-scale, micro-dune bedforms may be a signature of microturbulent flow structures.

At larger spatio-temporal scales, morphological dynamics are more closely related to external morphological controls. This is demonstrated in chapter 4 where the distribution of channel length changes in the pre-modification period (indicative of the spatial variations in planform dynamics) is shown to be closely related to the distribution of resistant clay plug deposits within the contemporary meander belt (as identified by Hudson and Kesel, 2000). Over longer timescales, the distribution of these deposits is found to correlate strongly with neotectonic activity and extensive

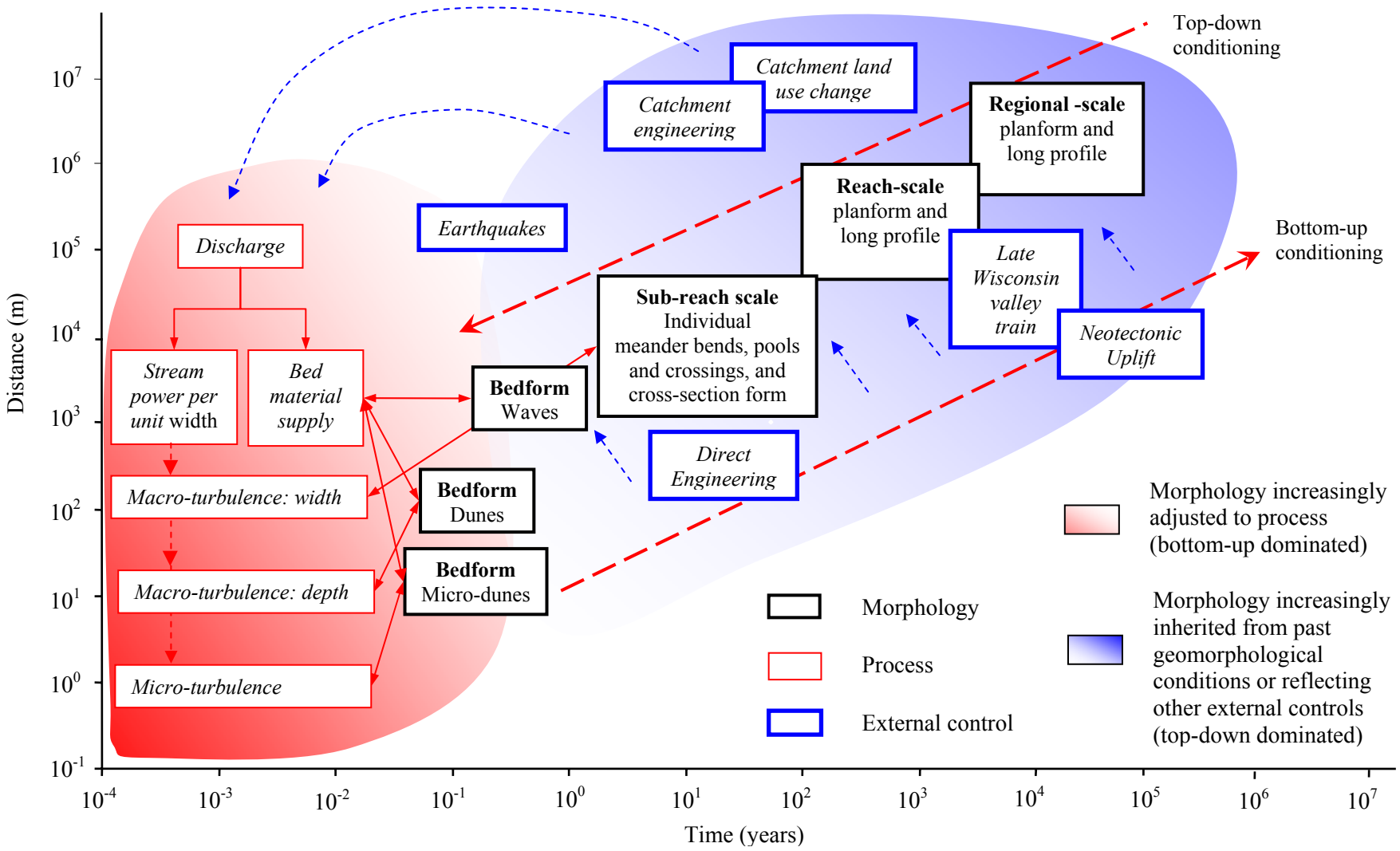

Figure 8.1 Representing spatially-distributed form-process feedback mechanisms in a scale-hierarchical framework

areas of coarse glacial outwash deposits in the alluvial valley. In chapter 5, it is proposed that the presence of deeper pools on the deltaic plain in relation to the alluvial valley reflects greater planform stability caused by more cohesive bank materials. Thus, at small spatio-temporal scales, observed morphology and morphological dynamics are largely process-driven from the 'bottom-up' whereas at larger spatio-temporal scales, 'top-down' contingent controls become increasingly important.

This hierarchy is important in terms of form resistance because it shows that regional-scale requirements for energy expenditure can be met by a series of internal morphological adjustments spanning a range of spatio-temporal scales. In this way, fluvial morphology can be described as self-organising to an optimum configuration. This is consistent with Phillips (1991) account of self-organisation in the wider landscape through 'multiple modes of adjustment.' The diversity of adjustments observed at each scale is a configurational product of spatially-distributed feedbacks between operating processes and diverse morphological boundary conditions caused by different reach or sub-reach histories. Hence, referring back to Simpson (1963), geomorphological behaviour is as much conditioned by spatial and temporal variations in the 'configurational' elements of the fluvial system, as the operation of 'immanent' processes.

Given that the morphological properties at any single scale within the hierarchy are conditioned by both top-down and bottom-up influences, but the relative strength of these is dependent on the relative position within the hierarchy of possible scales, it follows that different methodological approaches are appropriate to resolve geomorphological dynamics at different scales of analysis. This therefore supports the ideas of Church (1996; Table 1.3). In addition to the type of methodological approach, disentangling observed complexity at each scale, and identifying relationships between scales, relies upon using a range of analytical techniques. This is discussed in the following section.

8.4 Methodological approaches

From a methodological perspective, this analysis demonstrates that the multi-scaled and multivariate nature of alluvial channel dynamics can be adequately identified by adopting a GIS-based methodology and by applying a range of analytical techniques. Adoption of a GIS-based methodology is important for two reasons:

i) It allows easier and therefore, more detailed, analysis of older archival data sources such as historic planform maps and historic hydrographic surveys.

ii) It allows automated computation and visualisation of a wide range of morphological and process parameters.

Applying a range of analytical techniques at a range of scales emphasises the danger of relying on single parameter, single analytical technique, or single scale investigations to inform geomorphological behaviour. Chapter 4 demonstrated the dangers of drawing misleading conclusions from single parameter investigations because of miss-association (Mackin, 1963) or sensitivity to methods of computation. Miss-association can arise from relying on variables that do not adequately represent the property being investigated. For example, the sinuosity of a specific river reach may not necessarily be indicative of the formation of tighter bends that exert a greater form resistance (chapter 4). Sensitivity to method of computation is illustrated by the range of estimates of meander wavelength obtained from the three techniques used. The spatial and temporal pattern observed is heavily dependent on the technique used because each technique measures wavelength in a different way. Hence, dynamics can only be reliably reconstructed through parallel analysis of several complementary parameters.

Results presented in chapter 6 demonstrate the dangers of relying on single technique investigations. The conceptual model of geomorphological response presented by Biedenharn and Watson (1997) is misleading because it is based solely on changes of water surface elevation which do not account for changes in flow resistance and therefore, do not accurately reflect variations in the channel bed. In a similar fashion, Biedenharn and Thorne's (1994) assertion that mid-channel bars (crossings) are the active geomorphological feature of the contemporary Lower Mississippi

River is also misleading because, whilst this is supported if pool-crossing dynamics are considered longitudinally, it is not supported by analysis of cross-sectional changes.

Decomposition of the regional-scale concavity in the long profile in chapter 5 emphasises the danger of undertaking geomorphological investigations at single scales of analysis. A high proportion (95 percent) of the total variation can be described by a simple second-order polynomial function which may be suggestive of a relatively simple physical control. However, decomposition of the profile using a series of analytical techniques indicates that the profile is actually partly inherited form past geomorphological conditions, partly continually adjusting to long-term natural controlling variables and is partly a direct product of engineering modification. This shows that as a result large-scale spatially-distributed process-form feedbacks, morphological configurations can develop that appear relatively simple to interpret but are actually the result of a complex array of overlapping physical controls. Hence, the apparent concavity has little or no physical significance in its own right.

Together these findings therefore demonstrate that gaining understanding of the full complexity of large-scale geomorphological behaviour of river channels not only requires the undertaking of a number of parallel investigations, as stated by Thorne (2002), but these investigations must be based at a range of scales and performed by applying a series of appropriate analytical techniques. This supports Mackin (1963; 149) general view of empirical research:

> *'there is nothing wrong with it as a tool, but like most tools, how well it works depends on how intelligently it is used'.*

Thus, new technologies may be revolutionising the scales at which geomorphological dynamics can be observed on large alluvial rivers, but improving geomorphological understanding is ultimately dependent on the questions asked and the methodological approach adopted by the researcher.

8.5 Recommendations for further research

A series of recommendations for future research have arisen from this thesis. These may be based upon existing data sets or require the collection of new data sets.

8.5.1 Further research based on existing data sets

Analysis presented in this thesis has made only selective use of the range of spatial and temporal data sets available to the study (Table 2.4). Further advances in the understanding of large-scale geomorphological behaviour can be made in two ways:

First, the geomorphological response to imposed engineering intervention identified in chapter 6 using the decadal hydrographic surveys demonstrates the critical importance of repeated monitoring of the Lower Mississippi River over engineering timescales. It is recommended that this analysis is extended:

i) spatially to incorporate existing decadal hydrographic surveys within the USACE Memphis and New Orleans District so that geomorphological response is examined along the entire Lower Mississippi River from Cairo to the Head of Passes.

ii) temporally to incorporate the earliest hydrographic survey data sets (1879-93, 1911-21, and 1937-38). These have been digitised but were not considered in this thesis because the vertical datum has presently not been resolved to NGVD 1929. Processing of these early data sets would allow the long profile to be established for the pre-modification period, and hence an assessment of longer-term temporal changes in reach-scale slope and sub-reach scale pool-crossing configuration. It is therefore recommended that further efforts are made to resolve the vertical datum of early hydrographic surveys.

Second, it is recommended that existing annual hydrographic surveys for the USACE Vicksburg District, available in hardcopy format from the mid-1960s, are digitised to extend annual analysis beyond the 1991-2001 period considered in this study. Analysing changes in the pool-crossing configuration during this time period would

be particularly interesting because it would allow more detailed understanding to be developed of spatial and temporal configurational changes associated with the 1973-74 flood event.

8.5.2 Further research requiring new data sets

Understanding of geomorphological behaviour is conditioned by the available data sets. Most data sets collected in this thesis were collected as part of routine data monitoring programmes designed not explicitly for the purposes of geomorphological research. Although these data sets have proved extremely valuable to informing geomorphological behaviour at a range of spatio-temporal scales, routine measurements may be considered inappropropriate for informing geomorphological behaviour because the rate and nature of geomorphological dynamics are typically irregular in both time and space.

Given the range of new monitoring technologies available, it is important that future data collection efforts are focused on areas that will add most to the understanding of large-scale geomorphological behaviour. Two specific recommendations arise from this thesis. First, the major drawback with decadal and annual hydrographic survey data sets is that they have typically been collected at low flow stages, and therefore they do not contain adequate morphological information of the banks and bars that are exposed at such flows. As a result, analysis of morphological parameters computed using the 1-D step backwater modelling procedure in chapter 6 was restricted to a relatively low flow of 10 000 m^3s^{-1}. Although this analysis revealed interesting geomorphological changes, it is the near-bankfull flows which are thought to be of greatest geomorphological significance because of their association with dominant discharge (Wolman and Miller, 1960). Advances in airborne LiDAR technology (Woolard and Colby, 2002; Bielecki and Mueller, 2002; French, 2003) may allow hydrographic surveys at low flow stage to be combined with relatively rapid out-of-bank topographic surveys in the near future. It is therefore recommended that research is undertaken to examine the potential for surveying over-bank topography by such remote methods.

Second, to be more useful in informing larger-scale behaviour, there is a need to extend analysis at the sub-reach scale. This need can be partitioned in three ways:

i) 2-D topographic surface analysis in chapter 7 revealed that aggradation and degradation of Red Eye crossing, with the rise and fall of flow stage respectively, was not accompanied by clear reverse changes in the pool downstream at Missouri Bend. It is hypothesised that this is because the single beam and multi-beam sonar surveys of the sub-reach only extent into the upper portion of the downstream bend. It is recommended therefore that future surveys of individual sub-reaches include entire pool-crossing units.

ii) Analysis of a single case study sub-reach inherently invokes questions regarding its representativeness of other sub-reaches on the Lower Mississippi River. It is therefore recommended that sub-reach scale surveys are undertaken at a greater number of pool-crossing units, distributed throughout the alluvial valley and the deltaic plain. Sub-reaches should be selected to represent the diversity of planform configurations (relatively straight and very sinuous sub-reaches), the diversity of pool-crossing configurations, and the diversity of engineering interventions (dikes and bank revetments).

iii) It is recommended that a sampling strategy is developed at selected sub-reaches that allows the reconstruction of rates of bed material load movement through the coupling of 1-D and 2-D analytical techniques. This requires an increase in the temporal resolution of multi-beam sonar surveys. Providing estimates of rates of bed material movement through time between adjacent pool-crossing units is critical to improving explanation of observed longer-term changes in pool-crossing configuration.

APPENDIX A

The data files used in this thesis are stored on the accompanying CD-ROM. The contents can be viewed by opening the file titled '*CD Inventory.xls*' in Microsoft Excel. File titles that are colour-coded blue are Microsoft Excel files and will load automatically if selected from *CD Inventory.xls*. Data files are stored in two principal directories: raw data; and processed data. Within each directory, the data files are then stored according to the thesis chapter in which they are analysed.

REFERENCES

Abrahams, A. D. (1985) 'Lithologic control of bedrock meander dimensions in the Appalachian valley and ridge province: a comment', *Earth Surface Processes and Landforms*, 10, 635-638.

Ackers, P. and Charlton, F. G. (1970) 'Meander geometry arising from varying flows', *Journal of Hydrology*, 11, 232-252.

Allen, J. R. L. (1970) '*Physical processes of sedimentation*', Unwin University Books, London, 248pp.

Allen, J. R. L. (1983) 'River bedforms: progress and problems', in Collinson, J. D. and Lewin, J. (ed.), *Modern and ancient fluvial systems*, Blackwell, Oxford, 19-33.

Andrews, E. D. (1979) 'Scour and fill in a stream channel, East Fork River, western Wyoming', *United States Geological Survey Professional Paper 1117*.

Ashworth, P. J. and Ferguson, R. I. (1986) 'Interrelationships of channel processes, changes and sediments in a proglacial braided river', *Geografiska Annaler Series A - Physical Geography*, 68 (4), 361-371.

Autin, W. J. (1996) 'Pleistocene stratigraphy in the southern lower Mississippi Valley', *Engineering Geology*, 45 (1-4), 87-112.

Autin, W. J., Burns, S. F., Miller, B. J., Saucier, R. T. and Snead, J. I. (1991) 'Quaternary geology of the Lower Mississippi valley', in Morrison, R. B. (ed.), *Quaternary nonglacial geology: Conterminuous U.S.*, Geological Society of America, Boulder, CO, 547-582.

Bagnold, R. A. (1941) '*The physics of blown sand and desert dunes*', Methuen & Co. ltd., London, 265pp.

Bagnold, R. A. (1960) 'Some aspects of the shape of river meanders', *United States Geological Survey Professional Paper 282E*, 135-144.

Bak, P. and Chen, K. (1991) 'Self-organised criticality', *Scientific American*, 264, 26-33.

Bannister, A., Raymond, S. and Baker, R. (1998) '*Surveying*', Longman, Harlow, 502pp.

Barry, J. M. (1997) '*Rising tide: The great Mississippi flood of 1927 and how it changed America*', Simon & Schuster, New York, 524pp.

Bates, R. E. (1939) 'Geomorphic history of the Kickapoo Region, Wisconsin', *Bulletin of Geological Society of America*, 50, 819-880.

Beckinsale, R. P. and Chorley, R. J. (1991) '*The history of the study of landforms or the development of geomorphology*', Volume 3, Routledge, London, 496pp.

Best, J. L. (1996) 'The fluid dynamics of small-scale alluvial bedforms', in Carling, P. A. and Dawson, M. R. (eds.), *Advances in Fluvial Dynamics and Stratigraphy*, John Wiley & Sons, New York, 67-125.

Biedenharn, D. S. (April 2001) Personal communication, U.S. Army Corps of Engineers Waterways Experiment Station, Vicksburg, MS.

Biedenharn, D. S. and Thorne, C. R. (1994) 'Magnitude frequency analysis of sediment transport in the Lower Mississippi River', *Regulated Rivers-Research & Management*, 9 (4), 237-251.

Biedenharn, D. S., Thorne, C. R. and Watson, C. C. (2000) 'Recent morphological evolution of the Lower Mississippi River', *Geomorphology*, 34 (3-4), 227-249.

Biedenharn, D. S. and Watson, C. C. (1997) 'Stage adjustment in the Lower Mississippi River, USA', *Regulated Rivers: Research and Management*, 13, 517-536.

Bielecki, A. E. and Mueller, K. J. (2002) 'Origin of terraced hillslopes on active folds in the southern San Joaquin Valley, California', *Geomorphology*, 42 (1-2), 131-152.

Blench, T. (1969) '*Mobile-bed fluviology; A regime theory treatment of canals and rivers for engineers and hydrologists*', 2nd, University of Alberta Press, Edmonton, Alberta, Canada.

Box, G. E. and Jenkins, G. M. (1970) '*Time series analysis - forecasting and control*', Holden-Day, San Francisco, 553pp.

Braga, G. and Gervasoni, S. (1989) 'Evolution of the Po River: an example of the application of historic maps', in Petts, G. (ed.), *Historical Change of Large Alluvial Rivers: Western Europe*, John Wiley & Sons, 113-125.

Braun, D. D. (1983) 'Lithologic control of bedrock meander dimensions in the Appalachian Valley and Ridge province', *Earth Surface Processes and Landforms*, 8, 223-237.

Braun, D. D. (1985) 'Lithologic control of bedrock meander dimensions in the Appalachian Valley and Ridge province: a comment on a comment', *Earth Surface Processes and Landforms*, 10, 639-642.

Bravard, J. P. and Bethemont, J. (1989) 'Cartography of rivers in France', in Petts, G. (ed.), *Historical Change of Large Alluvial Rivers: Western Europe*, John Wiley & Sons, 95-111.

Brice, J. C. (1973) 'Meandering pattern of the White River in Indiana - an analysis', in Morisawa, M. (ed.), *Fluvial Geomorphology*, State University of New York, Binghampton, 180-200.

Brice, J. C. (1974) 'Evolution of meander loops', *Geological Society of America Bulletin*, 85, 581-586.

Brice, J. C. (1983) 'Planform properties of meandering rivers', in Elliott, C. M. (ed.), *River Meandering*, American Society of Civil Engineers, New Orleans, 1-15.

Bridge, J. S. (2003) '*Rivers and floodplains: forms, processes, and sedimentary record*', Blackwell, Oxford, 491pp.

Brookes, A. (1988) '*Channelized rivers: perspectives for environmental management*', John Wiley & Sons Ltd, Chichester, 326pp.

Brunsden, D. and Thornes, J. B. (1979) 'Landscape sensitivity and change', *Transactions of the Institute of British Geographers New Series 4*, 463-484.

Burnett, A. W. and Schumm, S. A. (1983) 'Alluvial-river response to neotectonic deformation in Louisiana and Mississippi', *Science*, 222, 49-50.

Carey, W. C. and Keller, M. D. (1957) 'Systematic changes in the beds of alluvial rivers', *Journal of the Hydraulics Division, American Society of Civil Engineers*, 83 (HY4).

Carling, P. A., Williams, J. J., Golz, E. and Kelsey, A. D. (2000) 'The morphodynamics of fluvial sand dunes in the River Rhine, near Mainz, Germany, part 2. Hydrodynamics and sediment transport', *Sedimentology*, 47 (1), 253-278.

Carson, M. A. and Lapointe, M. F. (1983) 'The inherent asymmetry of river meander planform', *Journal of Geology*, 91, 41-45.

Chang, T. P. and Toebes, G. H. (1970) 'A statistical comparison of meander planforms in the Wabash Basin', *Water Resources Research*, 6, 557-578.

Changnon, S. A. (1996) 'The lessons from the flood', in Changnon, S. A. (ed.), *The Great Flood of 1993*, Westview Press, Oxford, 300-320.

Chen, X. Q., Zong, Y. Q., Zhang, E. F., Xu, E. G. and Li, S. J. (2001) 'Human impacts on the Changjiang (Yangtze) River basin, China, with special reference to the impacts on the dry season water discharges into the sea', *Geomorphology*, 41, 111-123.

Chorley, R. J. (1962) 'Geomorphology and general system theory', *United States Geological Survey Professional Paper 500-B*, 10pp.

Chorley, R. J., Schumm, S. A. and Sugden, D. E. (1984) '*Geomorphology*', Methuen, London, 605pp.

Chow, V. T. (1959) '*Open channel hydraulics*', McGraw-Hill, Tokyo, 680pp.

Church, M. (1996) 'Space, time and the mountain - how do we order what we see?' in Rhoads, B. L. and Thorn, C. E. (ed.), *The Scientific Nature of Geomorphology*, John Wiley & Sons Ltd, Chichester, 147-170.

Clifford, N. J., Hardisty, J., French, J. R. and Hart, S. (1993) 'Downstream variation in bed material characteristics: a turbulence-controlled form-process feedback mechanism', in Best, J. L. and Bristow, C. S. (ed.), *Braided Rivers*, The Geological Society, London, 89-104.

Clifford, N. J. and Richards, K. S. (1992) 'The reversal hypothesis and the maintenance of riffle-pool sequences: a review and reappraisal', in Carling, P. A. and Petts, G. (ed.), *Lowland Floodplain Rivers: geomorphological perspectives*, Wiley, Chichester, 43-70.

Coates, D. R. and Vitek, J. D. (1980) '*Thresholds in geomorphology*', Allen and Unwin, London, 498pp.

Coleman, J. M. (1969) 'Brahmaputra River channel processes and sedimentation', *Sedimentary Geology*, 3, 129-239.

Curran, P. J., Milton, E. J., Atkinson, P. M. and Foody, G. M. (1998) 'Remote sensing from data to understanding', in Longley, P., Brooks, S., Macmillan, W. and McDonnell, R. (eds.), *Geocomputation: a primer*, John Wiley & Sons Ltd, Chichester, 33-59.

Dalrymple, R. W. (1984) 'Morphology and internal structure of sandwaves in the Bay of Fundy', *Sedimentology*, 31 (3), 365-382.

Dardeau, E. A. and Causey, E. M. (1990) 'Downward trend in Mississippi River suspended-sediment loads', *U.S. Army Corps of Engineers Potamology Program (P-1), Report 5*, Waterways Experiment Station, Vicksburg, MS, 67pp.

Davies, T. R. and Sutherland, A. J. (1980) 'Resistance to flow past deformable boundaries', *Earth Surface Processes*, 5, 175-179.

Davis, J. C. (2002) '*Statistics and data analysis in geology*', 3rd edition, John Wiley & Sons Ltd, London, 638pp.

Davis, W. M. (1899) 'The geographical cycle', *Geographical Journal*, 14, 481-504.

Denning, J. (1994) When the levee breaks *Civil Engineering*, 38-41.

Dinehart, R. L. (2002) 'Bedform movement recorded by sequential in tidal rivers', *Journal of Hydrology*, 258, 25-39.

Dixon, L. F. J., Barker, R., Bray, M., Farres, P., Hooke, J. M., Inkpen, R., Merel, A., Payne, D. and Shelford, A. (1998) 'Analytical photogrammetry for geomorphological research', in Lane, S. N., Richards, K. and Chandler, J. H. (eds.), *Landform Monitoring, Modelling and Analysis*, John Wiley and Sons Ltd, Chichester, 63-94.

Douglas, D. H. and Peucker, T. K. (1973) 'Algorithms for the reduction of the number of points required to represent a digitised line or its caricature', *The Canadian Cartographer*, 10 (2), 112-122.

Douglas, I. (1982) 'The unfulfilled promise: earth surface processes as a key to landform evolution', *Earth Surface Processes and Landforms*, 7, 101.

Downs, P. W. and Priestnall, G. (1999) 'System design for catchment-scale approaches to studying river channel adjustments using a GIS', *International Journal of Geographical Information Science*, 13 (3), 247-266.

Dunn, R., Harrison, A. R. and White, J. C. (1990) 'Positional accuracy and measurement error in digital databases of land use: an empirical study', *International Journal of Geographical Information Systems*, 4 (4), 385-398.

Dury, G. H. (1964) 'Principles of underfit streams', *United States Geological Survey Professional Paper, 452A*.

Dury, G. H. (1970) 'A resurvey of part of the Hawkesbury River, New South Wales, after 100 years', *Australian Geographical Studies*, 8, 121-132.

Elliott, D. O. (1932) '*The improvement of the lower Mississippi river for flood control and navigation*', U.S. Army Corps of Engineers, Waterways Experiment Station, Vicksburg, MS, 3 volumes.

Ferguson, R. I. (1975) 'Meander irregularity and wavelength estimation', *Journal of Hydrology*, 26, 315-333.

Ferguson, R. I. (1976) 'Disturbed periodic model for river meanders', *Earth Surface Processes*, 1, 337-347.

Ferguson, R. I. (1977) 'Meander sinuosity and direction variance', *Geological Society of America Bulletin*, 88, 212-214.

Ferguson, R. I. and Ashworth, P. J. (1992) 'Spatial patterns of bedload transport and channel change in braided and near-braided rivers', in Billi, P., Hey, R. D., Thorne, C. R. and Tacconi, P. (eds.), *Dynamics of Gravel-Bed Rivers*, Wiley, Chichester, 477-492.

Feringa, P. A. (1952) 'One hundred years improvement on the Lower Mississippi River', *U.S. Army Corps of Engineers*, 25pp.

Fisk, H. N. (1944) 'Geological investigation of the alluvial valley of the Lower Mississippi River', *U.S. Army Corps of Engineers Mississippi River Commission*, Vicksburg, MS, 78pp.

Fisk, H. N. (1947) 'Fine-grained alluvial deposits and their effects on Mississippi River activity', *U.S. Army Corps of Engineers, Mississippi River Commission*, Vicksburg, MS, 82pp.

Fisk, H. N. (1951) 'Mississippi river valley geology in relation to river regime', *The American Society of Civil Engineers*, (paper no. 2511), 667-682.

Fisk, H. N. and McFarlan, E. (1955) 'Late Quaternary deltaic deposits of the Lower Mississippi River', in: *The crust of the earth*, Special Paper 62, Geological Society of America, Boulder, CO, 279-302.

Fisk, H. N., McFarlan, E., Kolb, C. R. and Wilbert, L. J. (1954) 'Sedimentary framework of the modern Mississippi delta', *Journal of Sedimentary Petrology*, 24 (2), 76-99.

French, J. R. (2003) 'Airborne LiDAR in support of geomorphological and hydraulic modelling', *Earth Surface Processes and Landforms*, 28 (3), 321-335.

Friedkin, J. F. (1945) 'A laboratory study of the meandering of alluvial rivers', *US Army Corps of Engineers*, Vicksburg, MS, 40pp.

Furbish, D. J. (1991) 'Spatial autoregressive structure in meander evolution', *Geological Society of America Bulletin*, 103, 1576-1589.

Gardner, R. (1983) 'Introduction', in Gardner, R. and Scoging, H. (eds.), *Mega-geomorphology*, Clarendon, Oxford, 1-17.

Gilbert, G. K. (1887) 'Report on the geology of the Henry Mountains', *United States Geological and Geographical Survey*, Rocky Mountain Region, General Printing Office, Washington DC, 170pp.

Gill, D. (1970) 'Application of a statistical zonation method to a reservoir evaluation and digititised log analysis', *The American Association of Petroleum Geologists Bulletin*, 54 (5), 719-729.

Goff, J. R. and Ashmore, P. (1994) 'Gravel transport and morphological change in braided Sunwapta River, Alberta, Canada', *Earth Surface Processes and Landforms*, 19 (3), 195-212.

Gomez, B., Naff, R. L. and Hubbell, D. W. (1989) 'Temporal variations in bedload transport rates associated with migration of bedforms', *Earth Surface Processes and Landforms*, 14, 135-56.

Goudie, A. S. (1990) 'The global geomorphological future', *Zeitschrift Fur Geomorphologie*, Supplementband 73, 51-62.

Graf, W. L. (1992) 'Science, public-policy, and western American rivers', *Transactions of the Institute of British Geographers*, 17 (1), 5-19.

Graf, W. L. (2001) 'Damage control: restoring the physical integrity of America's rivers', *Annals of the Association of American Geographers*, 91 (1), 1-27.

Granger, C. W. J. (1969) 'Spatial data and time series analysis', in Scott, A. J. (ed.), *Studies in regional science*, Pion, London.

Granger, C. W. J. and Hatanaka, M. (1964) '*Spectral analysis of economic time series*', Princeton University Press, Princeton, N.J., 299pp.

Grebau, W. (April 2001) Personal communication, Vicksburg, MS.

Gregory, D. I. and Schumm, S. A. (1987) 'The effect of active tectonics on alluvial river morphology', in Richards, K. S. (ed.), *River Channels: Environment and Process*, Blackwell, Oxford, 41-68.

Gregory, K. J. (2000) '*The changing nature of physical geography*', Arnold, London, 368pp.

Guccione, M. J., Lafferty, R. H. and Cummings, L. S. (1988) 'Environmental constraints of human settlement in an evolving Holocene alluvial system, the Lower Mississippi Valley', *Geoarchaeology*, 3 (1), 65-84.

Gurnell, A. M., Bickerton, M., Angold, P., Bell, D., Morrissey, I., Petts, G. E. and Sadler, J. (1998) 'Morphological and ecological change on a meander bend: the role of hydrological processes and the application of GIS', *Hydrological Processes*, 12 (6), 981-993.

Hack, J. T. (1957) 'Studies of longitudinal stream profiles in Virginia and Maryland', *United States Geological Survey Professional Paper, 294B*, 59-63.

Hack, J. T. (1965) 'Postglacial drainage evolution and stream geometry in the Ontonagon area, Michigan', *United States Geological Survey, Professional Paper, 504-B*, 40pp.

Haltiner, J. P., Kondolf, G. M. and Williams, P. B. (1996) 'Restoration approaches in California', in Brookes, A. and Shields, F. D. J. (eds.), *River Channel Restoration: Guiding Principles for Sustainable Projects*, John Wiley & Sons Ltd, Chichester.

Harbor, D. J. (1998) 'Dynamics of bedforms in the Lower Mississippi River', *Journal of Sedimentary Research*, 68 (5), 750-762.

Harrison, S. (2001) 'On reductionism and emergence in geomorphology', *Transactions of the Institute of British Geographers*, 26 (3), 327-339.

Hart, E. D. and Downing, G. C. (1977) 'Positioning techniques and equipment for U.S. Army Corps of Engineers hydrographic surveys', *U.S. Army Corps of Engineers Technical Report H-77-10*, Vicksburg, MS, 166pp.

Harvey, A. C. (1993) '*Time series models*', 2nd edition, Harvester Wheatsheaf, London, 308pp.

Harvey, A. M. (1975) 'Some aspects of the relations between channel characteristics and riffle spacing in meandering streams', *American Journal of Science*, 275, 470-478.

Hawkins, D. M. and Merriam, D. F. (1973) 'Optical zonation of digitised sequential data', *Mathematical Geology*, 5 (4), 389-395.

Hawkins, D. M. and Merriam, D. F. (1974) 'Zonation of multivariate sequences of digitised geologic data', *Mathematical Geology*, 6 (3), 263-269.

Hey, R. D. (1976) 'Impact prediction on the physical environment', in O'Riordan, T. and Hey, R. D. (eds.), *Environmental Impact Assessment*, Saxon House, Farnborough, 71-81.

Hickin, E. J. (1977) 'The analysis of river planform responses to changes in discharge', in Gregory, K. J. (ed.), *River channel changes*, John Wiley & Sons Ltd, Chichester, 249-264.

Hoey, T. B. and Sutherland, A. J. (1991) 'Channel morphology and bedload pulses in braided rivers: A laboratory study', *Earth Surface Processes and Landforms*, 16, 447-462.

Hooke, J. M. (1977) 'The distribution and nature of river channel patterns: the example of Devon', in Gregory, K. J. (ed.), *River Channel Changes*, John Wiley & Sons Ltd, Chichester, 265-280.

Hooke, J. M. (1984) 'Changes in river meanders - a review of techniques and results of analyses', *Progress in Physical Geography*, 8 (4), 473-508.

Hooke, J. M. (1987) 'Changes in meander morphology', in Gardiner, V. (ed.), *International Geomorphology*, John Wiley & Sons, Chichester, 1, 591-609.

Hooke, J. M. (2003) 'River meander behaviour and instability: a framework for analysis', *Transactions of the Institute of British Geographers*, NS 28, 238-253.

Hooke, J. M. and Harvey, A. M. (1983) 'Meander changes in relation to bend morphology and secondary flows', in Collinson, J. D. and Lewin, J. (eds.), *Modern and ancient fluvial systems*, International Association on Sediment Special Publication, 6, 121-132.

Hooke, J. M. and Redmond, C. E. (1989) 'Use of cartographic sources for analysing river channel change with examples from Britain', in Petts, G. (ed.), *Historical Change of Large Alluvial Rivers*, John Wiley & Sons, 79-93.

Horton, R. E. (1945) 'Erosional development of streams and their drainage basins: hydrophysical approach to quantitative morphology', *Bulletin of Geological Society of America*, 56, 275-370.

Hudson, P. F. and Kesel, R. H. (2000) 'Channel migration and meander-bend curvature in the Lower Mississippi River prior to major human modification', *Geology*, 28 (6), 531-534.

Hulsing, H., Winchell, S. and Cobb, E. D. (1966) 'Velocity head coefficients in open channels', *U.S Geological Survey Professional Paper*, 27pp.

Humphreys, A. A. and Abbot, H. L. (1861) 'Report upon the Physics and Hydraulics of the Mississippi River', *U.S. Army Corps of Topographic Engineers, Professional Paper 13*, Washington D.C., 691pp.

Inglis, C. C. (1947) 'Meanders and their bearing on river training', *The Institute of Civil Engineers, Maritime and Waterways Engineering Division Paper 7*, 23pp.

IPCC (1996) '*Climate change 1995. The science of climate change*', Cambridge University Press, Cambridge.

Jackson, R. G. (1975) 'Hierarchical attributes and a unifying model of bed forms composed of cohesionless material and produced by a shearing flow', *Geological Society of America Bulletin*, 86, 1523-1533.

Jain, S. C. and Kennedy, J. F. (1974) 'The spectral evolution of sedimentary bed forms', *Journal of Fluid Mechanics*, 63 (2), 301-314.

Jefferson, M. (1902) 'The limiting widths of meander belts', *National Geographic Magazine*, 373-384.

Jibson, R. W., Keefer, D. K., Russ, D. P. and Crone, A. J. (1988) 'Landslides triggered by earthquakes in the central Mississippi valley, Tennessee and Kentucky', *United States Geological Survey Professional Paper 1336-C*, Washington DC, C1-C24.

Johnson, J. W. (1944) 'Rectangular artificial roughness in open channels', *Transactions of the American Geophysical Union*, 25, 906-914.

Johnson, S. (2001) '*Emergence: The connected lives of ants, brains, cities and software*', Penguin, London, 288pp.

Jones, C. (1997) '*Geographical Information Systems and Computer Cartography*', Longman, Harlow.

Jones, J. A. A. (1997) '*Global hydrology: processes, resources and environmental management*', Longman, Harlow, 399pp.

Julien, P. Y. and Klassen, G. J. (1995) 'Sand-dune geometry of large rivers during floods', *Journal of Hydraulic Engineering, American Society of Civil Engineers*, 121, 657-663.

Keller, E. A. (1971) 'Areal sorting of bed-load material: the hypothesis of velocity reversal', *Geological Society of America Bulletin*, 82, 753-756.

Keller, E. A. (1972) 'Development of alluvial stream channels: A five stage model', *Geological Society of America Bulletin*, 83, 1531-1536.

Keller, E. A. and Melhorn, W. N. (1978) 'Rhythmic spacing and origin of pools and riffles', *Geological Society of America Bulletin*, 89, 723-730.

Kellerhals, R. and Church, M. (1989) *'The morphology of large rivers: characterisation and management*', Proceedings of the International Large Rivers Symposium, Ontario, Canada, Canadian Special Publication of Fisheries and Aquatic Sciences 106.

Kennedy, B. A. (1972) "Bankfull' discharge and meander forms', *Area*, 4, 209-212.

Kennedy, B. A. (1992) 'Hutton to Horton - views of sequence, progression and equilibrium in geomorphology', *Geomorphology*, 5 (3-5), 231-250.

Keown, M. P., Dardeau, E. A. and Causey, E. M. (1981) 'Characterisation of the suspended-sediment regime and bed-material gradation of the Mississippi River Basin', *U.S Army Corps of Engineers Potamology Program (P-1) Report*, Vicksburg, MS, 44pp.

Kesel, R. H. (1988) 'The decline in the suspended load of the Lower Mississippi River and its influence on adjacent wetlands', *Environmental Geology and Water Sciences*, 11 (3), 271-281.

Kesel, R. H. (1989) 'The role of the Mississippi River in wetland loss in southeastern Louisiana, USA', *Environmental Geology and Water Sciences*, 13 (3), 183-193.

King, A. W. (1950) 'The study of the worlds plainlands', *Quaterly Journal of the Geological Society of London*, 106, 101-131.

Knighton, D. (1998) '*Fluvial forms and processes: a new perspective*', Arnold, London, 383pp.

Koellner, W. H. (1996) 'The flood's hydrology', in Changnon, S. A. (ed.), *The great flood of 1993*, Westview Press, Oxford, 68-100.

Kolb, C. R. (1963) 'Sediments forming the bed and banks of the Lower Mississippi River and their effects on river migration', *Sedimentology*, 2, 227-234.

Kostaschuk, R. and Villard, P. (1996) 'Flow and sediment transport over large subaqueous dunes: Fraser River, Canada', *Sedimentology*, 43 (5), 849-863.

Lane, E. W. (1947) *'The effect of cutting off bends in rivers*', University of Iowa Studies in Engineering, Proceedings of the Third Hydraulic Conference, University of Iowa, Iowa City, Iowa.

Lane, E. W. (1955) 'The importance of fluvial morphology in hydraulic engineering', *Proceedings, American Society of Civil Engineers*, 81, 1-17.

Lane, S. N. (1995) 'The dynamics of dynamic river channels', *Geography*, 80 (2), 147-162.

Lane, S. N. (1998) 'The use of digital terrain modelling in the understanding of dynamic river channel systems', in Lane, S. N., Richards, K. and Chandler, J. H. (eds), *Landform Monitoring, Modelling and Analysis*, John Wiley & Sons, 311-342.

Lane, S. N., Chandler, J. H. and Richards, K. S. (1994) 'Developments in monitoring and modelling small-scale river bed topography', *Earth Surface Processes and Landforms*, 19 (4), 349-368.

Lane, S. N. and Richards, K. S. (1997) 'Linking river channel form and process: time, space and causality revisited', *Earth Surface Processes and Landforms*, 22 (3), 249-260.

Lane, S. N., Richards, K. S. and Chandler, J. H. (1995) 'Morphological estimation of the time-integrated bed-load transport rate', *Water Resources Research*, 31 (3), 761-772.

Lane, S. N., Richards, K. S. and Chandler, J. H. (1996) 'Discharge and sediment supply controls on erosion and deposition in a dynamic alluvial channel', *Geomorphology*, 15 (1), 1-15.

Langbein, W. B. and Leopold, L. B. (1966) 'River meanders - theory of minimum variance', *United States Geological Survey Professional Paper, 422-H*, 15pp.

Leopold, L. B. (1994) '*A view of the river*', Harvard University Press, Cambridge, 281pp.

Leopold, L. B., Bagnold, R. A., Wolman, M. G. and Brush, L. M. J. (1960) 'Flow resistance in sinuous or irregular channels', *U.S. Geological Survey Professional Paper, 282-D*.

Leopold, L. B. and Emmett, W. W. (1983) 'Bedload movement and its relation to scour', in Elliott, C. M. (ed.), *River Meandering*, American Society of Civil Engineers, New Orleans, 640-649.

Leopold, L. B. and Maddock, T. (1953) 'The hydraulic geometry of stream channels and some physiographic implications', *United States Geological Survey Professional Paper 252*, 1-55.

Leopold, L. B. and Wolman, M. G. (1957) 'River channel patterns - braided, meandering and straight', *Professional Paper of the United States Geological Survey, 282B*, 85pp.

Leopold, L. B. and Wolman, M. G. (1960) 'River meanders', *Bulletin of Geological Society of America*, 71, 769-794.

Lewin, J. (1976) 'Initiation of bedforms and meanders in coarse-grained sediments', *Bulletin of Geological Society of America*, 87, 281-285.

Lewin, J. (1977) 'Channel pattern changes', in Gregory, K. J. (ed.), *River Channel Changes*, John Wiley & Sons Ltd, Chichester, 167-184.

Lisle, T. E. (1979) 'A sorting mechanism for a riffle-pool sequence', *Geological Society of America Bulletin*, 90, 1142-1157.

Mackin, J. H. (1948) 'Concept of a graded river', *Bulletin of Geological Society of America*, 59, 463-511.

Mackin, J. H. (1963) 'Rational and empirical methods of investigation in geology', in Albritton, C. C. (ed.), *The fabric of geology*, Addison-Wesley, Reading, Massachusetts, 135-163.

Maddock, T. (1969) 'The behaviour of straight open channels with moveable beds', *United States Geological Survey Professional Paper 622A*.

Martin, Y. and Church, M. (1995) 'Bed-material transport estimated from channel surveys - Vedder River, British-Columbia', *Earth Surface Processes and Landforms*, 20 (4), 347-361.

McDonnell, R. A. (2000) 'Hierarchical modelling of the environmental impacts of river impoundment based on a GIS', *Hydrological Processes*, 14 (11-12), 2123-2142.

Meade, R. H. (1981) 'Movement and storage of bed material during 1979 in East Fork River, Wyoming, USA', *IAHS Publication*, Christchurch.

Meade, R. H. (1985) 'Wavelike movement of bedload sediment, East Fork River, Wyoming', *Environmental Geological Water Science*, 7 (4), 215-225.

Meuller, J. E. (1968) 'Introduction to hydraulic and topographic sinuosity indexes', *Annals of the Association of American Geographers*, 58, 371-385.

Milne, J. A. (1982) 'Bed forms and bend-arc spacings of some coarse-bedload channels in upland Britain', *Earth Surface Processes and Landforms*, 7, 227-240.

Milne, J. A. and Sear, D. A. (1997) 'Modelling river channel topography using GIS', *International Journal of Geographical Information Science*, 11 (5), 499-519.

Moore, N. R. (1972) 'Improvement of the Lower Mississippi River and tributaries, 1931-1972', *U.S. Army Corps of Engineers, Mississippi River Commission*, Vicksburg, MS, 241pp.

Morrison, R. B. (1991) 'Introduction', in Morrison, R. B. (ed.), *Quaternary nonglacial geology: Conterminous U.S.*, Geological Society of America, Boulder, CO, 1-12.

Newson, M. D. (1992) '*Land, water, and development : river basin systems and their sustainable management*', Routledge, London, 351pp.

Nordin, C. F. and Algert, J. H. (1966) 'Spectral analysis of sand waves', *Journal of the Hydraulics Division, American Society of Civil Engineers*, 92, 95-114.

Nordin, C. F. and Queen, B. S. (1992) 'Particle size distributions of bed sediments along the thalweg of the Mississippi River, Cairo, Illinois to Head of Passes, September 1989', *U.S. Army Corps of Engineers Potamology Program (P-1), Report 7*, Lower Mississippi Valley Division Office, Vicksburg, MS, 93pp.

O'Neill, M. P. and Abrahams, A. D. (1984) 'Objective identification of pools and riffles', *Water Resources Research*, 20, 921-926.

Orlowski, L. A., Schumm, S. A. and Mielke, P. W. (1995) 'Reach classifications of the Lower Mississippi River', *Geomorphology*, 14 (3), 221-234.

Petts, G. (1995) 'Changing river channels: the geographical tradition', in Gurnell, A. M. and Petts, G. (ed.), *Changing River Channels*, John Wiley & Sons, 1-24.

Phillips, J. D. (1991) 'Multiple modes of adjustment in unstable river channel cross-sections', *Journal of Hydrology*, 123, 39-49.

Pitlick, J. C. (1997) 'A regional perspective of the hydrology of the 1993 Mississippi River Basin floods', *Annals of the Association of American Geographers*, 87 (1), 135-151.

Porter, D. A. and Guccione, M. J. (1994) 'Deglacial flood origin of the Charleston alluvial fan, Lower Mississippi alluvial valley', *Quaternary Research*, 41, 278-284.

Pratt, T. C. (1995) 'A comparison of a standard current meter discharge measurement technique to one that uses an Acoustic Doppler Current Profiler (ADCP) to measure discharge', Miscellaneous Paper HL-95-4, *U.S. Army Corps of Engineers*, Vicksburg, MS, 15pp.

Prince, H. (1997) '*Wetlands of the American Midwest: A historical geography of changing attitudes*', University of Chicago Press, Chicago, 395pp.

Ray, L. L. (1964) 'The Charleston, Missouri, alluvial fan', *United States Geological Survey Professional Paper, 501-B*, Washington DC, B130-B134.

Reisner, M. (1990) '*Cadillac desert: the American west and its disappearing water*', Penguin, New York, 582pp.

Renwick, W. H. (1992) 'Equilibrium, disequilibrium, and nonequilibrium landforms in the landscape', *Geomorphology*, 5 (3-5), 265-276.

Richards, K. S. (1976) 'Channel width and the riffle-pool sequence', *Geological Society of America Bulletin*, 87, 883-890.

Richards, K. S. (1976) 'The morphology of the riffle-pool sequence', *Earth Surface Processes*, 1, 71-88.

Richards, K. S. (1979) '*Stochastic processes in one-dimensional series*', CATMOG 23, 57pp.

Richards, K. S. (1982) '*Rivers, form and process in alluvial channels*', Methuen, London, 358pp.

Richards, K. S. (1987) 'Rivers: environment, process and form', in Richards, K. S. (ed.), *River Channels: Environment and Process*, Blackwell, Oxford, 1-13.

Richards, K.S. (1990) 'Real geomorphology', *Earth Surface Processes and Landforms*, 15 (3), 195-197.

Richards, K. S. (1999) 'The magnitude-frequency concept in fluvial geomorphology: a component of a degenerating research programme?' *Zietschrift fur Geomorphologies*, Suppl. Bd. 115, 1-18.

Richards, K. S., Brooks, S., Clifford, N., Harris, T. and Lane, S. N. (1996) 'Theory, measurement and testing in 'real' geomorphology and physical geography', in Stoddart, D. R. (ed.), *Process and Form in Geomorphology*, Routledge, London, 265-292.

Richards, K. S., Brunsden, D., Jones, D. K. C. and McCaig, M. (1987) 'Applied fluvial geomorphology: River engineering project appraisal in its geomorphological context', in Richards, K. S. (ed.), *River Channels: Environment and Process*, Blackwell, Oxford, 348-382.

Robbins, L. G. (1977) 'Suspended sediment and bed material studies on the Lower Mississippi River', Potamology Investigations, Report 300-1, *U.S. Army Corps of Engineers, Vicksburg District*, Vicksburg, MS.

Robinson, D. R. (2003) '*River rehabilitation in urban environments: morphology and design principles for the pool-riffle sequence*', University College London, London, 315pp.

Rubin, D. M. and McCulloch, D. S. (1980) 'Single and superimposed bedforms: A synthesis of San Francisco Bay and flume observations', *Sedimentary Geology*, 26, 207-231.

Saucier, R. T. (1994) 'Geomorphology and Quaternary geologic history of the Lower Mississippi River', *U.S. Army Engineer Waterways Experiment Station*, Vicksburg, MS, 364pp.

Sayer, A. (1992) '*Method in social science*', 2nd edition, Routledge, London, 313pp.

Sayre, W. W. and Albertson, M. L. (1961) 'Roughness spacing in rigid open channels', *A.S.C.E Journal of the Hydraulics Division*, 87, 121-150.

Schumm, S. A. (1969) 'River metamorphosis', *Journal of the Hydraulics Division, American Society of Civil Engineers*, 95, HY1, 255-273.

Schumm, S. A. (1985) 'Patterns of alluvial rivers', *Annual Review of Earth and Planetary Sciences*, 13, 5-27.

Schumm, S. A. and Galay, V. J. (1994) 'The River Nile in Egypt', in Schumm, S. A. and Winkley, B. R. (eds.), *The Variability of Large Alluvial Rivers*, American Society of Civil Engineers, 75-100.

Schumm, S. A. and Khan, H. R. (1972) 'Experimental study of channel patterns', *Geological Society of America Bulletin*, 83, 1755-1770.

Schumm, S. A. and Lichty, R. W. (1965) 'Time, space and causality in geomorphology', *American Journal of Science*, 263, 110-119.

Schumm, S. A., Rutherford, I. D. and Brooks, J. (1994) 'Pre-cutoff morphology of the Lower Mississippi River', in Schumm, S. A. and Winkley, B. R. (eds.), *The Variability of Large Alluvial Rivers*, American Society of Civil Engineers, 13-44.

Schumm, S. A., Watson, C. and Burnett, A. W. (1982) 'Investigation of Neotectonic activity within the Lower Mississippi Valley Division', *U.S Army Corps of Engineers*, Vicksburg, Mississippi, 168pp.

Schumm, S. A. and Winkley, B. R. (1994) 'The character of large alluvial rivers', in Schumm, S. A. and Winkley, B. R. (eds.), *The Variability of Large Alluvial Rivers*, American Society of Civil Engineers, 1-9.

Sear, D. A. and Milne, J. A. (2000) 'Surface modelling of upland river channel topography and sedimentology using GIS', *Physics and Chemistry of the Earth Part B-Hydrology Oceans and Atmosphere*, 25 (4), 399-406.

Simons, D. B. and Richardson, E. V. (1966) 'Resistance to flow in alluvial channels', *United States Geological Survey Professional Paper, 422-J*, Washington DC, J1-J61.

Simons, D. B., Richardson, E. V. and Nordin, C. F. (1965) 'Bedload equation for ripples and dunes', *U.S. Geological Survey Professional Paper, 462-H*.

Simons, D. B., Stevens, M. A. and Duke, J. H., Jr. (1973) 'Predicting stages on sand-bed rivers', *Journal of Waterways, Harbours and Coastal Engineering Division, American Society of Civil Engineers*, 99, 231-244.

Simpson, G. G. (1963) 'Historical science', in Albritton, C. C. (ed.), *The Fabric of Geology*, Addison-Wesley, Reading, Massachusetts, 24-48.

Simpson, M. R. and Oltmann, R. N. (1993) 'Discharge measurement system using an acoustic doppler current profiler with applications to large rivers and estuaries', *U.S. Geological Survey Water Supply Paper, 2395*, 17pp.

Smith, J. D. and McLean, S. R. (1977) 'Spatially averaged flow over a wavy surface', *Journal of Geophysical Research*, 82 (12), 1735-1746.

Smith, L. M. (1996) 'Fluvial geomorphic features of the Lower Mississippi alluvial valley', *Engineering Geology*, 45 (1-4), 139-165.

Speight, J. G. (1965) 'Meander spectra of the Angabunga River, Papua', *Journal of Hydrology*, 3, 1-15.

Stanley Consultants (1990) 'Lower Mississippi River hydraulic studies 1950-1988 (River mile 320 to 596)', *U.S. Army Corps of Engineers Vicksburg District*, Vicksburg, MS.

Stolum, H. (1998) 'Planform geometry and dynamics of meandering rivers', *Geological Society of America Bulletin*, 110 (11), 1485-1498.

Strahler, A. N. (1950) 'Davis's concept of slope development viewed in the light of recent quantitative investigations', *Annals of the Association of American Geographers*, 40, 209-13.

Strahler, A. N. (1952) 'Dynamic basis of geomorphology', *Bulletin of Geological Society of America*, 63, 923-938.

Sugden, D. E., Summerfield, M. A. and Burt, T. P. (1997) 'Editorial: Linking short-term geomorphic processes to landscape evolution', *Earth Surface Processes and Landforms*, 22 (3), 193-194.

Summerfield, M. A. (1991) '*Global geomorphology*', Longman, Harlow, 537pp.

Thakur, T. R. and Schiedegger, A. E. (1970) 'Chain model of river meanders', *Journal of Hydrology*, 12, 25-47.

Thorne, C. R. (1990) 'Effects of vegetation on riverbank erosion and stability', in Thornes, J. B. (ed.), *Vegetation and Erosion*, John Wiley & Sons Ltd, 125-144.

Thorne, C. R. (1997) 'Channel types and morphological classification', in Bathurst, J. C., Thorne, C. R. and Hey, R. D. (eds.), *Applied Fluvial Geomorphology for River Engineering and Management*, John Wiley & Sons Ltd, Chichester, 175-222.

Thorne, C. R. (2002) 'The geomorphic analysis of large alluvial rivers', *Geomorphology,* 44, 203-220.

Thorne, C. R., Russell, J. R. and Alam, M. K. (1993) 'Planform pattern and channel evolution of the Brahmaputra River, Bangladesh', in Best, J. L. and Bristow, C. S. (eds.), *Braided Rivers*, The Geological Society, London, 257-276.

Tinkler, K. J. (1971) 'Active valley meanders in south-central Texas and their wider implications', *Geological Society of America Bulletin*, 82, 1783-1800.

Toth, L. A. (1996) 'Restoring the hydrogeomorphology of the channelised Kissimmee River', in Brookes, A. and Shields, F. D. J. (eds.), *River Channel Restoration: Guiding Principles for Sustainable Projects*, John Wiley & Sons, Chichester, 369-383.

U. S. Army Corps of Engineers (2002) 'Engineer and design manual - hydrographic surveying', *U.S. Army Corps of Engineers Report Number EM 1110-2-1003*, Washington.

van den Berg, J. H. (1987) 'Bedform migration and bedload transport in some rivers and tidal environments', *Sedimentology*, 34, 681-98.

van Rijn, L. C. (1984) 'Sediment transport. Part III: Bedforms and alluvial roughness', *Journal of Hydraulic Engineering*, 110, 1733-54.

Walsh, S. J., Butler, D. R. and Malanson, G. P. (1998) 'An overview of scale, pattern, process relationships in geomorphology: a remote sensing and GIS perspective', *Geomorphology*, 21, 183-205.

Walters, W. H. and Simons, D. B. (1983) 'Long-term changes of Lower Mississippi River meander geometry', in Elliott, C. M. (ed.), *River Meandering*, American Society of Civil Engineers, New York, New Orleans, 318-329.

Webster, R. (1973) 'Automatic soil-boundary location from transect data', *Mathematical Geology*, 5 (1), 27-37.

Westaway, R. M., Lane, S. N. and Hicks, D. M. (2000) 'The development of an automated correction procedure for digital photogrammetry for the study of wide, shallow, gravel- bed rivers', *Earth Surface Processes and Landforms*, 25 (2), 209-226.

Williams, G. P. (1986) 'River meanders and channel size', *Journal of Hydrology*, 88, 147-164.

Winkley, B. R. (1977) 'Man-made cutoffs on the Lower Mississippi River, conception, construction, and river response', *U.S. Army Corps of Engineer Potamology Investigations Report 300-2*, Vicksburg, MS, 209pp.

Winkley, B. R. (1982) 'Response of the Lower Mississippi to river training and realignment', in Hey, R. D., Bathurst, J. C. and Thorne, C. R. (eds.), *Gravel Bed Rivers*, John Wiley & Sons, Chichester, 659-681.

Winkley, B. R. (1994) 'Response of the Lower Mississippi River to flood control and navigation improvements', in Schumm, S. A. and Winkley, B. R. (eds.), *The Variability of Large Alluvial Rivers*, American Society of Civil Engineers, New York, 45-74.

Wohl, E. E., Vincent, K. R. and Merritts, D. J. (1993) 'Pool and riffle characteristics in relation to channel gradient', *Geomorphology*, 6, 99-110.

Wolman, M. G. and Miller, J. P. (1960) 'Magnitude and frequency of forces in geomorphic processes', *Journal of Geology*, 68, 54-74.

Woolard, J. W. and Colby, J. D. (2002) 'Spatial characterization, resolution, and volumetric change of coastal dunes using airborne LIDAR: Cape Hatteras, North Carolina', *Geomorphology*, 48 (1-3), 269-287.

Worboys, M. F. (1995) '*GIS: A computing perspective*', Taylor & Francis, London, 376pp.

Worster, D. (1985) '*Rivers of empire*', Pantheon Books, New York, 402pp.

Yalin, M. S. (1964) 'Geometrical properties of sand waves', *Journal of the Hydraulics Division, American Society of Civil Engineers*, 90, 105-119.

Yalin, M. S. (1977) '*Mechanics of sediment transport*', Pergamon Press, Oxford.

Yalin, M. S. (1992) '*River mechanics*', Pergamon Press, Oxford, 219pp.

Yang, C. T. (1971) 'On river meanders', *Journal of Hydrology*, 13 (3), 231-253.

Yatsu, E. (1955) 'On the longitudinal profile of the graded river', *Transactions American Geophysical Union*, 35, 655-63.

Yin, H. F. and Li, C. G. (2001) 'Human impact on floods and flood disasters on the Yangtze River', *Geomorphology*, 41 (2-3), 105-109.